

Non-Covalent Interactions in Block Copolymers Synthesized via Living Polymerization Techniques

Brian Douglas Mather

Dissertation submitted to the Faculty of the
Virginia Polytechnic Institute and State University
in partial fulfillment of the requirements for the degree of

Doctor of Philosophy
in
Chemical Engineering

Timothy E. Long, Chair
Garth L. Wilkes, Co-Chair
James E. McGrath
Richey M. Davis
Aaron S. Goldstein

April 10, 2007
Blacksburg, Virginia

Keywords: Hydrogen bonding, Block Copolymer, Living Polymerization, Nitroxide
Mediated Polymerization, Ionomers, Morphology, AFM

Copyright 2007, Brian D. Mather

Non-Covalent Interactions in Block Copolymers Synthesized via Living Polymerization Techniques

Brian Douglas Mather

Abstract

Non-covalent interactions including nucleobase hydrogen bonding and ionic aggregation were studied in block and end-functional polymers synthesized via living polymerization techniques such as nitroxide mediated polymerization and anionic polymerization. Non-covalent interactions were expected to increase the effective molecular weight of the polymeric precursors through intermolecular associations and to induce microphase separation. The influence of non-covalent association on the structure/property relationships of these materials were studied in terms of physical properties (tensile, DMA, rheology) as well as morphological studies (AFM, SAXS).

Hydrogen bonding, a dynamic interaction with intermediate enthalpies (10-40 kJ/mol) was introduced through complementary heterocyclic DNA nucleobases such as adenine, thymine and uracil. Hydrogen bonding uracil end-functionalized polystyrenes and poly(alkyl acrylate)s were synthesized via nitroxide mediated polymerization from novel uracil-functionalized alkoxyamine unimolecular initiators. Terminal functionalization of poly(alkyl acrylate)s with hydrogen bonding groups increased the melt viscosity, and as expected, the viscosity approached that of nonfunctional analogs as temperature increased. The effects of hydrogen bonding were also evident in thermal (DSC) analysis and ^1H NMR spectroscopic investigations, and low molar mass polystyrenes exhibited glass transition temperatures that were consistent with a higher apparent molar mass.

A novel difunctional alkoxyamine, DEPN₂, was synthesized and utilized as an efficient initiator in nitroxide-mediated controlled radical polymerization of triblock copolymers. Complementary hydrogen bonding triblock copolymers containing adenine (A) and thymine (T) nucleobase-functionalized outer blocks were synthesized. These thermoplastic elastomeric block copolymers contained short nucleobase-containing outer blocks ($M_n \sim 1\text{K}-4\text{K}$) and *n*-butyl acrylate rubber blocks of variable length ($M_n \sim 14\text{K}-70\text{K}$). Hydrogen bonding interactions were observed for blends of the complementary nucleobase-functionalized block copolymers in terms of increased specific viscosity as well as higher scaling exponents for viscosity with solution concentration. In the solid state, the blends exhibited evidence of a complementary A-T hard phase, which formed upon annealing, and dynamic mechanical analysis (DMA) revealed higher softening temperatures. Morphological development of the block copolymers was studied using SAXS and AFM which revealed intermediate interdomain spacings and surface textures for the blends compared to the individual precursors. Hydrogen bonding interactions enabled the compatibilization of complementary hydrogen bonding guest molecules such as 9-octyladenine.

Ionic interactions, which possess stronger interaction energies than hydrogen bonds (~ 150 kJ/mol) were studied in the context of sulfonated poly(styrene-*b*-ethylene-*co*-propylene-*b*-styrene) block copolymers. As for hydrogen bonding block copolymers, only short block molecular weights of the sulfonated blocks (1K) were necessary to achieve microphase separation. Strong ionic interactions resulted in the development of a microphase separated physical network and greater extents for the rubbery

plateau in DMA analysis compared to sulfonic acid groups, which exhibit weak hydrogen bonding interactions. Small-angle X-ray scattering revealed trends in terms of inter-domain spacing as a function of center block molecular weight.

Multiple hydrogen bonding interactions were utilized to reversibly attach nucleobase-functional quaternary phosphonium ionic guests to complementary adenine-functionalized triblock copolymers. The ionic guest molecules formed optically clear blends with the adenine-functional block copolymer. The presence of the ionic groups resulted in screening of interchain hydrogen bonding interactions, leading to lower solution viscosity and lower softening temperatures for the hard phases. The incorporation of the phosphonium salt guest molecules induced a transition from a cylindrical to lamellar morphology due to increased volume fraction of the hard phase. The molecular recognition between a water-soluble uracil-functionalized phosphonium salt and an adenine-containing block copolymer surface was observed using quartz crystal microbalance with dissipation (QCM-D) measurements

In contrast to the physical networks consisting of sulfonated or hydrogen bonding block copolymers, covalent networks were synthesized using carbon-Michael addition chemistry of acetoacetate functionalized telechelic oligomers to diacrylate Michael acceptors. The thermomechanical properties of the networks based on poly(propylene glycol) oligomers were analyzed with respect to the molecular weight between crosslink points (M_c) and the critical molecular weight for entanglement (M_e). Kinetic analyses of the Michael additions were performed using ^1H NMR spectroscopy, and the influence of basic catalyst and concentration were elucidated. A novel acid-cleavable diacrylate crosslinker, dicumyl alcohol

diacrylate (DCDA), was synthesized. DCDA was utilized as a difunctional Michael acceptor in the synthesis of acid-cleavable crosslinked networks via base-catalyzed Michael addition of telechelic poly(ethylene glycol) bis(acetoacetate).

Overall, non-covalent interactions were introduced into block and end-functionalized polymers, resulting in associations between polymer chains and the formation of physical networks in the case of functional block copolymers. Effects of these non-covalent interactions on a number of physical properties were investigated. Covalent networks composed were also synthesized via Michael addition chemistry and the effect of precursor chain length was investigated.

Acknowledgements

First, I would like to thank my advisor, Prof. Timothy E. Long, for his guidance and inspiration over the course of my graduate career. Your wealth of ideas and contagious enthusiasm has never ceased to amaze me. It has been a pleasure working with you and I have learned a great deal. I am grateful for the summer research internship in 2000, which ultimately led me back to your group for graduate school. I also would like to thank my co-advisor, Prof. Garth L. Wilkes, who was always willing to share his wisdom and technical expertise. You have been a great co-advisor and important bridge to the Chemical Engineering department. Prof. James E. McGrath, Prof. Richey M. Davis and Prof. Aaron S. Goldstein have also been insightful and helpful committee members and teachers during my graduate career. I would also like to thank Prof. S. Richard Turner for his helpful discussions and his very practical class on the transition to industry. I would like to thank Prof. Judy S. Riffle, for being a great teacher in both presentation skills and polymer synthesis courses.

I would like to thank Laurie Good and Millie Ryan who have truly been lifesavers. They have always been willing to help and have also been good friends. I would like to thank Vicki Long, who has helped me many times in both technical work and organizing travel. Also, I would like to thank Tammy Jo Hiner, who has been instrumental during the interviewing process. I would like to also thank Angie Flynn, who is one of the primary organizers of the SURP program that brought me to VT.

I would like to thank the Macromolecular Architecture for Performance Multidisciplinary University Research Initiative (MAP MURI), which has provided funding for my research over the last several years. The MURI grant has also facilitated many

positive interactions with students and faculty in other universities (such as Prof. Ralph Colby at Penn State University and Prof. Geoff Coates at Cornell University). Dr. Cheryl Heisey, Rebecca Heath and Mary Dean Coleman served as organizers of the MAP MURI research program. I am thankful to Cheryl for editing my papers.

I would also like to thank Kraton Polymers and Rohm and Haas for supporting my research both financially and through collaborations. I would like to thank Dr. Carl Willis and Dr. Dale Handlin from Kraton Polymers for their insightful discussions. I would also like to thank Dr. Kevin Miller and Thomas Kauffman from Rohm and Haas, who collaborated with us through a grant from the Department of Energy.

I would also like to thank Dr. Carl Willis, Dr. Peter Pasman, Dr. Dale Handlin and Dan Goodwin with whom I spent an exciting summer at Kraton Polymers in Houston, TX in 2004. The internship was an excellent opportunity to learn about the industrial side of polymer research and has recently led to a patent application and a successful product launch.

I would like to thank Dr. Rick Beyer at the Army Research Laboratories in Aberdeen, MD who has been an excellent collaborator and has always been willing to share his expertise in X-ray scattering analysis of polymers. I enjoyed spending two weeks in Aberdeen with him learning about X-ray scattering and our collaboration has been fruitful.

The staff at Virginia Tech have been a great resource. I would especially like to acknowledge Steve McCartney for his help with microscopy, and Mark Flynn for his help with SEC analysis. Tom Glass, Geno Iannacone and Bill Bebout have also been a great help. Michael Berg and Carla Slebodnick have been great resources for single crystal X-ray diffraction. Jan McGinty has been a great resource for helping our research group to function

properly and keeping the stockroom working.

I would like to thank Prof. Hiroyuki Nishide and his student, Dr. Takeo Suga from Waseda University in Tokyo, Japan, with whom I have collaborated in the last year. They were excellent hosts during my two-week visit to Waseda in November of 2006.

I would also like to thank those that I worked with during undergraduate research. My first research experience was with Prof. James A. Brozik at the University of New Mexico. Dr. Douglas Loy taught my first class on polymers and hired me as a student intern at Sandia National Laboratories where I met Dr. Christopher Cornelius.

I would especially like to thank my research group including post-docs and undergraduates, whom I have enjoyed interacting with. You have been good friends and I have enjoyed the good times working together. Tomonori, Sharlene, Gozde, Serkan, Casey, Dave, Afia, Lars, Qin and Emily made the upstairs labs enjoyable. I valued the mentorship from Dave and Jeremy. Ann, Matt M., Matt G., Matt H., Matthew, Erika, Rebecca, Bill and Funda were also fun people to interact with. I would also like to thank Margaux Baker, a dedicated summer undergraduate student that I worked with from the University of Michigan.

My greatest appreciation and deepest thanks goes to my wife, Qian, who I was blessed to have met in graduate school. You have been my greatest inspiration and my constant companion during graduate school, providing me with great support. With your love, I believe I can achieve anything. I look forward to our life together in San Diego after graduation. I have to appreciate “Poly and the Mers” for the music and Halloween party that brought us together.

Finally, I would like to thank my parents, Doug Mather and Joan Voute, who supported

me throughout graduate school with their words of encouragement, numerous visits and occasional box of pomegranates. I have enjoyed your visits to B'burg, including floating down the New River, hiking up Dragon's tooth, or taking a dip in the Cascades. Thanks for helping to keep me sane through all of this. I would like to thank my wife's parents, Yunling Jiang and Baiyuan Zhang, who took great care of us during our stay in China. Last, but not least, I would like to thank my "little" brother, Joe and his wife Cheri. You two are a lovely couple, and I look forward to seeing the kids soon...

Attribution

Several colleagues and coworkers aided in the writing and research behind several of the chapters of this dissertation. A brief description of their background and their contributions are included here.

Prof. Timothy E. Long- Ph.D. (Department of Chemistry, Virginia Tech) is the primary Advisor and Committee Chair. Prof. Long provided the research direction for all work during the author's graduate study. Furthermore, Prof. Long also directed the composition of the chapters, extensively edited each chapter in this dissertation and is the corresponding author of all papers published.

Chapter 3: Michael Addition Reactions in Macromolecular Design for Emerging Technologies

Kalpana Viswanathan- Ph.D. (Department of Chemistry, Virginia Tech) currently at Guidant Corporation was a student in the author's group and contributed during her graduate studies to this chapter in terms of discussing the applications of the Michael addition reaction in sections 3.7 and 3.8.

Kevin M. Miller- Ph.D. (Department of Chemistry, University of Notre Dame) is employed by Rohm and Haas Company and worked in collaboration with the author on a project supported from Department of Energy. Kevin contributed to the discussion of the mechanism of the Michael addition reaction in sections 3.3.1 and 3.3.2.

Chapter 4: Synthesis of Chain End Functionalized Multiple Hydrogen Bonded Polystyrenes and Poly(alkyl acrylates) via Nitroxide Mediated Radical Polymerization

Jeremy R. Lizotte- Ph.D. (Department of Chemistry, Virginia Tech) currently at Eastman Chemical Company, was a member of the author's research group. His mentorship aided in the publication of this chapter and he contributed through helpful discussions.

Chapters 5 and 6: Supramolecular Triblock Copolymers Containing Complementary Nucleobase Molecular Recognition *and* Multiple Hydrogen Bonding for the Non-covalent Attachment of Ionic Functionality in Block Copolymers

Margaux B. Baker- Undergraduate student (Department of Chemical Engineering, University of Michigan) was a summer undergraduate intern who aided in the experimental work for this chapter, in particular in the synthesis of nucleobase functional block copolymers.

Frederick L. Beyer- Ph.D. (Polymer Science and Engineering, University of Massachusetts in Amherst) is a researcher at the Army Research Laboratory in Aberdeen, MD. Rick contributed to this work by carrying out extensive SAXS analysis and through editing the chapters.

Matthew D. Green- Undergraduate student (Department of Chemical Engineering, Virginia Tech) is an undergraduate researcher in the author's group and aided in solution rheological experiments described in this chapter.

Michael A.G. Berg- Ph.D. (Department of Chemistry, Virginia Tech) is an instructor at the Department of Chemistry at Virginia Tech. He contributed by obtaining X-ray

crystallographic structures for the compounds in these chapters.

Chapter 7: Novel Michael Addition Networks Containing Poly(propylene glycol) Telechelic Oligomers

Kevin M. Miller- Ph.D. contributed by synthesizing the bisAcAc terminated poly(propylene glycol)s which were further reacted in this study to form networks.

Chapter 8: Synthesis of an Acid-Labile Diacrylate Crosslinker for Cleavable Michael Addition Networks

Sharlene R. Williams- Graduate Student (Department of Chemistry, Virginia Tech) is a member of the author's research group and contributed through the synthesis of the bisAcAc terminated poly(ethylene glycol)

Chapter 9: Synthesis and Morphological Characterization of Sulfonated Triblock Copolymers: Influence of High Sulfonate Levels and Poly(ethylene-*co*-propylene) Molecular Weight

Frederick L. Beyer- Ph.D. contributed through teaching the author how to carry out SAXS analysis of the sulfonated block copolymers. Rick contributed further through scientific discussions and through editing the chapter.

Dale L. Handlin- Ph.D. (Polymer Science and Engineering, University of Massachusetts in Amherst) is a researcher at Kraton Polymers. Dale contributed to this chapter through scientific discussions as well as introducing a model for analyzing the tensile behavior of the

polymers studied.

Chapter 10: Morphological Analysis of Telechelic Ureido-Pyrimidone Functional Hydrogen Bonding Linear and Star-Shaped Poly(ethylene-*co*-propylene)s

Casey L. Elkins- Ph.D. (Department of Chemistry, Virginia Tech) was a member of the author's research group and is currently employed by DuPont Company. Casey carried out the synthesis of the UPy terminated polymers and published a paper on these prior to the studies that resulted in this chapter. Casey also contributed through editing this chapter and scientific discussions.

Frederick L. Beyer- Ph.D. contributed through teaching the author how to carry out SAXS analysis of the UPy terminated copolymers. Rick contributed further through numerous helpful discussions and editing the chapter.

Table of Contents

CHAPTER 1. INTRODUCTION	1
1.1 SCIENTIFIC RATIONALE AND PERSPECTIVE	1
CHAPTER 2. REVIEW OF THE LITERATURE – HYDROGEN BOND FUNCTIONALIZED BLOCK COPOLYMERS AND TELECHELIC HYDROGEN BONDING OLIGOMERS	5
2.1 FUNDAMENTALS OF HYDROGEN BONDING	5
2.2 PERFORMANCE ADVANTAGES OF HYDROGEN BONDING POLYMERS	11
2.3 HYDROGEN BONDING BLOCK COPOLYMERS	20
2.3.1 <i>Block Copolymers Involving Single Hydrogen Bonding Groups</i>	22
2.3.2 <i>Nucleobase Containing Hydrogen Bonding Block Copolymers</i>	28
2.3.3 <i>Block Copolymers Containing DNA Oligonucleotides</i>	37
2.3.4 <i>Block Copolymers Containing other Hydrogen Bonding Arrays</i>	40
2.3.5 <i>Order-Disorder Transitions (ODT) in Hydrogen Bonding Block Copolymers</i>	42
2.4 TELECHELIC HYDROGEN BOND FUNCTIONAL POLYMERS.....	43
2.5 COMBINING HYDROGEN BONDING WITH OTHER NON-COVALENT INTERACTIONS.....	55
2.6 REVERSIBLE ATTACHMENT OF GUEST MOLECULES VIA HYDROGEN BONDING	57
2.7 CONCLUSIONS AND SUMMARY	63
CHAPTER 3. REVIEW OF THE LITERATURE – MICHAEL ADDITION REACTIONS IN MACROMOLECULAR DESIGN FOR EMERGING TECHNOLOGIES	65
3.1 ABSTRACT	65
3.2 MOTIVATION AND SCIENTIFIC RATIONALE	65
3.3. INTRODUCTION TO THE MICHAEL ADDITION REACTION	70
3.3.1 <i>Mechanism of the Carbon-Michael Addition Reaction</i>	70
3.3.1.1 <i>Effect of Base Strength</i>	75
3.3.1.2 <i>Effect of Solvent</i>	76
3.3.1.3 <i>Effect of Substrate</i>	77
3.3.1.4 <i>Other Carbon-Michael Catalysts</i>	80
3.3.2 <i>Heteroatomic Donors in the Michael Addition Reaction</i>	85
3.3.2.1. <i>The aza-Michael Reaction</i>	85
3.3.2.2. <i>Thiols as Michael Donors</i>	95
3.4 LINEAR STEP GROWTH MICHAEL ADDITION POLYMERIZATIONS	98
3.4.1 <i>Overview</i>	98
3.4.2 <i>Poly(amido amine)s</i>	101
3.4.3 <i>Poly(imido sulfide)s</i>	111
3.4.4 <i>Poly(aspartamide)s</i>	117
3.4.5 <i>Poly(amino quinone)s</i>	123
3.4.6 <i>Step Growth Polymers Derived from Bisacetylene-Containing Monomers</i>	127
3.4.7 <i>Hydrogen transfer polymerization</i>	128
3.5 LINEAR CHAIN GROWTH MICHAEL ADDITION POLYMERIZATIONS	133

3.5.1. Anionic Polymerization of Methacrylates.....	134
3.5.2 Group Transfer Polymerization	141
3.5.3 Anionic Polymerization of α -cyanoacrylates.....	143
3.5.4 Living Radical Polymerization.....	145
3.6 SYNTHESIS OF BRANCHED POLYMERS VIA THE MICHAEL ADDITION REACTION.....	148
3.6.1 Dendrimers	149
3.6.2 Hyperbranched and Highly Branched Polymers	159
3.6.3 Graft Copolymers.....	172
3.7 NOVEL NETWORKS VIA THE MICHAEL ADDITION REACTION.....	177
3.7.1 Bismaleimide Networks and Composite Materials	177
3.7.2 Carbon Michael Addition Networks Utilizing Acetoacetate Chemistry	180
3.7.3 Curing Mechanisms Involving Michael Addition with Photocrosslinking or Sol-Gel Chemistry.....	185
3.7.4 Hydrogel Networks for Biomedical Applications	190
3.8 BIOCONJUGATES VIA THE MICHAEL ADDITION REACTION.....	207
3.8.1 Polymer-Protein and Polymer-Drug Conjugates.....	207
3.8.2 Coupling of Biological Molecules to Michael Addition Polymers	216
3.9 CONCLUSIONS AND FUTURE DIRECTIONS.....	217
3.10 ACKNOWLEDGEMENTS	218
CHAPTER 4. SYNTHESIS OF CHAIN END FUNCTIONALIZED MULTIPLE HYDROGEN BONDED POLYSTYRENES AND POLY(ALKYL ACRYLATES) VIA NITROXIDE MEDIATED RADICAL POLYMERIZATION	219
4.1 ABSTRACT	219
4.2 INTRODUCTION	220
4.3 EXPERIMENTAL.....	226
4.3.1 Materials	226
4.3.2 Synthesis of Uracil-TEMPO Unimolecular Initiator	226
4.3.3 Synthesis of Uracil-DEPN Unimolecular Initiator	227
4.3.4 Polymerizations of Styrene Using Uracil-TEMPO.....	228
4.3.5 Polymerizations of n-Butyl Acrylate Using Uracil-DEPN	229
4.3.6 Polymer Characterization.....	230
4.4 RESULTS AND DISCUSSION.....	231
4.4.1 Uracil-TEMPO and Uracil-DEPN Unimolecular Initiator Syntheses	231
4.4.2 Polymerizations of Styrene and n-Butyl Acrylate Using the Uracil Based Initiators.....	234
4.4.3 In-situ FTIR Monitoring of Polymerization Kinetics	238
4.4.4 Characterization of Hydrogen Bonding Using ^1H NMR Spectroscopy.....	244
4.4.5 Characterization of Hydrogen Bonding Using Melt Rheology.....	247
4.4.6 Thermal Analysis of Uracil Polystyrenes.....	251
4.5 CONCLUSION.....	255
4.6 ACKNOWLEDGEMENT	255
CHAPTER 5. SUPRAMOLECULAR TRIBLOCK COPOLYMERS CONTAINING COMPLEMENTARY NUCLEOBASE MOLECULAR RECOGNITION	256
5.1 ABSTRACT	256
5.2 INTRODUCTION	257

5.3 EXPERIMENTAL	265
5.3.1 Materials	265
5.3.2 Synthesis of DEPN₂	265
5.3.3 Polymerization of n-Butyl Acrylate with DEPN₂	267
5.3.4 Synthesis of Thymine-Containing Block Copolymer	267
5.3.5 Synthesis of Adenine-Containing Block Copolymer	268
5.3.6 Blends of Adenine and Thymine Functionalized Block Copolymers and Sample Preparation	269
5.3.7 Polymer Characterization	270
5.4 RESULTS AND DISCUSSION	272
5.4.1 Synthesis of a Novel Difunctional Alkoxyamine Initiator	272
5.4.2 Performance of DEPN₂ in the Homopolymerization of n-Butyl Acrylate	274
5.4.3 Synthesis of Nucleobase-Functionalized Hydrogen Bonding Block Copolymers	279
5.4.4 Complementary Hydrogen Bonding Interactions in Solution and Solid State	282
5.4.5 Morphological Investigations of Nucleobase-Functionalized Block Copolymers and Blends	292
5.4.6 Introduction of Guest Molecules to Hydrogen Bonding Block Copolymers	305
5.5 CONCLUSIONS	310
5.6 ACKNOWLEDGEMENT	310
CHAPTER 6. MULTIPLE HYDROGEN BONDING FOR THE NON-COVALENT ATTACHMENT OF IONIC FUNCTIONALITY IN BLOCK COPOLYMERS	311
6.1 ABSTRACT	311
6.2 INTRODUCTION	312
6.3 EXPERIMENTAL	317
6.3.1 Materials	317
6.3.2 Synthesis of 6-(trioctylphosphonium methyl)uracil chloride (UP⁺)	317
6.3.3 Synthesis of DEPN₂ Difunctional Alkoxyamine Initiator	318
6.3.4 Polymerization of n-Butyl Acrylate from DEPN₂ Nitroxide	320
6.3.5 Synthesis of Adenine Containing Block Copolymer	320
6.3.6 Characterization	321
6.4 RESULTS AND DISCUSSION	322
6.4.1 Synthesis and Characterization of a Novel Difunctional Initiator	322
6.4.2 Synthesis of Adenine Functional Block Copolymer	326
6.4.3 Compatible Blends of Adenine Functional Block Copolymer with Uracil Phosphonium Salt	328
6.4.4 Morphological Characterization of Phosphonium Salt Blends	330
6.4.5 Effect of Phosphonium Salt on Solution and Solid State Properties	334
6.5 CONCLUSION	336
6.6 ACKNOWLEDGMENT	336
CHAPTER 7. NOVEL MICHAEL ADDITION NETWORKS CONTAINING POLY(PROPYLENE GLYCOL) TELECHELIC OLIGOMERS	337
7.1 ABSTRACT	337
7.2 INTRODUCTION	338
7.3 EXPERIMENTAL	343
7.3.1 Materials	343
7.3.2 Synthesis of Acetoacetate Functionalized Poly(propylene glycol) (PPG bisAcAc)	344

7.3.3 Crosslinking Reactions.....	345
7.3.4 SEC and ¹ H NMR Analysis of the Crosslinking Process.....	345
7.3.5 ¹ H NMR Kinetics Experiments	345
7.3.6 Polymer Characterization.....	346
7.4 RESULTS AND DISCUSSION	347
7.4.1 Synthesis of Acetoacetate Functionalized Poly(propylene glycol) (PPG bisAcAc)	347
7.4.2 Synthesis of carbon-Michael Addition Networks	348
7.4.3 Characterization of the PPG bisAcAc / PEG diacrylate Networks	351
7.4.4 Sampling Experiments of the Crosslinking Reaction Involving SEC Analysis.....	363
7.4.5 Kinetic Investigations of the carbon-Michael Addition Crosslinking Reaction	367
7.5 CONCLUSIONS	371
7.6 ACKNOWLEDGEMENTS	371
CHAPTER 8. SYNTHESIS OF AN ACID-LABILE DIACRYLATE CROSSLINKER FOR CLEAVABLE MICHAEL ADDITION NETWORKS	372
8.1 ABSTRACT	372
8.2 INTRODUCTION	372
8.3 EXPERIMENTAL	377
8.3.1 Materials	377
8.3.2 Dicumyl alcohol diacrylate (DCDA).....	377
8.3.3 Poly(ethylene glycol) bis(acetoacetate)	378
8.3.4 Crosslinked Network Synthesis and Degradation	378
8.3.5 Characterization	379
8.4 RESULTS AND DISCUSSION	380
8.4.1 Synthesis of Acid-Cleavable Networks.....	380
8.4.2 Acid Catalyzed Degradation of Networks	383
8.4.3 Thermal Degradation of Networks	386
8.4.4 Mechanical Characterization of Networks	388
8.5 CONCLUSION	392
8.6 ACKNOWLEDGEMENT	392
CHAPTER 9. SYNTHESIS AND MORPHOLOGICAL CHARACTERIZATION OF SULFONATED TRIBLOCK COPOLYMERS: INFLUENCE OF HIGH SULFONATE LEVELS AND POLY(ETHYLENE-CO-PROPYLENE) MOLECULAR WEIGHT	393
9.1 ABSTRACT	393
9.2 INTRODUCTION	394
9.3 EXPERIMENTAL	399
9.3.1 Materials	399
9.3.2 Synthesis of Poly(styrene- <i>b</i> -isoprene- <i>b</i> -styrene) Triblock Copolymers.....	400
9.3.3 Hydrogenation of Poly(styrene- <i>b</i> -isoprene- <i>b</i> -styrene) Triblock Copolymers.....	401
9.3.4 Sulfonation of Poly(styrene- <i>b</i> -ethylene-co-propylene- <i>b</i> -styrene) Triblock Copolymers	402
9.3.5 Titration and Neutralization of Sulfonated Poly(styrene- <i>b</i> -ethylene-co-propylene- <i>b</i> -styrene)	402
9.3.6 Small Angle X-Ray Scattering (SAXS) Measurements	403
9.3.7 Atomic Force Microscopy (AFM) Measurements	404
9.3.8 Size Exclusion Chromatography.....	404

9.3.9 Dynamic Mechanical Analysis, Thermal and Rheological Studies	404
9.4 RESULTS AND DISCUSSION	405
9.4.1 Sulfonated SEPS Triblock Polymer Synthesis.....	405
9.4.2 Dynamic Mechanical Analysis (DMA) of Sulfonated SEPS Triblock Polymers.....	410
9.4.3 Tensile Characterization of Sulfonated SEPS Polymers	415
9.4.4 Rheological Studies of Sulfonated Block Copolymers	422
9.4.5 Small Angle X-Ray Scattering Characterization	425
9.4.6 Atomic Force Microscopy (AFM) Characterization.....	431
9.5 CONCLUSIONS	434
9.6 ACKNOWLEDGEMENTS	434
 CHAPTER 10. MORPHOLOGICAL ANALYSIS OF TELECHELIC UREIDO-PYRIMIDONE FUNCTIONAL HYDROGEN BONDING LINEAR AND STAR-SHAPED POLY(ETHYLENE-CO-PROPYLENE)S.....	
10.1 ABSTRACT	435
10.2 INTRODUCTION	436
10.3 EXPERIMENTAL	444
10.3.1 Materials	444
10.3.2 Polymer Characterization.....	444
10.3.3 Small-angle X-ray Scattering (SAXS) Measurements.....	445
10.3.4 Atomic Force Microscopy (AFM) Measurements	446
10.4 RESULTS AND DISCUSSION	446
10.4.1 Polymer Synthesis.....	446
10.4.2 Small-angle X-Ray Scattering Studies	450
10.4.3 Atomic Force Microscopy.....	458
10.5 CONCLUSIONS	461
10.6 ACKNOWLEDGEMENTS	461
 CHAPTER 11. REAL-TIME MONITORING OF MOLECULAR RECOGNITION OF COMPLEMENTARY IONIC GUEST MOLECULES WITH HYDROGEN BONDING BLOCK COPOLYMERS USING QUARTZ-CRYSTAL MICROBALANCE WITH DISSIPATION (QCM-D)...	
11.1 ABSTRACT.....	462
11.2 INTRODUCTION.....	463
11.3 EXPERIMENTAL.....	468
11.3.1 Materials	468
11.3.2 Polymerization of <i>n</i> -Butyl Acrylate from DEPN ₂	468
11.3.3 Synthesis of Adenine Containing Block Copolymer	469
11.3.4 Synthesis of Poly(styrene- <i>b</i> - <i>n</i> -butyl acrylate- <i>b</i> -styrene) Block Copolymer.....	469
11.3.5 Characterization	470
11.3.6 Quartz Crystal Microbalance with Dissipation (QCM-D) Measurements	471
11.4 RESULTS AND DISCUSSION	471
11.4.1 Synthesis of Nucleobase Functional Hydrogen Bonding Block Copolymers.....	471
11.4.2 Quartz Crystal Microbalance Measurements.....	474
11.4.3 X-ray Crystallographic Studies of Uracil Phosphonium Salt.....	484
11.5 CONCLUSIONS	488

11.6 ACKNOWLEDGEMENT	488
CHAPTER 12. INTRODUCTION OF CENTRAL DIESTER FUNCTIONALITY IN POLYSTYRENES USING LIVING RADICAL POLYMERIZATION FOR GRAFT POLYESTER SYNTHESIS.....	
12.1 ABSTRACT	489
12.2 INTRODUCTION	489
12.3 EXPERIMENTAL	494
12.3.1 <i>Materials</i>	494
12.3.2 <i>Polystyrene Diester Synthesis</i>	494
12.3.3 <i>Removal of DEPN from Polystyrene Diester</i>	495
12.3.4 <i>Graft Polyester Synthesis</i>	495
12.3.5 <i>Characterization</i>	497
12.4 RESULTS AND DISCUSSION	498
12.4.1 <i>Synthesis of DEPN-Terminated Polystyrene Diesters</i>	498
12.4.2 <i>Removal of DEPN End-groups from Polystyrene Diesters</i>	501
12.4.3 <i>Synthesis of Graft Copolymers</i>	506
12.5 CONCLUSION	512
12.6 ACKNOWLEDGEMENT	512
CHAPTER 13. FUTURE DIRECTIONS - INTRODUCTION OF CHIRAL HYDROGEN BONDING GUEST MOLECULES FOR INFLUENCE OF TACTICITY OF RADICAL POLYMERIZATIONS ...	
13.1 ABSTRACT	513
13.2 INTRODUCTION	513
13.3 EXPERIMENTAL	519
13.3.1 <i>Materials</i>	519
13.3.2 <i>Synthesis of 2',3',5'-trihexyladenosine (AdHex)</i>	519
13.3.3 <i>Synthesis of 1-(2-bromoethyl)thymine</i>	520
13.3.4 <i>Synthesis of 1-vinylthymine</i>	520
13.3.5 <i>Free radical polymerization of 1-vinylthymine</i>	521
13.3.6 <i>Polymerization of 1-vinylthymine in the Presence of a Chiral Auxiliary</i>	522
13.3.7 <i>Free radical polymerization of 1-vinylbenzylthymine</i>	522
13.3.8 <i>Polymerization of 1-vinylbenzylthymine in the Presence of a Chiral Auxiliary</i>	522
13.3.9 <i>Characterization</i>	523
13.4 RESULTS AND DISCUSSION	523
13.5 CONCLUSIONS	534
13.6 FUTURE WORK	534
13.7 ACKNOWLEDGEMENT	534
CHAPTER 14. FUTURE DIRECTIONS- RHEOLOGICAL STUDIES OF HYDROGEN BONDING COPOLYMERS WITH REVERSIBLE ATTACHMENT OF IONIC FUNCTIONALITY	
14.1 ABSTRACT	535
14.2 INTRODUCTION	536
14.3 EXPERIMENTAL	542
14.3.1 <i>Materials</i>	542
14.3.2 <i>Phosphonium Styrene Monomer Synthesis</i>	542

<i>14.3.3 Uracil Phosphonium Salt</i>	543
<i>14.3.4 Adenine Containing Copolymer</i>	543
<i>14.3.5 Phosphonium Salt Containing Copolymer</i>	544
<i>14.3.6 Blends of an Adenine Containing Copolymer with a Uracil Phosphonium Salt</i>	545
<i>14.3.7 Characterization</i>	545
14.4 RESULTS AND DISCUSSION	546
14.5 CONCLUSIONS	561
14.6 FUTURE WORK	561
14.7 ACKNOWLEDGEMENT	561
CHAPTER 15. OVERALL CONCLUSIONS	563
VITAE	566

List of Tables

Table 3.1. Step growth polymers derived from Michael addition polymerization.	100
Table 4.1. Target and experimental molecular weights for polystyrenes and poly(<i>n</i> -butyl acrylate)s synthesized using Uracil-TEMPO and Uracil-DEPN.	236
Table 4.2. Uracil functionalized polystyrene and poly(<i>n</i> -butyl acrylate) molecular weights determined using both GPC and NMR.	237
Table 4.3. Polymerization rate constants for various styrene to Uracil-TEMPO ratios.	241
Table 4.4 Glass transition temperatures for various uracil functionalized polystyrenes with molecular weights below the critical molecular weight.	254
Table 5.1. Molecular weight data for nucleobase-functionalized block copolymers and blends.	281
Table 5.2. Small-angle X-ray scattering results for hydrogen bonding block copolymers.	301
Table 7.1. Characterization of PPG bisAcAc precursors.	349
Table 7.2. Gel fractions for PPG bisAcAc / PEG diacrylate networks.	353
Table 7.3. Tensile properties of PPG-bisAcAc/ PEG diacrylate networks.	359
Table 7.4. Swelling properties of PPG bisAcAc / PEG diacrylate networks in ethanol and M_c values calculated from both swelling and tensile data.	362
Table 7.5. Kinetic data for the PPG bisAcAc / PEG diacrylate reaction using various basic catalysts. The pKa data is in aqueous solution.	370
Table 9.1. Compositional analysis of block copolymers.	409
Table 9.2. Tensile properties of sulfonated SEPS block copolymers and fitting parameters using model from van der Heide.	417
Table 9.3. Summary of scattering maxima position and Bragg spacing for sulfonated block copolymers.	428
Table 10.1. Molecular weight and molecular weight distribution of monofunctional, telechelic, and star-shaped polyisoprenes before and after hydrogenation and UPy functionalization.	448
Table 10.2. Scattering maxima and corresponding Bragg spacings for UPy functional poly(ethylene- <i>co</i> -propylene)s.	454
Table 11.1. Film thickness of adenine containing polymer using QCM and SEM.	475
Table 11.2. Effect of moisture uptake on frequency and dissipation of adenine containing polymer and control polymer.	479
Table 11.3. Adsorption of $UPPh_3^+$ on adenine-containing and control block copolymers.	483
Table 12.1. Molecular weight characterization of polystyrene diesters.	500
Table 14.1. Yarusso-Cooper fitting of scattering for 30 mol% phosphonium copolymer.	554

List of Figures

Figure 2.1. Degree of non-covalent polymerization as a function of association constant (K_a)	13
Figure 2.2. An Archimedean tile morphology for blends of poly(2-vinylpyridine- <i>b</i> -isoprene- <i>b</i> -vinylpyridine) with poly(styrene- <i>b</i> -4-hydroxystyrene)	25
Figure 2.3. Synthesis of adenine containing block copolymers via a ROMP methodology	32
Figure 2.4. Formation of cylindrical aggregates via multi-directional self-association bonding of adenine functional block copolymers.	33
Figure 2.5. Scheme for stepwise synthesis of oligonucleotides via coupling of phosphoramidite functionalized nucleosides.	38
Figure 2.6. Solution viscosity of (a) telechelic UPy functional PDMS and (b) benzyl protected analog in chloroform at 20 °C	46
Figure 2.7. UPy homodimer (left) and heterodimer (right) with Napy via tautomerization	50
Figure 2.8. Association of ditopic self-complementary tetraurea functional calixarenes.	54
Figure 2.9. Dual side chain non-covalent interaction modes including both hydrogen bonding and metal-ligand interactions.	56
Figure 2.10. Phase diagram of poly(isoprene- <i>b</i> -2-vinylpyridine) with octyl gallate.	61
Figure 3.1 a) Arthur Michael (1855-1942), who discovered the Michael addition reaction.	69
Figure 3.2. General carbon-Michael reaction mechanistic scheme.	72
Figure 3.3. Second Michael addition of acetoacetate group to methyl acrylate.	74
Figure 3.4. Michael Addition involving an alkyne acceptor.	79
Figure 3.5. Lewis-acid catalyzed Michael addition reaction.	82
Figure 3.6. Stereoselective Michael addition between enone and silyl enolate in the presence of $TiCl_4$	83
Figure 3.7. Phosphine catalyzed Michael addition reaction.	84
Figure 3.8. Aza-Michael addition reaction of dimethylamine with ethyl acrylate.	86
Figure 3.9. Aza-Michael addition of methyl amine to two equivalents of ethyl acrylate.	87
Figure 3.10. Higher reactivity of secondary amines in aza-Michael addition reactions.	89
Figure 3.11. Acid catalyzed aza-Michael addition.	90
Figure 3.12. Acid catalyzed aza-Michael addition to activated alkyne acceptors.	91
Figure 3.13. Lewis acid catalyzed aza-Michael reaction.	93
Figure 3.14. Stereoselective aza-Michael additions.	94
Figure 3.15. Regioselective Michael addition through preferential coordination of substrate carbonyls with lithium cations,	97
Figure 3.16. Poly(amido amine) synthesis via a) primary and b) secondary amines.	102
Figure 3.17. Poly(amino ester) synthesis from butanediol diacrylate and piperazine.	110
Figure 3.18. Poly(imido sulfide) synthesis from a bismaleimide precursor and hydrogen	

sulfide gas.	113
Figure 3.19. a) A typical poly(imido sulfide)s synthesis.	116
Figure 3.20. Thermally stable poly(aspartamide)s synthesized from arylene ether diamines.	119
Figure 3.21. Typical poly(amide aspartamide) polymerization.	122
Figure 3.22. Poly(amino quinone) synthesis involving peracetic acid as an oxidizing agent.	124
Figure 3.23. Polymerization of poly(thiophenylene)s via Michael addition and oxidation.	126
Figure 3.24. Poly(enone sulfide) synthesis via Michael addition step growth.	130
Figure 3.25. Hydrogen transfer polymerization of acrylamide to poly(β -alanine).	131
Figure 3.26. Anionic polymerization of methyl methacrylate from diphenylhexyl lithium.	135
Figure 3.27. Michael addition of heterocyclic nucleotide bases to acrylated anionic polystyrene.	138
Figure 3.28. Polymerization of macrocyclic ether acrylic monomers to form ion channels.	140
Figure 3.29. Group transfer polymerization of methyl methacrylate.	142
Figure 3.30. Water-initiated polymerization of ethyl α -cyanoacrylate.	144
Figure 3.31. Synthesis of a dihydroxyl functional ATRP initiator.	147
Figure 3.32. Divergent PAMAM dendrimer synthesis via alternating Michael addition and amidation.	150
Figure 3.33. Synthesis of PPI dendrimers via alternating Michael addition and hydrogenation.	154
Figure 3.34. Convergent dendrimer synthesis via dendron core-linking Michael addition reactions.	156
Figure 3.35. Crosslinkable dendrimer synthesis using Michael addition reactions.	158
Figure 3.36. Hyperbranched polymer synthesis via AB_2 Michael addition polymerization.	161
Figure 3.37. Hyperbranched poly(aspartamide)s via $A_2 + B_3$ polymerization.	163
Figure 3.38. Hyperbranched poly(ester amine)s from $A_2 + B_3$ polymerization with unequal reactivity in the B_3 monomer functional groups.	166
Figure 3.39. Homopolymerization of an AB_2 poly(amido amine) monomer.	169
Figure 3.40. Homopolymerization of an AB_2 poly(ester ether) monomer.	171
Figure 3.41. Graft copolymerization via grafting of thiol terminated PEG to pendant acryloxy side groups on a poly(ϵ -caprolactone) derivative.	174
Figure 3.42. Modification of chitin via Michael addition reaction with ethyl acrylate.	176
Figure 3.43. Crosslinking of bismaleimide networks via a combination of Michael addition and maleimide homopolymerization.	179
Figure 3.44. Carbon-Michael addition polymerization of acetoacetates with acrylates catalyzed by bases for network synthesis.	182
Figure 3.45. Network formation of PEG bis(vinyl sulfone) and protein dithiols.	192
Figure 3.46. a) Effect of pH on gel time for PEG bis(vinyl sulfone).	194
Figure 3.47. Release of albumin from PEG networks based on PEG tetraacrylate (black	

squares) and PEG octaacrylate (white triangles).	197
Figure 3.48. Protein-containing PEG networks via Michael addition crosslinking of PEG octaacrylate with dithiothreitol.	199
Figure 3.49. a) Swelling of PEG octaacrylate, dithiothreitol networks via initial solvent uptake followed by ester hydrolysis leading to degradation.....	200
Figure 3.50. Illustration of the stepwise synthesis of a PEG-based hydrogel by reacting multiarm vinyl sulfone-terminated PEG with small amounts of a monocysteine-containing adhesion peptide	203
Figure 3.51. Self-condensing dendrimer synthesized from PPI and acrylate initiated living PTMO.	206
Figure 3.52. Protein incorporation via Michael addition of thiol residues to PEG-acrylamide.	211
Figure 3.53. Drug delivery via polymer-drug conjugates.	213
Figure 4.1. Synthesis and polymerization from Uracil-TEMPO and Uracil-DEPN.....	233
Figure 4.2. In-situ FTIR kinetic plot of styrene and <i>n</i> -butyl acrylate polymerizations using Uracil-TEMPO and Uracil-DEPN	240
Figure 4.3. Evolution of molecular weight with conversion for the polymerizations of styrene and <i>n</i> -butyl acrylate	243
Figure 4.4. Chemical shift of uracil N-H protons as a function of molecular weight in CDCl ₃ at 10.4 wt%.....	246
Figure 4.5. Zero-shear melt viscosities for uracil functionalized poly(<i>n</i> -butyl acrylate)	249
Figure 4.6. Arrhenius analysis of the melt rheology data depicting the flow activation energies for functionalized and non functionalized poly(<i>n</i> -butyl acrylate)	250
Figure 4.7. Thermogravimetric and derivative traces for a polystyrene synthesized from Uracil-TEMPO.....	252
Figure 5.1. Synthesis of adenine and thymine nucleobase-functionalized triblock copolymers.	264
Figure 5.2. Synthesis of DEPN ₂ , difunctional alkoxyamine initiator, using copper-promoted reaction of an activated dihalide.....	273
Figure 5.3. SEC analysis of polymerization with time of <i>n</i> -butyl acrylate from DEPN ₂ and linear molecular weight versus conversion plot.....	276
Figure 5.4. SEC trace from a polymerization containing DEPN ₂ (difunctional) and Sty-DEPN (monofunctional) initiators.	278
Figure 5.5. Solution rheology of hydrogen bonding block copolymers (A3, T3 and their blend) in chloroform at 25 °C.	284
Figure 5.6. Zero-shear solution viscosities of the A3, T3 hydrogen bonding block copolymers and their 1:1 A:T blend A3/T3 as a function of concentration.....	287
Figure 5.7. Dynamic mechanical storage modulus and tan delta curves for adenine- and thymine-functionalized block copolymers.....	290
Figure 5.8. Expansion of high-temperature region of DMA storage modulus curves....	291
Figure 5.9. Tapping mode AFM phase images of thymine- (T2) and adenine-functionalized (A2) polymers before and after annealing.....	294
Figure 5.10. Tapping mode AFM phase images of A1, T1 and A1/T1 blend.	297

Figure 5.11. SAXS scattering profiles for nucleobase-containing polymers (A1, T1) and their 1:1 A:T blend.	302
Figure 5.12. Effect of annealing conditions on thymine-containing triblock copolymer (T1) sample. Scattering maxima in terms of q/q^* are denoted with arrows.	304
Figure 5.13. Chemical shift changes during introduction of 9-octyladenine to a thymine-containing triblock copolymer (T3).	307
Figure 5.14. Tapping mode AFM images of unannealed thymine-functionalized block copolymer (T2) spin coated on a silicon wafer from chloroform solutions containing (a) 0, (b) 0.4 and (c) 2.2 equivalents of 9-octyladenine.	309
Figure 6.1. Reversible attachment of UP^+ phosphonium salt to complementary nucleobase functionalized block copolymers.	314
Figure 6.2. ORTEP X-ray crystal structure of $DEPN_2$ difunctional alkoxyamine initiator	324
Figure 6.3. Number average molecular weight as a function of monomer conversion for the polymerization of <i>n</i> -butyl acrylate with $DEPN_2$	325
Figure 6.4. Synthesis of adenine containing triblock copolymers from $DEPN_2$ initiated poly(<i>n</i> -butyl acrylate).	327
Figure 6.5. DSC thermograms of adenine-containing block copolymer/ UP^+ blend.	329
Figure 6.6. Tapping mode AFM phase images of 1.5K-16.5K-1.5K adenine triblock UP^+ blend (A:U 1:1).	331
Figure 6.7. Small-angle X-ray scattering (SAXS) of 1.5K-16.5K-1.5K adenine triblock and UP^+ blend	332
Figure 6.8 Bright field TEM micrograph of adenine-containing polymer/ UP^+ blend stained with OsO_4	333
Figure 6.9 Dynamic mechanical temperature sweep for pure 1.5K-16.5K-1.5K adenine triblock copolymer and blend with 1 equivalent of UP^+	335
Figure 7.1. Synthesis of acetoacetate networks from acetoacetate functionalized PPG (PPG bisAcAc) using DBU as a basic catalyst.	341
Figure 7.2. Gel times for PPG bisAcAc / PEG diacrylate networks as a function of PPG molecular weight.	350
Figure 7.3. Storage modulus (E') plots for the PPG bisAcAc / PEG diacrylate networks with a 1.4:1.0 acrylate to acetoacetate ratio	355
Figure 7.4. Glass transition temperatures of PPG bisAcAc / PEG diacrylate networks as a function of inverse PPG molecular weight as determined by SEC (1.4:1.0 acrylate to acetoacetate ratio)	356
Figure 7.5. Stress-strain curves for PPG bisAcAc / PEG diacrylate networks containing 1.4:1.0 acrylate to acetoacetate ratios. Measurement was performed at 25 °C.	358
Figure 7.6. SEC traces from a PPG bisAcAc / PEG diacrylate crosslinking reaction.	365
Figure 7.7. Weight-average molecular weight as determined by SEC MALLS and refractive index versus acrylate conversion.	366
Figure 7.8. First-order rate analysis of acrylate concentration	369
Figure 8.1. 1H NMR spectrum of acid-cleavable diacrylate crosslinker, DCDA.	381
Figure 8.2. Synthesis of crosslinked networks via base catalyzed Michael addition.	382
Figure 8.3. Degradation reactions of Michael addition networks containing DCDA using	

p-toluenesulfonic acid.....	384
Figure 8.4. Pictures of the degradation of DCDA containing Michael addition networks using <i>p</i> -toluenesulfonic acid	385
Figure 8.5. Thermogravimetric analysis (TGA) and derivative weight loss curve for DCDA containing network.	387
Figure 8.6. Dynamic mechanical analysis (DMA) of acid cleavable diacrylate network.	389
Figure 8.7. Tensile analysis of acid-cleavable Michael addition network.	391
Figure 9.1. Synthesis of sulfonated block copolymers via sequential addition anionic polymerization	407
Figure 9.2. SEC analysis of aliquots removed from the polymerization reaction after each block (9K sample).....	408
Figure 9.3. Dynamic mechanical analysis of sulfonated SEPS polymers	412
Figure 9.4. Glass transition temperatures of sodium sulfonated SEPS copolymers as a function of rubber block molecular weight.....	414
Figure 9.5. Tensile curves for sulfonated SEPS block copolymers.	416
Figure 9.6. Typical tensile curve and fit from the model by van der Heide.	420
Figure 9.7. Trends in fitting moduli and molecular weight between crosslinks for the sodium sulfonated SEPS polymers.	421
Figure 9.8 Complex viscosity (a) and storage modulus (b) master curves of 5K and 17K samples ($T_r = 20\text{ }^\circ\text{C}$).	424
Figure 9.9. 1-D SAXS profiles for sulfonated block copolymers of varying rubber block molecular weights	427
Figure 9.10. Effect of neutralization on the scattering maxima in the sulfonated block copolymer (10K sample).....	430
Figure 9.11. Tapping mode AFM phase images of the sulfonated block copolymer series.	433
Figure 10.1. Ureidopyrimidone (UPy) quadruple hydrogen bonded dimer attached to poly(ethylene- <i>co</i> -propylene)s.	439
Figure 10.2. Representation of expected modes of association for different hydrogen bonding architectures in solution.	449
Figure 10.3. SAXS data for UPy-containing monofunctional (left chart) and telechelic (right chart) poly(ethylene- <i>co</i> -propylene)s polymers.	452
Figure 10.4. SAXS data showing the effect of functionality for 12 kg/mol polymers. ...	456
Figure 10.5. Scattering profile for star-shaped poly(ethylene- <i>co</i> -propylene) with UPy functional periphery and the 12K monofunctional polymer.....	457
Figure 10.6. Variable temperature tapping mode AFM images of the UPy star-shaped polymer.	460
Figure 11.1. Molecular recognition of uracil containing phosphonium salt with complementary hydrogen bonding block copolymer.....	467
Figure 11.2. Synthesis of hydrogen bonding triblock copolymers containing adenine and thymine nucleobases from difunctional DEPN terminated poly(<i>n</i> -butyl acrylate).473	
Figure 11.3. Tapping mode AFM a) height and b) phase images of adenine containing polymer spin coated on Si, from chloroform solution.	476

Figure 11.4. Changes in frequency (7 th overtone) with exposure to humid air, 25 °C....	478
Figure 11.5. Changes in frequency (7 th overtone) with exposure to UPPh ₃ ⁺ in water (0.5 wt%), 25 °C for adenine-containing and control block copolymer.....	482
Figure 11.6. Molecular structure of UPPh ₃ ⁺ (50% probability displacement ellipsoids), crystallized from ethanol.....	485
Figure 11.7. Molecular structure of UPPh ₃ ⁺ (50% probability displacement ellipsoids), crystallized from water/THF.....	487
Figure 12.1. Synthesis of polystyrene diesters from DEPN ₂ initiator.....	499
Figure 12.2. Removal of DEPN endgroups via heating with 1-dodecanethiol.....	502
Figure 12.3. ¹ H NMR spectrum of polystyrene diester (a) after removal of DEPN.....	503
Figure 12.4. ³¹ P NMR data showing loss of DEPN from polystyrene diester.....	504
Figure 12.5. TGA data showing loss of DEPN endgroup.....	505
Figure 12.6. Synthesis of graft polyester containing polystyrene arms.....	507
Figure 12.7. ¹ H NMR spectrum of polyester graft copolymer (400 MHz, acetone-d ₆)..	508
Figure 12.8. Graft polyester synthesis involving 1,4-cyclohexanedimethanol.....	509
Figure 12.9. AFM a) height and b) phase images of a graft polyester with polystyrene arms M _n = 5700 g/mol.....	511
Figure 13.1. Polymerization of a hydrogen bonded complex of a chiral auxiliary and a complementary hydrogen bonding monomer.....	518
Figure 13.2. Synthesis of a chloroform soluble chiral auxiliary (AdHex) for polymerization of complementary thymine or uracil-containing monomers.	524
Figure 13.3. Polymerization of 1-vinylbenzylthymine with and without added chiral auxiliary AdHex.....	527
Figure 13.4. ¹ H NMR spectra of poly(1-vinylbenzylthymine).....	528
Figure 13.5. Synthesis of 1-vinylthymine.....	531
Figure 13.6. ¹ H NMR spectrum of poly(1-vinylthymine) polymerized in the presence (a) and absence (b) of AdHex.....	533
Figure 14.1. Pictorial representation of ionic groups hydrogen bonded to a polymer chain.....	541
Figure 14.2. Synthesis of an adenine-containing random copolymer.....	547
Figure 14.3. Synthesis of a phosphonium styrene containing random copolymer.	549
Figure 14.4. DSC analysis of phosphonium styrene copolymer (30 mol%).	551
Figure 14.5. Small-angle X-ray scattering of 30 mol% phosphonium copolymer.	553
Figure 14.6. DMA analysis of 30 mol% phosphonium copolymer.....	556
Figure 14.7. DSC analysis of blends of adenine- and phosphonium-functional random copolymers and blend of adenine copolymer with uracil phosphonium salt.....	558
Figure 14.8. Rheological analysis of uracil phosphonium salt blend with adenine copolymer and comparisons with adenine and phosphonium copolymers.....	560

Chapter 1. Introduction

1.1 Scientific Rationale and Perspective

Recently, increasing attention has been devoted to the study of non-covalent interactions, particularly hydrogen bonding, in the construction and design of supramolecular materials.^{1,2} Hydrogen bonding enables the introduction of thermoreversible properties into macromolecules through the creation of specific non-covalent intermolecular interactions.³ The strength of these interactions is a strong function of temperature, solvent, humidity and pH, thus allowing control of properties through a number of environmental parameters. The strength of hydrogen bonding associations is further tunable via structural parameters and molecular design of the hydrogen bonding sites. Association strengths range from DNA nucleobases, which have association constants near 100 M^{-1} ,⁴ to self-complementary ureidopyrimidone (UPy) hydrogen bonding groups, which possess association constants near 10^7 M^{-1} .¹

Hydrogen bonding interactions are important for the development of self-assembling supramolecular materials, which are defined as materials in which monomeric units are reversibly bound via secondary interactions to form polymer-like structures that exhibit

¹ Brunsveld, L.; Folmer, B. J. B.; Meijer, E. W.; Sijbesma, R. P. Supramolecular Polymers. *Chem Rev* **2001**, 101, 4071-98.

² Ilhan, F.; Galow, T. H.; Gray, M.; Clavier, G.; Rotello, V. M. Giant Vesicle Formation through Self-Assembly of Complementary Random Copolymers. *J Am Chem Soc* **2000**, 122, 5895-6.

³ Yamauchi, K.; Lizotte, J. R.; Hercules, D. M.; Vergne, M. J.; Long, T. E. Combinations of Microphase Separation and Terminal Multiple Hydrogen Bonding in Novel Macromolecules. *J Am Chem Soc* **2002**, 124, 8599-604.

⁴ Kyogoku, Y.; Lord, R. C.; Rich, A. The Effect of Substituents on the Hydrogen Bonding of Adenine and Uracil Derivatives. *Proc Natl Acad Sci USA* **1967**, 57, 250-7.

polymeric properties in solution as well as in bulk.⁵ Researchers have used hydrogen bond functional polymers to direct the formation of large vesicles,⁶ reversibly attach polymers on surfaces,⁷ and reversibly attach functional small molecules on polymers.⁸ Long has incorporated quadruple hydrogen bonding self-complementary UPy multiple hydrogen bonding groups into random copolymers⁹ and also onto the chain end of homopolymers¹⁰ to introduce controlled rheological performance and thermoreversible properties into novel supramolecular structures.

In classical polymer science, hydrogen bonding interactions have already played a major role. From the hydrogen bonding in polyurethanes¹¹ to the structures of polypeptides¹² we can observe the cohesive effect hydrogen bonding interactions produce in macroscopic properties. More recently, elegant hydrogen bonding arrays were introduced into synthetic polymers and have yielded novel materials containing reversible linkages,

⁵ Brunsveld, L.; Folmer, B. J. B.; Meijer, E. W.; Sijbesma, R. P. Supramolecular Polymers. *Chem Rev* **2001**, 101, 4071-98.

⁶ Ilhan, F.; Galow, T. H.; Gray, M.; Clavier, G.; Rotello, V. M. Giant Vesicle Formation through Self-Assembly of Complementary Random Copolymers. *J Am Chem Soc* **2000**, 122, 5895-6.

⁷ Norsten, T. B.; Jeoung, E.; Thibault, R. J.; Rotello, V. M. Specific Hydrogen-Bond-Mediated Recognition and Modification of Surfaces Using Complementary Functionalized Polymers. *Langmuir* **2003**, 19, 7089-93.

⁸ Ilhan, F.; Gray, M.; Rotello, V. M. Reversible Side Chain Modification through Noncovalent Interactions. "Plug and Play" Polymers. *Macromolecules* **2001**, 34, 2597-601.

⁹ Yamauchi, K.; Lizotte, J. R.; Long, T. E. Thermoreversible Poly(alkyl acrylates) Consisting of Self-Complementary Multiple Hydrogen Bonding. *Macromolecules* **2003**, 36, 1083-8.

¹⁰ Yamauchi, K.; Lizotte, J. R.; Hercules, D. M.; Vergne, M. J.; Long, T. E. Combinations of Microphase Separation and Terminal Multiple Hydrogen Bonding in Novel Macromolecules. *J Am Chem Soc* **2002**, 124, 8599-604.

¹¹ McKeirnan, R. L.; Heintz, A. M.; Hsu, S. L.; Atkins, E. D. T. P., J; Gido, S. P. Influence of Hydrogen Bonding on the Crystallization Behavior of Semicrystalline Polyurethanes. *Macromolecules* **2002**, 35, 6970-4.

¹² Aggeli, A.; Bell, M.; Boden, N.; Keen, J. N.; Knowles, P. F.; McLeish, T. C. B.; Pitkeathly, M.; Radford, S. E. Responsive gels formed by the spontaneous self-assembly of peptides into polymeric β -sheet tapes *Nature* **1997**, 386, 259-62.

which are tuned with such environmental variables as temperature, moisture and solvent polarity. The resultant polymers often exhibit a stronger temperature dependence of melt viscosity, suggesting possible processability advantages.

The advantages of hydrogen bond containing materials are numerous. Beyond the novel rheological properties of hydrogen bonding systems, the introduction of hydrogen bonds often results in increased modulus and tensile strength, as well as increased polarity and adhesion. Hydrogen bonding interactions enable such diametrically opposed effects as the compatibilization of blends and the induction of microphase separation. They can also be used to create dynamic micelles in solution, the structure of which is tunable through the introduction of guest molecules, altering solvent polarity or introducing covalent crosslinks. In the case of block copolymers, the introduction of hydrogen bonding groups leads to a synergistic combination of microphase separation and hydrogen bonding associations. This results from associations between hydrogen bonding blocks, which reinforces microphase separation. The microphase separation, in turn, leads to increased local concentration of the hydrogen bonding groups in microphase separated domains, resulting in greater hydrogen bonding interactions. Furthermore, guest molecules may be sequestered in specific domains of the block copolymer allowing the reversible attachment of various functional groups.

In Chapter 2, we discuss the recent literature involving hydrogen bonding block and telechelic polymers. Chapter 3 focuses on literature describing the applications of Michael addition chemistry, which relates to the synthesis of covalent networks at ambient temperature. Chapters 4 and 5 describe the introduction of nucleobases to synthetic polymers and the resultant changes in properties which are observed. Chapter 6 and Chapter 11 discuss

the introduction of ionic guest molecules to hydrogen bonding polymers. Chapters 7 and 8 describe some of the research efforts involving Michael addition chemistry to synthesize networks based on telechelic functional oligomers. Chapter 9 pertains to the synthesis of sulfonated block copolymers, in which ionic interactions were studied. Chapter 10 discusses the application of SAXS to analyze the morphology of telechelic hydrogen bonding polymers. Chapter 12 presents efforts to utilize nitroxide mediated polymerization to create macromonomers for polyester synthesis. Chapter 13 relates preliminary experiments toward utilizing hydrogen bonding to influence stereocontrol in radical polymerizations. Chapter 14 centers on preliminary investigations of comparing covalent and hydrogen bonding attachment of ionic groups.

Chapter 2. Review of the Literature – Hydrogen Bond Functionalized Block Copolymers and Telechelic Hydrogen Bonding Oligomers

2.1 Fundamentals of Hydrogen Bonding

Hydrogen bonds are formed between molecules containing an electronegative atom possessing lone pairs of electrons (usually O, N or F), called acceptors (A) and molecules containing covalent bonds between hydrogen and an electronegative atom (usually O-H, N-H, S-H), called donors (D). The polarized nature of the X-H bond (X=O,N..) results in a highly electropositive hydrogen which is attracted toward bond formation with the electron rich electronegative acceptor atoms.

The preferred geometry of the hydrogen bond is a linear conformation, with the hydrogen atom positioned along the line connecting the heteroatoms. This preferred geometry, however, is not always obtained in nature due to the constraints of the neighboring covalent systems, which are much less easily distorted. This property of the hydrogen bond leads to its directionality. The strength of individual hydrogen bonds range from 1-10 kcal/mol¹³ which leads to longer, weaker bonds compared to covalent bonds (70-110 kcal/mol). Thus, when hydrogen bonds serve as the primary secondary interaction, the resultant structures are typically closer to thermodynamic equilibrium, and are quite dynamic with respect to changes in the environment. This is due to the simple fact that thermal energy (kT) more closely matches the bond strengths in these systems. For instance, an association energy of 3 kcal/mol leads to a 1% level of dissociation among units in a single

¹³ Coleman, M. M.; Graf, J. F.; Painter, P. C., Specific Interactions and the Miscibility of Polymer Blends. Technomic: Lancaster, PA, 1991.

component bulk liquid bound with this energy at ambient temperature.¹⁴ This figure obviously represents a time average; the typical lifetime of a hydrogen bond in water, for example is roughly 10^{-11} s.¹⁵

The acidity of the donor and the Lewis basicity of the acceptor play important roles in the strength of the interaction.^{16,17} Phenols, which possess a stronger acidity than aliphatic alcohols, produce stronger hydrogen bonds with acceptors. These properties, which are measured in terms of pK_a or pK_b , are founded in the electronic structure of the donors and acceptors and their ability to stabilize negative or positive charges, respectively. Electron withdrawing substituents such as fluorine increase the acidity of the hydrogen bond donors, as the case of the hexafluoroisopropanol group.¹⁸ In the extreme case, mixing a strongly acidic hydrogen bond donor with a strongly basic hydrogen bond acceptor results in an acid-base neutralization reaction and the formation of an ion pair. Coleman et al. discussed the fact that hydrogen bonding interactions are indeed founded in electrostatic attractive and repulsive interactions.¹⁴

¹⁴ Coleman, M. M.; Graf, J. F.; Painter, P. C., *Specific Interactions and the Miscibility of Polymer Blends*. Technomic: Lancaster, PA, 1991.

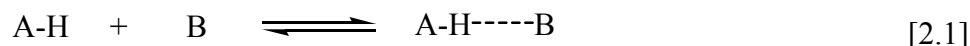
¹⁵ Conde, O.; Teixeira, Hydrogen bond dynamics in water studied by depolarized Rayleigh scattering. *J. J. Phys.* **1983**, 44, 525-9.

¹⁶ Beijer, F. H.; Sijbesma, R. P. V., J.A.J.M.; Meijer, E. W. K., H; Spek, A.L. Hydrogen-Bonded Complexes of Diaminopyridines and Diaminotriazines: Opposite Effect of Acylation on Complex Stabilities. *J. Org. Chem.* **1996**, 61, 6371-80.

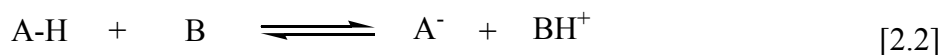
¹⁷ Kawakami, T.; Kato, T. Use of Intermolecular Hydrogen Bonding between Imidazolyl Moieties and Carboxylic Acids for the Supramolecular Self-Association of Liquid-Crystalline Side-Chain Polymers and Networks. *Macromolecules* **1998**, 31, 4475-9.

¹⁸ Liu, S.; Zhu, H.; Zhao, H.; Jiang, M.; Wu, C. Interpolymer Hydrogen-Bonding Complexation Induced Micellization from Polystyrene-*b*-poly(methyl methacrylate) and PS(OH) in Toluene. *Langmuir* **2000**, 16, 3712-7.

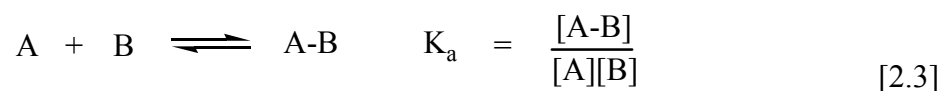
hydrogen bonding interaction



formation of ion pairs



The common measure of the strength of association or complexation is the association constant (K_a), defined in terms the equilibrium between associated and dissociated units:



The K_a value is a key measurement of the strength of the hydrogen bonding association and determines the dynamics of systems incorporating the hydrogen bonding groups. Thus, for weaker hydrogen bonding interactions, the lifetimes of associated species are shorter than for systems with higher association constants. This has a dramatic effect on material properties, such as relaxation rates, creep, modulus, melt viscosity etc. In order to tune the strength of the association constant, numerous molecular parameters are accessible. A common approach for increasing association strength is the incorporation of additional hydrogen bonding sites within a single hydrogen bonding array, termed “multiple hydrogen bonding”. Entropically, the association of two species is unfavorable, but this loss of entropy is not greatly increased from the association of additional pairs of donors and acceptors on the same two molecules. Single through quadruple hydrogen bonding units exist and even some cases of larger arrays containing six¹⁹ and eight²⁰ hydrogen bonds were synthesized

¹⁹ Zeng, H.; Miller, R. S.; Flowers, R. A.; Gong, B. A Highly Stable, Six-Hydrogen-Bonded Molecular Duplex. *J Am Chem Soc* **2000**, 122, 2635-44.

²⁰ Folmer, B. J. B.; Sijbesma, R. P.; Kooijman, H.; Spek, A. L.; Meijer, E. W. Cooperative Dynamics in Duplexes of Stacked Hydrogen-Bonded Moieties. *J Am Chem Soc* **1999**, 121, 9001-7.

and studied. Additionally, the strength of the hydrogen bonding interaction is tuned via the pattern of hydrogen bonding groups. Meijer, Lehn and Rotello have shown that a number of factors are important in the use of multiple hydrogen bonded systems.^{21,22} Alternation of donor and acceptor groups in a multiple hydrogen bonding array reduces the strength of the association via repulsive interactions of opposing adjacent donors or acceptors.^{23,24} Thus, Meijer's quadruple hydrogen bonding (DDAA) UPy group is designed with minimum alternation of donor and acceptor units.²³ When multiple hydrogen bonding groups are considered, the possibility of self-complementarity arises. The simplest case of self-complementarity is probably the carboxylic acid dimer, which contains two hydrogen bonds. In contrast, complementary hydrogen bonding arrays are found in DNA, which possesses both adenine-thymine (A-T) and cytosine-guanine (C-G) pairs. Another factor to consider in heterocyclic bases is the ability of the base to tautomerize into different forms.²⁵ This can lead to complexity in the behavior of the hydrogen bonding group, and different hydrogen bonding guests can shift the equilibrium between tautomers.²⁶

The reversible nature of the hydrogen bond is not limited to thermoreversibility,

²¹ Beijer, F. H.; Sijbesma, R. P. V.; J.A.J.M.; Meijer, E. W. K., H; Spek, A.L. Hydrogen-Bonded Complexes of Diaminopyridines and Diaminotriazines: Opposite Effect of Acylation on Complex Stabilities. *J. Org. Chem.* **1996**, 61, 6371-80.

²² Brunsveld, L.; Folmer, B. J. B.; Meijer, E. W.; Sijbesma, R. P. Supramolecular Polymers. *Chem Rev* **2001**, 101, 4071-98.

²³ Beijer, F. H.; Sijbesma, R. P.; Kooijman, H.; Spek, A. L.; Meijer, E. W. Strong Dimerization of Ureidopyrimidones via Quadruple Hydrogen Bonding. *J Am Chem Soc* **1998**, 120, 6761-9.

²⁴ Jorgensen, W. L.; Pranata, J. Importance of Secondary Interactions in Triply Hydrogen Bonded Complexes: Guanine-Cytosine vs Uracil-2,6-Diaminopyridine. *J Am Chem Soc* **1990**, 112, 2008-10.

²⁵ Lee, G. Y. C.; Chan, S. I. Tautomerism of Nucleic Acid Bases. 11. Guanine. *J Am Chem Soc* **1972**, 94, 3218-3229.

²⁶ Ligthart, G. B. W. L.; Ohkawa, H.; Sijbesma, R. P.; Meijer, E. W. Complementary Quadruple Hydrogen Bonding in Supramolecular Copolymers. *J Am Chem Soc* **2005**, 127, 810-811.

although that is the most commonly exploited and studied property of these systems. The hydrogen bond is also sensitive to other environmental factors, such as the polarity of the medium, and the presence of competitive solvents and water. Deans et al. observed that solvent polarity has a strong effect on hydrodynamic volume for self-associating polymers.²⁷ Thus, humidity and exposure to polar media are two other factors which are considerations in the application of hydrogen bonded materials. Another factor that strongly affects hydrogen bonding, as suggested in Eq. 1, is concentration. Lower concentrations of monomeric units leads to lower equilibrium concentrations of complexed units. Solution pH can also affect hydrogen bonding systems, leading to pH controlled thickening²⁸ in cases of interpolymer complexes between poly(acrylic acid) and poly(acrylamide). Complexes of poly(acrylic acid) and poly(*N*-vinylpyrrolidone) exhibit molecular weight dependent critical pHs below which stable complexes are formed due to a transition to polyelectrolyte species at higher pH.²⁹

The hydrogen bond is extensively used in nature, particularly in the construction of proteins,³⁰ DNA³¹ and RNA. In all cases, it performs the role of establishing a reversible structure which allows such processes as replication and transcription in DNA and reactions in enzymes and is key in many molecular recognition events in living organisms. One goal of modern science is to incorporate such functionality and dynamics into synthetic materials.

²⁷ Deans, R.; Ilhan, F.; Rotello, V. M. Recognition-Mediated Unfolding of a Self-Assembled Polymeric Globule. *Macromolecules* **1999**, 32, 4956-60.

²⁸ Sotiropoulou, M.; Bokias, G.; Staikos, G. Soluble Hydrogen-Bonding Interpolymer Complexes and pH-controlled Thickening Phenomena in Water. *Macromolecules* **2003**, 36, 1349-54.

²⁹ Nurkeeva, Z. S.; Mun, G. A.; Khutoryanskiy, V. V.; Bitekenova, A. B.; Dubolazov, A. V.; Esirkegenova, S. Z. *Eur. Phys. J* **2003**, 10, 65-8.

³⁰ Aggeli, A.; Bell, M.; Boden, N.; Keen, J. N.; Knowles, P. F.; McLeish, T. C. B.; Pitkeathly, M.; Radford, S. E. Responsive gels formed by the spontaneous self-assembly of peptides into polymeric β -sheet tapes *Nature* **1997**, 386, 259-62.

³¹ Voet, D.; Voet, J. G., *Biochemistry*. John Wiley and Sons: New York, 1995; p 1361.

In the case of DNA, hydrogen bonding performs in concert with numerous other non-covalent interactions such as electrostatic interactions and π - π stacking³² to yield the double helix structure and to give DNA its dynamic properties.

Numerous analytical tools are useful in the study of hydrogen bonding phenomenon. FTIR³³ and NMR³⁴ techniques as well as UV-vis³⁵ are useful for determining association constants or observing association phenomena. For very high association constant systems, more advanced techniques are requisite.³⁶ Rheology^{37,38} and mechanical analysis³⁹ are useful for determining the influence of hydrogen bonding interactions on thermal and mechanical properties, while microscopy (TEM, AFM) are primarily useful for studying changes in morphology. Solution rheology is a particularly useful tool for hydrogen bonded systems due to the ability to introduce solvents of varying dielectric constant and to study the

³² Vanommeslaeghe, K.; Mignon, P.; Loverix, S.; Tourwe, D.; Geerlings, P. Influence of Stacking on the Hydrogen Bond Donating Potential of Nucleic Bases. *Journal of Chemical Theory and Computation* **2006**, 2, 1444-52.

³³ Kyogoku, Y.; Lord, R. C.; Rich, A. The Effect of Substituents on the Hydrogen Bonding of Adenine and Uracil Derivatives. *Proc Natl Acad Sci USA* **1967**, 57, 250-7.

³⁴ Fielding, L. Determination of Association Constants (K_a) from Solution NMR Data. *Tetrahedron* **2000**, 56, 6151-70.

³⁵ Lutz, J. F.; Thunemann, A. F.; Rurack, K. DNA-like "Melting" of Adenine- and Thymine-Functionalized Synthetic Copolymers. *Macromolecules* **2005**, 38, 8124-6.

³⁶ Söntjens, S. H. M.; Sijbesma, R. P.; van Genderen, M. H. P.; Meijer, E. W. Stability and Lifetime of Quadruply Hydrogen Bonded 2-Ureido-4[1H]-pyrimidinone Dimers. *J Am Chem Soc* **2000**, 122, 7487-93.

³⁷ Yamauchi, K.; Lizotte, J. R.; Hercules, D. M.; Vergne, M. J.; Long, T. E. Combinations of Microphase Separation and Terminal Multiple Hydrogen Bonding in Novel Macromolecules. *J Am Chem Soc* **2002**, 124, 8599-604.

³⁸ Müller, M.; Dardin, A.; Seidel, U.; Balsamo, V.; Ivan, B.; Spiess, H. W.; Stadler, R. Junction Dynamics in Telechelic Hydrogen Bonded Polyisobutylene Networks. *Macromolecules* **1996**, 29, 2577-83.

³⁹ Reith, R. L.; Eaton, F. R.; Coates, W. G. Polymerization of Ureidopyrimidinone-Functionalized Olefins by Using Late-Transition Metal Ziegler-Natta Catalysts: Synthesis of Thermoplastic Elastomeric Polyolefins. *Angew. Chem. Int. Ed.* **2001**, 40, 2153-6.

hydrogen bonding interaction as a function of concentration.⁴⁰ Light scattering techniques (DLS, SLS) are often used to characterize micellar or aggregate structures resulting from hydrogen bonding associations in solution.^{41,42}

2.2 Performance Advantages of Hydrogen Bonding Polymers

Reversibility of the hydrogen bond confers unique properties to polymeric and supramolecular materials. In supramolecular science, reversible bonding is important because it allows the self assembly process to occur. Molecular recognition and self-organization are hailed as the mechanisms of supramolecular growth.⁴³ Controlled geometric placement of hydrogen bonding groups leads to efficient molecular recognition which is optimized through self-organization. Furthermore, the directionality of the hydrogen bond assists in the construction of supramolecular structures since random orientations of hydrogen bonding associations leading to disordered networks are not favored. In the field of polymer processing, thermoreversibility is of interest because of the promise for lower melt viscosities of hydrogen bonding polymers. Thus, a lower molecular weight hydrogen bonding polymer could potentially afford mechanical properties approaching those of a higher molecular weight non-functional polymer over a short time scale and yet exhibit

⁴⁰ Sijbesma, R. P.; Beijer, F. H.; Brunsveld, L.; Folmer, B. J. B.; Hirschberg, J. H. K. K.; Lange, R. F. M.; Lowe, J. K. L.; Meijer, E. W. Reversible Polymers Formed from Self-Complementary Monomers Using Quadruple Hydrogen Bonding. *Science* **1997**, 278, 1601-4.

⁴¹ Liu, G.; Zhou, J. First- and Zero-Order Kinetics of Porogen Release from the Cross-Linked Cores of Diblock Nanospheres. *Macromolecules* **2003**, 36, 5279-84.

⁴² Liu, L.; Jiang, M. Synthesis of Novel Triblock Copolymers Containing Hydrogen-Bond Interaction Groups via Chemical Modification of Hydrogenated Poly (styrene-*block*-butadiene-*block*-styrene). *Macromolecules* **1995**, 28, 8702-4.

⁴³ Kato, T. Supramolecular liquid-crystalline materials: molecular self-assembly and self-organization through intermolecular hydrogen bonding. *Supramolecular Science* **1996**, 3, 53-9.

lower melt viscosity when heated above the dissociation temperature of the hydrogen bonding groups.^{44,45} The hydrogen bonding polymer would exhibit a higher apparent molecular weight at room temperature according to viscosity measurements than it actually possessed.

In the case of ditopic molecules with two hydrogen bonding groups, linear non-covalent polymers can form in either solution or the solid state (Figure 2.1). In this case, the degree of non-covalent polymerization (DP) depends directly on the association constant (K_a) in the medium and the concentration of the molecule (c):⁴⁶

$$DP = 4K_a c / (-1 + (1 + 8K_a c)^{0.5}) \sim (2K_a c)^{0.5} \quad [2.4]$$

⁴⁴ Yamauchi, K.; Lizotte, J. R.; Hercules, D. M.; Vergne, M. J.; Long, T. E. Combinations of Microphase Separation and Terminal Multiple Hydrogen Bonding in Novel Macromolecules. *J Am Chem Soc* **2002**, 124, 8599-604.

⁴⁵ Yamauchi, K.; Kanomata, A.; Inoue, T.; Long, T. E. Thermoreversible Polyesters Consisting of Multiple Hydrogen Bonding (MHB). *Macromolecules* **2004**, 37, 3519-22.

⁴⁶ Xu, J.; Fogleman, E. A.; Craig, S. L. Structure and Properties of DNA-Based Reversible Polymers. *Macromolecules* **2004**, 37, 1863-70.

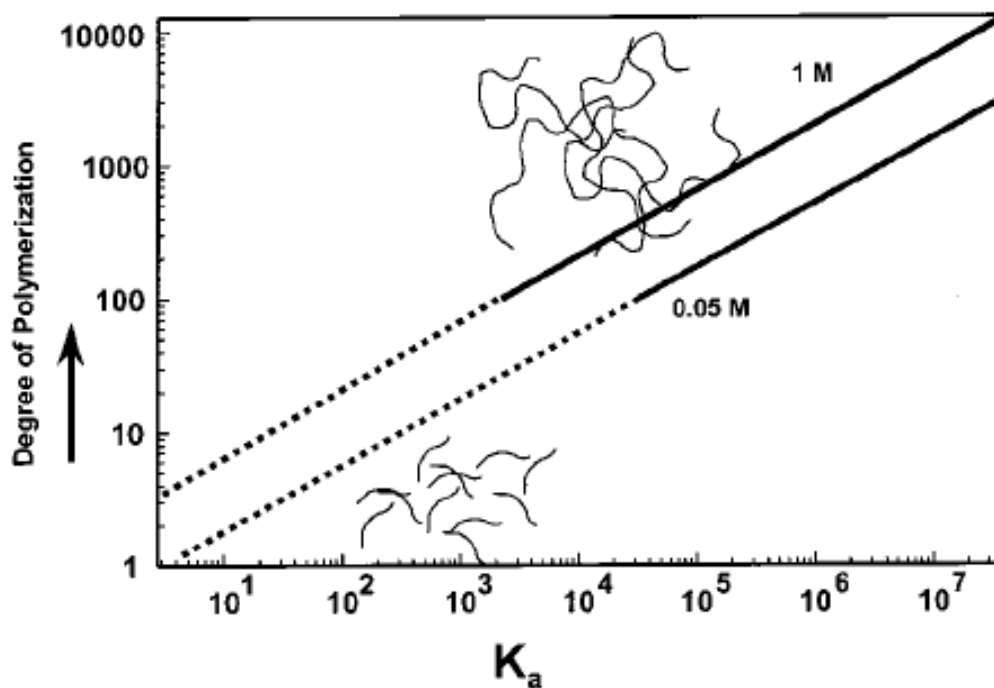


Figure 2.1. Degree of non-covalent polymerization as a function of association constant (K_a).

The effect of concentration is illustrated in the two parallel lines. Reprinted with permission from Brunsveld et al.⁴⁷ Copyright 2001 American Chemical Society.

⁴⁷ Brunsveld, L.; Folmer, B. J. B.; Meijer, E. W.; Sijbesma, R. P. Supramolecular Polymers. *Chem Rev* **2001**, 101, 4071-98.

Another feature of hydrogen bonding systems is that they are dynamic, and this often allows them to achieve the most thermodynamically favored state. This dynamic property of hydrogen bonding allows self-assembly to occur at ambient conditions, unlike many covalent polymerizations.⁴⁸ Rotello et al. were able to create a thermodynamic cycle to examine the competitive processes of self association of a hydrogen bonding polymer and association with a small molecule complementary guest in solution.⁴⁹ In the case of hydrogen bonded networks, the dynamic character leads to the presence of fewer network defects, such as dangling ends and unincorporated chains (sol). In support of this hypothesis, Meijer et al. observed a higher plateau modulus for a hydrogen bonded network compared to a covalent network.⁵⁰

Hydrogen bonding has improved mechanical properties in a number of systems and is often grouped with other non-covalent cohesive intermolecular interactions, performing the “glue” that sticks chains. Hydrogen bonding supramolecular assembly in conjunction with covalent polymer synthesis often leads to positive impact on mechanical properties such as stress at break and percent elongation⁵¹ as well as elastic modulus.⁵² Nissan theorized that for a solid in which hydrogen bonds dominate the mechanical properties such as ice or

⁴⁸ Saadeh, H.; Wang, L.; Yu, L. Supramolecular Solid-State Assemblies Exhibiting Electrooptic Effects. *J Am Chem Soc* **2000**, 122, 546-7.

⁴⁹ Deans, R.; Ilhan, F.; Rotello, V. M. Recognition-Mediated Unfolding of a Self-Assembled Polymeric Globule. *Macromolecules* **1999**, 32, 4956-60.

⁵⁰ Lange, R. F. M.; van Gurp, M.; Meijer, E. W. Hydrogen-bonded supramolecular polymer networks. *J. Polym. Sci. Part A. Polym. Chem.* **1999**, 37, 3657-70.

⁵¹ Reith, R. L.; Eaton, F. R.; Coates, W. G. Polymerization of Ureidopyrimidinone-Functionalized Olefins by Using Late-Transition Metal Ziegler-Natta Catalysts: Synthesis of Thermoplastic Elastomeric Polyolefins. *Angew. Chem. Int. Ed.* **2001**, 40, 2153-6.

⁵² Shandryuk, G. A.; Kuptsov, S. A.; Shatalova, A. M.; Plate, N. A.; Talroze, R. V. Liquid Crystal H-Bonded Polymer Networks under Mechanical Stress. *Macromolecules* **2003**, 36, 3417-23.

cellulose, that the Young's modulus scales with the number of hydrogen bonds per unit volume to the 1/3 power.⁵³ Hydrogen bonding results in increased glass transition temperature, due to restricted molecular mobility and temporary "crosslinks".⁵⁴ Hydrogen bonding interactions are credited, in part (along with phase separation), with the outstanding mechanical properties of polyurethanes. Wilkes and coworkers have recently shown that hydrogen bonding in model single unit hard segment poly(urethane urea)s leads to the development of ribbon-like hard phases containing stacks of hydrogen bonding urethanes or ureas which are disrupted upon addition of branching units in the hard phase or addition of hydrogen bond screening agents such as lithium chloride.⁵⁵ Further studies of single hard segment poly(urethane)s and poly(urea)s demonstrated that the symmetry of the hard segment precursor, which affects the packing ability of hydrogen bonding groups, have a dramatic influence on the thermal integrity of the hard phases. Model poly(urea)s based on *p*-phenylene diisocyanate and poly(tetramethylene oxide) possessed rubbery plateaus extending to 250 °C, while *meta* substitution led to rubbery plateaus extending only 100 °C.⁵⁶ McKeirnan et al. utilized variable temperature FTIR to show that the hydrogen bonds in polyurethanes persist up to temperatures beyond 100 °C and that, even in the melt, ~ 75% of

⁵³ Nissan, A. H. H-Bond Dissociation in Hydrogen Bond Dominated Solids. *Macromolecules* **1976**, *9*, 840-50.

⁵⁴ Yamauchi, K.; Lizotte, J. R.; Hercules, D. M.; Vergne, M. J.; Long, T. E. Combinations of Microphase Separation and Terminal Multiple Hydrogen Bonding in Novel Macromolecules. *J Am Chem Soc* **2002**, *124*, 8599-604.

⁵⁵ Sheth, J. P.; Wilkes, G. L.; Fornof, A. R.; Long, T. E.; Yilgor, I. Probing the Hard Segment Phase Connectivity and Percolation in Model Segmented Poly(urethane urea) Copolymers. *Macromolecules* **2005**, *38*, 5681-5.

⁵⁶ Sheth, J. P.; Klinedinst, D. B.; Wilkes, G. L.; Yilgor, E.; Yilgor, I. Role of chain symmetry and hydrogen bonding in segmented copolymers with monodisperse hard segments. *Polymer* **2005**, *46*, 7317-22.

the urethane linkages were involved in hydrogen bonding.⁵⁷

Hydrogen bonding interactions confer unique melt⁵⁸ and solution⁵⁹ rheological behavior. The temperature sensitivity of the hydrogen bond holds promise for increasing the temperature dependence of the melt viscosity while providing an effectively higher molecular weight at room temperature. Thus, lower molecular weight hydrogen bonding polymers may be employed. However, increased melt and solution viscosity are typically observed at temperatures where hydrogen bonds still exist. Lillya et al. showed that the zero-shear melt viscosity of a 650 g/mol carboxylic acid terminated poly(tetrahydrofuran) was 2.5 times that of the corresponding protected (ester) version telechelic carboxylic acid functionalized poly(THF).⁶⁰ This high melt viscosity dropped above 62 °C and 50 °C for the 650 g/mol and the 1000 g/mol polymers respectively. Rowan et al. have also observed sudden decreases in viscosity in hydrogen bonding systems.⁶¹ Based on sticky reptation theory that Leibler, Rubinstein and Colby developed,⁶² the terminal relaxation time (t_D) for a thermoreversible, hydrogen bonded network is longer than for a corresponding non-functionalized polymer. Rogovina et al. observed reversible network formation in self associating carboxyl

⁵⁷ McKeirnan, R. L.; Heintz, A. M.; Hsu, S. L.; Atkins, E. D. T. P., J; Gido, S. P. Influence of Hydrogen Bonding on the Crystallization Behavior of Semicrystalline Polyurethanes. *Macromolecules* **2002**, 35, 6970-4.

⁵⁸ Yamauchi, K.; Lizotte, J. R.; Long, T. E. Thermoreversible Poly(alkyl acrylates) Consisting of Self-Complementary Multiple Hydrogen Bonding. *Macromolecules* **2003**, 36, 1083-8

⁵⁹ Lele, A. K.; Mashelkar, R. A. Energetically crosslinked transient network (ECTN) model: implications in transient shear and elongation flows. *J. Non-Newtonian Fluid Mech.* **1998**, 75, 99-115.

⁶⁰ Lillya, C. P.; Baker, R. J.; Huette, S.; Winter, H. H.; Lin, H.-G.; Shi, J.; Dickinson, L. C.; Chien, J. C. W. Linear Chain Extension through Associative Termini. *Macromolecules* **1992**, 25, 2076-80.

⁶¹ Sivakova, S.; Bohnsak, D. A.; Mackay, M. E.; Suwanmala, P.; Rowan, S. J. Utilization of a Combination of Weak Hydrogen-Bonding Interactions and Phase Segregation to Yield Highly Thermosensitive Supramolecular Polymers. *J Am Chem Soc* **2005**, 127, 18202-11.

⁶² Leibler, L.; Rubinstein, M.; Colby, R. H. Dynamics of reversible networks. *Macromolecules* **1991**, 24, 4701-7.

functionalized poly(dimethylcarbosiloxane) with 0.5-2.5 mol% of the carboxylic acid group.⁶³ Müller, Seidel and Stadler conducted some of the first major rheological studies of multiple hydrogen bond functionalized polymers. They studied randomly functionalized, urazole and phenylurazole containing, anionically synthesized polybutadienes.⁶⁴ Increased plateau shear moduli, melt viscosity and a shifting of relaxation times to lower frequencies (longer times) were observed in randomly substituted urazole containing polybutadienes.⁶⁵ Zero shear viscosities, which are sensitive to molecular weight, but not to molecular weight distribution (MWD) were shown to increase with mol% phenylurazole substitution which gave an increasing “effective” molecular weight. The real part of the creep compliance at low shear rates (J_c^0), which is sensitive to changes in MWD but not to molecular weight was found to increase with increasing phenylurazole content due to the effective broadening in MWD in the thermoreversible network. Similar results were obtained from relaxation time spectra, where a broadening of the relaxation time distribution occurred for phenylurazole substituted polymers. Increased flow activation energies were also observed through fitting of Williams-Landel-Ferry (WLF) parameters for the shift factors of the storage modulus. Comparing plateau moduli above and below a frequency corresponding to the dissociation rate of the phenylurazoles led to the determination of the number of reversible contacts indicating that 60-70% of the phenylurazole groups were complexed at any one point in time.

⁶³ Rogovina, L. Z.; Vasilev, V. G.; Papkov, V. S.; Shchegolikhina, O. I.; Slonimskii, G. L.; Zhdanov, A. A. The peculiarities of physical network formation in carboxyl-containing poly(dimethylcarbosiloxane). *Macromol. Symp.* **1995**, 93, 135-42.

⁶⁴ Müller, M.; Seidel, U.; Stadler, R. Influence of hydrogen bonding on the viscoelastic properties of thermoreversible networks: analysis of the local complex dynamics. *Polymer* **1995**, 36, 3143-50.

⁶⁵ De Lucca Freitas, L.; Stadler, R. Thermoplastic Elastomers by Hydrogen Bonding. 3. Interrelations between Molecular Parameters and Rheological Properties. *Macromolecules* **1987**, 20, 2478-85.

The solution behavior of hydrogen bonding polymers is equally interesting compared to the solid state. In the dissolved state, polymers exhibit greater freedom to assume conformations which are thermodynamically favored. Furthermore, the dynamic nature of solutions allows rapid response to changes in environment. In solution, factors such as concentration and solvent dielectric constant are used to control the equilibrium between associated and dissociated states. For instance, Kwei et al. established that self-association of the 4-hydroxystyrene residues in symmetric poly(styrene-*b*-4-hydroxystyrene) diblock copolymers led to the formation of rod-like micelles in low polarity toluene which was not observed in the more polar THF solvent.⁶⁶ Reversible non-covalent crosslinking of similar polymers with 1,4-butanediamine induced micelle formation.⁶⁷ Placement of specific molecules within micelles was also achieved using hydrogen bonding.⁶⁸ Solvent dielectric constant strongly affects the solution rheological behavior of hydrogen bonding polymers. Solution rheological studies of UPy functional PMMA indicated that the solution viscosity increased with decreasing dielectric constant (polarity) of the solvent, and that the critical concentration for entanglement (C_e) decreased, presumably due to the higher effective molecular weight of the associated structures.⁶⁹ Furthermore, the slope of the viscosity versus concentration above C_e increased with decreasing solvent polarity, illustrating the

⁶⁶ Zhao, J. Q.; Pearce, E. M.; Kwei, T. K.; Jeon, H. S.; Kesani, P. K.; Balsara, N. P. Micelles Formed by a Model Hydrogen-Bonding Block Copolymer. *Macromolecules* **1995**, 28, 1972-8.

⁶⁷ Yoshida, E.; Kunugi, S. Micelle Formation of Nonamphiphilic Diblock Copolymers through Noncovalent Bond Cross-Linking. *Macromolecules* **2002**, 35, 6665-9.

⁶⁸ Zhang, W.; Shi, L.; An, Y.; Wu, K.; Gao, L.; Liu, Z.; Ma, R.; Meng, Q.; Zhao, C.; He, B. Adsorption of Poly(4-vinyl pyridine) Unimers into Polystyrene-Block-Poly(acrylic acid) Micelles in Ethanol Due to Hydrogen Bonding. *Macromolecules* **2004**, 37, 2924-9.

⁶⁹ McKee, M. G.; Elkins, C.; Long, T. E. Influence of self-complementary hydrogen bonding on solution rheology/electrospinning relationships. *Polymer* **2004**, 45, 8705-15.

effect of concentration on the equilibrium between associated and dissociated states. Hydrogen bonding was utilized to induce micelle formation. Chen and Jiang have studied micelle formation via hydrogen bonding between homopolymers of poly(4-vinylpyridine) and carboxylic acid terminated polystyrene or polyisoprene. They found that assemblies of these homopolymers formed micelles when selective solvents were added for either block.⁷⁰ The size of such micelles was controlled via the mass ratio of the two homopolymers.⁷¹ Furthermore, the polydispersity of the micelles changed with the solvent composition, and narrowed for less selective solvent mixtures.

Other potential applications for hydrogen bonding polymers exist, such as reversible attachment of guest molecules,⁷² reversible crosslinking,⁷³ better melt processing behavior,⁷⁴ self-healing materials,⁷⁵ shape-memory polymers,⁷⁶ recyclable thermosets,⁷⁵ induction of liquid crystallinity⁷⁷ induction of phase mixing⁷⁸ and demixing,⁷⁹ templated

⁷⁰ Chen, D.; Jiang, M. Strategies for Constructing Polymeric Micelles and Hollow Spheres in Solution via Specific Intermolecular Interactions. *Acc Chem Res* **2005**, 38, 494-502.

⁷¹ Wang, M.; Zhang, G.; Chen, D.; Jiang, M.; Liu, S. Noncovalently Connected Polymeric Micelles Based on a Homopolymer Pair in Solutions. *Macromolecules* **2001**, 34, 7172-8.

⁷² Ilhan, F.; Gray, M.; Rotello, V. M. Reversible Side Chain Modification through Noncovalent Interactions. "Plug and Play" Polymers. *Macromolecules* **2001**, 34, 2597-601.

⁷³ Thibault, R. J.; Hotchkiss, P. J.; Gray, M.; Rotello, V. M. Thermally Reversible Formation of Microspheres through Non-Covalent Polymer Cross-Linking. *J Am Chem Soc* **2003**, 125, 11249-52.

⁷⁴ Yamauchi, K.; Lizotte, J. R.; Hercules, D. M.; Vergne, M. J.; Long, T. E. Combinations of Microphase Separation and Terminal Multiple Hydrogen Bonding in Novel Macromolecules. *J Am Chem Soc* **2002**, 124, 8599-604.

⁷⁵ Lange, R. F. M.; van Gorp, M.; Meijer, E. W. Hydrogen-bonded supramolecular polymer networks. *J. Polym. Sci. Part A. Polym. Chem.* **1999**, 37, 3657-70.

⁷⁶ Liu, G.; Guan, C.; Xia, H.; Guo, F.; Ding, X.; Peng, Y. Novel Shape-Memory Polymer Based on Hydrogen Bonding. *Macromol Rapid Commun* **2006**, 27, 1100-4.

⁷⁷ Gulik-Krzywicki, T.; Fouquey, C.; Lehn, J. M. Electron microscopic study of supramolecular liquid crystalline polymers formed by molecular-recognition-directed self-assembly from complementary chiral components. *Proc. Natl. Acad. Sci. USA* **1993**, 90, 163-7.

⁷⁸ Kuo, S. W.; Chan, S. C.; Chang, F. C. Correlation of Material and Processing Time Scales with Structure Development in Isotactic Polypropylene Crystallization. *Macromolecules* **2003**, 36, 6653-61.

polymerization,⁸⁰ drug-selective chromatographic media,⁸¹ hydrogen bonded layer-by-layer assemblies⁸² and reinforcement of orientation of non-linear optic materials.⁸³

2.3 Hydrogen Bonding Block Copolymers

Hydrogen bonding telechelic and block copolymers both differ from randomly functionalized copolymers in that the placement of the hydrogen bonding groups is localized to specific region(s) in the polymer backbone. This typically leads to different behavior compared to random functionalization due to the presence of both phase separation and hydrogen bonding interactions. Thus, in the bulk state, many of these systems consist of separated domains of hydrogen bonding groups or blocks and non-hydrogen bonded regions.

One particular advantage of introducing hydrogen bonding groups as substituents in one particular block of a block copolymer structure is the multiplicative and cooperative effects of the hydrogen bonding interactions due to the multitude of adjacent hydrogen bonding groups.⁸⁴ Hogen-Esch et al. observed the association constants of poly(4-vinylpyridine-*b*-NLO) with poly(4-hydroxystyrene-*b*-styrene) (a good hydrogen

⁷⁹ de Lucca Freitas, L.; Jacobi, M. M.; Goncalves, G. Microphase Separation Induced by Hydrogen Bonding in a Poly(1,4-butadiene)-block poly(1,4-isoprene) Diblock Copolymers An Example of Supramolecular Organization via Tandem Interactions. *Macromolecules* **1998**, 31, 3379-82.

⁸⁰ Khan, A.; Haddleton, D. M.; Hannon, M. J.; Kukulj, D.; Marsh, A. Hydrogen Bond Template-Directed Polymerization of Protected 5'-Acryloylnucleosides. *Macromolecules* **1999**, 32, 6560-4.

⁸¹ Kugimiya, A.; Mukawa, T.; Takeuchi, T. Synthesis of 5-fluorouracil-imprinted polymers with multiple hydrogen bonding interactions. *Analyst* **2001**, 126, 772-4.

⁸² Wang, L.; Fu, Y.; Wang, Z.; Fan, Y.; Zhang, X. Investigation into an Alternating Multilayer Film of Poly(4-Vinylpyridine) and Poly(acrylic acid) Based on Hydrogen Bonding. *Langmuir* **1999**, 15, 1360-3.

⁸³ Huggins, K. E.; Son, S.; Stupp, S. I. Two-Dimensional Supramolecular Assemblies of a Polydiacetylene. 1. Synthesis, Structure, and Third-Order Nonlinear Optical Properties. *Macromolecules* **1997**, 30, 5305-12.

⁸⁴ Pan, J.; Chen, M.; Warner, W.; He, M.; Dalton, L.; Hogen-Esch, T. E. Synthesis and Self-Assembly of Diblock Copolymers through Hydrogen Bonding. Semiquantitative Determination of Binding Constants. *Macromolecules* **2000**, 33, 7835-41.

bonding donor) of 4.5 to $7.9 \times 10^5 \text{ M}^{-1}$ and poly(2-hydroxyethyl methacrylate-*b*-methyl methacrylate) (a poor hydrogen bonding donor) of $4.4 \times 10^3 \text{ M}^{-1}$ in toluene/CH₂Cl₂ (99:1) mixtures. These values are much higher than those expected for a single vinylpyridine-hydroxystyrene hydrogen bonding interaction. Brus et al. found that the cooperativity of association of poly(4-vinyl pyridine) and poly(4-hydroxystyrene) increased with degree of polymerization and reached a maximum at a 1:1 functional group molar ratio.⁸⁵

Also, only short hydrogen bonding blocks are necessary to achieve phase separation, due to the influence of the associations on the tendency of block copolymers to microphase separate. Although this tendency is often measured through the Flory-Huggins interaction parameter χ ,^{86, 87} hydrogen bonding interactions must be accounted for through additions of other parameters into thermodynamic treatments, since χ refers to non-specific interactions and is repulsive, whereas hydrogen bonding is attractive. Painter and Coleman have thoroughly discussed thermodynamic treatments of hydrogen bonding effects in polymer blend miscibility, and considerations must be made for screening and accessibility of hydrogen bonding interactions (since they are directional) as well as the competition between self-association and complementary association.^{88, 89} In some cases, single hydrogen

⁸⁵ Kriz, J.; Dybal, J.; Brus, J. Cooperative Hydrogen Bonds of Macromolecules. 2. Two-Dimensional Cooperativity in the Binding of Poly(4-vinylpyridine) to Poly(4-vinylphenol). *J Phys Chem B* **2006**, 110, 18338-46.

⁸⁶ Leibler, L. Theory of Microphase Separation in Block Copolymers. *Macromolecules* **1980**, 13, 1602-17.

⁸⁷ Lee, K. M.; Han, C. D. Microphase Separation Transition and Rheology of Side-Chain Liquid-Crystalline Block Copolymers. *Macromolecules* **2002**, 35, 3145-56.

⁸⁸ Coleman, M.M.; Painter, P.C. Hydrogen Bonded Polymer Blends. *Prog. Polym. Sci.* **1995**, 20, 1-59.

⁸⁹ Coleman, M.M.; Painter, P.C. Prediction of the Phase Behaviour of Hydrogen-Bonded Polymer Blends. *Aust. J. Chem.* **2006**, 59, 499-507.

bonding groups at the chain ends phase separate from the bulk polymer.^{90,91} This is particularly possible when hydrogen bonding interactions take place in multiple directions, facilitating the organization of the chain ends.⁹²

2.3.1 Block Copolymers Involving Single Hydrogen Bonding Groups

Hydrogen bonding block copolymers containing single hydrogen bonding groups have drawn attention due to the simplicity of their preparation via anionic polymerization techniques of commonly available monomers. One specific template that has occupied researchers is poly(vinylpyridine) which is often blended with complementary poly(methacrylic acid)⁹³ or poly(4-hydroxystyrene). Anionic polymerization possesses a weakness in these cases due to the sensitivity of anionic polymerization to protic functionality. Thus, protecting group strategies are often employed. In the case of 4-hydroxystyrene, silyl protecting groups are employed and in the case of methacrylic acid residues, *tert*-butyl ester protecting groups are employed. Another strategy involves post-polymerization modification. Liu and Jiang introduced carboxylic acid groups and hydroxyl groups into SEBS polymers via Friedel-Crafts acylation and subsequent oxidation

⁹⁰ Lillya, C. P.; Baker, R. J.; Huette, S.; Winter, H. H.; Lin, H.-G.; Shi, J.; Dickinson, L. C.; Chien, J. C. W. Linear Chain Extension through Associative Termini. *Macromolecules* **1992**, *25*, 2076-80.

⁹¹ Sivakova, S.; Bohnsak, D. A.; Mackay, M. E.; Suwanmala, P.; Rowan, S. J. Utilization of a Combination of Weak Hydrogen-Bonding Interactions and Phase Segregation to Yield Highly Thermosensitive Supramolecular Polymers. *J Am Chem Soc* **2005**, *127*, 18202-11.

⁹² Kautz, H.; van Beek, D. J. M.; Sijbesma, R. P.; Meijer, E. W. Cooperative End-to-End and Lateral Hydrogen-Bonding Motifs in Supramolecular Thermoplastic Elastomers. *Macromolecules* **2006**, *39*, 4265-7.

⁹³ Jiang, S.; Gopfert, A.; Abetz, V. Novel Morphologies of Block Copolymer Blends via Hydrogen Bonding. *Macromolecules* **2003**, *31*, 6171-7.

or reduction of the ketone functional groups.⁹⁴ Other strategies involve protecting group chemistry. In the case of 4-hydroxystyrene blocks, a silyl protected monomer is polymerized and deprotected after completion of the reaction.

Block copolymers containing complementary monomers such as 2-vinylpyridine and 4-hydroxystyrene or methacrylic acid were shown to produce novel morphologies in which the complementary segments are mixed in domains which are phase separated from the bulk polymer.⁹⁵ Abetz et al. blended poly(styrene-*b*-butadiene-*b*-*tert*-butyl methacrylate-*co*-methacrylic acid) (SBT/A) with poly(styrene-*b*-2-vinylpyridine) (SV) to obtain a compatibilized blend. The degree of hydrogen bonding interaction was varied through controlling the level of hydrolysis of the *tert*-butyl methacrylate residues to methacrylic acid residues. For partially hydrolyzed SBT polymers (18-51% hydrolyzed), blending with SV led to a transition from a double gyroid or lamellar morphology (SBT/A---A/TBS) to hcp V-T/A cylinders in B lamella alternating with S lamella. Matsushita et al. carried out a similar study in which poly(2-vinylpyridine-*b*-isoprene-*b*-2-vinylpyridine) triblocks with a mole fraction of vinylpyridine of 0.07 and poly(styrene-*b*-4-hydroxystyrene) with 4-hydroxystyrene mole fraction of 0.14 were blended in either a 1:1 or 2:1 2-vinylpyridine to 4-hydroxystyrene

⁹⁴ Liu, L.; Jiang, M. Synthesis of Novel Triblock Copolymers Containing Hydrogen-Bond Interaction Groups via Chemical Modification of Hydrogenated Poly (styrene-*block*-butadiene-*block*-styrene). *Macromolecules* **1995**, *28*, 8702-4.

⁹⁵ Asari, T.; Matsuo, S.; Takano, A.; Matsushita, Y. Three-Phase Hierarchical Structures from AB/CD Diblock Copolymer Blends with Complemental Hydrogen Bonding Interaction. *Macromolecules* **2005**, *38*, 8811-5.

ratio.⁹⁶ Archimedean tile morphologies resulted which consisted of rows of vinylpyridine with 4-hydroxystyrene cylinders staggered between isoprene and styrene lamella for the 1:1 ratio or hexagons of styrene in an isoprene matrix with 2-vinylpyridine with 4-hydroxystyrene cylinders at the corners of the styrene hexagons (Figure 2.2). Matsushita et al. established the 4-hydroxystyrene / 2-vinylpyridine hydrogen bonding interaction from ¹H NMR where a shifting of the OH proton was visible with the addition of vinylpyridine containing copolymers.

⁹⁶ Asari, T.; Arai, S.; Takano, A.; Matsushita, Y. Archimedean Tiling Structures from ABA/CD Block Copolymer Blends Having Intermolecular Association with Hydrogen Bonding. *Macromolecules* **2006**, 39, 2232-7.

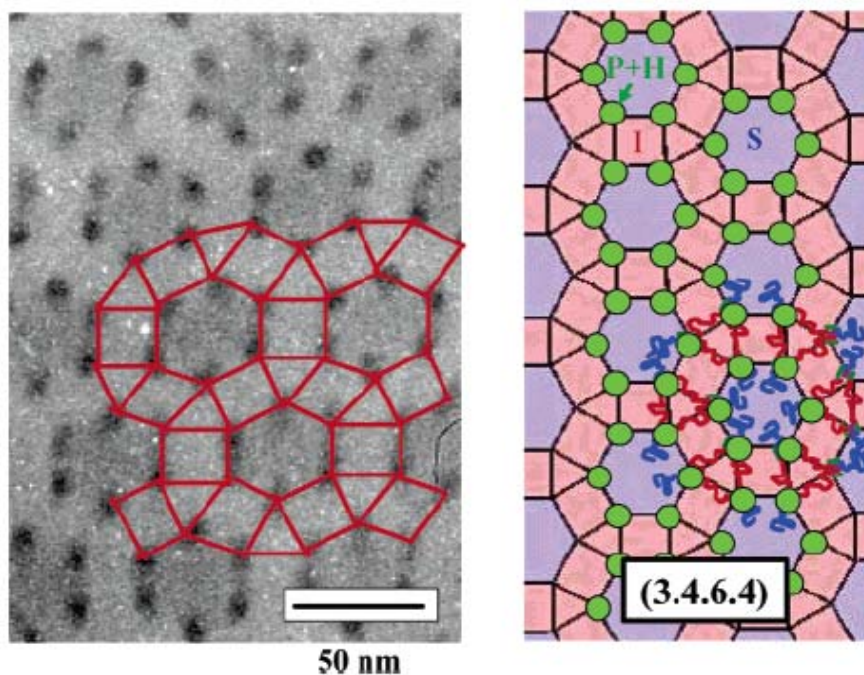


Figure 2.2. An Archimedean tile morphology for blends of poly(2-vinylpyridine-*b*-isoprene-*b*-vinylpyridine) with poly(styrene-*b*-4-hydroxystyrene) in a 2:1 vinylpyridine to hydroxystyrene blend. The vinylpyridine/hydroxystyrene domains are the cylinders at the vertices of polystyrene hexagons within a polyisoprene continuous phase. Reprinted with permission from Asari et al.⁹⁷ Copyright 2006, American Chemical Society.

⁹⁷ Asari, T.; Arai, S.; Takano, A.; Matsushita, Y. Archimedean Tiling Structures from ABA/CD Block Copolymer Blends Having Intermolecular Association with Hydrogen Bonding. *Macromolecules* **2006**, 39, 2232-7.

Painter and Coleman developed theoretical treatments to describe hydrogen bonding in polymer blends.^{98,99} In general, the compatibilization of blends reduces the sizes of the domains present and increases the mechanical properties while reducing melt viscosity, as Huang et al. observed in studies of blending syndiotactic polystyrene with a thermoplastic polyurethane using a poly(styrene-*b*-4-vinylpyridine) block copolymer.¹⁰⁰ The reduction of interfacial tension through the use of hydrogen bonding block copolymers is the primary mechanism to improve blend miscibility. Blends of poly(2,5-dimethyl-1,4-phenylene oxide) (PPO) and poly(ethylene-*co*-acrylic acid) were compatibilized using poly(styrene-*b*-2-ethyl-2-oxazoline) due to the hydrogen bonding interactions of the amine and the carboxylic acid and the compatibility of the polystyrene block with PPO.¹⁰¹ Tensile strength and elongation of blends increased as domain size decreased with the addition of a small amount (~5 wt%) of the poly(styrene-*b*-2-ethyl-2-oxazoline). Frechet and Kramer have pursued living anionic and atom transfer radical polymerization (ATRP) of block and graft copolymers of styrene and 4-hydroxystyrene for strengthening the interface between polystyrene and poly(4-vinylpyridine).¹⁰² The hydrogen bonding between the

⁹⁸ Coleman, M. M.; Graf, J. F.; Painter, P. C., Specific Interactions and the Miscibility of Polymer Blends. Technomic: Lancaster, PA, 1991.

⁹⁹ Painter, P. C.; Veytsman, B.; Kumar, S.; Shenoy, S.; Graf, J. F.; Xu, Y.; Coleman, M. M. Intramolecular Screening Effects in Polymer Mixtures. 1. Hydrogen-Bonded Polymer Blends. *Macromolecules* **1997**, 30, 932-42.

¹⁰⁰ Xu, S.; Chen, B.; Tang, T.; Huang, B. Syndiotactic polystyrene/thermoplastic polyurethane blends using poly(styrene-*b*-4-vinylpyridine) diblock copolymer as a compatibilizer. *Polymer* **1999**, 40, 3399-406.

¹⁰¹ Xu, S.; Zhao, H.; Tang, T.; Dong, L.; Huang, B. Effect and mechanism in compatibilization of poly(styrene-*b*-2-ethyl-2-oxazoline) diblock copolymer in poly(2,6-dimethyl-1,4-phenylene oxide)/poly(ethylene-*ran*-acrylic acid) blends. *Polymer* **1999**, 40, 1537-45.

¹⁰² Edgecombe, B. D.; Stein, J. A.; Frechet, J. M. J.; Xu, Z.; Kramer, E. J. The Role of Polymer Architecture in Strengthening Polymer-Polymer Interfaces: A Comparison of Graft, Block, and Random Copolymers Containing Hydrogen-Bonding Moieties. *Macromolecules* **1998**, 31, 1292-304.

poly(4-hydroxystyrene) block and the poly(4-vinylpyridine) led to strong interactions which allowed the use of poly(4-hydroxystyrene) blocks that were below the entanglement molecular weight (M_c). In contrast, the polystyrene blocks possessed molecular weights above M_c , which allowed some degree of entanglement with the polystyrene side of the interface.

Often, self-association and multiple modes of association of hydrogen bonding groups leads to complexity in the behavior of hydrogen bonded systems in which complementary hydrogen bonding groups are involved. Kwei et al. synthesized poly(styrene-*b*-vinylphenyldimethylsilanol) polymers via anionic polymerization of silane (Si-H) containing monomers and subsequent post-polymerization oxidation with dimethyldioxirane.¹⁰³ The stronger acidity of the silanol group compared to the hydroxyl group was expected to result in greater hydrogen bonding donating capabilities. However, self-association of the silanol residues was found to play a large role in the behavior of these copolymers. Block copolymers with a range of 11-33% conversion to silanol groups were miscible with the weak hydrogen bond accepting homopolymer poly(*n*-butyl methacrylate) whereas higher or lower conversions led to macrophase separation. Blends of the 21% silanol block copolymer with the stronger hydrogen bond acceptor poly(4-vinylpyridine) or poly(*N*-vinylpyrrolidone) formed clear films in all cases and exhibited hydrogen bonding through changes in the FTIR spectrum.

¹⁰³ Han, Y. K.; Pearce, E. M.; Kwei, T. K. Poly(styrene-*b*-vinylphenyldimethylsilanol) and Its Blends with Homopolymers. *Macromolecules* **2000**, 33, 1321-9.

2.3.2 Nucleobase Containing Hydrogen Bonding Block Copolymers

Nucleobase containing hydrogen bonding block copolymers are typically synthesized via techniques which are amenable to protic functionality of the hydrogen bonding groups such as living radical or metathesis polymerization techniques. Also, nucleobase functional polymers are synthesized via post-polymerization techniques, although these are typically hampered from incomplete conversion and side reactions. Nucleobase associations possess strengths in the range of 100 M^{-1} (A-T, two hydrogen bonds) to 10^4 M^{-1} (C-G, three hydrogen bonds) which places them between simple single hydrogen bonds and synthetic quadruple, or higher multiple hydrogen bonding interactions.^{104,105} Recent computational studies on the energy of hydrogen bonding interactions in DNA duplexes revealed values of $\sim 14 \text{ kcal/mol}$ for the A-T pair and $\sim 27 \text{ kcal/mol}$ for the C-G pair.¹⁰⁶ For adenine-uracil (A-U) hydrogen bonds in chloroform, the association energy was determined experimentally from an Arrhenius plot of association constants, yielding a value of 6.2 kcal/mol .¹⁰⁷ Nucleobases are complementary in nature, so that specific pairs such as adenine and thymine or uracil (A-T, A-U) or cytosine and guanine (C-G) are typically employed. Rowan et al. noted that the behavior of the isolated nucleobases in synthetic polymers is quite different from their

¹⁰⁴ Kyogoku, Y.; Lord, R. C.; Rich, A. The Effect of Substituents on the Hydrogen Bonding of Adenine and Uracil Derivatives. *Proc Natl Acad Sci USA* **1967**, 57, 250-7.

¹⁰⁵ Thomas, G. J.; Kyogoku, Y. Hypochromism Accompanying Purine-Pyrimidine Association Interactions. *J Am Chem Soc* **1967**, 89, 4170-5.

¹⁰⁶ Sponer, J.; Jurecka, P.; Hobza, P. Accurate Interaction Energies of Hydrogen-Bonded Nucleic Acid Base Pairs. *J. Am. Chem. Soc.* **2004**, 126, 10142-51.

¹⁰⁷ Kyogoku, Y.; Lord, R. C.; Rich, A. An Infrared Study of Hydrogen Bonding between Adenine and Uracil Derivatives in Chloroform Solution. *J Am Chem Soc* **1967**, 89, 496-504.

behavior in DNA where they bond to a complementary base.¹⁰⁸ Multiple association modes are also possible for these nucleobases, including the primary Watson-Crick mode which is present in DNA and the less commonly observed Hoogsteen association mode,¹⁰⁹ as well as several self-association modes. The self-association modes of typical nucleobases are extremely weak in nature and exhibit association constants less than 10 M^{-1} .¹¹⁰ As in DNA, other non-covalent interactions such as π - π stacking are often present with these heterocyclic bases.

As for DNA, synthetic nucleobase containing polymers have exhibited a “melting” in solution due to the unraveling of cooperatively associated chains. One must note, however, that the structure of the associated species was not elucidated and likely possesses little resemblance to the double helix of DNA. Lutz et al. observed this melting phenomenon in mixtures of random copolymers of adenine and thymine functionalized styrenic monomers, 9-(4-vinylbenzyl)adenine and 1-(vinylbenzyl) thymine, with dodecylmethacrylate.^{111, 112} These copolymers organized in low-dielectric constant organic solvents (chloroform and dioxane) at concentrations near $3 \times 10^{-5} \text{ M}^{-1}$. A decrease in the UV absorbance near 260 nm for the complex compared to the individual copolymers suggesting the formation of stacked

¹⁰⁸ Sivakova, S.; Bohnsak, D. A.; Mackay, M. E.; Suwanmala, P.; Rowan, S. J. Utilization of a Combination of Weak Hydrogen-Bonding Interactions and Phase Segregation to Yield Highly Thermosensitive Supramolecular Polymers. *J Am Chem Soc* **2005**, 127, 18202-11.

¹⁰⁹ Ghosal, G.; Muniyappa, K. Hoogsteen base-pairing revisited: Resolving a role in normal biological processes and human diseases. *Biochemical and Biophysical Research Communications* **2006**, 343, 1-7.

¹¹⁰ Kyogoku, Y.; Lord, R. C.; Rich, A. The Effect of Substituents on the Hydrogen Bonding of Adenine and Uracil Derivatives. *Proc Natl Acad Sci USA* **1967**, 57, 250-7.

¹¹¹ Lutz, J. F.; Thunemann, A. F.; Rurack, K. DNA-like “Melting” of Adenine- and Thymine-Functionalized Synthetic Copolymers. *Macromolecules* **2005**, 38, 8124-6.

¹¹² Lutz, J. F.; Thunemann, A. F.; Nehring, R. Preparation by Controlled Radical Polymerization and Self-Assembly via Base-Recognition of Synthetic Polymers Bearing Complementary Nucleobases. *J Polym Sci, Part A: Polym Chem* **2005**, 43, 4805-18.

nucleotide base pairs. The hypochromic effect, which is also observed in DNA, increased with solution concentration due to a shift to a more associated state. The hypochromic effect diminished with heating, as a result of thermal disruption of the hydrogen bonded complex, and a characteristic “melting” temperature was measured at 325 K, much as in the melting of A-T DNA oligonucleotides at 325 K.

Haddleton et al. reported on the use of ATRP for the synthesis of uridine and adenosine functionalized methacrylate homopolymers as well as end-functionalization using uridine and adenosine functional initiators.¹¹³ These uridine and adenosine monomers consisted of the nucleotide bases uracil and adenine connected to the five membered deoxyribose sugars present in DNA, and subsequently bonded to methacrylate groups. In their study, silyl protecting groups were employed on the hydroxyl groups of the uridine and adenosine monomers to improve their solubility in organic solvents. Narrow polydispersities were obtained, however, molecular weights of the hydrogen bonding homopolymers were typically low (<10000 g/mol). Glass transition temperatures for the hydrogen bonding methacrylate homopolymers, even at these low molecular weights were near 140 °C.

van Hest et al. synthesized nucleobase functional block copolymers containing thymine via ATRP of a thymine methacrylate monomer from a PEG-macroinitiator.¹¹⁴ This polymer was introduced into the polymerization of an adenine containing methacrylate monomer in order to attempt to template the polymerization of the adenine containing monomer. Instead, however, a rate enhancement of the adenine monomer polymerization reaction was observed.

¹¹³ Marsh, A.; Khan, A.; Haddleton, D. H.; Hannon, M. J. Atom Transfer Polymerization: Use of Uridine and Adenosine Derivatized Monomers and Initiators. *Macromolecules* **1999**, 32, 8725-31.

¹¹⁴ Spijker, H. J.; Dirks, A. J.; van Hest, J. C. M. Unusual rate enhancement in the thymine assisted ATRP process of adenine monomers. *Polymer* **2005**, 46, 8528-35.

Similar rate enhancements were observed with the addition of a thymine small molecule, suggesting that competitive coordination of the adenine groups to the copper ATRP catalyst occurred, which slowed reaction rates and was disrupted due to the hydrogen bonding association to thymine.

Sleiman et al. have synthesized adenine functional block copolymers using ring-opening metathesis polymerization (ROMP) of substituted oxonorbornene monomers (Figure 2.3).¹¹⁵ The adenine containing block copolymers self-assembled during evaporation from dilute solutions into cylindrical shaped structures (Figure 2.4). The ability to form these structures was attributed to the ability of adenine to hydrogen bond in two directions with neighboring adenine molecules. Apparently, low degrees of crystallinity in the adenine homopolymers were observed from WAXS and DSC. Novel, non-covalent protecting chemistry involving addition of complementary succinimide was utilized to improve the conversion of the adenine containing monomer.

Inaki, who has synthesized a wide range of nucleobase functionalized random and homopolymers,¹¹⁶ has also synthesized block copolymers containing thymine and uracil groups in the main chain, through ring-opening cationic and anionic polymerization of cyclic derivatives of the nucleobases.¹¹⁷

¹¹⁵ Bazzi, H.; Sleiman, H. Adenine-Containing Block Copolymers via Ring-Opening Metathesis Polymerization: Synthesis and Self-Assembly into Rod Morphologies. *Macromolecules* **2002**, 35, 9617-20.

¹¹⁶ Inaki, Y. Synthetic Nucleic Acid Analogs. *Prog Polym Sci* **1992**, 17, 515-70.

¹¹⁷ Inaki, Y.; Futagawa, H.; Takemoto, K. *Polymerization of cyclic derivatives of uracil and thymine*. *J Polym Sci, Polym Chem Ed* 1980, 18, 2959-69.

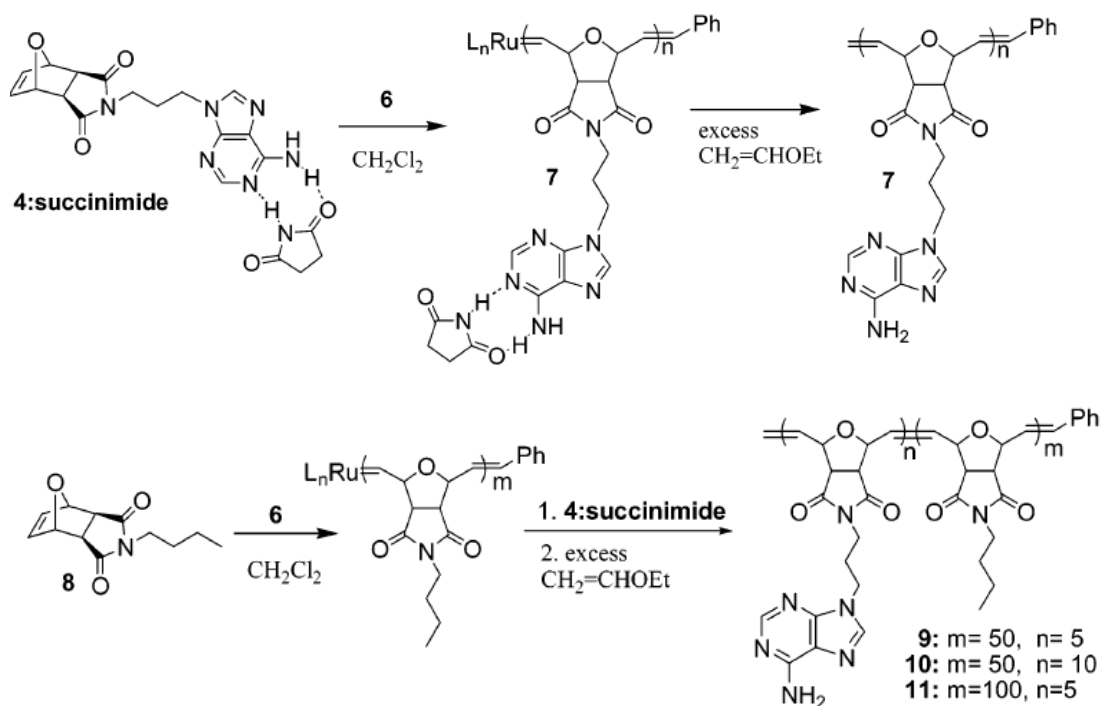


Figure 2.3. Synthesis of adenine containing block copolymers via a ROMP methodology.

Reprinted with permission from Bazzi and Sleiman¹¹⁸ Copyright 2002 American Chemical Society.

¹¹⁸ Bazzi, H.; Sleiman, H. Adenine-Containing Block Copolymers via Ring-Opening Metathesis Polymerization: Synthesis and Self-Assembly into Rod Morphologies. *Macromolecules* **2002**, *35*, 9617-20.

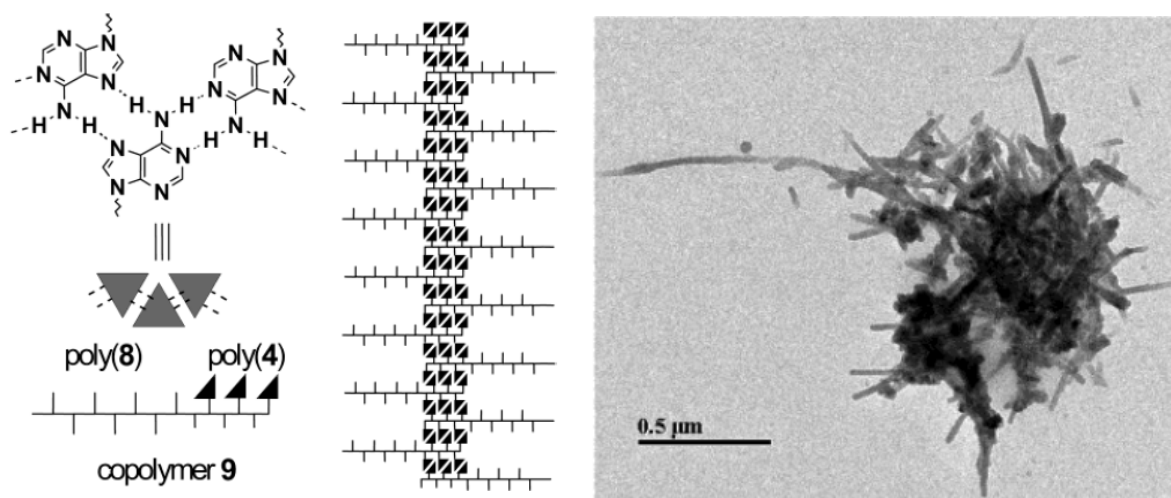


Figure 2.4. Formation of cylindrical aggregates via multi-directional self-association bonding of adenine functional block copolymers. Reprinted with permission from Bazzi and Sleiman¹¹⁹ Copyright 2005, American Chemical Society.

¹¹⁹ Bazzi, H.; Sleiman, H. Adenine-Containing Block Copolymers via Ring-Opening Metathesis Polymerization: Synthesis and Self-Assembly into Rod Morphologies. *Macromolecules* **2002**, *35*, 9617-20.

Hydrogen bonding in nucleobase functionalized block copolymers was utilized to template nanostructured materials in solution for potential drug delivery applications. In work from Liu et al., crosslinkable and hydrogen bonding functionality were introduced in the form of poly(2-cinnamoyloxyethyl methacrylate-*co*-2-thyminylacetoxyethyl methacrylate-*b-tert*-butyl acrylate). Complementary, non-crosslinkable poly(2-hydrocinnamoyloxyethyl methacrylate-*co*-9-adeninylacetoxyethyl methacrylate) was also synthesized. These complementary polymers were solution blended in chloroform/cyclohexane mixtures to produce micelles containing the nucleotide pairs with soluble *tert*-butyl acrylate blocks extending into solution.¹²⁰ Photocrosslinking of these micelles and subsequent extraction of the adenine functionalized polymers resulted in porous nanospheres, which absorbed adenine from solution more rapidly than non-extracted or non-crosslinked micelles. Kinetics varying from first order for low molar mass porogens to zero order for higher molar mass porogens were observed, which suggested potential applications in drug delivery.¹²¹ In a related study, Hu and Liu produced mixed micelles from poly(2-cinnamoyloxyethyl methacrylate-*co*-2-thyminylacetoxyethyl methacrylate-*b-tert*-butyl acrylate) and poly(2-cinnamoyloxyethyl methacrylate-*co*-9-adeninylacetoxyethyl methacrylate-*b*-styrene).^{122, 123} These mixed micelles were photocrosslinked and then the *tert*-butyl acrylate blocks were hydrolyzed to

¹²⁰ Zhou, J.; Li, Z.; Liu, G. Diblock Copolymer Nanospheres with Porous Cores. *Macromolecules* **2002**, 35, 3690-6.

¹²¹ Liu, G.; Zhou, J. First- and Zero-Order Kinetics of Porogen Release from the Cross-Linked Cores of Diblock Nanospheres. *Macromolecules* **2003**, 36, 5279-84.

¹²² Hu, J.; Lui, G. Chain Mixing and Segregation in B-C and C-D Diblock Copolymer Micelles. *Macromolecules* **2005**, 38, 8058-65.

¹²³ Yan, X.; Liu, G.; Hu, J.; Willson, C. G. Coaggregation of B-C and D-C Diblock Copolymers with H-Bonding C Blocks in Block-Selective Solvents. *Macromolecules* **2006**, 39, 1906-12.

produce poly(acrylic acid) residues, which phase separated from the styrene functionalized block copolymer tails in the micellar corona, as observed in TEM. The phase separation resulted in either two-faced appearance or flower-like patterns in the corona.

Lehn and Rotello's groups extensively studied diacyldiaminopyridines which form triple hydrogen bonded associated structures with uracil and thymine groups.^{124 -127} Rotello et al. studied the formation of vesicles from mixtures of randomly functionalized complementary copolymers containing thymine groups and another with diacyldiaminopyridine units.¹²⁸ The complementary flavin guest molecule was incorporated into the ~ 3 μm spherical vesicles. Bis(thymine) functional small molecules served as non-covalent crosslinkers when mixed with randomly functionalized diacyldiaminopyridine functionalized polystyrene.¹²⁹ In chloroform solution, mixing of these complementary units led to the formation of ~ 1 μm microgels. Temperature dependent turbidity measurements at 700 nm showed that clearing of the solutions was obtained upon heating to 50 °C due to thermal disruption of hydrogen bonding and turbidity was reproducibly obtained upon

¹²⁴ Gulik-Krzywicki, T.; Fouquey, C.; Lehn, J. M. Electron microscopic study of supramolecular liquid crystalline polymers formed by molecular-recognition-directed self-assembly from complementary chiral components. *Proc. Natl. Acad. Sci. USA* **1993**, 90, 163-7.

¹²⁵ Sanyal, A.; Norsten, T. B.; Uzun, O.; Rotello, V. M. Adsorption/Desorption of Mono- and Diblock Copolymers on Surfaces Using Specific Hydrogen Bonding Interactions. *Langmuir* **2004**, 20, 5958-64.

¹²⁶ Stubbs, L. P.; Weck, M. Towards a Universal Polymer Backbone: Design and Synthesis of Polymeric Scaffolds Containing Terminal Hydrogen-Bonding Recognition Motifs at Each Repeating Unit. *Chem Eur J* **2003**, 9, 992-9.

¹²⁷ Carroll, J. B.; Waddon, A. J.; Nakade, H.; Rotello, V. M. "Plug and Play" Polymers. Thermal and X-ray Characterizations of Noncovalently Grafted Polyhedral Oligomeric Silsesquioxane (POSS)-Polystyrene Nanocomposites. *Macromolecules* **2003**, 36, 6289-91.

¹²⁸ Ilhan, F.; Galow, T. H.; Gray, M.; Clavier, G.; Rotello, V. M. Giant Vesicle Formation through Self-Assembly of Complementary Random Copolymers. *J Am Chem Soc* **2000**, 122, 5895-6.

¹²⁹ Thibault, R. J.; Hotchkiss, P. J.; Gray, M.; Rotello, V. M. Thermally Reversible Formation of Microspheres through Non-Covalent Polymer Cross-Linking. *J Am Chem Soc* **2003**, 125, 11249-52.

cooling back to room temperature. Rotello has further demonstrated reversible attachment of diacyldiaminopyridine containing styrenic copolymers to thymine modified surfaces using XPS and quartz crystal microbalances to measure the adsorption. The adsorbed polymer was easily removed via washing with hydrogen bond screening solvents such as chloroform/ethanol mixtures but was retained upon washing with chloroform.¹³⁰ Non-covalent attachment of diacyldiaminopyridine functionalized polyoligosilsequioxanes (POSS) to thymine functionalized polystyrene was also studied.¹³¹ Stubbs and Weck also examined ROMP homopolymers of diacyldiaminopyridine and diacyldiaminotriazine functionalized norbornenes.¹³² Due to the propensity for self-association of these hydrogen bonding units, homopolymers precipitated from solution during polymerization. The polymers were re-dissolved slowly through the addition of 1-butylthymine in chloroform. To avoid precipitation during polymerization, the authors utilized non-covalent protecting chemistry with the addition of 1-butylthymine.

Block copolymers containing the diacyldiaminopyridine group were also synthesized. Starting with poly(*tert*-butyl acrylate-*b*-hydroxyethylmethacrylate), block copolymers synthesized from ATRP, Li et al. carried out post-polymerization esterification of the hydroxyl groups with a carboxylic acid containing acrylamide functionalized

¹³⁰ Sanyal, A.; Norsten, T. B.; Uzun, O.; Rotello, V. M. Adsorption/Desorption of Mono- and Diblock Copolymers on Surfaces Using Specific Hydrogen Bonding Interactions. *Langmuir* **2004**, 20, 5958-64.

¹³¹ Carroll, J. B.; Waddon, A. J.; Nakade, H.; Rotello, V. M. "Plug and Play" Polymers. Thermal and X-ray Characterizations of Noncovalently Grafted Polyhedral Oligomeric Silsesquioxane (POSS)-Polystyrene Nanocomposites. *Macromolecules* **2003**, 36, 6289-91.

¹³² Stubbs, L. P.; Weck, M. Towards a Universal Polymer Backbone: Design and Synthesis of Polymeric Scaffolds Containing Terminal Hydrogen-Bonding Recognition Motifs at Each Repeating Unit. *Chem Eur J* **2003**, 9, 992-9.

diacyldiaminopyridine hydrogen bonding crosslinker.¹³³ The unreacted hydroxyl groups were then reacted with methacrylic anhydride to introduce further crosslinkable groups. The block copolymers hydrogen bonded with alkyl functional thymines and uracils in non-selective solvents as observed in FTIR spectra. The introduction of a selective solvent (cyclohexane) produced micelles which were then crosslinked in solution. Extraction of the alkyl functional thymines or uracils through dialysis led to hollow nanospheres. Binding isotherms of the nanospheres with the thymine or uracil containing molecules were obtained.

2.3.3 Block Copolymers Containing DNA Oligonucleotides

Conjugates of synthetic polymers with DNA oligonucleotides were also synthesized. Matsushita et al. utilized the phosphoramidite route to incorporate nucleotide bases in a stepwise fashion from a hydroxyl containing polymer precursor.¹³⁴ Coupling of thymidine phosphoramidite to polymeric hydroxyl groups was achieved with benzimidazoleum triflate (Figure 2.5). Oxidation with *tert*-butyl hydroperoxide led to the formation of phosphodiester bonds. The addition of acid allowed deprotection of the remaining hydroxyl groups of the deoxyribose sugar linkage, enabling repetition of the chemistry to generate multiple thymidine residues. Matsushita et al. synthesized anionic deuterated polystyrenes with five terminal thymidine units which formed a cylindrical morphology. Microphase separation was also visible for a single terminal thymidine unit.

¹³³ Li, Z.; Ding, J.; Day, M.; Tao, Y. Molecularly Imprinted Polymeric Nanospheres by Diblock Copolymer Self-Assembly. *Macromolecules* **2006**, 39, 2629-36.

¹³⁴ Noro, A.; Nagata, Y.; Tsukamoto, M.; Hayakawa, Y.; Takano, A.; Matsushita, Y. Novel Synthesis and Characterization of Bioconjugate Block Copolymers Having Oligonucleotides. *Biomacromolecules* **2005**, 6, 2328-33.

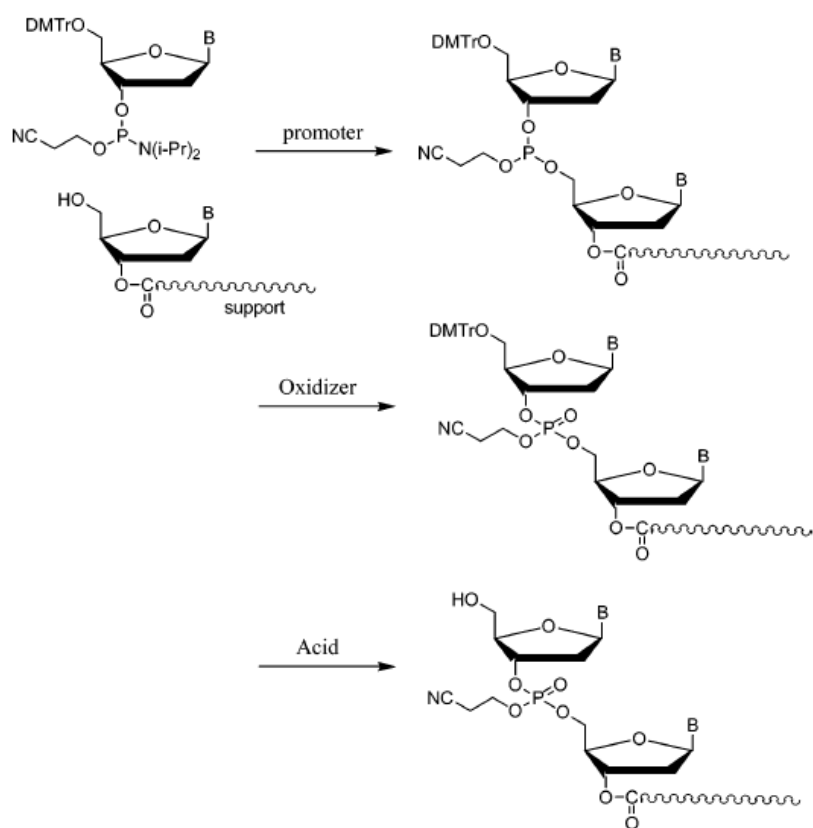


Figure 2.5. Scheme for stepwise synthesis of oligonucleotides via coupling of phosphoramidite functionalized nucleosides. Reprinted with permission from Noro et al.¹³⁵

Copyright 2005, American Chemical Society.

¹³⁵ Noro, A.; Nagata, Y.; Tsukamoto, M.; Hayakawa, Y.; Takano, A.; Matsushita, Y. Novel Synthesis and Characterization of Bioconjugate Block Copolymers Having Oligonucleotides. *Biomacromolecules* **2005**, *6*, 2328-33.

In work from Craig et al., DNA oligonucleotides were synthesized consisting of 8-base self-complementary sequences repeated twice in the same molecule to create ditopic linear self assembly.¹³⁶ The association of these molecules resulted in a degree of polymerization of roughly 10, corresponding to a molecular weight of 182000 g/mol at 0.54 mM concentration in water. Injections of varying volumes of the associated polymer onto a size exclusion chromatograph resulted in decreasing apparent molecular weight for smaller injection volumes, which was consistent with dilution leading to a lower effective molecular weight. The solution viscosity exhibited a slope discontinuity from 1.8 to 3.7, indicating a transition from dilute to semi-dilute unentangled behavior, which is characteristic of high molecular weight polymers. The radius of gyration (R_g) of the associated structures scaled with $M_w^{0.7}$, indicating rod-like behavior typical of DNA. The introduction of flexible PEG spacers between the self-complementary 8-base sequences led to the formation of associated cyclic structures and slow reorganization into linear, high molecular weight species.

Watson et al. synthesized ROMP homopolymers and block copolymers from hydroxyl containing norbornene monomers.¹³⁷ The hydroxyl functional groups were phosphoramidated and attached to DNA oligonucleotides. Complementary DNA oligonucleotide containing ROMP polymers were mixed in solution resulted in precipitation of the hydrogen bonded complex. Heating of this complex produced a melting point similar to that observed in pure DNA oligonucleotides near 75 °C. Gold nanoparticles containing DNA strands were complexed with complementary difunctional polymeric oligonucleotides,

¹³⁶ Xu, J.; Fogleman, E. A.; Craig, S. L. Structure and Properties of DNA-Based Reversible Polymers. *Macromolecules* **2004**, 37, 1863-70.

¹³⁷ Watson, K. J.; Park, S. J.; Im, J. H.; Nguyen, S. B. T.; Mirkin, C. A. DNA-Block Copolymer Conjugates. *J Am Chem Soc* **2001**, 123, 5592-3.

resulting in aggregation of the gold nanoparticles into a network structure as observed with TEM and surface plasmon resonance.

Peptide nucleic acids (PNAs) are a class of polymers with peptide or pseudopeptide backbones and pendant nucleotide bases. PNAs typically lack the helicity of DNA but benefit from stronger association and solubility in organic solvents. Berry et al. polymerized hydroxyethylacrylate from a bromo functional PNA hexamer via ATRP.¹³⁸ This poly(hydroxyethyl acrylate-*b*-PNA) associated with a PNA with three complementary arms, resulting in an apparent molecular weight three times higher than the precursor. Solution phase “melting” of these PNA assemblies occurred at 30 °C. Biologically inspired hydrogen bonding block copolymers containing peptide sequences¹³⁹ or polysaccharide¹⁴⁰ blocks were also studied recently. Klok et al. studied the synthesis of poly(styrene-*b*- γ -benzyl-L-glutamate) copolymers.¹⁴¹

2.3.4 Block Copolymers Containing other Hydrogen Bonding Arrays

Sleiman’s group also studied hydrogen bonding ROMP block copolymers containing dicarboximide hydrogen bonding groups as the polar, hydrogen bonding block and alkylated

¹³⁸ Wang, Y.; Armitage, B. A.; Berry, G. C. Reversible Association of PNA-Terminated Poly(2-hydroxyethyl acrylate) from ATRP. *Macromolecules* **2005**, 38, 5846-8.

¹³⁹ Arimura, H.; Ohya, Y.; Ouchi, T. Formation of Core-Shell Type Biodegradable Polymeric Micelles from Amphiphilic Poly(aspartic acid)-*block*-Polylactide Diblock Copolymer. *Biomacromolecules* **2005**, 6, 720-5.

¹⁴⁰ Bosker, W. T. E.; Agoston, K.; Cohen Stuart, M. A.; Norde, W.; Timmermans, J. W.; Slaghek, T. M. Synthesis and Interfacial Behavior of Polystyrene-Polysaccharide Diblock Copolymers. *Macromolecules* **2003**, 36, 1982-7.

¹⁴¹ Klok, H. A.; Langenwalter, J. F.; Lecommandoux, S. Self-Assembly of Peptide-Based Diblock Oligomers. *Macromolecules* **2000**, 33, 7819-26.

dicarboximide residues as a hydrophobic block.¹⁴² Upon addition of water to a THF solution of the block copolymers, large (100-300 nm) spherical aggregates formed which were stained with CsOH, which deprotonated the dicarboximide groups. These polymers are capable of hydrogen bonding with adenine due to the similarity of the dicarboximide group to thymine and uracil. In another paper, Sleiman described the ROMP of ABC and BAC triblock copolymers containing dicarboximide groups (A) and complementary diacyldiaminopyridine groups (C) as well as a blocked, alkylated dicarboximide monomer (B). The placement of the complementary groups on opposite ends of the block copolymer (ABC) resulted in large aggregates in chloroform solution as well as micelles, while placement of these complementary blocks adjacent to one another did not result in aggregate formation, suggesting a tendency toward intramolecular association.¹⁴³

Rotello et al. studied diaminotriazine randomly functionalized polystyrenes, which exhibited strong intramolecular self-association leading to five-fold decreased radius of gyration (R_g) values compared to nonfunctional polystyrenes in low polarity solvents such as chloroform.¹⁴⁴ The absence of acyl groups on diaminotriazine led to stronger self-association and open more modes of self-association due to the presence of additional N-H protons. The self-association of the diaminotriazine functional polymers led to lower association constants with complementary flavin guests. Through a study of the temperature dependence

¹⁴² Dalphond, J.; Bazzi, H.; Kahrim, K.; Sleiman, H. Synthesis and Self-Assembly of Polymers Containing Dicarboximide Groups by Living Ring-Opening Metathesis Polymerization. *Macromol Chem Phys* **2002**, 203, 1988-94.

¹⁴³ Bazzi, H.; Bouffard, J.; Sleiman, H. Self-Complementary ABC Triblock Copolymers via Ring-Opening Metathesis Polymerization. *Macromolecules* **2003**, 36, 7899-902.

¹⁴⁴ Deans, R.; Ilhan, F.; Rotello, V. M. Recognition-Mediated Unfolding of a Self-Assembled Polymeric Globule. *Macromolecules* **1999**, 32, 4956-60.

of the association constants between polymeric diaminotriazine and flavin as well as monomeric diaminotriazine and flavin, entropic and enthalpic thermodynamic parameters were deduced for the polymer unfolding process required to allow the association with flavin. Based on comparing the enthalpy of unfolding (-4.66 kcal/mol) with that of association (7.00 kcal/mol), it was proposed that two hydrogen bonds were involved in the self-associated folded chain while three were involved in the associated complex.

2.3.5 Order-Disorder Transitions (ODT) in Hydrogen Bonding Block Copolymers

Order-disorder transitions occur when a phase separated block copolymer melt is heated to the point that the phase separated domains begin mixing. In block copolymers containing hydrogen bonding functionality, hydrogen bonding interactions often control miscibility. Thus the thermoreversibility of the hydrogen bonding interactions plays a role in the ODT. Wang et al. studied order-disorder transitions in hydrogen bonding hydroxyl functionalized diblock dendrons. In their work, poly(benzyl ether) and poly(ester) containing dendrons were coupled and peripheral hydroxyl groups on the poly(ester) dendron were subsequently deprotected. SAXS indicated a lamellar morphology which disordered at 50 °C, which corresponded to transition from bound to free hydroxyl absorbances in FTIR measurements.¹⁴⁵

¹⁴⁵ Yuan, F.; Wang, W.; Yang, M.; Zhang, X.; Li, J.; Li, H.; He, B.; Minch, B.; Lieser, G.; Wegner, G. Layered Structure and Order-to-Disorder Transition in a Block Codendrimer Caused by Intermolecular Hydrogen Bonds. *Macromolecules* **2006**, 39, 3982-5.

Lee and Han studied low molecular weight poly(styrene-*b*-isoprene) diblocks synthesized anionically in THF.¹⁴⁶ The high 1,2- and 3,4- enchainment produced from the polar polymerization solvent resulted in the absence of microphase separation between the blocks. Upon hydroboration-oxidation of the isoprene double bonds, hydroxyl groups were selectively introduced to the isoprene units and microphase separation was obtained. An order-disorder transition temperature near 195 °C was obtained for a poly(styrene-*b*-hydroxylated isoprene) with block molecular weights of 14K-3K, and the ODT was much higher for longer hydroxylated isoprene blocks. In-situ FTIR indicated the loss of hydrogen bonds between hydroxyl groups near the ODT that was measured using melt rheology.

2.4 Telechelic Hydrogen Bond Functional Polymers

Telechelic hydrogen bonding is a second method of obtaining localized hydrogen bonding functionality. Although the ability to increase the association strength via cooperative hydrogen bonding of neighboring groups is sacrificed, more well-defined supramolecular structures are attainable. The effect of telechelic hydrogen bonding groups diminishes with increasing molecular weight, however, in low molecular weight systems even weak hydrogen bonding groups lead to significant changes in properties.¹⁴⁷ Recently, attention has centered on strong telechelic hydrogen bonding, since the degree of association

¹⁴⁶ Lee, K. M.; Han, C. D. Order-Disorder Transition Induced by the Hydroxylation of Homogeneous Polystyrene-*block*-polyisoprene Copolymer. *Macromolecules* **2002**, 35, 760-9.

¹⁴⁷ Lillya, C. P.; Baker, R. J.; Huette, S.; Winter, H. H.; Lin, H.-G.; Shi, J.; Dickinson, L. C.; Chien, J. C. W. Linear Chain Extension through Associative Termini. *Macromolecules* **1992**, 25, 2076-80.

of telechelic polymers depends on the association constant raised to the one-half power.¹⁴⁸ Meijer¹⁴⁹⁻¹⁵¹ and Long^{152,153} have extensively studied the self-complementary quadruple hydrogen bonding unit 2-ureido-4[1H]-pyrimidone (UPy). This DDAA quadruple hydrogen array forms very strong self-associated dimers in solution, with association constants near $6 \times 10^7 \text{ M}^{-1}$ in chloroform and dimer lifetimes of 170 ms in chloroform.¹⁵⁴ Telechelic functionalization of molecules with UPy was shown to result in the formation of hydrogen bonded extended chain structures where the degree of polymerization (as determined from solution viscosity) depended on the solution concentration.¹⁵⁵ Much like a step-growth condensation polymerization, this leads to sensitivity of the non-covalent degree of polymerization on monofunctional end-cappers and the formation of cycles are observed in cases where the spacer between the UPy groups is bent.

¹⁴⁸ Xu, J.; Fogleman, E. A.; Craig, S. L. Structure and Properties of DNA-Based Reversible Polymers. *Macromolecules* **2004**, *37*, 1863-70.

¹⁴⁹ Brunsveld, L.; Folmer, B. J. B.; Meijer, E. W.; Sijbesma, R. P. Supramolecular Polymers. *Chem Rev* **2001**, *101*, 4071-98.

¹⁵⁰ Ligthart, G. B. W. L.; Ohkawa, H.; Sijbesma, R. P.; Meijer, E. W. Complementary Quadruple Hydrogen Bonding in Supramolecular Copolymers. *J Am Chem Soc* **2005**, *127*, 810-11.

¹⁵¹ Hirschberg, J. H. K. K.; Beijer, F. H.; van Aert, H. A.; Magusin, P. C. M. M.; Sijbesma, R. P.; Meijer, E. W. Supramolecular Polymers from Linear Telechelic Siloxanes with Quadruple-Hydrogen-Bonded Units. *Macromolecules* **1999**, *32*, 2696-705.

¹⁵² Yamauchi, K.; Lizotte, J. R.; Hercules, D. M.; Vergne, M. J.; Long, T. E. Combinations of Microphase Separation and Terminal Multiple Hydrogen Bonding in Novel Macromolecules. *J Am Chem Soc* **2002**, *124*, 8599-604.

¹⁵³ McKee, M. G.; Elkins, C.; Long, T. E. Influence of self-complementary hydrogen bonding on solution rheology/electrospinning relationships. *Polymer* **2004**, *45*, 8705-15

¹⁵⁴ Söntjens, S. H. M.; Sijbesma, R. P.; van Genderen, M. H. P.; Meijer, E. W. Stability and Lifetime of Quadruply Hydrogen Bonded 2-Ureido-4[1H]-pyrimidinone Dimers. *J Am Chem Soc* **2000**, *122*, 7487-93.

¹⁵⁵ Sijbesma, R. P.; Beijer, F. H.; Brunsveld, L.; Folmer, B. J. B.; Hirschberg, J. H. K. K.; Lange, R. F. M.; Lowe, J. K. L.; Meijer, E. W. Reversible Polymers Formed from Self-Complementary Monomers Using Quadruple Hydrogen Bonding. *Science* **1997**, *278*, 1601-4.

Some of the earliest telechelic UPy containing polymers were based on oligomeric (DP = 2, 100) poly(dimethylsiloxane).¹⁵⁶ The degrees of association observed through melt rheological measurements ranged from 100 to 20 and decreased with increasing molecular weight. The activation energy also decreased with increasing molecular weight and was lower for a benzyl protected precursor (37 kJ/mol). A rubbery plateau was observed in melt rheological experiments for the short (DP = 2) telechelic polymer, indicating entanglements in the melt and associated structures with molecular weight above M_c . Solution rheological measurements indicated that solution viscosity scaled with concentration to the 3.9, whereas a benzyl protected analogue produced a scaling value of 1.06 (Figure 2.6). The higher exponent for the hydrogen bonded compound was consistent with the Cates model for concentration dependent association.¹⁵⁷

¹⁵⁶ Hirschberg, J. H. K. K.; Beijer, F. H.; van Aert, H. A.; Magusin, P. C. M. M.; Sijbesma, R. P.; Meijer, E. W. Supramolecular Polymers from Linear Telechelic Siloxanes with Quadruple-Hydrogen-Bonded Units. *Macromolecules* **1999**, 32, 2696-705.

¹⁵⁷ Cates, M. E. Reptation of living polymers: dynamics of entangled polymers in the presence of reversible chain-scission reactions. *Macromolecules* **1987**, 20, 2289-96.

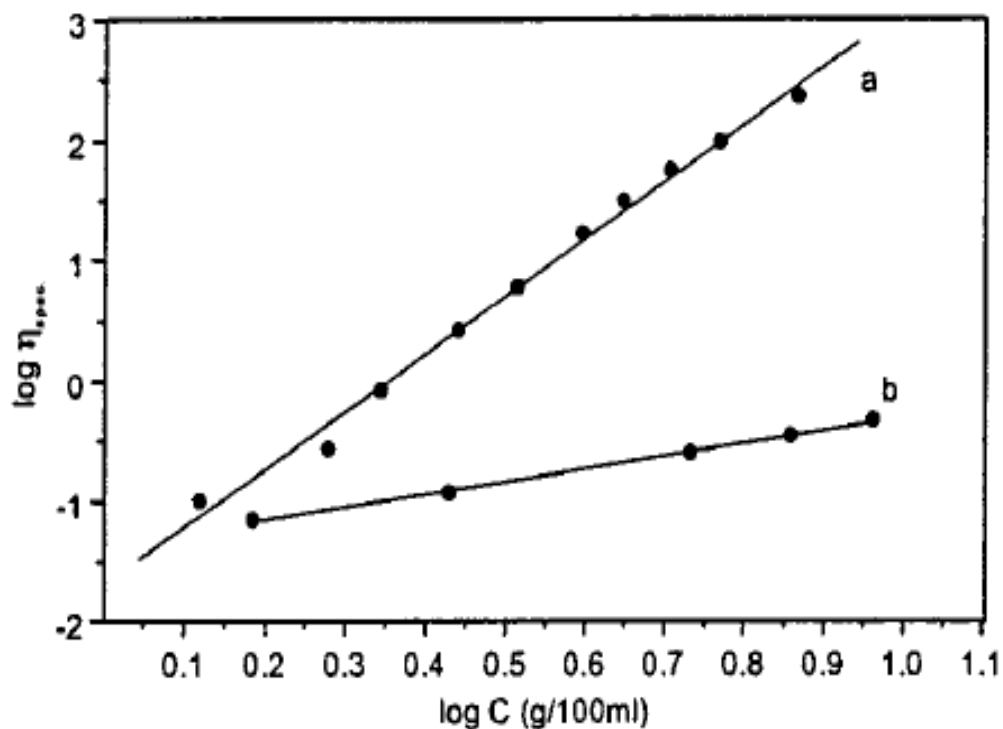


Figure 2.6. Solution viscosity of (a) telechelic UPy functional PDMS and (b) benzyl protected analog in chloroform at 20 °C. Reprinted with permission from Hirschberg et al.¹⁵⁸

Copyright 1999, American Chemical Society.

¹⁵⁸ Hirschberg, J. H. K. K.; Beijer, F. H.; van Aert, H. A.; Magusin, P. C. M. M.; Sijbesma, R. P.; Meijer, E. W. Supramolecular Polymers from Linear Telechelic Siloxanes with Quadruple-Hydrogen-Bonded Units. *Macromolecules* **1999**, 32, 2696-705.

Meijer et al. functionalized poly(ethylene oxide-*co*-propylene oxide) three-arm star oligomers of $M_n = 6000$ g/mol (2000 g/mol arms) with UPy and urethane hydrogen bonding groups.¹⁵⁹ Due to the presence of three terminal UPy units, non-covalent networks could form. Thus, the authors observed the formation of elastic solids from the viscous liquid precursors, as well as increased solution viscosity in chloroform with increased concentration dependence due to the concentration dependence of the hydrogen bonding association. In melt rheological studies, plateaus in the storage modulus were observed, which were not present in the oligomeric precursor and resembled those expected for high molecular weight polymers. A urea-terminated analog exhibited a higher plateau modulus than the UPy containing polymer, which was attributed to the formation of stacked arrays of hydrogen bonding groups instead of simple dimers. In contrast, a covalent polyurethane network prepared with the same oligomeric precursor exhibited a lower plateau modulus than the UPy functional oligomers, which was attributed to the formation of a more thermodynamically perfect network for the UPy polymer, due to the reversibility of the hydrogen bonding interactions in comparison to the irreversible covalent bonds.

Due to the fact that the UPy group preferentially associates into dimers in both the solution and solid state, the introduction of only two telechelic UPy groups leads to increased effective molecular weight, without evidence of phase separation or elastic character for low- T_g precursor. In recent work, Meijer et al. have placed urea and urethane groups

¹⁵⁹ Lange, R. F. M.; van Gurp, M.; Meijer, E. W. Hydrogen-bonded supramolecular polymer networks. *J. Polym. Sci. Part A. Polym. Chem.* **1999**, 37, 3657-70.

adjacent to telechelic UPy group, resulting in elastic behavior due to phase separation.¹⁶⁰ These urethane and urea groups were responsible for lateral stacking of the chain ends, much like that Wilkes et al. observed in model single hard segment polyurethanes and polyureas.^{161,162} The lateral stacking of these telechelic hydrogen bonding groups gives rise to fibril-like structures in surface morphology as observed from AFM, and more pronounced stacking is observed for the stronger hydrogen bonding urea functional copolymers. The presence of the UPy group increased the strain at break four-fold compared to simple telechelic urea functionality due to the non-covalent chain extension and effectively more difficult chain pullout from the hydrogen bonded fibrils.

Li et al. have synthesized naphthyridine (Napy) complementary hydrogen bonding arrays for UPy.¹⁶³ These Napy groups associate to one particular tautomer of UPy with K_a values near those of the UPy homodimerization ($5 \times 10^6 \text{ M}^{-1}$) (Figure 2.7). Solution rheological studies involving mixtures of bis(UPy) and bis(Napy) low molar mass compounds indicated that solution viscosity remained high as the bis(Napy) was added to the bis(UPy), until more than one equivalent was added, upon which time the solution viscosity decreased.¹⁶⁴

¹⁶⁰ Kautz, H.; van Beek, D. J. M.; Sijbesma, R. P.; Meijer, E. W. Cooperative End-to-End and Lateral Hydrogen-Bonding Motifs in Supramolecular Thermoplastic Elastomers. *Macromolecules* **2006**, *39*, 4265-7.

¹⁶¹ Sheth, J. P.; Wilkes, G. L.; Fornof, A. R.; Long, T. E.; Yilgor, I. Probing the Hard Segment Phase Connectivity and Percolation in Model Segmented Poly(urethane urea) Copolymers. *Macromolecules* **2005**, *38*, 5681-5.

¹⁶² Sheth, J. P.; Klinedinst, D. B.; Wilkes, G. L.; Yilgor, E.; Yilgor, I. Role of chain symmetry and hydrogen bonding in segmented copolymers with monodisperse hard segments. *Polymer* **2005**, *46*, 7317-22.

¹⁶³ Li, X. Q. K.; Jiang, X.; Wang, X. Z.; Li, Z. T. Novel multiply hydrogen-bonded heterodimers based on heterocyclic ureas. Folding and stability. *Tetrahedron* **2004**, *60*, 2063-9.

¹⁶⁴ Ligthart, G. B. W. L.; Ohkawa, H.; Sijbesma, R. P.; Meijer, E. W. Complementary Quadruple Hydrogen Bonding in Supramolecular Copolymers. *J Am Chem Soc* **2005**, *127*, 810-11.

Recently, Meijer et al. functionalized a semicrystalline polyoctenamer synthesized using ROMP with telechelic Napy functionality, and blended it with telechelic UPy functionalized poly(ethylene-*co*-propylene).¹⁶⁵ This resulted in the microphase separated structures via AFM, whereas mixtures of non-functional analogs resulted in macrophase separation. Thus, hydrogen bonding was utilized to effectively connect the blocks of a multiblock polymer.

¹⁶⁵ Scherman, O. A.; Ligthart, G. B. W. L.; Ohkawa, H.; Sijbesma, R. P.; Meijer, E. W. Olefin metathesis and quadruple hydrogen bonding: A powerful combination in multistep supramolecular synthesis. *Proc Natl Acad Sci USA* **2006**, 103, 11850-5.

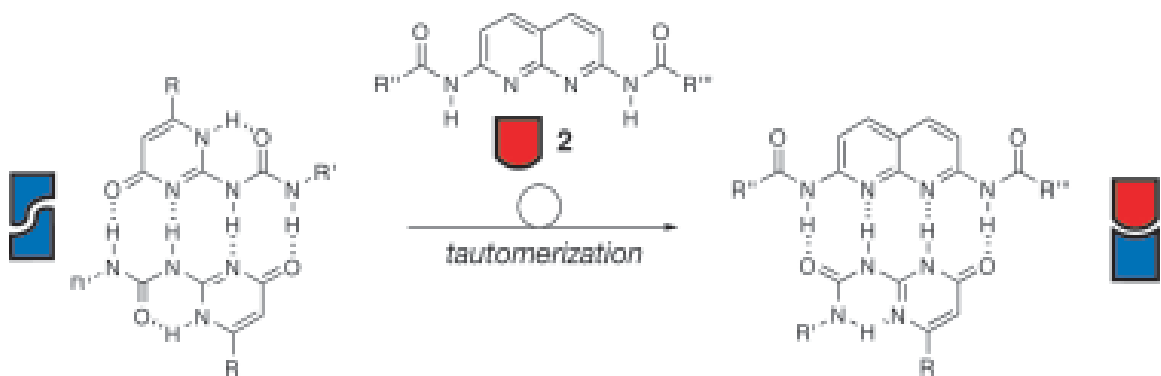


Figure 2.7. UPy homodimer (left) and heterodimer (right) with Napy via tautomerization.

Reprinted from Scherman et al.¹⁶⁶ Copyright 2006 with permission from the National Academy of Sciences, U.S.A.

¹⁶⁶ Scherman, O. A.; Ligthart, G. B. W. L.; Ohkawa, H.; Sijbesma, R. P.; Meijer, E. W. Olefin metathesis and quadruple hydrogen bonding: A powerful combination in multistep supramolecular synthesis. *Proc Natl Acad Sci USA* **2006**, 103, 11850-5.

Long et al. studied the end-functionalization of polystyrene, polyisoprene and poly(isoprene-*b*-styrene) with UPy groups.¹⁶⁷ The introduction of the hydrogen bonding groups lead to increased T_g and melt viscosities, with a decrease in melt viscosity at 80 °C, which was attributed to hydrogen bonding dissociation. Long et al. also studied the terminal functionalization of star-shaped and linear poly(ethylene-*co*-propylene)s.¹⁶⁸ This resulted in dramatic increases in melt viscosity, particularly in the case of the star-shaped polymer, and a shift of the terminal region to longer times. Recently, Long et al. telechelically end-functionalized poly(ester)s with UPy via post-polymerization reaction with an isocyanate containing UPy.¹⁶⁹ Melt rheological analysis indicated higher viscosity for the UPy containing polymer with a dramatic decrease near 80 °C to levels comparable to a nonfunctional analog. Tensile strength and elongation of the UPy containing polyester matched those of a nonfunctional polyester with twice the molecular weight, however, melt viscosity was lower than for this high molecular weight polyester.

Telechelic nucleobase functional polymers have also gathered attention recently. Long et al. has synthesized complementary nucleobase (thymine, adenine and purine) end-functional polystyrenes via Michael addition to terminal acrylate groups, introduced via

¹⁶⁷ Yamauchi, K.; Lizotte, J. R.; Hercules, D. M.; Vergne, M. J.; Long, T. E. Combinations of Microphase Separation and Terminal Multiple Hydrogen Bonding in Novel Macromolecules. *J Am Chem Soc* **2002**, 124, 8599-604.

¹⁶⁸ Elkins, C.; Viswanathan, K.; Long, T. E. Synthesis and Characterization of Star-Shaped Poly(ethylene-*co*-propylene) Polymers Bearing Terminal Self-Complementary Multiple Hydrogen-Bonding Sites. *Macromolecules* **2006**, 39, 3132-9.

¹⁶⁹ Yamauchi, K.; Kanomata, A.; Inoue, T.; Long, T. E. Thermoreversible Polyesters Consisting of Multiple Hydrogen Bonding (MHB). *Macromolecules* **2004**, 37, 3519-22.

post-functionalization of anionic hydroxyl terminated polystyrene.¹⁷⁰ The hydrogen bonding groups were found to associate via ¹H NMR studies, in which chemical shift changes of hydrogen bonded protons were found to diminish on heating to 95 °C, indicating thermoreversible association. Rowan et al. functionalized poly(tetramethylene oxide) with acylated adenine and cytosine nucleobases.¹⁷¹ The film forming, solid-like properties of the films were attributed to the weak self-association of the adenine and cytosine groups (< 5 M⁻¹), in concert with phase separation, which increased the hydrogen bonding association via concentration of the hydrogen bonding units. Rheological and x-ray scattering data studies on the adenine functionalized polymer indicated the formation of stacks of the benzyl protected adenine units showing the presence of π -stacking, which diminished on heating above 70 °C. Blockage of the hydrogen bonding properties via alkyl substitution at the hydrogen bonding (NH) protons resulted in reversion of the functional polymer to a liquid state. The protected cytosine containing polymers did not exhibit π -stacking interactions, likely due to the bulky aliphatic *tert*-butyl containing acyl group, but exhibited gel-like behavior in rheological studies.

Binder et al. compatibilized blends of polyisobutylene and a bisphenol A containing poly(ether ketone) using telechelic complementary hydrogen bonding.¹⁷² First, a thymine and diaminopyridine hydrogen bonding pair with an association constant near 800 M⁻¹ was

¹⁷⁰ Yamauchi, K.; Lizotte, J. R.; Long, T. E. Synthesis and Characterization of Novel Complementary Multiple-Hydrogen Bonded (CMHB) Macromolecules via a Michael Addition. *Macromolecules* **2002**, 35, 8745-50.

¹⁷¹ Sivakova, S.; Bohnsak, D. A.; Mackay, M. E.; Suwanmala, P.; Rowan, S. J. Utilization of a Combination of Weak Hydrogen-Bonding Interactions and Phase Segregation to Yield Highly Thermosensitive Supramolecular Polymers. *J Am Chem Soc* **2005**, 127, 18202-11.

¹⁷² Binder, W. H.; Bernstorff, S.; Kluger, C.; Petraru, L.; Kunz, M. J. Tunable Materials from Hydrogen-Bonded Pseudo Block Copolymers. *Adv Mater* **2005**, 17, 2824-8.

employed. This resulted in microphase separation as observed from TEM and SAXS. From variable temperature SAXS studies, the blend was stable up to 250 °C, at which point the poly(ether ketone) phase reached T_g and macrophase separation occurred. A stronger Janus wedge and barbituric acid hydrogen bonding pair with an association constant near $10^4 - 10^6 \text{ M}^{-1}$ resulted in stability of the blend to nearly 80 °C above the poly(ether ketone) glass transition.

Craig and coworkers developed a calixarene with four terminal urea groups in a radial, cone-shaped geometry (Figure 2.8).¹⁷³ The self-complementarity of this hydrogen bonding calixarene exhibited association constants of $10^6 - 10^8 \text{ M}^{-1}$, and required a central solvent molecule as a space filling guest (either *o*-dichlorobenzene or chloroform). The strong hydrogen bonding of ditopic calixarenes led to the observation of an overlap concentration (C^*) in the solution viscosity versus concentration profile as well as the ability to draw fibers from solution. Furthermore, the introduction of a tetrafunctional calixarene resulted in non-covalent networks in which greater than 99% of the material was associated at only 5 wt% concentration. The gels behaved as solids on short time scales but flowed over longer time scales.

¹⁷³ Castellano, R. K.; Clark, R.; Craig, S. L.; Nuckolls, C.; Rebek, J. Emergent mechanical properties of self-assembled polymeric capsules. *Proc Natl Acad Sci USA* **2000**, 97, 12418-21.

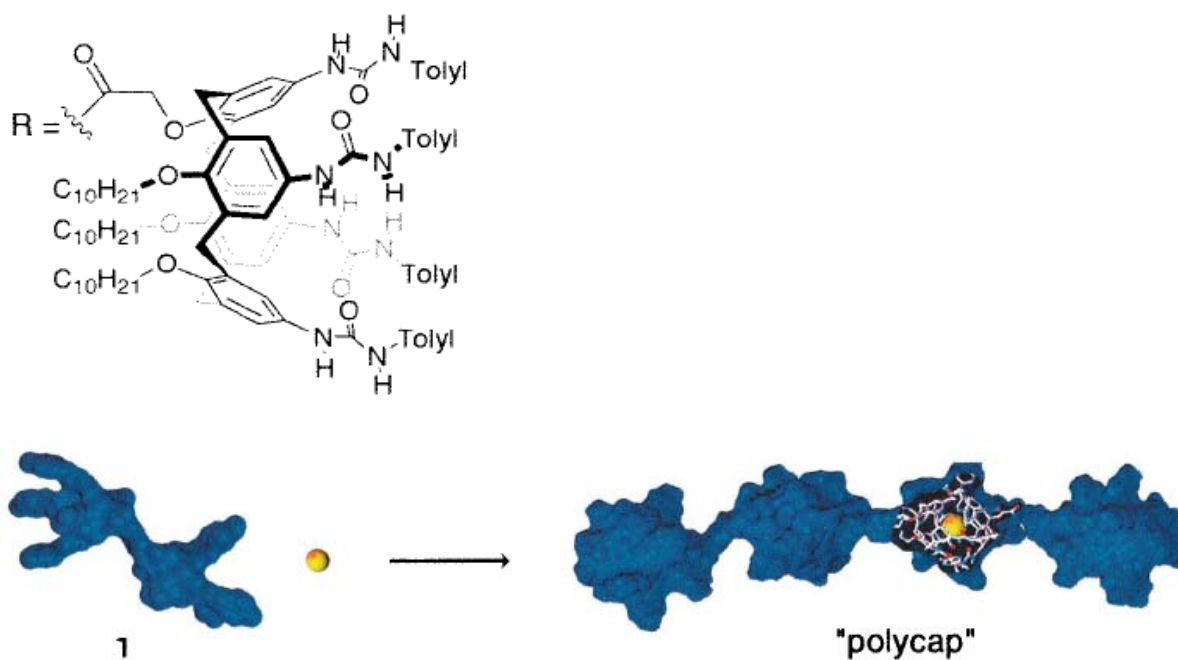


Figure 2.8. Association of ditopic self-complementary tetraurea functional calixarenes. Reprinted from Castellano et al.¹⁷⁴ Copyright 2000, with permission from the National Academy of Sciences, U.S.A.

¹⁷⁴ Castellano, R. K.; Clark, R.; Craig, S. L.; Nuckolls, C.; Rebek, J. Emergent mechanical properties of self-assembled polymeric capsules. *Proc Natl Acad Sci USA* **2000**, 97, 12418-21.

2.5 Combining Hydrogen Bonding with other Non-Covalent Interactions

The combining of multiple non-covalent interactions is currently a topic of intense study. DNA, the paradigm of supramolecular assembly is built up from interactions including hydrogen bonding, electrostatic interactions¹⁷⁵ due to the charged phosphodiester linkages, hydrophobic interactions and π - π stacking of the nucleobases.¹⁷⁶ This combination of non-covalent interactions enables DNA to perform functions such as replication and protein synthesis necessary for life.¹⁷⁷ As in DNA, combining multiple non-covalent assembly mechanisms results in versatility and tunable properties, particularly when the interaction mechanisms respond to different stimuli. Recently, Weck et al. have introduced both metal-ligand and hydrogen bonding interactions into ROMP block copolymers (Figure 2.9).¹⁷⁸ The polymers consisted of blocks of palladium sulfur-carbon-sulfur (SCS) pincer complexes (which bind nitrile groups), and diacyldiaminopyridine (which binds to thymine) functionalized ROMP monomers. The presence of the metal coordinating groups was found not to affect the hydrogen bonding capabilities of the diacyldiaminopyridine containing block copolymers, suggesting orthogonality of the association mechanisms.

¹⁷⁵ Herbert, H. E.; Halls, M. D.; Hratchian, H. P.; Raghavachari, K. Hydrogen-Bonding Interactions in Peptide Nucleic Acid and Deoxyribonucleic Acid: A Comparative Study. *Journal of Physical Chemistry B* **2006**, 110, 3336-43.

¹⁷⁶ Vanommeslaeghe, K.; Mignon, P.; Loverix, S.; Tourwe, D.; Geerlings, P. Influence of Stacking on the Hydrogen Bond Donating Potential of Nucleic Bases. *Journal of Chemical Theory and Computation* **2006**, 2, 1444-52.

¹⁷⁷ Voet, D.; Voet, J. G., *Biochemistry*. John Wiley and Sons: New York, 1995; p 1361.

¹⁷⁸ Nair, K. P.; Pollino, J. M.; Weck, M. Noncovalently Functionalized Block Copolymers Possessing Both Hydrogen Bonding and Metal Coordination Centers. *Macromolecules* **2006**, 39, 931-40.

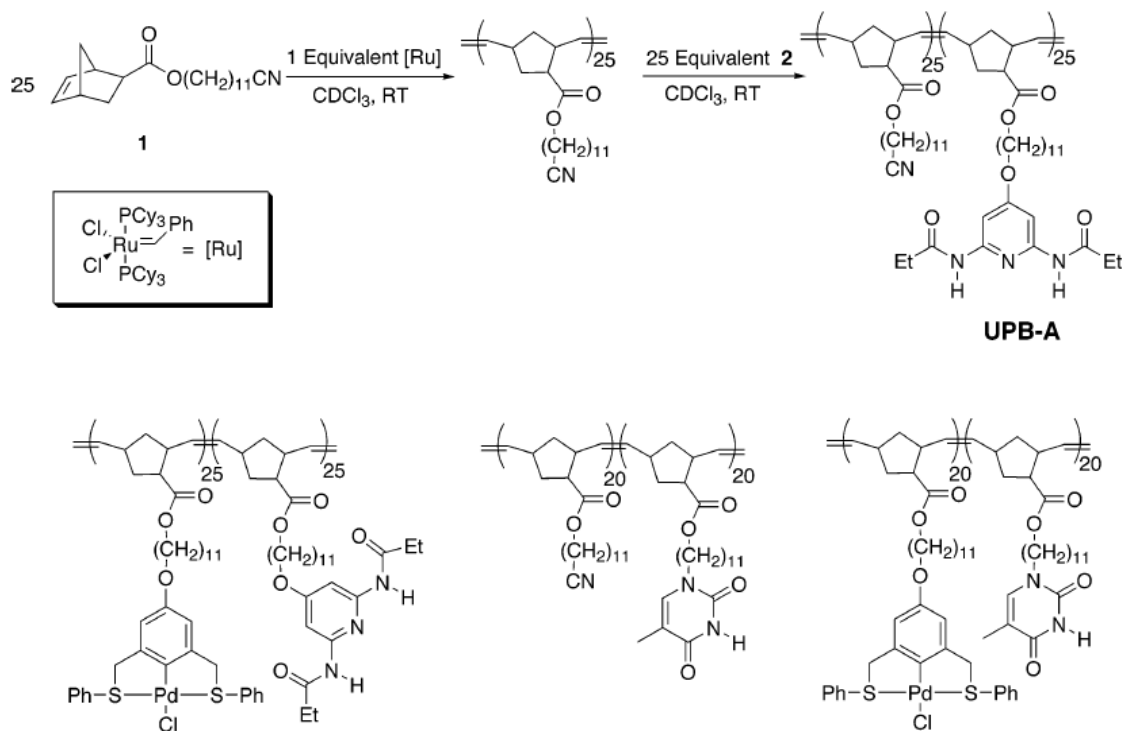


Figure 2.9. Dual side chain non-covalent interaction modes including both hydrogen bonding and metal-ligand interactions. Reprinted with permission from Nair et al.¹⁷⁹ Copyright 2006, American Chemical Society.

¹⁷⁹ Nair, K. P.; Pollino, J. M.; Weck, M. Noncovalently Functionalized Block Copolymers Possessing Both Hydrogen Bonding and Metal Coordination Centers. *Macromolecules* **2006**, 39, 931-40.

Recently, Schubert reported on the use of both metal-ligand and UPy hydrogen bonding interactions in the main chain using a heterotelechelic poly(ϵ -caprolactone).¹⁸⁰ Highly associated non-covalent polymers were formed on the addition of iron salts to a poly(ϵ -caprolactone) containing UPy and terpyridine end groups. Sudden decreases in melt viscosity at temperatures ranging from 100 to 127 °C were attributed to dynamics of the metal-ligand associations. Replacing iron with zinc salt decreased the temperature of this transition to 70-80 °C.

2.6 Reversible Attachment of Guest Molecules via Hydrogen Bonding

Reversible attachment of small molecules through recognition processes in hydrogen bonding polymers is an area of current interest. Even in homopolymer blended with small molecule hydrogen bonding groups, novel morphologies and behaviors are observed. In work from ten Brinke et al.,¹⁸¹ poly(4-vinylpyridine) was blended with the small molecule pentadecylphenol. At a ratio of pyridine to phenol of 1:1, a microphase separated texture composed of lamella was observed from SAXS in which a second diffraction maxima occurs at two times the primary scattering maximum ($2q^*$). Heating this blend resulted in a marked decrease and broadening of the SAXS maxima at 65 °C, which was attributed to a transition from a microphase separated morphology to a homogeneous system. This ODT was

¹⁸⁰ Hofmeier, H.; Hoogenboom, R.; Wouters, M. E. L.; Schubert, U. S. High Molecular Weight Supramolecular Polymers Containing Both Terpyridine Metal Complexes and Ureidopyrimidinone Quadruple Hydrogen-Bonding Units in the Main Chain. *J Am Chem Soc* **2005**, 127, 2913-21.

¹⁸¹ Ruokolainen, J.; Torkkeli, M.; Serimaa, R.; Komanschek, E.; ten Brinke, G.; Ikkala, O. Order-Disorder Transition in Comblike Block Copolymers Obtained by Hydrogen Bonding between Homopolymers and End-Functionalized Oligomers: Poly(4-vinylpyridine)-Pentadecylphenol. *Macromolecules* **1997**, 30, 2002-7.

confirmed with rheological measurements in which the storage modulus G' exhibited a sudden decrease at 65 °C, and G' and G'' began to follow scaling relationships expected for homopolymer melts ($G' \sim \omega^2$, $G'' \sim \omega$).

In the case of hydrogen bonding block copolymers, reversible attachment of guests holds promise to place guest molecules in specific domains and to influence the size and morphology of those domains. The morphology of block copolymers is classically controlled using changes in the volume fractions of various blocks, which are related to the relative molecular weights of each block. In AB diblock copolymers, this ranges from spherical dispersed phases at low volume fractions to cylinders and gyroid structures with increasing volume fraction and finally lamella at near equal volume fractions for the two monomers. The introduction of small molecule hydrogen bonding groups serves to control this volume fraction through selective incorporation into particular domains, thereby influencing the morphology. For example, ten Brinke et al. studied blends of pentadecylphenol and poly(styrene-*b*-4-vinylpyridine).^{182,183} In this case, two length scales were observed: a longer length scale (20-90 nm) corresponding to microphase separation between polystyrene and poly(4-vinylpyridine) blocks and a smaller length scale (3.5 nm) corresponding to lamellar structure in the poly(4-vinylpyridine)-pentadecylphenol comb domains.

¹⁸² Polushkin, E.; Alberda van Ekenstein, G. O. R.; Knaapila, M.; Ruokolainen, J.; Torkkeli, M.; Serimaa, R.; Bras, W.; Dolbnya, I.; Ikkala, O.; ten Brinke, G. Intermediate Segregation Type Chain Length Dependence of the Long Period of Lamellar Microdomain Structures of Supramolecular Comb-Coil Diblocks. *Macromolecules* **2001**, 34, 4917-22.

¹⁸³ Alberda van Ekenstein, G.; Polushkin, E.; Nijland, H.; Ikkala, O.; ten Brinke, G. Shear Alignment at Two Length Scales: Comb-Shaped Supramolecules Self-Organized as Cylinders-within-Lamellar Hierarchy. *Macromolecules* **2003**, 36, 3684-8.

In block lamellar diblock copolymers, the molecular weight dependence of the long period typically follows a dependence on molecular weight to the 0.67 power in the case of strong phase separation ($D \sim N^{0.67}$). However, in the case of poly(styrene-*b*-4-vinylpyridine) with pentadecylphenol an exponent of 0.8 was observed suggesting weaker phase separation, which was attributed to the partial miscibility of the pentadecylphenol with the styrenic lamella. High shear stability of hydrogen bonded pentadecylphenol and poly(4-vinylpyridine) groups below their ODT was demonstrated at strains of 100% and 0.5 Hz frequency. In the case of poly(styrene-*b*-4-vinylpyridine) blends with pentadecylphenol, shearing was a useful means of orienting the lamella parallel to the shear direction and the hydrogen bonded comb structure was re-developed upon cooling.¹⁸⁴ Shearing of blends with cylindrical morphology resulted in the orientation of the hexagonally packed cylinders along the shear direction. The soluble pentadecylphenol was extracted from the oriented cylinders of poly(4-vinylpyridine) using methanol, resulting in a nanoporous structure.¹⁸⁵

ten Brinke's group has also studied the hydrogen bonding attachment of octyl gallate (an octyl functionalized trihydroxybenzene) to poly(isoprene-*b*-vinylpyridine) block copolymers containing small 2- or 4-vinylpyridine blocks of 10 - 28 units.¹⁸⁶ For 4-vinylpyridine block copolymers, the morphologies consisted of cylinders of 4-vinylpyridine

¹⁸⁴ Makinen, R.; Ruokolainen, J.; Ikkala, O.; De Moel, K.; ten Brinke, G.; De Odorico, W.; Stamm, M. Orientation of Supramolecular Self-Organized Polymeric Nanostructures by Oscillatory Shear Flow. *Macromolecules* **2000**, 33, 3441-6.

¹⁸⁵ Makki-Ontto, R.; de Moel, K.; de Odorico, W.; Ruokolainen, J.; Stamm, M.; ten Brinke, G.; Ikkala, O. "Hairy Tubes": Mesoporous Materials Containing Hollow Self-Organized Cylinders with Polymer Brushes at the Walls. *Adv Mater* **2001**, 13, 117-21.

¹⁸⁶ Bondzic, S.; DeWit, J.; Polushkin, E.; Schouten, A. J.; ten Brinke, G.; Ruokolainen, J.; Ikkala, O.; Dolbnya, I.; Bras, W. Self-Assembly of Supramolecules Consisting of Octyl Gallate Hydrogen Bonded to Polyisoprene-*block*-poly(vinylpyridine) Diblock Copolymers. *Macromolecules* **2004**, 37, 9517-24.

and octyl gallate in a polyisoprene matrix and cylinder diameters increased with octyl gallate content. This was unsurprising given that the hard phase weight fraction ranged from 15.8 wt% to 25.2 wt%. For the poly(2-vinylpyridine) blocks, the attachment led to different morphologies depending on the amount of octyl gallate present. The morphology shifted to lamellar morphology with increasing octyl gallate content, and the morphologies exhibited temperature dependence such that the lamellar morphology showed a decrease in lamellar spacing with temperature and a transition to cylindrical morphology at 150 °C (Figure 2.10). Shifting of the morphology and the changing sizes of the morphological features was attributed to dissociation of hydrogen bonding guests and the poly(2-vinylpyridine) blocks were thought to relax from a stretched state upon the dissociation of the octyl gallate. Hydrogen bonding was observed to decrease with heating above 100 °C using FTIR so that at 190 °C, almost all of the pyridine groups were not hydrogen bonded.

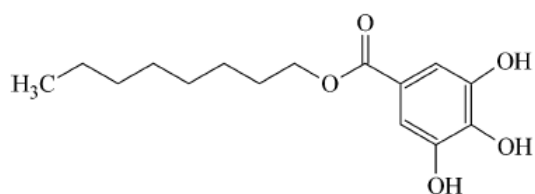
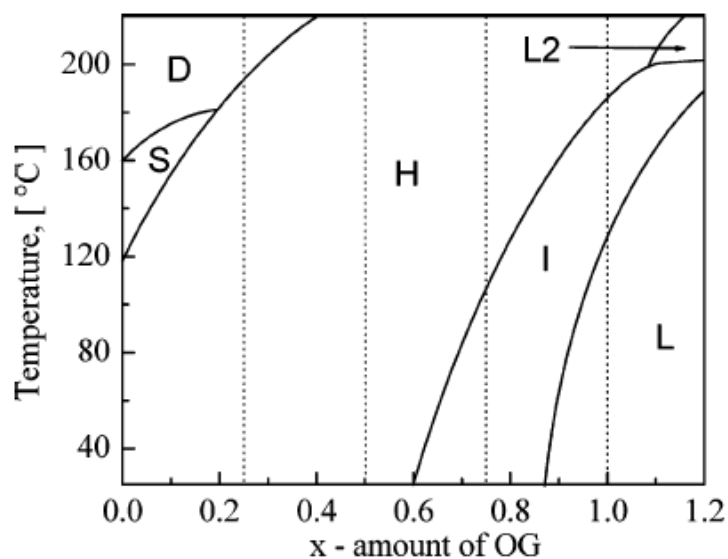


Figure 2.10. Phase diagram of poly(isoprene-*b*-2-vinylpyridine) with octyl gallate, indicating the transition between different morphologies with octyl gallate content and temperature. (D = disordered, S = spherical, H = hexagonal, L = lamellar, L2 = lamellar with reduced spacing and I = intermediate state). Reprinted with permission from Bondzic et al.¹⁸⁷ Copyright 2004, American Chemical Society.

¹⁸⁷ Bondzic, S.; DeWit, J.; Polushkin, E.; Schouten, A. J.; ten Brinke, G.; Ruokolainen, J.; Ikkala, O.; Dolbnya, I.; Bras, W. Self-Assembly of Supramolecules Consisting of Octyl Gallate Hydrogen Bonded to Polyisoprene-*block*-poly(vinylpyridine) Diblock Copolymers. *Macromolecules* **2004**, 37, 9517-24.

Thomas et al. studied the reversible attachment of liquid crystalline side chains to poly(acrylic acid-*b*-styrene) block copolymers via hydrogen bonding of imidazole groups to mesogens.¹⁸⁸ The reversibility of the attachment of the mesogens, which tended to form smectic phases, was proposed to play an integral role in the ability of these block copolymers to undergo reorientation of the lamella relative to external electrodes with an alternating electric field above T_g . Comparisons with covalently bound chromophores showed that reorientation of the lamella did not occur. Further studies involving poly(methacrylic acid-*b*-styrene) with imidazole containing mesogens allowed the fabrication of temperature dependent photonic bandgap materials which exhibited reflectivity maxima that reversibly changed as a function of temperature from 560 to 569 nm from 40 to 70 °C.¹⁸⁹

Recently, ten Brinke and Ikkala's group demonstrated the attachment of ionic molecules (zinc dodecylbenzene sulfonate) to poly(styrene-*b*-4-vinylpyridine) via coordination of the zinc ions to the pyridine rings.¹⁹⁰ These blends possessed lamellar morphology, even at low weight fractions (0.23) of the 4-vinylpyridine and zinc dodecylbenzene sulfonate, possibly due to the strength of the ionic interactions. Strong segregation due to ionic interactions often leads to altered morphology in ionomers.¹⁹¹

¹⁸⁸ Chao, C. Y.; Li, X.; Ober, C. K.; Osuji, C.; Thomas, E. L. Orientational Switching of Mesogens and Microdomains in Hydrogen Bonded Side-Chain Liquid-Crystalline Block Copolymers Using AC Electric Fields. *Adv Funct Mater* **2004**, 14, 364-70.

¹⁸⁹ Osuji, C.; Chao, C. Y.; Bitá, I.; Ober, C. K.; Thomas, E. L. Temperature-Dependent Photonic Bandgap in a Self-Assembled Hydrogen Bonded Liquid-Crystalline Block Copolymer. *Adv Funct Mater* **2002**, 12, 753-58.

¹⁹⁰ Valkama, S.; Ruotsalainen, T.; Kosonen, H.; Ruokolainen, J.; Torkkeli, M.; Serimaa, R.; ten Brinke, G.; Ikkala, O. Amphiphiles Coordinated to Block Copolymers as a Template for Mesoporous Materials. *Macromolecules* **2003**, 36, 3986-91.

¹⁹¹ Mani, S.; Weiss, R. A.; Williams, C. E.; Hahn, S. F. Microstructure of Ionomers Based on Sulfonated Block Copolymers of Polystyrene and Poly(ethylene-*alt*-propylene). *Macromolecules* **1999**, 32, 3663-70.

Although the crystallinity of the zinc dodecylbenzene sulfonate was suppressed in the blends, a lamellar packing present in the pure salt was observed in the blends, indicating a lamella within lamella structure. The zinc salt was selectively removed using methanol washes.

2.7 Conclusions and Summary

Hydrogen bonding interactions have gained significant attention recently, as a means of introducing novel, thermoreversible interactions to polymers, influencing both physical property performance as well as morphology and processing behavior. The recent development of multiple hydrogen bonding groups which associate more strongly than single hydrogen bonds has led to greater control of physical and mechanical properties.

The introduction of hydrogen bonding groups in block copolymers leads to increased hydrogen bonding interactions through locally increased hydrogen bonding group concentration and cooperativity of the hydrogen bonding groups. Increased χ parameters in hydrogen bonding block copolymers result in improved phase separation and the need for fewer repeating units to achieve phase separation. This phase separation often exhibits a greater temperature dependence and order-disorder transitions are linked directly to the hydrogen bonding phenomenon. In the case of complementary hydrogen bonding groups, such as nucleobases, introduction of guest molecules and complexation of complementary polymer blocks is achievable. Interesting morphologies are observed in both the solution and solid state for hydrogen bonding block copolymers.

Telechelic hydrogen bonding functionality has been the focus of great attention in recent years. Telechelic functionality results in a simpler system for studying hydrogen

bonding, although microphase separation can still complicate the system in the solid state. Self-complementary quadruple hydrogen bonding ureidopyrimidone (UPy) groups have been a strong focus in this area. Solution rheology is a particularly powerful tool for studying these systems and both concentration and the present of “chain blocker” monofunctional hydrogen bonding groups control the effective molecular weight in solution.

Chapter 3. Review of the Literature – Michael Addition Reactions in Macromolecular Design for Emerging Technologies

(Mather, B.D.; Viswanathan, K.; Miller, K.M.; Long, T.E. *Progress in Polymer Science* 2006, 31, 487-531) Reproduced with permission. Copyright 2006 Elsevier.

3.1 Abstract

The Michael addition reaction is a versatile synthetic methodology for the efficient coupling of electron poor olefins with a vast array of nucleophiles. This review outlines the role of the Michael addition reaction in polymer synthesis with attention to applications in emerging technologies including biomedical, pharmaceutical, optoelectronic, composites, adhesives, and coatings. Polymer architectures, which broadly range from linear thermoplastics to hyperbranched polymers and networks are achievable. The versatility of the Michael reaction in terms of monomer selection, solvent environment, and reaction temperature permits the synthesis of sophisticated macromolecular structures under conditions where other reaction processes will not operate. The utility of the Michael addition in many biological applications such as gene delivery, polymer drug conjugates, and tissue scaffolds is related to macromolecular structure.

3.2 Motivation and Scientific Rationale

The Michael addition reaction, which is also commonly termed conjugate addition, has recently gained increased attention as a polymer synthesis strategy for tailored

macromolecular architectures. The Michael addition, named for Arthur Michael, is a facile reaction between nucleophiles and activated olefins and alkynes in which the nucleophile adds across a carbon-carbon multiple bond.¹⁹² The Michael addition benefits from mild reaction conditions, high functional group tolerance, a large host of polymerizable monomers and functional precursors as well as high conversions and favorable reaction rates.¹⁹³ The Michael reaction lends itself to both step growth¹⁹⁴ and chain growth polymerization¹⁹⁵ and has been employed in the synthesis of linear, graft, hyperbranched, dendritic and network polymers. Furthermore, post-polymerization modification¹⁹⁶ and coupling of biological and synthetic polymers are often facilitated by the Michael reaction.¹⁹⁷ These features make the Michael addition reaction well-suited to numerous emerging technologies including biomedical applications such as gene transfection,¹⁹⁸ cell scaffolds¹⁹⁹ and tissue replacements.¹⁹³

The Michael addition reaction enables a wide range of polymers from diverse monomers, and corresponding polymers are prepared in environments in which other

¹⁹² Michael, A. On the addition of sodium acetacetic ether and analogous sodium compounds to unsaturated organic ethers. *Am Chem J* **1887**, 9, 115.

¹⁹³ Vernon, B.; Tirelli, N.; Bachi, T.; Haldimann, D.; Hubbell, J. Water-borne, in situ crosslinked biomaterials from phase-segregated precursors. *J Biomed Mater Res* **2003**, 64A, 447-56.

¹⁹⁴ Vaccaro, E.; Scola, D. A. New applications of polyaminoquinones. *CHEMTECH* **1999**, 29, 15-23.

¹⁹⁵ van Beylen, M.; Bywater, S.; Smets, G.; Swarc, M.; Worsfold, D. J. Developments in anionic polymerization - a critical review. *Adv Polym Sci* **1988**, 86, 87-143.

¹⁹⁶ Tokura, S.; Nishi, N.; Nishimura, S.; Ikeuchi, Y. Studies on chitin X. Cyanoethylation of chitin. *Polym J* **1983**, 15, 553-6.

¹⁹⁷ Morpurgo, M.; Veronese, F. M.; Kachensky, D.; Harris, J. M. Preparation and characterization of poly(ethylene glycol) vinyl sulfone. *Bioconjug Chem* **1996**, 7, 363-8.

¹⁹⁸ Richardson, S. C. W.; Patrick, N. G.; Stella Man, Y. K.; Ferruti, P.; Duncan, R. Poly(amidoamine)s as potential nonviral vectors: ability to form interpolyelectrolyte complexes and to mediate transfection in vitro. *Biomacromolecules* **2001**, 2, 1023-8.

¹⁹⁹ Ferruti, P.; Bianchi, S.; Ranucci, E.; Chiellini, F.; Caruso, V. Novel poly(amido-amine)-based hydrogels as scaffolds for tissue engineering. *Macromol Biosci* **2005**, 5, 613-22.

polymerization mechanisms will not operate. In biological applications such as protein derivitization the mild Michael addition reaction conditions are favorable since high temperatures, oxidizing radicals, and organic solvents are not feasible.²⁰⁰ Furthermore, the Michael addition has recently found utility for the synthesis of crosslinked polymers such as hydrogels,²⁰¹ thermoset resins,²⁰² and coatings, where rapid cure and high conversions are necessary for performance. Few polymerizations offer sufficient rates to permit room temperature cure, and industrial coatings are often limited to toxic and environmentally hazardous isocyanate containing monomers. The Michael addition proceeds rapidly at room temperature, offers low cure times, and involves less toxic precursors. Non-linear optical materials were also realized using the Michael addition, which benefits from the absence of volatile byproducts.²⁰³ The Michael addition is also ubiquitous in classical polymer chemistry, such as the anionic polymerization of alkyl methacrylates and cyanoacrylates.

The Michael addition involves the addition of a nucleophile, also called a “Michael donor,” to an activated electrophilic olefin, the “Michael acceptor”, resulting in a “Michael adduct”, as shown in Figure 3.1b. Although the Michael addition is generally considered the addition of enolate nucleophiles to activated olefins, a wide range of functional groups possess sufficient nucleophilicity to perform as Michael donors. Reactions involving

²⁰⁰ Elbert, D. L.; Pratt, A. B.; Lutolf, M. P.; Halstenberg, S.; Hubbell, J. A. Protein delivery from materials formed by self-selective conjugate addition reactions. *J Contr Rel* **2001**, 76, 11-25.

²⁰¹ Rizzi, S. C.; Hubbell, J. A. Recombinant protein-co-PEG networks as cell-adhesive and proteolytically degradable hydrogel matrixes. Part I: Development and physicochemical characteristics. *Biomacromolecules* **2005**, 6, 1226-38.

²⁰² Pavlinec, J.; Moszner, N. Photocured polymer networks based on multifunctional β -ketoesters and acrylates. *J Polym Sci Part A: Polym Chem* **1997**, 10, 165-78.

²⁰³ Abbotto, A.; Beverina, L.; Chirico, G.; Facchetti, A.; Ferruti, P. G., M; Pagani, G. A. Crosslinked poly(amido-amine)s as superior matrices for chemical incorporation of highly efficient organic nonlinear optical dyes. *Macromol Rapid Commun* **2003**, 24, 397-402.

non-enolate nucleophiles such as amines, thiols, and phosphines are typically referred to as “Michael-type additions”. In this review we will refer to Michael-type addition reactions with all nucleophilic donors as Michael additions. The Michael acceptor possesses an electron withdrawing and resonance stabilizing activating group, which stabilizes the anionic intermediate. Michael addition acceptors are far more numerous and varied than donors, due to the plethora of electron withdrawing activating groups that enable the Michael addition to olefins and alkynes. Acrylate esters, acrylonitrile, acrylamides, maleimides, alkyl methacrylates, cyanoacrylates and vinyl sulfones serve as Michael acceptors and are commercially available. Less common, but equally important, vinyl ketones, nitro ethylenes, α,β -unsaturated aldehydes, vinyl phosphonates, acrylonitrile, vinyl pyridines, azo compounds and even β -keto acetylenes and acetylene esters also serve as Michael acceptors.²⁰⁴

²⁰⁴ Gimbert, C.; Lumbierres, M.; Marchi, C.; Moreno-Manas, M.; Sebastian, R. M.; Vallribera, A. Michael additions catalyzed by phosphines. An overlooked synthetic method. *Tetrahedron* **2005**, 61, 8598-605.



b)

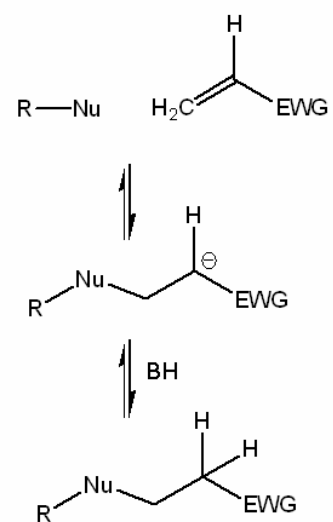


Figure 3.1 a) Arthur Michael (1855-1942), who discovered the Michael addition reaction. b) Schematic depiction of the Michael addition reaction. Nu = nucleophile, EWG = electron withdrawing group, BH = protic source to neutralize Michael adduct.

3.3. Introduction to the Michael Addition Reaction

The Michael reaction typically refers to the base-catalyzed addition of a nucleophile such as an enolate anion (Michael donor) to an activated α,β -unsaturated carbonyl-containing compound (Michael acceptor) as in Figure 3.1b.^{205 - 209} However, over the years, the scope of this reaction has increased dramatically to include a broad range of acceptors and the Michael-type additions of non-carbon donors. Due to the many types of Michael additions in the literature, we will focus here on investigating the mechanism and kinetics of only a few examples, namely the carbon-carbon bond forming Michael addition (referred to as the carbon-Michael addition), nitrogen (amine or aza) Michael additions, and the reaction of thiols with Michael acceptors.

3.3.1 Mechanism of the Carbon-Michael Addition Reaction

One of the most well-known carbon-Michael transformations is the base-catalyzed addition of ethyl acetoacetate to methyl acrylate.²¹⁰ The mechanism of the reaction is fairly straightforward, with every step being in equilibrium and thermodynamically dependent on the relative strengths of the base and the type of acetoacetate. The acetoacetate is first

²⁰⁵ Bergman, E. D.; Ginsburg, D.; Pappo, R. The Michael reaction. *Org React* **1959**, 10, 179-556.

²⁰⁶ Little, R. D.; Masjedizadeh, M. R.; Wallquist, O.; McLoughlin, J. I. The Intramolecular Michael reaction. *Org React* **1995**, 47, 315-552.

²⁰⁷ Jung, M. E., Stabilized nucleophiles with electron deficient alkenes and alkynes. In *Comprehensive Organic Synthesis*, Trost, B. M., Ed. Pergamon: Oxford, 1991.

²⁰⁸ Michael, A. J. Ueber die addition von natriumäcetessig- und natriummälonsäureathern zu den aethern ungesättigter sauren. *Prakt Chem* **1887**, 35, 349-56.

²⁰⁹ Connor, R.; McClellan, W. R. The Michael condensation. V. The influence of the experimental conditions and the structure of the acceptor upon the condensation. *J Org Chem* **1938**, 3, 570-7.

²¹⁰ Albertson, N. F. Alkylation with non-ketonic Mannich bases. Amino-thiazoles and pyrrole. *J Am Chem Soc* **1948**, 70, 669-70.

deprotonated by the base, providing an enolate anion (Michael donor) in equilibrium (Figure 3.2). The enolate anion then reacts in a 1,4-conjugate addition to the olefin of the acrylate (Michael acceptor). The carbonyl of the acrylate stabilizes the resulting anion until proton transfer occurs, regenerating the base. The overall driving force for the conjugate addition is the enthalpic change that accompanies replacement of a π -bond with a σ -bond. Thus, there is the preference for 1,4-addition over 1,2-addition. In some cases however, kinetically controlled reaction conditions can afford attack at the carbonyl carbon rather than at the β -carbon of the olefin.^{211,212}

From Figure 3.2, one can observe that the rate determining step is the attack of the enolate anion on the activated olefin. The reaction rate is therefore second order overall and first order with respect to the enolate anion and the olefin acceptor. The concentration of the enolate is a function of the base strength and the K_{eq} of the deprotonation of the active methylene proton. It follows that the equilibrium constant is dependent on the relative strength of the base and the structure of the acetoacetate.

²¹¹ Little, R. D.; Masjedizadeh, M. R.; Wallquist, O.; McLoughlin, J. I. The intramolecular Michael reaction. *Org React* **1995**, 47, 315-52.

²¹² Schultz, A. G.; Lee, Y. K. Conjugate and direct addition of ester enolates to cyclohexenone. Selective control of reaction composition. *J Org Chem* **1976**, 41, 4044-5.

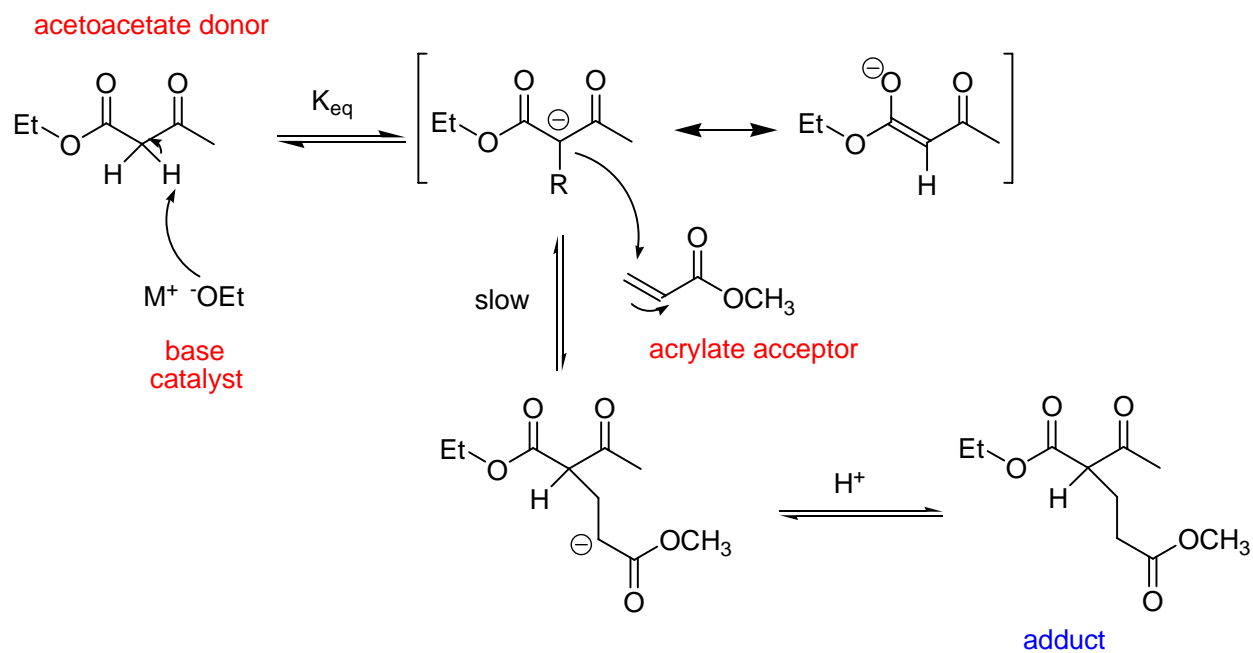
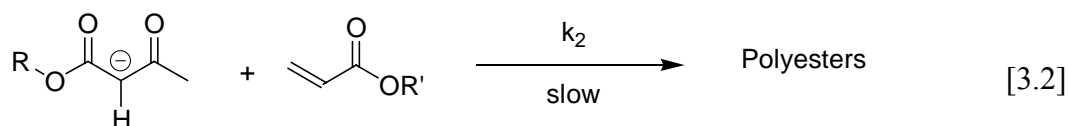
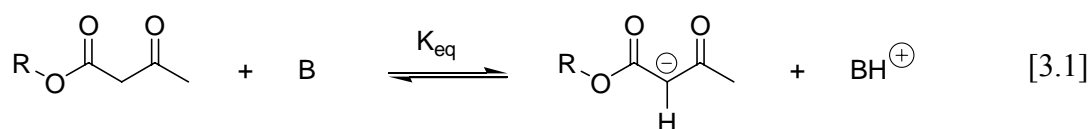


Figure 3.2. General carbon-Michael reaction mechanistic scheme.

It is important to note that the product of the first Michael addition has a remaining active methylene proton which can undergo a second addition to another acrylate (Figure 3.3). Clemens et al. have documented that the second pK_a is expected to have a value of 13 (versus the pK_a of the initial active proton of 12).²¹³ The second deprotonation therefore has a different equilibrium constant (K_{eq}) and it is assumed that the concentration of the first Michael adduct will be low. As a result, the concentration of the enolate at any rate (especially in the early stages of the reaction) is not strongly affected by this second reaction. It follows that a rate law can be determined for the above reaction sequence. Writing the reactions in terms of the Michael addition, we arrive at the kinetic equations:



And subsequent rate equations:

$$K_{eq} = [\text{AcAc}^-][\text{BH}^+] / [\text{AcAc}][\text{B}] \quad [3.3]$$

$$\text{Rate} = k_2[\text{AcAc}^-][\text{Acrylate}] = k_2K_{eq}([\text{B}] / [\text{BH}^+])[\text{AcAc}][\text{Acrylate}] \quad [3.4]$$

²¹³ Clemens, R. J.; Rector, F. D. A comparison of catalysts for crosslinking acetoacetylated resins via the Michael reaction. *J Coat Tech* **1989**, 61, 83-91.

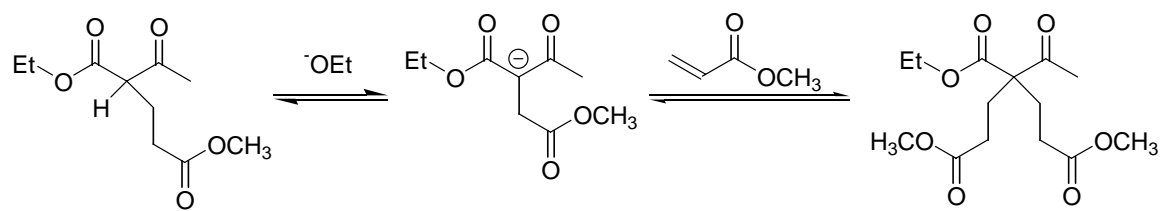


Figure 3.3. Second Michael addition of acetoacetate group to methyl acrylate.

3.3.1.1 Effect of Base Strength

The choice of base catalyst has a tremendous effect on the reaction kinetics. As previously noted, the concentration of the enolate and therefore the value of K_{eq} is highly dependent on the relative base strength. For strong bases, K_{eq} will lie far to the right and the concentration of the enolate anion is then approximately equal to the concentration of the base (achieving a steady state concentration). In the resulting rate expression (Eq. 3.5), there is a pseudo first-order dependence on acrylate concentration, where k_{obs} is a function of base concentration.

$$\text{Rate} = k_{obs}[\text{Acrylate}] \quad [3.5]$$

In the case of weaker base catalysts, K_{eq} has a moderate value, but is not large. This introduces the equilibrium constant into the rate law and results in second order behavior (Eq. 3.4). Clemens et al. completed an extensive study on the effect of base strength on reaction kinetics and molecular weight when the Michael addition is used to prepare crosslinked acetoacetate resins for thermoset coatings.²¹⁴ In a model study, Clemens analyzed the activity of weaker bases such as TMG (tetramethylguanidine), triethylamine, DBU (1,8-diazabicyclo[5.4.0]undec-7-ene), and DBN (1,5-diazabicyclo[4.3.0]non-5-ene) and found that the rate of the reaction was dependent on catalyst concentration as indicated in Eq. 3.4. For strong bases such as hydroxide, a steady-state concentration of enolate anion is achieved and pseudo-first order kinetics were observed (Eq. 3.5).

²¹⁴ Clemens, R. J.; Rector, F. D. A comparison of catalysts for crosslinking acetoacetylated resins via the Michael reaction. *J Coat Tech* **1989**, 61, 83-91.

The pK_a of the Michael donor is important to the choice of base catalyst, which must have a pK_a for its conjugate acid in the same range as the Michael donor. Stronger bases such as tetramethylguanidine, with a pK_a of 13.6 in its protonated form, are needed in the case of the carbon Michael addition of enolates due to the high pK_a of the acetoacetate groups ($pK_{a1} \sim 12$, $pK_{a2} \sim 13.6$). Base catalysts are often unnecessary in the case of amines, because of the strong nucleophilicity of the nitrogen atom, whereas weak bases aid in deprotonation of thiols.

3.3.1.2 Effect of Solvent

Typical solvents for the carbon-Michael reaction include methanol, ethanol, diethyl ether, tetrahydrofuran, benzene, xylene, dioxane and mixtures of these solvents. Initially, protic solvents were desirable in the carbon-Michael reaction to promote rapid proton transfer and to stabilize charged intermediates, however, Schlessinger's group has shown that high yielding reactions were also achieved using aprotic solvents.²¹⁵⁻²¹⁷ The choice of solvent strongly depends on the solubility of the catalyst, donor, and acceptor as well as sensitivity to side reactions. For example, if the reactants or products are susceptible to alcoholysis (ester exchange or hydrolysis), self-condensation of the substrate or the 'retro-Michael' reaction, a non-hydroxylic solvent is desirable.^{218,219} In some cases, reactions are carried out in the

²¹⁵ Cregge, R. J.; Herrmann, J. L.; Richman, J. E.; Romanent, R. F.; Schlessinger, R. H. The conjugate addition of a glyoxalate derived carbonyl anion equivalent and its application to the synthesis of 1,4-dicarbonyl compounds. *Tet Lett* **1973**, 14, 2595-98.

²¹⁶ Herrmann, J. L.; Richman, J. E.; Schlessinger, R. H. A highly reactive carbonyl anion equivalent derived from ethyl glyoxalate and its conjugate addition to Michael receptors. *Tet Lett* **1973**, 14, 2599-602.

²¹⁷ Cregge, R. J.; Herrmann, J. L.; Schlessinger, R. H. A versatile and reactive Michael receptor for the synthesis of 1,4-dicarbonyl compounds. *Tet Lett* **1973**, 14, 2603-6.

²¹⁸ Bergman, E. D.; Ginsburg, D.; Pappo, R. The Michael reaction. *Org React* **1959**, 10, 179-556.

absence of solvent, especially for network or coating applications.

3.3.1.3 Effect of Substrate

As mentioned before, the initial step of the carbon-Michael addition is deprotonation of an active methylene proton. Thus, donors must stabilize the resulting negative charge. Examples of functional groups which stabilize enolate donors include ketones, aldehydes, nitriles, amides, nitrones, sulfones, malonates and acetoacetates. A great deal of thought must be directed to the selection of the proper donor and base, and knowledge of the pK_a of these various species is critical. Furthermore, strongly bases such as hydroxide and methoxide may promote side reactions such as ester hydrolysis, so non-nucleophilic bases are often desirable.

Acceptors in the carbon-Michael addition are typically olefins that are activated for nucleophilic attack. The resulting anion from nucleophilic attack of the donor must also be stabilized for the reaction to occur. Thus, the use of α,β -unsaturated carbonyl compounds is prevalent in Michael addition chemistry. The reactivity of the acceptor will decrease if the substituent is electron rich, such as in the case of alkyl, aryl or carboethoxy substituted olefins such as styrene derivatives or vinyl ethers. Sterics are also an important factor. The larger the groups substituted at the α and β positions, the slower the reaction rate, although this can be offset by stronger polar effects.^{220,221} Differences in reactivity between

²¹⁹ Bickel, C. L. The addition of malonic esters to an acetylenic ketone. *J Am Chem Soc* **1950**, 72, 1022-3.

²²⁰ Connor, R.; McClellan, W. R. The Michael condensation. V. The influence of the experimental conditions and the structure of the acceptor upon the condensation. *J Org Chem* **1938**, 3, 570-7.

²²¹ Ingold, C. K.; Perren, E. A.; Thorpe, J. F. Ring-chain tautomerism. III. The occurrence of tautomerism of the three-carbon (glutaconic) type between a homocyclic compound and its unsaturated open-chain isomeride. *J Chem Soc* **1922**, 121, 1765-89.

acceptors require differences in nucleophilicity of the Michael donors. For instance, alkyl methacrylates are relatively poor Michael acceptors. Thus, stronger nucleophiles such as carbanions are necessary for successful Michael addition to alkyl methacrylates. Better acceptors such as alkyl acrylate or acrylamide groups readily accept amine and thiol nucleophiles.

Alkynes have also been utilized as Michael acceptors. In Figure 3.4, electron-rich enamines react readily with activated alkynes in refluxing ethanol.²²² Products of Michael reactions with alkynes have the additional variables of stereochemistry of the unsaturated product, and regiochemistry of addition for disubstituted alkynes acceptors.

²²² Wang, M. X.; Miao, W. S.; Cheng, Y.; Huang, Z. T. A systematic study of reaction of heterocyclic enamines with electrophilic alkynes: a simple and efficient route to 2-pyridinone-fused heterocycles. *Tetrahedron* **1999**, 55, 14611-22.

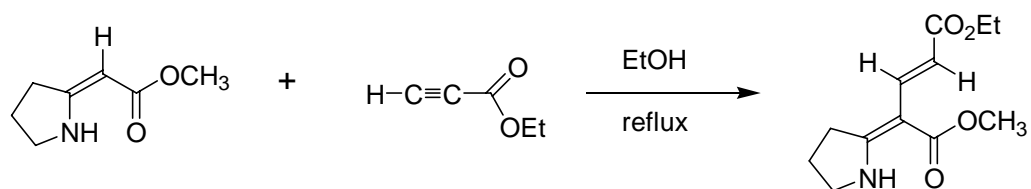


Figure 3.4. Michael Addition involving an alkyne acceptor.

3.3.1.4 Other Carbon-Michael Catalysts

Although base-catalysis is most prominently used in the carbon-Michael addition, the reaction is also catalyzed with acids, particularly in the case of Lewis acids. Some of the earlier examples include the use of boron trifluoride, aluminum trichloride, and zinc chloride.²²³ In these cases, the Lewis acid coordinates to the carbonyl of the acrylate to activate the olefin (Figure 3.5). The coordinated complex will then react with the nucleophile to obtain the same adduct as in the base-catalyzed Michael addition. In the case where silyl enolates are donors, the reaction is often referred to as the Mukaiyama-Michael reaction.

Researchers have used Lewis acid complexes to their advantage over the years, especially in the area of enantioselective additions. For example, Heathcock's group has shown that silyl enolates will react enantioselectively with α,β -unsaturated ketones in the presence of TiCl_4 (Figure 3.6).²²⁴ In the area of enantioselective carbon-Michael additions, the reader is directed to two recent reviews published on the subject.^{225,226}

Phosphines also catalyze the carbon-Michael reaction.²²⁷ The reaction sequence begins with nucleophilic attack of the phosphine on the β -position of the olefin, generating a reactive phosphonium ylid (Figure 3.7). The resulting anion can then either react as a

²²³ Hauser, C. R.; Breslow, D. S. Condensations. XII. A general theory for certain carbon-carbon condensations effected by acidic and basic reagents. *J Am Chem Soc* **1940**, 62, 2389-92.

²²⁴ Heathcock, C. H.; Uehling, D. E. Acyclic stereoselection. Part 34. Stereoselection in the Michael addition reaction. 4. Diastereofacial preferences in Lewis acid-mediated additions of enolsilanes to chiral enones. *J Org Chem* **1986**, 51, 279-80.

²²⁵ Sibi, M.; Manyem, S. Enantioselective conjugate additions. *Tetrahedron* **2000**, 56, 8033-61.

²²⁶ Krause, N.; Hoffman-Röder, A. Recent advances in catalytic enantioselective Michael additions. *Synthesis* **2001**, 2, 171-96.

²²⁷ Gimbert, C.; Lumbierres, M.; Marchi, C.; Moreno-Manas, M.; Sebastian, R. M.; Vallribera, A. Michael additions catalyzed by phosphines. An overlooked synthetic method. *Tetrahedron* **2005**, 61, 8598-605.

nucleophile or as a base. If an acetoacetate is present in the reaction, the ylid deprotonates the acetoacetate first, which adds to the β -position of another olefin in a Michael fashion. Proton transfer then results in regeneration of the initial olefin and the phosphine catalyst.

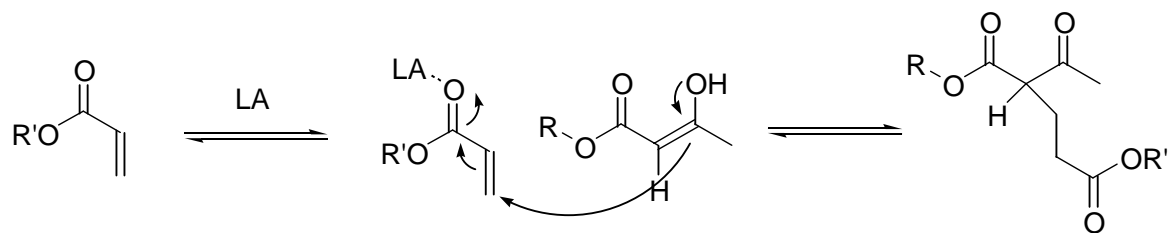


Figure 3.5. Lewis-acid catalyzed Michael addition reaction.

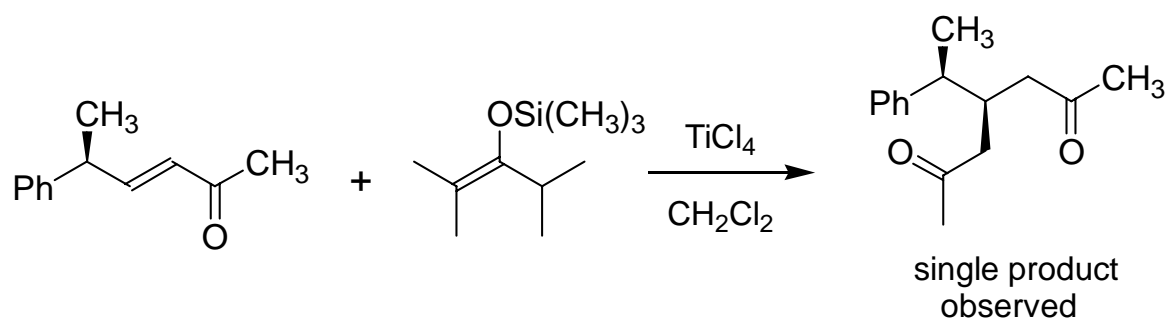


Figure 3.6. Stereoselective Michael addition between enone and silyl enolate in the presence of TiCl_4 .

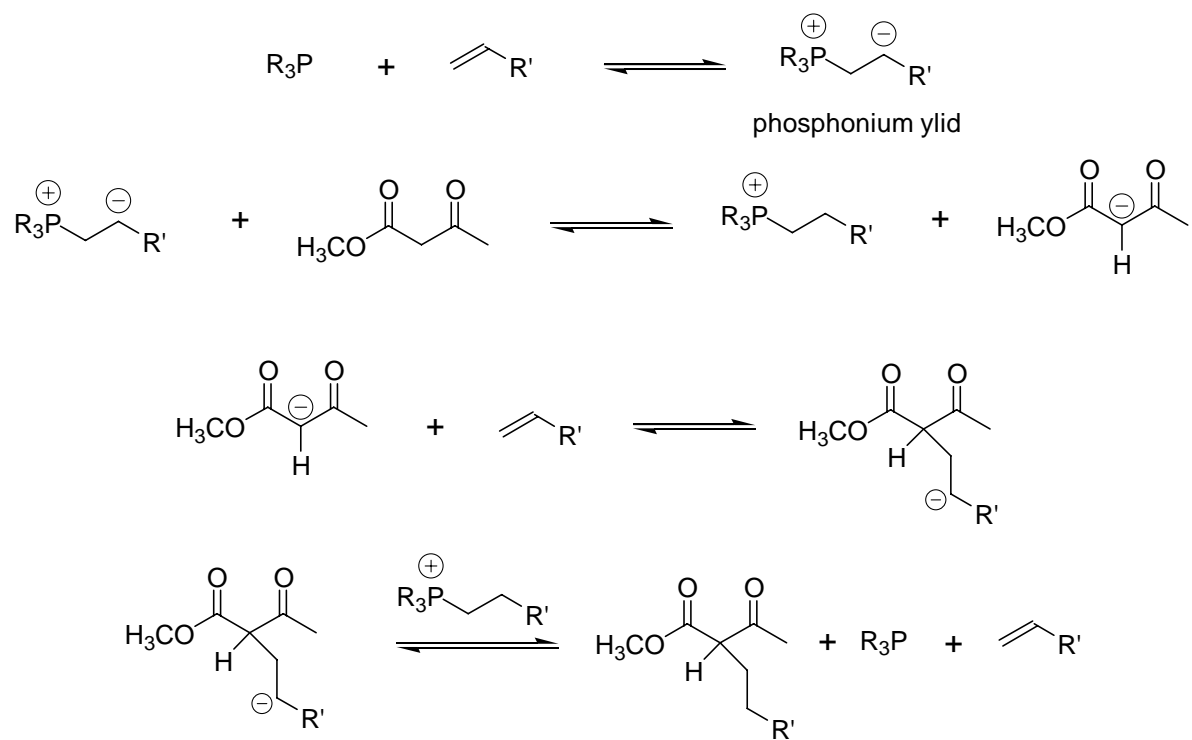


Figure 3.7. Phosphine catalyzed Michael addition reaction.

3.3.2 Heteroatomic Donors in the Michael Addition Reaction

Carbon-based nucleophiles represent only one class of donors used in Michael addition reactions. Heteroatomic nucleophiles involving nitrogen, sulfur, oxygen and phosphorus have also been used. In this section, two of these additions will be discussed: the aza-Michael reaction (amines) and the thiol Michael addition reaction. These are of primary importance due to the presence of sulfur and nitrogen nucleophiles in biological systems.

3.3.2.1. The aza-Michael Reaction

The nitrogen-donor version of the Michael addition is often referred to as the aza-Michael reaction. Since only a few concepts will be touched upon here, the reader is encouraged to investigate several reviews for additional information.^{228 - 231} Since amines can act as both nucleophiles and bases, no additional base is typically needed in these reactions. The reaction tends to follow second-order kinetics based on the concentration of the olefin acceptor and the amine (Figure 3.8).

Primary amines can react with two equivalents of acceptor to form tertiary amines. In some cases, this second addition affects the observed kinetics, especially as the concentration of the secondary amine increases. An example is the reaction of methyl amine with ethyl acrylate, giving an excellent yield of the tertiary amine (Figure 3.9).²³²

²²⁸ Jung, M. E., Stabilized nucleophiles with electron deficient alkenes and alkynes. In *Comprehensive Organic Synthesis*, Trost, B. M., Ed. Pergamon: Oxford, 1991.

²²⁹ Wabnitz, T. C.; Yu, J. Q.; Spencer, J. B. Evidence that protons can be the active catalyst in Lewis acid mediated hetero-Michael addition reactions. *Chem Eur J* **2004**, 10, 484-93.

²³⁰ Wabnitz, T. C.; Yu, J. Q.; Spencer, J. B. A general, polymer-supported acid catalyzed hetero-Michael addition. *Syn Lett* **2003**, 7, 1070-2.

²³¹ Wabnitz, T. C.; Spencer, J. B. A general, Brønsted acid-catalyzed hetero-Michael addition of nitrogen, oxygen, and sulfur nucleophiles. *Org Lett* **2003**, 5, 2141-4.

²³² McElvain, S. M.; Rorig, K. Piperidine derivatives. XVIII. The condensation of aromatic aldehydes with 1-methyl-4-piperidone. *J Am Chem Soc* **1948**, 70, 1820-5.

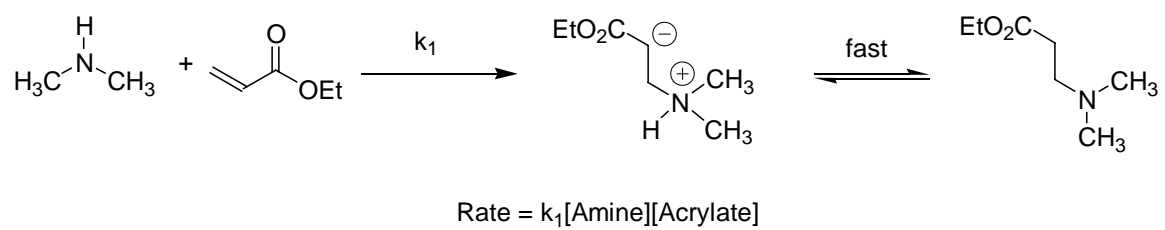


Figure 3.8. Aza-Michael addition reaction of dimethylamine with ethyl acrylate.

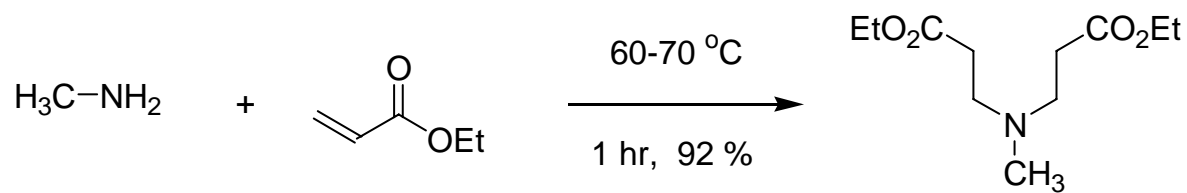


Figure 3.9. Aza-Michael addition of methyl amine to two equivalents of ethyl acrylate.

In the aza-Michael reaction, secondary amines are more nucleophilic than primary amines and are therefore more reactive. However, it is worth noting that this is highly dependent on the electronic and steric environment of the amine. For example, 1,4-butanediol diacrylate was allowed to react with 1-(2-aminoethyl)piperazine in an equimolar ratio (Figure 3.10).²³³ During the initial part of the experiment, it was found that there was exclusive reaction with the secondary amine present in the piperazine ring. Only upon longer reaction times, did reaction occur with the primary amine, which led to polymerization.

Acid catalyzed aza-Michael additions have also been studied extensively. Spencer and coworkers have determined a general and efficient way of reacting carbamates (NHCOOR) with α,β -unsaturated carbonyl compounds (Figure 3.11), providing precursors to β -amino acids.²³⁴

Vedejs and Gringas have also shown that acids catalyze the aza-Michael addition.²³⁵ In Figure 3.12, a tertiary amine, as the donor, adds to the alkyne in the presence of catalytic *p*-toluenesulfonic acid. The resulting intermediate further undergoes a Claisen rearrangement and proton transfer to afford the final α,β -unsaturated amine.

²³³ Wu, D.; Liu, Y.; He, C.; Chung, T.; Goh, S. Effects of chemistries of trifunctional amines on mechanisms of Michael addition polymerizations with diacrylates. *Macromolecules* **2004**, *37*, 6763-70.

²³⁴ Wabnitz, T. C.; Yu, J. Q.; Spencer, J. B. Evidence that protons can be the active catalyst in Lewis acid mediated hetero-Michael addition reactions. *Chem Eur J* **2004**, *10*, 484-93.

²³⁵ Vedejs, E.; Gringas, M. Aza-claisen rearrangements initiated by acid-catalyzed Michael addition. *J Am Chem Soc* **1994**, *116*, 579-88.

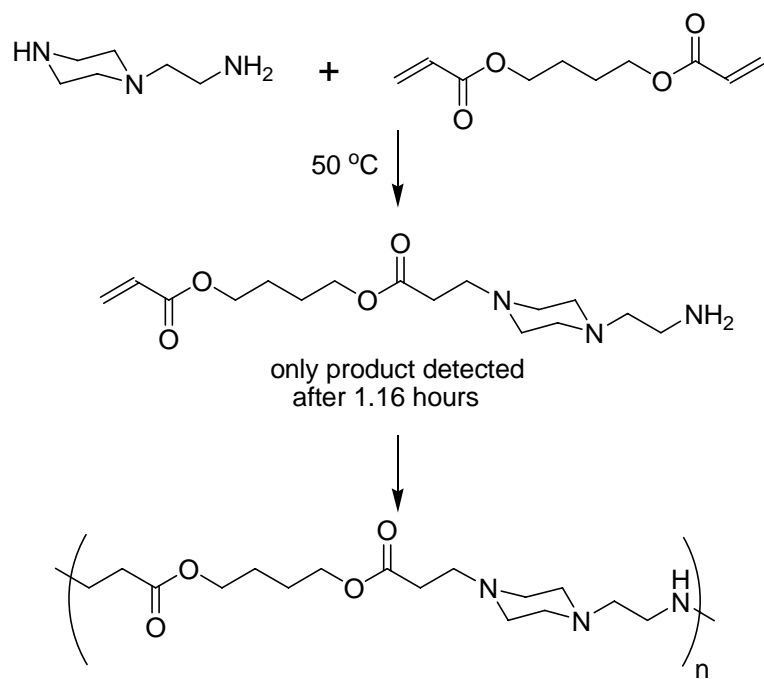


Figure 3.10. Higher reactivity of secondary amines in aza-Michael addition reactions.

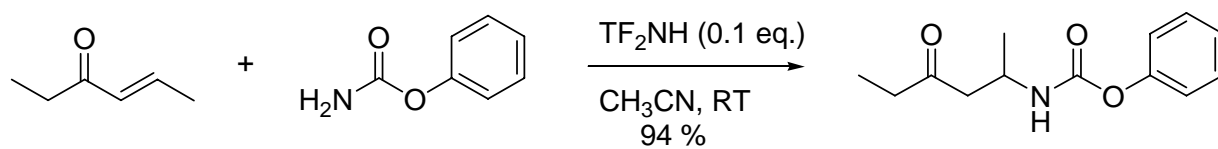


Figure 3.11. Acid catalyzed aza-Michael addition.

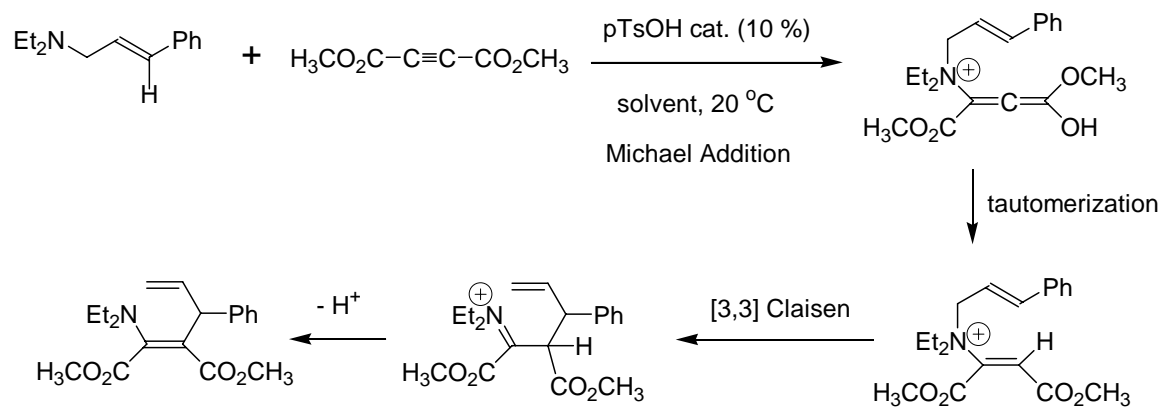


Figure 3.12. Acid catalyzed aza-Michael addition to activated alkyne acceptors.

Lewis acids have also been used to catalyze the aza-Michael reaction, as in Figure 3.13. The mechanism is thought to occur in an analogous fashion to the carbon-Michael addition where the Lewis acid coordinates to the carbonyl of the α,β -unsaturated olefin. However, Spencer has reported that, in the case of weakly basic amine nucleophiles, Brønstead acids that are formed during the reaction may catalyze the reaction.²³⁶

The ability to generate β -amino carbonyl compounds has become increasingly important to the natural product and pharmaceutical areas. The aza-Michael reaction is a key transformation which enables the preparation of such compounds. Jørgensen was the first to report the enantioselective conjugate amine additions (Figure 3.14).²³⁷ The TiCl_2 -BINOL Lewis acid catalyst coordinates with the *N*-acyloxazolidinone, creating a chiral environment in which the primary amine will preferentially attack from one face of the complex, resulting in the formation of one major diastereomer. The oxazolidinone ring is then removed to afford the β -amino acid. Although the enantioselectivity is low (maximum enantiomeric excess of 42 %), the proof of concept was accomplished. The area has grown significantly and Sibi has published two reviews which discuss stereoselective aza-Michael additions to generate β -amino acids.^{238,239}

²³⁶ Wabnitz, T. C.; Yu, J. Q.; Spencer, J. B. Evidence that protons can be the active catalyst in Lewis acid mediated hetero-Michael addition reactions. *Chem Eur J* **2004**, 10, 484-93.

²³⁷ Falborg, L.; Jørgensen, K. A. Asymmetric titanium-catalysed Michael addition of *O*-benzylhydroxylamine to α,β -unsaturated carbonyl compounds: synthesis of β -amino acid precursors. *J Chem Soc, Perkin Trans 1: Org Bio-org Chem* **1996**, 23, 2823-6.

²³⁸ Sibi, M.; Manyem, S. Enantioselective conjugate additions. *Tetrahedron* **2000**, 56, 8033-61.

²³⁹ Liu, M.; Sibi, M. P. Recent advances in the stereoselective synthesis of β -amino acids. *Tetrahedron* **2002**, 58, 7991-8035.

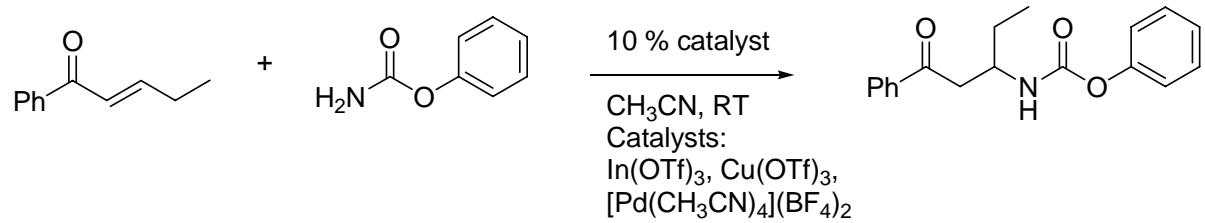


Figure 3.13. Lewis acid catalyzed aza-Michael reaction.

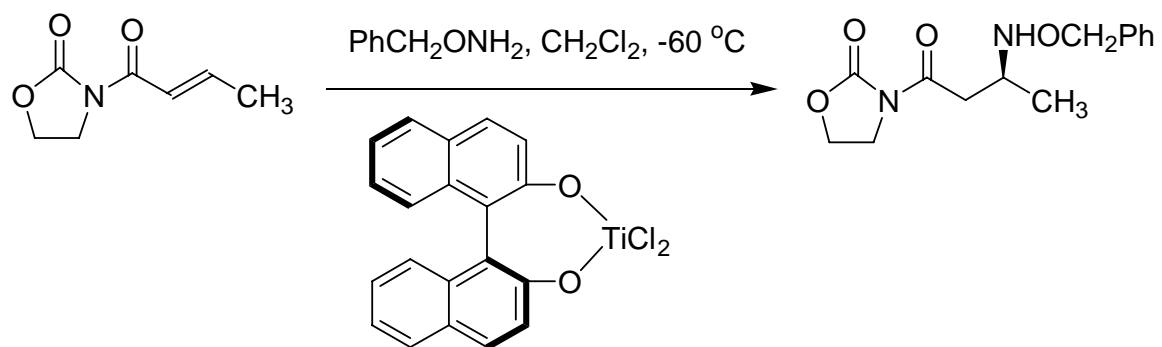


Figure 3.14. Stereoselective aza-Michael additions.

3.3.2.2. Thiols as Michael Donors

Thiols can also be used as heteroatomic donors in the Michael addition. Many of the same reaction scenarios that were described above can be directly applied to the addition of thiols to activated olefins. Thiols are generally more nucleophilic than amines, although bases are often used to deprotonate them due to their comparatively higher acidity. The thiolate anion is often the active species in Michael additions involving thiols. The thiol Michael addition reaction rates increase with pH due to the increased concentration of the thiolate anion.²⁴⁰ The thiol group is a useful Michael donor in biological systems where thiols are present on proteins in cysteine residues. One primary side reaction in thiol Michael additions is disulfide bond formation, which often prompts the use of protecting group chemistry.

Regioselective Michael additions of thiols to asymmetrically substituted fumarate esters or amides was achieved using lithium salts as Lewis acids or base catalysts to alter the charge environment around the double bond through coordination of carbonyls or deprotonation of the thiol (Figure 3.15).²⁴¹ Enantioselective Michael additions of thiols to methacrylates and other 1-alkyl acrylates was accomplished with chiral lanthanide catalysts to enantiomeric excesses as high as 90 % ee.²⁴² Enzyme catalysis of the thiol addition to 2-butenal was

²⁴⁰ Rizzi, S. C.; Hubbell, J. A. Recombinant protein-*co*-PEG networks as cell-adhesive and proteolytically degradable hydrogel matrixes. Part I: Development and physicochemical characteristics.

Biomacromolecules **2005**, 6, 1226-38.

²⁴¹ Kamimura, A.; Murakami, N.; Kawahara, F.; Yokota, K.; Omata, Y.; Matsuura, K.; Oishi, Y.; Morita, R.; Mitsudera, H.; Suzukawa, H.; Kakehi, A.; Shiraic, M.; Okamoto, H. On the regioselectivity for the Michael addition of thiols to unsymmetrical fumaric derivatives. *Tetrahedron* **2003**, 59, 9537-46.

²⁴² Emori, E.; Arai, T.; Sasai, H.; Shibasaki, M. A catalytic Michael addition of thiols to α,β -unsaturated carbonyl compounds: asymmetric Michael additions and asymmetric protonations. *J Am Chem Soc* **1998**, 120, 4043-4.

shown with *Candida antarctica* lipase B.²⁴³ Surprisingly, aqueous sodium dodecyl sulfate solutions perform as powerful catalysts of the Michael additions of thiols or amines to enones.²⁴⁴ Firouzabadi et al. proposed that the accelerating effect of the sodium dodecyl sulfate related to the concentrating of the hydrophobic species into the micellar core.

²⁴³ Carlqvist, P.; Svedendahl, M.; Branneby, C.; Hult, K.; Brinck, T.; Berglund, P. Exploring the active-site of a rationally redesigned lipase for catalysis of Michael-type additions. *Chem Bio Chem* **2005**, *6*, 331-6.

²⁴⁴ Firouzabadi, H.; Iranpoor, N.; Jafari, A. A. Micellar solution of sodium dodecyl sulfate (SDS) catalyzes facile Michael addition of amines and thiols to α,β -unsaturated ketones in water under neutral conditions. *Adv Synth Catal* **2005**, *347*, 655-61.

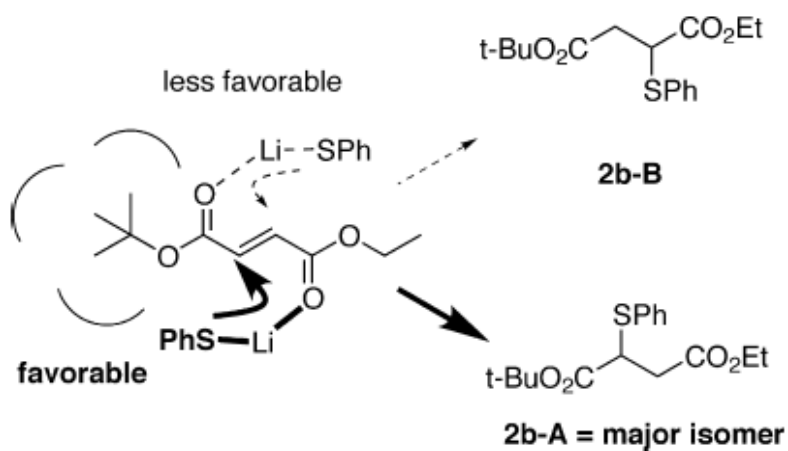


Figure 3.15. Regioselective Michael addition through preferential coordination of substrate carbonyls with lithium cations, reprinted from *Tetrahedron*, 59, Kamimura et al. “On the regioselectivity for the Michael addition of thiols to unsymmetrical fumaric derivatives,” 9537-46, Copyright 2003, with permission from Elsevier.²⁴⁵

²⁴⁵ Kamimura, A.; Murakami, N.; Kawahara, F.; Yokota, K.; Omata, Y.; Matsuura, K.; Oishi, Y.; Morita, R.; Mitsudera, H.; Suzukawa, H.; Kakehi, A.; Shiraic, M.; Okamoto, H. On the regioselectivity for the Michael addition of thiols to unsymmetrical fumaric derivatives. *Tetrahedron* **2003**, 59, 9537-46.

3.4 Linear Step Growth Michael Addition Polymerizations

3.4.1 Overview

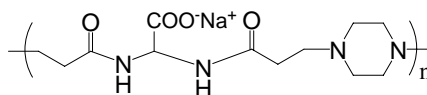
Significant earlier attention was devoted to linear step growth Michael addition polymerizations. Polymers that were produced via Michael addition polymerizations have ranged from segmented elastomers to high- T_g engineering thermoplastics. Both rigid, amorphous, aromatic systems as well as semicrystalline aliphatic systems were pursued and a wide variety of monomers were employed. Numerous examples of step growth Michael addition polymerizations exist, however, a few main classifications exist, outlined in Table 1. Perhaps the earliest example is poly(amido amine)s, which were synthesized from bisacrylamides and diamines. A second class of step growth polymers are derived from bismaleimides and diamines, a type of poly(imido amine) referred to as poly(aspartamide)s in the literature. Thiol nucleophiles are involved in the synthesis of poly(imido sulfide)s, which are also based on bismaleimide monomers. Analogous poly(ester sulfide)s and poly(amino ester)s synthesized from diacrylates are potentially biodegradable due to the hydrolytic instability of the ester linkages. Poly(amino quinone)s are a unique class of polymers which possess redox activity²⁴⁶ and serve as anticorrosion coatings on metals. α,β -unsaturated alkyne esters and ketones also serve as Michael acceptors in some cases and step growth polymerizations based on amine and thiol nucleophiles were pursued. Finally, hydrogen transfer polymerization allows the synthesis of polyamides and polyesters from AB-type Michael addition polymerizations. The high conversion of the Michael addition

²⁴⁶ Phama, M. C.; Hubert, S.; Piro, B.; Maurel, F.; Le Daob, H.; Takenouti, H. Investigations of the redox process of conducting poly(2-methyl-5-amino-1,4-naphthoquinone) (PMANQ) film. Interactions of quinone–amine in the polymer matrix. *Syn Met* **2004**, 140, 183-97.

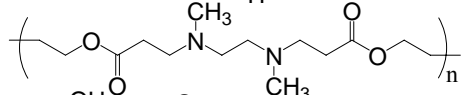
reaction and lack of side reactions are prerequisites for high molecular weight in step growth polymerizations, which is clearly obtained in numerous subsequent examples.

Table 3.1. Step growth polymers derived from Michael addition polymerization.

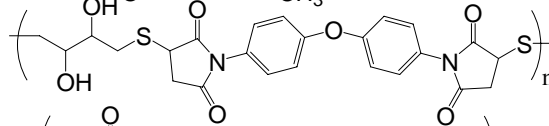
Poly(amido amine)



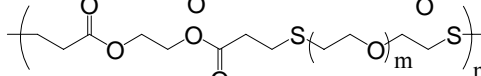
Poly(amino ester)



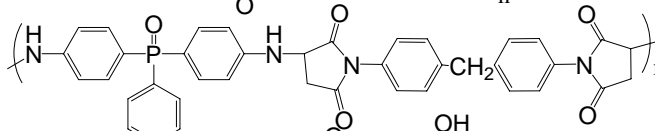
Poly(imido sulfide)



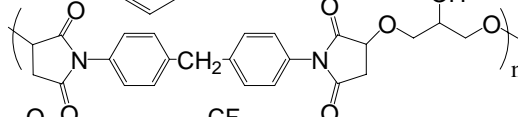
Poly(ester sulfide)



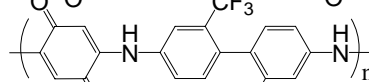
Poly(aspartamide)



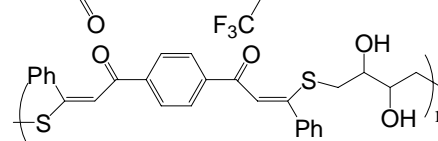
Poly(imido ether)



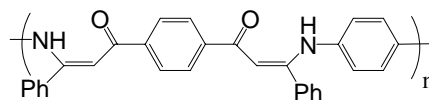
Poly(amino quinone)



Poly(enone sulfide)



Poly(enamine ketone)



3.4.2 Poly(amido amine)s

Poly(amido amines) are synthesized through the reaction of secondary diamines with bisacrylamides at 15 to 60 °C in water for durations of hours to days. Also, primary amines, which have difunctionality in the Michael addition are employed in poly(amido amine) synthesis (Figure 3.16). Ferruti et al. synthesized linear poly(amido amine)s from a range of monomers including piperazine bisacrylamide and *N,N'*-dimethyl-1,6-hexanediamine.^{247,248} The poly(amido amine) polymerizations occurred rapidly at room temperature in protic media such as alcohol and water without catalyst. The rate of the Michael addition polymerization increased with protic solvents and was less dependent on solvent polarity or dielectric constant. Generally, these polymerizations do not proceed to high molecular weight in aprotic solvents. The rate of these polymerizations increased with the basicity of the secondary diamines, and with lower steric hindrance.²⁴⁹ For instance, polymerization rates increased in the order: *N,N'*-diisopropylethylenediamine < *N,N'*-dimethylethylenediamine < 2-methylpiperazine < piperazine.

²⁴⁷ Ferruti, P.; Marchisio, M. A.; Duncan, R. Poly(amido-amine)s: biomedical applications. *Macromol Rapid Commun* **2002**, 23, 332-55.

²⁴⁸ Ferruti, P.; Marchisio, M. A.; Barbucci, R. Synthesis, physico-chemical properties and biomedical applications of poly(amido-amine)s. *Polymer* **1985**, 26, 1336-48.

²⁴⁹ Danusso, F.; Ferruti, P. Synthesis of tertiary amine polymers. *Polymer* **1970**, 11, 88-113.

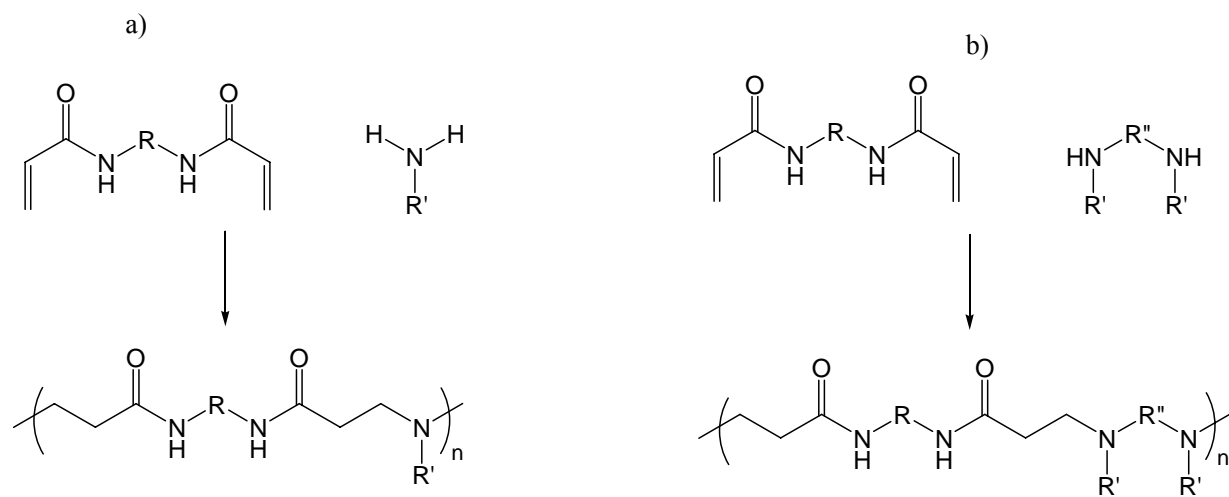


Figure 3.16. Poly(amido amine) synthesis via a) primary and b) secondary amines.

Numerous variations of poly(amido amine) polymerizations exist. Amino acids may be copolymerized with bisacrylamides, as long as triethylamine is added to deprotonate the amino acid zwitterion and an amino acid with low steric bulk is employed. Successful polymerization occurred with glycine, taurine and β -alanine. Peptide oligomers may also be used as comonomers as long as the amine terminus is a simple amino acid such as glycine. Monomers such as divinylsulfones and diacrylates²⁵⁰ can replace bisacrylamides as Michael acceptors. Segmented poly(amido amine ether)s were derived from PEG bis(piperazine) monomers.²⁵¹ Other routes to poly(amido amine)s yield different ordering of amido and amino functionalities including homopolymerization of protected aminoacrylamides with in-situ deprotection. Yet another route is the reaction of activated acrylic acid derivatives with secondary diamines through amidation and the also Michael addition.²⁵² Hydrazine and alkylated hydrazines were also employed in the synthesis of poly(amido amine)s, however, if excess bisacrylamide monomer is used, then crosslinking occurs with residual NH groups along the polymer backbone at long reaction times.^{253,254} Thermal stability of aliphatic poly(amido amine)s is fairly low, and thermal decomposition occurs near 200 °C. Poly(amido phosphine)s are synthesized in a similar manner to poly(amido amine)s, with the

²⁵⁰ Sun, G.; Wu, D.; Liua, Y.; Hea, C.; Chung, T. S.; Goh, S. H. pH-controllable cyclic threading/dethreading of polypseudorotaxane obtained from cyclodextrins and poly(amino ester). *Polymer* **2005**, 46, 3355-62.

²⁵¹ Ranucci, E.; Ferruti, P. Block copolymers containing poly(ethylene glycol) and poly(amido-amine) or poly(amido-thioether-amine) segments. *Macromolecules* **1991**, 24, 3747-52.

²⁵² Rusconi, L.; Tanzi, M.; Ferruti, P.; Angiolini, L.; Barbucci, R.; Casolaro, M. Synthesis of tertiary poly(amido-amine)s with amido- and amino-groups randomly arranged along the macromolecular chain. *Polymer* **1982**, 23, 1233-6.

²⁵³ Danusso, F.; Ferruti, P. Synthesis of tertiary amine polymers. *Polymer* **1970**, 11, 88-113.

²⁵⁴ Malgesini, B.; Ferruti, P.; Manfredi, A.; Casolaro, M.; Chiellini, F. Synthesis, acid-base properties and preliminary cell compatibility evaluation of amphoteric poly(amido-hydrazine)s. *J Bioact Compat Polym* **2005**, 20, 377-94.

exception that free radical inhibitors are employed to prevent radical catalyzed addition of the phosphines to the bisacrylamides. Poly(amido phosphine)s exhibit greater thermal stability than poly(amido amines), with decomposition temperatures near 360 °C.

Aliphatic poly(amido amines) often possess crystallinity and are water soluble due to the presence of tertiary amines in the backbone, which undergo partial protonation in water. Poly(amido amine)s exhibit a tendency toward amide hydrolysis. Ferruti et al. demonstrated increased solution viscosity versus time during polymerizations at high temperatures (100 °C) in water, with a subsequent decrease in viscosity at later times. This attribute along with low toxicity of the amino acid degradation products enables poly(amido amine)s as degradable pro-drug conjugates.²⁵⁵ Poly(amido amine)s based on hydrazine were found to decrease in molecular weight by a factor of four over 2 d in water at physiological conditions, and were also found to possess low cytotoxicity.²⁵⁶

Linear and crosslinked poly(amido amine)s were found to complex with heparin, an anticoagulant in the human body.²⁵⁷ In medical practice, when heparin levels are too high in the body, protamine sulfate is administered, which is also an anticoagulant. A solution to this problem is the use of linear or crosslinked poly(amido amine)s to remove heparin from the blood stream. Poly(amido amine)s selectively remove heparin over other plasma components and do not cause hemolysis or affect other properties of blood such as

²⁵⁵ Ferruti, P.; Ranucci, E.; Sartore, L.; Bignotti, F.; Marchisio, M. A.; Bianciardi, P.; Veronese, F. M. Recent results on functional polymers and macromonomers of interest as biomaterials or for biomaterial modification. *Biomaterials* **1994**, 15, 1235-41.

²⁵⁶ Malgesini, B.; Ferruti, P.; Manfredi, A.; Casolaro, M.; Chiellini, F. Synthesis, acid-base properties and preliminary cell compatibility evaluation of amphoteric poly(amido-hydrazine)s. *J Bioact Compat Polym* **2005**, 20, 377-94.

²⁵⁷ Ferruti, P.; Marchisio, M. A.; Duncan, R. Poly(amido-amine)s: biomedical applications. *Macromol Rapid Commun* **2002**, 23, 332-55.

prothrombin time. The poly(amido amine)s were also recycled through removal of heparin upon treatment with alkaline solutions of pH 11. Heparin, when coated on non-physiological objects, reduces the thrombus formation response of the human body. Thus, poly(amido amine)s also find utility in creating non-thrombogenic surfaces through covalent attachment to surfaces. Ferruti et al. developed synthetic methods for surface attachment of poly(amido amine)s to Dacron™ and poly(vinyl chloride) (PVC) using Michael addition of terminal acrylamide groups with surface tethered amine groups.²⁵⁸ These surfaces readily adsorbed heparin without heparin release.

Ferruti et al. reacted ethylene sulfide with piperazine to yield dithiol monomers which were polymerized with bisacrylamides. The resultant polymers were quaternized with methyl iodide, yielding water soluble antimicrobial polyelectrolytes.²⁵⁹ These polymers exhibited antimicrobial activity even against resistant strains such as *Pseudomonas aeruginosa*. The polymers also possessed surprisingly low rates of hemolysis relative to commercial antimicrobial polymers.

Ferruti et al. investigated further biomedical applications of poly(amido amine)s in creating platinum (II) complexes with antitumor activity.²⁶⁰ Polymer-drug conjugates have improved the effectiveness of drugs through a combination of increased solubility and slow drug release. The net result is called the enhanced permeability and retention (EPR) effect.

²⁵⁸ Ferruti, P.; Marchisio, M. A.; Barbucci, R. Synthesis, physico-chemical properties and biomedical applications of poly(amido-amine)s. *Polymer* **1985**, 26, 1336-48.

²⁵⁹ Ferruti, P.; Ranucci, E.; Sartore, L.; Bignotti, F.; Marchisio, M. A.; Bianciardi, P.; Veronese, F. M. Recent results on functional polymers and macromonomers of interest as biomaterials or for biomaterial modification. *Biomaterials* **1994**, 15, 1235-41.

²⁶⁰ Ferruti, P.; Ranucci, E.; Trotta, F.; Gianasi, E.; Evagorou, E.; Wasil, M.; Wilson, G.; Duncan, R. Synthesis, characterization and antitumor activity of platinum (II) complexes of novel functionalized poly(amido amine)s. *Macromol Chem Phys* **1999**, 200, 1644-54.

Linear poly(amido amine)s based on 2-methylpiperazine, carboxylated bisacrylamides, and amino- β -cyclodextrin moieties were complexed directly with cisplatin. The degree of cisplatin complexation and release rate of platinum increased for polymers containing the cyclodextrin moiety. Release was suppressed however, with the carboxylated bisacrylamide, and non-carboxylated bisacrylamides were also studied. Both in-vivo and in-vitro toxicity of most complexes were lower than pure cisplatin, and similar antitumor activities were observed. Earlier work on poly(amido amine)s revealed effectiveness in reducing tumor metastasis in Lewis lung tumors and Sarcoma 180 carcinoma implanted in mice.²⁶¹ The reduction in cancer metastasis was attributed to specific interactions of these charged polymers with cell membranes. Neuse et al. also studied poly(amido amine) complexes of cisplatin, using 1,2-dihydroxylated, 1,2-dicarboxylated or 1-hydroxy-2-carboxyl functional amine monomers that chelate to the platinum center.²⁶²

Recently, Ferruti et al. devoted considerable effort to studying the delivery of genes and proteins via complexation with poly(amido amine)s. One advantage of poly(amido amine)s is rapid protonation and expansion at low pH inside tumor cells which releases the genes or proteins and a compact geometry at plasma pH 7.4 to effectively hold the desired agent prior to delivery. Small angle neutron scattering (SANS) studies revealed that decreasing the pH of aqueous poly(amido amine)s solutions increases the radius of gyration from ~2 nm to 8

²⁶¹ Ferruti, P.; Danusso, F.; Franchi, G.; Polentarutti, N.; Garattini, S. Effects of a series of new synthetic high polymers on cancer metastases? *J Med Chem* **1973**, 16, 496-9.

²⁶² Johnson, M. T.; Komane, L. L.; N'Da, D. D.; Neuse, E. W. Polymeric drug carriers functionalized with pairwise arranged hydroxyl and/or carboxyl groups for platinum chelation. *J Appl Polym Sci* **2005**, 96, 10-19.

nm.²⁶³ Furthermore, poly(amido amine)s possess dramatically lower toxicity than conventional non-viral vectors such as poly(ethylene imine). In some cases, poly(amido amine)s were prepared that exhibited a “stealth” behavior and maintained long circulatory lifetimes.²⁶⁴ Duncan et al. recently investigated poly(amido amine)s that contained covalently bound endosomolytic protein melittin (a main component of bee venom).²⁶⁵ These conjugates were less toxic than pure melittin and were found to possess pH-selective hemolytic properties at pH 5.5 and not at pH 7.4 at low concentrations of the conjugates. Some of the conjugates were also effective in delivering the non-permeant toxin gelonin into cells. Segmented copolymers based on poly(amido amine)s containing carboxylic acid and hydroxyl functional blocks also showed promising endosomolytic and gelonin delivery activity.²⁶⁶ Gene transfection studies of poly(amido amine)s have also demonstrated successful polyplex formation with λ Hind III DNA and transfection of β -galactosidase into HepG2 cells, with similar transfection efficiency as Lipofectin[®] and poly(ethylene imine).²⁶⁷ Ferruti et al. coupled bovine serum albumin and human serum albumin to poly(amido amine)s based on piperazine and piperazine bisacrylamide through Michael addition of

²⁶³ Griffiths, P. C.; Paul, A.; Khayat, Z.; Wan, K. W.; King, S. M.; Grillo, I.; Schweins, R.; Ferruti, P.; Franchini, J.; Duncan, R. Understanding the mechanism of action of poly(amidoamine)s as endosomolytic polymers: correlation of physicochemical and biological properties. *Biomacromolecules* **2004**, *5*, 1422-7.

²⁶⁴ Richardson, S.; Ferruti, P.; Duncan, R. Poly(amidoamine)s as potential endosomolytic polymers: evaluation in vitro and body distribution in normal and tumour-bearing animals. *J Drug Target* **1999**, *6*, 391-404.

²⁶⁵ Lavignac, N.; Lazenby, M.; Franchini, J.; Ferruti, P.; Duncan, R. Synthesis and preliminary evaluation of poly(amidoamine)–melittin conjugates as endosomolytic polymers and/or potential anticancer therapeutics. *Int J Pharmaceutics* **2005**, *300*, 102-12.

²⁶⁶ Lavignac, N.; Lazenby, M.; Foka, P.; Malgesini, B.; Verpilio, I.; Ferruti, P.; Duncan, R. Synthesis and endosomolytic properties of poly(amidoamine) block copolymers. *Macromol Biosci* **2004**, *4*, 922-9.

²⁶⁷ Richardson, S. C. W.; Patrick, N. G.; Stella Man, Y. K.; Ferruti, P.; Duncan, R. Poly(amidoamine)s as potential nonviral vectors: ability to form interpolyelectrolyte complexes and to mediate transfection in vitro. *Biomacromolecules* **2001**, *2*, 1023-8.

protein amine groups to terminal acrylamide groups on the poly(amido amine)s.²⁶⁸ The reaction was conducted under mild conditions (pH 8 to 8.5, 25 °C) to high conversion and the coupled product was verified by size exclusion chromatography (SEC).

Poly(amino ester)s are similar to poly(amido amine)s, however, they utilize diacrylates instead of bisacrylamides. Langer et al. studied the use of Michael addition step growth linear poly(amino ester)s as gene transfection agents (Figure 3.17).²⁶⁹ Like poly(amido amine)s, poly(amino ester)s have benefits over conventional gene transfection agents (such as poly(ethylene imine) or poly(L-lysine)) due to their low cytotoxicity as well as biodegradability into low toxicity byproducts. Furthermore, the structure and degradability of the poly(amino ester)s are tailored through the incorporation of a wide range of diamines and diacrylates. Langer et al. obtained high molecular weight poly(amino ester)s (32000 g/mol) and performed successful complexation with plasmid DNA. The absence of a *retro*-Michael addition in these systems eliminates the possibility of carcinogenic diacrylate production during degradation. The degradability of these transfection agents is expected to aid in the release of the DNA inside the cell.

Non-biological applications of poly(amido amine)s also exist. Recently, Ferruti et al. examined the introduction of NLO chromophores into both linear and crosslinked poly(amido amine)s.²⁷⁰ The Michael addition chemistry was well-suited to the primary amine containing

²⁶⁸ Ranucci, E.; Bignotti, F.; Paderno, P. L.; Ferruti, P. Modification of albumins by grafting poly(amido amine) chains. *Polymer* **1995**, 36, 2989-94.

²⁶⁹ Lynn, D. M.; Langer, R. Degradable poly(β -amino esters): synthesis, characterization, and self-assembly with plasmid DNA. *J Am Chem Soc* **2000**, 122, 10761-8.

²⁷⁰ Abbotto, A.; Beverina, L.; Chirico, G.; Facchetti, A.; Ferruti, P. G., M; Pagani, G. A. Crosslinked poly(amido-amine)s as superior matrices for chemical incorporation of highly efficient organic nonlinear optical dyes. *Macromol Rapid Commun* **2003**, 24, 397-402.

chromophores and mild reaction conditions prevented chromophore degradation.²⁷¹ Initial studies showed that solution optical properties of the chromophores such as two photon pumped fluorescence were maintained in the polymer.

²⁷¹ Abbotto, A.; Beverina, L.; Chirico, G. F., A; Ferruti, P.; Pagani, G. A. Design and synthesis of new functional polymers for nonlinear optical applications. *Syn Met* **2003**, 139, 629-32.

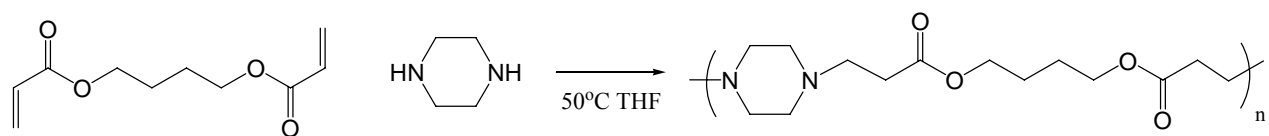


Figure 3.17. Poly(amino ester) synthesis from butanediol diacrylate and piperazine.

3.4.3 Poly(imido sulfide)s

Maleimides possess two carbonyl groups conjugated to the double bond, presenting a highly electron poor double bond susceptible to reaction with a range of nucleophiles. Poly(imido sulfide)s result from the step growth polymerization of dithiols with bismaleimide monomers. White and Scaia polymerized aromatic dithiols with aromatic bismaleimides in *m*-cresol with catalytic amounts of tri-*n*-butylamine at 80 to 100 °C.²⁷² The acidity of the *m*-cresol prevented the anionic homopolymerization of the maleimide groups upon reaction with thiolate anions, which would have resulted in crosslinking. The poly(imido sulfide)s containing aromatic thiol units were susceptible to degradation from bases such as diethylamine in aprotic solvents which was attributed to *retro*-Michael addition regeneration of the maleimide group. Aliphatic dithiol-containing polymers were less susceptible to depolymerization. Poly(imido sulfide)s with molecular weights ranging from 70000 to 450000 g/mol possessed glass transition temperatures from 185 to 212 °C. Semicrystalline poly(imido sulfide)s were produced through the reaction of aliphatic dithiols with aliphatic bismaleimides.²⁷³ Melting temperatures of approximately 77 °C were observed. Semicrystalline poly(imido sulfide)s possessed stresses at break near 12 MPa and elongations of 120%. Thermal decomposition of the poly(imido sulfide)s occurred between 336 to 380 °C, and likely resulted from a *retro*-Michael addition depolymerization. Hydrogen sulfide serves as an effective dithiol in the synthesis of poly(imido sulfide)s and reacts very rapidly with bismaleimides in the presence of catalytic quantities of amines such as

²⁷² White, J. E.; Scaia, M. D. Polymerization of *N,N'*-bismaleimido-4,4'-diphenylmethane with arenedithiols. Synthesis of some new polyimidosulphides. *Polymer* **1984**, 25, 850-4.

²⁷³ White, J. E.; Scaia, M. D. Synthesis and properties of some new polyimidosulfides with highly mobile backbones. *J Polym Sci: Polym Chem Edn* **1984**, 22, 589-96.

N,N,N',N'-tetramethylethylenediamine (TMEDA) or acids such as acetic acid (Figure 3.18).²⁷⁴ Poly(imido sulfide)s were also attained from biscitraconimides (methyl substituted maleimides), which resulted in geminal substitution of the sulfide group on the maleimide ring at the same position as the methyl group.²⁷⁵

²⁷⁴ Crivello, J. V. Polyimidothioethers. *J Polym Sci: Polym Chem Edn* **1976**, 14, 159-82.

²⁷⁵ Giana, C.; Giana, V. Synthesis of new polyimidosulfides by Michael addition of bis(1-mercapto-2-ethylether) and amido thiosulfide oligomers. *Des Mon Polym* **2005**, 8, 145-58.

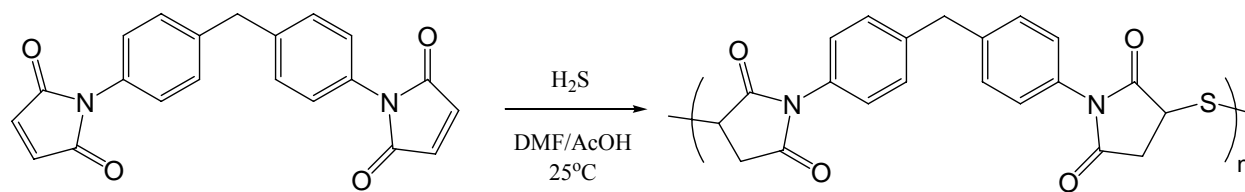


Figure 3.18. Poly(imido sulfide) synthesis from a bismaleimide precursor and hydrogen sulfide gas.

Segmented polymers based on poly(imido sulfide) chemistry were developed by Crivello and Juliano.²⁷⁶ These polymers were synthesized in an analogous fashion to polyurethanes, starting with an oligomeric “soft block” consisting of a thiol terminated polysulfide (Thiokol™ resin) and reacting with an excess of aromatic bismaleimide monomer in cresol with tri-*n*-butylamine catalyst at room temperature. The reactive oligomer is chain extended through reaction with hydrogen sulfide to produce the poly(imido sulfide) “hard block”. The poor thermal stability of the polysulfide oligomers limited the processing temperature of the polymers to less than 150 °C, but tensile strengths as high as 10 MPa and 500% elongation were obtained. The thermal instability limited the choice of bismaleimide monomer to maintain a T_g that was less than 100 °C. These segmented poly(imido sulfide)s exhibited two glass transition temperatures in dynamic mechanical analysis, indicating the presence of microphase separation. The rubbery plateau (service window) ranged from -30 to 130 °C. Increasing the hard segment content above 30 wt% led to higher tensile strengths with lower extensibilities and poor processability. The polysulfide containing segmented elastomers benefited from excellent solvent resistance.

Dix et al. showed that changing between protic and aprotic monomers in aprotic solvents controlled the topology of poly(imido sulfide)s (Figure 3.19).²⁷⁷ Bismaleimides were reacted with oligomeric dithiols as well as low molar mass dithiols in the presence of catalytic quantities of triethylamine. Oligomeric bithiols reacted with

²⁷⁶ Crivello, J. V.; Juliano, P. C. Polyimidothioether-polysulfide block polymers. *J Polym Sci: Polym Chem Edn* **1975**, 13, 1819-42.

²⁷⁷ Dix, L. R.; Ebdon, J. R.; Hodge, P. Chain extension and crosslinking of telechelic oligomers-II. Michael additions of bithiols to bismaleimides, bismaleates and bis(acetylene ketone)s to give linear and crosslinked polymers. *Eur Polym J* **1995**, 31, 653-8.

N,N'-bismaleimido-4,4'-diphenylmethane to create crosslinked networks due to the reaction of the carbanion formed upon Michael addition with additional maleimide groups. The use of a protic small molecule dithiol monomer, dithiothreitol, resulted in linear polymers without crosslinking, due to protonation of the carbanions by hydroxyl groups on dithiothreitol. Triethylamine does not initiate maleimide polymerization, but deprotonates thiols which are capable of polymerizing maleimides. For example, an oligomeric dithiol was reacted with excess monofunctional maleimide in the presence of triethylamine resulting in anionic polymerization of the maleimide from the chain ends of the oligomeric dithiol.

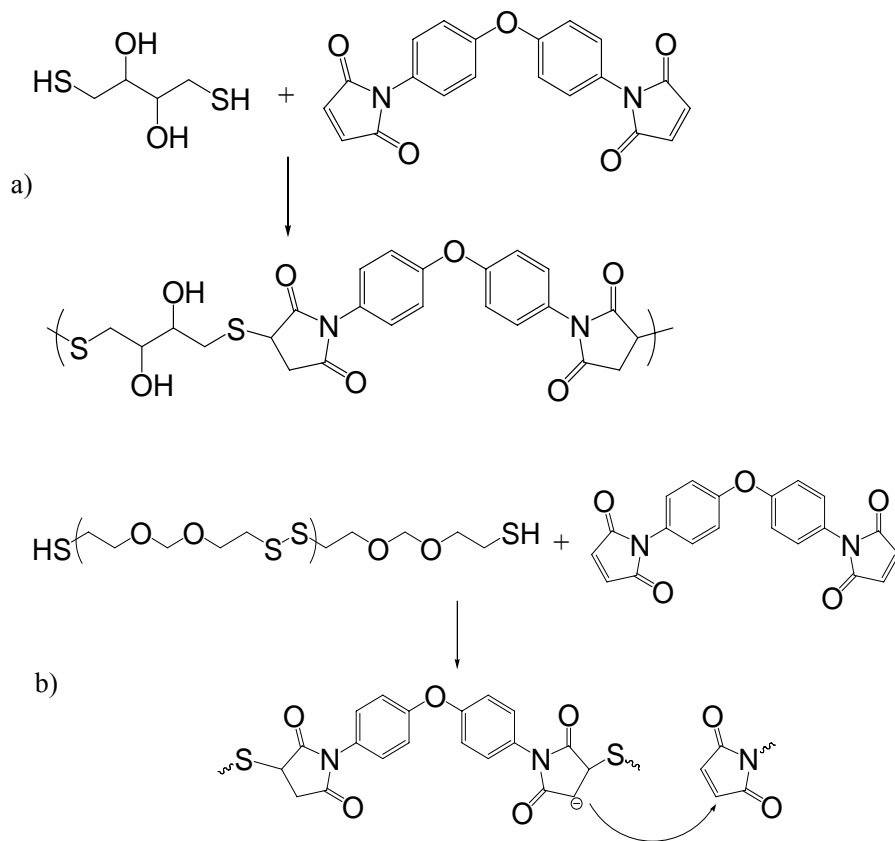


Figure 3.19. a) A typical poly(imido sulfide)s synthesis. b) Possible crosslinking side reaction through maleimide homopolymerization observed for aprotic oligomeric dithiols.

The acrylic analog to poly(imido sulfide)s, poly(ester sulfide)s, were synthesized using PEG dithiol and butanediol diacrylate or PEG diacrylate using triethylamine base catalyst.²⁷⁸ Varying the length of the PEG spacer enabled hydrophilicity control. The reaction kinetics were studied in a number of aprotic solvents and increased in the order benzene < dioxane << chloroform with increasing dielectric constant. Weight average molecular weights ranged from 5000 to 28000 g/mol and glass transition temperatures from -50 to -60 °C were observed. Crystallinity was observed in selected poly(ester sulfide)s.

3.4.4 Poly(aspartamide)s

Poly(aspartamide)s are a class of condensation polymers derived from bismaleimides and diamine monomers. Poly(aspartamide)s exhibit properties similar to polyimides yet benefit from a facile, one-pot synthesis and increased solubility in organic solvents relative to aromatic polyimides and polyamides.²⁷⁹ Poly(aspartamide) synthesis relies on a facile Michael addition of the amine functional group to the maleimide double bond and does not require a high temperature poly(amic acid) cyclization reaction as for polyimides.

Crivello synthesized poly(aspartamide)s through the reaction of aromatic diamines with aromatic bismaleimides in cresol at 110 °C for 3 d with catalytic amounts of acetic acid.²⁸⁰ The lower basicity of the aromatic amines allowed the use of acetic acid, which activated the

²⁷⁸ Tomasi, S.; Bizzarri, R.; Solaro, R.; Chiellini, E. Poly(ester-sulfide)s from oligo(oxyethylene)dithiols and bis(acrylates). *J Bioact Compat Polym* **2002**, 17, 3-21.

²⁷⁹ Wu, C. S.; Liu, Y. L.; Chiu, Y. S. Synthesis and characterization of new organosoluble polyaspartamides containing phosphorus. *Polymer* **2002**, 43, 1773-9.

²⁸⁰ Crivello, J. V. Polyaspartamides: condensation of aromatic diamines and bismaleimide compounds. *J Polym Sci: Polym Chem Edn* **1973**, 11, 1185-200.

maleimide group, through protonation.²⁸¹ Model reactions suggested that the polymerization mechanism involved charged intermediates due to increased rates in polar solvents. The poly(aspartamide)s exhibited glass transition temperatures near 210 °C and thermal decomposition temperatures near 350 °C. This decomposition occurred at the same temperature (TGA) in both air and nitrogen atmospheres, suggesting that depolymerization occurred rather than oxidation. The poly(aspartamide)s possessed tensile strengths near 95 MPa and elongations of 5.5%. Flexural strengths and moduli as high as 140 MPa and 3.1 GPa, respectively, were reported.

Liaw studied poly(aspartamide)s based on arylene ether diamines with improved thermal stability and 10% weight loss temperatures near 400 °C (Figure 3.20).²⁸² The molecular weight of the poly(aspartamide)s increased with increasing monomer concentration, from $M_n = 7,900$ at 0.38 M to $M_n = 12,800$ at 1.0 M. Weight average molecular weights ranged from 24000 to 68000 g/mol.

²⁸¹ White, J. E.; Snider, D. A. Reactions of diaminoalkanes with bismaleimides: synthesis of some unusual polyimides. *J Appl Polym Sci* **1984**, 29, 891-9.

²⁸² Liaw, D. J.; Liaw, B. Y.; Chen, J. J. Synthesis and characterization of new soluble polyaspartimides derived from bis(3-ethyl-5-methyl-4-maleimidophenyl)methane and various diamines. *Polymer* **2001**, 42, 867-72.

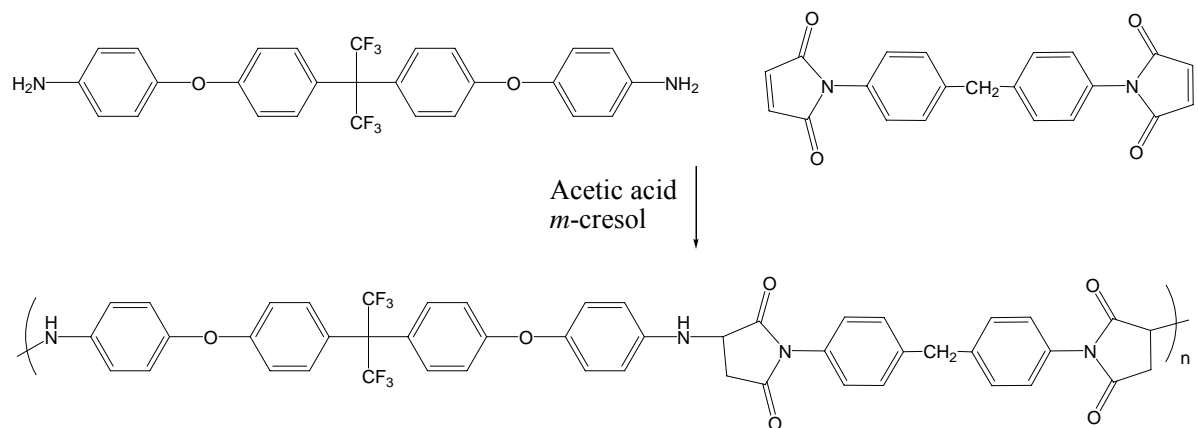


Figure 3.20. Thermally stable poly(aspartamide)s synthesized from arylene ether diamines.

White and Scaia synthesized amorphous elastomeric poly(aspartamide)s via the polymerization of aliphatic secondary diamines and aliphatic bismaleimides.²⁸³ Acetic acid was used in the polymerization of aromatic diamines and bismaleimides but not with aliphatic diamines due to the tendency to protonate the amine groups and prevent polymerization. The poly(aspartamide)s undergo slow crosslinking at ambient conditions likely due to Michael addition reaction of amine and maleimide end groups and subsequent homopolymerization of the maleimide group. Amorphous poly(aspartamide)s possessed elongations of 1700%, stresses at break near 9.3 MPa, and glass transition temperatures ranging from 0 to 86 °C.

Poly(aspartamide)s have potential application in second order non-linear optical (NLO) materials due to their high glass transition temperatures (~260 to 290 °C) which help maintain the critical orientation of the NLO chromophores. In addition, poly(aspartamide)s do not exhibit poling interferences due to water evolution as seen with polyimides during cyclization of the precursor poly(amic acid). Wu et al. used Michael addition to obtain an NLO-containing poly(aspartamide) pre-polymer with maleimide end groups that was thermally cured to obtain the final product.²⁸⁴ At higher curing temperatures, the glass transition temperature of the cured poly(aspartamide)s appeared to increase, which demonstrated that curing continued to 250 °C.

Poly(amide aspartamide)s are similar to poly(aspartamide)s with the exception that

²⁸³ White, J. E.; Scaia, M. D. Synthesis and properties of some new polyimidosulfides with highly mobile backbones. *J Polym Sci: Polym Chem Edn* **1984**, 22, 589-96.

²⁸⁴ Wu, W.; Wang, D.; Zhu, P.; Wang, P.; Ye, C. Thermally stable second-order nonlinear optical addition-type polyimides functionalized by diamine chromophore. *J Polym Sci Part A: Polym Chem* **1999**, 37, 3598–605.

polymerization occurs via both Michael addition of amines and maleimides and amidation reactions of amines and carboxylic acids.²⁸⁵ Poly(amide aspartamide)s are synthesized through a step growth polymerization of an AA' monomer containing a carboxylic acid and a maleimide functional group with a B₂ diamine monomer such as those shown in Figure 3.21. The polymers are thus synthesized in a sequential process beginning with the Michael addition of the nucleophilic amine groups to the maleimide group followed by the amidation at the carboxylic acid. These polymers are controllably branched through the addition of AB₂ monomers. One drawback of the poly(amide aspartamide)s is their relatively low thermal stability, with typical thermal degradation temperatures of 300 to 360 °C at 10% weight loss. The char yields of the polymers increased on end-capping the carboxylic acid end groups with aniline.

²⁸⁵ Wu, C. S.; Tsai, S. H.; Liu, Y. L. One-pot synthesis of linear and branched poly(amide aspartimide)s with good solubility in organic solvents. *J Polym Sci Part A: Polym Chem* **2005**, 43, 1923-9.

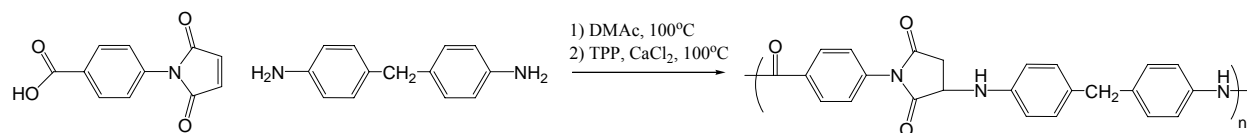


Figure 3.21. Typical poly(amide aspartamide) polymerization. The first heating step produces the Michael adduct while the second step promotes amide bond formation.

Oxygen nucleophiles are also effective in step growth polymerizations with bismaleimides. Hulubei and Rusu copolymerized glycerol and phenolphthalein with aliphatic bismaleimides resulting in poly(imido ethers).²⁸⁶ The reaction was performed in NMP using triethylamine or 2-mercaptobenzothiazole as catalysts at 85 to 115 °C for 2 to 3 d. In the case of glycerol, the difference in reactivity of the secondary and primary alcohols allowed synthesis of pendant hydroxyl polymers. Thermogravimetric analysis revealed initial weight losses ranging from 215 to 400 °C. Polymerization of bismaleimides with phenols was successful in solution (95 to 110 °C) and in the melt (180 °C), and fiber-glass reinforced composites were prepared.²⁸⁷

3.4.5 Poly(amino quinone)s

Poly(amino quinone)s are synthesized from primary diamines and quinone, through Michael additions on both sides of the quinone (Figure 3.22).²⁸⁸ The unsaturated nature of the quinone is maintained in the polymer, using either excess quinone or other oxidizing agents. Use of peracetic acid leads to improved yields and simplified purification. Poly(amino quinone)s have recently found application in anticorrosion coatings and moisture resistant adhesives. Numerous traditional adhesives suffer from delamination from solid surfaces in the presence of water. This is due to a stronger interaction of water with the surface.

²⁸⁶ Hulubei, C.; Rusu, E. New functional poly(bismaleimide-ether)s: synthesis and characterization. *Polym Plast Technol Eng* **2001**, 40, 117-31.

²⁸⁷ Taranu, V.; Pecincu, S. Preparation and properties of poly(bismaleimide ethers). *Macromol Reports* **1994**, A31, 45-52.

²⁸⁸ Vaccaro, E.; Scola, D. A. New applications of polyaminoquinones. *CHEMTECH* **1999**, 29, 15-23.

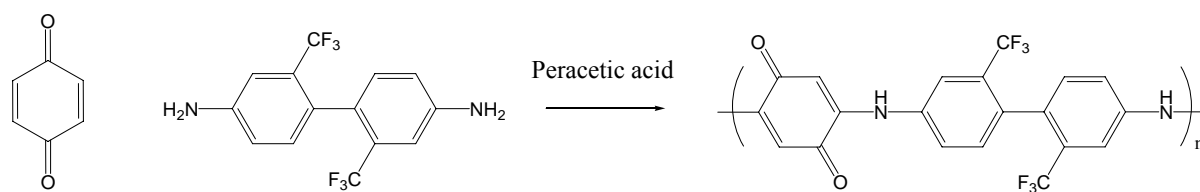


Figure 3.22. Poly(amino quinone) synthesis involving peracetic acid as an oxidizing agent.

Poly(amino quinone)s, however, displace water on metal surfaces and bind preferentially. The strong interaction of these polymers with metal surfaces is thought to arise from the electron donating capabilities of the quinone group. Poly(amino quinone)s inhibit corrosion on stainless steel surfaces even in the presence of sulfuric acid, through the formation of a protective coating that forms spontaneously on the metal surface. These corrosion inhibiting coatings are used for ship hull protection as well as protection of magnetic particles on data storage media. Diamino quinone containing polyimides are used to improve the corrosion resistance of interlayer dielectrics in microelectronics.²⁸⁹ Poly(amino quinone)s have also been introduced into polyolefins and polyurethanes.

Similar to poly(amino quinone)s are poly(thiophenylene)s formed from aromatic dithiols and bis(1,4-phenylenediimine)s, depicted in Figure 3.23. The product of the Michael addition between the thiol groups and this nitrogen analog to quinone aromatizes through proton transfer to the imine nitrogens resulting in a poly(thiophenylene) with pendant amino groups.²⁹⁰ The polymerization proceeds without a catalyst. These polymers exhibit electroresponsive behavior and are redox active under acidic conditions. The number average molecular weight of the polymer was 5,400 g/mol and the glass transition temperature was 131 °C.

²⁸⁹ Han, M.; Bie, H.; Nikles, D. E.; Warren, G. W. Amine–quinone polyimide: a new high-temperature polymer and its use to protect iron against corrosion. *J Polym Sci Part A: Polym Chem* **2000**, 38, 2893-9.

²⁹⁰ Yamamoto, K.; Higuchi, M.; Takai, H.; Nishiumi, T. Novel synthesis of electroresponsive poly(thiophenylene) through a Michael-type addition. *Org Lett* **2001**, 3, 131-4.

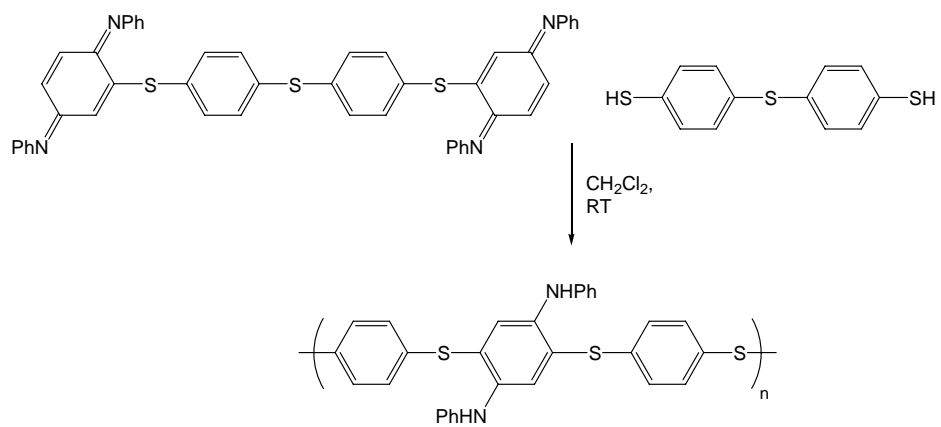


Figure 3.23. Polymerization of poly(thiophenylene)s via Michael addition and oxidation.

3.4.6 Step Growth Polymers Derived from Bisacetylene-Containing Monomers

Numerous step growth Michael addition polymers are synthesized from bisacetylenic precursors. The acetylene bond reacts electrophilically when conjugated to electron withdrawing groups, in a similar fashion to an olefin as noted earlier. Typical functional groups that serve as Michael receptors are conjugated acetylene ketones and conjugated acetylene esters. These carbon-carbon triple bond Michael acceptors react with oxygen, sulfur and amine nucleophiles and adducts possess the additional feature of stereochemistry at the double bond.²⁹¹ Michael addition polymers based on acetylenic precursors possess surprising thermal stability and produce remarkably tough thermoplastics.

Sinsky et al. studied poly(enamine ketone)s synthesized through the Michael addition reaction of aromatic diamines with aromatic bis(alkynone)s.²⁹² These nucleophilic additions to acetylenic compounds result primarily in *Z* isomer formation. The reactions were performed in *m*-cresol at 100 °C without catalyst. Glass transition temperatures between 198 and 235 °C were obtained and thermogravimetric decomposition temperatures were nearly 300 °C. The poly(enamine ketone)s were tough thermoplastics, with tensile strengths of 85 MPa (63 MPa at 93 °C), tensile moduli of 2.27 GPa, and elongations of 4%.

Bass et al. synthesized poly(enone sulfide)s, the sulfur analog to poly(enamine ketone)s through the reaction of aromatic dithiols (e.g. 1,3-benzenedithiol) with aromatic internal bis(alkynone)s in *m*-cresol at room temperature with *N*-methyl morpholine as a catalyst at

²⁹¹ Dickstein, J. I.; Miller, S. I., Nucleophilic attacks on acetylenes. In *The chemistry of the carbon-carbon triple bond. Part 2*, Patai, S., Ed. Wiley: New York, 1978; pp 813-955.

²⁹² Sinsky, M. S.; Bass, R. G.; Connell, J. W. Poly(enamine ketones) from aromatic diacetylenic diketones and aromatic diamines. *J Polym Sci Part A: Polym Chem* **1986**, 24, 2279-95.

temperatures from 25 to 40 °C.²⁹³ The polymers had moderately high glass transition temperatures ($T_g \sim 107$ to 156 °C) and thermal decomposition temperatures near 330 °C. Tough, clear films were obtained from solution casting and exhibited tensile strengths of 78 MPa and tensile moduli near 3.2 GPa. Dix et al. also synthesized poly(enone sulfide)s from internal bis(alkynone)s and found a *Z:E* ratio of 60/40 (Figure 3.24).²⁹⁴ Model reactions of thiols with phenylacetylene resulted in almost exclusive formation of the *Z* isomer.²⁹⁵

3.4.7 Hydrogen transfer polymerization

Nylon-3 type polyamides are also synthesized via a Michael addition process. The base catalyzed polymerization of acrylamide to poly(β -alanine), as shown in Figure 3.25, was originally proposed as an anionic chain growth process, which occurred with proton transfer of the amide NH_2 on the growing chain end to the enolate carbanion. This process was described as a “hydrogen transfer polymerization.” However, it was later classified as a step growth polymerization due to proton transfer from the growing enolate carbanion to amide NH_2 groups on other monomers. Bush and Breslow demonstrated this via monitoring molecular weight as a function of monomer conversion.²⁹⁶ At very short reaction times, high monomer conversion was achieved but high molecular weight product was not obtained

²⁹³ Bass, R. G.; Cooper, E.; Hergenrother, P. M.; Connell, J. W. Poly(enone sulfides) from the addition of aromatic dithiols to aromatic dipropynones. *J Polym Sci Part A: Polym Chem* **1987**, *25*, 2395-407.

²⁹⁴ Dix, L. R.; Ebdon, J. R.; Hodge, P. Chain extension and crosslinking of telechelic oligomers-II. Michael additions of bithiols to bismaleimides, bismaleates and bis(acetylene ketone)s to give linear and crosslinked polymers. *Eur Polym J* **1995**, *31*, 653-8.

²⁹⁵ Truce, W. E.; Simms, J. A. Stereospecific reactions of nucleophilic agents with acetylenes and vinyl-type halides. IV. The stereochemistry of nucleophilic additions of thiols to acetylenic hydrocarbons. *J Am Chem Soc* **1956**, *78*, 2756-9.

²⁹⁶ Bush, L. W.; Breslow, D. S. The mechanism of hydrogen transfer polymerization. *Macromolecules* **1968**, *1*, 189-90.

suggesting initial dimerization and trimerization. Longer reaction times led to high molecular weight poly(β -alanine). These polymerizations were typically conducted at 80 to 120 °C in aprotic solvents such as DMF in the presence of radical inhibitors. Further work from Lim et al. demonstrated that branching occurred in these polymerizations in aprotic solvents due to propagation of both enolate and amide anions, which are formed before and after hydrogen transfer, respectively.²⁹⁷

²⁹⁷ Camino, G.; Lim, S. L.; Trossarelli, L. Branching in the base catalyzed hydrogen transfer polymerization of acrylamide in *N*-methyl-2-pyrrolidone at 100°C. *Eur Polym J* **1977**, 13, 479-81.

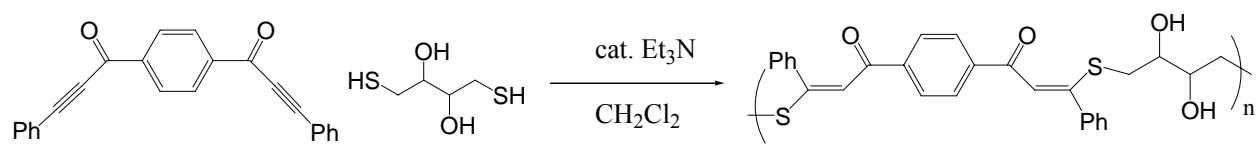


Figure 3.24. Poly(enone sulfide) synthesis via Michael addition step growth.

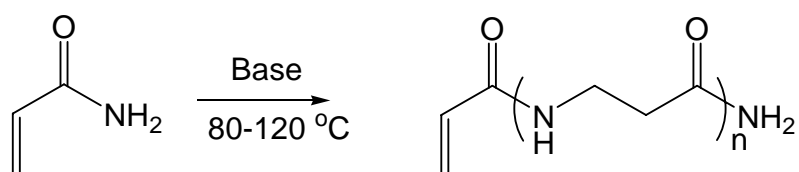


Figure 3.25. Hydrogen transfer polymerization of acrylamide to poly(β -alanine).

Hydrogen transfer polymerization of acrylamide in the presence of carbon black and *n*-butyl lithium was effective in grafting of poly(β -alanine) onto the carbon black via polymerization from surface lithium alkoxides.²⁹⁸ The grafted carbon black showed improved dispersability in water and organic solvents, and grafting ratios of 60 to 80% were achieved. Recently, the hydrogen transfer polymerization process was applied to *N*-acetylacrylamide and *N*-benzoylacrylamide and the proton transfer mechanism was preserved despite the steric hindrance and lower acidity of the amide NH groups.²⁹⁹ Hydrogen transfer polymerization was also achieved with *N*-acryloyl-*N'*-*p*-tolylureas,³⁰⁰ *p*-styrenesulfonamides, heterocyclic base containing acrylamides,³⁰¹ and maleimide.

In a similar nature to the hydrogen transfer polymerization of acrylamide, hydroxyalkyl acrylates are also polymerizable through Michael addition chemistry as AB monomers. The polymerization of hydroxyethyl acrylate was performed at temperatures from 85 to 150 °C in the presence of free radical inhibitors using bases such as sodium hydride and potassium *tert*-butoxide as initiators.³⁰² Molecular weights as high as 9000 g/mol were obtained and hydroxyethyl acrylate polymerized more effectively than hydroxyethyl methacrylate. The primary side reaction in these polymerizations is the disproportionation of hydroxyethyl

²⁹⁸ Tsubokawa, N.; Nagano, Y.; Sone, Y. Grafting of poly(β -alanine) onto carbon black: The hydrogen transfer polymerization of acrylamide catalyzed by *n*-butyllithium in the presence of carbon black. *J Appl Polym Sci* **1984**, 29, 985-93.

²⁹⁹ Iwamura, T.; Tomita, I.; Suzuki, M.; Endo, T. Hydrogen-transfer polymerization behavior of *N*-acrylacrylamide. *J Polym Sci Part A: Polym Chem* **2000**, 38, 430-5.

³⁰⁰ Iwamura, T.; Tomita, I.; Suzuki, M.; Endo, T. Hydrogen-transfer polymerization of vinyl monomers derived from *p*-tolyl isocyanate and acrylamide derivatives. *React Funct Polym* **1999**, 40, 115-22.

³⁰¹ Kondo, K.; Tanioku, S.; Takemoto, K. Functional monomers and polymers. LI. On the synthesis and polymerization of acryloylaminomethyl derivatives of nucleic acid bases. *Polym J* **1979**, 1, 81-2.

³⁰² Gibas, M.; Korytkowska-Walach, A. Polymerization of 2-hydroxyethyl acrylate and methacrylate via Michael-type addition. *Polym Bull* **2003**, 51, 17-22.

acrylate to ethylene glycol diacrylate and ethylene glycol.

3.5 Linear Chain Growth Michael Addition Polymerizations

A classic example of Michael addition polymerization is the anionic chain-growth polymerization of methacrylate monomers. This review is not intended to comprehensively review anionic polymerization but rather to place the Michael addition in context for trends in polymer synthesis strategies. Anionic polymerization has been reviewed extensively in the literature.³⁰³⁻³⁰⁵ The relatively low reactivity of the methacrylate, as noted earlier, towards Michael addition chemistry demands a stronger nucleophile, thus carbanionic species such as diphenylhexyllithium and nitrogen anions such as lithium diisopropyl amide are suitable for the polymerization of alkyl methacrylates. One current limitation is the requirement for cryogenic temperatures to prevent potential nucleophilic attack of the enolate anion on ester groups. Group transfer polymerization, which was developed in the mid-1980s, enabled polymerization at ambient temperatures due to the use of a reversible silyl protecting group that was proposed to stabilize the propagating chain end. Anionic polymerization was demonstrated with acrylamides and acrylate monomers, later, and this may complicate step growth processes in some cases.³⁰⁶ The polymerization of cyanoacrylates is another chain

³⁰³ van Beylen, M.; Bywater, S.; Smets, G.; Swarc, M.; Worsfold, D. J. Developments in anionic polymerization - a critical review. *Adv Polym Sci* **1988**, 86, 87-143.

³⁰⁴ Teyssie, P.; Baran, J.; Dubois, P.; Jerome, R.; Wang, J. S.; Yu, J.; Yu, Y.; Zundel, T. Living anionic polymerization of (meth)acrylic esters. New mechanistic concepts and resulting materials. *Macromol Symp* **1998**, 132, 303-7.

³⁰⁵ Hirao, A.; Hayashi, M. Recent advance in syntheses and applications of well-defined end-functionalized polymers by means of anionic living polymerization. *Acta Polymerica* **1999**, 50, 219-31.

³⁰⁶ Reetz, M. T.; Ostarek, R. Polymerization of acrylic acid esters initiated by tetrabutylammonium alkyl- and aryl- thiolates. *J Chem Soc Chem Commun* **1988**, 3, 213-5.

growth Michael addition process. Cyanoacrylates are initiated with very poor nucleophiles, such as water, due to the electron poor olefin and strong resonance contributions of the adjacent cyano and ester groups. Cyanoacrylate polymerizations are widely used in rapid cure adhesives, and adhesive products possessing extremely high bond strengths.

3.5.1. Anionic Polymerization of Methacrylates

Anionic polymerization of alkyl methacrylates is an established chain growth polymerization technique which relies upon Michael addition chemistry. Anionic polymerization is known for producing polymers of controlled molecular weights and narrow polydispersity. Anionic polymerization is particularly suited for well-defined block copolymers³⁰⁷ and star-shaped polymers via chain-end coupling strategies. A further advantage of anionic polymerization is the potential for controlling tacticity, which was achieved for the sterically bulky *tert*-butyl methacrylate monomer in toluene by Long et al.³⁰⁸ Anionic polymerization is generally initiated using alkyllithium initiators with sufficient nucleophilicity to attack alkyl methacrylate monomers. However, due to the potential side reaction of the carbanionic chain end with ester carbonyls, the reaction must be conducted at low temperatures and with sterically hindered carbanions such as diphenylhexyllithium.³⁰⁷ These bulky carbanions react selectively at the double bond, resulting in an enolate Michael adduct, as shown in Figure 3.26.

³⁰⁷ Long, T. E.; Broske, A. D.; Bradley, D. J.; McGrath, J. E. Synthesis and characterization of poly(*tert*-butyl methacrylate-*b*-isoprene-*b*-*tert*-butyl methacrylate) block copolymers by anionic techniques. *J Polym Sci Part A: Polym Chem* **1989**, 27, 4001-12.

³⁰⁸ Allen, R. D.; Long, T. E.; McGrath, J. E. Synthesis of tactic poly(alkyl methacrylate) homo- and copolymers. *Polym Sci Tech* **1985**, 31, 347-62.

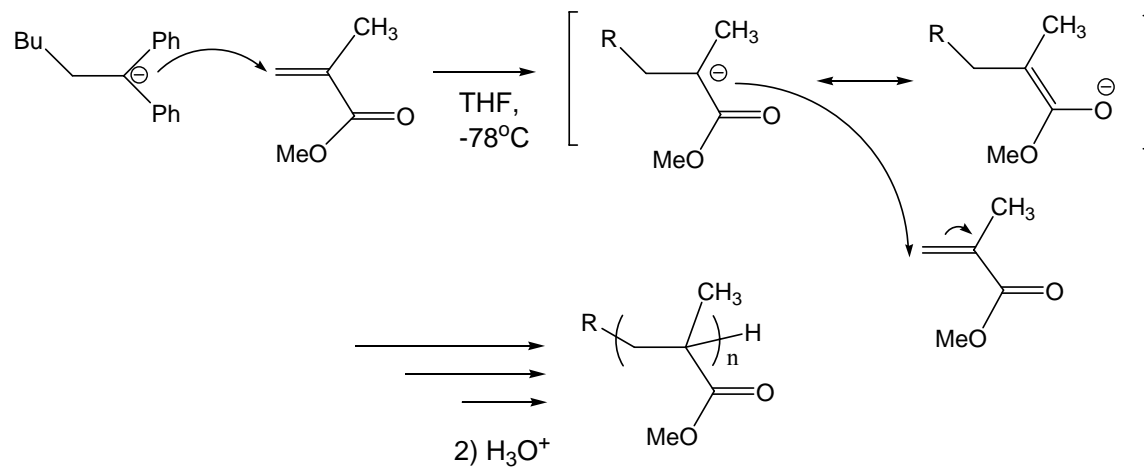


Figure 3.26. Anionic polymerization of methyl methacrylate from diphenylhexyl lithium.

The strong nucleophilicity of the anionic PMMA growing chain end was used in chain end functionalization strategies in numerous cases.³⁰⁹ For example, addition of di-*tert*-butyl maleate at the end of the polymerization results in succinate ester end groups.³¹⁰ These end groups were then pyrolyzed to produce reactive anhydrides capable of imide coupling with amine functional polymers. Long et al. achieved end functionalization with hydrogen bonding groups via Michael addition of heterocyclic base pairs to acrylated polystyrenes (Figure 3.27).³¹¹ Termination of the anionic polymerization of styrene with ethylene oxide created hydroxyl functionality which allowed esterification with acryloyl chloride. Michael addition of nucleotide bases then allowed facile functionalization of the polystyrene chains, without detracting from hydrogen bonding properties. Adenine and thymine functionalized polystyrene demonstrated association in ¹H NMR spectroscopic investigations.

Long et al.^{312,313} as well as Muller et al.³¹⁴ studied the synthesis of diene / acrylic, styrene / acrylic and all acrylic triblock copolymers containing *tert*-butyl methacrylate, which were later hydrolyzed and neutralized to obtain carboxylate block ionomers. The bulkier

³⁰⁹ Hirao, A.; Hayashi, M. Recent advance in syntheses and applications of well-defined end-functionalized polymers by means of anionic living polymerization. *Acta Polymerica* **1999**, 50, 219-31.

³¹⁰ Cernohous, J. J.; Macosko, C. W.; Hoyer, T. R. Anionic synthesis of polymers functionalized with a terminal anhydride group. *Macromolecules* **1997**, 30, 5213-9.

³¹¹ Yamauchi, K.; Lizotte, J. R.; Long, T. E. Synthesis and characterization of novel complementary multiple-hydrogen bonded (CMHB) macromolecules via a Michael addition. *Macromolecules* **2002**, 35, 8745-50.

³¹² Long, T. E.; Broske, A. D.; Bradley, D. J.; McGrath, J. E. Synthesis and characterization of poly(*tert*-butyl methacrylate-*b*-isoprene-*b*-*tert*-butyl methacrylate) block copolymers by anionic techniques. *J Polym Sci Part A: Polym Chem* **1989**, 27, 4001-12.

³¹³ Deporter, C. D.; Long, T. E.; McGrath, J. E. Methacrylate-based block ionomers. I. Synthesis of block ionomers derived from *t*-butyl methacrylate and alkyl methacrylates. *Polym Int* **1994**, 33, 205-16.

³¹⁴ Ludwigs, S.; Boker, A.; Abetz, V.; Muller, A. H. E.; Krausch, G. Phase behavior of linear polystyrene-*block*-poly(2-vinylpyridine)-*block*-poly(*tert*-butyl methacrylate) triblock terpolymers. *Polymer* **2003**, 44, 6815-23.

ester alkyl prohibits carbonyl ester attack at room temperature. Long et al. also established the utility of lithium diisopropylamide (LDA) as an initiator for methacrylate polymerizations in THF at -78 °C, despite the relatively low nucleophilicity of the hindered amide ion.³¹⁵ Anionic polymerization of acrylates,³¹⁶ maleimides, vinyl ketones³¹⁷ and acrylamides³¹⁸ are also known.

³¹⁵ Long, T. E.; Guistina, R. A.; Schell, B. A.; McGrath, J. E. Hindered lithium dialkylamide initiators for the living anionic polymerization of methacrylic esters. *J Polym Sci Part A: Polym Chem* **1994**, *32*, 2425-30.

³¹⁶ Reetz, M. T.; Ostarek, R. Polymerization of acrylic acid esters initiated by tetrabutylammonium alkyl- and aryl- thiolates. *J Chem Soc Chem Commun* **1988**, *3*, 213-5.

³¹⁷ Catterall, E.; Lyons, A. R. Organometal initiated polymerization of vinyl ketones. I. *n*-Butyllithium initiated polymerization of methyl isopropenyl ketone. *Eur Polym J* **1971**, *7*, 839-48.

³¹⁸ Kodaira, T.; Tanahashi, H.; Hara, K. Cyclopolymerization XVII. Anionic cyclopolymerization tendency of *N*-methyldiacrylamide and *N*-substituted dimethacrylamides. *Polym J* **1990**, *22*, 649-59.

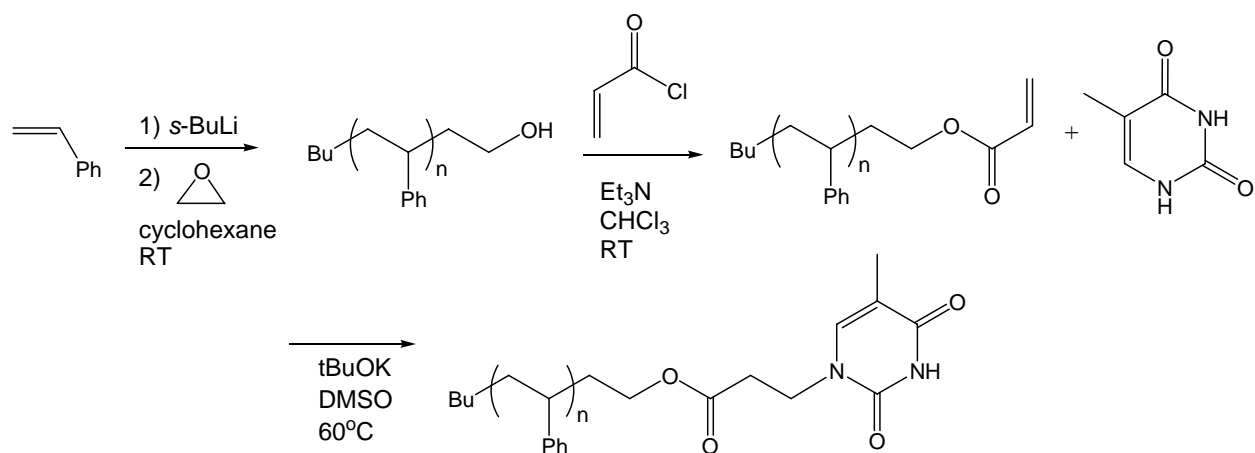


Figure 3.27. Michael addition of heterocyclic nucleotide bases to acrylated anionic polystyrene.

In some cases, anionically polymerized methacrylates have been designed for biologically related applications. For instance, Okamoto et al. synthesized macrocyclic ether containing acrylic monomers which polymerized anionically to obtain highly isotactic polymers capable of functioning as synthetic ion channels in hexadecyl phosphate vesicles (Figure 3.28).³¹⁹ In contrast, radical polymerization of macrocyclic ether monomers yielded atactic polymer with dramatically lower ion transport.

³¹⁹ Habaue, S.; Morita, M.; Okamoto, Y. Stereospecific anionic polymerization of α -(hydroxymethyl)acrylate derivatives affording novel vinyl polymers with macrocyclic side chains. *Polymer* **2002**, 43, 3469-74.

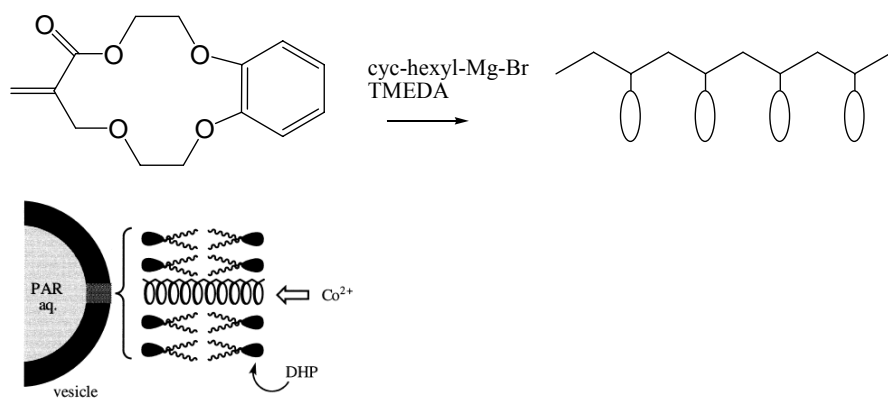


Figure 3.28. Polymerization of macrocyclic ether acrylic monomers to form ion channels. Reprinted from *Polymer*, 43, Okamoto, et al. “Stereospecific anionic polymerization of α -(hydroxymethyl)acrylate derivatives affording novel vinyl polymers with macrocyclic side chains,” 3469-74, Copyright 2002, with permission from Elsevier.³²⁰

³²⁰ Habaue, S.; Morita, M.; Okamoto, Y. Stereospecific anionic polymerization of α -(hydroxymethyl)acrylate derivatives affording novel vinyl polymers with macrocyclic side chains. *Polymer* **2002**, 43, 3469-74.

3.5.2 Group Transfer Polymerization

Commonly, anionic polymerization of alkyl methacrylates is conducted at cryogenic temperatures. Such temperatures are generally not industrially feasible, except in the cationic polymerization of isobutylene, and significant research effort was directed towards a methodology that was amenable to higher temperatures. Group transfer polymerization (GTP) is a polymerization methodology that was developed in the mid-1980s by DuPont as a method of producing narrow polydispersity methacrylate and acrylate polymers and block polymers above room temperature.³²¹ GTP is conveniently conducted at 80 °C using a silyl ketene acetal initiator in the presence of a nucleophilic anionic catalyst (Figure 3.29). Initially, GTP was believed to proceed through a transfer of a silyl protecting group from the enolate oxygen on the chain end to monomers during the propagation step.³²² This initial mechanism has largely been disproven in favor of a dissociative anionic polymerization mechanism which involves a reversible dissociation of the silyl protecting group from the enolate oxygen, aided by anionic catalysts (HF_2^- , bibenzoate anion). The position of the equilibrium between the free enolate and the silyl protected enolate determines the rate of the polymerization. Similar to anionic polymerizations, the reaction is terminated through the addition of a protic species such as methanol. GTP is currently used by DuPont to produce acrylic block copolymers for pigment dispersing applications in automotive paints.³²¹

³²¹ Webster, O. W. Group transfer polymerization: Mechanism and comparison with other methods for controlled polymerization of acrylic monomers. *Adv Polym Sci* **2004**, 167, 1-34.

³²² Webster, O. W.; Hertler, W. R.; Sogah, D. Y.; Farnham, W. B.; RajanBabu, T. V. Group-transfer polymerization. 1. A new concept for addition polymerization with organosilicon initiators. *J Am Chem Soc* **1983**, 105, 5706-8.

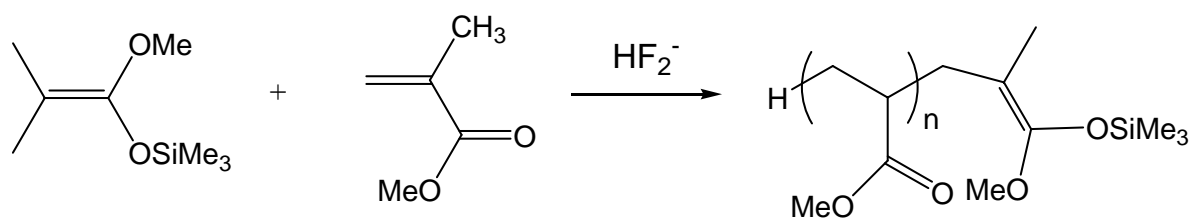


Figure 3.29. Group transfer polymerization of methyl methacrylate.

3.5.3 Anionic Polymerization of α -cyanoacrylates

Cyanoacrylates are a class of monomers which undergo rapid anionic polymerization initiated by weak nucleophiles such as water, as shown in Figure 3.30. These rapidly polymerizing monomers are used primarily in the adhesives industry as a high strength rapid setting adhesives.³²³ The added electron withdrawing character of the nitrile group facilitates anionic polymerization of these monomers. Unlike conventional anionic polymerization, however, molecular weight control is absent. Klemarczyk studied the polymerization of ethyl cyanoacrylate using phosphine and amine initiators.³²⁴ The initiated monomer species is zwitterionic, which makes it an effective nucleophile towards further monomer addition. Primary and secondary amines initiate more slowly than tertiary amines due to proton transfer after the first addition of monomer, which results in a neutral, less reactive adduct. In terms of current biomedical applications, octyl cyanoacrylate has recently found application as a tissue adhesive and gained FDA approval for surgical use.³²⁵ This monomer polymerizes on contact with a wound and maintains flexibility due to the pendant octyl chain and furthermore possesses low water solubility.

³²³ Klemarczyk, P., Cyanoacrylate instant adhesives. In *Adhesion Science and Engineering*, Dillard, D. A.; Pocius, A. V., Eds. Elsevier: Amsterdam, 2002; pp 847-67.

³²⁴ Klemarczyk, P. The isolation of a zwitterionic initiating species for ethyl cyanoacrylate (ECA) polymerization and the identification of the reaction products between 1°, 2°, and 3° amines with ECA. *Polymer* **2001**, 42, 2837-48.

³²⁵ Singer, A. J.; Thode, H. C. A review of the literature on octyl cyanoacrylate tissue adhesive. *Amer J Surgery* **2004**, 187, 238-48.

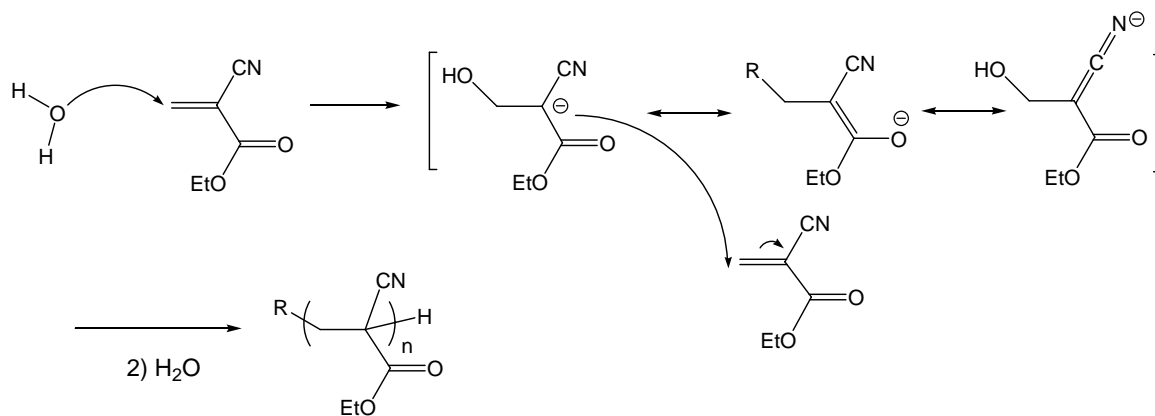


Figure 3.30. Water-initiated polymerization of ethyl α -cyanoacrylate.

3.5.4 Living Radical Polymerization

Living radical polymerization encompasses several techniques for producing well-defined homopolymers, block copolymers, and star polymers. Due to the radical nature of this polymerization methodology, a wider range of monomers are accessible compared to traditional anionic polymerization and less stringent purification techniques are required. Numerous living radical polymerization methods are currently known, including atom transfer radical polymerization (ATRP) which involves activated alkyl halides and metal catalysts,³²⁶ stable free radical polymerization (SFRP) which utilizes nitroxides,³²⁷ and reversible addition fragmentation chain transfer polymerization (RAFT) which typically utilizes dithioester or dithiocarbamate chain transfer reagents.³²⁸ Michael addition reactions have recently proven useful in many of these living radical polymerization strategies.

Functional initiation is of interest for the synthesis of well-defined polymers with the potential for block copolymer synthesis, coupling with proteins or reaction with surfaces. Recently, Michael addition was used to synthesize an ATRP initiator containing two hydroxyl groups.³²⁹ This novel dihydroxyl initiator allowed the synthesis of Y-shaped polymers via a combination of ATRP on the initial alkyl halide site and post polymerization conversion of the hydroxyl groups to alkyl halides which allowed polymerization of a second monomer (Figure 3.31). Matyjaszewski et al. recently studied the synthesis of ATRP ligands through

³²⁶ Matyjaszewski, K.; Xia, J. Atom transfer radical polymerization. *Chem Rev* **2001**, 101, 2921-90.

³²⁷ Hawker, C. J.; Bosman, A. W.; Harth, E. New polymer synthesis by nitroxide mediated living radical polymerizations. *Chem Rev* **2001**, 101, 3661-88.

³²⁸ Moad, G.; Mayadunne, R. T. A.; Rizzardo, E.; Skidmore, M.; Thang, S. H. Synthesis of novel architectures by radical polymerization with reversible addition fragmentation chain transfer. *Macromol Symp* **2003**, 192, 1-12.

³²⁹ Cai, Y.; Armes, S. P. Synthesis of well-defined Y-shaped zwitterionic block copolymers via atom-transfer radical polymerization. *Macromolecules* **2005**, 38, 271-9.

the Michael addition reaction of tris(aminoethyl)amine with several acrylates, resulting in ligands that were suitable for the polymerization of methacrylic, acrylic and styrenic monomers in nonpolar media.³³⁰ Matyjaszewski et al. also synthesized ATRP ligands containing dimethoxymethylsilylpropyl acrylate, which aided in post-polymerization catalyst removal via passage through silica gel and coupling of the complexes to the silica gel via sol-gel reactions. Shen et al. synthesized novel diaminopyridine (DAP) containing ATRP ligands through acrylation of DAP followed by Michael addition using bis(diethylaminoethyl)amine.³³¹ Silica gel modified with thymine residues created hydrogen bonded associations with these DAP ATRP ligands which dissociated at reaction temperatures, allowing polymerization to occur. After cooling the reaction, re-association allowed removal and recycling of the catalyst.

Synthesis of functional polymers is also achieved through post-polymerization strategies based on the Michael addition. For example, hydroxyl functionalized RAFT polymerized PMMA were synthesized using hydrolysis of the dithioester end groups followed by Michael addition with hydroxyethyl acrylate to the thiol group.³³²

³³⁰ Gromada, J.; Spanswick, J.; Matyjaszewski, K. Synthesis and ATRP activity of new TREN-based ligands. *Macromol Chem Phys* **2004**, 205, 551-66.

³³¹ Ding, S.; Yang, J.; Radosz, M.; Shen, Y. Atom transfer radical polymerization of methyl methacrylate via reversibly supported catalysts on silica gel via self-assembly. *J Polym Sci Part A: Polym Chem* **2004**, 42, 22-30.

³³² Lima, V.; Jiang, X.; Brokken-Zijp, J.; Schoenmakers, P.; Klumperman, B.; van der Linde, R. Synthesis and characterization of telechelic polymethacrylates via RAFT polymerization *J Polym Sci Part A: Polym Chem* **2005**, 43, 959-73.

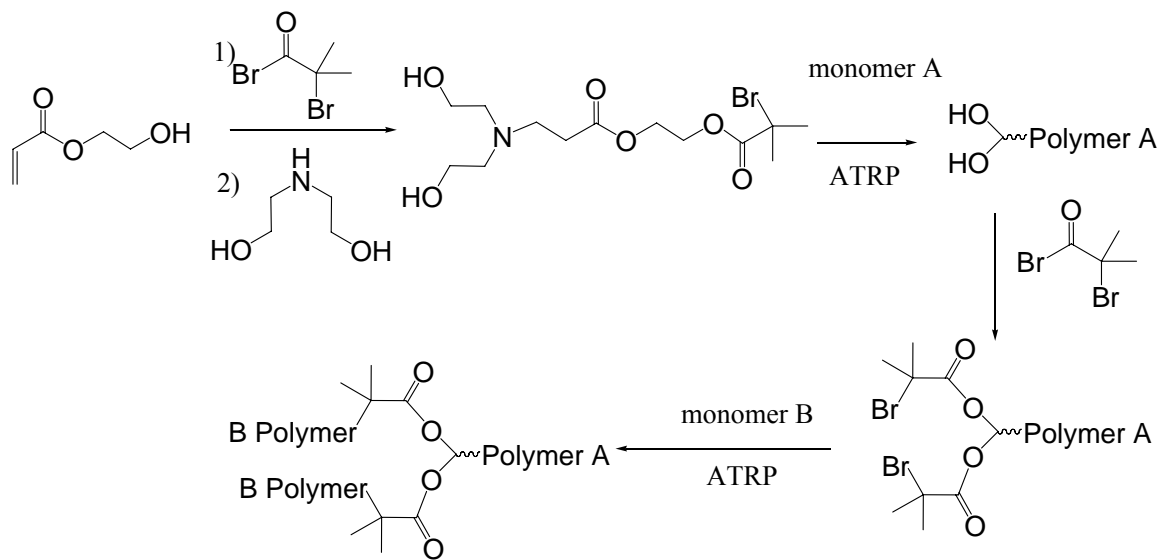


Figure 3.31. Synthesis of a dihydroxyl functional ATRP initiator.

3.6 Synthesis of Branched Polymers via the Michael Addition Reaction

Branched polymers encompass a wide range of topologies, ranging from hyperbranched to graft and dendritic polymers. Michael addition polymerization mechanisms were broadly applied to each of these topological designs. Hyperbranched polymers have gained interest recently, due to a large number of functional termini and processing advantages in terms of lower melt viscosity relative to linear polymers of equivalent molecular weight. Michael addition provides the means to incorporate numerous types of terminal functionalities due to an inherent functional group tolerance and wide variety of monomers. Graft copolymers are also of increasing interest given the similarity to block copolymers and the ability to control the graft density and graft length. Graft copolymers often possess microphase separated morphologies and offer elastomeric properties. Dendrimers have traditionally been synthesized using Michael addition reactions, and in fact, Tomalia et al. synthesized the first dendrimer, poly(amido amine) (PAMAM) using Michael addition. Dendrimers and hyperbranched polymers, are interesting due to a plurality of functional groups. However, the absence of entanglements often limits the use of dendrimers to non-structural and mechanically non-demanding applications. Dendrimers based on Michael addition reactions are used in numerous applications, including biomedical applications and gene delivery.^{333,334}

³³³ Bielinska, A.; Kukowska-Latallo, J. F.; Johnson, J.; Tomalia, D. A.; Baker, J. R. Regulation of in vitro gene expression using antisense oligonucleotides or antisense expression plasmids transfected using starburst PAMAM dendrimers. *Nuc Acid Res* **1996**, *24*, 2176-82.

³³⁴ Kubasiak, L.; Tomalia, D. A., Cationic dendrimers as gene transfection vectors: Dendri-poly(amido amines) and dendri-poly(propyleneimines). In *Polymeric Gene Delivery*, Amiji, M. M., Ed. CRC Press: Boca Raton, FL, 2005; pp 133-57.

3.6.1 Dendrimers

Michael addition reactions are ideal for dendrimer synthesis due to the low probability of side reactions and mild reaction conditions. In the first dendrimer synthesis, dendritic poly(amido amine)s were synthesized via the alternating Michael addition of methyl acrylate to amine substrates (ammonia, $f = 3$; ethylenediamine, $f = 4$) and aminolysis of the resultant esters with excess ethylene diamine.³³⁵ As depicted in Figure 3.32, the PAMAM dendrimer synthesis is divergent, beginning from a small molecule core and enlarging as further generations are added. The high conversion and facile nature of the Michael addition led to nearly monodisperse individual dendrimer molecules as revealed using electron microscopy.³³⁶ The Michael addition was most efficient in methanol, while aprotic solvents led to incomplete alkylation of amine groups. *Retro*-Michael additions fragmented the dendrimer molecules at elevated temperature (80 °C) in solution.³³⁷

³³⁵ Tomalia, D.; Naylor, A. M.; Goddard, W. A. Starburst dendrimers: Molecular-level control of size, shape, surface chemistry. *Angew Chem Int Ed* **1990**, 29, 138-175.

³³⁶ Tomalia, D. A.; Baker, H.; Dewald, J.; Hall, M.; Kallos, G.; Martin, S.; Roeck, J.; Ryder, J.; Smith, P. Dendritic macromolecules: Synthesis of starburst dendrimers. *Macromolecules* **1986**, 19, 2466-8.

³³⁷ Tomalia, D. A.; Baker, H.; Dewald, J.; Hall, M.; Kallos, G.; Martin, S.; Roeck, J.; Ryder, J.; Smith, P. A new class of polymers: starburst-dendritic macromolecules. *Polym J* **1985**, 17, 117-32.

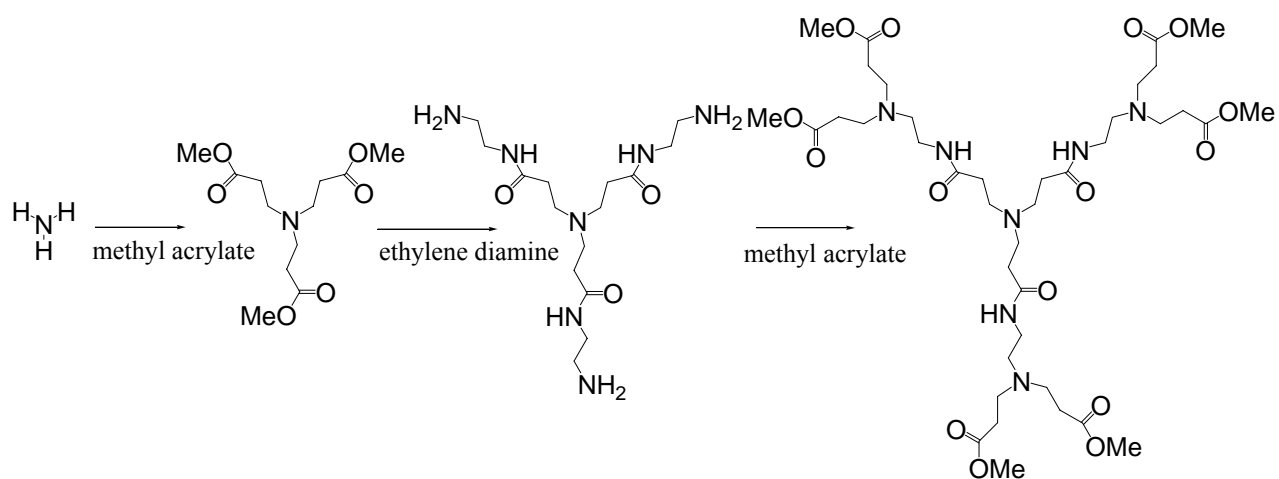


Figure 3.32. Divergent PAMAM dendrimer synthesis via alternating Michael addition and amidation.

PAMAM dendrimers are effective gene transfection agents due to the plurality of terminal amine groups available to complex with the negatively charged DNA phosphate backbone. In aqueous solution, protonation of the terminal amine groups produces a cationic charge that favors complexation with DNA. A DNA-polymer complex must have a net positive charge in order to pass through a cell membrane. The PAMAM dendrimers effectively transfected genes for β -galactosidase expression, luciferase expression, and also antisense genes that selectively suppress luciferase genes.³³⁸ PAMAM dendrimers received significant attention for effectiveness in gene transfection and numerous transfection studies were performed on diverse eukaryotic cell lines. Studies found increased transfection efficiency for higher generation dendrimers.³³⁹ Higher generations were necessary to obtain efficient coverage of DNA, as higher generations possessed sizes close to the histone octamer. Heating the dendrimers in aqueous solution led to fragmentation, likely through *retro*-Michael additions and solvolysis, which significantly improved transfection. In fact, a commercial gene transfection agent, Superfectin™, is based on fragmented PAMAM dendrimers. PAMAM dendrimers of numerous sizes possess very low cytotoxicity and in-vivo studies have also showed low toxicity.

Amine terminated PAMAM dendrimers were recently used to eliminate prion proteins from scrapie infected neuroblastoma cells.³⁴⁰ Higher generation PAMAM dendrimers were

³³⁸ Bielinska, A.; Kukowska-Latallo, J. F.; Johnson, J.; Tomalia, D. A.; Baker, J. R. Regulation of in vitro gene expression using antisense oligonucleotides or antisense expression plasmids transfected using starburst PAMAM dendrimers. *Nuc Acid Res* **1996**, *24*, 2176-82.

³³⁹ Kubasiak, L.; Tomalia, D. A., Cationic dendrimers as gene transfection vectors: Dendri-poly(amido amines) and dendri-poly(propyleneimines). In *Polymeric Gene Delivery*, Amiji, M. M., Ed. CRC Press: Boca Raton, FL, 2005; pp 133-57.

³⁴⁰ Supattapone, S.; Nguyen, H. O. B.; Cohen, F.; Prusiner, S. B.; Scott, M. R. Elimination of prions by branched polyamines and implications for therapeutics. *Proc Natl Acad Sci USA* **1999**, *96*, 14529-34.

more effective in removing the prion proteins and were most effective below pH 4, suggesting the importance of ammonium charge and activity in the lysosomal or endosomal regions. The importance of branching was demonstrated through the comparison of linear and branched poly(ethylene imine) controls. The ability to remove prions occurred at noncytotoxic dendrimer concentrations.

A second common dendrimer is poly(propylene imine) (PPI), marketed under the trade name Astramol™.³⁴¹ PPI dendrimers are accessed through the Michael addition of primary diamines with acrylonitrile followed by hydrogenation of the nitrile groups to amines and repeated reaction with acrylonitrile (Figure 3.33). First through fifth generation dendrimers are commercially produced in this manner. PPI dendrimers were recently synthesized with poly(propylene oxide) Jeffamine® cores, allowing greater flexibility and less steric congestion of the dendrimer molecules.³⁴² The terminal nitrile groups of poly(propylene imine) dendrimers are hydrolyzed under acidic conditions to obtain peripheral carboxylic acid functionality, but this often leads to degradation or discoloration of the polymer. Meijer et al. developed a route to carboxylic acid functional dendrimers via hydrogenation of the peripheral nitriles followed by the Michael addition of methyl acrylate and basic hydrolysis of the resultant ester functionalities.³⁴³ In contrast to PAMAM dendrimers, PPI dendrimers

³⁴¹ Froehling, P.; Brackman, J. Properties and applications of poly(propylene imine) dendrimers and poly(ester amide) hyperbranched polymers. *Macromol Symp* **2000**, 151, 581-9.

³⁴² Froimowicz, P.; Gandinib, A.; Strumia, M. New polyfunctional dendritic linear hybrids from terminal amine polyether oligomers (Jeffamine): synthesis and characterization. *Tet Lett* **2005**, 46, 2653-7.

³⁴³ van Duijvenbode, R. C.; Rajanayagam, A.; Koper, G. J. M.; Baars, M. W. P. L.; de Waal, B. F. M.; Meijer, E. W.; Borkovec, M. Synthesis and protonation behavior of carboxylate-functionalized poly(propyleneimine) dendrimers. *Macromolecules* **2000**, 33, 46-52.

have less potential for gene transfection and higher cytotoxicity.³⁴⁴ Lower toxicity was achieved with PPI dendrimers containing ether and ester linkages, synthesized by the Michael addition of alcohols to acrylonitrile, reduction of the nitrile, Michael addition to methyl acrylate, and reduction back to alcohol terminal groups.³⁴⁵

³⁴⁴ Kubasiak, L.; Tomalia, D. A., Cationic dendrimers as gene transfection vectors: Dendri-poly(amido amines) and dendri-poly(propyleneimines). In *Polymeric Gene Delivery*, Amiji, M. M., Ed. CRC Press: Boca Raton, FL, 2005; pp 133-57.

³⁴⁵ Krishna, T. R.; Jayaraman, N. Synthesis of poly(propyl ether imine) dendrimers and evaluation of their cytotoxic properties. *J Org Chem* **2003**, 68, 9694-704.

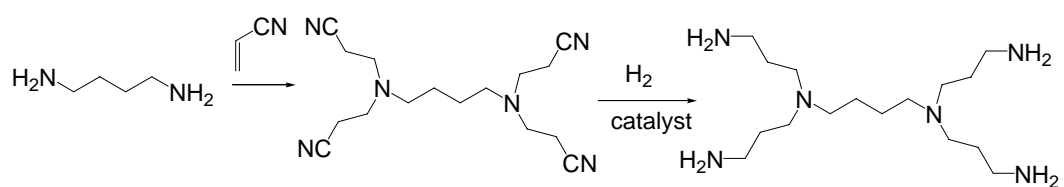


Figure 3.33. Synthesis of PPI dendrimers via alternating Michael addition and hydrogenation.

Majoral et al. developed novel dendrons containing Michael acceptors consisting of $\text{CH}_2=\text{CH}-\text{P}=\text{N}-\text{P}=\text{S}-(\text{O}-\text{R})_2$ or $\text{CH}_2=\text{CH}-\text{P}=\text{N}-\text{P}=\text{O}-(\text{O}-\text{R})_2$ groups at the dendrimer core. This allowed convergent synthesis of dendrimers via coupling of the dendrons through Michael addition with primary diamine donors (Figure 3.34).^{346,347}

³⁴⁶ Maraval, V.; Laurent, R.; Merino, S.; Caminade, A. M.; Majoral, J. P. Michael-type addition of amines to the vinyl core of dendrons 2. Application to the synthesis of multidendritic systems. *Eur J Org Chem* **2000**, 21, 3555-68.

³⁴⁷ Maraval, V.; Laurent, R.; Donnadiou, B.; Mauzac, M.; Caminade, A. M.; Majoral, J. P. Rapid synthesis of phosphorus-containing dendrimers with controlled molecular architectures: first example of surface-block, layer-block, and segment-block dendrimers issued from the same dendron. *J Am Chem Soc* **2000**, 122, 2499-511.

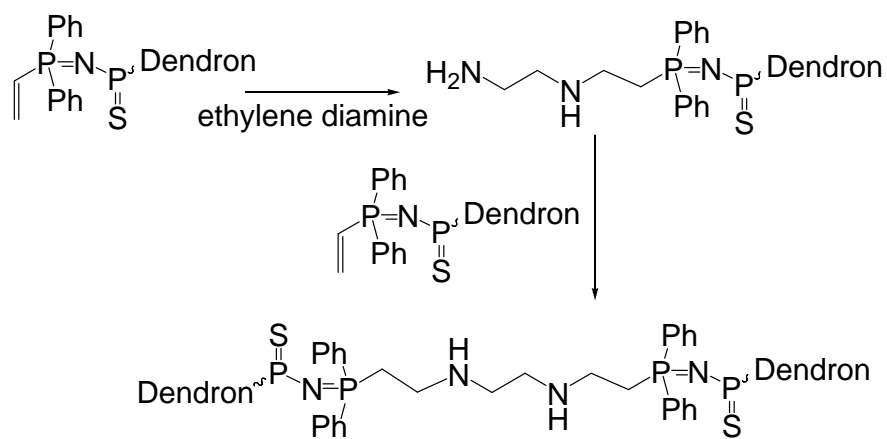


Figure 3.34. Convergent dendrimer synthesis via dendron core-linking Michael addition reactions.

Peripheral modification of dendrimers was also accomplished via Michael reactions with pendant Michael donors or acceptors. For instance, mesogenic cyanobiphenyl acrylates were introduced onto amine terminated poly(propylene imine) dendrimers resulting in liquid crystalline dendrimer molecules.³⁴⁸ Michael addition of acryloxyethyl methacrylate to amine terminated dendrimers resulted in photocrosslinkable dendrimer methacrylates.³⁴⁹ The Michael addition scheme was the only successful functionalization methodology as reaction with isocyanatoethyl methacrylate or acetoacetoxy methacrylate resulted in insoluble, crystalline products and reaction with methacrylic anhydride did not completely functionalize the terminal amines. The methacrylated dendrimers exhibited nearly quantitative cure reactions as determined through differential scanning calorimetry (DSC). In Figure 3.35, dendritic acrylate oligomers were also synthesized through the Michael addition of trimethylolpropane triacrylate (TMPTA) with ethylene diamine in a 5:1 ratio.^{350,351} The desired product possessed a TPMTA:EDA ratio of 4:1, however, network formation occurred under these conditions. The branched oligoacrylates resembled dendrimers with low viscosities and facile cure conditions using UV-photocuring techniques. Purification of these dendrimers was achieved primarily through precipitation.

³⁴⁸ Yonetake, K.; Masuko, T.; Morishita, T.; Suzuki, K.; Ueda, M.; Nagahata, R. Poly(propyleneimine) dendrimers peripherally modified with mesogens. *Macromolecules* **1999**, 32, 6578-86.

³⁴⁹ Moszner, N.; Volkel, T.; Liechtenstein, S. Synthesis, characterization and polymerization of dendrimers with methacrylic end groups. *Macromol Chem Phys* **1996**, 197, 621-31.

³⁵⁰ Xu, D. M.; Zhang, K. D.; Zhu, X. L. A novel dendritic acrylate oligomer: synthesis and UV curable properties. *J Appl Polym Sci* **2004**, 92, 1018-22.

³⁵¹ Xu, D. M.; Zhang, K. D.; Zhu, X. L. Synthesis and characterization of dendrimers from ethylene diamine and trimethylolpropane triacrylate. *J Macromol Sci Part A: Pure Appl Chem* **2005**, 42, 211-9.

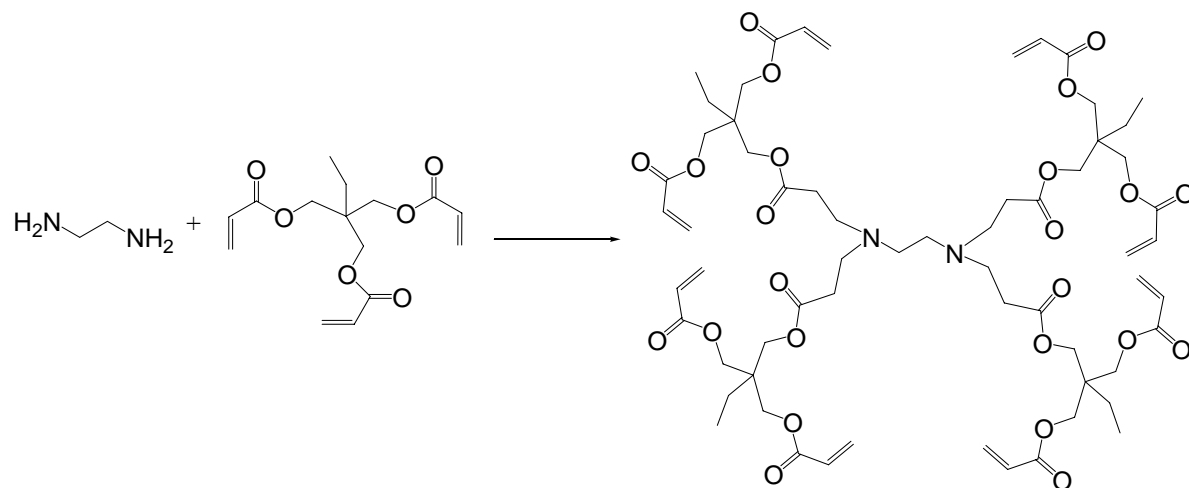


Figure 3.35. Crosslinkable dendrimer synthesis using Michael addition reactions.

3.6.2 Hyperbranched and Highly Branched Polymers

Hyperbranched polymers were initially developed as inexpensive, one-pot substitutes for dendrimers, but have developed a unique character over the last several years. Hyperbranched polymers were traditionally approached from asymmetric monomer synthesis (AB_n monomers). Difficult monomer synthesis is a major disadvantage of the AB_n method due to a lack of commercial AB_n monomer sources. Recently, $A_n + B_m$ approaches were used to synthesize hyperbranched polymers, enabling a much wider range of monomers and topologies. A further development is the use of oligomeric A_n or B_m monomers, resulting in “highly branched polymers”, which allows control of the molecular weight between branch points, an important parameter that affects degree of entanglement and has performance implications.³⁵² Michael addition reactions were successfully applied to both the AB_2 and $A_n + B_m$ strategies for hyperbranched polymer synthesis.

In a conventional AB_2 hyperbranching polymerization, Endo et al. conducted acetoacetylation of hydroxyethyl acrylate through a reaction with diketene.³⁵³ This produced an AB_2 monomer that was capable of producing hyperbranched Michael addition polymers in the presence of base catalyst (Figure 3.36). Polymerization of this novel monomer in the presence of DBU resulted in number average molecular weights between 2000 and 12000 g/mol with dispersities between 1.4 and 3.5 and degrees of branching between 43 and 83%. A high ratio of dendritic to linear units was observed, suggesting

³⁵² Unal, S.; Lin, Q.; Maurey, T. H.; Long, T. E. Tailoring the degree of branching: preparation of poly(ether ester)s via copolymerization of poly(ethylene glycol) oligomers (A_2) and 1,3,5-benzenetricarbonyl trichloride (B_3). *Macromolecules* **2005**, 38, 3246-54.

³⁵³ Kim, Y. B.; Kim, H. K.; Nishida, H.; Endo, T. Synthesis and characterization of hyperbranched poly(β -ketoester) by the Michael addition. *Macromol Mater Eng* **2004**, 289, 923-6.

greater reactivity of the *mono*-Michael adduct towards the acrylate group compared to the reactivity of the original acetoacetate group.

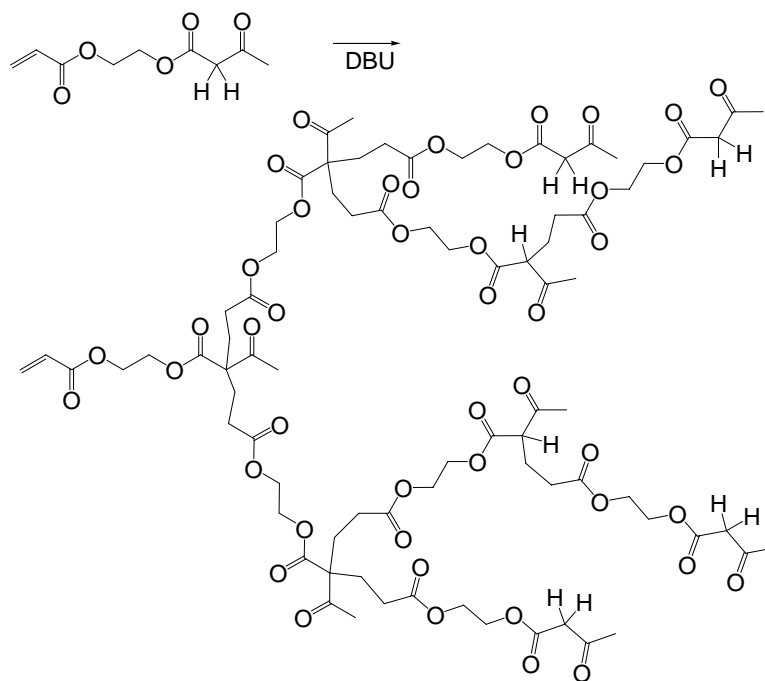


Figure 3.36. Hyperbranched polymer synthesis via AB₂ Michael addition polymerization.

Trumbo studied the step growth polymerization of low molar mass diacrylates (tripropylene glycol diacrylate) with bisacetoacetates³⁵⁴ and bisacetoacetamides.³⁵⁵ These systems formed branched structures due to the difunctionality of the acetoacetate group. Gelation of the reaction mixture was avoided with an excess of bisacetoacetate monomer and through conducting the reaction in solution with a relatively mild base catalyst (DBU). Weight average molecular weights as high as 437000 g/mol were observed, however broad dispersities ($M_w/M_n \sim 10$) were typical, which further suggested branching in this system. Decreases in molecular weight and dispersity with reaction time were observed during these polymerizations, suggesting the occurrence of a *retro*-Michael addition and subsequent equilibration.

Hyperbranched poly(aspartamide)s were synthesized from bismaleimides and aromatic triamines using the A_2+B_3 methodology.³⁵⁶ The reaction stoichiometry was limiting in bismaleimide, thus controlling the extent of the reaction and favoring secondary amine terminated products. The hyperbranched polymers exhibited degrees of branching near 0.51 and 0.69, high glass transition temperatures (~ 210 to 250 °C) as well as equivalent thermal stability to analogous linear polymers. In Figure 3.37, a tris(4-aminophenyl)phosphine oxide triamine was used to create polymers with higher thermal stability and also to allow degree of branching determination through ^{31}P NMR.

³⁵⁴ Trumbo, D. L. Michael addition polymers from 1,4- and 1,3-benzenedimethanol diacetoacetates and tripropylene glycol diacrylate. *Polym Bull* **1991**, 26, 265-70.

³⁵⁵ Trumbo, D. L. Michael addition polymers from bisacetoacetates II. 2,2-dimethyl-1,3-bis(acetoacetyl)-propanediol and *N,N*-bis(acetoacetyl)-1,4-piperazine. *Polym Bull* **1991**, 26, 481-5.

³⁵⁶ Liu, Y. L.; Tsai, S. H.; Wu, C. S.; Jeng, R. J. Preparation and characterization of hyperbranched polyaspartimides from bismaleimides and triamines. *J Polym Sci Part A: Polym Chem* **2004**, 42, 5921-8.

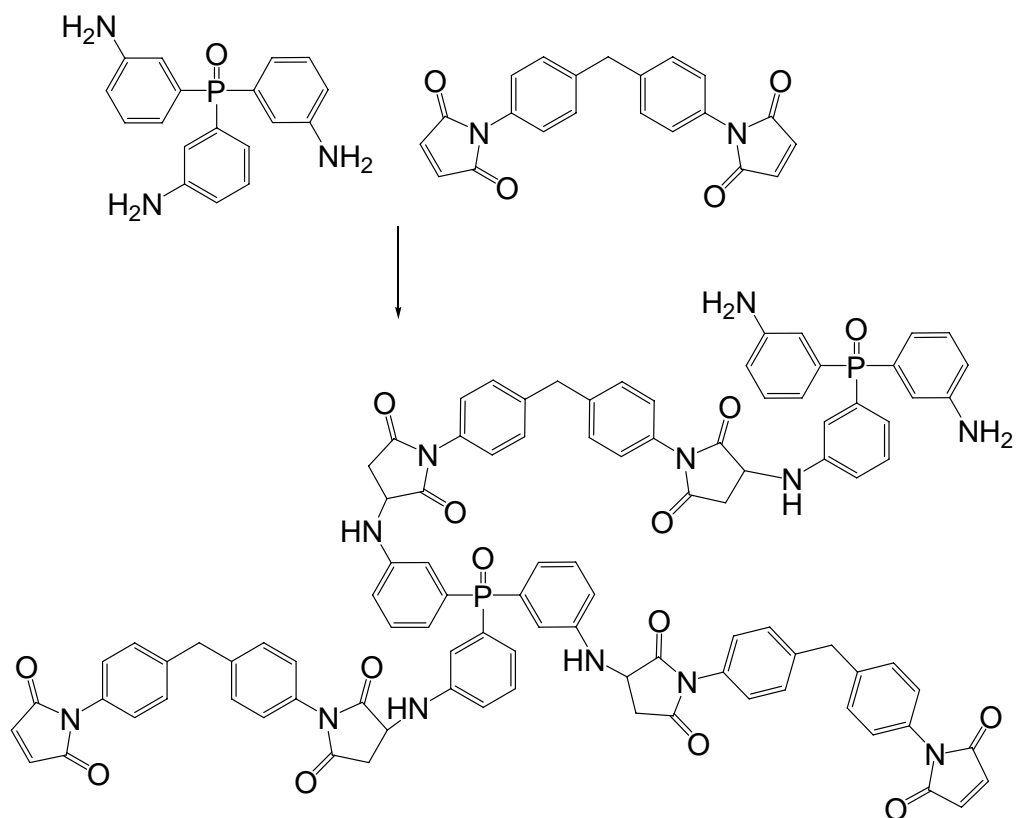


Figure 3.37. Hyperbranched poly(aspartamide)s via A₂ + B₃ polymerization.

Feng et al. studied hyperbranched poly(amino ester)s that were synthesized from piperazine and trimethylolpropane triacrylate in molar ratios ranging from 1:1.08 to 1:2.³⁵⁷ These hyperbranched polymers formed aggregates in acetone/acidic water, which were proposed to contain a hydrophobic acrylate rich core and a hydrophilic, protonated amine periphery. The aggregates were crosslinked using UV light via reaction of residual acrylate groups. The size of the aggregates (DLS, TEM) decreased upon crosslinking and were smaller for higher molecular weight polymers, suggesting a packing efficiency limitation with the higher molecular weight, more disperse, polymers. Enhanced aggregation of similar poly(amino ester)s was achieved through reaction of peripheral amine groups with long chain acyl halides.³⁵⁸

Wu et al. studied the effect of unequal functional group reactivity in a hyperbranching $A_2 + B_3$ system with a butanediol diacrylate A_2 and a trifunctional amine B_3 containing both primary ($f = 2$) and secondary ($f = 1$) amines (Figure 3.38).³⁵⁹ For an equimolar $A_2:B_3$ ratio, 1H NMR studies indicated that secondary amines were consumed prior to primary amines. The secondary amine that was formed from reaction of the primary amine and the acrylate group was not consumed, and thus a predominantly linear product was obtained despite the functionality of the monomers. The reactivity of the amines was secondary > primary >> formed secondary. If the $A_2:B_3$ ratio was increased, participation of the formed secondary

³⁵⁷ Tang, L.; Fang, Y.; Feng, J. Structure, solution aggregation and UV curing of hyperbranched poly(ester amine)s with terminal acrylate groups. *Polym J* **2005**, 37, 255-61.

³⁵⁸ Tang, L.; Fang, Y.; Tang, X. Influence of alkyl chains of amphiphilic hyperbranched poly(ester amine)s on the phase-transfer performances for acid dye and the aggregation behaviors at the interface. *J Polym Sci Part A: Polym Chem* **2005**, 43, 2921-30.

³⁵⁹ Wu, D.; Liu, Y.; He, C.; Chung, T.; Goh, S. Effects of chemistries of trifunctional amines on mechanisms of Michael addition polymerizations with diacrylates. *Macromolecules* **2004**, 37, 6763-70.

amine during the reaction of the primary amine occurred, thus resulting in a branched product. If the steric hindrance at the secondary amine position was increased, the primary amine was the most reactive and the reaction proceeded at the formed secondary amine during the reaction and again the product was branched. Thus, both the level of substitution of the amine groups and the stoichiometric ratio of the reactants controlled the degree of branching. Degrees of branching that ranged from 30 to 40% and weight average molecular weights as high as 23,500 g/mol were obtained.

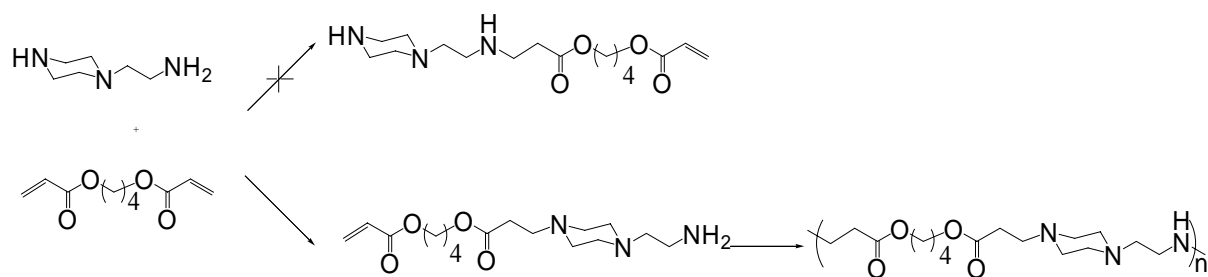


Figure 3.38. Hyperbranched poly(ester amine)s from A₂ + B₃ polymerization with unequal reactivity in the B₃ monomer functional groups.

Wu et al. also studied hyperbranched poly(amino ester)s that were synthesized using two equivalents of butanediol acrylate and one equivalent of 1-(2-aminoethyl)piperazine.³⁶⁰ Due to the higher reactivity of the secondary cyclic amine, the Michael addition with butanediol diacrylate occurred preferentially. The primary amino group reacted second, resulting in the in-situ generation of an AB₂ intermediate that undergoes a branching at the secondary amine formed from the primary amine. The ratio of R_h to R_g of 1.0 as measured by SAXS and DLS demonstrated the hyperbranched nature of the polymers. The hyperbranched polymers had number average molecular weights of 29000 to 38000 g/mol and dispersities of 3.4 to 3.7.

In similar work, Gao et al. synthesized hyperbranched polymers from diethanolamine and methyl acrylate.³⁶¹ The reaction proceeded through an initial Michael addition reaction to form an ester diol AB₂ monomer in-situ that self-condensed at elevated temperature (150 °C) through transesterification in the presence of a zinc acetate catalyst. Number average molecular weights as high as 268000 g/mol were observed with a polydispersity of 2.4. Crosslinking occurred when the temperature in the second stage exceeded 160 °C, whereas lack of polycondensation occurred if the temperature was less than 120 °C. The degree of branching of these polymers was roughly 55%. These polymers degraded rapidly in water to form self-buffered pH 7 solutions, suggesting them as good candidates for drug delivery.

Hyperbranched poly(amido amine) hydrochloride polyelectrolytes were synthesized through the Michael addition polymerization of AB₂ monomers based on ammonium alkyl

³⁶⁰ Wu, D.; Liu, Y.; Chen, L.; He, C.; Chung, T. S.; Goh, S. H. "2A₂ + BB'B" approach to hyperbranched poly(amino ester)s. *Macromolecules* **2005**, 38, 5519-25.

³⁶¹ Gao, C.; Xu, Y.; Yan, D.; Chen, W. Water-soluble degradable hyperbranched polyesters: novel candidates for drug delivery? *Biomacromolecules* **2003**, 4, 704-12.

acrylamides, as shown in Figure 3.39.³⁶² The lack of nucleophilicity of the ammonium group toward the acrylamide functionality required the use of high temperatures (210 °C) in order to drive the polymerization. It was postulated that a small equilibrium concentration of free amine that exists at these high temperatures undergoes the Michael addition. The shorter alkylene spacer (n = 2) between the acrylamide group and the ammonium group resulted in faster reaction, and an intramolecular deprotonation through a six membered cyclic transition state was proposed. Model reactions suggested that the ammonium group reacts twice with acrylamide functionalities, resulting in a highly branched product. ¹⁵N NMR was used to characterize the degree of branching in these materials. Signals from linear units were not observed, corroborating the highly branched nature of the polymer. This methodology is a more facile route to hyperbranched polymers resembling PAMAM dendrimers.

³⁶² Hobson, L. J.; Feast, W. J. Poly(amido amine) hyperbranched systems: synthesis, structure and characterization. *Polymer* **1999**, 40, 1279-97.

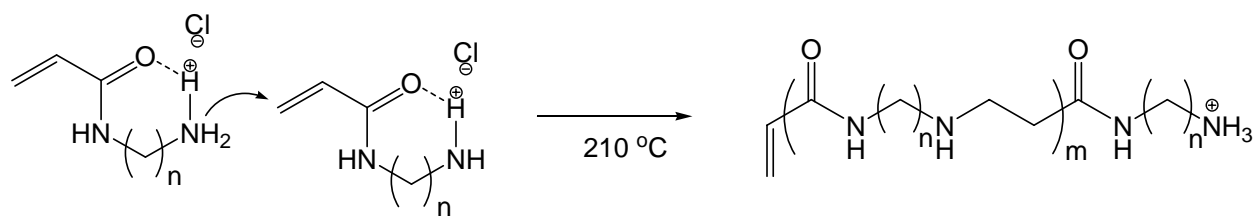


Figure 3.39. Homopolymerization of an AB₂ poly(amido amine) monomer.

Kadokawa et al. studied the triphenylphosphine initiated Michael addition polymerization of 2,2-bis(hydroxymethyl)propyl acrylate to yield phosphonium containing hyperbranched polymers of 1,200 to 2,700 g/mol, as shown in Figure 3.40.³⁶³ This is one of the few examples of oxygen based nucleophiles involved in a Michael addition polymerization. Degrees of branching near 50% were obtained. Similar polymers were produced through initiation using sodium hydride. The poor quality of the oxygen nucleophile for Michael addition is evident in the reaction temperatures (80 to 100 °C, with free radical inhibitors).³⁶⁴

³⁶³ Kadokawa, J.; Kaneko, Y.; Yamada, S.; Ikuma, K.; Tagaya, H.; Chiba, K. Synthesis of hyperbranched polymers via proton transfer polymerization of acrylate monomer containing two hydroxy groups.

Macromol Rapid Commun **2000**, 21, 362-8.

³⁶⁴ Kadokawa, J.; Ikuma, K.; Tagaya, H. Polymerization of acrylate monomer containing two hydroxyl groups initiated with sodium hydride for synthesis of hyperbranched polymer. *J Macromol Sci Pure Appl Chem* **2002**, A39, 879-88.

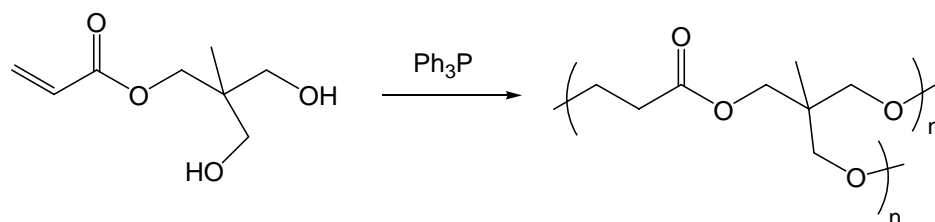


Figure 3.40. Homopolymerization of an AB₂ poly(ester ether) monomer.

Highly branched gene transfection agents were synthesized through the reaction of low molecular weight linear PEI with PEG diacrylate.³⁶⁵ The polymers clearly did not represent linear topologies due to branching in the PEI as well as reaction at multiple amine sites along the polymer backbone. The presence of ester groups in the polymers facilitated degradation. The half-lives of the polymers in PBS at 37 °C were approximately 8 d. The polymers demonstrated complex formation with plasmid DNA and transfection studies were performed. Branched gene transfection agents were also synthesized via reaction of trimethylolpropane triacrylate with primary amines such as *N,N*-dimethylethylenediamine.³⁶⁶ Polyplex formation with plasmid DNA was verified with dynamic light scattering and transfection into various human and mouse cell lines exhibited transfection efficiencies similar to poly(ethylene imine). The branched nature of the poly(amino ester)s slowed polymer degradation and hence controlled the release of the plasmid DNA. The branched poly(amino ester)s showed little or no cytotoxicity.

3.6.3 Graft Copolymers

Graft copolymers are synthesized through numerous routes including chain or step growth polymerization of macromonomers and post-polymerization grafting. Ferruti et al. examined graft copolymer synthesis using poly(amido amine)s.³⁶⁷ PEG chains with weight

³⁶⁵ Park, M. R.; Han, K. O.; Han, I. K.; Cho, M. H.; Nah, J. W.; Choi, Y. J.; Cho, C. S. Degradable polyethylenimine-*alt*-poly(ethylene glycol) copolymers as novel gene carriers. *J Contr Rel* **2005**, 105, 367-80.

³⁶⁶ Kim, T.; Seo, H. J.; Choi, J. S.; Yoon, J. K.; Baek, J.; Kim, K.; Park, J. S. Synthesis of biodegradable cross-linked poly(β -amino ester) for gene delivery and its modification, inducing enhanced transfection efficiency and stepwise degradation. *Bioconjugate Chem* **2005**, 16, 1140-8.

³⁶⁷ Vansteenkiste, S.; Schacht, E.; Ranucci, E.; Ferruti, P. Synthesis of a new family of poly(amido-amine)s carrying poly(oxyethylene) side chains. *Makromol Chem* **1992**, 193, 937-43.

average molecular weight of 750 g/mol were incorporated into poly(amido amine) backbones using monoamine terminated PEG as a comonomer. As a second route, PEG-NH₂ was first reacted with excess bisacrylamide monomer to obtain a PEG bisacrylamide, which was polymerized with piperazine. In both cases, vapor pressure osmometry indicated that the molecular weights obtained were quite low (~3000 g/mol). Ferruti concluded that the reactivity of the PEG-NH₂ in the polymerization was lower than typical small molecule amines. Ferruti et al. also studied poly(amido amine)s grafted to polyethylene via a post-polymerization strategy, although Michael addition was not involved in the coupling.³⁶⁸

Jerome et al. utilized γ -acryloxy- ϵ -caprolactone as a graftable comonomer in copolymerizations with ϵ -caprolactone.³⁶⁹ In Figure 3.41, pendant acrylate groups were introduced into poly(ϵ -caprolactone), permitting grafting of thiol terminated oligomeric PEG ($M_n = 900$ g/mol). The Michael addition reaction of various thiols (mercaptoacetic acid and triphenylmethane thiol) with PEG-acrylate model compounds proceeded to completion. However, conversions of only 65% and 70% were obtained with PEG-thiol and mercaptoacetic acid, respectively, in grafting studies with poly(γ -acryloxy- ϵ -caprolactone-*co*- ϵ -caprolactone).

³⁶⁸ Martuscelli, E.; Nicolais, L.; Riva, F.; Ferruti, P.; Provenzale, L. Synthesis and characterization of a potentially non-thrombogenic polyethylene-poly(amido amine) graft copolymer. *Polymer* **1978**, *19*, 1063-6.

³⁶⁹ Rieger, J.; van Butsele, K.; Lecomte, P.; Detrembleur, C.; Jerome, R.; Jerome, C. Versatile functionalization and grafting of poly(ϵ -caprolactone) by Michael-type addition. *Chem Comm* **2005**, *2*, 274-6.

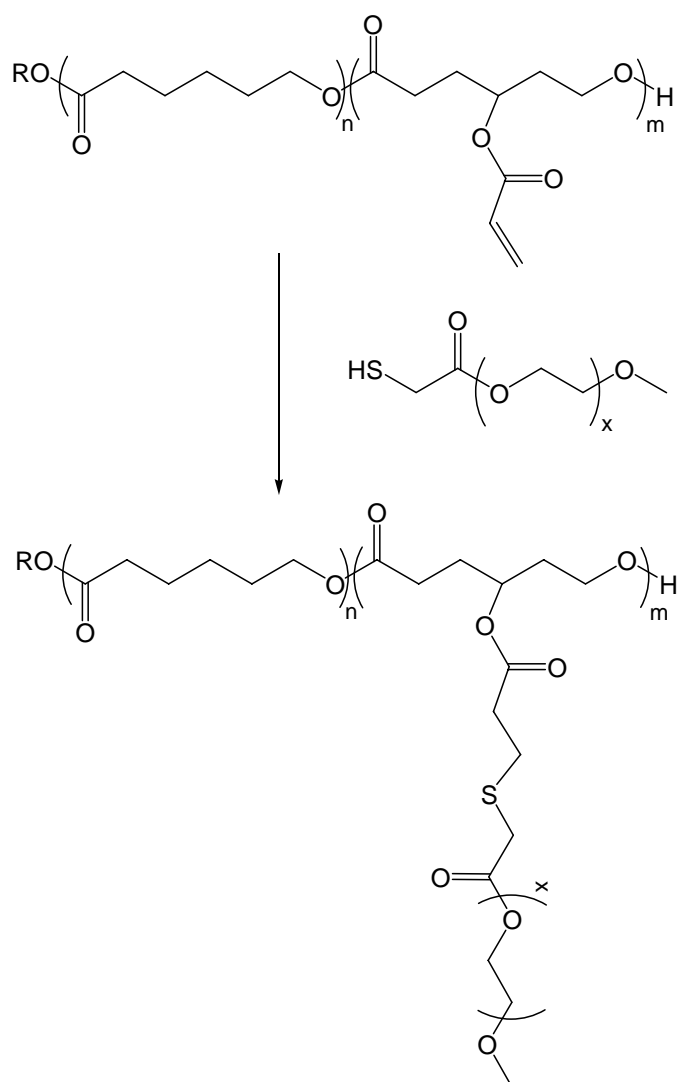


Figure 3.41. Graft copolymerization via grafting of thiol terminated PEG to pendant acryloxy side groups on a poly(ϵ -caprolactone) derivative.

Much work was done in the area of “grafting to” syntheses utilizing the Michael addition, especially in the case of biopolymers such as chitin and chitosan. These materials typically possess poor solubility, which is improved through grafting techniques. Modification of chitosan with poly(amido amine) dendrimers was achieved by reacting chitosan surface amine groups with methyl acrylate followed by alternate reactions with ethylene diamine and further methyl acrylate.³⁷⁰ The heterogeneity and steric hindrance of the backbone resulted in imperfect dendrimers. Grafting of living cationic poly(methyl oxazoline) and poly(isobutyl vinyl ether) onto the pendant amine groups of the grafted poly(amido amine) dendrimers was achieved successfully. Modification of chitin with small molecules was also achieved through Michael addition to pendant amine groups. Reaction with acrylonitrile yielded cyanoethylated chitin³⁷¹ and reaction with ethyl acrylate afforded ester-containing chitin³⁷² (Figure 3.42).

³⁷⁰ Tsubokawa, N.; Takayama, T. Surface modification of chitosan powder by grafting of 'dendrimer-like' hyperbranched polymer onto the surface. *React Funct Polym* **2000**, 43, 341-50.

³⁷¹ Tokura, S.; Nishi, N.; Nishimura, S.; Ikeuchi, Y. Studies on chitin X. Cyanoethylation of chitin. *Polym J* **1983**, 15, 553-6.

³⁷² Aoi, K.; Seki, T.; Okada, M.; Sato, H.; Mizutani, S.; Ohtani, H.; Tsuge, S.; Shiogai, Y. Synthesis of a novel *N*-selective ester functionalized chitin derivative and water-soluble carboxyethylchitin. *Macromol Chem Phys* **2000**, 201, 1701-8.

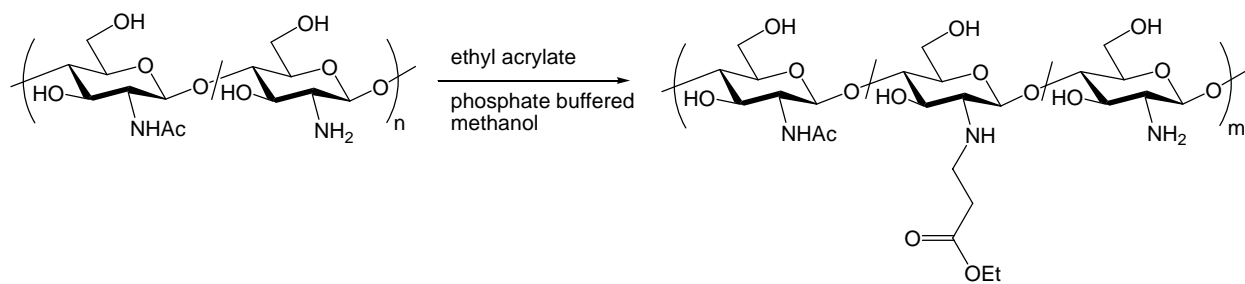


Figure 3.42. Modification of chitin via Michael addition reaction with ethyl acrylate.

3.7 Novel Networks via the Michael Addition Reaction

Network polymers that are synthesized via Michael addition reactions offer applications in diverse areas such as drug delivery systems, high performance composites, and coatings. Networks are often synthesized through a combination of Michael addition step growth chemistry combined with chain growth polymerization using photoinitiated radical or anionic processes. The Michael addition is suited to the formation of well-defined networks due to the commercial availability or facile synthesis of narrow molecular weight distribution functional oligomers. Commercially available reactive oligomers include PEG diacrylate and numerous oligomeric diamines such as Jeffamine[®]. Several classes of Michael addition networks are currently of interest.

3.7.1 Bismaleimide Networks and Composite Materials

Currently, bismaleimide based networks are used in high performance fiber-reinforced composite materials³⁷³ and also in thermoset resins. These materials have applications in the aerospace industry due to their high temperature strength, mechanical robustness, and low density.³⁷⁴ In the absence of other components, bismaleimides crosslink through chain growth type reactions at high temperature to form highly crosslinked, high-T_g networks. Vitrification in these systems leads to incomplete conversion of maleimide groups. Brittleness is the primary drawback of these homopolymerized networks. Efforts to reduce the crosslink density and hence the brittleness of these thermosets have involved Michael

³⁷³ Fry, C. G.; Lind, A. C. Curing of bismaleimide polymers: a solid-state ¹³C-NMR study. *New Polym Mater* **1990**, 2, 235-54.

³⁷⁴ Curliss, D. B.; Cowans, B. A.; Caruthers, J. M. Cure reaction pathways of bismaleimide polymers: a solid-state ¹⁵N NMR investigation. *Macromolecules* **1998**, 31, 6776-82.

addition chain extension reactions with primary or secondary diamines to consume some of the maleimide functional groups.³⁷⁵ The chain extension process results in greater toughness and improved mechanical properties for composites. The introduction of diamines such as methylene dianiline (MDA) causes a low temperature Michael addition polymerization (<180 °C) during initial curing, followed on further heating (180 to 220 °C) with a crosslinking homopolymerization of the maleimide groups (Figure 3.43).^{376,377} Under certain conditions, secondary amines formed during the initial Michael addition undergo further Michael addition crosslinking with maleimide groups. Hyperbranched amine terminated polyamides were also investigated as components of bismaleimide networks, successfully improving the toughness of these systems.³⁷⁸

³⁷⁵ Wu, C. S.; Liu, Y. L.; Chiu, Y. S. Synthesis and characterization of new organosoluble polyaspartamides containing phosphorus. *Polymer* **2002**, 43, 1773-9.

³⁷⁶ Curliss, D. B.; Cowans, B. A.; Caruthers, J. M. Cure reaction pathways of bismaleimide polymers: a solid-state ¹⁵N NMR investigation. *Macromolecules* **1998**, 31, 6776-82.

³⁷⁷ Baek, J. B.; Ferguson, J. B.; Tan, L. S. Room-temperature free-radical-induced polymerization of 1,1'-(methylenedi-1,4-phenylene)bismaleimide via a novel diphenylquinoxaline-containing hyperbranched aromatic polyamide. *Macromolecules* **2003**, 36, 4385-96.

³⁷⁸ Kumar, A. A.; Alagar, M.; Rao, R. M. V. G. K. Synthesis and characterization of siliconized epoxy-1, 3-bis(maleimido)benzene intercrosslinked matrix materials. *Polymer* **2002**, 43, 693-702.

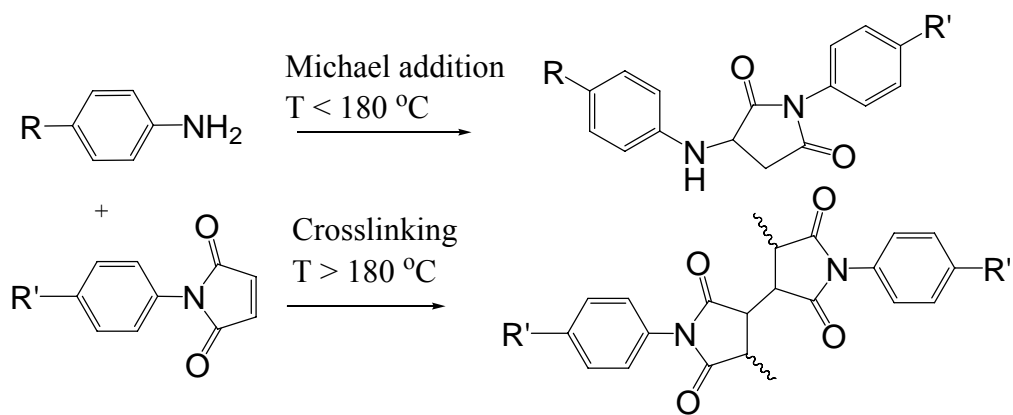


Figure 3.43. Crosslinking of bismaleimide networks via a combination of Michael addition and maleimide homopolymerization.

Kumar et al. incorporated bismaleimide crosslinking systems into silicon-containing epoxy resin networks.³⁷⁹ The bismaleimides increased the flexural and tensile modulus, but decreased fracture toughness of the epoxy networks by introducing a more rigid, higher T_g component. This network reinforcement was due to the thermal cure and Michael addition reactions between the bismaleimide and the amines from the epoxy resin and the added diamine.

Bismaleimide networks are useful as NLO materials as well as composites due to their high glass transition temperatures and crosslink densities. These features are attractive for NLO materials for maintenance of the chromophore orientation. Furthermore, the absence of volatile by-products during cure allows poling during this process. Wu et al. synthesized a diamine NLO chromophore and incorporation into bismaleimide networks resulted in nonlinear optical coefficients as high as $d_{33} = 60$ pm/V at 1064 nm.³⁸⁰ Upon heating, the second harmonic generation (SHG) was stable to 120 °C, although the cure process was continued 250 °C in order to maximize crosslinking. Maintenance of the poling field during the cooling process maximized the NLO properties.

3.7.2 Carbon Michael Addition Networks Utilizing Acetoacetate Chemistry

Considerable interest in Michael addition networks from acetoacetate and acrylate precursors has recently emerged. These networks are interesting due to the relatively low toxicity of the components and their room temperature processing in the absence of UV

³⁷⁹ Kumar, A. A.; Alagar, M.; Rao, R. M. V. G. K. Synthesis and characterization of siliconized epoxy-1, 3-bis(maleimido)benzene intercrosslinked matrix materials. *Polymer* **2002**, 43, 693-702.

³⁸⁰ Wu, W.; Zhang, Z.; Zhang, X. Synthesis of NLO diamine chromophore and its use in the preparation of functional polyimides. *Des Mon Polym* **2004**, 5, 423-34.

radiation. Furthermore, functionalization of common polyols with the acetoacetate group is achieved through transesterification with *tert*-butylacetoacetate³⁸¹ or reaction with diketene precursors³⁸² providing a facile route to crosslinkable precursors from a wide variety of hydroxyl containing feedstocks.

Room temperature thermosetting coatings is one of the primary applications of Michael addition networks. The Michael addition mechanism is advantageous as neither UV radiation nor heat are required, both of which could be deleterious to the substrate and require additional processing equipment. The base catalyzed carbon Michael addition of acetoacetylated resins to acrylate acceptors, as depicted in Figure 3.44, is an ideal route to crosslinked networks due to the difunctionality of the acetoacetate group and the absence of undesirable toxic amine and malodorous thiol nucleophiles in industrial processes. Acrylic monomers and oligomers are useful candidates for the formation of coatings and adhesives with highly reduced volatile organic compounds (VOCs) and improved material performance properties. Although UV curing is not necessary for network formation, the presence of photocrosslinkable groups in these systems allows tandem Michael and radical curing mechanisms.

³⁸¹ Witzeman, J. S.; Nottingham, W. D. Transacetoacetylation with *tert*-butyl acetoacetate: synthetic applications. *J Org Chem* **1991**, 56, 1713-8.

³⁸² Clemens, R. J.; Hyatt, J. A. Acetoacetylation with 2,2,6-trimethyl-4H-1,3-dioxin-4-one: A convenient alternative to diketene. *J Org Chem* **1985**, 50, 2431-5.

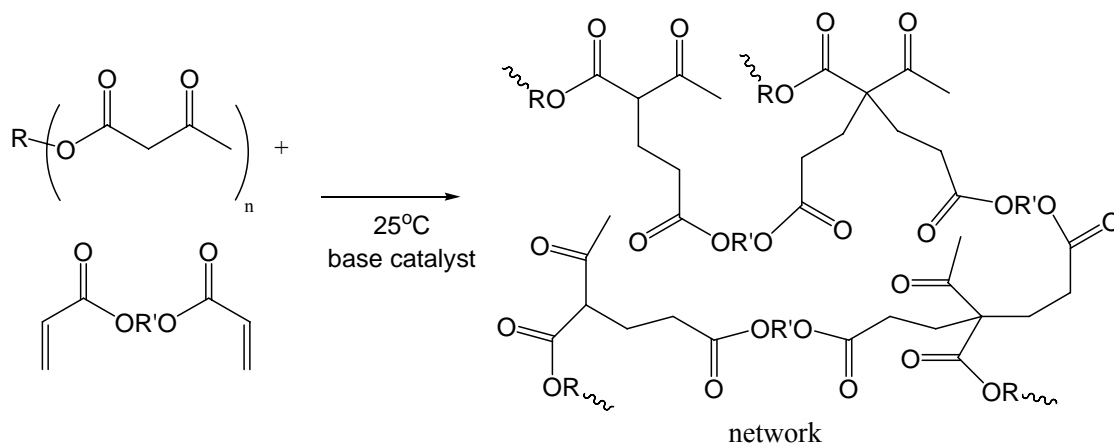


Figure 3.44. Carbon-Michael addition polymerization of acetoacetates with acrylates catalyzed by bases for network synthesis.

Clemens and Rector studied the carbon Michael addition reaction between model compounds, and concluded that the reaction mechanism involved an equilibrium deprotonation of the acetoacetate and subsequent rate limiting addition of the enolate to the acrylate group.³⁸³ Thus, the rate of the reaction was unaffected by the acetoacetate concentration but was directly proportional to the base catalyst concentration. The effect of various catalysts was investigated and as expected, higher basicity led to faster reaction kinetics. Typical base catalysts included DBU and TMG as well as hydroxide and methoxide bases. A striking difference, however, was observed in the degree to which bisadducts of acrylates with acetoacetates formed as a function of catalyst. Amidine and guanidine bases resulted in higher formation of bisadducts while monoadducts were favored by methoxide and hydroxide bases. Weaker bases such as triethylamine were not strong enough to deprotonate the acetoacetate groups and did not catalyze the Michael addition reaction effectively.

Clemens and Rector prepared crosslinked coatings consisting of randomly functionalized acetoacetylated precursors such as methyl methacrylate / acetoacetyloxyethyl methacrylate random copolymers with low molar mass multiacrylates such as trimethylolpropane triacrylate.³⁸³ The level of functionality of the methacrylate copolymers strongly influenced cure times, with a doubling of the acetoacetate functionality resulting in a 75% reduction in cure time. Acetoacetylated cellulose was also investigated, and the more rigid character of the polymer coupled with the lack of a spacer between the backbone and the acetoacetate groups resulted in slower cure reactions. One disadvantage of the Michael

³⁸³ Clemens, R. J.; Rector, F. D. A comparison of catalysts for crosslinking acetoacetylated resins via the Michael reaction. *J Coat Tech* **1989**, 61, 83-91.

crosslinked coatings was hydrolytic instability that was attributed to hydrolysis of the ester linkages in the presence of the base catalyst. Heat treatments reduced the hydrolytic instability of the network.

Marsh described the use of high solids acetoacetate-containing resins for coatings applications.³⁸⁴ High solids polyester resins containing hydroxyl groups were synthesized and acetoacetylated to various levels. It was found that increasing levels of acetoacetyl groups lowered the T_g of the polyester resins significantly to yield solvent-free low viscosity resins. The crosslinking of the pendant acetoacetyl groups using Michael type reactions with electron deficient olefins and DBU base catalyst (pH = 12.6) afforded formaldehyde- and isocyanate-free room temperature curable coatings.

Tung published a review on the performance of coatings made from multifunctional acrylate resins containing reactive diluents and acid blocked catalysts and compared them to two-package polyurethanes.³⁸⁵ The use of a formic acid neutralized DBU catalyst yielded better pot life and humidity resistance of the coatings when compared to the highly basic DBU catalyst. It was found that incorporation of 10 to 15 mol% of a reactive diluent such as 2,2,4-trimethyl-1,3-pentane-bis(acetoacetate) resulted in low VOC coatings with desirable ultimate properties. Various multifunctional acrylate crosslinkers were investigated to determine the influence of crosslinker functionality on the resulting resin properties. A mixture of tri- and tetraacrylates produced the best hardness, flexibility, solvent resistance, humidity resistance, adhesion, and weatherability compared to the triacrylates or

³⁸⁴ Marsh, S. J. Acetoacetate chemistry- crosslinking versatility for high-solids coatings resins. *Am Chem Soc, Div Polym Chem: Polym Prepr* **2003**, 44, 52-3.

³⁸⁵ Tung, C. C. Recent advances in isocyanate free coatings: use of acetoacetylated polymers in Michael crosslinking technology. *Surface Coatings, Australia* **1999**, 36, 10-15.

hexaacrylates.

3.7.3 Curing Mechanisms Involving Michael Addition with Photocrosslinking or Sol-Gel Chemistry

Cure mechanisms using a combination of Michael addition and photoinitiated radical curing are currently of interest due to higher crosslink densities and functional group conversions. The use of multifunctional acrylate monomers in the carbon Michael addition networks is ideal for photocrosslinking. Residual acrylate dangling ends must be limited to maximize chemical and physical durability. Moszner and Rheinberger synthesized networks from multiacrylates such as PEG diacrylates, trimethylolpropane triacrylate, and pentaerythritol tetraacrylate with bisacetoacetates such as PEG bis(acetoacetate) and hexanediol bis(acetoacetate) using DBN base catalyst.³⁸⁶ Isothermal DSC studies revealed less than 25% of the double bonds were consumed via Michael addition during cure. The conversion of acrylate groups increased for longer, more flexible, spacers to approximately 71%. Subsequent photocuring of the Michael addition networks using camphorquinone/*N*-(2-cyanoethyl)-*N*-methylaniline resulted in dramatically improved hardness and conversion of the acrylate groups. Moy et al. developed photocrosslinked networks from crosslinkable oligomers that were synthesized using Michael addition with an excess of multiacrylates relative to acetoacetate precursors.³⁸⁷ The Michael addition of

³⁸⁶ Moszner, N.; Rheinberger, V. Reaction behavior of monomeric β -ketoesters, 4) Polymer network formation by Michael reaction of multifunctional acetoacetates with multifunctional acrylates. *Macromol Rapid Commun* **1995**, 16, 135-8.

³⁸⁷ Moy, T. M.; Hilliard, L.; Powell, D.; Loza, R. Liquid oligomers containing unsaturation. US Patent 5,945,489, 1999.

acetoacetoxyethyl methacrylate with multifunctional acrylates is another route to photocrosslinkable methacrylate oligomers. The ketone-containing oligomers were capable of self-initiation in UV light due to Norrish type cleavage reactions. Klee et al. conducted Michael addition using diamines and acryloxyethyl methacrylate to create crosslinkable branched multimethacrylate oligomers for dental composites with lower shrinkage upon photocrosslinking.³⁸⁸ Dammann and coworkers demonstrated the formation of liquid oligomeric Michael adducts by reacting di-, tri- and tetraacrylates with ethyl acetoacetate in a specific ratio in the presence of catalytic amounts of epoxide and quaternary ammonium salt. These compositions were further crosslinked to obtain coatings, laminates, and adhesives.³⁸⁹

Pavlinec and Moszner further studied crosslinked networks from poly(propylene glycol) bis(acetoacetate) or pentaerythritol tetrakis(acetoacetate) and pentaerythritol tetraacrylate cured with DBN.³⁹⁰ In these Michael addition networks, a 2:1 ratio of acrylate to acetoacetate was studied. The residual acrylate groups in the networks were studied using FTIR, following the acrylate vinyl absorbance at 810 cm^{-1} . The concentration of residual unreacted acrylate groups was lowest for networks that were prepared using poly(propylene glycol) bis(acetoacetate)s due to the molecular mobility and long distance between crosslink points. Higher conversion of reactive functional groups for longer precursors was also

³⁸⁸ Klee, J. E.; Neidhart, F.; Flammersheim, H. J.; Mulhaupt, R. Monomers for low shrinking composites, 2a. Synthesis of branched methacrylates and their application in dental composites. *Macromol Chem Phys* **1999**, 200, 517-23.

³⁸⁹ Dammann, L. G.; Gould, M. L. Liquid uncrosslinked Michael addition oligomers prepared in the presence of a catalyst having both an epoxy moiety and a quaternary salt. US Patent 6,706,414, 2004.

³⁹⁰ Pavlinec, J.; Moszner, N. Photocured polymer networks based on multifunctional β -ketoesters and acrylates. *J Polym Sci Part A: Polym Chem* **1997**, 10, 165-78.

observed in photocrosslinking studies of diacrylate oligomers.³⁹¹ Ambient temperature aging and thermal postcure treatments to 200 °C increased the conversion of acrylate groups from 88% to nearly 97%. The gel fractions that were obtained for the Michael addition networks ranged from 87% to 94%. The combination of Michael addition curing with free radical photocuring was also investigated with the addition of photoinitiators, excess pentaerythritol tetraacrylate, and PEG dimethacrylate monomers to selected compositions. The stability of the methacrylate against Michael addition prevented interference between the two cure mechanisms performed in a stepwise manner, beginning with a dark Michael cure and ending with the photocure. In the photocured systems, lower viscosity during the Michael addition stage was attributed to the additional PEG dimethacrylate monomer and excess acrylate monomer. This was postulated to improve the cure process by improving molecular mobility and homogeneity.

Michael reactions between multifunctional acrylates and acetoacetates have found widespread applications in the formation of radiation curable coatings, printing ink formulations, and adhesives. UV curable ink formulations have gained importance as a substitute to solvent-based ink systems. Currently available UV curable ink formulations exhibit rapid curing under commercial line speeds, however, large quantities of photoinitiator such as benzophenone are required to ensure complete curing throughout the thickness of the film for printing applications. These photoinitiators are known to be toxic, expensive and also cause odor and color in the material. In order to overcome this issue, current studies have involved the use of liquid oligomeric Michael adducts formed from multifunctional

³⁹¹ Kurdikar, D. L.; Peppas, N. A. A kinetic study of diacrylate photopolymerizations. *Polymer* **1994**, 35, 1004-11.

acrylates by reaction with Michael donors such as acetoacetate compounds, which are amenable to further crosslinking under UV irradiation.³⁹² Through the incorporation of suitable additives such as acrylic monomers and oligomers, vinyl monomers, vinyl ethers, and primary and secondary amines, ink formulations were modified to obtain rheological and adhesion characteristics that were desirable for printing applications on many different kinds of substrates.

Recently Liu et al. described the formation of renewable and environmentally benign wood adhesives based on derivatized soy protein using the Michael addition crosslinking approach.³⁹³ Soy proteins used as renewable wood adhesives suffer from low shear strength and moisture resistance. In order to improve the properties of the adhesive, the authors first maleated the soy protein isolates (SPI) using maleic anhydride, which was then reacted with poly(ethylene imine) via Michael addition. Wood composites that were bonded with adhesive exhibited shear strength of 7.0 MPa as compared to 2.0 MPa of those bonded using SPI. In addition the joints also gained water resistance.

In addition to the application of the Michael addition in the formation of crosslinked coatings, the formation of reactive intermediates through Michael additions which are subsequently crosslinked using other mechanisms yields useful coatings and adhesives. This strategy has often involved sol-gel chemistry of the Michael adducts to form networks. For example, Wilkes et al. have reported the formation of bis- and tris(maleimide)

³⁹² Narayansarathy, S.; Gould, M.; Zaranec, A.; Hahn, L. Radiation-curable inks and coatings from novel multifunctional acrylate oligomers. *Technical Conference Proceedings-UV & EB Technology Expo & Conference, Charlotte NC, May 2004*, 447-59.

³⁹³ Liu, Y.; Li, K. New wood adhesive based on modified soy protein. *Abstracts of Papers, 229th ACS National Meeting, Cell-143, March 2005*.

functionalized trialkoxysilanes by Michael addition reaction between 3-aminopropyl triethoxysilanes and corresponding maleimides.³⁹⁴ The functionalized silanes were crosslinked via sol-gel methods and used as protective coatings on polycarbonate substrates exhibiting enhanced abrasion resistance. Tilley et al. recently described the use of the Michael addition reaction for the preparation of acrylate-functionalized silane coupling agents to introduce acrylate functionality to colloidal silica particles.³⁹⁵ Such acrylate functionalized silica particles were used as toughness enhancers for UV-curable acrylic coatings. Incorporation of these functionalized silica particles into a wide variety of organic matrices such as polyesters, epoxies, and polyurethanes was demonstrated. Such inorganic oxide modified coatings exhibited much greater micro-hardness and abrasion resistance compared to commercially prepared coatings. In a recent patent disclosure, Kobayashi et al. reported the synthesis of an acryloxy-functional silicone composition curable by high-energy radiation.³⁹⁶ The silicones consisted of a mixture of multifunctional acrylates, amino-functional alkoxy silanes, organofunctional alkoxy silanes, and colloidal silica. The resultant coatings exhibited excellent storage stability, transparency, adhesiveness, water repellency, and abrasion resistance. Zhu et al. also demonstrated the formation of a trimethoxysilane coupling agents containing *O*-butyrylchitosan via Michael addition of 3-acryloxypropyltrimethoxysilane with the amino groups of the butyrylchitosan.³⁹⁷

³⁹⁴ Tamami, B.; Betrabet, C.; Wilkes, G. L. Synthesis and application of abrasion resistant coating materials based on functionalized bis and tris maleimides. *Polym Bull* **1993**, 30, 293-9.

³⁹⁵ Misra, M.; Tilley, G. A. Hybrid inorganic-organic UV-curable abrasion resistant coatings. *Surf Coatings Int* **1998**, 81, 594-5.

³⁹⁶ Nakashima, H.; Wakita, M.; Kobayashi, H. Acryloxy-functional silicone composition curable by high-energy radiation. World Patent Appl. 2004078863, 2004.

³⁹⁷ Zhu, A.; Wu, H.; Shen, J. Preparation and characterization of a novel Si-containing crosslinkable *O*-butyrylchitosan. *Coll Polym Sci* **2004**, 282, 1222-7.

Crosslinking of the modified silanes derivatives resulted in colorless, flexible elastomeric coatings at 20 mol% incorporation of the modified silane. The resulting hydrogel films possessed good antithrombogenic properties as determined by blood-clotting and platelet adhesion.

3.7.4 Hydrogel Networks for Biomedical Applications

Michael addition networks find application in areas beyond composites and coatings. Recently, numerous biomedical applications were investigated. Hubbell et al. studied in-vivo gelling networks based on multifunctional thiols and multiacrylates as injectable tissue reinforcement.³⁹⁸ Currently two mechanical ranges of in-vivo biomaterials exist: low modulus gels which are used for drug delivery and high modulus bone cements. An intermediate strength material (0.5-50 MPa) is desirable for tissue reinforcement of intervertebral disc annuli. Michael addition networks based on thiol and acrylate precursors are ideal due to the ability to control gelation with the addition of a basic catalyst, the absence of free thiols in the bloodstream, and the faster rate of the thiol-acrylate Michael addition in comparison to potential Michael reactions with amines in the bloodstream. Metters and Hubbell also recently demonstrated the biodegradability of these networks via slow hydrolysis of ester bonds adjacent to sulfide linkages, which leads to degradation on the order of days to weeks.³⁹⁹ In a separate work, Hubbell et al. showed that the length of the alkyl spacer between the ester and the sulfide controlled the hydrolysis rate of these poly(ester

³⁹⁸ Vernon, B.; Tirelli, N.; Bachi, T.; Haldimann, D.; Hubbell, J. Water-borne, in situ crosslinked biomaterials from phase-segregated precursors. *J Biomed Mater Res* **2003**, 64A, 447-56.

³⁹⁹ Metters, A.; Hubbell, J. Network formation and degradation behavior of hydrogels formed by Michael-type addition reactions. *Biomacromolecules* **2005**, 6, 290-301.

sulfide)s, with higher degradation rates occurring for shorter alkyl spacers.⁴⁰⁰ Both dispersion type and reverse emulsion type polymers were synthesized via mixing network components with basic PBS. Reverse emulsion type networks exhibited a slower change in shear storage modulus with time near the gel point and higher ultimate compressive strengths (6.7 MPa vs. 1.8 MPa) due to greater continuity of the organic phase. Dispersion networks exhibited rapid increases in shear storage modulus near the gel point, due to the percolation of dispersed crosslinking particles. Both materials exhibited maximum deformations near 37%. Modulus increased with increased amounts of tetraacrylate precursors versus diacrylate precursors.

Rizzi and Hubbell developed protein containing hydrogel networks for tissue repair applications.⁴⁰¹ Cysteine-functionalized recombinant proteins containing sequences for integrin receptor ligation were synthesized and crosslinked with PEG bis(vinyl sulfone) (Figure 3.45). Integrin receptors are cellular receptors which play important roles in tissue development processes. These networks were stable to aqueous solution and did not exhibit hydrolytic degradation. Thus, protease cleavable units were introduced into the proteins to enable biodegradability. Glutamic acid units were placed strategically near cysteine residues to inhibit disulfide bond formation prior to crosslinking, while glycine residues were used to prevent hindrance of the Michael addition.

⁴⁰⁰ Schoenmakers, R. G.; van de Wetering, P.; Elbert, D. L.; Hubbell, J. A. The effect of the linker on the hydrolysis rate of drug-linked ester bonds. *J Contr Rel* **2004**, 95, 291-300.

⁴⁰¹ Rizzi, S. C.; Hubbell, J. A. Recombinant protein-co-PEG networks as cell-adhesive and proteolytically degradable hydrogel matrixes. Part I: Development and physicochemical characteristics. *Biomacromolecules* **2005**, 6, 1226-38.

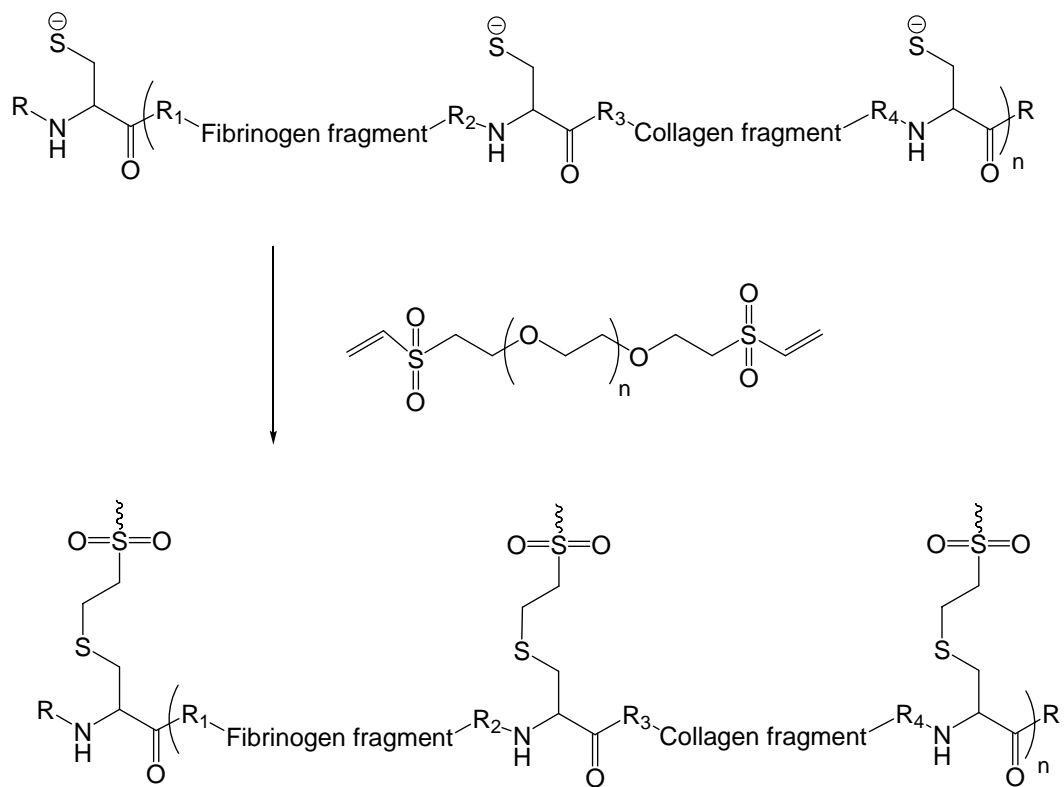


Figure 3.45. Network formation of PEG bis(vinyl sulfone) and protein dithiols.

Previous work on cysteine containing peptides revealed that positively charged arginine groups adjacent to cysteine lower the pK_a of the cysteine group, accelerating Michael reaction by a factor of 2 and decreasing gel time by a factor of 2.5.⁴⁰² Numerous charged residues were also used to enhance solubility of the proteins. The crosslinking kinetics were studied using rheological measurements, which showed increasing storage modulus with time during the crosslinking reaction. The gel time decreased with increasing pH, due to the fact that the thiolate ion is the active species in the Michael addition reaction with vinyl sulfone groups. A maxima in G' and minimum in gel time was found for a ratio of thiol to vinyl sulfone (SH:VS) slightly greater than unity and differed with protein precursor. This non-stoichiometric maximum was likely due to disulfide bond formation during reaction. Higher storage modulus and lower swelling were generally observed with an increased molar ratio of thiol to vinyl sulfone (Figure 3.46). A potential explanation for this phenomenon was decreased accessibility of reactive sites for crosslinking at lower SH:VS ratios. In similar work featuring non-degrading peptides with two cysteine residues, higher elastic modulus and lower swelling were observed for PEG bis(vinyl sulfone)s of higher functionality (3 to 8 arms) due to increased crosslink density.⁴⁰² Network elastic moduli in these systems reached a maximum at pH 8, likely because of slower kinetics at pH < 8 and greater disulfide bond formation at pH > 8. Furthermore, precursor concentration strongly influenced mechanical properties due to the propensity for cyclization reactions in dilute conditions.

⁴⁰² Lutolf, M. P.; Hubbell, J. A. Synthesis and physicochemical characterization of end-linked poly(ethylene glycol)-*co*-peptide hydrogels formed by Michael-type addition. *Biomacromolecules* 2003, 4, 713-22.

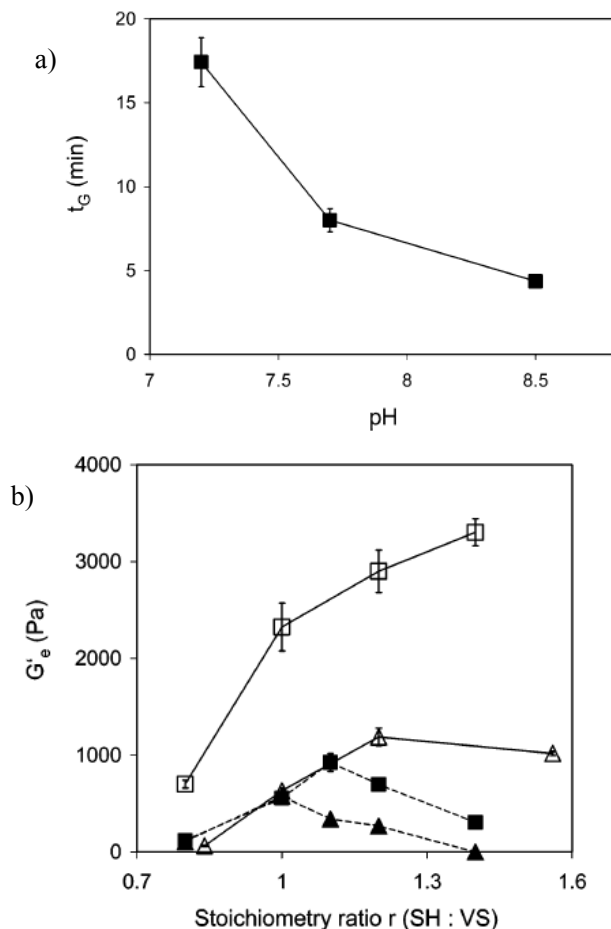


Figure 3.46. a) Effect of pH on gel time for PEG bis(vinyl sulfone). Gel time decreases at higher pH due to the greater thiolate anion concentration.

b) Effect of thiol to vinyl sulfone ratio (SH:VS) on the storage modulus of PEG-protein networks. The G' maxima occurs at ratios slightly greater than unity suggesting disulfide formation.

Reproduced from “Recombinant protein-*co*-PEG networks as cell-adhesive and proteolytically degradable hydrogel matrixes. Part I: Development and physicochemical characteristics,” Rizzi and Hubbell, Copyright 2005 with permission from the American Chemical Society.⁴⁰³

⁴⁰³ Rizzi, S. C.; Hubbell, J. A. Recombinant protein-*co*-PEG networks as cell-adhesive and proteolytically degradable hydrogel matrixes. Part I: Development and physicochemical characteristics. *Biomacromolecules* **2005**, 6, 1226-38.

Michael addition networks were also developed for protein drug delivery applications. Protein drugs often suffer from rapid clearance from the bloodstream due to removal by the liver or kidneys. The use of drug delivery devices allows steady and long lasting delivery of protein drugs. Many current drug delivery materials such as poly(lactide)s can potentially denature the protein drug due to changes in pH associated with degradation byproducts. Another issue with current drug delivery materials is incorporating the protein into the material. Hubbell et al. studied Michael addition networks based on PEG multiacrylate and PEG dithiol that overcame many of these problems via incorporating bovine serum albumin protein during synthesis in aqueous media at physiological pH without denaturing the protein (Figure 3.47).⁴⁰⁴ The crosslinking of these Michael addition networks required no basic catalyst or UV light that could potentially harm the protein as in photocuring of acrylate networks. Furthermore, the ester bonds in the PEG networks were degradable, allowing release of the protein as the network swells. The thiol-acrylate Michael addition reaction proceeded without significant side reactions with protein based amine nucleophiles, preserving the chemistry of the protein drugs. Furthermore, protein based free thiols are uncommon in extracellular proteins, lending greater selectivity to the approach. In cases where free thiols do exist, they are often confined to sterically hindered locations in the tertiary structure of the protein. Hubbell et al. introduced the protein as well-defined ~100 μm solid particles which were embedded into the Michael addition network during curing.⁴⁰⁴ The release rate of the networks was tuned via the functionality of the PEG multiacrylate. PEG triacrylate networks resulted in rapid release of the protein. PEG tetraacrylate

⁴⁰⁴ Elbert, D. L.; Pratt, A. B.; Lutolf, M. P.; Halstenberg, S.; Hubbell, J. A. Protein delivery from materials formed by self-selective conjugate addition reactions. *J Contr Rel* **2001**, 76, 11-25.

networks released protein over the course of 4 d at a linear rate of 20% per day. PEG octaacrylate networks exhibited a slower release with a release rate of 10 to 15% per day. Hydrolytic degradation was observed in the swelling kinetics of these networks. A decrease in gel time with increasing solution pH (up to pH 8.2) indicated that the thiolate anion is the active species in the Michael addition with the acrylate.

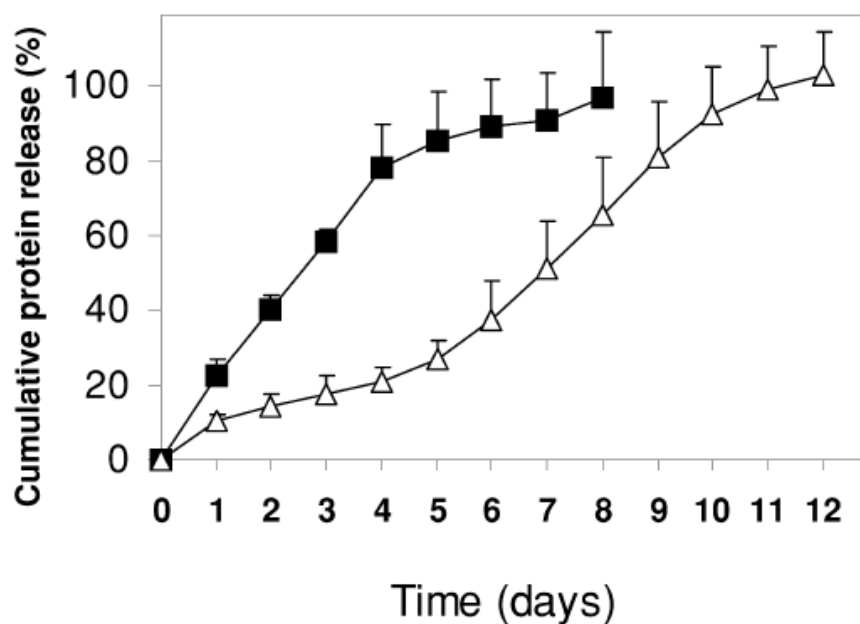


Figure 3.47. Release of albumin from PEG networks based on PEG tetraacrylate (black squares) and PEG octaacrylate (white triangles). The lower functionality of the PEG tetraacrylate leads to lower crosslink density and more rapid release. Reprinted from J. Control Rel, 76, Hubbell et al. "Protein delivery from materials formed by self-selective conjugate addition reactions," 11-25, Copyright 2001, with permission from Elsevier.⁴⁰⁵

⁴⁰⁵ Elbert, D. L.; Pratt, A. B.; Lutolf, M. P.; Halstenberg, S.; Hubbell, J. A. Protein delivery from materials formed by self-selective conjugate addition reactions. *J Contr Rel* **2001**, 76, 11-25.

Hubbell et al. also studied protein drug delivery using Michael addition hydrogel networks from eight-arm PEG octaacrylate with dithiothreitol (Figure 3.48).⁴⁰⁶ The protein drug human growth hormone (hGH), which suffers from rapid clearance was incorporated into these hydrogels without covalent attachment. Currently, daily administrations of this drug are required for treatment of the hormone deficiency as well as Turner's syndrome and renal failure. The crosslink density of the networks is controlled with the use of varying molecular weights of PEG octaacrylate, thereby influencing the drug diffusion. As shown in Figure 3.49, the drug release rate was tuned to occur over periods from hours to months by changing the crosslink density of the networks. The ester sulfide linkages produced in the network degraded at a significantly faster rate than in free radically crosslinked acrylic networks, presumably due to neighboring group effects from the thioether group. Thus, the diffusion coefficient in these networks increases with time. The degradation rate of these networks varied from weeks to months and was directly related to the crosslink density.

⁴⁰⁶ an de Wetering, P.; Metters, A. T.; Schoenmakers, R. G.; Hubbell, J. A. Poly(ethylene glycol) hydrogels formed by conjugate addition with controllable swelling, degradation, and release of pharmaceutically active proteins. *J Contr Rel* **2005**, 102, 619-27.

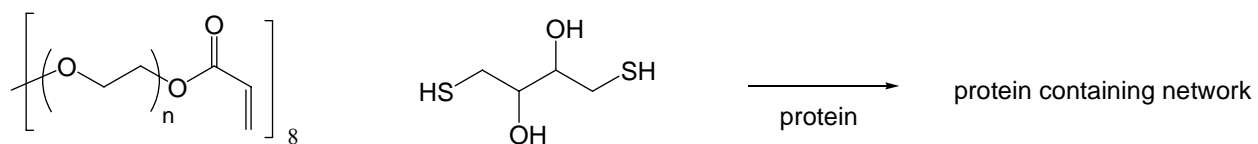


Figure 3.48. Protein-containing PEG networks via Michael addition crosslinking of PEG octaacrylate with dithiothreitol. Human growth factor protein (hGH) was incorporated by mixing.

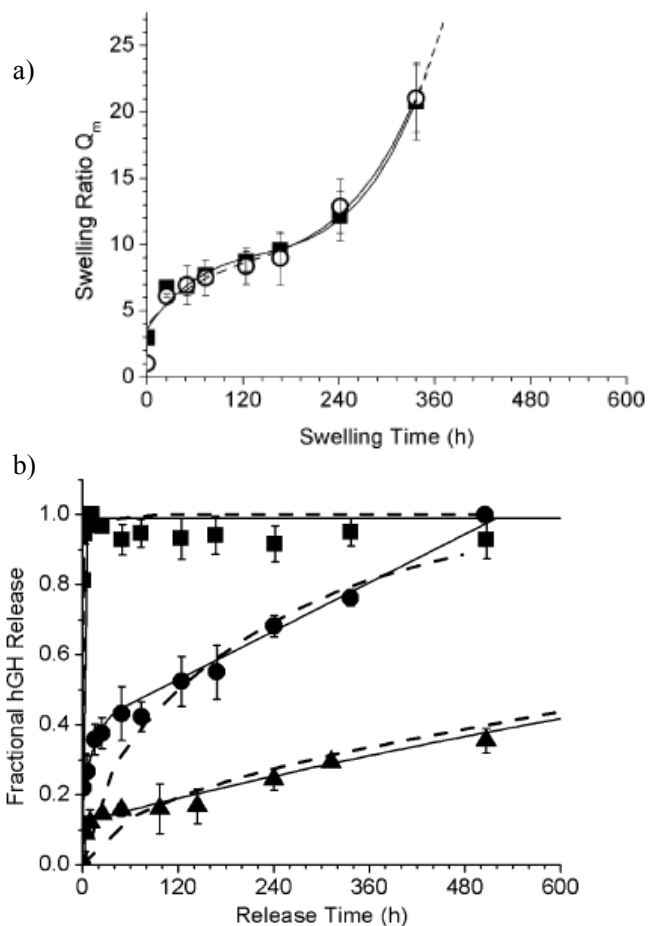


Figure 3.49. a) Swelling of PEG octaacrylate, dithiothreitol networks via initial solvent uptake followed by ester hydrolysis leading to degradation. b) Release kinetics of hGH protein from networks as a function of PEG octaacrylate molecular weight (squares 10000 g/mol, circles 10000 g/mol mixed with 2000 g/mol (50:50), triangles 2000 g/mol). Reprinted from *J Control Rel*, 102, van de Wetering et al. "The effect of the linker on the hydrolysis rate of drug-linked ester bonds," 619-27, Copyright 2005, with permission from Elsevier.⁴⁰⁷

⁴⁰⁷ Schoenmakers, R. G.; van de Wetering, P.; Elbert, D. L.; Hubbell, J. A. The effect of the linker on the hydrolysis rate of drug-linked ester bonds. *J Contr Rel* **2004**, 95, 291-300.

Hubbell et al. also studied synthetic cell encapsulation networks.⁴⁰⁸ These networks were synthesized from physically gelled four-arm Pluronics[®] (poly(ethylene oxide-*b*-propylene oxide-*b*-ethylene oxide)) functionalized with acrylate groups and thiols. These hydrogels have potential applications in cell encapsulation. The propensity of the thiol groups to undergo disulfide bond formation prompted the use of the thioacetic ester protecting group which was deprotected during crosslinking. The reversible physical gelation process for Pluronics occurred in aqueous solution when a cold, slightly acidic medium (5 °C, pH = 6.8) was increased both in temperature and pH (37 °C, pH = 7.4). Once the physical gel formed, the covalent crosslinking via the Michael addition reaction produced gels, which were biodegradable due to the presence of ester groups. Degradation in PBS at physiological conditions occurred over periods of 1 to 2 weeks.

In order to mimic the extracellular matrix and guide the growth of cells, synthetic matrices should be biocompatible, resistant to non-specific adsorption of proteins, degradable via cell- secreted matrix metalloproteinases (MMPs), and further promote cell-adhesion. Extending on an earlier study, Hubbell et al. synthesized hydrogels comprising multiarm vinyl sulfone-terminated PEG, a monocysteine containing adhesion protein, and a bis(cysteine) metalloprotein substrate protein. The adhesion peptide was introduced to provide adhesion sites on the surface of the hydrogel matrix. The unreacted vinyl sulfone groups were reacted with the bis(cysteine) terminated MMP substrate peptide. Figure 3.50 depicts the stepwise formation of the hydrogel containing the adhesion proteins and the MMP

⁴⁰⁸ Cellesia, F.; Tirellia, N.; Hubbell, J. A. Towards a fully-synthetic substitute of alginate: development of a new process using thermal gelation and chemical cross-linking. *Biomaterials* **2004**, 25, 5115-24.

substrate proteins as well as the attack on the substrate protein by a metalloproteinase.⁴⁰⁹ Analysis of the activity of an MMP to various substrates in the 3D hydrogel indicated that the invasion of the cells was dependent on the enzymatic sensitivity of the substrate peptide and the rate of this process was dependent on the adhesion peptide concentration. Also the invasion of the cells decreased with an increase in crosslink density at lower PEG molecular weights. In order to demonstrate the capability of these hydrogels to promote tissue growth a bone protein containing hydrogel was placed in a rat cranial defect. Bone regeneration was observed after 4 weeks of hydrogel implantation and depended on the MMP sensitivity of the networks.^{409,410} Enhanced bone regeneration was observed due to the additional affinity sites for the bone protein in the matrix.⁴¹¹ Similarly, the covalent incorporation of a vascular endothelial growth factor in the hydrogel matrix alongside adhesion peptides and MMP substrate peptides aided the regeneration of human endothelial cells and formation of new vascularized tissue in place of the biomaterial.⁴¹²

⁴⁰⁹ Lutolf, M. P.; Lauer-Fields, J. L.; Schmoekel, H. G.; Metters, A.; Weber, F. E.; Fields, G. B.; Hubbell, J. A. Synthetic matrix metalloproteinase-sensitive hydrogels for the conduction of tissue regeneration: Engineering cell-invasion characteristics. *Proc Natl Acad Sci USA* **2003**, 100, 5413-8.

⁴¹⁰ Lutolf, M. P.; Raeber, G. P.; Zisch, A. H.; Tirelli, N.; Hubbell, J. A. Cell-responsive synthetic hydrogels. *Adv Mater* **2003**, 15, 888-92.

⁴¹¹ Pratt, A. B.; Weber, F. E.; Schmoekel, H. G.; Müller, R.; Hubbell, J. A. Synthetic extracellular matrices for in situ tissue regeneration. *Biotechnol Bioeng* **2004**, 86, 27-36.

⁴¹² Zisch, A. H.; Lutolf, M. P.; Ehrbar, M.; Raeber, G. P.; Rizzi, S. C.; Davies, N.; Schmoekel, H.; Bezuidenhout, D.; Djonov, V.; Zilla, P.; Hubbell, J. A. Cell-demanded release of VEGF from synthetic, biointeractive cell growth matrices for vascularized tissue growth. *FASEB* **2003**, 17, 2260-2.

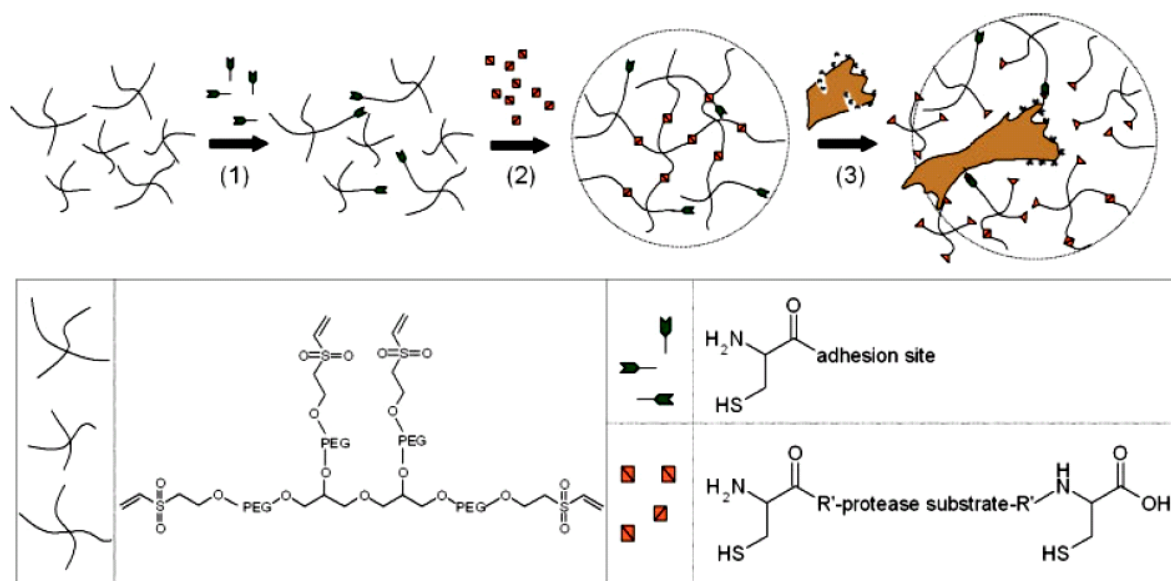


Figure 3.50. Illustration of the stepwise synthesis of a PEG-based hydrogel by reacting multiarm vinyl sulfone-terminated PEG with small amounts of a monocysteine-containing adhesion peptide (1) followed by reaction of excess bis(cysteine) containing MMP substrate peptide (2). Attack of a cell-secreted MMP is also shown (3). Structures of the multiarm vinyl sulfone-terminated PEG (cross lines); monocysteine-containing adhesion peptide (green wedge shaped arrows), and bis(cysteine) containing MMP substrate peptide (orange divided squares) are shown in the legend. Reprinted from Proc Natl Acad Sci, 100, Lutolf et al., “Synthetic matrix metalloproteinase-sensitive hydrogels for the conduction of tissue regeneration: Engineering cell-invasion characteristics.” 5413-8, Copyright 2003, with permission from the National Academy of Sciences, U.S.A.⁴¹³

⁴¹³ Lutolf, M. P.; Lauer-Fields, J. L.; Schmoekel, H. G.; Metters, A.; Weber, F. E.; Fields, G. B.; Hubbell, J. A. Synthetic matrix metalloproteinase-sensitive hydrogels for the conduction of tissue regeneration: Engineering cell-invasion characteristics. *Proc Natl Acad Sci USA* **2003**, 100, 5413-8.

Ferruti et al. studied tissue scaffolds consisting of crosslinked poly(amido amine) hydrogels based on 2,2-bisacrylamidoacetic acid, which was crosslinked using primary diamines.⁴¹⁴ The networks degraded completely within 10 d in Dulbecco's medium at physiological conditions, and cytotoxicity tests using direct contact with fibroblast cell lines demonstrated the non-cytotoxic nature of both networks as well as the degradation products. Bovine serum albumin was also incorporated into selected networks, through mixing with the network precursors prior to crosslinking. Ferruti et al. developed hydrogels containing agmatine, a guanidine functionalized amine precursor that resembles the RGD (arginine glycine aspartic acid) tripeptide, an agent for promoting cell adhesion.⁴¹⁵ The mechanical performance of these tissue scaffolds improved and degradation decreased through the use of a multi-amine functionalized crosslinker molecule, which was also synthesized through poly(amido amine) chemistry.

Goethals et al. reacted living cationic, acryloyloxybutyl triflate initiated poly(tetramethylene oxide) (PTMO) with Astramol™ dendrimers to produce acrylate functionalized dendrimers (Figure 3.51).⁴¹⁶ The presence of both amine and acrylate groups on the dendrimer molecules resulted in rapid gel formation with gel fractions of 88 to 99%. The pot life varied from 25 to 125 min with the molecular weight of the PTMO changing from 1000 to 4000 g/mol. Higher degrees of swelling and higher tensile elongations were observed for higher molecular weight PTMO precursors. The pot life was also affected by

⁴¹⁴ Ferruti, P.; Bianchi, S.; Ranucci, E.; Chiellini, F.; Caruso, V. Novel poly(amido-amine)-based hydrogels as scaffolds for tissue engineering. *Macromol Biosci* **2005**, *5*, 613-22.

⁴¹⁵ Ferruti, P.; Bianchi, S.; Ranucci, E. Novel agmatine-containing poly(amidoamine) hydrogels as scaffolds for tissue engineering. *Biomacromolecules* **2005**, *6*, 2229-35.

⁴¹⁶ Tanghe, L. M.; Goethals, E. J.; du Prez, F. Segmented polymer networks containing amino-dendrimers. *Polym Int* **2003**, *52*, 191-7.

the temperature of the reaction from 45 min at 25 °C to 4 min at 65 °C. The gel fraction increased with the incorporation of four PTMO arms as opposed to two arms.

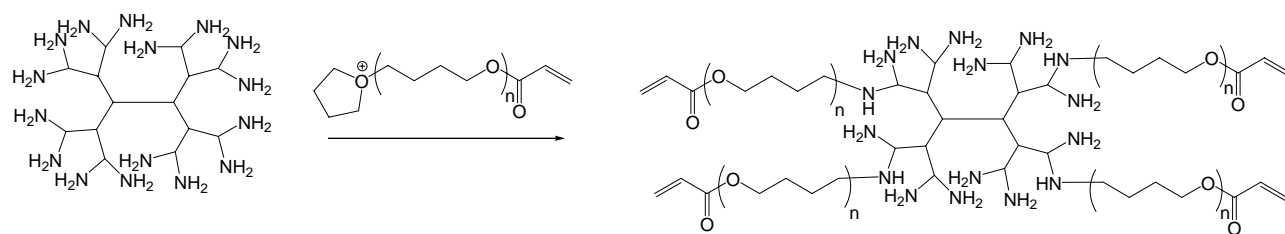


Figure 3.51. Self-condensing dendrimer synthesized from PPI and acrylate initiated living PTMO.

3.8 Bioconjugates via the Michael Addition Reaction

Strong interest in bioconjugates has developed in recent years. Bioconjugates consist of synthetic polymers covalently bound to biopolymers (proteins, polysaccharides, polynucleotides, antibodies) or bioactive species (pharmaceuticals). These materials possess special properties that make them useful in biomedical applications and fundamental studies. Coupling synthetic polymers to biomaterials is useful for numerous reasons. Polymer-protein bioconjugates may possess “stealth” properties, resisting clearance from the bloodstream in terms of excretion from the liver or kidneys, thus increasing circulatory lifetimes of protein drugs. Furthermore, recognition properties may be imparted to synthetic polymers through the incorporation of receptor proteins. Recognition properties are important in artificial organs and implants as well as in biosensors. Polymer-protein and polymer-drug conjugates were used to improve solubility and circulation time within the body. In some cases, biomolecule linking using Michael addition chemistry was studied. Thus, Roy et al. used Michael addition to create sugar-protein conjugates from sialyloligosaccharides.⁴¹⁷

3.8.1 Polymer-Protein and Polymer-Drug Conjugates

Poly(ethylene glycol) (PEG) is the most common synthetic polymer for coupling with proteins. PEG is a non-biodegradable polymer ideal for coupling to proteins due to its biocompatibility and nonabsorbent properties with respect to proteins. Currently, numerous

⁴¹⁷ Roy, R.; Laferriere, C. A. Michael addition as the key step in the syntheses of sialyloligosaccharide-protein conjugates from *N*-acryloylated glycopyranosylamines. *J Chem Soc Chem Commun* **1990**, 23, 1709-11.

functional PEGs are commercially available for applications in protein pegylation.⁴¹⁸ Michael addition of protein-bound thiol groups to maleimide functionalized PEG is one of the most common methods of polymer-protein conjugate synthesis. A second route is through Michael addition of thiol groups to vinyl sulfone functionalized PEG, resulting in greater hydrolytic stability. PEG containing two maleimide functional groups was used for mimicking the heavy chain end of antibodies and is also useful for binding two proteins in close proximity.⁴¹⁸ The coupling of thiol groups on cysteine residues with polymeric Michael acceptors benefits from several advantages. The Michael addition chemistry occurs readily at physiological conditions and is selective to thiol-containing proteins over amine nucleophiles. The reaction also produces no potentially toxic byproducts.⁴¹⁹ Hubbell et al. studied the reactivity of protein-bound cysteine residues as a function of charge environment.⁴²⁰ Positively charged residues placed adjacent to the cysteine resulted in a lower pK_a of the cysteine group and increased Michael addition to PEG diacrylates. Negatively charged residues produced the opposite effect. The specific order of the residues adjacent to the cysteine groups had no apparent effect on reaction kinetics. Vinyl sulfone functionalized PEG molecules reacted selectively with cysteine residues over lysine residues at pH 8 and possessed greater hydrolytic stability. Harris et al. coupled reduced

⁴¹⁸ Harris, J. M.; Kozlowski, A. Poly(ethylene glycol) derivatives with proximal reactive groups. US Patent 6,664,331, 2003.

⁴¹⁹ Heggli, M.; Tirelli, N.; Zisch, A.; Hubbell, J. A. Michael-type addition as a tool for surface functionalization. *Bioconjug Chem* **2003**, 14, 967-73.

⁴²⁰ Lutolf, M. P.; Tirelli, N.; Cerritelli, S.; Cavalli, L.; Hubbell, J. A. Systematic modulation of Michael-type reactivity of thiols through the use of charged amino acids. *Bioconjug Chem* **2001**, 12, 1051-6.

ribonuclease with PEG vinyl sulfone.⁴²¹ Reaction with lysine residues required a higher pH of 9.3 but was still dramatically slower than the reaction with cysteine at comparable pH.

Lysine residues of proteins also serve as functional group handles for the Michael reaction of acrylamides. This strategy benefits from the lack of dimerization of lysine residues in comparison to cysteine residues. A large number of protein-modifying PEG reagents are directed toward reaction with the amine groups contained in lysine residues. Such reagents include activated acylating agents such as *N*-hydroxysuccinimidyl ester-PEG (NHS-PEG). However, attachment to lysine residues is disadvantageous when the lysine residues are critical to protein binding or enzymatic active sites. Examples of proteins that show diminished activity upon pegylation using lysine targeting modified PEGs are asparaginase, α -galactosidase, and CD4.⁴²² The reaction with lysine groups is also less controlled and often results in multiple PEG attachments due to the presence of numerous lysine residues. The use of cysteine via Michael addition to PEG reagents is advantageous in these cases and further benefits from the lack of synthetic byproducts. Thus, Kogan synthesized a maleimide terminated PEG capable of reaction with free cysteine residues in proteins.⁴²²

Hubbell et al. have performed a great deal of work in the area of polymer-protein conjugates, often favoring the method of cysteine Michael addition.⁴²³ PEG bisacrylamide and PEG diacrylate were studied as PEG substrates for coupling with proteins via the

⁴²¹ Morpurgo, M.; Veronese, F. M.; Kachensky, D.; Harris, J. M. Preparation and characterization of poly(ethylene glycol) vinyl sulfone. *Bioconjug Chem* **1996**, *7*, 363-8.

⁴²² Kogan, T. P. The synthesis of substituted methoxy-poly(ethyleneglycol) derivatives suitable for selective protein modification. *Syn Comm* **1992**, *22*, 2417-24.

⁴²³ Elbert, D. L.; Hubbell, J. A. Conjugate addition reactions combined with free-radical cross-linking for the design of materials for tissue engineering. *Biomacromolecules* **2001**, *2*, 430-41.

Michael addition. Residual acrylamide or acrylate groups permitted free radical crosslinking of the resulting pegylated proteins to create hydrogels with embedded proteins that serve as tissue scaffolds. The reaction of the acrylamide groups with cysteines was more than an order of magnitude slower than the corresponding acrylate reaction, but the acrylamide group possesses superior hydrolytic stability. The more hydrolytically stable and more Michael reactive vinyl sulfone linkage could not be used due to its inability to polymerize free radically. The tissue scaffold environment is critical to inducing particular phenotypes to embedded cells. PEG is well known to possess low adhesion to proteins, which allows the study of specific cell-adhesion agents such as RGD protein. Thus, Hubbell et al. introduced RGD protein to PEG bisacrylamide and formed networks (Figure 3.52).⁴²⁴ These networks were treated with cells that spread on the surfaces of the network, clearly well-adhered. Furthermore, the mechanical properties of the crosslinked tissue scaffolds were sufficient to produce durable materials.

⁴²⁴ Elbert, D. L.; Hubbell, J. A. Conjugate addition reactions combined with free-radical cross-linking for the design of materials for tissue engineering. *Biomacromolecules* **2001**, 2, 430-41.

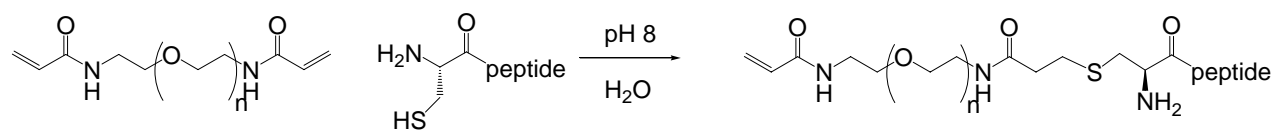


Figure 3.52. Protein incorporation via Michael addition of thiol residues to PEG-acrylamide.

Polymer-drug conjugates are of special interest in anticancer therapy where numerous drugs have improved performance in comparison with the parent drug.⁴²⁵ Conjugates of interest include poly(*N*-(2-hydroxypropyl)methacrylamide) doxorubicin, poly(glutamic acid)-paclitaxel and PEG-camptothecin. Several reasons exist for the improved performance of these conjugates including improved solubility, lower toxicity, and longer retention in the bloodstream. Furthermore, some conjugates benefit from the enhanced vascular permeability and retention (EPR) effect, in which drugs are preferentially absorbed into tumor tissue and not released (Figure 3.53). In fact, one reason for the lower toxicity of the polymer-drug conjugates is the absence of nonspecific uptake into nontargeted tissues and organs. Generally, polymer-drug conjugates must contain a hydrolysable or enzyme-cleavable linker to allow cellular uptake of the drug molecules at the tumor site. In some cases, linkers are introduced that cleave via lysosomal cysteine proteases. Generally, polymers used in these composites must either biodegrade or possess low enough molecular weight (< 30000 g/mol) to allow removal through the kidneys.

⁴²⁵ Duncan, R.; Gac-Breton, S.; Keane, R.; Musila, R.; Sat, Y. N.; Satchi, R.; Searle, F. Polymer-drug conjugates, PDEPT and PELT: basic principles for design and transfer from the laboratory to clinic. *J Contr Rel* **2001**, 74, 135-46.

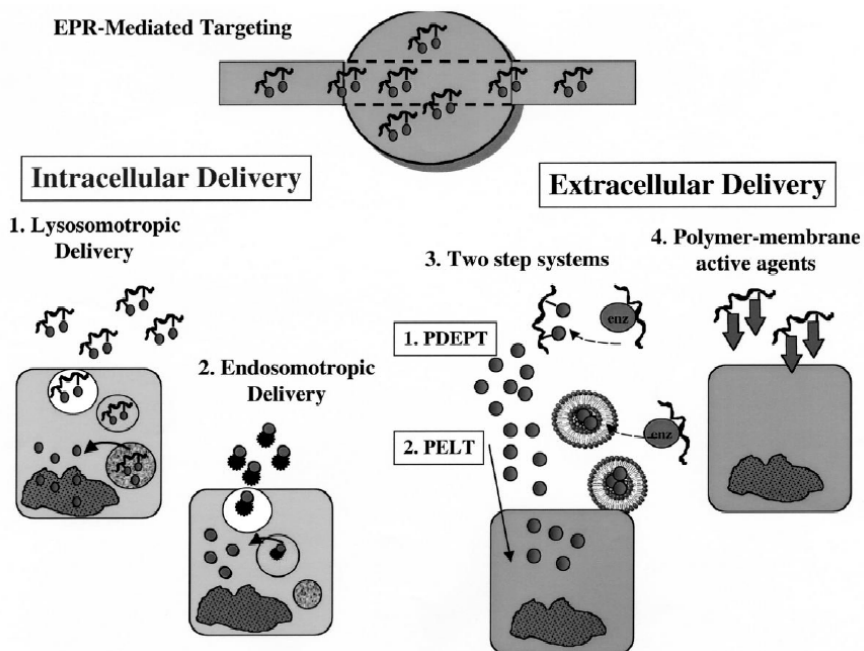


Figure 3.53. Drug delivery via polymer-drug conjugates. Enhanced permeability and retention (EPR) mechanism of drug delivery relies on preferential permeation of the conjugate followed by drug release, without reverse permeation. Reprinted from *J Control Rel*, 74, Duncan et al., “Polymer–drug conjugates, PDEPT and PELT: basic principles for design and transfer from the laboratory to clinic,” 135-46, Copyright 2001, with permission from Elsevier.⁴²⁶

⁴²⁶ Duncan, R.; Gac-Breton, S.; Keane, R.; Musila, R.; Sat, Y. N.; Satchi, R.; Searle, F. Polymer–drug conjugates, PDEPT and PELT: basic principles for design and transfer from the laboratory to clinic. *J Contr Rel* **2001**, 74, 135-46.

Goodson and Katre accomplished pegylation of recombinant interleukin-2 protein using PEG-maleimide.⁴²⁷ Interleukin-2 is a glycosylated protein that serves important functions in the immune system and is useful as an anticancer drug. The recombinant interleukin-2 was modified to include a cysteine site for Michael addition at the glycosidic linkage of the original protein, thereby preventing inhibition of the protein. The conjugation of recombinant interleukin-2 to PEG-maleimide resulted in an increase in hydrodynamic size and solubility, increasing systemic exposure four fold. An increase in hydrodynamic size results in less glomerular kidney filtration compared to the unmodified protein. Katre et al. showed a systematic decrease in clearance with increasing effective molecular weight up to 70000 g/mol above which the rate of clearance was almost constant, possibly due to a different mechanism of clearance.⁴²⁸ In previous work, modification of interleukin-2 via amine groups on lysine residues resulted in reduced bioactivity of the protein.⁴²⁹

Jaspers et al. studied recombinant staphylokinase pegylated at artificially introduced cysteine sites using PEG-maleimide.⁴³⁰ Staphylokinase is an enzyme that is used to treat acute myocardial infarction, through thrombolysis of blood clots within blood vessels. Numerous sites on the enzyme were targeted for introduction of the cysteine residue. The

⁴²⁷ Goodson, R. J.; Katre, N. V. Site-directed pegylation of recombinant interleukin-2 at its glycosylation site. *Bio/technology* **1990**, 8, 343-6.

⁴²⁸ Knauf, M. J.; Bell, D. P.; Hirtzer, P.; Luo, Z. P.; Young, J. D.; Katre, N. V. Relationship of effective molecular size to systemic clearance in rats of recombinant interleukin-2 chemically modified with water-soluble polymers. *J Biol Chem* **1988**, 263, 15064-70.

⁴²⁹ Katre, N. V.; Knauf, M. J.; Laird, W. J. Chemical modification of recombinant interleukin 2 by polyethylene glycol increases its potency in the murine Meth A sarcoma model. *Proc Natl Acad Sci USA* **1987**, 84, 1487-91.

⁴³⁰ Vanwetswinkel, S.; Plaisance, S.; Zhi-yong, Z.; Vanlinthout, I.; Brepoels, K.; Lasters, I.; Collen, D.; Jaspers, L. Pharmacokinetic and thrombolytic properties of cysteine-linked polyethylene glycol derivatives of staphylokinase. *Blood* **2000**, 95, 936-42.

circulatory lifetime of the staphlokinase was increased through pegylation while thrombolytic activity was maintained. The plasma clearance rates of the staphlokinase conjugate decreased with increasing PEG molecular weight. Clinical trials revealed successful restoration of circulation for patients suffering from acute myocardial infarction.⁴³¹

Currently, strong interest exists in functionalizing polymers with the RGD protein to promote cell adhesion for tissue scaffolds. The RGD protein selectively promotes cell adhesion, while avoiding nonspecific adsorption of proteins. Furthermore, cell spreading, a change in the cellular morphology occurs in the presence of the RGD coating, indicating cell signaling has occurred. Hubbell et al. used a hetero-bifunctional PEG containing *N*-hydroxysuccinimide and vinyl sulfone linkages to couple the RGD containing peptides via cysteine linkages to the PEG and then to couple the PEG-RGD to poly(L-lysine).⁴³²

Surface grafting of biological molecules was achieved using the Michael addition reaction.⁴³³ Model systems to achieve protein grafted surfaces were studied using PEG acrylated surfaces coupled to cysteine containing proteins such as portions of the Platelet factor 4 protein. A modification route beginning with thiol functionalized surfaces was also pursued, however, the surface grafted thiols were unreactive.

⁴³¹ Collen, M. D.; Sinnaeve, P.; Demarsin, E.; Moreau, H.; De Maeyer, M.; Jespers, L.; Laroche, Y.; van de Werf, F. Polyethylene glycol-derivatized cysteine-substitution variants of recombinant staphylokinase for single-bolus treatment of acute myocardial infarction. *Circulation* **2000**, 102, 1766-72.

⁴³² van de Vondele, S.; Voros, J.; Hubbell, J. A. RGD-grafted poly-L-lysine-graft-(polyethylene glycol) copolymers block non-specific protein adsorption while promoting cell adhesion. *Biotech Bioeng* **2003**, 82, 784-90.

⁴³³ Heggli, M.; Tirelli, N.; Zisch, A.; Hubbell, J. A. Michael-type addition as a tool for surface functionalization. *Bioconjug Chem* **2003**, 14, 967-73.

3.8.2 Coupling of Biological Molecules to Michael Addition Polymers

In addition to the Michael reaction as a strategy to couple synthetic polymers to biological molecules, it is also useful in the synthesis of polymers that will be coupled to biological molecules. Numerous Michael addition polymers are useful as precursors for bioconjugates due to their biocompatibility and biodegradability. Poly(amido amine)s are an excellent example of a biocompatible, biodegradable Michael addition polymers. Both linear poly(amido amine)s and dendritic poly(amido amine)s (PAMAM) proved useful in forming bioconjugates.

Ferruti et al. synthesized poly(amido amine) drug conjugates of the anticancer drug mitomycin C, which was bound to pendant hydroxyl groups on the poly(amido amine). In-vivo studies showed similar antitumor activity for the conjugate compared to mitomycin C as well as lower toxicity values.⁴³⁴ Poly(amido amine) dendrimers were also used to facilitate the release of the toxic anticancer drug 5-fluorouracil via covalent incorporation onto the terminal amines on the dendrimer structure.⁴³⁵ Higher generation dendrimers released larger amounts of 5-fluorouracil, with complete release occurring over the period of about one week.

Glycodendrimers are dendrimers containing saccharide residues on the peripheral functional groups. Glycodendrimer interactions with proteins are often more pronounced than with individual saccharides due to increased “valency”. However, the density of functional groups at the dendrimer surface may potentially lead to steric hindrance of the

⁴³⁴ Ferruti, P.; Marchisio, M. A.; Duncan, R. Poly(amido-amine)s: biomedical applications. *Macromol Rapid Commun* **2002**, 23, 332-55.

⁴³⁵ Zhuo, R. X.; Du, B.; Lu, Z. R. In vitro release of 5-fluorouracil with cyclic core dendritic polymer. *J Contr Rel* **1999**, 57, 249-57.

sugar groups. Meijer et al. introduced peripheral sugar groups at various distances from the surface of PPI dendrimers using alkyl spacers of various lengths, thus reducing steric congestion.⁴³⁶

3.9 Conclusions and Future Directions

This review outlined the current applications of the Michael addition to polymer synthesis. The Michael addition reaction serves important roles in polymer synthesis, allowing the development of novel polymers from diverse monomer feedstocks. Polymers of numerous different topologies including linear, dendritic, hyperbranched and network polymers are enabled. Both step growth and chain growth techniques are utilized. The flexibility of the Michael reaction in terms of monomer functionality, solvent environment, and conversion at ambient or near ambient temperature allows the production of sophisticated macromolecular systems for technologically important applications. Other advantages include a general lack of sensitivity to oxygen and the absence of low molar mass byproducts which require removal.

The applications of Michael addition polymers are as diverse as their compositions and topologies, ranging from networks for coatings and adhesives to linear, biodegradable polymers for gene transfection or drug delivery. Several Michael addition polymers such as poly(amido amine)s benefit from biocompatibility and non-toxic degradation products. Michael addition also serves as a synthetic tool for coupling polymers with biological

⁴³⁶ Peerlings, H. W. I.; Nepogodiev, S. A.; Stoddart, J. F.; Meijer, E. W. Synthesis of spacer-armed glucodendrimers based on the modification of poly(propylene imine) dendrimers. *Eur J Org Chem* **1998**, 9, 1879-86.

systems such as proteins and enzymes. The ability to carry out the Michael addition under physiological conditions permits novel tissue replacements, cell scaffolds and direct application.

One aspect of the Michael addition largely unused in polymer science is the ability to carry out stereospecific Michael additions. The application of special catalysts to achieve stereospecific Michael addition may yield polymers with improved biological applications and potential crystallinity. Chirality is particularly important in biological systems including recognition processes with proteins. Another likely future direction for Michael addition polymerizations is the increased use of bio-based reactants. The number of bio-based precursors entering the market and the multitude of functionalities available for Michael addition chemistry are growing. Many of these materials are amenable to modification for introduction into Michael addition systems. Furthermore, the tolerance of the Michael reaction to protic impurities allows the use of less well-defined feed streams.

3.10 Acknowledgements

This material is based upon work supported by the US Army Research Laboratory and US Army Research Office under grant number DAAD19-02-1-0275 Macromolecular Architecture for Performance (MAP) MURI.

The authors would like to acknowledge the financial support of Rohm and Haas Company and the Department of Energy (DE-FG36-04GO14317).

Chapter 4. Synthesis of Chain End Functionalized Multiple Hydrogen Bonded Polystyrenes and Poly(alkyl acrylates) via Nitroxide Mediated Radical Polymerization

(Mather, B.D.; Lizotte, J.R.; Long, T.E. *Macromolecules* **2004**, 37(25), 9331-7) Reproduced with permission. Copyright 2004, American Chemical Society

4.1 Abstract

Hydrogen bonding uracil functionalized polystyrenes and poly(alkyl acrylate)s were synthesized via nitroxide mediated polymerization. Quantitative chain end functionalization was achieved using novel uracil containing TEMPO- and DEPN-based alkoxyamine unimolecular initiators. Polymerizations were conducted at 130 °C and yielded functionalized homopolymers with narrow molecular weight distributions ($M_w/M_n = 1.20$) and predictable molecular weights. Polymerizations of both *n*-butyl acrylate and styrene using the DEPN- and TEMPO-based alkoxyamines resulted in molecular weight control over a wide range of conversions. Terminal functionalization of poly(alkyl acrylate)s with hydrogen bonding groups increased the melt viscosity, and as expected, the viscosity approached that of the nonfunctional analogues as temperature was increased. The hydrogen bonding effect was also evident in thermal (DSC) analysis and ^1H NMR spectroscopic investigations, and low molar mass polystyrenes exhibited glass transition temperatures that were consistent with a higher apparent molar mass. ^1H NMR spectroscopy confirmed the presence of a single hydrogen

bonding group at the chain terminus, which was consistent with a well-defined initiation process for two families of novel alkoxyamines.

4.2 Introduction

Stable free radical polymerization (SFRP), which is often also described as nitroxide mediated polymerization (NMP), is well established as a controlled radical polymerization methodology.^{437 - 440} In a similar fashion to other controlled radical polymerization methodologies, the process relies on an equilibrium between dormant propagating chains and a low concentration of propagating radicals. The relatively high rate of initiation relative to propagation and the reduction of transfer or termination events through reversible capping of the growing radical chain end has led to the classification of this polymerization methodology as “living”. The systematic variation of the monomer weight to the moles of initiator leads to predictable molecular weights and relatively low polydispersities ($M_w/M_n \sim 1.20$). Stable free radical polymerization offers functional group tolerance, which is typical of radical polymerizations. This tolerance provides versatility that is often not easily achieved with other living polymerization techniques and less stringent purification techniques are required compared to living anionic polymerization. Moreover, stable free

⁴³⁷ Hawker, C.J.; Bosman, A.W.; Harth, E. New Polymer Synthesis by Nitroxide Mediated Living Radical Polymerizations. *Chem. Rev.* **2001**, 101, 3661-88.

⁴³⁸ Matyjaszewski, K., Advances in controlled/living radical polymerization. American Chemical Society: Washington, 2003; Vol. 854, p 2-9.

⁴³⁹ Hawker, C. J.; Hedrick, J. L.; Malmstrom, E.; Trollsas, M.; Stehling, U. M.; Waymouth, R. M., Solvent-free polymerizations and processes: minimization of conventional organic solvents In *ACS Symposium Series*, Long, T. E.; Hunt, M. O., Eds. 1998; Vol. 713, pp 127-39.

⁴⁴⁰ Bisht, H. S.; Chatterjee, A. K. Living Free-Radical Polymerization-A Review. *J. Macromol. Sci., Polym. Rev.* **2001**, 41, 139-73.

radical polymerization⁴³⁷⁻⁴⁴⁰ enables the synthesis of block,⁴⁴¹ graft, star^{442, 443} and hyperbranched⁴⁴⁴ topologies in a similar fashion to other living polymerization processes.

Rizzardo et.al. initially described stable free radical polymerization^{445,446} and later Georges et al. examined bimolecular initiators which primarily involved TEMPO (2,2,6,6-tetramethylpiperidinyloxy), conventional radical initiators (AIBN, BPO), and styrenic monomers.⁴⁴⁷ This method proved very effective for styrenic monomers. Furthermore, the typical reaction rates initially were quite slow, and often days were required to reach high conversion. More recently, other monomers such as acrylates, dienes, and acrylamides were successfully polymerized using nitroxides such as DEPNO (*N-tert-butyl-N-(1-diethylphosphono-2,2-dimethylpropyl)-N-oxy*l), which contains a hydrogen alpha to the nitroxide functionality.^{448 - 451} Polymerizations, which utilized this

⁴⁴¹ Robin, S.; Guerret, O.; Couturier, J. L.; Pirri, R.; Gnanou, Y. Synthesis and Characterization of Poly(styrene-*b*-*n*-butyl acrylate-*b*-styrene) Triblock Copolymers Using a Dialkoxyamine as Initiator. *Macromolecules* **2002**, 35, 3844-8.

⁴⁴² Pasquale, A. J.; Long, T. E. Synthesis of star-shaped polystyrenes via nitroxide-mediated stable free-radical polymerization. *J. Polym. Sci.: Part A. Polym. Chem.* **2001**, 39, 216-23.

⁴⁴³ Bosman, A. W.; Vestberg, R.; Heumann, A.; Fréchet, J. M. J.; Hawker, C. J. A Modular Approach toward Functionalized Three-Dimensional Macromolecules: From Synthetic Concepts to Practical Applications. *J. Am. Chem. Soc.* **2003**, 125, 715-28.

⁴⁴⁴ Hawker, C. J. "Living" Free Radical Polymerization: A Unique Technique for the Preparation of Controlled Macromolecular Architectures. *Acc. Chem. Res.* **1997**, 30, 373-82.

⁴⁴⁵ Solomon, D.H.; Rizzardo, P.; Cacioli, P. Polymerization process and polymers produced thereby. U.S. Patent. 4581429, 1986.

⁴⁴⁶ Moad, G.; Rizzardo, E.; Solomon, D. H. Selectivity of the reaction of free radicals with styrene. *Macromolecules* **1982**, 15, 909-14.

⁴⁴⁷ Veregin, R. P. N.; Georges, M. K.; Kazmaier, P. M.; Hamer, G. K. Free radical polymerizations for narrow polydispersity resins: electron spin resonance studies of the kinetics and mechanism. *Macromolecules* **1993**, 26, 5316-20.

⁴⁴⁸ Benoit, D.; Chaplinski, V.; Braslau, R.; Hawker, C. J. Development of a Universal Alkoxyamine for "Living" Free Radical Polymerizations. *J. Am. Chem. Soc.* **1999**, 121, 3904-20.

⁴⁴⁹ Diaz, T.; Fischer, A.; Jonquieres, A.; Brembilla, A.; Lochon, P. Controlled Polymerization of Functional Monomers and Synthesis of Block Copolymers Using a β -Phosphonylated Nitroxide. *Macromolecules* **2003**, 36, 2235-41.

family of nitroxides, exhibited greater propagation rates than the styrene / TEMPO systems, and this observation was attributed to the lower C-ON bond strengths due to steric strain.⁴⁵¹

Stable free radical polymerization is a premier method for obtaining chain end functionality due to recent advances in alkoxyamine “unimolecular” initiator synthesis. Unimolecular initiators have the added advantage over bimolecular initiator systems due to defined stoichiometry between the initiating fragment and the nitroxide. This feature leads to better control of molecular weight and polydispersity,⁴⁵² and many synthetic methods were discovered earlier for the preparation of alkoxyamine unimolecular initiators. For example, Wu et.al. conducted a radical capping reaction between AIBN initiated styrene and TEMPO.⁴⁵³ An alternate method involved hydrogen abstraction from benzylic sites using *t*-butyl peroxide and in-situ radical capping with nitroxide.⁴⁵² Hawker⁴⁵⁴ and Schmidt-Naake⁴⁵⁵ have employed manganese complexes, e.g. Jacobsen’s catalyst, to directly react styrene olefinic sites with nitroxides. Moreover, in a scheme that is reminiscent of atom transfer radical processes, nitroxides also react with an activated halide through a

⁴⁵⁰ Benoit, D.; Harth, E.; Fox, P.; Waymouth, R. M.; Hawker, C. J. Accurate Structural Control and Block Formation in the Living Polymerization of 1,3-Dienes by Nitroxide-Mediated Procedures. *Macromolecules* **2000**, 33, 363-70.

⁴⁵¹ Le Mercier, C.; Lutz, J. F.; Marque, S.; Le Moigne, F.; Tordo, P.; Lacroix-Desmazes, P.; Boutevin, B.; Couturier, J. L.; Guerret, O.; Martschke, R.; Sobek, J.; Fischer, H., In *ACS Symposium Series*, American Chemical Society: Washington, 2000; Vol. 768, pp 108-22.

⁴⁵² Hawker, C. J.; Barclay, G. G.; Orellana, A.; Dao, J.; Devonport, W. Initiating Systems for Nitroxide-Mediated "Living" Free Radical Polymerizations: Synthesis and Evaluation. *Macromolecules* **1996**, 29, 5245-54.

⁴⁵³ Wang, D.; Bi, X.; Wu, Z. Convenient Synthesis and Application of a New Unimolecular Initiator. *Macromolecules* **2000**, 33, 2293-5.

⁴⁵⁴ Dao, J.; Benoit, D.; Hawker, C.J. A versatile and efficient synthesis of alkoxyamine LFR initiators via manganese based asymmetric epoxidation catalysts *J. Polym. Sci., Part A: Polym. Chem.* **1998**, 36, 2161-7.

⁴⁵⁵ Bothe, M.; Schmidt-Naake, G. An Improved Catalytic Method for Alkoxyamine Synthesis - Functionalized and Biradical Initiators for Nitroxide-Mediated Radical Polymerization. *Macromol. Rapid Commun.* **2003**, 24, 609-13.

copper promoted coupling reaction.^{456,457} The particular functionality of interest in our work was multiple hydrogen bonding chain end functionality, which was easily accessed using earlier synthetic strategies for unimolecular initiators.

Multiple hydrogen bonding has recently gained attention in the field of macromolecular and supramolecular chemistry due to the pioneering work of Meijer,⁴⁵⁸ Stadler,⁴⁵⁹ Lehn⁴⁶⁰ and others.^{461,462} The use of multiple hydrogen bonding sites in conjunction with conventional oligomers and polymers has resulted in thermoreversible mechanical and rheological properties which are tunable based on the strength of the hydrogen bond.^{461,462} For example, Meijer introduced a self-complementary 2-ureido-4[1H]-pyrimidone quadruple hydrogen bonding array at the ends a trifunctional oligomeric poly(propylene glycol-*co*-ethylene glycol) copolymer and a thermoreversible network with film forming

⁴⁵⁶ Diaz, T.; Fischer, A.; Jonquieres, A.; Brebilla, A.; Lochon, P. Controlled Polymerization of Functional Monomers and Synthesis of Block Copolymers Using a β -Phosphonylated Nitroxide. *Macromolecules* **2003**, 36, 2235-41.

⁴⁵⁷ Matyjaszewski, K.; Woodworth, B. E.; Zhang, X.; Gaynor, S.; Metzner, Z. Simple and Efficient Synthesis of Various Alkoxyamines for Stable Free Radical Polymerization. *Macromolecules* **1998**, 31, 5955-7.

⁴⁵⁸ Lange, R. F. M.; van Gulp, M.; Meijer, E. W. Hydrogen-bonded supramolecular polymer networks. *J. Polym. Sci. Part A. Polym. Chem.* **1999**, 37, 3657-70.

⁴⁵⁹ Müller, M.; Dardin, A.; Seidel, U.; Balsamo, V.; Ivan, B.; Spiess, H. W.; Stadler, R. Junction Dynamics in Telechelic Hydrogen Bonded Polyisobutylene Networks. *Macromolecules* **1996**, 29, 2577-83.

⁴⁶⁰ Berl, V.; Schmutz, M.; Krische, M.J.; Khoury, R.G.; Lehn, J.-M. Supramolecular Polymers Generated from Heterocomplementary Monomers Linked through Multiple Hydrogen-Bonding Arrays—Formation, Characterization, and Properties. *Chem. Eur. J.* **2002**, 8, 1227-44.

⁴⁶¹ Yamauchi, K.; Lizotte, J. R.; Long, T. E. Thermoreversible Poly(alkyl acrylates) Consisting of Self-Complementary Multiple Hydrogen Bonding. *Macromolecules* **2003**, 36, 1083-8.

⁴⁶² Yamauchi, K.; Lizotte, J. R.; Hercules, D. M.; Vergne, M. J.; Long, T. E. Combinations of Microphase Separation and Terminal Multiple Hydrogen Bonding in Novel Macromolecules. *J Am Chem Soc* **2002**, 124, 8599-604.

capability and elastomeric mechanical properties was observed.⁴⁵⁸ Long⁴⁶² and Coates⁴⁶³ have also investigated the introduction of pyrimidones in a random fashion in a copolymer using both radical and coordination polymerization methods respectively. The hydrogen bonding motif offers unique thermoreversibility and the influence on physical properties is quite evident in melt rheology. This design strategy offers promise for improved melt processability with equivalent polymer properties at temperatures below hydrogen bond dissociations and also enables potentially recyclable thermoreversible networks.

In biological systems, hydrogen bonding plays an essential role in protein folding and in maintaining the structure of DNA and RNA. For example, the reversibility of the hydrogen bonds that are between base pairs in the DNA structure permits the transcription process.⁴⁶⁴ In protein folding, hydrogen bonds establish the α -helix and β -sheet secondary structures. Introduction of nucleic acid base pairs (adenine, thymine, uracil, guanine, cytosine) into polymers is achievable via numerous means such as post polymerization end group functionalization of well-defined anionically synthesized polymers⁴⁶⁵ or conventional radical polymers,⁴⁶⁶ synthesis of functionalized (meth)acrylic or vinyl monomers followed by conventional radical homopolymerization⁴⁶⁷ or copolymerization,^{468,469} alternating radical

⁴⁶³ Reith, R. L.; Eaton, F. R.; Coates, W. G. Polymerization of Ureidopyrimidinone-Functionalized Olefins by Using Late-Transition Metal Ziegler-Natta Catalysts: Synthesis of Thermoplastic Elastomeric Polyolefins. *Angew. Chem. Int. Ed.* **2001**, 40, 2153-6.

⁴⁶⁴ Nir, E.; Kleinermands, K.; de Vries, M.S. *Nature* **2000**, 408, 949-51.

⁴⁶⁵ Yamauchi, K.; Lizotte, J. R.; Long, T. E. Synthesis and Characterization of Novel Complementary Multiple-Hydrogen Bonded (CMHB) Macromolecules via a Michael Addition. *Macromolecules* **2002**, 35, 8745-50.

⁴⁶⁶ Ilhan, F.; Galow, T. H.; Gray, M.; Clavier, G.; Rotello, V. M. Giant Vesicle Formation through Self-Assembly of Complementary Random Copolymers. *J Am Chem Soc* **2000**, 122, 5895-6.

⁴⁶⁷ Inaki, Y. Synthetic nucleic acid analogs. *Prog. Polym. Sci.* **1992**, 17, 515-70.

⁴⁶⁸ Khan, A.; Haddleton, D. M.; Hannon, M. J.; Kukulj, D.; Marsh, A. Hydrogen Bond Template-Directed Polymerization of Protected 5'-Acryloylnucleosides. *Macromolecules* **1999**, 32, 6560-4.

polymerization with maleic anhydrides,⁴⁷⁰ living cationic and anionic ring-opening polymerization of cyclic base pair derivatives⁴⁷¹ or post-polymerization functionalization of poly(ethylene imine) and polypeptides.⁴⁷² The incorporation of base pairs leads to molecular recognition ability,^{473, 474} metal ligation,⁴⁶⁹ photocrosslinking (thymine),⁴⁷⁴ photoresists^{474,475} and selective chromatographic media.⁴⁷⁴

The present work, which involves controlled radical polymerization, offers the advantage of controlled molecular weights and uracil placement without strenuous anionic techniques or potentially incomplete post polymerization modification. Hydrogen bonding units that are comprised of the uracil nucleic acid base are introduced into styrenic and acrylic polymers using a new family of functionalized initiators. The expected self-association of these units was probed using a number of techniques including melt rheology and ¹H NMR spectroscopy.

⁴⁶⁹ Srivatsan, S. G.; Parvez, M.; Verma, S. Modeling of Prebiotic Catalysis with Adenylated Polymeric Templates: Crystal Structure Studies and Kinetic Characterization of Template-Assisted Phosphate Ester Hydrolysis. *Chem. Eur. J.* **2002**, 8, 5184-91.

⁴⁷⁰ Han, M.J.; Park, S.M.; Park, J.Y.; Yoon, S.H. Polynucleotide analogs. 3. Synthesis, characterization, and physicochemical properties of poly(thymidylic acid) analogs. *Macromolecules* **1992**, 25, 3534-9.

⁴⁷¹ Inaki, Y.; Futagawa, H.; Takemoto, K. Polymerization of cyclic derivatives of uracil and thymine. *J. Polym. Sci., Part A: Polym. Chem.* **1980**, 18, 2959-69

⁴⁷² Overberger, C.G.; Inaki, Y. Graft copolymers containing nucleic acid bases and L- α -amino acids. *J. Polym. Sci., Part A: Polym. Chem.* **1979**, 17, 1739-58.

⁴⁷³ Ilhan, F.; Galow, T. H.; Gray, M.; Clavier, G.; Rotello, V. M. Giant Vesicle Formation through Self-Assembly of Complementary Random Copolymers. *J Am Chem Soc* **2000**, 122, 5895-6.

⁴⁷⁴ Inaki, Y. Synthetic nucleic acid analogs. *Prog. Polym. Sci.* **1992**, 17, 515-70.

⁴⁷⁵ Han, M.J.; Chang, J.Y. Polynucleotide analogues. *Adv. in Polym. Sci.* **2000**, 153, 1-36

4.3 Experimental

4.3.1 Materials

Copper powder (45 μm , 99%), copper (II) triflate (98%), and 2,2,6,6-tetramethylpiperidinyloxy (TEMPO, 98%) were obtained from Acros and used as received. Copper (I) bromide (99.999%), 4,4'-dinonylbipyridine (dNbpy, 97%) and 6-chloromethyluracil (98%) were obtained from Aldrich and used as received. Styrene (99%, Aldrich), *n*-butyl acrylate (99%, Aldrich), dimethyl sulfoxide (DMSO, 99.9%, Aldrich), *N,N*-dimethyl formamide (DMF, 99%, EM Science) and *N,N,N',N'',N'''*-pentamethyldiethylenetriamine (PMDETA, 99%, Aldrich) were distilled from calcium hydride and stored under nitrogen at 0 °C. DEPN was synthesized according to a procedure in the earlier literature.⁴⁷⁶

4.3.2 Synthesis of Uracil-TEMPO Unimolecular Initiator

6-Chloromethyluracil (1.69 g, 10.5 mmol), TEMPO (1.64 g, 10.4 mmol) and dNbpy (170 mg, 0.42 mmol) were dissolved in dimethyl sulfoxide (DMSO, 10 mL). Dichloromethane (20 mL) and THF (10 mL) were added to the reaction mixture. The solution was subjected to three freeze-pump-thaw degassing cycles, warmed to room temperature, and cannulated into a nitrogen filled flask containing a stir bar, copper (II) triflate (37 mg, 0.10 mmol), and copper powder (0.670 g, 10.6 mmol). The reaction mixture was heated to 70 °C and stirred vigorously for 24 h. The contents of the reaction were

⁴⁷⁶ Grimaldi, S.; Finet, J. P.; Le Moigne, F.; Zeghdaoui, A.; Tordo, P.; Benoit, D.; Fontanille, M.; Gnanou, Y. Acyclic β -Phosphonylated Nitroxides: A New Series of Counter-Radicals for "Living"/Controlled Free Radical Polymerization. *Macromolecules* **2000**, 33, 1141-7.

precipitated into water, gravity filtered, and washed with water. The resultant product was dissolved in acetone and purified using flash chromatography on a silica column. The acetone was removed using rotary evaporation and the product was dried under high vacuum at room temperature for 24 h. Uracil-TEMPO was obtained as a white solid (mp 205-207 °C) in 24% yield. ¹H NMR (400 MHz, CDCl₃), 1.1-1.6 ppm (br multiplet, 18H from TEMPO including methyls at 1.1 ppm), 4.6 ppm (d, *J* = 1.2 Hz, N-O-CH₂-C=C: 2H), 5.6 ppm (br s, C=CH-C=O: 1H), 8.5 ppm (br, N-H: 2H). ¹³C NMR (100 MHz, DMSO-d₆), 16.9 ppm, 20.3 ppm, 31.2 ppm, 32.8 ppm (TEMPO 2° and 1° carbons), 60.1 ppm (TEMPO quaternary carbons), 73.6 ppm (CH₂-O-N), 96.8 ppm (C=CH-C=O), 151.8 ppm (NH-C=O-NH), 153.0 ppm (C=CH-C=O), 164.5 ppm (C=CH-C=O). FAB MS: *m/z* = 282.1794 amu (experimental), *m/z* = 282.1818 amu (theoretical).

4.3.3 Synthesis of Uracil-DEPN Unimolecular Initiator

6-Chloromethyluracil (1.82 g, 11.4 mmol), DEPN (3.00 g, 10.2 mmol) and PMDETA (3.51 g, 20.4 mmol) were dissolved in DMSO (20 mL). Dichloromethane (40 mL) was added to the reaction mixture. The solution was subjected to three freeze-pump-thaw degassing cycles, warmed to room temperature, and transferred under nitrogen into a nitrogen filled flask containing a stir bar, copper (I) bromide (1.16 g, 8.2 mmol), and copper powder (0.51 g, 8.2 mmol). The reaction mixture was stirred vigorously for 24 h at ambient temperature. Dichloromethane (300 mL) was added to the reaction mixture and the contents were washed with deionized water 5 times, dried over sodium sulfate, and decanted. The solvent was removed using rotary evaporation at ambient temperature and the resulting green

oil was subjected to column chromatography on silica, and eluting with acetone. The acetone was removed using rotary evaporation and the product was dried under high vacuum at room temperature for 24 h. Uracil-DEPN was obtained as a white solid (mp 137-141 °C) in 71% yield. ¹H NMR (400 MHz, CDCl₃), 1.16 ppm (two s, two C(CH₃)₃: 18H), 1.2-1.36 ppm (m, ethoxy CH₃: 6H), 3.30 ppm (d, *J*_{P-H} = 25 Hz -N-CHC(CH₃)₃-PO(OEt)₂: 1H), 3.95-4.22 ppm (m, ethoxy CH₂: 4H), 4.37 ppm and 4.91 ppm (two d, *J* = 11 Hz, CH₂-O-N: 2H), 5.48 ppm (br s, C=CH-C=O: 1H), 8.31 ppm (br, C-NH-C=O), 11.79 ppm (br, O=C-NH-C=O: 1H). ¹³C NMR (100 MHz, CDCl₃), 16.2 ppm (ethoxy CH₃), 27.7 ppm (N-C(CH₃)₃), 30.3 ppm (C-C(CH₃)₃), 36.3 ppm (C-C(CH₃)₃), 60.3 ppm, 61.7 ppm (P-O-CH₂, *J*_{C-P} = 144 Hz), 62.5 (N-C(CH₃)₃), 67.6 ppm and 69.0 ppm (N-CH-P, *J*_{C-P} = 140 Hz), 73.5 ppm (CH₂-O-N), 99.6 ppm (C=CH-C=O), 150.0 ppm (NH-C=O-NH), 151.1 ppm (C=CH-C=O), 164.2 ppm (C=CH-C=O). FAB MS: *m/z* = 420.2271 amu (experimental), *m/z* = 420.2263 amu (theoretical).

4.3.4 Polymerizations of Styrene Using Uracil-TEMPO

A 100-mL round-bottomed flask containing a magnetic stirring bar was charged with Uracil-TEMPO (100 mg, 0.35 mmol), sealed with a septum-capped three-way glass adaptor connected to a vacuum line, and flushed through repeated vacuum / nitrogen cycles before distilled styrene monomer (30 mL, 259 mmol) was introduced via syringe. The solution was further degassed with multiple freeze-pump-thaw cycles using a dry ice / isopropanol bath and warmed to room temperature. The in-situ FTIR probe was inserted into a 100-mL three-necked flask, and the system was septum sealed and flushed with nitrogen for 30

minutes. The degassed solution was transferred under an inert atmosphere into the three-necked flask and immersed in an oil bath, which was maintained at 130 °C. Samples (2-3 mL) were removed from the reaction at hourly intervals using a syringe. All samples, as well as the final product, were isolated via precipitation into a large excess of isopropanol after first diluting with an equal volume of THF, and subsequently dried overnight under vacuum at elevated temperature (~80-100 °C). The final polymer product had $M_n = 47,200$ g/mol and $M_w/M_n = 1.22$ (SEC MALLS), which agrees well with the molecular weight calculated based on monomer conversion as measured using in-situ FTIR spectroscopy (47,100 g/mol, 62% conversion).

4.3.5 Polymerizations of *n*-Butyl Acrylate Using Uracil-DEPN

Polymerizations involving *n*-butyl acrylate and Uracil-DEPN were conducted in an analogous fashion to those involving styrene and Uracil-TEMPO, however, an additional 0.5 equivalents of DEPN were added to the reaction mixture prior to degassing. A small excess of nitroxide was shown earlier to improve control of nitroxide mediated acrylate polymerizations.^{477,478} Uracil-DEPN initiator (120 mg, 0.29 mmol) and DEPN (42 mg, 0.14 mmol) were added to a 100-mL round bottom flask containing a magnetic stirring bar. The flask was sealed with a septum-capped three-way glass adaptor, connected to a vacuum line, and flushed through repeated vacuum / nitrogen cycles before distilled *n*-butyl acrylate

⁴⁷⁷ Benoit, D.; Grimaldi, S.; Robin, S.; Finet, J. P.; Tordo, P.; Gnanou, Y. Kinetics and Mechanism of Controlled Free-Radical Polymerization of Styrene and *n*-Butyl Acrylate in the Presence of an Acyclic β -Phosphonylated Nitroxide. *J. Am. Chem. Soc.* **2000**, 122, 5929-39.

⁴⁷⁸ Lacroix-Desmazes, P.; Lutz, J. F.; Chauvin, F.; Severac, R.; Boutevin, B. Living Radical Polymerization: Use of an Excess of Nitroxide as a Rate Moderator. *Macromolecules* **2001**, 34, 8866-71.

monomer (28.5 mL, 200 mmol) and distilled DMF (10 mL) were introduced via syringe. The solution was further degassed with multiple freeze-pump-thaw cycles using a dry ice / isopropanol bath and warmed to room temperature. The in-situ FTIR probe was inserted into a 100-mL three-neck flask, and the system was septum sealed and flushed with nitrogen for 30 minutes. The degassed solution was transferred under nitrogen atmosphere into the three-necked flask and immersed in an oil bath, which was maintained at 130 °C. Samples (2-3 mL) were removed from the reaction at hourly intervals using a syringe. All samples, as well as the final product, were isolated via precipitation into a large excess of methanol/water (9:1), and subsequently vacuum dried overnight at elevated temperature (~80-100 °C). The final polymer product had $M_n = 44600$ and $M_w/M_n = 1.17$ (SEC MALLS), which agrees well with the molecular weight calculated from monomer conversion (42700, 48% conversion).

4.3.6 Polymer Characterization

Size exclusion chromatography (SEC) was performed at 40 °C in chloroform or THF at a flow rate of 1 mL/min using a Waters size exclusion chromatographer equipped with an autosampler, three 5 μ m PLgel Mixed-C columns, a Waters 2410 refractive index (RI) detector, and a miniDAWN multiangle laser light scattering (MALLS) detector operating at 690 nm, which was calibrated with polystyrene standards. The refractive index increment (dn/dc) was calculated online. SEC of uracil-polystyrenes in *N*-methylpyrrolidone containing 0.05 M LiBr was performed using a Waters size exclusion chromatographer equipped with a 2414 refractive index detector, which was calibrated using polystyrene

standards. In-situ FTIR spectroscopic analysis was performed using an ASI ReactIR 1000 attenuated total reflectance (ATR) spectrometer.^{200, 201} Differential scanning calorimetry (DSC) was performed under a nitrogen flush at a heating rate of 10 °C/min on a PE Pyris 1 instrument, which was calibrated using indium (mp = 156.60 °C) and zinc (mp = 419.47 °C) standards. Glass transition temperatures were measured as the mid-point of the transition. Thermogravimetric analysis (TGA) was performed under a nitrogen atmosphere at a heating rate of 10 °C/min using a TA Instruments Hi-Res TGA 2950. NMR spectroscopic data was collected in either CDCl₃ or DMSO-d₆ on a Varian 400 MHz spectrometer at ambient temperature. Melt rheology was performed on a stress-controlled, TA Instruments Advanced Rheometer 1000 using a 1 kPa oscillatory stress and a 62.45 rad/s shear rate in a 25 mm diameter parallel plate geometry with a plate separation distance of 1 mm.

4.4 Results and Discussion

4.4.1 Uracil-TEMPO and Uracil-DEPN Unimolecular Initiator Syntheses

The Uracil-TEMPO unimolecular initiator was synthesized analogously to non-hydrogen bonding alkoxyamines discussed in the literature (Figure 4.1).⁴⁷⁹ A copper (I) species, which is generated from Cu⁰ and copper (II) triflate, reductively cleaves the C-Cl bond in 6-chloromethyluracil, and TEMPO efficiently caps the resulting allylic radical in solution. A similar approach was used for Uracil-DEPN synthesis, however, copper (I)

⁴⁷⁹ Matyjaszewski, K.; Woodworth, B. E.; Zhang, X.; Gaynor, S.; Metzner, Z. Simple and Efficient Synthesis of Various Alkoxyamines for Stable Free Radical Polymerization. *Macromolecules* **1998**, 31, 5955-7.

bromide was introduced rather than generated in-situ.⁴⁸⁰ These synthetic methods are convenient, but are limited to activated halides, such as benzylic halides or α -halocarbonyl compounds, due to the instability of the radical generated from non-activated alkyl halides. In this work, it was demonstrated that the conjugated enone activates the chloride on 6-chloromethyluracil, and enables the one-step synthesis of a unimolecular initiator containing a site for hydrogen bonding.

⁴⁸⁰ Diaz, T.; Fischer, A.; Jonquieres, A.; Brebilla, A.; Lochon, P. Controlled Polymerization of Functional Monomers and Synthesis of Block Copolymers Using a β -Phosphonylated Nitroxide. *Macromolecules* **2003**, 36, 2235-41.

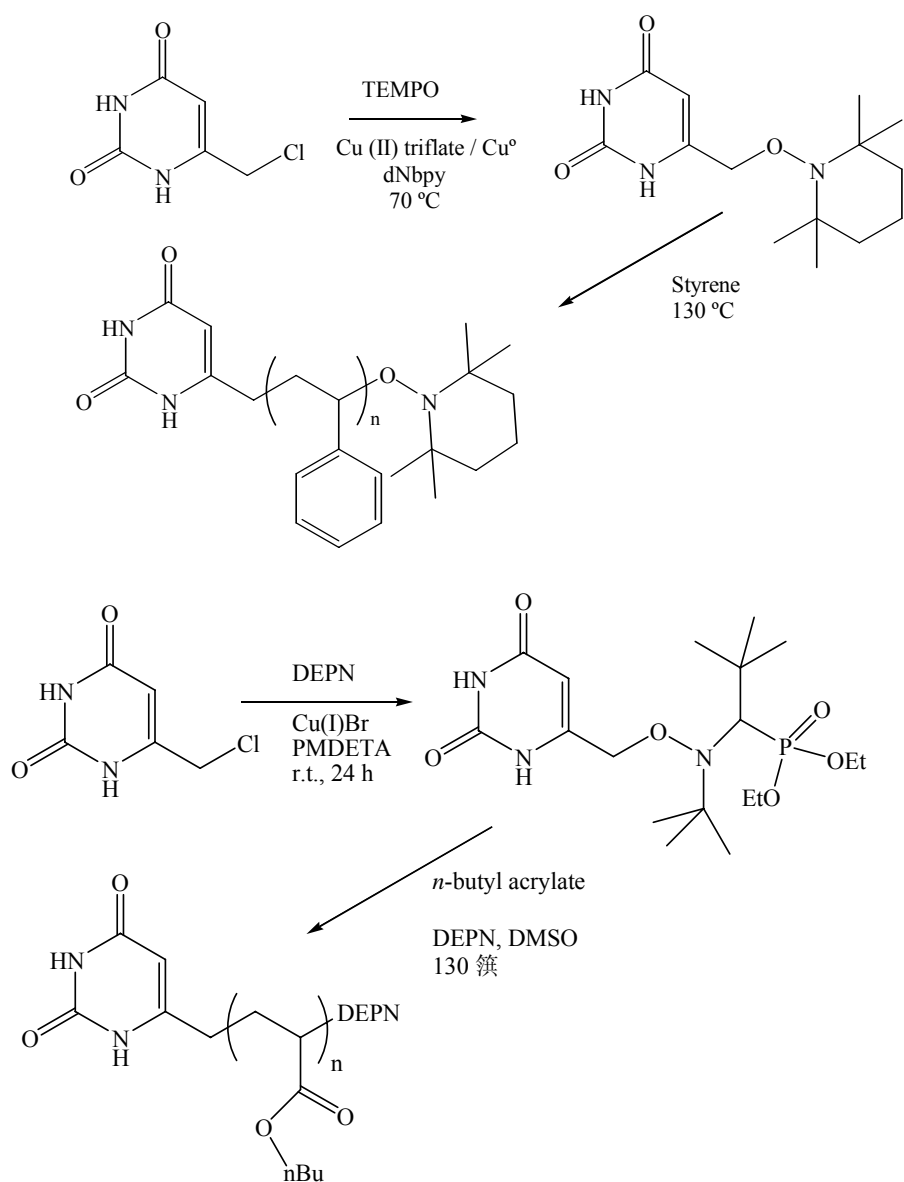


Figure 4.1. Synthesis and polymerization from Uracil-TEMPO and Uracil-DEPN.

4.4.2 Polymerizations of Styrene and *n*-Butyl Acrylate Using the Uracil Based Initiators

Polystyrenes and poly(*n*-butyl acrylates) with molecular weights ranging from 4500 g/mol to 42000 g/mol with narrow molecular weight distributions were synthesized using Uracil-TEMPO and Uracil-DEPN. The polymerization reactions were colorless and exhibited significant increases in viscosity but typically were not allowed to vitrify. The polymer products were colorless and similar in appearance to polymers that were prepared using conventional azo or peroxide initiators. In some experiments, polymerizations were performed using 25 vol % DMSO or DMF to study the effect of hydrogen bond screening solvents on the polymerization, however, statistically significant effects on the kinetics or the molecular weight evolution with conversion were not observed.

Good agreement was obtained between experimental molecular weights and molecular weights calculated from monomer conversion as measured using in-situ FTIR spectroscopy ($g_{\text{styrene}} / \text{mol}_{\text{initiator}} \times \% \text{ conversion}$) (Table 4.1). Typically, low conversions (~50%) were targeted due to the risk of side reactions at higher conversion such as nitroxide degradation and chain termination which can lead to broadened polydispersities.⁴⁸¹ ¹H NMR spectroscopy was utilized to verify the presence of the uracil end group through comparison of the NMR number average molecular weights with SEC results (Table 4.2). In the case of polystyrenes, the ratio of the integration of the aromatic protons to the integration of the alkene proton of the uracil end group allowed the accurate calculation of NMR number average molecular weights for values less than 25000. For poly(*n*-butyl

⁴⁸¹ Moffat, K.; Hamer, G. K.; Georges, M. K. Stable Free Radical Polymerization Process: Kinetic and Mechanistic Study of the Thermal Decomposition of MB-TMP Monitored by NMR and ESR Spectroscopy. *Macromolecules* **1999**, 32, 1004-12.

acrylate)s, the ratio of the integration of the CH₂ protons that are α to the acrylate ester to the integration of the alkene proton of the uracil end group was used to calculate molecular weights. Similar calculations were performed using protons α to the nitroxide end groups, and comparable results were obtained. In the case of uracil functionalized polystyrenes, ¹H NMR spectroscopy also allowed the verification of TEMPO methyl resonances near 0.5 ppm.

Table 4.1. Target and experimental molecular weights for polystyrenes and poly(*n*-butyl acrylate)s synthesized using Uracil-TEMPO and Uracil-DEPN.

Monomer/Initiator	Target ^a M _n	GPC ^b M _n	M _w /M _n
Styrene/U-TEMPO	7100	8000	1.10
Styrene/U-TEMPO	13200	13000	1.27
Styrene/U-TEMPO	27000	25200	1.26
Styrene/U-TEMPO	36500	39800	1.26
Styrene/U-TEMPO	43700	45700	1.21
Styrene/U-TEMPO	69900	75200	1.27
Styrene/U-TEMPO	84400	99200	1.28
nBA/U-DEPN	4100	5900	1.20
nBA/U-DEPN	9100	9800	1.22
nBA/U-DEPN	11700	13700	1.12
nBA/U-DEPN	19500	19100	1.12
nBA/U-DEPN	27000	26100	1.11
nBA/U-DEPN	35600	33300	1.18
nBA/U-DEPN	42500	44600	1.17

^a Target = % conversion × (g_{monomer} / moles_{init}) (conversion measured using in-situ FTIR)

^b MALLS, 40 °C

Table 4.2. Uracil functionalized polystyrene and poly(*n*-butyl acrylate) molecular weights determined using both GPC and NMR.

Monomer/Initiator	GPC ^a M _n	NMR ^b M _n	M _w /M _n
Styrene/U-TEMPO	4500	4800	1.07
Styrene/U-TEMPO	7800	7000	1.04
Styrene/U-TEMPO	10500	9400	1.04
Styrene/U-TEMPO	14600	14400	1.05
Styrene/U-TEMPO	21600	21500	1.26
nBA/U-DEPN	5900	5500	1.20
nBA/U-DEPN	13700	13400	1.12
nBA/U-DEPN	16700	15300	1.09
nBA/U-DEPN	19100	21000	1.12
nBA/U-DEPN	26100	28500	1.11
nBA/U-DEPN	33000	33800	1.14
nBA/U-DEPN	40600	48800	1.19

^a MALLS, 40 °C

^b 400 MHz, CDCl₃, r.t., using uracil alkene proton.

4.4.3 In-situ FTIR Monitoring of Polymerization Kinetics

In-situ FTIR spectroscopy is a powerful, state-of-the-art analytical technique for monitoring numerous organic reactions. The primary strengths of this technique include kinetic analyses, determining reaction order, and obtaining real-time conversion information. The ASI ReactIR instrument is equipped with a diamond-composite/stainless steel probe, which allows the monitoring of reactions under a wide range of pressures (up to 100 psi), temperatures (up to 300 °C) and aggressive reagents. Our research laboratories have devoted significant attention to the kinetic analyses of nitroxide-mediated polymerization using in-situ FTIR spectroscopy.^{482,483}

The polymerization kinetics of styrene and *n*-butyl acrylate using the uracil based initiators at 130 °C revealed pseudo-first order polymerization kinetics, which is expected for radical polymerizations, and is indicative of a constant number of propagating centers (Figure 4.2). The absorbance at 907 cm⁻¹, which corresponds to the vinyl CH₂ wag of styrene, was used to determine the styrene concentration based on a calibration curve that was constructed from a range of styrene / polystyrene compositions at 130 °C. The average observed rate constant ($k_{\text{obs}} = k_p$) for Uracil-TEMPO initiated styrene polymerization of approximately $3.0 \times 10^{-5} \text{ s}^{-1}$ was 50% higher than literature values for TEMPO mediated polymerization of styrene at 132 °C using a similar method.⁴⁸⁴ It is possible that this difference arises from the

⁴⁸² Pasquale, A. J.; Lizotte, J. R.; Williamson, D. T.; Long, T. E. The allure of "molecular videos": In-situ infrared spectroscopy of polymerization processes. *Polym. News* **2002**, 27, 272-83.

⁴⁸³ Lizotte, J. R.; Erwin, B. M.; Colby, R. H.; Long, T. E. Investigations of thermal polymerization in the stable free-radical polymerization of 2-vinylnaphthalene. *J. Polym. Sci., Part A: Polym. Chem.* **2002**, 40, 583-90.

⁴⁸⁴ Pasquale, A. J.; Long, T. E. Real-Time Monitoring of the Stable Free Radical Polymerization of Styrene via in-Situ Mid-Infrared Spectroscopy. *Macromolecules* **1999**, 32, 7954-7.

use of a unimolecular initiating system in this work as opposed to the bimolecular reaction previously employed since stoichiometric mismatch in the latter case could lead to excess nitroxide. Furthermore, the use of a calibration curve in analyzing the in-situ FTIR spectroscopic data may have also contributed to this difference since calibration was not used in the cited reference. Interestingly, for various ratios of Uracil-TEMPO to styrene, nearly identical rate constants were obtained (Table 4.3), which is consistent with the observations of Fischer⁴⁸⁵ and others,⁴⁸⁶ that the amount of initiator did not affect the polymerization rate. Similar equilibrium concentrations of active radicals exist in these polymerizations, however, these active radicals are in equilibrium with differing numbers of dormant chains, which leads to different molecular weights at various [M]:[I] ratios.

⁴⁸⁵ Fischer, A.; Brembilla, A.; Lochon, P. Nitroxide-Mediated Radical Polymerization of 4-Vinylpyridine: Study of the Pseudo-Living Character of the Reaction and Influence of Temperature and Nitroxide Concentration. *Macromolecules* **1999**, 32, 6069-72.

⁴⁸⁶ Fukuda, T.; Terauchi, T.; Goto, A.; Ohno, K.; Tsujii, Y.; Miyamoto, T. Mechanisms and Kinetics of Nitroxide-Controlled Free Radical Polymerization. *Macromolecules* **1996**, 29, 6393-8.

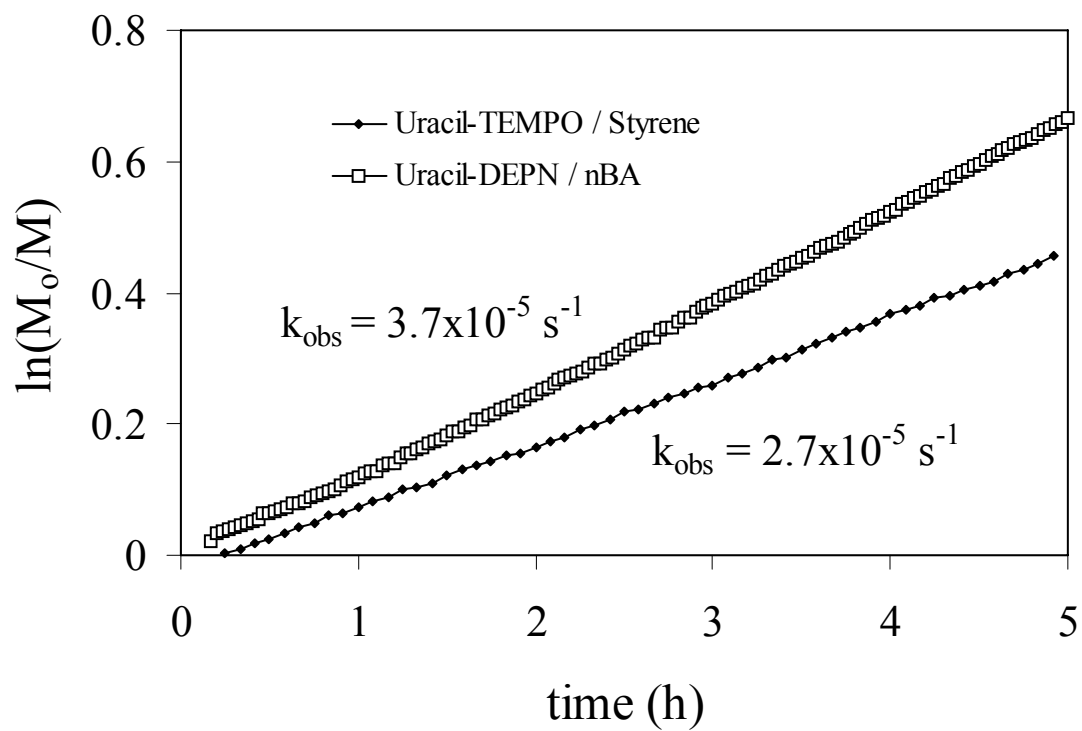


Figure 4.2. In-situ FTIR kinetic plot of styrene and *n*-butyl acrylate polymerizations using Uracyl-TEMPO and Uracyl-DEPN at 130 °C. [Styrene]:[U-TEMPO] = 1460 (bulk), [nBA]:[U-DEPN] = 695 (25 vol% DMSO).

Table 4.3. Polymerization rate constants for various styrene to Uracil-TEMPO ratios.

Moles monomer : Moles initiator	$k_{\text{obs}}^{\text{a}}$ (s^{-1})
366:1	3.02×10^{-5}
488:1	3.12×10^{-5}
732:1	2.97×10^{-5}
1460:1	2.69×10^{-5}
1740:1	3.06×10^{-5}

^a Determined by in-situ FTIR, 130 °C

During in-situ FTIR spectroscopic investigations of the *n*-butyl acrylate polymerizations, calibration curves were obtained for known mixtures of *n*-butyl acrylate and poly(*n*-butyl acrylate) at an absorbance maximum centered at 968 cm⁻¹. The rate constant of polymerization of *n*-butyl acrylate using the Uracil-DEPN unimolecular initiator in DMSO was 3.7 x 10⁻⁵ s⁻¹ at an initiator concentration of 7.4 mM. This rate constant appears low considering that DEPN based styrene polymerizations were shown earlier to proceed at significantly faster rates than analogous TEMPO mediated polymerizations.⁴⁸⁷ Faster rate constants were reported for *n*-butyl acrylate polymerizations at a lower temperature (120 °C) without additional DEPN (~1 x 10⁻⁴ s⁻¹).⁴⁸⁸ It is presumed that the slower kinetics in this work is due to the introduction of 0.5 equivalents of additional nitroxide relative to initiator into the polymerizations, which is known to slow polymerization kinetics.^{489,490}

The evolution of molecular weight with conversion was obtained through a combination of sampling techniques and in-situ FTIR spectroscopy (Figure 4.3). In the case of both unimolecular initiators, number average molecular weights increased in proportion to monomer conversion, with a proportionality constant equal to grams of monomer divided by moles of initiator.

⁴⁸⁷ Grimaldi, S.; Finet, J. P.; Le Moigne, F.; Zeghdaoui, A.; Tordo, P.; Benoit, D.; Fontanille, M.; Gnanou, Y. Acyclic β -Phosphonylated Nitroxides: A New Series of Counter-Radicals for "Living"/Controlled Free Radical Polymerization. *Macromolecules* **2000**, 33, 1141-7.

⁴⁸⁸ Benoit, D.; Grimaldi, S.; Robin, S.; Finet, J. P.; Tordo, P.; Gnanou, Y. Kinetics and Mechanism of Controlled Free-Radical Polymerization of Styrene and *n*-Butyl Acrylate in the Presence of an Acyclic β -Phosphonylated Nitroxide. *J. Am. Chem. Soc.* **2000**, 122, 5929-39.

⁴⁸⁹ Benoit, D.; Chaplinski, V.; Braslau, R.; Hawker, C. J. Development of a Universal Alkoxyamine for "Living" Free Radical Polymerizations. *J. Am. Chem. Soc.* **1999**, 121, 3904-20.

⁴⁹⁰ Lacroix-Desmazes, P.; Lutz, J. F.; Chauvin, F.; Severac, R.; Boutevin, B. Living Radical Polymerization: Use of an Excess of Nitroxide as a Rate Moderator. *Macromolecules* **2001**, 34, 8866-71.

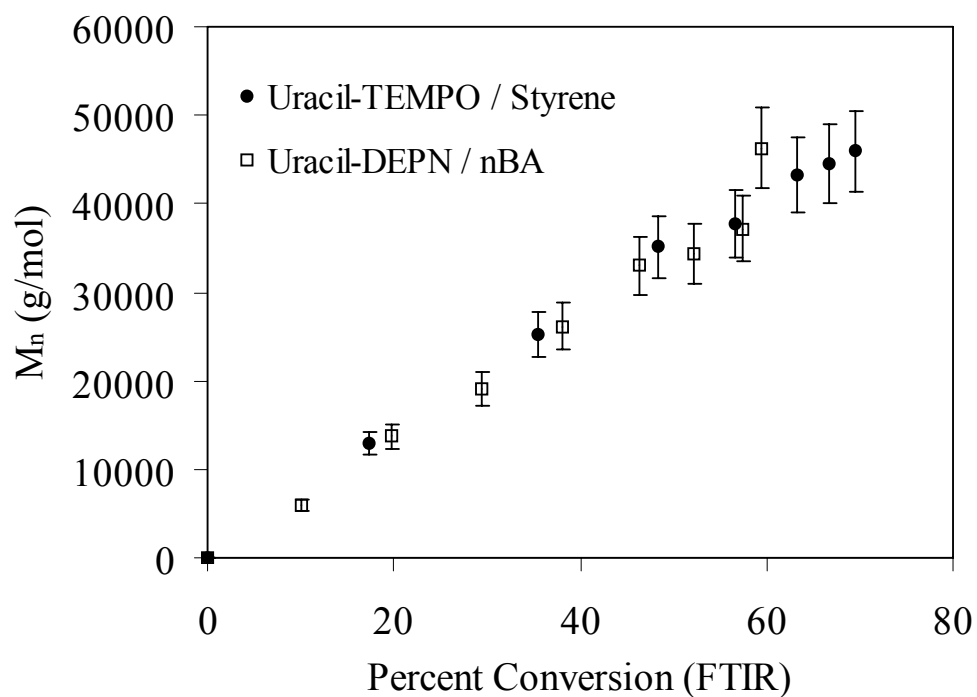


Figure 4.3. Evolution of molecular weight with conversion for the polymerizations of styrene and *n*-butyl acrylate from Uracil-TEMPO and Uracil-DEPN at 130 °C with 25 vol% DMSO.

[Styrene]:[U-TEMPO] = 730, [nBA]:[U-DEPN] = 695.

4.4.4 Characterization of Hydrogen Bonding Using ^1H NMR Spectroscopy

Dilution affects the position of the equilibrium between individual and associated hydrogen bonding groups in the system, as is suggested in the definition of the association constant. Diluting a system composed of associating species should shift the equilibrium toward the unassociated species. Thus, changing the concentration of the uracil end group in CDCl_3 induced a change in the degree of hydrogen bonding which resulted in a change in the chemical shift of one of the N-H protons. Rather than changing the concentration of the polymer in solution, samples of uracil functionalized polystyrene of different molecular weights were dissolved in chloroform-d at an identical concentration of 10.4 wt%. This relatively high solution concentration was chosen due to the ease of observing the N-H protons in ^1H NMR spectroscopy as concentration increases. As the molecular weight of the polystyrenes increased, the chemical shift decreased, which indicated less hydrogen bonding interaction for the higher molecular weight polymer chains due to the lower chain end concentration (Figure 4.4). Attempts to fit the chemical shift vs. concentration data to dimeric self-association models were unsuccessful, which suggested a higher stoichiometry for the complex.⁴⁹¹ However, the trend permitted the construction of a calibration curve for prediction of molecular weights for these polymers based on ^1H NMR spectroscopy. The uracil group is known to associate in several possible geometries due to the presence of both imide and lactam units in the uracil ring.⁴⁹² This is expected to lead to an association

⁴⁹¹ Chen, J. S.; Shirts, R. B. Iterative determination of the NMR monomer shift and dimerization constant in a self-associating system. *J. Phys. Chem.* **1985**, 89, 1643-46

⁴⁹² Beijer, F. H.; Sijbesma, R. P. V., J.A.J.M.; Meijer, E. W. K., H; Spek, A.L. Hydrogen-Bonded Complexes of Diaminopyridines and Diaminotriazines: Opposite Effect of Acylation on Complex Stabilities. *J. Org. Chem.* **1996**, 61, 6371-80.

constant that reflects a combination of several complexes, but this should not hinder the measurement of the association constant.

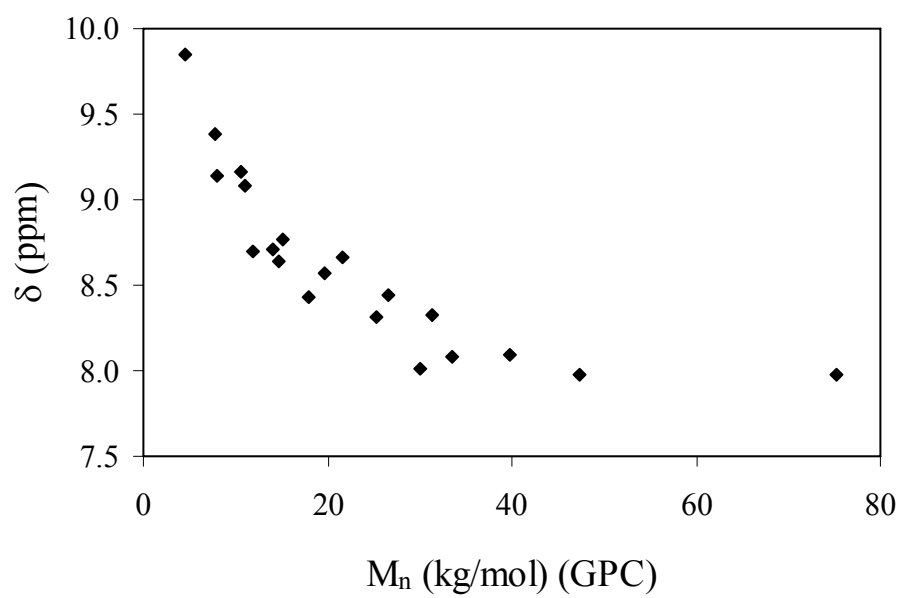


Figure 4.4. Chemical shift of uracil N-H protons as a function of molecular weight in CDCl_3 at 10.4 wt%.

Earlier observations of associations during SEC analysis for hydrogen bonding polymers has prompted SEC in more polar eluents.⁴⁹³ Comparison of SEC measurements of uracil polystyrenes in NMP containing LiBr, a hydrogen bond screening agent, versus chloroform suggested that significant hydrogen bonding did not occur during the SEC analysis. Furthermore, the agreement of the SEC molecular weight data with target molecular weights as well as those obtained via NMR spectroscopic analysis suggest the absence of associations at the concentrations employed in SEC.

4.4.5 Characterization of Hydrogen Bonding Using Melt Rheology

The low glass transition temperature of poly(*n*-butyl acrylate) permits melt rheology experiments over a temperature range that spans both associated and dissociated states of the hydrogen bonding group, as the thermal dissociation of hydrogen bonding groups may occur at temperatures from 50 °C to 130 °C.^{494 - 497} Melt rheology was performed on two samples of poly(*n*-butyl acrylate), one possessing the uracil end group ($M_n = 25,400$ g/mol, $M_w/M_n = 1.17$) and another possessing a 1-phenylethyl group ($M_n = 24000$ g/mol, $M_w/M_n = 1.16$). Zero shear viscosities were collected over a temperature range from 20 °C to 100 °C (Figure

⁴⁹³ Zheng, W.; Angelopoulos, M.; Epstein, A. J.; MacDiarmid, A. G. Experimental Evidence for Hydrogen Bonding in Polyaniline: Mechanism of Aggregate Formation and Dependency on Oxidation State. *Macromolecules* **1997**, *30*, 2953-55.

⁴⁹⁴ Yamauchi, K.; Lizotte, J. R.; Hercules, D. M.; Vergne, M. J.; Long, T. E. Combinations of Microphase Separation and Terminal Multiple Hydrogen Bonding in Novel Macromolecules. *J Am Chem Soc* **2002**, *124*, 8599-604.

⁴⁹⁵ Yamauchi, K.; Lizotte, J. R.; Long, T. E. Thermoreversible Poly(alkyl acrylates) Consisting of Self-Complementary Multiple Hydrogen Bonding. *Macromolecules* **2003**, *36*, 1083-8.

⁴⁹⁶ Müller, M.; Dardin, A.; Seidel, U.; Balsamo, V.; Ivan, B.; Spiess, H. W.; Stadler, R. Junction Dynamics in Telechelic Hydrogen Bonded Polyisobutylene Networks. *Macromolecules* **1996**, *29*, 2577-83

⁴⁹⁷ Lillya, C. P.; Baker, R. J.; Huette, S.; Winter, H. H.; Lin, H.-G.; Shi, J.; Dickinson, L. C.; Chien, J. C. W. Linear Chain Extension through Associative Termini. *Macromolecules* **1992**, *25*, 2076-80.

4.5). Melt viscosity enhancements were clearly observed for the uracil functionalized polyacrylate with nearly equivalent molecular weight. However, there was a stronger temperature dependence for the melt viscosity of the uracil functionalized poly(*n*-butyl acrylate), and dissociation of the hydrogen bonding groups appeared near 80 °C. An Arrhenius analysis of the zero shear viscosities revealed a higher flow activation energy for the uracil functionalized acrylate (54 kJ/mol vs. 48 kJ/mol) (Figure 4.6). The correlation coefficient for the linear fit used to calculate the activation energy was 0.996 in both cases. Based on the fact that flow activation energy is independent of molecular weight,⁴⁹⁸ the data suggests a more than dimeric association of the uracil end groups.

⁴⁹⁸ Wilkes, G. L. An overview of the basic rheological behavior of polymer fluids with an emphasis on polymer melts. *J. Chem. Educ.* **1981**, 58, 880-92.

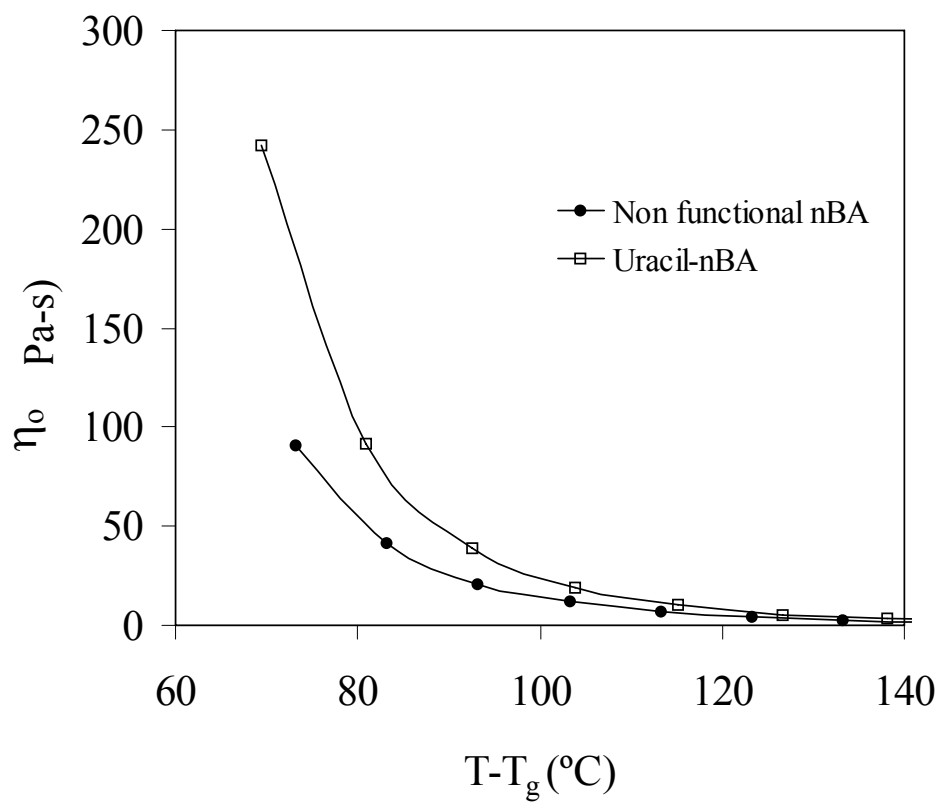


Figure 4.5. Zero-shear melt viscosities for uracil functionalized poly(*n*-butyl acrylate) ($M_n = 25400$, $M_w/M_n = 1.17$) and non functionalized poly(*n*-butyl acrylate) ($M_n = 24000$, $M_w/M_n = 1.16$).

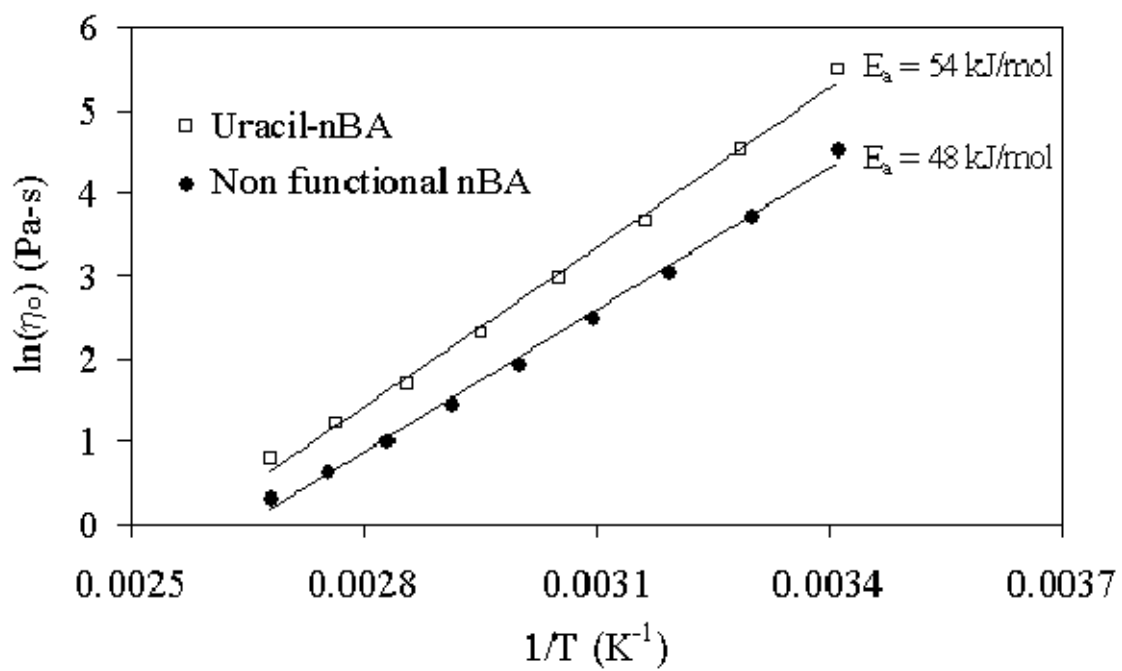


Figure 4.6. Arrhenius analysis of the melt rheology data depicting the flow activation energies for functionalized and non functionalized poly(*n*-butyl acrylate).

4.4.6 Thermal Analysis of Uracil Polystyrenes

Thermogravimetric analysis (TGA) was performed on the lower molecular weight uracil functionalized polystyrene samples ($M_n < 15000$ g/mol). A two-step degradation process was observed in each case (Figure 4.7). The weight loss during the first step (195 - 250 °C) decreased with increasing molecular weight. A two-step degradation process is not normally observed with non-functional polystyrene, but was reported earlier for TEMPO-functionalized polystyrene at similar temperatures.⁴⁹⁹ In order to determine whether the 1st stage degradation involved the loss of TEMPO, an isothermal degradation experiment was performed in which a uracil functionalized polystyrene ($M_n = 7800$ g/mol, $M_w/M_n = 1.04$, SEC MALLS) was heated to 230 °C for 30 min under nitrogen inside the TGA furnace. The sample remained completely soluble in $CDCl_3$, but a slightly brown color developed, and the 1H NMR spectrum indicated the presence of the uracil group in the polymer (the uracil alkene proton at 5.4 ppm) and the loss of the TEMPO group (the geminal dimethyl protons at 0.5 ppm, and benzylic ether proton at 4.1 ppm). The molecular weight calculated using the uracil alkene proton peak ($M_n = 7500$ g/mol) was similar to the value obtained from 1H NMR spectroscopy before degradation ($M_n = 7000$ g/mol). Gel permeation chromatography showed that the molecular weight had increased slightly and that the distribution had also broadened ($M_n = 8100$, $M_w/M_n = 1.27$), possibly due to coupling events. A resonance in the spectrum for the degraded polymer at 3.1 ppm likely represents benzylic protons at head to head linkages formed during styrenic radical combination.⁴⁹⁹

⁴⁹⁹ Roland, A. I.; Schmidt-Naake, G. Thermal degradation of polystyrene produced by nitroxide-controlled radical polymerization. *J. Anal. App. Pyrol.* **2001**, 58-9, 143-54.

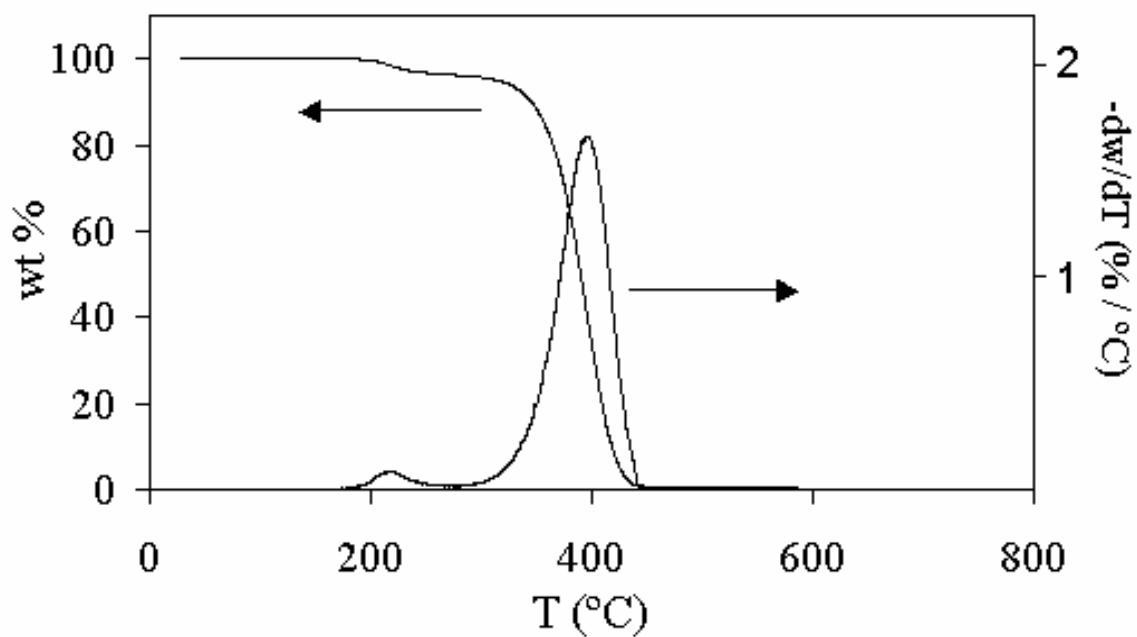


Figure 4.7. Thermogravimetric and derivative traces for a polystyrene synthesized from Uracil-TEMPO ($M_n = 4500$, $M_w/M_n = 1.07$).

A series of uracil functionalized polystyrenes with molecular weights between 5000 and 15000 g/mol were subjected to DSC analysis in order to determine their glass transition temperatures. All samples had approximately the same glass transition temperature (Table 4.4), despite the fact that molar masses were below 15000 g/mol, where non-associating end groups typically contribute to a lower glass transition temperature.⁵⁰⁰ Lin has demonstrated that the glass transition temperature of polystyrene decreases markedly as a function of molar mass below M_e .⁵⁰¹ The data suggests that the higher end group concentrations for lower molecular weight samples resulted in larger T_g enhancements. Similar behavior was observed in UPy functionalized polystyrenes.¹

⁵⁰⁰ Fetters, L. J.; Lohse, D. J.; Milner, S. T. Packing Length Influence in Linear Polymer Melts on the Entanglement, Critical, and Reptation Molecular Weights. *Macromolecules* **1999**, 32, 6847-51.

⁵⁰¹ Lin, Y. H. Entanglement and the molecular weight dependence of polymer glass transition temperature. *Macromolecules* **1990**, 23, 5292-94.

Table 4.4 Glass transition temperatures for various uracil functionalized polystyrenes with molecular weights below the critical molecular weight.

M_n (GPC ^a)	T_g ^b (°C)
4500	101
7800	102
10500	102
14600	101

^a MALLS, CHCl₃, 40 °C

^b DSC: 10 °C/min, N₂, 2nd heat

4.5 Conclusion

Novel uracil-containing alkoxyamines containing both TEMPO and DEPN were synthesized and used in the stable free radical polymerization of styrene and *n*-butyl acrylate. The resulting hydrogen bonding polymers exhibited narrow molecular weight distributions ($M_w/M_n \sim 1.20$) and controlled molecular weights, which are characteristic of stable free radical polymerizations. Linear progression of number average molecular weight with conversion was observed. The rate constant of *n*-butyl acrylate polymerization ($3.7 \times 10^{-5} \text{ s}^{-1}$) was slightly greater than that for styrene polymerization ($3.0 \times 10^{-5} \text{ s}^{-1}$), however, it was lower than typical literature values probably due to the quantity of excess nitroxide present. Also, the styrene polymerization rate constant was higher than literature values possibly due to excess nitroxide which may be present in bimolecular systems, but absent in unimolecular initiation.

Characterization of the polymers using ^1H NMR and melt rheology demonstrated the presence of the hydrogen bonding interaction. Furthermore, a stronger temperature dependence of melt viscosity was observed with uracil functionalized poly(*n*-butyl acrylate)s. Thermogravimetric analysis combined with pyrolysis experiments showed that the uracil-polystyrenes lost TEMPO in a first stage degradation from 195 to 250 °C but that the uracil groups remained on the polymer.

4.6 Acknowledgement

This material is based upon work supported by the U.S. Army Research Laboratory and the U.S. Army Research Office under contract/grant number DAAD19-02-1-0275 Macromolecular Architecture for Performance (MAP) MURI.

Chapter 5. Supramolecular Triblock Copolymers Containing Complementary Nucleobase Molecular Recognition

(Mather, B.D.; Baker, M.B; Beyer, F.L; Green, M.D.; Berg, M.A.G.; Long, T.E.

Macromolecules, submitted)

5.1 Abstract

A novel difunctional alkoxyamine initiator, DEP_N₂, was synthesized and utilized as an efficient initiator in nitroxide-mediated controlled radical polymerization of triblock copolymers. Complementary hydrogen bonding triblock copolymers containing adenine (A) and thymine (T) nucleobase-functionalized outer blocks were synthesized. These thermoplastic elastomeric block copolymers contained short nucleobase-containing outer blocks ($M_n \sim 1\text{K}-4\text{K}$) and *n*-butyl acrylate rubber blocks of variable length ($M_n \sim 14\text{K}-70\text{K}$). Hydrogen bonding interactions were observed for blends of the complementary nucleobase-functionalized block copolymers through increased specific viscosity as well as higher scaling exponents for specific viscosity as a function of solution concentration compared to the individual block copolymers. In the solid state, the blends exhibited evidence of a hard phase consisting of a mixture of complementary adenine and thymine functional blocks, which formed upon annealing, and dynamic mechanical analysis (DMA) revealed higher softening temperatures compared to individual block copolymers. Morphological development of the block copolymers was studied using SAXS and AFM, which revealed intermediate interdomain spacings and surface textures for the blends

compared to the individual precursors. Hydrogen bonding interactions enabled the compatibilization of complementary hydrogen bonding guest molecules such as 9-octyladenine.

5.2 Introduction

Hydrogen bonding enables the introduction of thermoreversible properties into macromolecules through the creation of specific non-covalent intermolecular interactions.⁵⁰² Due to the reversible properties it imparts, hydrogen bonding has been studied in the context of both supramolecular⁵⁰³ and macromolecular⁵⁰⁴ systems. The strength of these interactions is highly dependent on temperature,⁵⁰⁵ solvent,⁵⁰⁶ humidity⁵⁰⁷ and pH,⁵⁰⁸ thus allowing control of properties through a number of environmental parameters. The resulting polymers often exhibit a stronger temperature dependence of melt viscosity than non-hydrogen bonding polymers, suggesting possible advantages in melt processing.⁵⁰⁹ The

⁵⁰² Yamauchi, K.; Lizotte, J. R.; Hercules, D. M.; Vergne, M. J.; Long, T. E. Combinations of Microphase Separation and Terminal Multiple Hydrogen Bonding in Novel Macromolecules. *J Am Chem Soc* **2002**, 124, 8599-604.

⁵⁰³ Brunsveld, L.; Folmer, B. J. B.; Meijer, E. W.; Sijbesma, R. P. Supramolecular Polymers. *Chem Rev* **2001**, 101, 4071-98.

⁵⁰⁴ Ilhan, F.; Galow, T. H.; Gray, M.; Clavier, G.; Rotello, V. M. Giant Vesicle Formation through Self-Assembly of Complementary Random Copolymers. *J Am Chem Soc* **2000**, 122, 5895-6.

⁵⁰⁵ Lutz, J. F.; Thunemann, A. F.; Rurack, K. DNA-like "Melting" of Adenine- and Thymine-Functionalized Synthetic Copolymers. *Macromolecules* **2005**, 38, 8124-6.

⁵⁰⁶ Deans, R.; Ilhan, F.; Rotello, V. M. Recognition-Mediated Unfolding of a Self-Assembled Polymeric Globule. *Macromolecules* **1999**, 32, 4956-60.

⁵⁰⁷ Söntjens, S. H. M.; Sijbesma, R. P.; van Genderen, M. H. P.; Meijer, E. W. Stability and Lifetime of Quadruply Hydrogen Bonded 2-Ureido-4[1H]-pyrimidinone Dimers. *J Am Chem Soc* **2000**, 122, 7487-93.

⁵⁰⁸ Sotiropoulou, M.; Bokias, G.; Staikos, G. Soluble Hydrogen-Bonding Interpolymer Complexes and pH-controlled Thickening Phenomena in Water. *Macromolecules* **2003**, 36, 1349-54.

⁵⁰⁹ Yamauchi, K.; Kanomata, A.; Inoue, T.; Long, T. E. Thermoreversible Polyesters Consisting of Multiple Hydrogen Bonding (MHB). *Macromolecules* **2004**, 37, 3519-22.

strength of hydrogen bonding associations is further tunable via structural and geometric parameters as well as molecular design of the hydrogen bonding sites.^{510 - 513} Association strengths range from 10^2 M^{-1} for DNA nucleobases,⁵¹⁴ to self-complementary ureidopyrimidone (UPy) hydrogen bonding groups,⁵¹⁵ which possess association constants on the order of 10^7 M^{-1} .

Sivakova and Rowan recently reviewed the use of nucleobases in supramolecular assembly and hydrogen bonding polymers.⁵¹⁶ Rowan et al. noted that the behavior of the isolated nucleobases in synthetic polymers is quite different from their behavior in DNA where they are bound to a complementary base.⁵¹⁷ Multiple complementary association modes are possible for nucleobases, including the classical Watson-Crick mode⁵¹⁶ which is present in DNA as well as the less commonly observed Hoogsteen association mode.⁵¹⁸

⁵¹⁰ Beijer, F. H.; Sijbesma, R. P.; Kooijman, H.; Spek, A. L.; Meijer, E. W. Strong Dimerization of Ureidopyrimidones via Quadruple Hydrogen Bonding. *J Am Chem Soc* **1998**, 120, 6761-9.

⁵¹¹ Beijer, F. H.; Sijbesma, R. P. V., J.A.J.M.; Meijer, E. W. K., H.; Spek, A.L. Hydrogen-Bonded Complexes of Diaminopyridines and Diaminotriazines: Opposite Effect of Acylation on Complex Stabilities. *J. Org. Chem.* **1996**, 61, 6371-80.

⁵¹² Jorgensen, W. L.; Pranata, J. Importance of Secondary Interactions in Triply Hydrogen Bonded Complexes: Guanine-Cytosine vs Uracil-2,6-Diaminopyridine. *J Am Chem Soc* **1990**, 112, 2008-10.

⁵¹³ Pranata, J.; Wierschke, S. G.; Jorgensen, W. L. OPLS potential functions for nucleotide bases. Relative association constants of hydrogen-bonded base pairs in chloroform. *J Am Chem Soc* **1991**, 113, 2810-9.

⁵¹⁴ Kyogoku, Y.; Lord, R. C.; Rich, A. The Effect of Substituents on the Hydrogen Bonding of Adenine and Uracil Derivatives. *Proc Natl Acad Sci USA* **1967**, 57, 250-7.

⁵¹⁵ Brunsveld, L.; Folmer, B. J. B.; Meijer, E. W.; Sijbesma, R. P. Supramolecular Polymers. *Chem Rev* **2001**, 101, 4071-98.

⁵¹⁶ Sivakova, S.; Rowan, S. J. Nucleobases as supramolecular motifs. *Chem Soc Rev* **2005**, 34, 9-21.

⁵¹⁷ Sivakova, S.; Bohnsak, D. A.; Mackay, M. E.; Suwanmala, P.; Rowan, S. J. Utilization of a Combination of Weak Hydrogen-Bonding Interactions and Phase Segregation to Yield Highly Thermosensitive Supramolecular Polymers. *J Am Chem Soc* **2005**, 127, 18202-11.

⁵¹⁸ Ghosal, G.; Muniyappa, K. Hoogsteen base-pairing revisited: Resolving a role in normal biological processes and human diseases. *Biochemical and Biophysical Research Communications* **2006**, 343, 1-7.

Furthermore, nucleobases exhibit several weak self-association modes ($K_a < 10 \text{ M}^{-1}$),⁵¹⁴ which compete with the complementary association modes.

Hydrogen bonding block copolymers differ from randomly functionalized copolymers since the placement of the hydrogen bonding groups is localized to a specific region of the polymer backbone. This leads to a dramatic difference in morphology and physical properties due to a potential synergy between microphase separation and hydrogen bonding interactions. Multiplicative and cooperative effects of the neighboring hydrogen bonding groups lead to stronger associations^{519,520} which reinforce microphase separation. Specific hydrogen bonding can increase the tendency of block copolymers to microphase separate through strong associations between chains. Therefore, only short hydrogen bonding blocks are necessary to achieve microphase separation.⁵²¹ In some cases, microphase separation can occur even for a single hydrogen bonding group at the chain ends (i.e. telechelic functionality).⁵²² Others have noted the synergy between microphase separation and hydrogen bonding.⁵²³ Nowick et al. also observed enhanced hydrogen bonding interactions

⁵¹⁹ Pan, J.; Chen, M.; Warner, W.; He, M.; Dalton, L.; Hogen-Esch, T. E. Synthesis and Self-Assembly of Diblock Copolymers through Hydrogen Bonding. Semiquantitative Determination of Binding Constants. *Macromolecules* **2000**, 33, 7835-41.

⁵²⁰ Kriz, J.; Dybal, J.; Brus, J. Cooperative Hydrogen Bonds of Macromolecules. 2. Two-Dimensional Cooperativity in the Binding of Poly(4-vinylpyridine) to Poly(4-vinylphenol). *J Phys Chem B* **2006**, 110, 18338-46.

⁵²¹ Leibler, L. Theory of Microphase Separation in Block Copolymers. *Macromolecules* **1980**, 13, 1602-17.

⁵²² Sivakova, S.; Bohnsak, D. A.; Mackay, M. E.; Suwanmala, P.; Rowan, S. J. Utilization of a Combination of Weak Hydrogen-Bonding Interactions and Phase Segregation to Yield Highly Thermosensitive Supramolecular Polymers. *J Am Chem Soc* **2005**, 127, 18202-11.

⁵²³ Brunsveld, L.; Folmer, B. J. B.; Meijer, E. W.; Sijbesma, R. P. Supramolecular Polymers. *Chem Rev* **2001**, 101, 4071-98.

through localization of nucleobases in sodium dodecyl sulfate micellar cores in aqueous media.⁵²⁴

Others have previously synthesized nucleobase-containing block copolymers via living polymerization techniques such as atom transfer radical polymerization (ATRP)^{525 - 530} and ring opening metathesis polymerization (ROMP).^{531,532} Van Hest et al. synthesized thymine-functionalized block copolymers via ATRP of a thymine methacrylate monomer from a PEG-macroinitiator.⁵³³ Thymine-containing, cinnamate-functionalized photocrosslinkable block copolymers were synthesized via ATRP.^{526 -530} Hydrogen bonding interactions facilitated association of guest molecules into the core of micelles which were formed in selective solvents. The micelles were then photocrosslinked and the hydrogen bonding guest molecules were extracted, resulting in hollow nanospheres for potential drug

⁵²⁴ Nowick, J. S.; Chen, J. S.; Noronha, G. Molecular recognition in micelles: the roles of hydrogen bonding and hydrophobicity in adenine-thymine base-pairing in SDS micelles. *J Am Chem Soc* **1993**, 115, 7636-44.

⁵²⁵ Spijker, H. J.; Dirks, A. J.; van Hest, J. C. M. Unusual rate enhancement in the thymine assisted ATRP process of adenine monomers. *Polymer* **2005**, 46, 8528-35.

⁵²⁶ Zhou, J.; Li, Z.; Liu, G. Diblock Copolymer Nanospheres with Porous Cores. *Macromolecules* **2002**, 35, 3690-6.

⁵²⁷ Liu, G.; Zhou, J. First- and Zero-Order Kinetics of Porogen Release from the Cross-Linked Cores of Diblock Nanospheres. *Macromolecules* **2003**, 36, 5279-84.

⁵²⁸ Hu, J.; Lui, G. Chain Mixing and Segregation in B-C and C-D Diblock Copolymer Micelles. *Macromolecules* **2005**, 38, 8058-65.

⁵²⁹ Yan, X.; Liu, G.; Hu, J.; Willson, C. G. Coaggregation of B-C and D-C Diblock Copolymers with H-Bonding C Blocks in Block-Selective Solvents. *Macromolecules* **2006**, 39, 1906-12.

⁵³⁰ Li, Z.; Ding, J.; Day, M.; Tao, Y. Molecularly Imprinted Polymeric Nanospheres by Diblock Copolymer Self-Assembly. *Macromolecules* **2006**, 39, 2629-36.

⁵³¹ Bazzi, H.; Sleiman, H. Adenine-Containing Block Copolymers via Ring-Opening Metathesis Polymerization: Synthesis and Self-Assembly into Rod Morphologies. *Macromolecules* **2002**, 35, 9617-20.

⁵³² Nair, K. P.; Pollino, J. M.; Weck, M. Noncovalently Functionalized Block Copolymers Possessing Both Hydrogen Bonding and Metal Coordination Centers. *Macromolecules* **2006**, 39, 931-40.

⁵³³ Spijker, H. J.; Dirks, A. J.; van Hest, J. C. M. Unusual rate enhancement in the thymine assisted ATRP process of adenine monomers. *Polymer* **2005**, 46, 8528-35.

delivery applications. Sleiman et al. have synthesized adenine-functionalized block copolymers through ROMP of substituted oxonorbornene monomers, and subsequently formed cylindrical-shaped structures during evaporation from dilute solution.⁵³¹ Weck et al. recently demonstrated the combination of nucleobase hydrogen bonding and metal-ligand coordination interactions in block copolymers synthesized via ROMP.⁵³⁴ Matsushita et al. have also synthesized nucleoside-containing block copolymers using stepwise phosphoramidite coupling techniques.⁵³⁵ Significant effort was also devoted to studying nucleobase-containing homopolymers and random polymers.^{536 - 542}

Nitroxide mediated polymerization (NMP) is a well established controlled radical polymerization methodology which enables block copolymer synthesis with a wide range of acrylic and styrenic monomers.⁵⁴³ Controlled radical polymerization techniques are

⁵³⁴ Nair, K. P.; Pollino, J. M.; Weck, M. Noncovalently Functionalized Block Copolymers Possessing Both Hydrogen Bonding and Metal Coordination Centers. *Macromolecules* **2006**, 39, 931-40.

⁵³⁵ Noro, A.; Nagata, Y.; Tsukamoto, M.; Hayakawa, Y.; Takano, A.; Matsushita, Y. Novel Synthesis and Characterization of Bioconjugate Block Copolymers Having Oligonucleotides. *Biomacromolecules* **2005**, 6, 2328-33.

⁵³⁶ Ilhan, F.; Galow, T. H.; Gray, M.; Clavier, G.; Rotello, V. M. Giant Vesicle Formation through Self-Assembly of Complementary Random Copolymers. *J Am Chem Soc* **2000**, 122, 5895-6.

⁵³⁷ Lutz, J. F.; Thunemann, A. F.; Rurack, K. DNA-like "Melting" of Adenine- and Thymine-Functionalized Synthetic Copolymers. *Macromolecules* **2005**, 38, 8124-6.

⁵³⁸ Marsh, A.; Khan, A.; Haddleton, D. H.; Hannon, M. J. Atom Transfer Polymerization: Use of Uridine and Adenosine Derivatized Monomers and Initiators. *Macromolecules* **1999**, 32, 8725-31.

⁵³⁹ Lutz, J. F.; Thunemann, A. F.; Nehring, R. Preparation by Controlled Radical Polymerization and Self-Assembly via Base-Recognition of Synthetic Polymers Bearing Complementary Nucleobases. *J Polym Sci, Part A: Polym Chem* **2005**, 43, 4805-18.

⁵⁴⁰ Puskas, J. E.; Dahman, Y.; Margaritas, A.; Cunningham, M. F. Novel Thymine-Functionalized Polystyrenes for Applications in Biotechnology. 2. Adsorption of Model Proteins. *Biomacromolecules* **2004**, 5, 1412-21.

⁵⁴¹ Brahme, N. M.; Smith, W. T. Synthesis of Some Graft Copolymers of Uracil. *J Polym Sci, Part A: Polym Chem* **1984**, 22, 813-20.

⁵⁴² Kaye, H. Cyclopolymerization of *N*-Vinyluracil. *Macromolecules* **1971**, 4, 147-52.

⁵⁴³ Hawker, C. J.; Bosman, A. W.; Harth, E. New Polymer Synthesis by Nitroxide Mediated Living Radical Polymerizations. *Chem. Rev.* **2001**, 101, 3661-88.

particularly suited for the hydrogen bonding block copolymers, due to tolerance for protic functionality⁵⁴³ and absence of residual catalyst metals, which were demonstrated to coordinate to nucleobases and affect polymerization kinetics.⁵⁴⁴ Despite the many advantages of nitroxide-mediated polymerization, only one brief report exists in the prior literature regarding synthesis of nucleobase-functionalized block copolymers using NMP.⁵⁴⁵ In the present work, *N-tert-butyl-N-(1-diethylphosphono-2,2-dimethylpropyl)-N-oxyl* (DEPN, Scheme 1) nitroxide is utilized, which was developed earlier by Gnanou and Tordo, and is capable of mediating the polymerization of acrylic monomers.⁵⁴⁶ In order to achieve symmetric triblock copolymers in two synthetic steps, a novel difunctional alkoxyamine initiator (DEPN₂, Figure 5.1) was utilized in the present polymerizations. The use of difunctional initiation is further advantageous due to the difficulties in crossover from styrenic to acrylic monomers that are observed in nitroxide mediated polymerization.⁵⁴⁷ Furthermore, alkoxyamine initiators facilitate controlled molecular weights due to the 1:1 stoichiometry between the initiating fragment and the nitroxide and allow chain-end functionality as reported earlier in our laboratories.^{548,549}

⁵⁴⁴ Spijker, H. J.; Dirks, A. J.; van Hest, J. C. M. Unusual rate enhancement in the thymine assisted ATRP process of adenine monomers. *Polymer* **2005**, 46, 8528-35.

⁵⁴⁵ Saito, K.; Ingalls, L.; Warner, J. C. Core-Bound Nanomicelles Base on Hydrogen Bonding and Photocrosslinking of Thymine *Polym Prep* **2006**, 47, 829-30.

⁵⁴⁶ Grimaldi, S.; Finet, J. P.; Le Moigne, F.; Zeghdaoui, A.; Tordo, P.; Benoit, D.; Fontanille, M.; Gnanou, Y. Acyclic β -Phosphonylated Nitroxides: A New Series of Counter-Radicals for "Living"/Controlled Free Radical Polymerization. *Macromolecules* **2000**, 33, 1141-7.

⁵⁴⁷ Robin, S.; Gnanou, Y. Triblock copolymers based on styrene and *n*-butyl acrylate by nitroxide-mediated radical polymerization: problems and solutions. . *Macromolecular Symposia* **2001**, 165, 43-53.

⁵⁴⁸ Mather, B. D.; Lizotte, J. R.; Long, T. E. Synthesis of Chain End Functionalized Multiple Hydrogen Bonded Polystyrenes and Poly(alkyl acrylates) Using Controlled Radical Polymerization. *Macromolecules* **2004**, 37, 9331-7.

In this manuscript, we discuss combinations of nitroxide-mediated radical polymerization with complementary adenine (A) and thymine (T) nucleobase hydrogen bonding in block copolymer architectures (Figure 5.1). Furthermore, we examine the effects of hydrogen bonding in blends of complementary nucleobase-functionalized block copolymers. Due to the atactic polymer backbone in the present work, a well-ordered double helical complex is not predicted as suggested from the structure of DNA. Instead, associated structures are more likely to consist of multiple polymer chains with one or more associated A-T nucleobase pairs. Future work will involve substitution on tactic polymers to ascertain the effects of tacticity on organization of the intermolecular association.

⁵⁴⁹ Robin, S.; Guerret, O.; Couturier, J. L.; Pirri, R.; Gnanou, Y. Synthesis and Characterization of Poly(styrene-*b*-*n*-butyl acrylate-*b*-styrene) Triblock Copolymers Using a Dialkoxamine as Initiator. *Macromolecules* **2002**, 35, 3844-8.

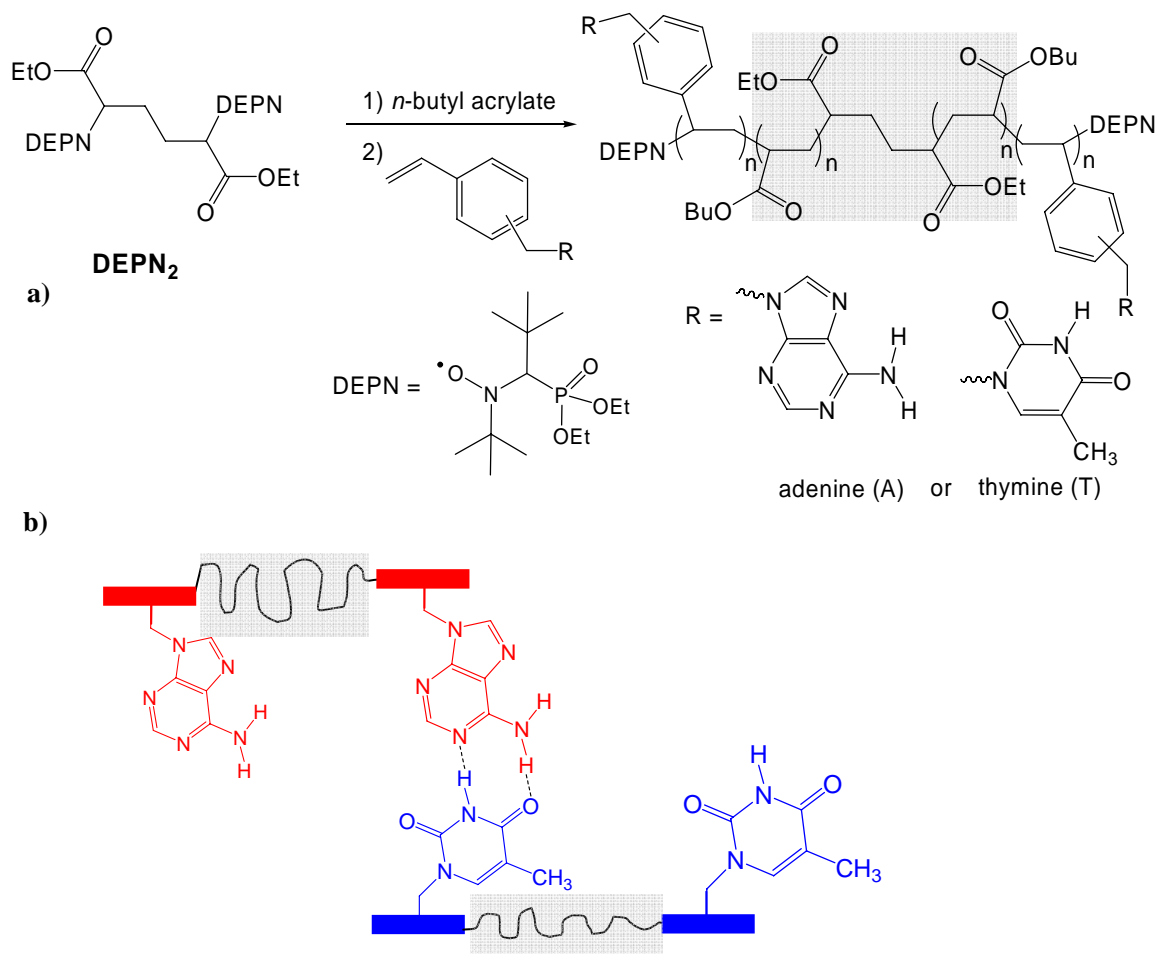


Figure 5.1. Synthesis of adenine and thymine nucleobase-functionalized triblock copolymers.(a) Pictorial representation of hydrogen bonding association of complementary adenine and thymine block copolymers in polymer blends.(b)

5.3 Experimental

5.3.1 Materials

n-Butyl acrylate (99%) was purchased from Aldrich and purified using an alumina column and subsequent vacuum distillation from calcium hydride. Diethyl-*meso*-2,5-dibromoadipate (98%), copper (I) bromide (99.999%), *N,N,N',N'',N''*-pentamethyldiethylenetriamine (PMDETA) (98%) and *N,N*-dimethylformamide (DMF, anhydrous, 99.8%) were purchased from Aldrich and used without further purification. Copper powder (45 μ m, 99%) was purchased from Acros and used as received. DEPN,⁵⁵⁰ Styryl-DEPN,⁵⁵¹ 1-vinylbenzyl thymine,⁵⁵² 9-vinylbenzyl adenine,⁵⁵³ and 9-octyladenine⁵⁵⁴ were synthesized according to the previous literature.

5.3.2 Synthesis of DEPN₂

DEPN (2.0 g, 6.8 mmol) and diethyl-*meso*-2,5-dibromoadipate (1.36 g, 3.8 mmol) were charged to a one-necked 100-mL round-bottomed flask containing a magnetic stirbar. CH₂Cl₂ (30 mL) was added and the solution was degassed with three freeze-pump-thaw cycles. In a

⁵⁵⁰ Grimaldi, S.; Finet, J. P.; Le Moigne, F.; Zeghdaoui, A.; Tordo, P.; Benoit, D.; Fontanille, M.; Gnanou, Y. Acyclic β -Phosphonylated Nitroxides: A New Series of Counter-Radicals for "Living"/Controlled Free Radical Polymerization. *Macromolecules* **2000**, 33, 1141-7.

⁵⁵¹ Diaz, T.; Fischer, A.; Jonquieres, A.; Brembilla, A.; Lochon, P. Controlled Polymerization of Functional Monomers and Synthesis of Block Copolymers Using a β -Phosphonylated Nitroxide. *Macromolecules* **2003**, 36, 2235-41.

⁵⁵² Sedlak, M.; Simunek, P.; Antonietti, M. Synthesis and ¹⁵NMR Characterization of 4-Vinylbenzyl Substituted Bases of Nucleic Acids. *J Heterocyclic Chem* **2003**, 40, 671-75.

⁵⁵³ Srivatsan, S. G.; Parvez, M.; Verma, S. Modeling of Prebiotic Catalysis with Adenylated Polymeric Templates: Crystal Structure Studies and Kinetic Characterization of Template-Assisted Phosphate Ester Hydrolysis. *Chem. Eur. J.* **2002**, 8, 5184-91.

⁵⁵⁴ Bunton, C. A.; Wolfe, B. B. Acid and micellar catalysis of the decomposition of 9-alkylpurine-6-diazotates. *J Am Chem Soc* **1974**, 96, 7747-52.

second 100-mL round-bottomed flask, PMDETA (2.34 g, 13.6 mmol) was dissolved in 20 mL CH₂Cl₂ and subjected to the same degassing. In a third 100-mL round-bottomed flask containing a stirbar, CuBr (0.78 g, 5.47 mmol) and Cu powder (0.35 g, 5.47 mmol) were purged with nitrogen gas. After degassing, the liquid reagents were transferred using a cannula into the flask containing the copper powder and CuBr. The reaction was stirred at 25 °C for 24 h, diluted with CH₂Cl₂ (200 mL), and washed repeatedly with water (10 x 100 mL), to remove copper compounds. The organic layer was then dried over sodium sulfate and evaporated. The product was separated on silica, eluting with ethyl acetate : hexane (1:1). The difunctional alkoxyamine initiator based on DEPN nitroxide (DEPN₂, as shown in Scheme 1) was isolated as a mixture of diastereomers. FAB MS: $m/z = 789.4842 [M+H]^+$ experimental, $m/z = 789.48$ theoretical. A peak for the monofunctional product was not observed ($m/z = 574.5$). ¹H NMR (400 MHz, CDCl₃, 25 °C) (δ, ppm): 1.0-1.2 ppm (s, tBu, 36H), 1.2-1.4 ppm (m, ester CH₃, 18H), 1.6-2.4 ppm (br s, linker CH₂, 4H), 3.1-3.6 ppm (m, DEPN CH, 2H), 3.9-4.2 ppm (m, CH₃, 12H), 4.4-4.5 ppm (m, COCH, 2H). ¹³C NMR (101 MHz, CDCl₃, 25 °C) (δ, ppm): 13.90, 13.98, 14.03, 16.08, 16.14, 16.32, 16.35, 16.41, 16.47, 26.46, 26.52, 26.67, 26.96, 27.53, 27.56, 27.89, 27.95, 28.12, 29.38, 29.44, 29.89, 29.93, 30.12, 30.18, 34.48, 35.09, 35.16, 35.21, 35.49, 35.58, 35.64, 58.82, 58.89, 60.22, 60.27, 60.32, 60.40, 60.62, 61.57, 61.66, 61.96, 62.03, 62.23, 62.30, 68.62, 68.90, 69.99, 70.27, 75.31, 76.85, 77.20, 81.52, 81.87, 86.31, 86.74, 171.46, 172.74, ³¹P NMR (162 MHz, CDCl₃, 25 °C) (δ, ppm): 24.91, 25.00, 25.20, 25.59, 25.63, 25.82.

Meso diastereomer of DEPN₂: The *meso* diastereomer was isolated from the partly crystalline fractions, which eluted first during chromatographic purification of DEPN₂.

Further separation was achieved via triturating the semicrystalline mixture with hexane. m.p. = 139.5-141.5 °C. ¹H NMR (400 MHz, CDCl₃, 25 °C) (δ, ppm): 1.03 (s, *N*-tBu, 18H), 1.06 (s, *C*-tBu, 18H), 1.24 (m, ester CH₃, 18H), 1.55-2.40 (br, linker CH₂, 4H), 3.18 (d, *J* = 25 Hz, DEPN CH, 2H), 3.85-4.20 (m, OCH₂, 12H), 4.25-4.46 (br, OCH, 2H). ¹³C NMR (101 MHz, CDCl₃, 25 °C) (δ, ppm): 13.95, 16.31 (dd, *J*₁ = 28.4 Hz, *J*₂ = 6.2 Hz), 27.94, 28.57, 29.31 (d, *J* = 6.2 Hz), 35.59 (d, *J* = 5.4 Hz), 58.69 (d, *J* = 7 Hz), 61.05 (d, *J* = 95 Hz), 61.80 (d, *J* = 6.1 Hz), 69.71 (d, *J* = 138 Hz), 86.65, 172.89. ³¹P NMR (162 MHz, CDCl₃, 25 °C) (δ, ppm): 25.67.

5.3.3 Polymerization of *n*-Butyl Acrylate with DEPN₂

DEPN₂ (106 mg, 0.134 mmol) and DEPN (17 mg, 0.057 mmol) were weighed into a 100-mL round-bottomed flask containing a magnetic stirbar. The flask was sealed with a three-way joint allowing introduction of reagents via syringe, application of vacuum, and nitrogen. The flask was evacuated to 60 mtorr and refilled with high-purity nitrogen three times. Purified *n*-butyl acrylate (25 mL, 174 mmol) was added and the mixture was degassed with three freeze-pump-thaw cycles. Finally, the flask was immersed in an oil bath thermostated at 130 °C for 75 min. After the polymerization, residual monomer was removed in vacuo (60 mtorr, 40 °C, 6 h). SEC analysis in THF revealed molecular weight data $M_n = 23,700$, $M_w/M_n = 1.11$.

5.3.4 Synthesis of Thymine-Containing Block Copolymer

Poly(*n*-butyl acrylate) homopolymer (208 mg, $M_n = 23,700$) and 1-vinylbenzylthymine

(56 mg, 0.23 mmol) were added to a 50-mL round-bottomed flask with a magnetic stirbar. The flask was sealed with a three-way joint and evacuated to 60 mtorr and refilled with high-purity nitrogen three times. DMF (2 mL) was then syringed into the flask and the mixture was degassed with three freeze-pump-thaw cycles. The flask was then immersed in an oil bath at 120 °C for 2 h. After the polymerization, the polymer was isolated via precipitation into methanol. ¹H NMR spectroscopy (CDCl₃ + DMSO-d₆) revealed block molecular weights T_{2.0K}-nBA_{23.7K}-T_{2.0K}. ¹H NMR (400 MHz, CDCl₃ + DMSO-d₆ (1:1 w/w), 25 °C) (δ, ppm): 0.86 (t, CH₃, 3H) 1.29 (q, COOCH₂CH₂CH₂CH₃, 2H), 1.5 (br, CH₂-CH-COO and COOCH₂CH₂-), 1.7 (br, CH₂-CH-COO-, 1H), 2.1 (br, CH-COO-, 1H) , 3.9 (br, COOCH₂, 2H) , 4.7 (br, Ph-CH₂, 2H), 6.3 (br, Ph, 2H), 6.9 (br, Ph, 2H), 7.2 (br s, N-C=CH, 1H), 11.0 (s, NH, 1H).

5.3.5 Synthesis of Adenine-Containing Block Copolymer

Poly(*n*-butyl acrylate) homopolymer (170 mg, M_n = 23,700) and 9-vinylbenzyladenine (77 mg, 0.31 mmol) were added to a 50-mL round-bottomed flask with a magnetic stirbar. The flask was sealed with a three-way joint and evacuated to 60 mtorr and refilled with high-purity nitrogen three times. DMF (1 mL) was then syringed into the flask and the mixture was degassed with three freeze-pump-thaw cycles. The flask was then immersed in an oil bath at 120 °C for 2 h. After the polymerization, the polymer was isolated via precipitation into methanol. ¹H NMR spectroscopy revealed block molecular weights A_{2.8K}-nBA_{23.7K}-A_{2.8K}. ¹H NMR (400 MHz, DMSO-d₆, 25 °C) (δ, ppm): 0.86 (t, CH₃, 3H) 1.30 (q, COOCH₂CH₂CH₂CH₃, 2H), 1.5 (br, CH₂-CH-COO and COOCH₂CH₂-), 1.75 (br,

$CH_2-CH-COO^-$, 1H), 2.2 (br, $CH-COO^-$, 1H), 4.0 (br, $COOCH_2$, 2H), 5.2 (br, $Ph-CH_2$, 2H), 6.3 (br, Ph , 2H), 6.9 (br, Ph , 2H), 7.6 (br, NH_2 , 2H), 8.1 (br, adenine ring protons, 2H).

5.3.6 Blends of Adenine and Thymine Functionalized Block Copolymers and Sample Preparation

An example of solution blending is provided for the A1 and T1 pair. Adenine containing block copolymer $A_{1.5K}-nBA_{15.9K}-A_{1.5K}$ (0.300 g, 0.19 mmol A) and thymine containing block copolymer $T_{1.8K}-nBA_{13.9K}-T_{1.8K}$ (0.216 g, 0.19 mmol T) were weighed into a vial containing a magnetic stirbar and chloroform (10 mL) was added. The vial was sealed and stirred for 18 h until the solid polymer was no longer visible. Films were cast in PTFE molds from solution and dried in a vacuum oven at 40 °C, with subsequent storage in a dessicator. Films were annealed at 155 °C under vacuum or 200 °C under nitrogen for 18 h.

For DMA and SAXS, polymer samples were cast from chloroform in PTFE molds and were dried under vacuum at 40 °C, with subsequent storage in a dessicator. In some cases (A1, T1, A1/T1), melt pressing (160 °C, 5 min) between PTFE films was necessary to obtain uniform films. Subsequent annealing steps were performed at 155 °C under vacuum for 18 h or at 135 °C under vacuum for A3, T3, A3/T3. In some cases, annealing at 200 °C for 18 h was performed under nitrogen.

For AFM studies, polymer films were solution cast from chloroform (~0.5 wt% polymer) on silicon wafers at 3000 rpm, which resulted in thickness values near 100 nm. Prior cleaning of the silicon wafers consisted of rinsing with chloroform and drying under a high pressure nitrogen stream. Annealing of the AFM film samples was conducted at 155 °C

under vacuum or 200 °C under nitrogen for 18 h.

5.3.7 Polymer Characterization

In-situ FTIR spectroscopic analysis was performed using a Mettler-Toledo ReactIR 1000 attenuated total reflectance (ATR) spectrometer equipped with a diamond composite (DiComp™) probe.^{555,564, 48} Reaction kinetics were determined through the measuring the consumption of *n*-butyl acrylate, which was monitored with the disappearance of the acrylate absorbance at 968 cm⁻¹. Size exclusion chromatography (SEC) was performed at 40 °C in HPLC grade THF at 1 mL/min using a Waters size-exclusion chromatographer equipped with an autosampler, 3 in-line 5 μm PLgel MIXED-C columns. Detectors included a Waters 410 differential refractive index (DRI) detector operating at 880 nm, and a Wyatt Technologies miniDAWN multiangle 690 nm laser light scattering (MALLS) detector, calibrated with PS standards. All reported molecular weight values are absolute molecular weights obtained using the MALLS detector. ¹H NMR spectroscopic data was collected in CDCl₃ or mixtures of CDCl₃ and DMSO-d₆ and (2:1) on a Varian 400 MHz spectrometer at 25 °C. FAB MS was conducted in positive ion mode on a JEOL HX110 Dual Focusing Mass Spectrometer using xenon ion bombardment, polyethylene glycol (PEG) standards and a 3-nitrobenzyl alcohol matrix.

DMA was conducted in film tension mode on 9.5 mm x 6.0 mm x 0.6 mm (l x w x t) rectangular strips on a TA Instruments Q800 DMA at a 3 °C/min scan rate, 1 Hz frequency.

⁵⁵⁵ Pasquale, A. J.; Lizotte, J. R.; Williamson, D. T.; Long, T. E. The allure of "molecular videos": In-situ infrared spectroscopy of polymerization processes. *Polym News* **2002**, 27, 272-83.

⁵⁵⁶ Lizotte, J. R.; Long, T. E. Stable Free-Radical Polymerization of Styrene in Combination with 2-Vinylnaphthalene Initiation *Macromol Chem Phys* **2003**, 204, 570-6.

Solution rheology measurements were conducted on a TA Instruments G2 Rheometer in concentric cylinder geometry in chloroform. Melt rheology was performed using a TA Instruments AR2000 rheometer at 1 Hz frequency and 2.5 % strain at 160 °C.

A Veeco MultiMode™ scanning probe microscope was used for tapping-mode AFM imaging. Samples were imaged at a set-point ratio of 0.6 at magnifications of 500 nm x 500 nm. Veeco's Nanosensor silicon tips having spring constants of 10-130 N/m were utilized for imaging.

For SAXS, $\text{Cu}_{K\alpha}$ X-ray radiation was generated using a Rigaku Ultrax18 rotating anode X-ray generator operated at 45 kV and 100 mA. A nickel filter was used to eliminate all wavelengths but the $\text{Cu}_{K\alpha}$ doublet, with an average wavelength of $\lambda = 1.542 \text{ \AA}$. The exact beam center and the sample-to-detector distance of approximately 1.5 m were calibrated using silver behenate.⁵⁵⁷ The 3 m camera uses 3-pinhole collimation (300, 200 and 600 μm), and a sample-to-detector distance of approximately 1.5 m. Two-dimensional data sets were collected using a Molecular Metrology 2D multi-wire area detector. The data were corrected for detector noise, sample absorption, and background scattering, followed using azimuthal averaging to obtain intensity as a function of the scattering vector, $I(q)$, where $q = 4\pi \cdot \sin(\theta)/\lambda$ and 2θ is the scattering angle. The data were then placed on an absolute scale using a 1.07 mm thick type 2 glassy carbon sample, previously calibrated at the Advanced Photon Source in the Argonne National Laboratory, as a secondary standard. All data processing and analysis were done using Wavemetrics IGOR Pro 5.04 software and IGOR procedures written by Dr. Jan Ilavsky of Argonne National Laboratory.

⁵⁵⁷ Huang, T. C.; Toraya, H.; Blanton, T. N.; Wu, Y. X-ray powder diffraction analysis of silver behenate, a possible low-angle diffraction standard. *J Appl Cryst* **1993**, 26, 180-4.

5.4 Results and Discussion

5.4.1 Synthesis of a Novel Difunctional Alkoxyamine Initiator

A novel, difunctional alkoxyamine initiator based on DEPN, (DEPN₂), was synthesized via conventional copper-promoted atom transfer radical addition techniques from a commercially available dihalide precursor (Figure 1).⁵⁵⁸ DEPN₂ contains four chiral centers, which leads to the existence of 16 diastereomers, and typically an oily product. The chemical structure of DEPN₂ was confirmed via ¹H, ¹³C and ³¹P NMR spectroscopies as well as fast atom bombardment (FAB) mass spectrometry, however, the presence of multiple diastereomers complicated the spectral assignments. A *meso* diastereomer of DEPN₂ (Figure 5.2) was isolated via chromatography in a crystalline form, and this was subjected to X-ray crystallography,⁵⁵⁹ conclusively confirming the identity of the initiator. Unlike previously described difunctional alkoxyamine initiators,⁵⁶⁰ DEPN₂ possesses a non-hydrolyzable linker in the main chain, which provides protection against hydrolytic degradation of the final polymer.

⁵⁵⁸ Matyjaszewski, K.; Woodworth, B. E.; Zhang, X.; Gaynor, S.; Metzner, Z. Simple and Efficient Synthesis of Various Alkoxyamines for Stable Free Radical Polymerization. *Macromolecules* **1998**, 31, 5955-7.

⁵⁵⁹ Mather, B. D. Baker, M.B.; Beyer, F.L.; Green, M.D.; Berg, M.A.G.; Long, T.E. Multiple Hydrogen Bonding for the Reversible Attachment of Ionic Functionality in Block Copolymers. *Macromolecules* **2007**, *submitted*.

⁵⁶⁰ Robin, S.; Guerret, O.; Couturier, J. L.; Pirri, R.; Gnanou, Y. Synthesis and Characterization of Poly(styrene-*b*-*n*-butyl acrylate-*b*-styrene) Triblock Copolymers Using a Dialkoxyamine as Initiator. *Macromolecules* **2002**, 35, 3844-8.

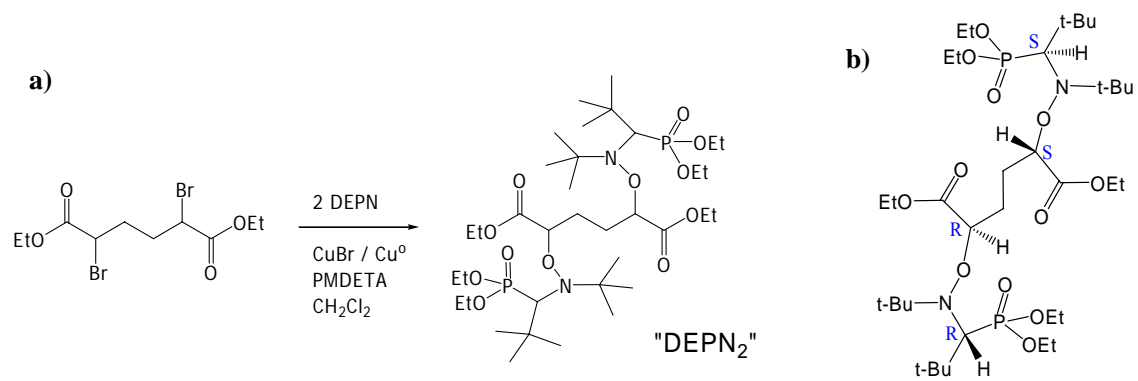


Figure 5.2. Synthesis of DEP₂N₂, difunctional alkoxyamine initiator, using copper-promoted reaction of an activated dihalide. (a) Crystalline meso diastereomer of DEP₂N₂. (b)

5.4.2 Performance of DEPN₂ in the Homopolymerization of *n*-Butyl Acrylate

The target nucleobase-containing block copolymers possess hydrogen bonding styrenic outer blocks and a rubbery poly(*n*-butyl acrylate) central block (Figure 5.1). Thus, initial studies focused on evaluating the performance of DEPN₂ in *n*-butyl acrylate polymerization. Poly(*n*-butyl acrylate) offers a low glass transition temperature, which provides a wide service window for block copolymers ($T_g = -40\text{ }^\circ\text{C}$).⁵⁶¹ Additional DEPN (0.4 equiv.) was added to maintain control of the *n*-butyl acrylate polymerizations, which was shown previously to be necessary in the polymerization of acrylic monomers.⁵⁶²

In order to probe the performance of DEPN₂ in the homopolymerization of *n*-butyl acrylate, kinetic studies were coupled with absolute molecular weight determination using SEC analysis. In-situ FTIR, which is a useful technique for monitoring reactions in real-time,⁵⁶³ was employed to study the kinetics of the *n*-butyl acrylate homopolymerization through monitoring the disappearance of the acrylate absorbance at 968 cm^{-1} as previously reported.⁵⁶⁴ The DEPN₂ initiated polymerizations of *n*-butyl acrylate exhibited *pseudo* first-order kinetics, which was consistent with a controlled radical polymerization. SEC analysis of fractions that were removed from the reaction produced a linear molecular weight (M_n) versus conversion profile, which indicated a constant number of propagating chain ends that is consistent with a living polymerization process (Figure 5.3). Furthermore, SEC traces

⁵⁶¹ Brandrup, J.; Immergut, E. H., *Polymer Handbook*. 3rd ed.; Wiley: New York, 1989.

⁵⁶² Lacroix-Desmazes, P.; Lutz, J. F.; Chauvin, F.; Severac, R.; Boutevin, B. Living Radical Polymerization: Use of an Excess of Nitroxide as a Rate Moderator. *Macromolecules* **2001**, *34*, 8866-71.

⁵⁶³ Pasquale, A. J.; Lizotte, J. R.; Williamson, D. T.; Long, T. E. *Polym News* **2002**, *27*, 272-83.

⁵⁶⁴ Mather, B. D.; Lizotte, J. R.; Long, T. E. Synthesis of Chain End Functionalized Multiple Hydrogen Bonded Polystyrenes and Poly(alkyl acrylates) Using Controlled Radical Polymerization. *Macromolecules* **2004**, *37*, 9331-7.

were unimodal with narrow polydispersities ($M_w/M_n \sim 1.10$), providing additional evidence for controlled radical polymerization.

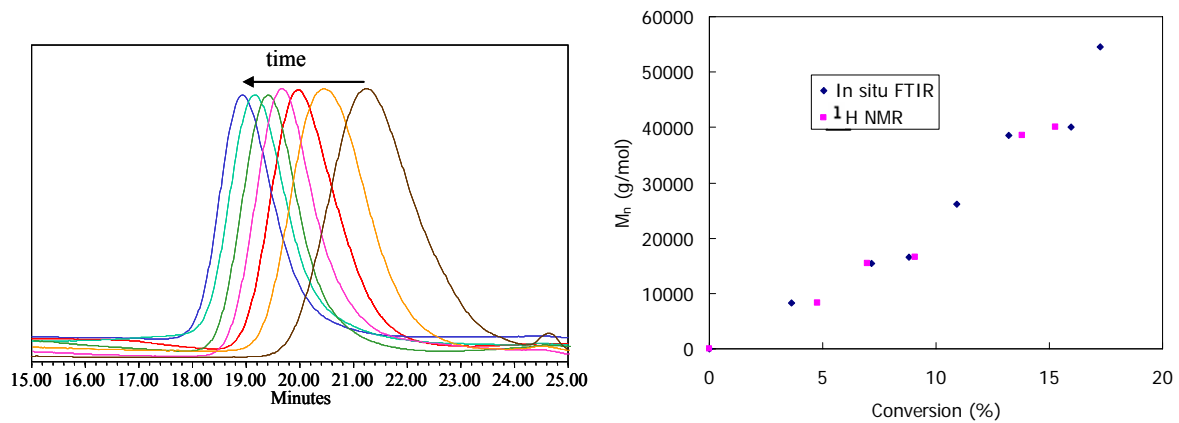


Figure 5.3. SEC analysis of polymerization with time of *n*-butyl acrylate from $DEPN_2$ and linear molecular weight versus conversion plot.

Once the control of *n*-butyl acrylate polymerization with DEPN₂ was established, it was necessary to demonstrate the difunctional nature of DEPN₂, which is essential to the synthesis of well-defined triblock copolymers. This was accomplished using a technique that was developed in the earlier literature, whereby *n*-butyl acrylate polymerizations were conducted with initiator mixtures of DEPN₂ and a monofunctional alkoxyamine initiator Sty-DEPN.⁵⁶⁵ Assuming equal propagation rates for Sty-DEPN and the two initiating sites of DEPN₂, the molecular weight of the polymer formed with DEPN₂ should be higher (doubled compared to the Sty-DEPN initiated polymers). As shown in Figure 5.4, the SEC analysis of these polymers exhibited a bimodal molecular weight distribution with a 2:1 molecular weight ratio of the two peaks, which confirmed our assumption and the difunctional nature of DEPN₂.

⁵⁶⁵ Diaz, T.; Fischer, A.; Jonquieres, A.; Brebilla, A.; Lochon, P. Controlled Polymerization of Functional Monomers and Synthesis of Block Copolymers Using a β -Phosphonylated Nitroxide. *Macromolecules* **2003**, 36, 2235-41.

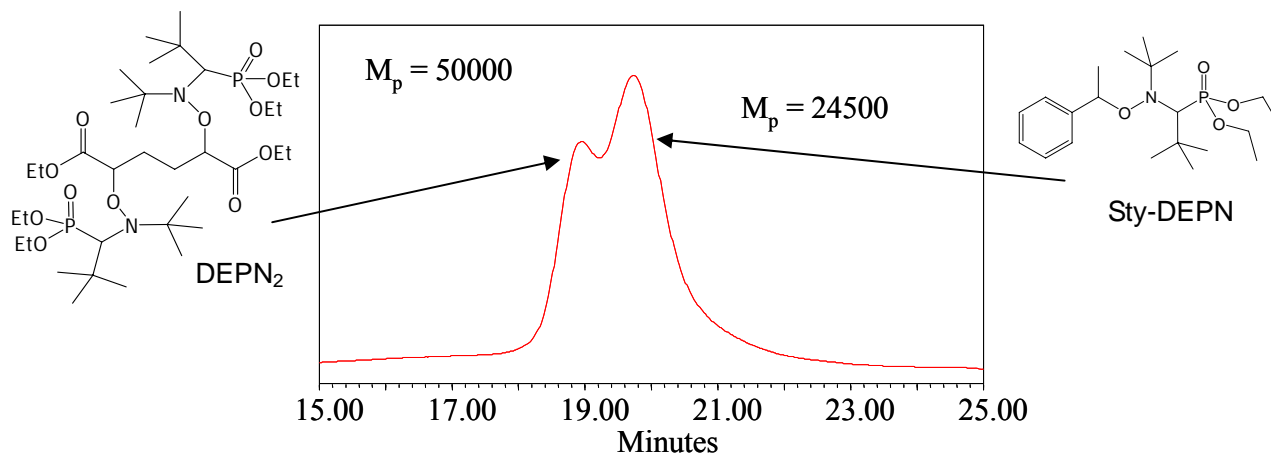


Figure 5.4. SEC trace from a polymerization containing DEPN_2 (difunctional) and Sty-DEPN (monofunctional) initiators.

5.4.3 Synthesis of Nucleobase-Functionalized Hydrogen Bonding Block Copolymers

Initial efforts in the synthesis of block copolymers using DEPN₂ focused on optimizing the conditions for the synthesis of non-hydrogen bonding poly(styrene-*b*-*n*-butyl acrylate-*b*-styrene) triblock copolymers. Block copolymerization, which was performed in a similar fashion to literature procedures,⁵⁶⁶ was conducted in the absence of solvent at 120 °C without additional DEPN for the preparation of poly(styrene-*b*-*n*-butyl acrylate-*b*-styrene) triblock copolymers. Copolymerization reactions resulted in low polydispersities ($M_w/M_n = 1.17$) and unimodal SEC traces for a range of styrene block molecular weights (15K to 26K). Furthermore, optically clear, elastic block copolymer films were formed from solution casting, and AFM imaging revealed microphase separated surface morphologies.

Nucleobase-functionalized block copolymers were synthesized using analogous conditions to those for the synthesis of styrenic triblock copolymers. Adenine and thymine hydrogen bonding groups were introduced via nucleobase-containing styrenic monomers, 1-vinylbenzylthymine and 9-vinylbenzyladenine (Figure 5.1). In contrast to the bulk polymerizations of non-functional styrenic block copolymers, solvent (DMF) was employed to dissolve the solid nucleobase-containing monomers, which resulted in homogeneous polymerizations. Purified polymer products were obtained through precipitation into methanol, which removed residual monomers and solvent. ¹H NMR spectroscopy verified the presence of the nucleobases and quantified the degree of polymerization of the outer blocks, based on the SEC molecular weight of the poly(*n*-butyl acrylate) precursor block

⁵⁶⁶ Robin, S.; Guerret, O.; Couturier, J. L.; Pirri, R.; Gnanou, Y. Synthesis and Characterization of Poly(styrene-*b*-*n*-butyl acrylate-*b*-styrene) Triblock Copolymers Using a Dialkoxamine as Initiator. *Macromolecules* **2002**, 35, 3844-8.

(Table 5.1, see Experimental for chemical shift values). Adenine-containing polymers with increasing poly(*n*-butyl acrylate) molecular weight were denoted as A1-A3, and thymine-containing polymers were denoted T1-T3. SEC analysis was also performed on the nucleobase-functionalized triblock copolymers in THF, which confirmed narrow molecular weight distributions and unimodal traces for the final triblock copolymers. However, SEC was not suitable for the determination of the number average molecular weights of the hydrogen bonding block due to the relatively short block lengths. Thus, ¹H NMR spectroscopy was used to calculate the molecular weights for the shorter hydrogen bonding outer blocks. Blends of the complementary adenine- and thymine-containing polymers of similar rubbery block molecular weights, denoted as A1/T1, A2/T2 and A3/T3, with a 1:1 ratio of adenine to thymine functional groups, were created via solution blending. These blends enabled investigations into the effects of complementary hydrogen bonding on the mechanical, rheological, thermal, and morphological properties of the triblock copolymers.

Table 5.1. Molecular weight data for nucleobase-functionalized block copolymers and blends.

Polymer	Triblock Molecular Weights	Total Molecular Weight (M_n)	Precursor M_w/M_n^a	Weight % nucleobase monomer
A1	A _{1.5K} -nBA _{16.5K} -A _{1.5K}	19.5K	1.26	15
A2	A _{2.8K} -nBA _{23.7K} -A _{2.8K}	29.3K	1.11	19
A3	A _{2.3K} -nBA _{62.3K} -A _{2.3K}	66.9K	1.23	7
T1	T _{1.8K} -nBA _{13.9K} -T _{1.8K}	17.5K	1.23	21
T2	T _{2.0K} -nBA _{23.7K} -T _{2.0K}	27.7K	1.11	14
T3	T _{1.4K} -nBA _{69.9K} -T _{1.4K}	72.7K	1.22	4

^aSEC: THF, 40 °C, MALLS

5.4.4 Complementary Hydrogen Bonding Interactions in Solution and Solid State

Hydrogen bonding interactions in polymers typically manifest themselves in both the solid and solution state through changes in glass transition temperature, modulus, and viscosity. Hydrogen bond association constants (K_a) are commonly characterized in the solution state, using ^1H NMR⁵⁶⁷ or FTIR⁵⁶⁸ spectroscopy to examine changes in the chemical environment and bonding. These studies are typically performed in low dielectric constant solvents such as chloroform or toluene, in order to facilitate stronger hydrogen bonding interactions while maintaining solubility of the polar heterocycles.⁵⁶⁹ Our attempts to study complementary hydrogen bonding in the block copolymers using ^1H NMR spectroscopy were unsuccessful due to disappearance of the resonances for the hydrogen bonding groups in spectra collected in low polarity solvents such as CDCl_3 , presumably due to solution aggregation. This was particularly evident for the adenine-functionalized block copolymer (A2), where the nucleobase-functionalized blocks were visible in DMSO-d_6 , but not in CDCl_3 . ^1H NMR titration experiments of T3 with 9-octyladenine revealed expected chemical shift changes for the thymine NH (from 10.4 to 11.7 ppm upon addition of 2.1 equiv 9-octyladenine). High solution viscosities and low concentrations of hydrogen bonding groups also complicated FTIR analysis in solution.

⁵⁶⁷ Fielding, L. Determination of Association Constants (K_a) from Solution NMR Data. *Tetrahedron* **2000**, 56, 6151-70.

⁵⁶⁸ Kyogoku, Y.; Lord, R. C.; Rich, A. An Infrared Study of Hydrogen Bonding between Adenine and Uracil Derivatives in Chloroform Solution. *J Am Chem Soc* **1967**, 89, 496-504.

⁵⁶⁹ Sijbesma, R. P.; Beijer, F. H.; Brunsveld, L.; Folmer, B. J. B.; Hirschberg, J. H. K. K.; Lange, R. F. M.; Lowe, J. K. L.; Meijer, E. W. Reversible Polymers Formed from Self-Complementary Monomers Using Quadruple Hydrogen Bonding. *Science* **1997**, 278, 1601-4.

Solution rheological experiments are often employed for the study of hydrogen bonding systems, due to the sensitivity of viscosity to polymer structure in solution and the ability to tune the strength of hydrogen bonding through solvent polarity.^{570- 572} Solution rheological studies were performed on the hydrogen bonding block copolymers in chloroform as a relatively low dielectric constant solvent. These studies were performed at a constant nucleobase concentration of 1.20 M, which led to different polymer concentrations among the samples due to slight differences in nucleobase block molecular weight. The presence of the complementary hydrogen bonding interaction in solution was evident from the higher solution viscosities of the blend, which possessed an intermediate polymer concentration due to different nucleobase block molecular weights for the precursor polymers. The zero-shear viscosity of the blend was more than three times higher than the individual polymers (Figure 5.5), which suggested significant intermolecular hydrogen bonding associations in solution. At the concentrations studied, the polymer solutions exhibited Newtonian behavior with the absence of shear thinning.

⁵⁷⁰ Sijbesma, R. P.; Beijer, F. H.; Brunsveld, L.; Folmer, B. J. B.; Hirschberg, J. H. K. K.; Lange, R. F. M.; Lowe, J. K. L.; Meijer, E. W. Reversible Polymers Formed from Self-Complementary Monomers Using Quadruple Hydrogen Bonding. *Science* **1997**, 278, 1601-4.

⁵⁷¹ Karikari, A.; Mather, B. D.; Long, T. E. Association of Star-Shaped Poly(D,L-lactide)s Containing Nucleobase Multiple Hydrogen Bonding. *Biomacromolecules* **2007**, 8, 302-8.

⁵⁷² Lange, R. F. M.; van Gurp, M.; Meijer, E. W. Hydrogen-bonded supramolecular polymer networks. *J. Polym. Sci. Part A. Polym. Chem.* **1999**, 37, 3657-70.

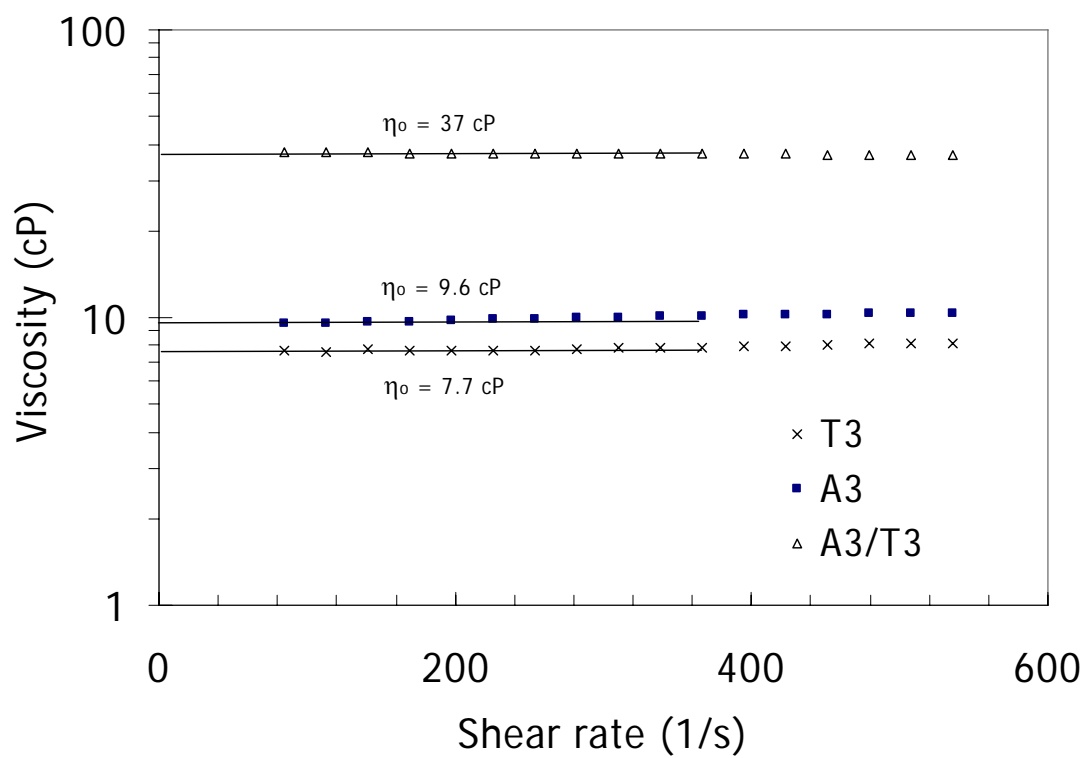


Figure 5.5. Solution rheology of hydrogen bonding block copolymers (A3, T3 and their blend) in chloroform at 25 °C.

The zero-shear solution viscosity of the hydrogen bonding triblock copolymers was also studied as a function of concentration in the semi-dilute unentangled regime.⁵⁷³ In studying the concentration dependence of the zero-shear specific solution viscosity, different scaling exponents of the solution viscosities were observed compared to non-associating polymers. Typically, the zero-shear viscosity scales as $C^{1.25}$, for polymers below their entanglement concentration (C_e), while above C_e , viscosity scales as $C^{3.7}$ assuming that the polymer is dissolved in a good solvent.⁵⁷⁴ As shown in Figure 5.6, the introduction of hydrogen bonding groups led to scaling exponents of 1.4 ± 0.02 and 1.6 ± 0.02 for the thymine- and adenine-functionalized triblock copolymers respectively due to the weak self association of the nucleobases ($K_{A-A} \sim K_{T-T} < 5 \text{ M}^{-1}$).⁵⁷⁵ The errors in the scaling exponents were obtained from statistical analysis of the linear regression, as described earlier.⁵⁷⁶ The blend of the two polymers led to the highest exponent of 2.1 ± 0.02 and the greater slope as a function of hydrogen bonding strength was presumed to result from the concentration dependence of the hydrogen bonding equilibrium.⁵⁷⁷ In the case of adenine and thymine hydrogen bonding groups, neglecting self-association modes, the equilibrium can be written as:

$$K_a = \frac{[AT]}{[A][T]} \quad [5.1]$$

⁵⁷³ de Gennes, P. G., *Scaling Concepts in Polymer Physics*. Cornell Univ: Ithaca, NY, 1979.

⁵⁷⁴ Colby, R. H.; Rubinstein, M. Two-parameter scaling for polymers in Θ solvents. *Macromolecules* **1990**, *23*, 2753-7.

⁵⁷⁵ Kyogoku, Y.; Lord, R. C.; Rich, A. The Effect of Substituents on the Hydrogen Bonding of Adenine and Uracil Derivatives. *Proc Natl Acad Sci USA* **1967**, *57*, 250-7.

⁵⁷⁶ Gaskins, K. *Organic Self-Assembled Thin Films for Second Order Nonlinear Optics*. Masters Thesis, Virginia Tech, 2004.

⁵⁷⁷ Sijbesma, R. P.; Beijer, F. H.; Brunsveld, L.; Folmer, B. J. B.; Hirschberg, J. H. K. K.; Lange, R. F. M.; Lowe, J. K. L.; Meijer, E. W. Reversible Polymers Formed from Self-Complementary Monomers Using Quadruple Hydrogen Bonding. *Science* **1997**, *278*, 1601-4.

where [A], [T] and [AT] are the concentrations of adenine, thymine and the associated complex of adenine and thymine and K_a is the association constant (130 M^{-1}).⁵⁷⁵ Thus, as the concentration of the individual nucleobases increases, the concentration of the complex must increase to satisfy the equilibrium. In the case of hydrogen bonding associations between polymers with multiple nucleobases, this leads to increased effective molecular weight of the supramolecular structures with increasing concentration. As Meijer has established, the formation of associated structures may be considered as a non-covalent step-growth process.⁵⁷⁸ Since solution viscosity is a strong function of molecular weight, association is expected to lead to increased solution viscosity scaling exponents with concentration. Long et al. previously observed higher scaling exponents above C_e for PMMA which was randomly functionalized with ureidopyrimidone (UPy) quadruple hydrogen bonding groups.⁵⁷⁹

⁵⁷⁸ Brunsveld, L.; Folmer, B. J. B.; Meijer, E. W.; Sijbesma, R. P. Supramolecular Polymers. *Chem Rev* **2001**, 101, 4071-98.

⁵⁷⁹ McKee, M. G.; Elkins, C.; Long, T. E. Influence of self-complementary hydrogen bonding on solution rheology/electrospinning relationships. *Polymer* **2004**, 45, 8705-15.

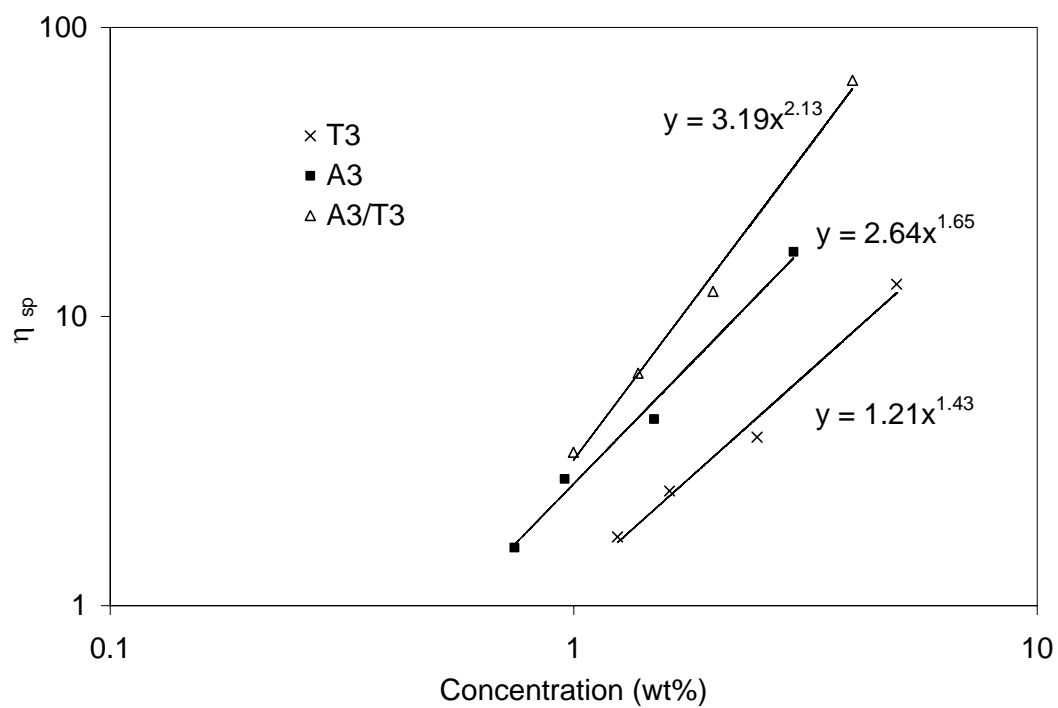


Figure 5.6. Zero-shear solution viscosities of the A3, T3 hydrogen bonding block copolymers and their 1:1 A:T blend A3/T3 as a function of concentration.

Dynamic mechanical analysis (DMA) was utilized to examine the effects of hydrogen bonding on the thermomechanical behavior of the individual triblock copolymers as well as their complementary blends. Modulus versus temperature plots at a constant frequency (1 Hz) confirmed the multiphase nature of the block copolymers (A3 and T3, Figure 5.7). The soft phase glass transition temperature (T_g) occurred at $-30\text{ }^\circ\text{C}$ in each case whereas the hard phase T_g occurred around $140\text{ }^\circ\text{C}$ for the A3 and $110\text{ }^\circ\text{C}$ for T3. This was consistent with measurements of the T_g of adenosine-functionalized methacrylate homopolymers synthesized by Haddleton et al., which possessed T_g values near $140\text{ }^\circ\text{C}$ even for molecular weights below 10K.⁵⁸⁰ A blend of the complementary adenine and thymine-containing polymers (A:T = 1:1 mole ratio), cast from solution, revealed a comparable softening temperature ($140\text{ }^\circ\text{C}$). The absence of multiple softening transitions suggested the presence of a single hard phase consisting of mixed adenine and thymine-containing polymer chains.

The samples were annealed at temperatures above the glass transitions ($T_{\text{anneal}} = 135\text{ }^\circ\text{C}$), in order to obtain thermodynamically favored morphologies, which may be inaccessible due to strong hydrogen bonding interactions at ambient temperature. Block copolymers typically require thermal annealing steps above the highest T_g , in order to achieve development of the morphology.^{581 - 583} Due to strong intermolecular interactions, it was presumed that

⁵⁸⁰ Marsh, A.; Khan, A.; Haddleton, D. H.; Hannon, M. J. Atom Transfer Polymerization: Use of Uridine and Adenosine Derivatized Monomers and Initiators. *Macromolecules* **1999**, 32, 8725-31.

⁵⁸¹ Jeusette, M.; Leclere, P.; Lazzaroni, R.; Simal, F.; Vaneecke, J.; Lardot, T.; Roose, P. New "All-Acrylate" Block Copolymers: Synthesis and Influence of the Architecture on the Morphology and the Mechanical Properties. *Macromolecules* **2007**, 40, 1055-65.

⁵⁸² Marcos, A. G.; Pusel, T. M.; Thomann, R.; Pakula, T.; Okrasa, L.; Geppert, S.; Gronski, W.; Frey, H. Linear-Hyperbranched Block Copolymers Consisting of Polystyrene and Dendritic Poly(carbosilane) Block. *Macromolecules* **2006**, 39, 971-7.

⁵⁸³ Tsarkova, L.; Horvat, A.; Krausch, G.; Zvelindovsky, A. V.; Sevink, G. J. A.; Magerle, R. Defect Evolution in Block Copolymer Thin Films via Temporal Phase Transitions. *Langmuir* **2006**, 22, 8089-95.

nucleobase-functionalized block copolymers required annealing at higher temperatures. In DMA experiments, the individual adenine- and thymine-functionalized triblock copolymers did not exhibit significant change in their softening points upon annealing. In contrast with the individual triblock copolymers, the blend (A3/T3) exhibited a significant increase in the length of the rubbery plateau upon annealing, which extended to 150 °C (Figure 5.8). This was attributed to formation of a hard phase consisting of associated adenine and thymine functionalized blocks, that possessed greater thermomechanical integrity than the individual components, which exhibited relatively weaker self-complementary (A-A, T-T) hydrogen bonding. The presence of the associated hard phase was revealed with AFM studies for the A2, T2, A2/T2 series.

For samples containing higher hard block weight fractions (A1, T1), a longer rubbery plateau were observed (160 °C, not shown), and a similar, but less pronounced, enhancement in hard phase thermal integrity for the blend upon annealing was also observed. Storage modulus values at the rubbery plateau were also significantly higher ($E'_{A1} = 0.6$ MPa, $E'_{T1} = 1.1$ MPa, 80 °C) than those for the A3, T3 set due to the higher hard phase volume fraction.

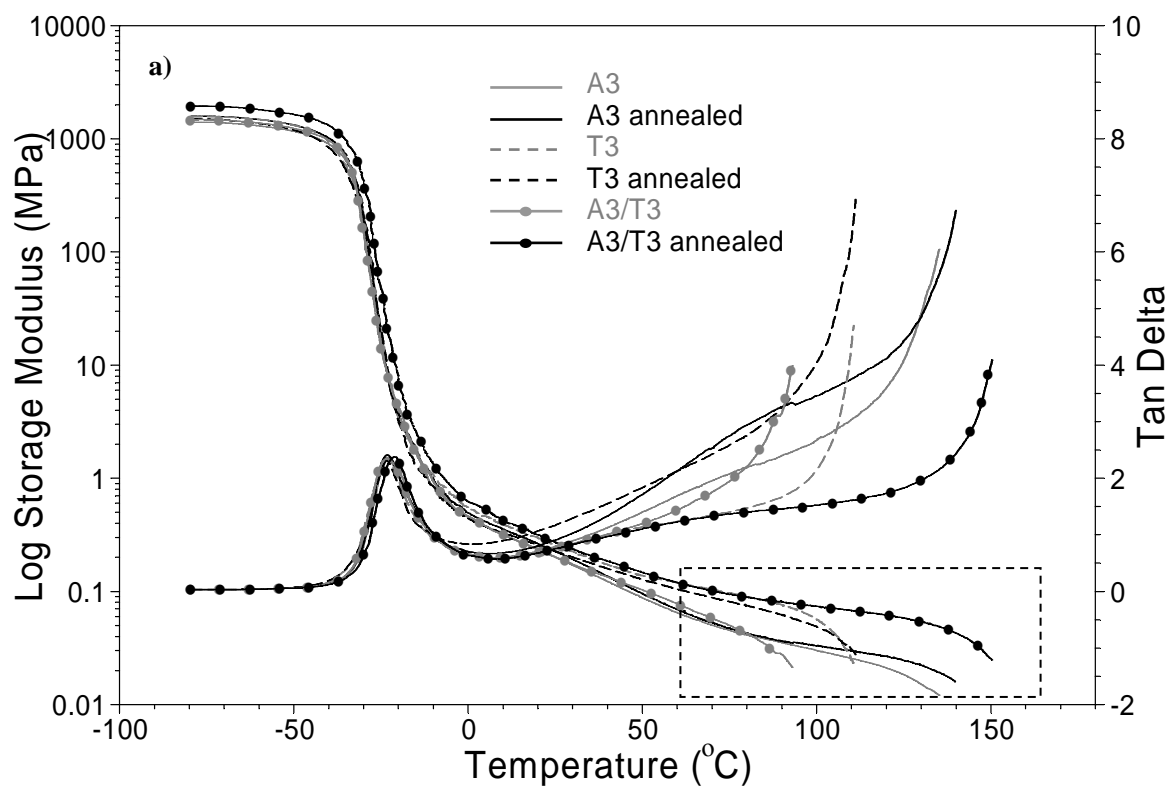


Figure 5.7. Dynamic mechanical storage modulus and tan delta curves for adenine- and thymine-functionalized block copolymers A3, T3 and their blend A3/T3 (A:T = 1:1). Black lines represent samples that were annealed at 135 °C for 18 h under vacuum and gray lines represent unannealed samples. DMA conditions: film tension mode, 1 Hz, 3 °C/min, N₂.

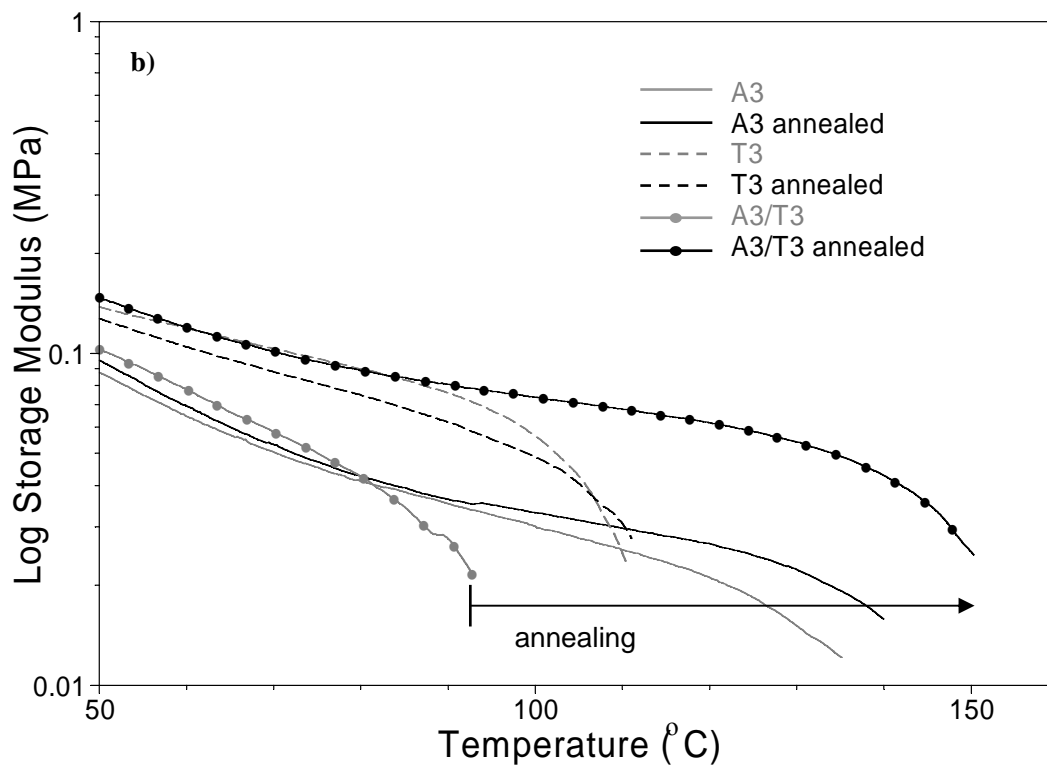


Figure 5.8. Expansion of high-temperature region of DMA storage modulus curves.

5.4.5 Morphological Investigations of Nucleobase-Functionalized Block Copolymers and Blends

AFM allows imaging of surface texture and morphology of microphase separated structures and is frequently applied to block copolymer films.^{584,585} For both adenine- and thymine-containing polymers, AFM revealed intriguing surface morphologies, which consisted of hard domains of the nucleobase-functionalized styrene (light color) dispersed in a soft matrix of poly(*n*-butyl acrylate) (dark color) (Figure 5.9). Adenine- and thymine-functionalized block copolymers with identical rubber block molecular weights, (A2 and T2), as well as their solution-cast equimolar nucleobase (1:1 A:T) blends, were spin-coated on silicon and imaged with AFM in tapping mode. Studies were conducted before and after annealing at 155 °C, which facilitated morphological development of the films. Unannealed samples exhibited microphase separation with generally poor shape development of domains and lack of ordering. Annealing produced distinct morphological features, with clear boundaries emerging between phases and development of short range order. Although AFM does not provide a definitive identification of bulk morphology, the thymine-containing block copolymer (T2) produced an apparent “end-on” cylindrical or possibly spherical morphology (Figure 5.9). The presence of a cylindrical morphology was consistent with the moderate weight fraction of the outer blocks (14 wt%). The positioning of the hard domains appeared to indicate some degree of short-range hexagonally-closest

⁵⁸⁴ Hobbs, J. N.; Register, R. A. Imaging Block Copolymer Crystallization in Real Time with the Atomic Force Microscope. *Macromolecules* **2006**, 39, 703-10.

⁵⁸⁵ Ott, H.; Abetz, V.; Altstadt, V.; Thomann, Y.; Pfau, A. Comparative study of a block copolymer morphology by transmission electron microscopy and scanning force microscopy. *J Microscopy* **2002**, 205, 106-8.

packed (hcp) order. AFM images of A2 resembled cylindrical morphologies where cylinders were lying in the plane of the image. The AFM image could possibly also be attributed to a lamellar morphology, but the weight fraction of the hard phase was more consistent with a cylindrical morphology. Hobbs and Register observed similar images corresponding to cylindrical morphology in melts of poly(1,4-butadiene-*b*-3,4-isoprene).⁵⁸⁶ Tsarkova et al. observed strikingly similar images of cylindrical morphologies of poly(styrene-*b*-butadiene) melts.⁵⁸⁷ The blend of the two polymers (A2/T2) exhibited a morphology with an intermediate appearance, presumably indicating the presence of cylinders lying both in the plane and perpendicular to the plane. The absence of macrophase separation in the blend suggested the compatibility of the complementary nucleobase functionalized hard blocks due to the hydrogen bonding ability of the adenine and thymine blocks. This supposition was reinforced with SAXS analysis, which indicated an averaged, intermediate Bragg spacing, and no evidence of multiple interdomain spacings, which is discussed in the following section. Furthermore, Choo et al. showed that thymine- and adenine-containing small molecules associate in the solid state into co-crystalline forms, upon simple grinding of a blend of the individual crystalline solids.⁵⁸⁸

⁵⁸⁶ Hobbs, J. N.; Register, R. A. Imaging Block Copolymer Crystallization in Real Time with the Atomic Force Microscope. *Macromolecules* **2006**, *39*, 703-10.

⁵⁸⁷ Tsarkova, L.; Horvat, A.; Krausch, G.; Zvelindovsky, A. V.; Sevink, G. J. A.; Magerle, R. Defect Evolution in Block Copolymer Thin Films via Temporal Phase Transitions. *Langmuir* **2006**, *22*, 8089-95.

⁵⁸⁸ Etter, M. C.; Reutzel, S. M.; Choo, C. G. Self-organization of Adenine and Thymine in the Solid State. *J Am Chem Soc* **1993**, *115*, 4411-2.

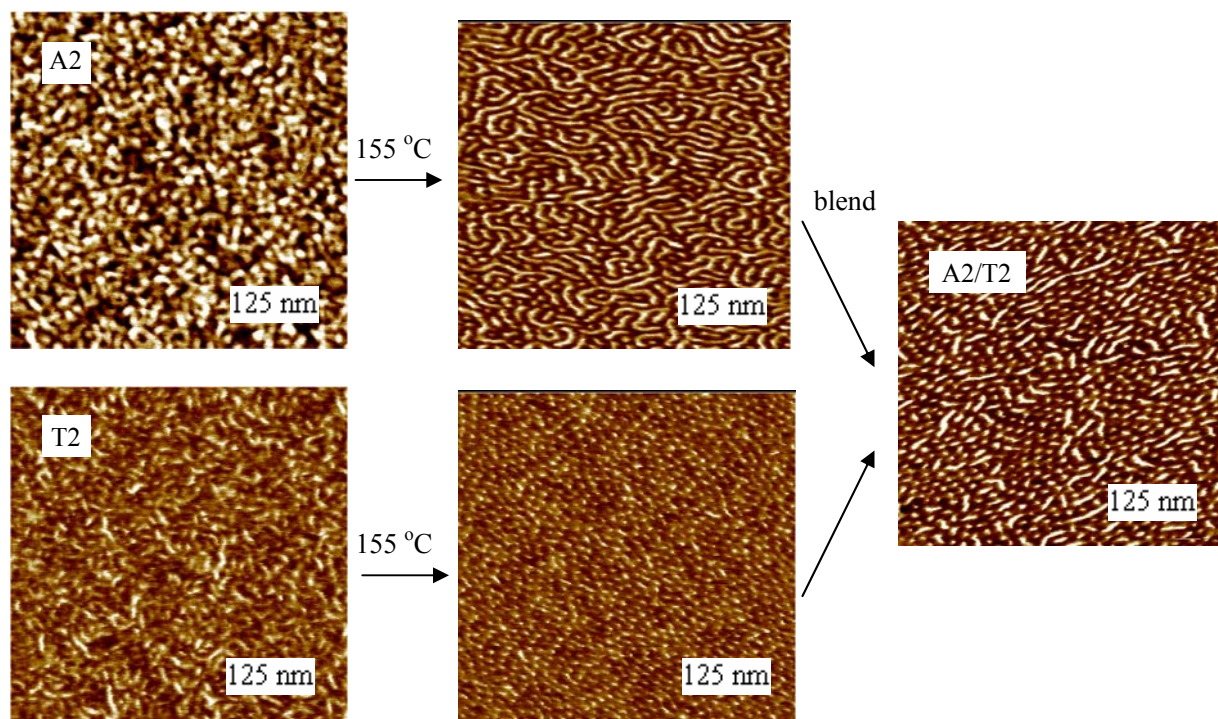


Figure 5.9. Tapping mode AFM phase images of thymine- (T2) and adenine-functionalized (A2) polymers before and after annealing as well as A2/T2 blend. Samples were spin-coated on a silicon wafer, from chloroform solution. Annealing was performed at 155 °C under vacuum for 18 h. Film thickness ~ 100 nm. Images are 500 nm x 500 nm.

Analogous AFM studies were conducted for the A1, T1 and A1/T1 set (Figure 5.10) which contained slightly higher nucleobase weight fractions (15-21 wt% for A1, T1 and A1/T1 versus 14-19 wt% for the A2, T2 and A2/T2 set) and slightly shorter rubber block molecular weights (13.9K or 15.9K vs. 23.7K). As seen with the A2 and T2 series, the unannealed samples exhibited poor morphological development. Annealing at 155 °C resulted in images that were similar to A2, resembling the “in plane” cylindrical morphology. Interestingly, the A1/T1 blend exhibited the least clear surface texture, possibly due to the strength of the complementary A-T hydrogen bonding interactions preventing clear morphological development. The higher softening temperatures for the hard phases of T1 and T2 (160 °C), suggested that annealing at 155 °C was insufficient. In order to probe the effect of annealing at higher temperatures on block polymers containing the higher levels of nucleobases, annealing experiments were conducted on the A1, T1, A1/T1 series at temperatures near 200 °C (Figure 5.10). Interestingly, annealing at temperatures near 200 °C enabled organization into “end-on” cylindrical morphologies for A1 and A1/T1 at the surface, and hcp ordering was observed as evidenced from the hexagonal shape of the Fourier transform of the AFM phase images. For the T1 sample, a well ordered cylindrical “in-plane” surface morphology was observed at 190 °C, followed by the beginning of a transition to “end-on” arrangement at 210 °C. SAXS experiments (discussed in the next section) conducted on the A1, T1 and A1/T1 set, annealed at 200 °C and 155 °C confirmed the cylindrical morphology in all cases. The hindered rearrangement of the thymine-containing polymer may have resulted from the fact that it possessed the highest nucleobase weight fraction (19 wt%) and lowest poly(*n*-butyl acrylate) block molecular weight (13.9K).

Roose et al. also observed a transition upon annealing of “cylinders in the plane” to “end-on” cylinders for a poly(methyl methacrylate-*b*-methyl acrylate-*co*-ethylhexyl acrylate-*b*-methyl methacrylate).⁵⁸⁹ The higher surface energy of the PMMA blocks was thought to result in the minimization of surface area of the hard domains, driving the system to the “end-on” morphology. In the present system, it is assumed that the polar nucleobase-containing blocks possess a higher surface energy than the poly(*n*-butyl acrylate) block, resulting in similar behavior.

⁵⁸⁹ Jeusette, M.; Leclere, P.; Lazzaroni, R.; Simal, F.; Vaneecke, J.; Lardot, T.; Roose, P. New “All-Acrylate” Block Copolymers: Synthesis and Influence of the Architecture on the Morphology and the Mechanical Properties. *Macromolecules* **2007**, *40*, 1055-65.

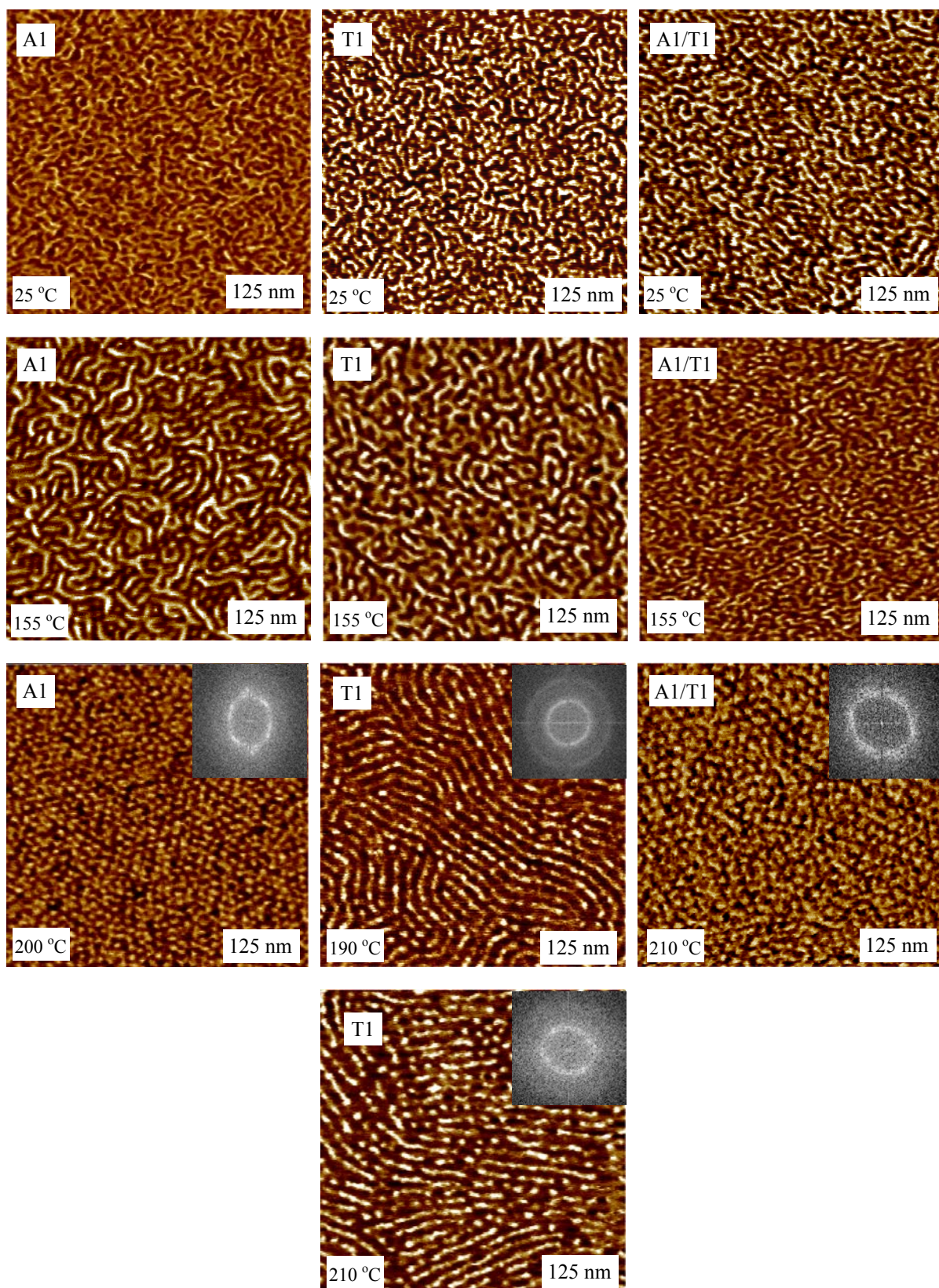


Figure 5.10. Tapping mode AFM phase images of A1, T1 and A1/T1 blend. Samples were spin-coated on silicon wafers, from chloroform solution. Annealing was performed at

temperatures indicated in the lower left corners of each image, under vacuum for 18 h. Film thicknesses ~ 100 nm. Images are 500 nm x 500 nm. Setpoint ratio ~ 0.6 . Insets are Fourier transforms (FFTs) of the phase images.

While AFM was successful in characterizing the surface morphology of the block copolymers, SAXS enabled characterization of the bulk morphology of the nucleobase-functionalized block copolymers. SAXS experiments were conducted on individual adenine- and thymine-functionalized triblock copolymer as well as the corresponding 1:1 A:T blends. SAXS confirmed the presence of microphase separation in all hydrogen bonding triblock copolymers, through the presence of a primary scattering maximum at scattering vector q^* . The primary scattering maximum was used to determine the interdomain (Bragg) spacing present in each sample ($d = 2\pi/q^*$), shown in Table 5.2. The interdomain spacing measured from SAXS (12-20 nm) were similar to those observed with AFM. Additional secondary scattering maxima were observed in some cases, allowing morphological assignments. In the case of $\sim 15K$ poly(*n*-butyl acrylate) block samples (A1, T1), each individual polymer produced cylindrical morphology, as evidenced from the positions of the scattering maxima ($q/q^* = 1, \sqrt{3}, \sqrt{7}$)⁵⁹⁰ (Figure 5.11). The expected maximum at $q/q^* = 2$ was not observed, but was believed to exist as a small shoulder on the peak at $q/q^* = \sqrt{3}$. The blend of the complementary block copolymers (A:T = 1:1) produced a similar cylindrical morphology with a Bragg spacing that was intermediate between the individual polymers. This trend of intermediate Bragg spacings for the blends was observed for the A2, T2 set as well and suggested the intimate mixing of the complementary hydrogen bonding hard blocks producing an averaged interdomain spacing. For the $\sim 24K$ poly(*n*-butyl acrylate) block samples (A2, T2), secondary scattering peaks were not clearly resolved, which may be due to the casting conditions. The highest rubber block molecular

⁵⁹⁰ Mani, S.; Weiss, R. A.; Hahn, S. F.; Williams, C. E.; Cantino, M. E.; Khairallah, L. H. Microstructure of block copolymers of polystyrene and poly(ethylene-*alt*-propylene). *Polymer* **1998**, 10, 2023-33.

weight samples (A3, T3) produced multiple scattering maxima, which were also attributed to cylindrical morphology.

Table 5.2. Small-angle X-ray scattering results for hydrogen bonding block copolymers.

Polymer	Triblock Molecular Weights	w _{Nu} ^a (%)	q* (Å ⁻¹)	d (nm)	q ₂ (Å ⁻¹)	q ₃ (Å ⁻¹)	Morphology ^b
A1	A _{1.5K} -nBA _{16.5K} -A _{1.5K}	15	0.042	15.0	0.072	0.112	cyl
A2	A _{2.8K} -nBA _{23.7K} -A _{2.8K}	19	0.044	14.3	-	-	-
A3	A _{2.3K} -nBA _{62.3K} -A _{2.3K}	7	0.029	21.7	0.052	-	cyl
T1	T _{1.8K} -nBA _{13.9K} -T _{1.8K}	21	0.039	16.1	0.069	0.111	cyl
T2	T _{2.0K} -nBA _{23.7K} -T _{2.0K}	14	0.052	12.1	-	-	-
T3	T _{1.4K} -nBA _{69.9K} -T _{1.4K}	4	0.032	19.6	0.054	-	cyl
A1/T1	N/A	18	0.040	15.7	0.074	0.121	cyl
A2/T2	N/A	16	0.046	13.7	-	-	-
A3/T3	N/A	6	0.033	19.0	0.058	-	cyl

^a Weight percent of nucleobase-functionalized block.

^b Assignments from SAXS maxima.

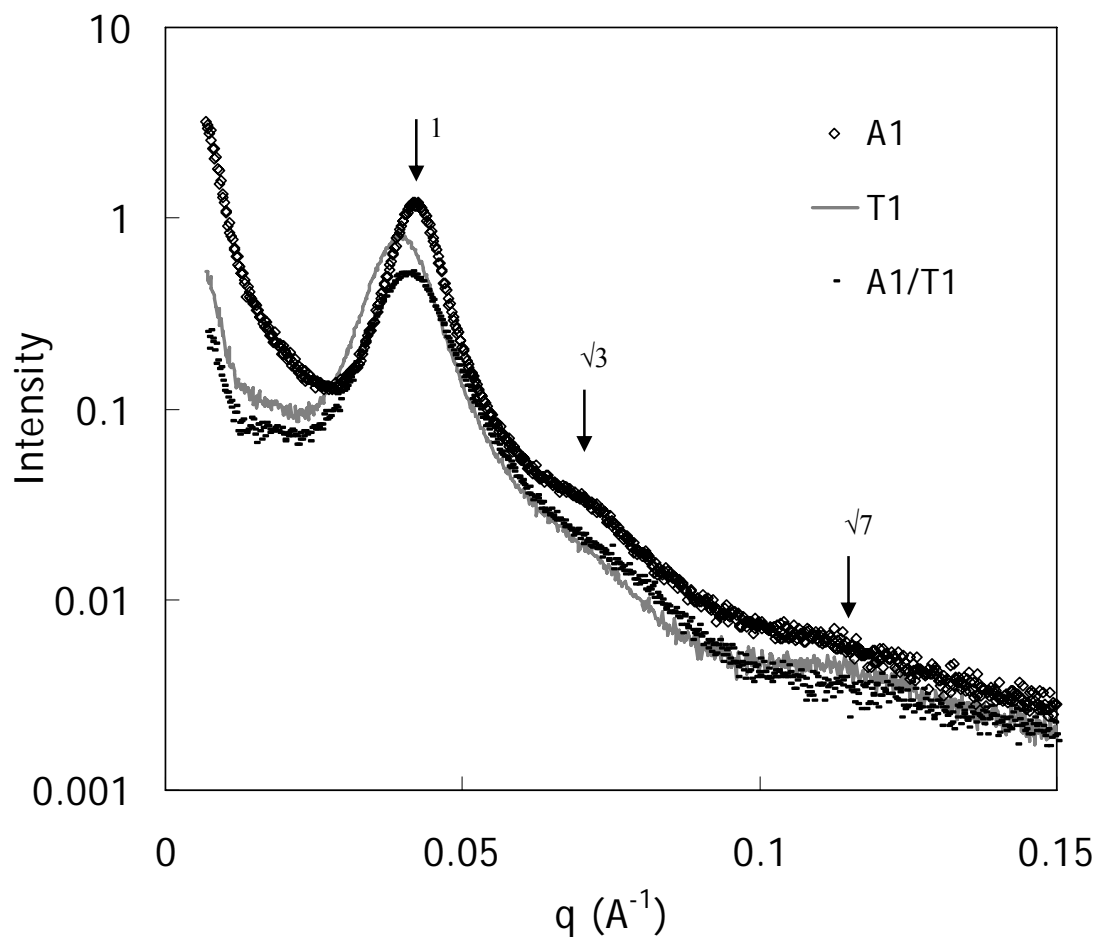


Figure 5.11. SAXS scattering profiles for nucleobase-containing polymers (A1, T1) and their 1:1 A:T blend. All samples annealed under vacuum at 155 °C for 18 h. Scattering maxima in terms of q/q^* are denoted with arrows.

Annealing studies with subsequent SAXS analysis were performed on the thymine-containing triblock copolymer with the highest nucleobase weight fraction (T1, 21 wt%). As the annealing temperature increased, the scattering profile changed dramatically (Figure 5.12). Narrowing of the scattering maxima and the appearance of several readily discernable secondary maxima were observed. Annealing at 200 °C appeared to result in the clearest development of morphology in this sample, revealing scattering maxima of $q/q^* = 1, \sqrt{3}, 2, \sqrt{7}, 3, 2\sqrt{3}$, which corresponded to hexagonal closest packed (hcp) cylindrical morphology. Furthermore, the scattering maximum at $q/q^* = 2$ was observed as a clear shoulder on the maximum at $q/q^* = \sqrt{3}$. This suggested that elevated temperatures near 200 °C were necessary to achieve well-developed morphologies for the triblock copolymers with higher nucleobase weight fraction.

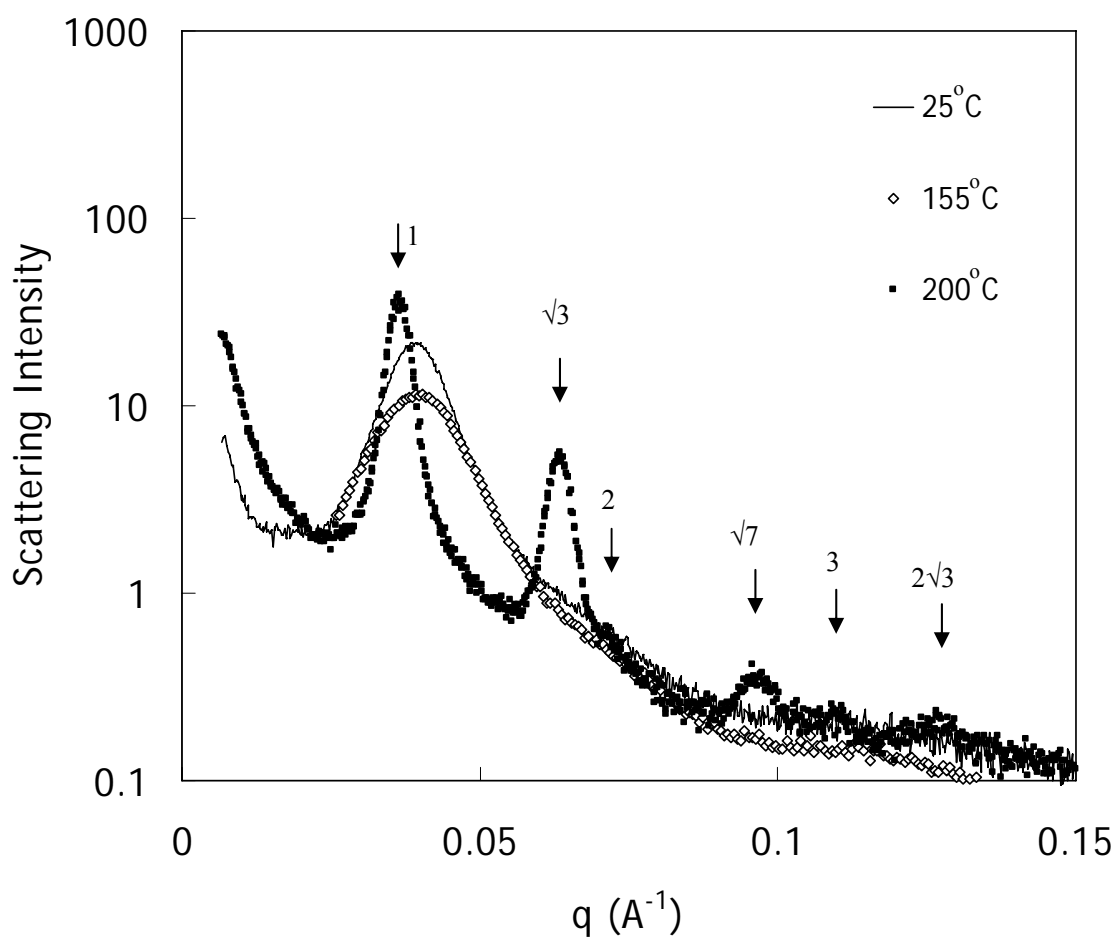


Figure 5.12. Effect of annealing conditions on thymine-containing triblock copolymer (T1) sample. Scattering maxima in terms of q/q^* are denoted with arrows.

The adenine-containing triblock copolymer A1, and blend of adenine- and thymine-containing block copolymers (A1/T1) were also annealed at 200 °C, but did not exhibit the development of the order apparent in the T1 sample annealed at 200 °C. SAXS profiles of adenine-containing samples that were annealed at 200 °C resembled samples annealed at 155 °C. This may have resulted from possible crosslinking side reactions including nucleophilic attack of the adenine NH₂ to the *n*-butyl acrylate ester. In dynamic mechanical measurements, heating of the adenine containing polymers above 200 °C resulted in crosslinking as evidenced from increasing storage modulus (E') and insolubility in solvents which previously dissolved the polymers. Melt rheological experiments at 150 and 160 °C indicated thermal stability at these reduced temperatures, and nearly constant shear storage modulus (G') and viscosity values were observed in the melt at 160 °C.

5.4.6 Introduction of Guest Molecules to Hydrogen Bonding Block Copolymers

Hydrogen bonding interactions will facilitate the introduction of guest molecules containing complementary recognition units. Others have shown the recognition of guest molecules through hydrogen bonding interactions in both solution⁵⁹¹ and the solid state.⁵⁹² Rotello et al. have used three-point hydrogen bonding between diacyldiaminopyridines and thymine to attach guest molecules containing flavin⁵⁹³ or POSS⁵⁹² to polystyrene. Guest

⁵⁹¹ Thibault, R. J.; Hotchkiss, P. J.; Gray, M.; Rotello, V. M. Thermally Reversible Formation of Microspheres through Non-Covalent Polymer Cross-Linking. *J Am Chem Soc* **2003**, 125, 11249-52.

⁵⁹² Carroll, J. B.; Waddon, A. J.; Nakade, H.; Rotello, V. M. "Plug and Play" Polymers. Thermal and X-ray Characterizations of Noncovalently Grafted Polyhedral Oligomeric Silsesquioxane (POSS)-Polystyrene Nanocomposites. *Macromolecules* **2003**, 36, 6289-91.

⁵⁹³ Ilhan, F.; Galow, T. H.; Gray, M.; Clavier, G.; Rotello, V. M. Giant Vesicle Formation through Self-Assembly of Complementary Random Copolymers. *J Am Chem Soc* **2000**, 122, 5895-6.

molecules also increase the solubility of hydrogen bonding polymers through screening self-association of the polymer, thereby maintaining the homogeneity during polymerization reactions.⁵⁹⁴

A complementary alkylated adenine-containing small molecule guest (9-octyladenine, see Figure 5.14 for structure) was introduced into a thymine-containing block copolymer (T2 and T3). ¹H NMR titrations of T3 with 9-octyladenine indicated shifts in the peak position of the thymine NH proton to higher field (from 10.4 to 11.7 ppm) upon the addition of 2.2 equivalents of 9-octyladenine (Figure 5.13). The curvature of the chemical shift data with increasing adenine concentration was consistent with typical NMR titration experiments in the literature.⁵⁹⁵ Fitting this chemical shift data using the Benesi-Hildebrand method⁵⁹⁵ produced an association constant of $K_a = 40 \text{ M}^{-1}$ and demonstrated the non-covalent attachment of 9-octyladenine in the solution state. Unlike the association of the complementary triblock copolymers, where associations led to disappearance of the nucleobase resonances, the attachment of the guest molecule does not create restrictions on the motion of the polymer in solution, which makes ¹H NMR spectroscopic observation of the hydrogen bonding interaction feasible.

⁵⁹⁴ Stubbs, L. P.; Weck, M. Towards a Universal Polymer Backbone: Design and Synthesis of Polymeric Scaffolds Containing Terminal Hydrogen-Bonding Recognition Motifs at Each Repeating Unit. *Chem Eur J* **2003**, *9*, 992-9.

⁵⁹⁵ Fielding, L. Determination of Association Constants (K_a) from Solution NMR Data. *Tetrahedron* **2000**, *56*, 6151-70.

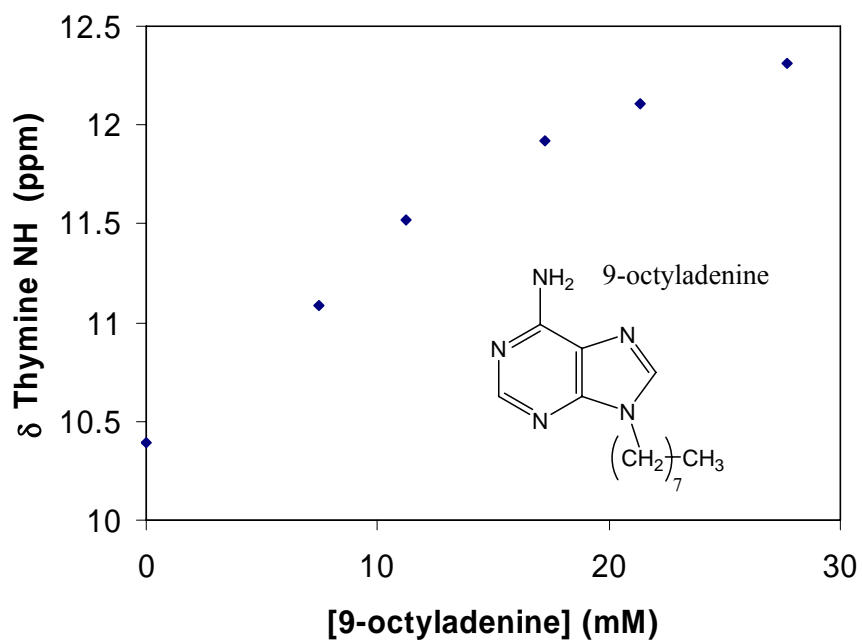


Figure 5.13. Chemical shift changes during introduction of 9-octyladenine to a thymine-containing triblock copolymer (T3).

For blends of 9-octyladenine with T2 in the solid state, AFM images indicated selective incorporation of the small molecule into the adenine-containing hard domains, as evidenced from increased phase contrast and greater hard phase continuity (Figure 5.14). The addition of 9-octyladenine present in the samples corresponded to 5 wt% for 0.4 equivalents, and 24 wt% for 2.2 equivalents. Future efforts will be devoted to studying non-covalent attachment of other functionalities via hydrogen bonding interactions.

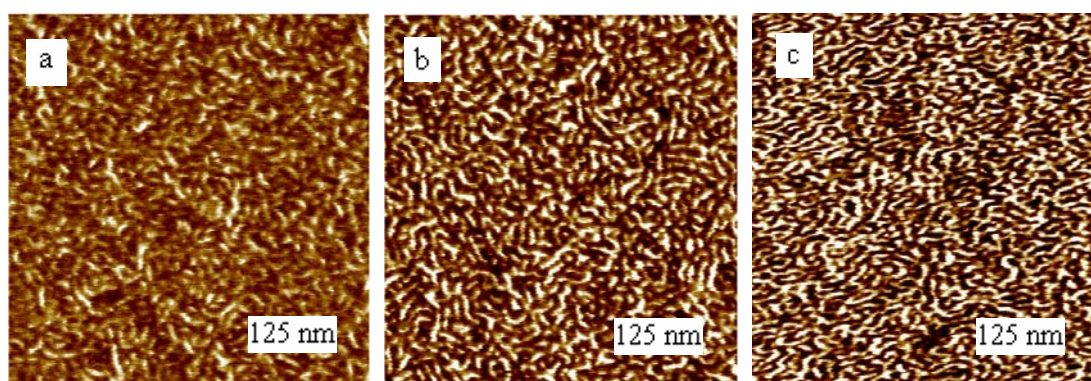


Figure 5.14. Tapping mode AFM images of unannealed thymine-functionalized block copolymer (T2) spin coated on a silicon wafer from chloroform solutions containing (a) 0, (b) 0.4 and (c) 2.2 equivalents of 9-octyladenine.

5.5 Conclusions

Nucleobase-functionalized triblock copolymers with adenine and thymine containing outer blocks were synthesized for the first time via nitroxide mediated radical polymerization involving a novel difunctional initiator. Hydrogen bonding interactions in blends of complementary polymers led to associations in solution that were manifested through dramatic increases in viscosity. Increased solution viscosity scaling exponents with concentration indicated the influence of the hydrogen bonding equilibrium through increased effective molecular weight. In the solid state, hydrogen bonding led to compatibilization of the blends through the formation of an associated A-T hard phase. Morphological investigations of the individual block copolymers as well as their complementary blends revealed intermediate domain spacings and surface textures for blends of the complementary block copolymers. The introduction of complementary guest molecules resulted in selective uptake into nucleobase containing domains.

5.6 Acknowledgement

The authors would like to thank Funda Senyurt for helpful discussions during the writing of the manuscript. The authors would like to acknowledge Kraton Polymers for complementary funding and Dr. Carl Willis of Kraton Polymers for insightful discussions. This material is based upon work supported by, or in part by, the U.S. Army Research Laboratory and the U.S. Army Research Office under grant number DAAD19-02-1-0275 Macromolecular Architecture for Performance (MAP) MURI.

Chapter 6. Multiple Hydrogen Bonding for the Non-covalent Attachment of Ionic Functionality in Block Copolymers

(Mather, B.D.; Baker, M.B.; Beyer, F.L.; Green, M.D.; Berg, M.A.G.; Long T.E., *Macromolecules*, submitted)

6.1 Abstract

Multiple hydrogen bonding interactions were utilized to reversibly attach nucleobase functional phosphonium salt guests to complementary functionalized triblock copolymers. Novel adenine-containing triblock copolymers were synthesized *via* nitroxide mediated polymerization using a novel difunctional alkoxyamine initiator. Ionic interactions were introduced *via* a novel uracil-containing phosphonium salt (UP^+), which formed optically clear blends with the adenine functional block copolymer. An apparent 3.4 fold decrease in solution viscosity upon addition of UP^+ to the block copolymer in chloroform (4.2 wt%, 25 °C) suggested a screening of adenine-adenine hydrogen bonding interactions. Morphological investigations revealed unique surface textures for the UP^+ block copolymer blends compared with the pure adenine-containing block copolymer. Small-angle X-ray scattering revealed a transition from cylindrical to lamellar morphologies upon incorporation of the phosphonium salt. Dynamic mechanical measurements indicated an increased rubbery plateau due to the greater hard phase volume fraction, and a softening at lower temperatures than the pure adenine-containing block copolymer due to hydrogen bond screening.

6.2 Introduction

The introduction of electrostatic interactions to diverse macromolecular architectures has received significant attention for several decades.⁵⁹⁶⁻⁵⁹⁹ Ionomers, which are defined as a class of lightly charged (≤ 15 mol%) ion-containing polymers, possess electrostatic interactions with enthalpies near ~ 200 kJ/mol.⁶⁰⁰ The Coulombic forces enable the formation of nanometer-scale aggregates⁶⁰¹ resulting in improved thermo-mechanical properties, increased toughness, improved chemical resistance, and opportunities for self-healing substrates.^{602,603} A further advantage of ion-containing polymers is the ability to conduct ions, which suggests applications in ion-conducting membranes, fuel cells, electromechanical devices, water purification membranes, and breathable textiles for protection from chemical and biological reagents.⁶⁰⁴⁻⁶⁰⁷

⁵⁹⁶ Eisenberg, A.; Hird, B.; Moore, R. B. A New Multiplet-Cluster Model for the Morphology of Random Ionomers. *Macromolecules* **1990**, *23*, 4098-107.

⁵⁹⁷ Mani, S.; Weiss, R. A.; Williams, C. E.; Hahn, S. F. Microstructure of Ionomers Based on Sulfonated Block Copolymers of Polystyrene and Poly(ethylene-*alt*-propylene). *Macromolecules* **1999**, *32*, 3663-70.

⁵⁹⁸ Lowry, S. R.; Mauritz, K. A. An investigation of ionic hydration effects in perfluorosulfonate ionomers by Fourier transform infrared spectroscopy. *J. Am. Chem. Soc.* **1980**, *102*, 4665-7.

⁵⁹⁹ Kabanov, A. V.; Bronich, T. K.; Kabanov, V. A.; Yu, K.; Eisenberg, A. Spontaneous Formation of Vesicles from Complexes of Block Ionomers and Surfactants. *J. Am. Chem. Soc.* **1998**, *120*, 9941-2.

⁶⁰⁰ Hird, B.; Eisenberg, A. Sizes and Stabilities of Multiplets and Clusters in Carboxylated and Sulfonated Styrene Ionomers. *Macromolecules* **1992**, *25*, 6466-74.

⁶⁰¹ Benetatos, N. M.; Heiney, P. A.; Winey, K. I. Reconciling STEM and X-ray Scattering Data from a Poly(styrene-*ran*-methacrylic acid) Ionomer: Ionic Aggregate Size. *Macromolecules* **2006**, *39*, 5174-6.

⁶⁰² Eisenberg, A.; Kim, J.-S.; *Introduction to Ionomers*; Wiley: New York 1998.

⁶⁰³ Kalista, S. J. M.S. Thesis, Virginia Tech, 2003.

⁶⁰⁴ Hickner, M. A.; Ghassemi, H.; Kim, Y. S.; Einsla, B. R.; McGrath, J. E. Alternative Polymer Systems for Proton Exchange Membranes (PEMs). *Chem Rev* **2004**, *104*, 4587-611.

⁶⁰⁵ Akle, B.; Leo, D. J.; Hickner, M. A.; McGrath, J. E. Correlation of capacitance and actuation in ionomeric polymer transducers. *J Mater Sci* **2005**, *40*, 3715-24.

⁶⁰⁶ Rivin, D.; Meermeier, G.; Schneider, N. S.; Vishnyakov, A.; Neimark, A. V. Simultaneous Transport of Water and Organic Molecules through Polyelectrolyte Membranes. *J. Phys. Chem. B* **2004**, *108*, 8900-9.

⁶⁰⁷ Zhou, J.; Li, Z.; Liu, G. Diblock Copolymer Nanospheres with Porous Cores. *Macromolecules* **2002**, *35*, 3690-6.

Despite the attractive physical properties of ionomers, melt processing often suffers due to relatively high viscosities that are attributed to ionic aggregates (which can persist to temperatures exceeding 300 °C).⁶⁰⁸ Earlier efforts have attempted to address this potential limitation, and for example, the processability of sulfonated poly(ethylene-*co*-propylene-*co*-diene) (EPDM) improved upon the addition of zinc stearate, which “plasticized” the ionic aggregates.⁶⁰⁹ Herein, we provide the first report of complementary hydrogen bonding as a reversible linkage for attachment of phosphonium cations to block copolymers (Figure 6.1). This manuscript demonstrates the general concept of reversible ionic site attachment to block copolymers, which dissociate from the block copolymer above the dissociation temperature for hydrogen bonding.

⁶⁰⁸ Lu, X.; Steckle, W. P.; Hsiao, B.; Weiss, R. A. Thermally Induced Microstructure Transitions in a Block Copolymer Ionomer. *Macromolecules* **1995**, 28, 2831-9.

⁶⁰⁹ Duvdevani, I.; Lundberg, R. D.; Wood-Cordova, C.; Wilkes, G. L., Coulombic Interactions in Macromolecular Systems. In *ACS Symposium Series*, Eisenberg, A.; Bailey, F. E., Eds. American Chemical Society: Washington DC, 1986; Vol. 302, pp 185-99.

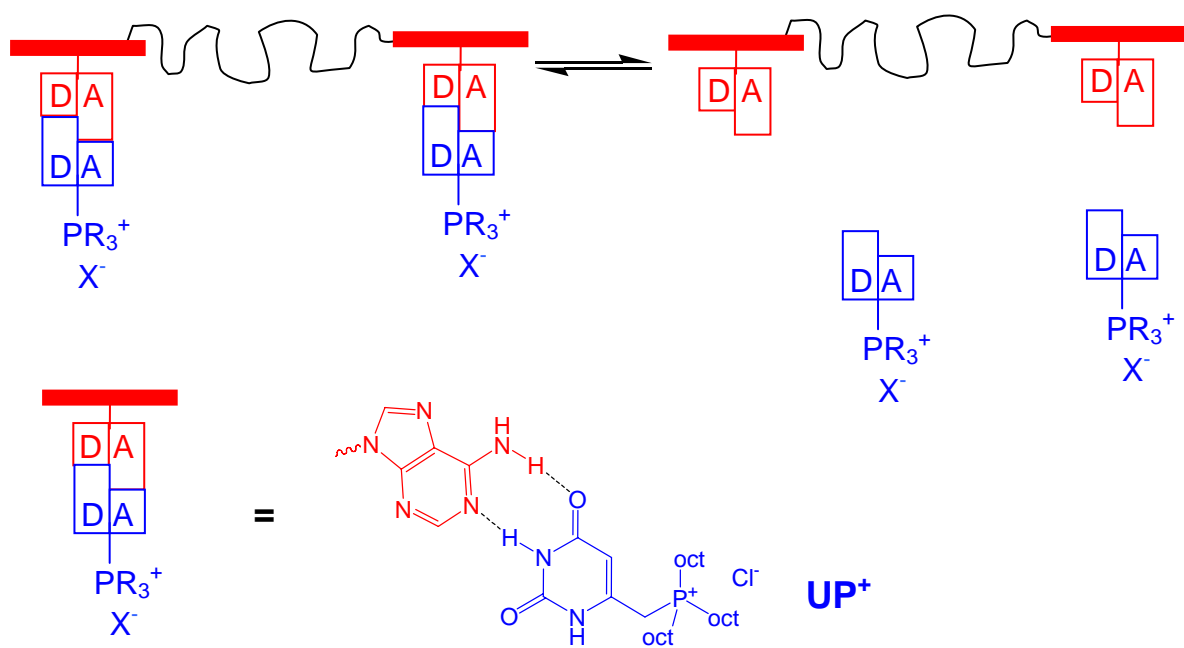


Figure 6.1. Reversible attachment of UP⁺ phosphonium salt to complementary nucleobase functionalized block copolymers.

Hydrogen bonding, in contrast to non-directional electrostatic interactions, exhibits lower enthalpies (10-40 kJ/mol) and greater specificity, which enables molecular recognition and lower melt viscosities using multiple hydrogen bonding arrays such as ureido pyrimidones (UPy) and nucleobase pairs.^{610 - 615} This manuscript describes the synergy of complementary hydrogen bonding in nanostructured block copolymers with guest molecules containing electrostatic interactions. Earlier researchers have reported coordination of metal sulfonates to pyridine containing block copolymers, however, the potential synergy of complementary hydrogen bonding with electrostatic interactions was not reported.⁶¹⁶ Other researchers have reported the reversible attachment of neutral guest molecules via hydrogen bonding interactions and for example, non-covalent attachment of mesogens resulted in supramolecular liquid crystalline assemblies.^{617 - 621}

⁶¹⁰ Sijbesma, R. P.; Beijer, F. H.; Brunsveld, L.; Folmer, B. J. B.; Hirschberg, J. H. K. K.; Lange, R. F. M.; Lowe, J. K. L.; Meijer, E. W. Reversible Polymers Formed from Self-Complementary Monomers Using Quadruple Hydrogen Bonding. *Science* **1997**, *278*, 1601-4.

⁶¹¹ Yamauchi, K.; Lizotte, J. R.; Hercules, D. M.; Vergne, M. J.; Long, T. E. Combinations of Microphase Separation and Terminal Multiple Hydrogen Bonding in Novel Macromolecules. *J Am Chem Soc* **2002**, *124*, 8599-604.

⁶¹² Mather, B. D.; Lizotte, J. R.; Long, T. E. Synthesis of Chain End Functionalized Multiple Hydrogen Bonded Polystyrenes and Poly(alkyl acrylates) Using Controlled Radical Polymerization. *Macromolecules* **2004**, *37*, 9331-7.

⁶¹³ Yamauchi, K.; Lizotte, J. R.; Long, T. E. Synthesis and Characterization of Novel Complementary Multiple-Hydrogen Bonded (CMHB) Macromolecules via a Michael Addition. *Macromolecules* **2002**, *35*, 8745-50.

⁶¹⁴ Nair, K. P.; Pollino, J. M.; Weck, M. Noncovalently Functionalized Block Copolymers Possessing Both Hydrogen Bonding and Metal Coordination Centers. *Macromolecules* **2006**, *39*, 931-40.

⁶¹⁵ Noro, A.; Nagata, Y.; Tsukamoto, M.; Hayakawa, Y.; Takano, A.; Matsushita, Y. Novel Synthesis and Characterization of Bioconjugate Block Copolymers Having Oligonucleotides. *Biomacromolecules* **2005**, *6*, 2328-33.

⁶¹⁶ Valkama, S.; Ruotsalainen, T.; Kosonen, H.; Ruokolainen, J.; Torkkeli, M.; Serimaa, R.; ten Brinke, G.; Ikkala, O. Amphiphiles Coordinated to Block Copolymers as a Template for Mesoporous Materials. *Macromolecules* **2003**, *36*, 3986-91.

⁶¹⁷ Kumar, U.; Kato, T.; Fréchet, J. M. J. Use of intermolecular hydrogen bonding for the induction of liquid crystallinity in the side chain of polysiloxanes. *J. Am. Chem. Soc.* 1992, *114*, 6630-9.

Phosphonium cations have received recent attention in our laboratories due to higher thermal stabilities relative to ammonium analogs. Earlier evidence indicates that the onset of decomposition of tetraoctylammonium bromide occurs at 170 °C due to Hofmann elimination, whereas the analogous phosphonium salt exhibits thermal stability to 260 °C.^{622,623} Despite bulky organic substitution on the phosphonium cation, others have recently reported random copolymers containing covalently bound phosphonium cations, which result in nanoscale ionic aggregation and concomitant thermoplastic elastomeric behavior.^{624,625}

Novel hydrogen bonding triblock copolymers containing adenine were synthesized *via* nitroxide mediated polymerization. A novel difunctional initiator, which does not introduce hydrolytically unstable ester linkages that lead to molecular weight loss, permitted the

⁶¹⁸ Thibault, R. J.; Hotchkiss, P. J.; Gray, M.; Rotello, V. M. Thermally Reversible Formation of Microspheres through Non-Covalent Polymer Cross-Linking. *J Am Chem Soc* **2003**, 125, 11249-52.

⁶¹⁹ van Ekenstein, G. A.; Polushkin, E.; Nijland, H.; Ikkala, O.; ten Brinke, G. Shear Alignment at Two Length Scales: Comb-Shaped Supramolecules Self-Organized as Cylinders-within-Lamellar Hierarchy. *Macromolecules* **2003**, 36, 3684-8.

⁶²⁰ Kato, T.; Kihara, H.; Ujiie, S.; Uryu, T.; Frechet, J. M. J. Structures and Properties of Supramolecular Liquid-Crystalline Side-Chain Polymers Built through Intermolecular Hydrogen Bonds. *Macromolecules* **1996**, 29, 8734-9.

⁶²¹ Burd, C.; Weck, M. Self-Sorting in Polymers. *Macromolecules* **2005**, 38, 7225-30.

⁶²² Xie, W.; Xie, R.; Pan, W. P.; Hunter, D.; Koene, B.; Tan, L. S.; Vaia, R. Thermal Stability of Quaternary Phosphonium Modified Montmorillonites. *Chem. Mater.* **2002**, 14, 4837-45.

⁶²³ Burch, R. R.; Manring, L. E. *N*-Alkylation and Hofmann elimination from thermal decomposition of R₄N⁺ salts of aromatic polyamide polyanions: synthesis and stereochemistry of *N*-alkylated aromatic polyamides. *Macromolecules* **1991**, 24, 1731-5.

⁶²⁴ Parent, J. S.; Penciu, A.; Guillen-Castellanos, A.; Liskova, A.; Whitney, R. A. Synthesis and Characterization of Isobutylene-Based Ammonium and Phosphonium Bromide Ionomers. *Macromolecules* **2004**, 37, 7477-83.

⁶²⁵ Arjunan, P.; Wang, H.-C.; Olkusz, J. A., *Functional Polymers*. American Chemical Society: Washington DC, 1998; Vol. 704, p 199-216.

formation of symmetric outer blocks, reduced the number of subsequent monomer additions, and enabled a single crossover reaction.

6.3 Experimental

6.3.1 Materials

n-Butyl acrylate (99%) was purchased from Aldrich and purified using an alumina column and subsequent vacuum distillation from calcium hydride. Diethyl-*meso*-2,5-dibromoadipate (98%), copper (I) bromide (99.999%), *N,N,N',N'',N'''*-pentamethyldiethylenetriamine (PMDETA, 98%), trioctylphosphine (90%) and 6-chloromethyluracil (98%) were purchased from Aldrich and used without further purification. Copper powder (45 μ m, 99%) was purchased from Acros and used as received. DEPN nitroxide,⁶²⁶ Styryl-DEPN,⁶²⁷ and 9-vinylbenzyl adenine⁶²⁸ were synthesized according to the previous literature.

6.3.2 Synthesis of 6-(trioctylphosphonium methyl)uracil chloride (UP⁺)

6-chloromethyluracil (1.001 g, 6.232 mmol) and trioctylphosphine (3.25 mL, 2.70 g, 7.29 mmol) were charged to a 100 mL round-bottomed flask containing a magnetic stirbar.

⁶²⁶ Grimaldi, S.; Finet, J. P.; Le Moigne, F.; Zeghdaoui, A.; Tordo, P.; Benoit, D.; Fontanille, M.; Gnanou, Y. Acyclic B-Phosphonylated Nitroxides: A New Series of Counter-Radicals for "Living"/Controlled Free Radical Polymerization. *Macromolecules* **2000**, 33, 1141-7.

⁶²⁷ Diaz, T.; Fischer, A.; Jonquieres, A.; Brembilla, A.; Lochon, P. Controlled Polymerization of Functional Monomers and Synthesis of Block Copolymers Using a B-Phosphonylated Nitroxide. *Macromolecules* **2003**, 36, 2235-41.

⁶²⁸ Srivatsan, S. G.; Parvez, M.; Verma, S. Modeling of Prebiotic Catalysis with Adenylated Polymeric Templates: Crystal Structure Studies and Kinetic Characterization of Template-Assisted Phosphate Ester Hydrolysis. *Chem. Eur. J.* **2002**, 8, 5184-91.

Ethanol (40 mL) was added and a condenser was fitted to the flask. The reactions was heated to reflux using an external oil bath for 24 h. Excess solvent was removed using rotary evaporation. The resulting waxy solid was washed with diethyl ether and was dried overnight at room temperature under high vacuum. UP⁺ was obtained as a light brown solid (m.p. 179-181 °C) in 88% yield. ¹H NMR (400 MHz, DMSO-d₆, 25 °C) δ (ppm): 0.86 (t, 9H, *J* = 6.8 Hz), 1.26 (m, 24H), 1.37 (m, 6H), 1.49 (m, 6H), 2.37 (m, 6H), 3.77 (d, 2H, *J* = 15 Hz), 5.55 (m, 1H), 11.15 (s, 1H), 11.47 (s, 1H). ¹³C NMR (101 MHz, DMSO-d₆, 25 °C) δ (ppm): 13.96, 17.61, 18.06, 20.52, 22.08, 28.27, 28.8, 30.06, 31.22, 102.08, 145.18, 150.95, 163.37. ³¹P NMR (162 MHz, DMSO-d₆, 25 °C) δ (ppm): 33.68 ppm. FAB MS: *m/z* = 495.4056 [M-Cl]⁺ (experimental), *m/z* = 495.41 (theoretical).

6.3.3 Synthesis of DEPN₂ Difunctional Alkoxyamine Initiator

DEPN nitroxide (2.0 g, 6.8 mmol) and diethyl-*meso*-2,5-dibromoadipate (1.36 g, 3.8 mmol) were charged to a one-necked 100-mL round-bottomed flask containing a magnetic stirbar. Dichloromethane (30 mL) was added and the solution was degassed with three freeze-pump-thaw cycles. In a second 100-mL round-bottomed flask, PMDETA (2.34 g, 13.6 mmol) was dissolved in 20 mL CH₂Cl₂ and subjected to the same degassing. In a third 100-mL round-bottomed flask containing a stirbar, CuBr (0.78 g, 5.47 mmol) and Cu powder (0.35 g, 5.47 mmol) were purged with nitrogen gas. After degassing, the liquid reagents were cannulated into the flask containing the copper powder and CuBr. The reaction was stirred for 24 h at 25 °C under nitrogen, diluted with CH₂Cl₂ (200 mL), and washed repeatedly with water (10 x 100 mL), to remove copper compounds. The organic layer was then dried over

sodium sulfate and evaporated. The product was separated on silica, eluting with ethyl acetate : hexane (1:1). DEPN₂ was isolated as a mixture of diastereomers. Purified yield = 49%. ¹H NMR (400 MHz, CDCl₃, 25 °C) δ (ppm): 1.0-1.2 (s, tBu, 36H), 1.2-1.4 (m, ester CH₃, 18H), 1.6-2.4 (br, linker CH₂, 4H), 3.1-3.6 (m, DEPN CH, 2H), 3.9-4.2 (m, CH₃, 12H), 4.4-4.5 (m, COCH, 2H). ¹³C NMR (101 MHz, CDCl₃, 25 °C) δ (ppm): 172.74, 171.46, 86.74, 86.31, 81.87, 81.52, 77.20, 76.85, 75.31, 70.27, 69.99, 68.90, 68.62, 62.30, 62.23, 62.03, 61.96, 61.66, 61.57, 60.62, 60.40, 60.32, 60.27, 60.22, 58.89, 58.82, 35.64, 35.58, 35.49, 35.21, 35.16, 35.09, 34.48, 30.18, 30.12, 29.93, 29.89, 29.44, 29.38, 28.12, 27.95, 27.89, 27.56, 27.53, 26.96, 26.67, 26.52, 26.46, 16.47, 16.41, 16.35, 16.32, 16.14, 16.08, 14.03, 13.98, 13.90. ³¹P NMR (162 MHz, CDCl₃, 25 °C) δ (ppm): 25.82, 25.63, 25.59, 25.20, 25.00, 24.91. FAB MS: *m/z* = 789.4842 [M+H]⁺ experimental, *m/z* = 789.48 theoretical. No peak for the monofunctional initiator was observed (*m/z* = 574.5).

Meso diastereomer of DEPN₂: The *meso* diastereomer was isolated from the partly crystalline first fractions obtained during chromatographic purification of DEPN₂. Further separation was achieved via washing the crystals with hexane. m.p. = 139.5-141.5 °C. ¹H NMR (400 MHz, CDCl₃, 25 °C) δ (ppm): 1.03 (s, *N*-tBu, 18H), 1.06 (s, *C*-tBu, 18H), 1.24 (m, ester CH₃, 18H), 1.55-2.40 (br, linker CH₂, 4H), 3.18 (d, *J* = 25 Hz, DEPN CH, 2H), 3.85-4.20 (m, OCH₂, 12H), 4.25-4.46 (br, OCH, 2H). ¹³C NMR (101 MHz, CDCl₃, 25 °C) δ (ppm): 172.89, 86.65, 69.71(d, *J* = 138 Hz), 61.80 (d, *J* = 6.1 Hz), 61.05 (d, *J* = 95 Hz), 58.69 (d, *J* = 7 Hz), 35.59 (d, *J* = 5.4 Hz), 29.31 (d, *J* = 6.2 Hz), 28.57, 27.94, 16.31 (dd, *J*₁ = 28.4 Hz, *J*₂ = 6.2 Hz), 13.95. ³¹P NMR (162 MHz, CDCl₃, 25 °C) δ (ppm): 25.67.

6.3.4 Polymerization of *n*-Butyl Acrylate from DEPN₂ Nitroxide

DEPN₂ alkoxyamine (212 mg, 0.269 mmol) and DEPN nitroxide (31 mg, 0.106 mmol) were weighed into a 100-mL round-bottomed flask containing a magnetic stirbar. The flask was sealed with a three-way joint allowing syringing of reagents and application of vacuum and nitrogen. The flask was evacuated to 60 mtorr and refilled with high-purity nitrogen three times. Purified *n*-butyl acrylate (30 mL, 209 mmol) was added via syringe and the mixture was degassed with repeated freeze-pump-thaw cycles. Finally, the flask was immersed in an oil bath at 122 °C for 3 h. After the polymerization, residual monomer was removed with high vacuum stripping. Yield = 5.82 g polymer (Conversion = 22%). SEC analysis revealed molecular weight data $M_n = 16,500$, $M_w/M_n = 1.24$.

6.3.5 Synthesis of Adenine Containing Block Copolymer

Poly(*n*-butyl acrylate) homopolymer (4.83 g, $M_n = 16,500$) and 9-vinylbenzyl adenine¹³ (9-VBA, 0.990 g, 3.94 mmol) were added to a 100-mL round-bottomed flask with a magnetic stirbar. The flask was sealed with a three-way joint and evacuated to 60 mtorr and refilled with high-purity nitrogen three times. DMF (15 mL) was then syringed into the flask and the mixture stirred until homogeneous and then degassed repeatedly with freeze-pump-thaw cycles. The flask was immersed in an oil bath at 120 °C for 5 h. After the polymerization, the polymer was isolated via precipitation twice into methanol. ¹H NMR (400 MHz, DMSO-d₆:CDCl₃, 1:1, 25 °C) revealed block molecular weights 1.5K-16.5K-1.5K. The final product was dried for 24 h under high vacuum at room temperature and stored in a desiccator. The adenine triblock copolymer formed a clear, elastomeric polymer.

6.3.6 Characterization

Size exclusion chromatography (SEC) was performed at 40 °C in HPLC grade tetrahydrofuran at 1 mL/min using a Waters size-exclusion chromatographer equipped with an autosampler, 3 in-line 5 µm PLgel MIXED-C columns. Detectors included a Waters 410 differential refractive index (DRI) detector operating at 880 nm, and a Wyatt Technologies miniDAWN multiangle 690 nm laser light scattering (MALLS) detector, calibrated with PS standards. NMR spectroscopic data was collected on a Varian 400 MHz spectrometer at 25 °C. A Veeco MultiMode™ scanning probe microscope was used for tapping-mode AFM. Polymer films were solution cast from chloroform on silicon. Samples were imaged at a set-point ratio of 0.6-0.7. Veeco's Nanosensor silicon tips having spring constants of 10-130 N/m were utilized for imaging. Solution rheology measurements were conducted on a TA Instruments G2 Rheometer in concentric cylinder geometry. DSC was conducted on a TA Instruments Q1000 DSC under nitrogen at a heating rate of 10 °C/min. X-ray data was collected on an Oxford Diffraction Xcalibur™ diffractometer equipped with a Sapphire™ 3 CCD detector. The data collection routine, unit cell refinement, and data processing were carried out with the program CrysAlis(v1.171, Oxford Diffraction: Wroclaw, Poland, 2004).

Small-angle X-ray Scattering (SAXS) Measurements. $\text{Cu}_{K\alpha}$ X-ray radiation was generated using a Rigaku Ultrax18 rotating anode X-ray generator operated at 45 kV and 100 mA. A nickel filter was used to eliminate all wavelengths but the $\text{Cu}_{K\alpha}$ doublet, with an average wavelength of $\lambda = 1.542 \text{ \AA}$. The exact beam center and the sample-to-detector distance of approximately 1.5 m were calibrated using silver behenate. The 3 m camera uses 3-pinhole collimation (300, 200 and 600 µm), and a sample-to-detector distance of

approximately 1.5 m. Two-dimensional data sets were collected using a Molecular Metrology 2D multi-wire area detector. The data were corrected for detector noise, sample absorption, and background scattering, followed by azimuthal averaging to obtain intensity as a function of the scattering vector, $I(q)$, where $q = 4\pi \cdot \sin(\theta)/\lambda$ and 2θ is the scattering angle. The data were then placed on an absolute scale using a type 2 glassy carbon sample 1.07 mm thick, previously calibrated at the Advanced Photon Source in the Argonne National Laboratory, as a secondary standard. All data processing and analysis were done using Wavemetrics IGOR Pro 5.04 software and IGOR procedures written by Dr. Jan Ilavsky of Argonne National Laboratory.

6.4 Results and Discussion

6.4.1 Synthesis and Characterization of a Novel Difunctional Initiator

The difunctional alkoxyamine initiator, which is depicted as DEP_N₂ in Figure 6.2, was synthesized from *N-tert*-butyl-*N*-(1-diethylphosphono-2,2-dimethylpropyl)-*N*-oxyl (DEPN) and diethyl-2,5-dibromoadipate using conventional atom transfer radical addition techniques.^{629 - 631} The chemical structure of DEP_N₂, which consists of a mixture of diastereomers, was confirmed using NMR spectroscopy and mass spectrometry, and the *meso*

⁶²⁹ Matyjaszewski, K.; Woodworth, B. E.; Zhang, X.; Gaynor, S.; Metzner, Z. Simple and Efficient Synthesis of Various Alkoxyamines for Stable Free Radical Polymerization. *Macromolecules* **1998**, 31, 5955-7.

⁶³⁰ Lacroix-Desmazes, P.; Lutz, J. F.; Chauvin, F.; Severac, R.; Boutevin, B. Living Radical Polymerization: Use of an Excess of Nitroxide as a Rate Moderator. *Macromolecules* **2001**, 34, 8866-71.

⁶³¹ Diaz, T.; Fischer, A.; Jonquieres, A.; Brembilla, A.; Lochon, P. Controlled Polymerization of Functional Monomers and Synthesis of Block Copolymers Using a β -Phosphonylated Nitroxide. *Macromolecules* **2003**, 36, 2235-41.

diastereomer was isolated in a crystalline form, which allowed structural determination using X-ray crystallography (Figure 6.2).

In situ FTIR spectroscopy was used to probe the kinetics of DEPN₂ initiated homopolymerization of *n*-butyl acrylate. As expected for the difunctional initiator, the polymerizations exhibited typical *pseudo* first-order kinetics and linear molecular weight versus conversion profiles (Figure 6.3) with narrow molecular weight distributions ($M_w/M_n \sim 1.10$). The difunctional nature of DEPN₂ was demonstrated via polymerization of *n*-butyl acrylate using mixtures of DEPN₂ and a monofunctional alkoxyamine initiator (Styryl-DEPN). Bimodal molecular weight distributions with a ratio of peak molecular weights of 2:1 were observed, which was consistent with both monofunctional and difunctional species.

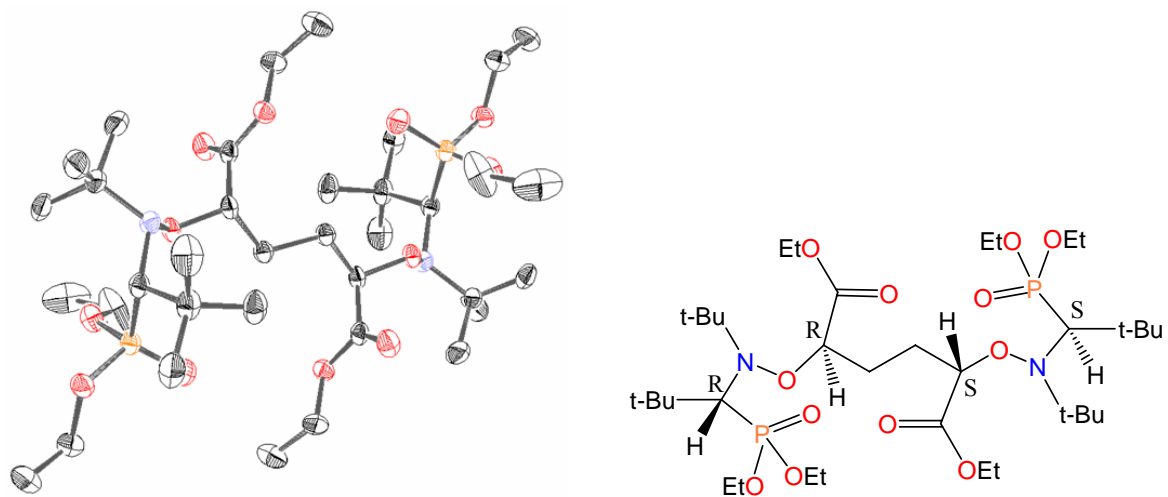


Figure 6.2. ORTEP X-ray crystal structure of DEPn₂ difunctional alkoxyamine initiator (hydrogen atoms omitted for clarity).

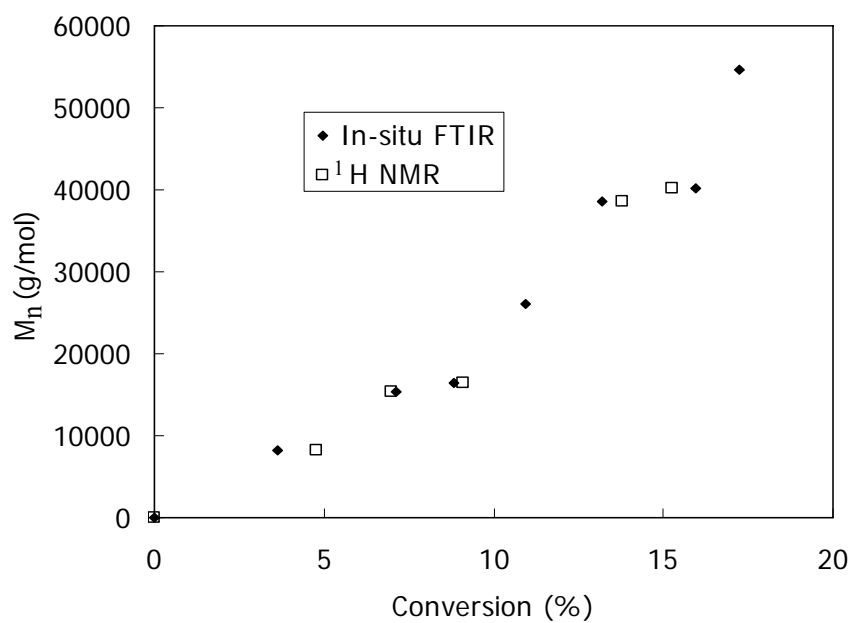


Figure 6.3. Number average molecular weight as a function of monomer conversion for the polymerization of *n*-butyl acrylate with DEPN_2 .

6.4.2 Synthesis of Adenine Functional Block Copolymer

An adenine functionalized styrenic monomer, 9-vinylbenzyladenine (9-VBA), was introduced after isolation of the telechelic DEPN functionalized poly(*n*-butyl acrylate) (Figure 6.4). ¹H NMR spectroscopy was used to verify the presence of the adenine containing repeat units and allowed quantification of the degree of polymerization of the outer blocks. Block molecular weights of 1.5K-16.5K-1.5K were calculated from ¹H NMR data, assuming an accurate SEC molecular weight for the rubber block ($M_n = 16500$). Size exclusion chromatography (SEC) in tetrahydrofuran revealed a narrow molecular weight distribution and monomodal traces for the final triblock copolymer, which was consistent with a well-defined polymerization process. SEC was not suitable for the determination of hydrogen bonding block molecular weights due to the relatively short block lengths. Thus, ¹H NMR was used to calculate the molecular weight for the shorter hydrogen bonding outer block.

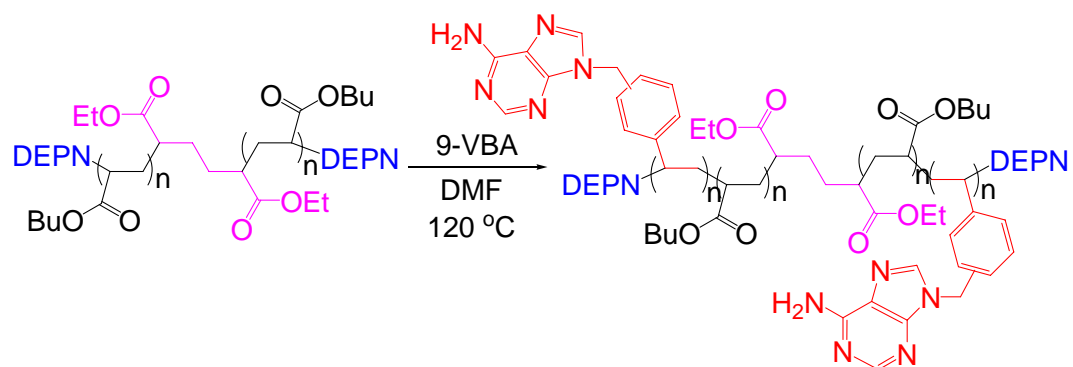


Figure 6.4. Synthesis of adenine containing triblock copolymers from DEPN₂ initiated poly(*n*-butyl acrylate).

6.4.3 Compatible Blends of Adenine Functional Block Copolymer with Uracil Phosphonium Salt

A novel uracil-containing phosphonium salt (UP^+) was synthesized in a single step from 6-chloromethyl uracil and trioctylphosphine. UP^+ exhibited an onset of weight loss at 280 °C using thermogravimetric analysis (TGA) as well as solubility in a wide range of common organic solvents. In blends of the phosphonium salt with adenine containing block polymers solution-cast from chloroform, crystallization and melting transitions of the phosphonium salt were absent from differential scanning calorimetry (DSC) thermograms (Figure 6.5). Furthermore, the solution-cast films were optically clear. In sharp contrast, solution-cast films of the phosphonium salt with non-functionalized poly(*n*-butyl acrylate) homopolymer resulted in opaque, macrophase separated, films.

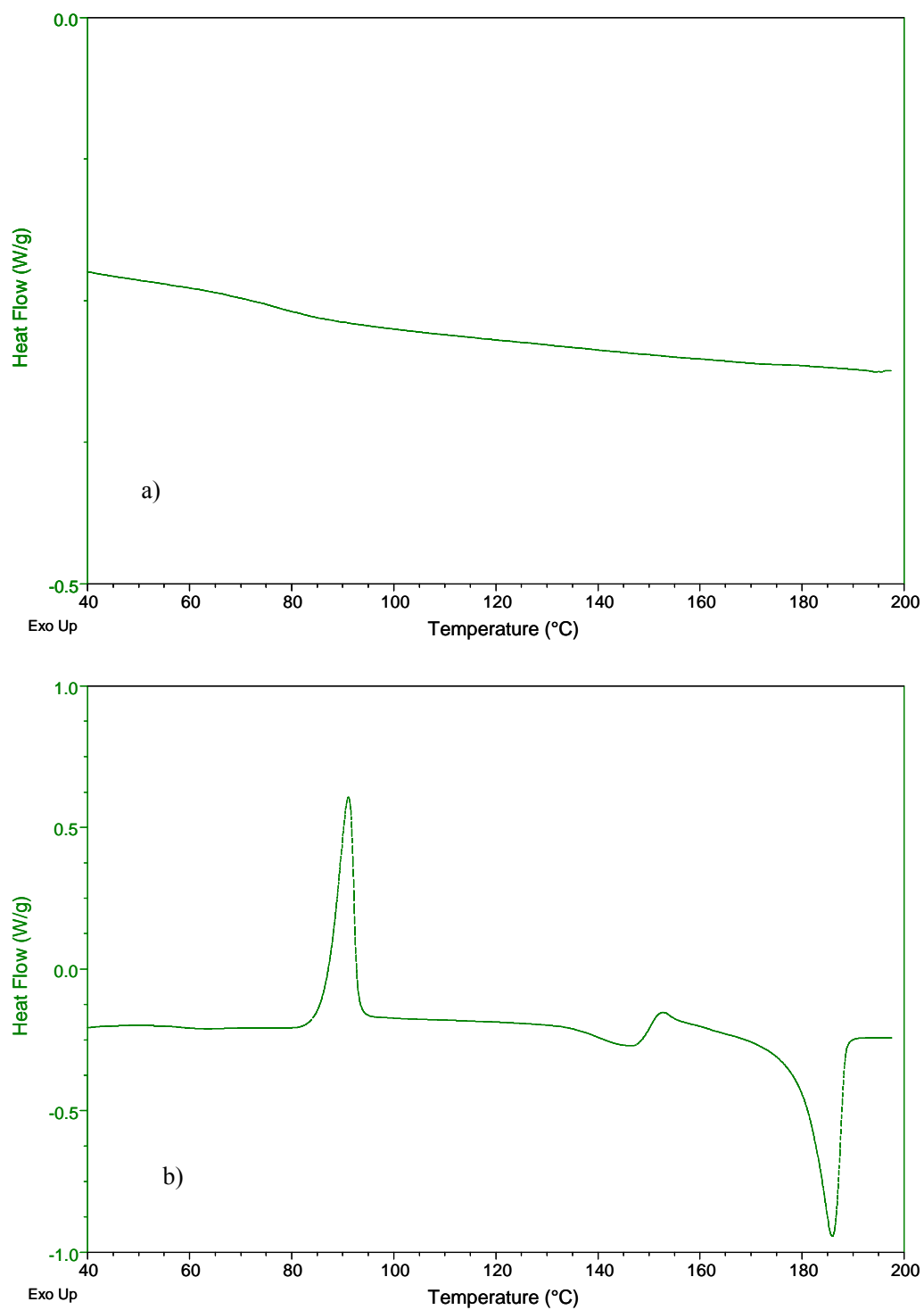


Figure 6.5. DSC thermograms of adenine-containing block copolymer/UP⁺ blend (a) and UP⁺ (b). Heating rate 10 °C/min, 2nd heat, N₂.

6.4.4 Morphological Characterization of Phosphonium Salt Blends

Morphological investigations with atomic force microscopy (AFM) revealed unique surface textures for the UP⁺ block copolymer blends compared with the pure adenine block copolymer (Figure 6.6). Annealing at temperatures from 155 to 200 °C under vacuum or nitrogen played a significant role in the surface morphology of the hydrogen bonding block copolymers containing the phosphonium salt. Significant differences in terms of the orientation of the domains relative to the surface were observed at each annealing temperature. The morphology of the blends near the surface appeared to resemble a lamellar morphology to a greater extent than the pure adenine containing block copolymer. Corresponding SAXS data (Figure 6.7) revealed that the addition of the phosphonium salt resulted in a shift in morphology from cylindrical to lamellar structures. The addition of one equivalent of phosphonium salt corresponded with a change in hard phase from 15 to 37 wt%. Transmission electron microscopy (Figure 6.8) of the phosphonium salt adenine polymer blend further supported the assignment of a lamellar morphology and revealed similar lamellar spacing (20 nm) compared to SAXS (15 nm). Reducing the concentration of the phosphonium salt to less than stoichiometric levels (0.53 equiv) also resulted in a transition to a lamellar morphology as determined through SAXS measurements.

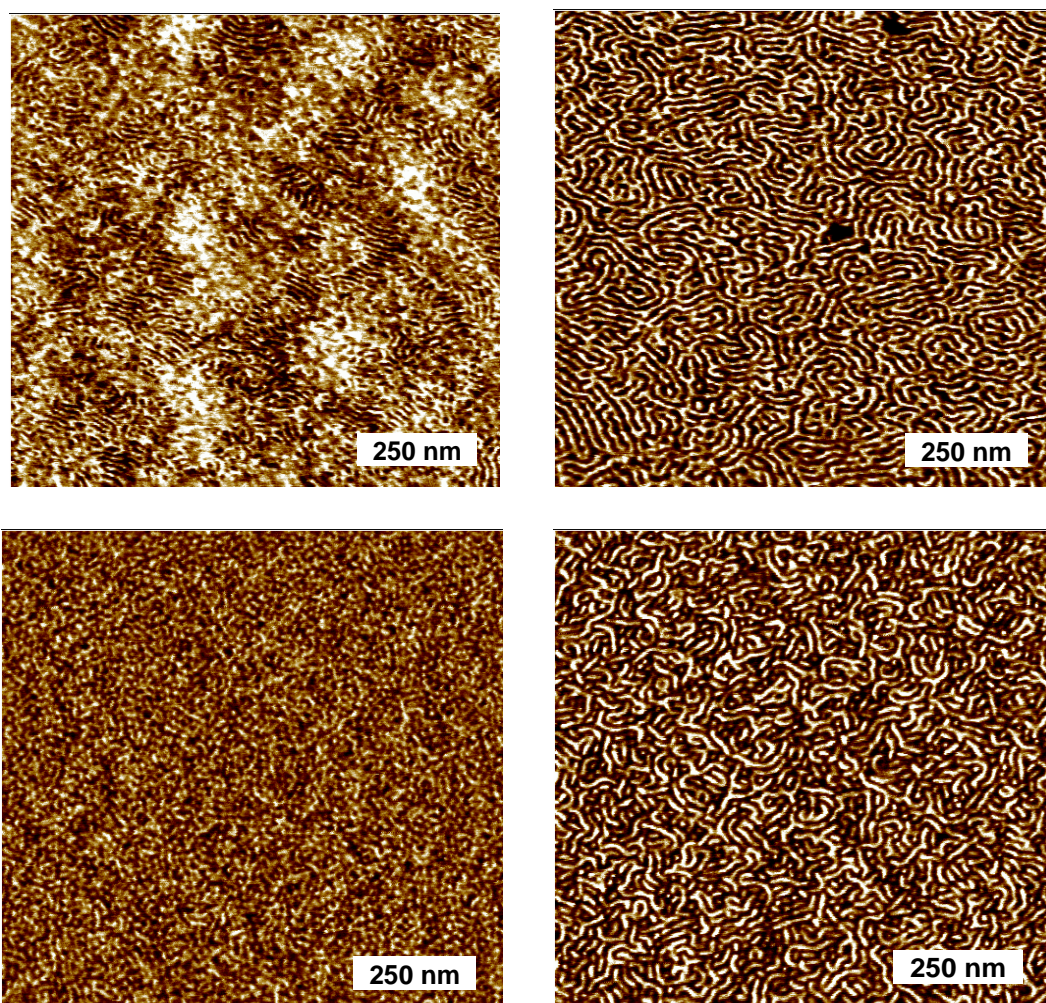


Figure 6.6. Tapping mode AFM phase images of 1.5K-16.5K-1.5K adenine triblock UP⁺ blend (A:U 1:1) annealed at (a) 155 °C (b) 170 °C (c) 200 °C. (d) pure adenine triblock copolymer annealed at 155 °C. Setpoint ratio = 0.6. All samples spin-coated on silicon and annealed for 18 h under vacuum. Silicon surfaces were cleaned prior to spin-coating via chloroform rinsing and drying with high-pressure nitrogen. Film thickness values were approximately 100 nm.

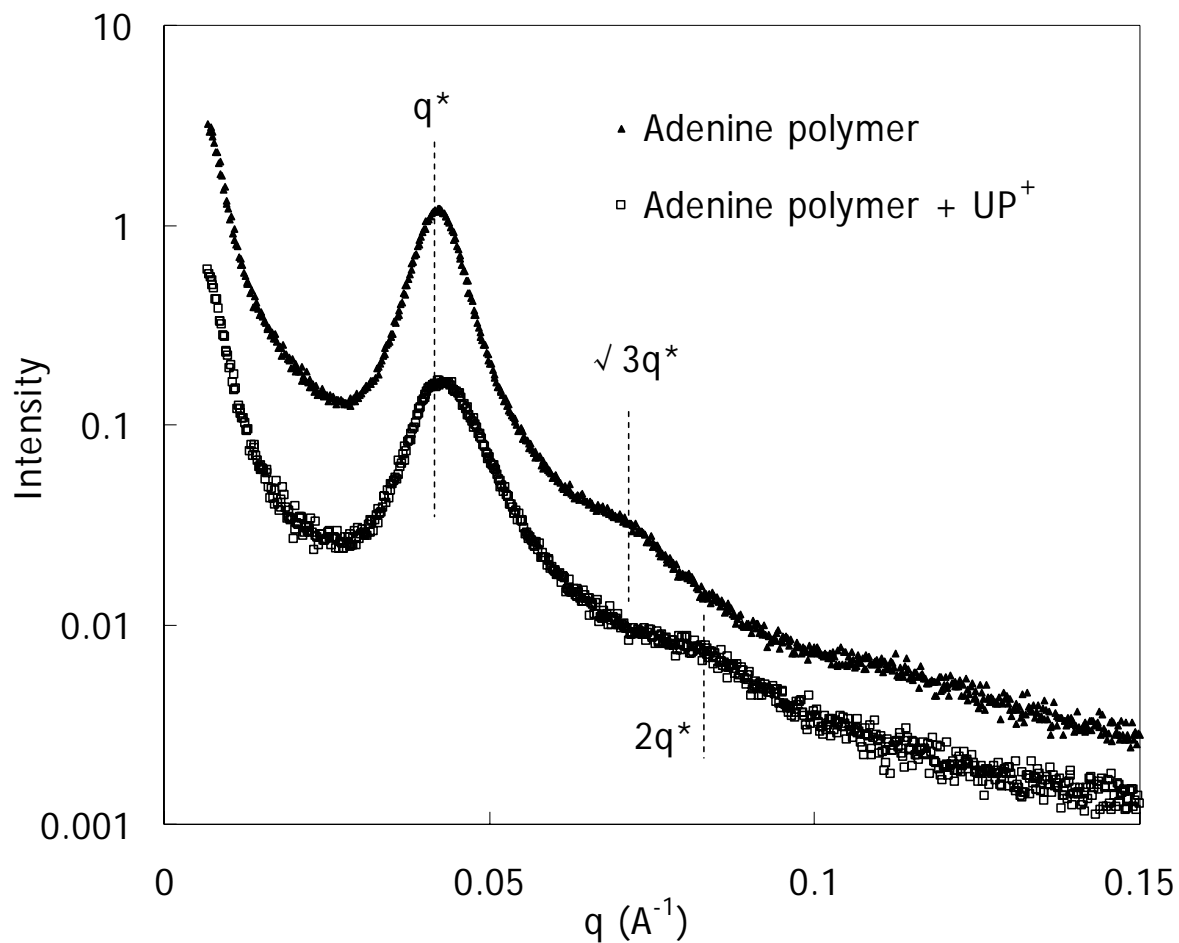


Figure 6.7. Small-angle X-ray scattering (SAXS) of 1.5K-16.5K-1.5K adenine triblock and UP⁺ blend (A:U 1:1) annealed 155 °C for 18 h under vacuum.

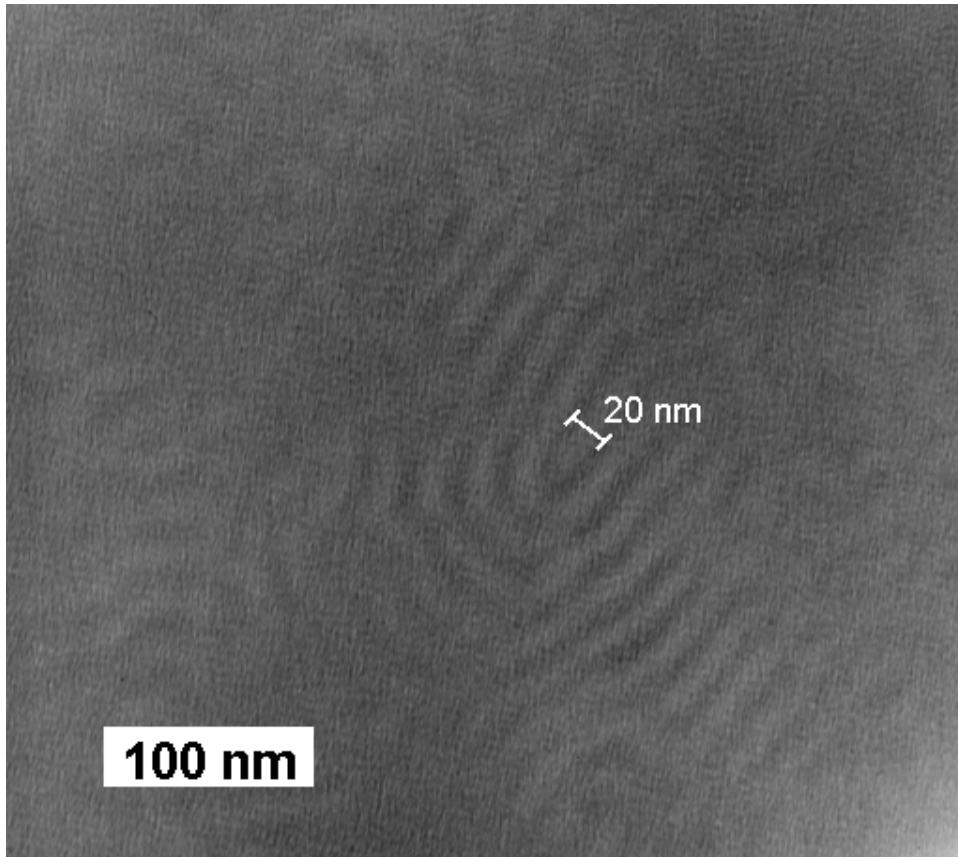


Figure 6.8 Bright field TEM micrograph of adenine-containing polymer/UP⁺ blend stained with OsO₄.

6.4.5 Effect of Phosponium Salt on Solution and Solid State Properties

Solution rheological studies of UP⁺ modified adenine containing triblock copolymers were conducted in chloroform, which favors hydrogen bonding interactions due to a relatively low dielectric constant. An apparent 3.4 fold decrease in solution viscosity of the block copolymer solution (4.2 wt%, 25 °C) was observed upon the addition of one equivalent UP⁺. This suggested a screening effect of the adenine-adenine self association between polymer chains and further indicated the effectiveness of the hydrogen bonding interaction.

Dynamic mechanical (DMA) studies on the adenine polymer UP⁺ blends revealed that the glass transition temperature of the rubber phase did not change significantly (Figure 6.9). The rubber phase T_g of the blend was -32 °C versus -29 °C for the pure adenine polymer according to the maximum of the loss modulus curve, indicating selective incorporation of UP⁺ into the hard phase. Furthermore, the rubbery plateau modulus increased from 0.7 to 14.6 MPa at 25°C, consistent with the increased hard phase volume fraction from 15 to 37 wt%. Interestingly, for the blend with UP⁺, the softening of the hard phase occurred at lower temperatures (170 vs 230 °C) again suggesting a screening effect of the adenine-adenine intermolecular hydrogen bonds.

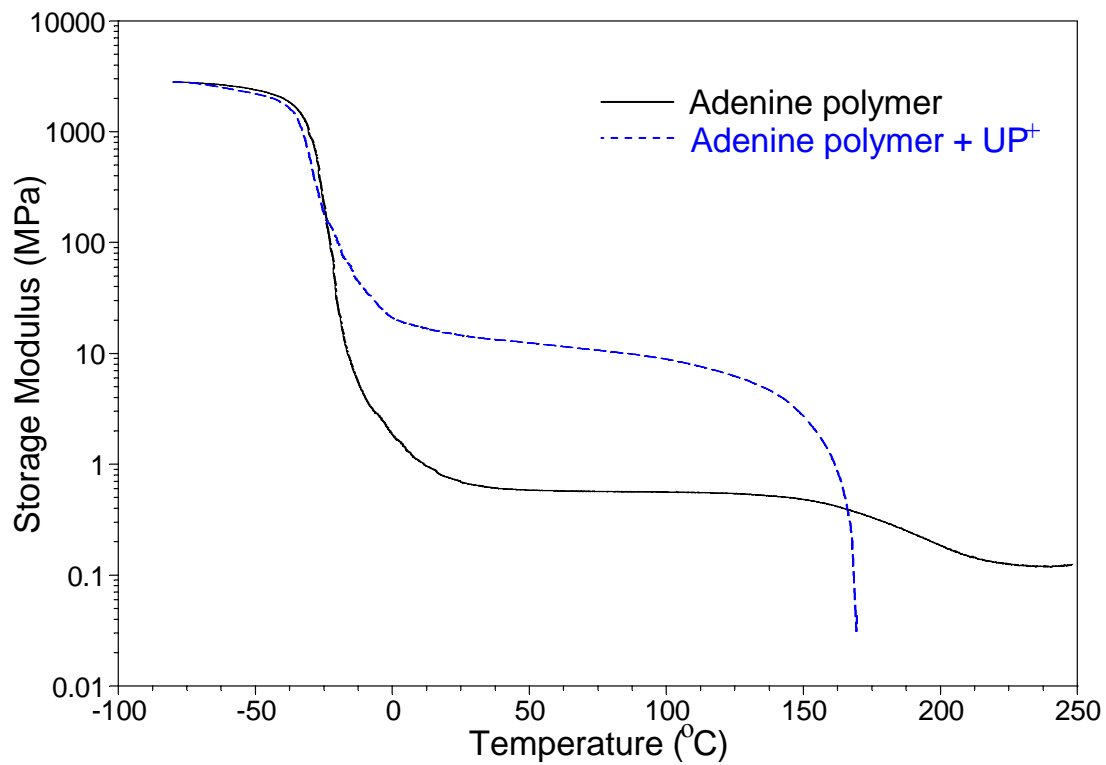


Figure 6.9 Dynamic mechanical temperature sweep for pure 1.5K-16.5K-1.5K adenine triblock copolymer and blend with 1 equivalent of UP⁺.

6.5 Conclusion

In conclusion, this manuscript defines a novel general strategy for the introduction of thermally stable ionic sites to block copolymers *via* reversible complementary hydrogen bonding. Novel adenine containing block copolymer precursors were synthesized using a novel difunctional initiator. Subsequent blending with unique phosphonium cation containing complementary hydrogen bonding guests was conducted. Influences on surface morphology, solution viscosity, and mechanical properties were observed.

6.6 Acknowledgment

The authors would like to acknowledge Emily B. Anderson and Erika M. Borgerding for electron microscopy. This material is based upon work supported by the U.S. Army Research Laboratory and the U.S. Army Research Office under contract/grant number DAAD19-02-1-0275 Macromolecular Architecture for Performance Multidisciplinary University Research Initiative (MAP MURI).

Chapter 7. Novel Michael Addition Networks Containing Poly(propylene glycol) Telechelic Oligomers

(Mather, B.D.; Miller, K.M.; Long, T.E. *Macromolecular Chemistry and Physics* 2006, 207, 1324-33.) Reproduced with permission, Copyright Wiley 2006.

7.1 Abstract

Poly(propylene glycol) oligomers with molecular weights ranging from 1000 to 8000 g/mol were end-functionalized with acetoacetate groups and subsequently crosslinking using carbon-Michael addition with PEG diacrylate. Gel fraction analysis, dynamic mechanical analysis (DMA), thermogravimetric analysis (TGA), tensile, and swelling measurements were utilized to characterize the networks. The thermomechanical properties of the networks were analyzed with respect to the molecular weight between crosslink points (M_c) and the critical molecular weight for entanglement (M_e). Sampling experiments during crosslinking revealed the evolution of molecular weight with time and monomer conversion. Kinetic analyses of the Michael additions were performed using ^1H NMR spectroscopy, and the influence of basic catalyst and concentration were elucidated.

7.2 Introduction

The Michael addition reaction has received significant attention as a versatile tool in the synthesis of novel polymeric network structures.^{632 - 640} The Michael addition reaction offers mild conditions, functional group tolerance, and readily available precursors. More recently, the carbon-Michael addition has demonstrated utility in the synthesis of polymeric networks, which offer promise as high performance coatings, adhesives and laminates. The carbon-Michael addition involves the reaction of enolate type nucleophiles such as acetoacetate esters in the presence of base with α,β -unsaturated carbonyl compounds such as acrylate esters. A wide range of basic catalysts are available for the synthesis of carbon-Michael addition networks, including both organic (amidine) and inorganic (hydroxide, carbonate) bases. The strength of the basic catalyst is critical in determining the rate of the Michael addition due to the equilibrium for deprotonation of the acetoacetate ester.

⁶³² Metters, A.; Hubbell, J. Network formation and degradation behavior of hydrogels formed by Michael-type addition reactions. *Biomacromolecules* **2005**, *6*, 290-301.

⁶³³ B.D. Mather, K. Viswanathan, K.M. Miller, T.E. Long Michael Addition Reactions in Macromolecular Design for Emerging Technologies. *Prog. Polym. Sci.* **2006**, *31*, 487-531.

⁶³⁴ Vernon, B.; Tirelli, N.; Bachi, T.; Haldimann, D.; Hubbell, J. Water-borne, in situ crosslinked biomaterials from phase-segregated precursors. *J Biomed Mater Res* **2003**, *64A*, 447-456.

⁶³⁵ Beckley, R.S.; Kauffman, T.F.; Zajackowski, M.J.; Whitman, D.W. Michael addition compositions. U.S. Pat. Appl., 2005245721, 2005.

⁶³⁶ Rizzi, S. C.; Hubbell, J. A. Recombinant protein-co-PEG networks as cell-adhesive and proteolytically degradable hydrogel matrixes. Part I: Development and physicochemical characteristics. *Biomacromolecules* **2005**, *6*, 1226-38.

⁶³⁷ van de Wetering, P.; Metters, A. T.; Schoenmakers, R. G.; Hubbell, J. A. Poly(ethylene glycol) hydrogels formed by conjugate addition with controllable swelling, degradation, and release of pharmaceutically active proteins. *J Contr Rel* **2005**, *102*, 619-27.

⁶³⁸ Clemens, R.J. Low temperature Michael addition reactions. U.S. Patent 5017649, 1991.

⁶³⁹ Moszner, N.; Rheinberger, V. Reaction behavior of monomeric β -ketoesters, 4) Polymer network formation by Michael reaction of multifunctional acetoacetates with multifunctional acrylates. *Macromol Rapid Commun* **1995**, *16*, 135-38.

⁶⁴⁰ Marsh, S. J. Acetoacetate chemistry- crosslinking versatility for high-solids coatings resins. *Am Chem Soc, Div Polym Chem: Polym Prepr* **2003**, *44*, 52-53.

Due to the presence of two acidic protons on the acetoacetate group, difunctionality of the acetoacetate group is often observed.⁶⁴¹ The acidities of the two acetoacetate protons differ significantly ($pK_{a1} \sim 12$, $pK_{a2} \sim 13$), and this difference in reactivity leads to different network structures depending on the strength of the basic catalyst.⁶⁴² For, instance, Clemens and Rector observed higher Michael bis-adduct formation for amidine bases compared to more mono-adducts for inorganic bases.⁶⁴² The Michael addition reaction provides advantages over classical urethane bond forming reactions due to the elimination of highly toxic isocyanates and also exhibits competitive rates compared to urethane formation, allowing efficient curing at room temperature.

A wide range of hydroxyl functional telechelic oligomers are readily converted to acetoacetate and acrylate functionality. In this work, hydroxyl terminated poly(propylene glycol) (PPG) telechelic oligomers were functionalized with acetoacetate groups via a facile, uncatalyzed transesterification with *tert*-butyl acetoacetate (tBAA).⁶⁴³ These bis(acetoacetate) precursors were subsequently crosslinked with PEG diacrylate (575 g/mol) using the base catalyzed Michael addition (Figure 7.1). The ACCLAIM™ PPGs served as ideal oligomeric precursors for this reaction due to near difunctionality of these oligomers, which are prepared in the absence of base and do not possess allylic end groups. The synthesis of networks via telechelic functionalized oligomers provides a convenient method

⁶⁴¹ Kim, Y. B.; Kim, H. K.; Nishida, H.; Endo, T. Synthesis and characterization of hyperbranched poly(β -ketoester) by the Michael addition. *Macromol Mater Eng* **2004**, 289, 923-6.

⁶⁴² Clemens, R. J.; Rector, F. D. A comparison of catalysts for crosslinking acetoacetylated resins via the Michael reaction. *J Coat Tech* **1989**, 61, 83-91.

⁶⁴³ Witzeman, J. S.; Nottingham, W. D. Transacetoacetylation with *tert*-butyl acetoacetate: synthetic applications. *J Org Chem* **1991**, 56, 1713-8.

for creating model networks with controlled molecular weights between crosslink points. The resulting model networks are considered more well-defined than typical sulfur or peroxide vulcanized rubbers and often possess better mechanical properties due to the presence of fewer dangling ends.^{644,645} Crosslinking telechelic oligomers to form model networks was previously accomplished with polysiloxanes via hydrosilation of vinyl terminated and SiH terminated oligomers,^{646 - 652} but other efforts involve telechelic polyethers,^{653 - 655} polyisobutylenes,⁶⁵⁶ polyurethanes,⁶⁵⁷ and polyimides.⁶⁵⁸

⁶⁴⁴ Mark, J.E. Some Interesting Things about Polysiloxanes. *Acc Chem Res* **2004**, *37*, 946-53.

⁶⁴⁵ Mark, J.E. New developments and directions in the area of elastomers and rubberlike elasticity. *Macromol Symp* **2003**, *201*, 77-84.

⁶⁴⁶ Batra, A.;Cohen, C.; Archer, L. Stress Relaxation of End-Linked Polydimethylsiloxane Elastomers with Long Pendent Chains. *Macromolecules* **2005**, *38*, 7174-80.

⁶⁴⁷ Meyers, K.O.; Bye, M.L.; Merrill, E.W. Model Silicone Elastomer Networks of High Junction Functionality: Synthesis, Tensile Behavior, Swelling Behavior, and Comparison with Molecular Theories of Rubber Elasticity. *Macromolecules* **1980**, *13*, 1045-53.

⁶⁴⁸ Urayama, K.; Miki, T.; Takigawa, T.; Kohjiya, S. Damping Elastomer Based on Model Irregular Networks of End-Linked Poly(Dimethylsiloxane). *Chem Mater* **2004**, *16*, 173-178.

⁶⁴⁹ Hedden, R. C.; Saxena, H.; Cohen, C. Mechanical Properties and Swelling Behavior of End-Linked Poly(diethylsiloxane) Networks. *Macromolecules* **2000**, *33*, 8676-84.

⁶⁵⁰ Kawamura, T.; Urayama, K.; Kohjiya, S. Multiaxial Deformations of End-Linked Poly(dimethylsiloxane) Networks. 1. Phenomenological Approach to Strain Energy Density Function. *Macromolecules* **2001**, *34*, 8252-60.

⁶⁵¹ Braun, J. L.; Mark, J. E.; Eichinger, B. E. Formation of Poly(dimethylsiloxane) Gels. *Macromolecules* **2002**, *35*, 5273-82.

⁶⁵² Shefer, A.; Gottlieb, M. Effect of crosslinks on the glass transition temperature of end-linked elastomers. *Macromolecules* **1992**, *25*, 4036-42.

⁶⁵³ Jong, L.; Stein, R. S. Synthesis, characterization, and rubber elasticity of end-linked poly(tetrahydrofuran) elastomer. *Macromolecules* **1991**, *24*, 2323-29.

⁶⁵⁴ Lee, B. P.; Dalsin, J. L.; Messersmith, P. B. Synthesis and Gelation of DOPA-Modified Poly(ethylene glycol) Hydrogels. *Biomacromolecules* **2002**, *3*, 1038-47.

⁶⁵⁵ Andrady, A. L.; Sefcik, M. D. Glass transition in poly(propylene glycol) networks. *J Polym Sci: Polym Phys Ed* **1983**, *21*, 2453-63.

⁶⁵⁶ Lackey, J. E.; Chang, V. S. C.; Kennedy, J. P.; Zhang, Z. M.; Sung, P. H.; Mark, J. E. Polyisobutylene model elastomers prepared using demonstrably complete end-linking reactions. 2. Elongation moduli of the trifunctional networks prepared from the three-arm polymers. *Polym Bull* **1984**, *11*, 19-24.

⁶⁵⁷ Mark, J. E.; Sung, P. H. Chain extension studies relevant to the completeness of end-linking in elastomeric polyurethane networks. *Rubber Chem Tech* **1982**, *55*, 1464-8.

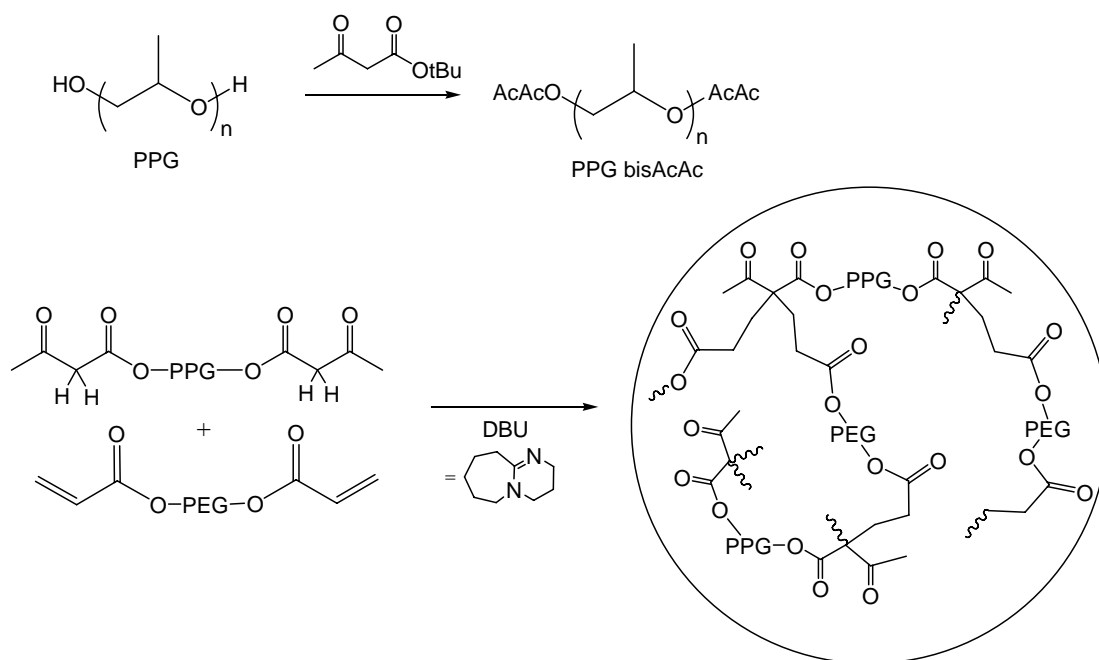


Figure 7.1. Synthesis of acetoacetate networks from acetoacetate functionalized PPG (PPG bisAcAc) using DBU as a basic catalyst.

⁶⁵⁸ Zhuang, H.; Sankarapandian, M. S.; Ji, Q.; McGrath, J. E. Thermosetting polyetherimides. The influence of reactive endgroup type and oligomer molecular weight on synthesis, network formation, adhesion strength, and thermal properties. *J Adhesion* **1999**, 71, 231-62.

A range of PPGs of various molecular weights are available, allowing investigations of the effect of the molecular weight between crosslink points relative to the critical molecular weight for entanglement. The molecular weight between crosslink points (M_c) and crosslink density are critical parameters in network synthesis, affecting such mechanical properties as modulus, strength, and toughness as well as swelling.^{659- 661} Recent attention involves studies of the effect of the molecular weight between crosslink points as a function of the entanglement molecular weight (M_e).^{662- 664} The entanglement molecular weight of PPG ($M_e = 7700$ g/mol)⁶⁶⁵ is in the range of commercially available ACCLAIM™ oligomers. Furthermore, PPG is an atactic, amorphous polymer, which avoids the complexities of strain induced crystallization that is typically observed in elastomers based on poly(tetramethylene oxide) (PTMO) or poly(ϵ -caprolactone) (PCL).

A number of authors have examined the effect of entanglements on networks.^{666- 668} It

⁶⁵⁹ Mark, J. E. New developments and directions in the area of elastomers and rubberlike elasticity. *Macromol Symp* **2003**, 201, 77-84.

⁶⁶⁰ Andraday, A. L.; Sefcik, M. D. Glass transition in poly(propylene glycol) networks. *J Polym Sci: Polym Phys Ed* **1983**, 21, 2453-63.

⁶⁶¹ Zhuang, H.; Sankarapandian, M. S.; Ji, Q.; McGrath, J. E. The influence of reactive endgroup type and oligomer molecular weight on synthesis, network formation, adhesion strength, and thermal properties. *J Adhesion* **1999**, 71, 231-62.

⁶⁶² Erman, B.; Mark, J. E., Structures and properties of rubberlike networks. Oxford University Press: New York, 1997.

⁶⁶³ Sung, P. H.; Pan, S. J.; Mark, J. E.; Chang, V. S. C.; Lackey, J. E.; Kennedy, J. P. Polyisobutylene model elastomers prepared using demonstrably complete end-linking reactions. 1. Elongation moduli of the trifunctional and tetrafunctional networks prepared from the linear polymers. *Polym Bull* **1983**, 9, 375-81.

⁶⁶⁴ Bhawe, D. M.; Cohen, C.; Escobedo, F. A. Effect of chain stiffness and entanglements on the elastic behavior of end-linked elastomers. *J Chem Phys* **2005**, 123, 014909-1/0124909/11.

⁶⁶⁵ Aharoni, S. M. On entanglements of flexible and rodlike polymers. *Macromolecules* **1983**, 16, 1722-28.

⁶⁶⁶ Dossin, L. M.; Graessley, W. W. Rubber Elasticity of Well-Characterized Polybutadiene Networks. *Macromolecules* **1979**, 12, 123-30.

is generally accepted that both crosslink points and entanglements, which are trapped during curing, contribute to the elastic moduli of networks.⁶⁶⁹ Mazich and Samus have stated that trapped entanglements, also known as topological constraints, can account for 20 to 90% of the elastic modulus in networks.⁶⁷⁰ The contribution to the elastic modulus from entanglements increases as crosslink density decreases and the molecular weight between crosslink points increases. Rubinstein and Panyukov recently developed a model which separates contributions to the elastic modulus from classical phantom network crosslink points and entanglements.⁶⁷¹

The objective of this work was to study the effect of poly(propylene glycol) precursor molecular weight on the mechanical properties of carbon-Michael addition networks in relation to the critical molecular weight for entanglement. Additionally, the gelation process was studied in relation to predictions from Flory's theory. Efforts were also devoted to studying the kinetics of the crosslinking reaction as a function of the basic catalyst employed.

7.3 Experimental

7.3.1 Materials

tert-Butyl acetoacetate (tBAA, 98%), poly(ethylene glycol) diacrylate ($M_n = 575$ g/mol),

⁶⁶⁷ Smedberg, A.; Hjertberg, T.; Gustafsson, B. The role of entanglements in network formation in unsaturated low density polyethylene. *Polymer* **2004**, 45, 4867-75.

⁶⁶⁸ Hvidt, S., In *Physical Networks: Polymers and Gels*, Burchard, W.; Ross-Murphy, S. B., Eds. Elsevier: New York, 1988; pp 125-32.

⁶⁶⁹ Termonia, Y., In *Synthesis, Characterization and Theory of Polymeric Networks and Gels*, Aharoni, S. M., Ed. Plenum Press: New York, 1992; pp 201-207.

⁶⁷⁰ Mazich, K. A.; Samus, M. A. Role of entanglement couplings in threshold fracture of a rubber network. *Macromolecules* **1990**, 23, 2478-83.

⁶⁷¹ Rubinstein, M.; Panyukov, S. Elasticity of Polymer Networks. *Macromolecules* **2002**, 35, 6670-86.

neopentyl glycol diacrylate, 1,8-diazabicyclo[5.4.0]undec-7-ene (DBU, 98%), tetramethylammonium hydroxide pentahydrate (TMAH) (97%) and 1,1,3,3-tetramethylguanidine (TMG, 99%), sodium methoxide (NaOMe, 25 wt% in methanol), were purchased from Aldrich and used as received. Arcol™ poly(propylene glycol) diol (1000 g/mol) (Bayer Co.), potassium *tert*-butoxide (KOtBu, 97%, TCI), and potassium carbonate (99%, EM Science) were used as received. 2000, 4000, and 8000 g/mol poly(propylene glycol) bis(acetoacetates) (PPG bisAcAc) were synthesized from ACCLAIM™ poly(propylene glycol) diols using a method similar to the one described below.

7.3.2 Synthesis of Acetoacetate Functionalized Poly(propylene glycol) (PPG bisAcAc)

Arcol™ poly(propylene glycol) (10.0 g, 10 mmol) and 6.3 g (40 mmol, 4 equiv) tBAA were charged to a two-necked 100 mL flask, equipped with a short-path distillation head, receiving flask, and magnetic stirbar. The mixture was maintained at 150 °C for 4 h and gentle vacuum (100 mm Hg) was applied to remove the *tert*-butanol byproduct and excess tBAA. An additional 6.3 g tBAA were added and heating continued for another 5 h at 150 °C in order to ensure quantitative functionalization. Aspirator vacuum (~100 mmHg) and finally high vacuum (0.1 mmHg) at 150 °C were applied to remove volatile starting reagents and reaction byproducts. ¹H NMR (400 MHz, CDCl₃): δ = 1.12 ppm (br, PPG CH₃), δ = 1.24 ppm (dd, 6H, CHCH₃OAcAc), δ = 2.26 ppm (s, 6H, COCH₂COCH₃), δ = 3.4 ppm (br, PPG CH), δ = 3.6 ppm (br, PPG CH₂), δ = 5.08 ppm (m, 4H, CH₂CHCH₃OAcAc), δ = 5.29 ppm (s, enol C=CH-C=O), δ = 12.09 ppm (s, enol OH).

7.3.3 Crosslinking Reactions

2000 g/mol PPG bisAcAc (4.00 g, 2.00 mmol) and PEG diacrylate (1.60 g, 2.78 mmol, 1.40 equiv.) were mixed to form a homogeneous, clear, blend. DBU catalyst (50 mg, 1.25 wt% relative to PPG bisAcAc) was added and mixed thoroughly. The homogeneous reaction mixture was transferred to a Teflon™ mold and cured at ambient temperature for 48 h. A dramatic increase in viscosity indicated that gelation occurred within minutes.

7.3.4 SEC and ¹H NMR Analysis of the Crosslinking Process

4000 g/mol PPG bisAcAc (2.25 g, 0.563 mmol), PEG diacrylate (440 mg, 0.765 mmol, 1.40 equiv.) were mixed initially, and potassium carbonate (50% aq) catalyst (28 mg, 0.101 mmol, 0.16 equiv.) was added and mixed thoroughly. Samples (~ 100 mg) were periodically removed from the crosslinking reaction prior to the gel point, rapidly quenched with acidified THF (~10 mL + 1 drop 35 wt. % HCl) and immediately dried using rotary evaporation and reduced pressure (0.1 mmHg) for 18 h at 25 °C. ¹H NMR and SEC analysis were used to determine PEG acrylate end group conversion and product molecular weight, respectively.

7.3.5 ¹H NMR Kinetics Experiments

Kinetic analyses of the Michael addition reaction were performed using ¹H NMR spectroscopy. A stock reaction mixture of 2000 g/mol PPG bisAcAc (2.00 g, 1.00 mmol) and PEG diacrylate (0.800 g, 1.39 mmol) was prepared, and 200 mg was added to each NMR tube with 800 mg DMSO-d₆. The ¹H NMR spectra were collected upon addition of the

DBU catalyst (13.2 μL) with a microliter syringe. The tube was vigorously shaken prior to insertion into the spectrometer. ^1H NMR spectra were collected at regular intervals and the conversion was reported as the ratio of the acrylate integration relative to the initial integration, based on the PPG ether methylene and methyne ($\text{CH}_2 + \text{CH}$, $\delta = 3.5$ ppm) resonances as an internal reference. In the case of overlapping catalyst resonances, the acrylate integrations were referenced to the PPG methyl groups ($\delta = 1.1$ ppm). The use of a relatively high concentration of reagents allowed determination of conversion with 4 scans, allowing measurements over ca. 30 seconds. Identical reactions external to the NMR instrument were performed in parallel to determine gel points.

7.3.6 Polymer Characterization

Size exclusion chromatography (SEC), was performed at 40 $^\circ\text{C}$ in THF at a flow rate of 1 mL/min using a Waters size exclusion chromatograph equipped with an autosampler, three 5 μm PLgel Mixed-C columns, a Waters 2410 refractive index (RI) detector operating at 880 nm, and a miniDAWN multiangle laser light scattering (MALLS) detector operating at 690 nm, which was calibrated with narrow polydispersity polystyrene standards. The refractive index increment (dn/dc) was calculated online. ^1H NMR spectroscopic data were collected on a Varian 400 MHz spectrometer at ambient temperature. Gel fraction analysis was performed using soxholet extraction in refluxing ethanol for 12 h followed by drying in a vacuum oven for 18 h at 80 $^\circ\text{C}$. Gel fractions were determined according to conventional, gravimetric approaches.⁶⁷² Dynamic mechanical measurements were conducted on a TA

⁶⁷² Elzubair, A.; Suarez, J. C. M.; Bonelli, C. M. C.; Mano, E. B. Gel fraction measurements in gamma-irradiated ultra high molecular weight polyethylene. *Polymer Testing* **2003**, 22, 647-9.

Instruments Q-800 DMA under nitrogen at a heating rate of 3 °C/min at 1 Hz frequency in film tension mode. Tensile characterization was performed on an Instron model 4411 at 0.5"/min crosshead speed using miniature dogbone specimens and manual grips at ambient conditions.

7.4 Results and Discussion

7.4.1 Synthesis of Acetoacetate Functionalized Poly(propylene glycol) (PPG bisAcAc)

The functionalization of PPG via transesterification with tBAA (Figure 7.1) is a more facile route than previous techniques involving diketene or 2,2,6-trimethyl-4*H*-1,3-dioxin-4-one, which involve either noxious or difficult to synthesize reagents, respectively.⁶⁷³ The relative ease of functionalization of alcohols with acetoacetate groups enables the incorporation of numerous precursors into carbon-Michael addition networks. In addition, the wide variety of acrylate functionalized molecules which are commercially available or readily synthesized, further diversifies the Michael addition networks. Simple vacuum distillation of excess tBAA starting material and *tert*-butanol byproduct was the only necessary purification step.

A comparison of NMR based number average molecular weights of the PPG bisAcAc with the SEC molecular weights was performed. The ratio of the integrations of the AcAc methyl resonances ($\delta = 2.26$ ppm) with the PPG methyl resonances ($\delta = 1.12$ ppm) was used to calculate the NMR number average molecular weight. The comparison of molecular

⁶⁷³ Clemens, R. J.; Hyatt, J. A. Acetoacetylation with 2,2,6-trimethyl-4*H*-1,3-dioxin-4-one: A convenient alternative to diketene. *J Org Chem* **1985**, 50, 2431-5.

weights from the different methods indicated nearly 100 % functionalization for the 1000 and 2000 g/mol PPG bisAcAc, however, lower levels of functionalization were observed for the 4000 and 8000 g/mol precursors (Table 7.1).

7.4.2 Synthesis of carbon-Michael Addition Networks

The acetoacetate functionalized PPGs of molecular weights ranging from 1000 to 8000 g/mol were successfully crosslinked via the Michael addition reaction with PEG diacrylate. The gel times of the reaction mixtures increased with increasing PPG molecular weight, but were generally less than 8 min in all cases (Figure 7.2). This was attributed to a lower concentration of functional groups for higher molecular weight PPG oligomers. In order to ensure high conversions at room temperature, 48 h cure times were employed, however, heat (65°C) was also used for curing the 8000 g/mol PPG bisAcAc. The crosslinked networks were optically clear, except for the 8000 g/mol PPG bisAcAc, which was translucent. The difference for the 8000 g/mol PPG bisAcAc sample was attributed to the high molecular weight of the PPG oligomer causing macrophase separation between the PPG and the PEG as well as the lower functionality of the 8000 g/mol PPG bisAcAc precursor.

Table 7.1. Characterization of PPG bisAcAc precursors.

PPG bisAcAc	M_n (g/mol) ($^1\text{H NMR}$) ^a	M_n (g/mol) (SEC) ^b	M_w/M_n	Degree of functionalization ^c (%)
1000	1300	1200	1.10	100
2000	2400	2400	1.05	100
4000	4300	4700	1.01	92
8000	10900	8300	1.02	76

^a determined from the ratio of PPG CH_3 ($\delta = 1.12$ ppm) to AcAc CH_3 ($\delta = 2.26$ ppm)

^b 40 °C, THF, MALLS

^c ratio of SEC M_n to $^1\text{H NMR } M_n$

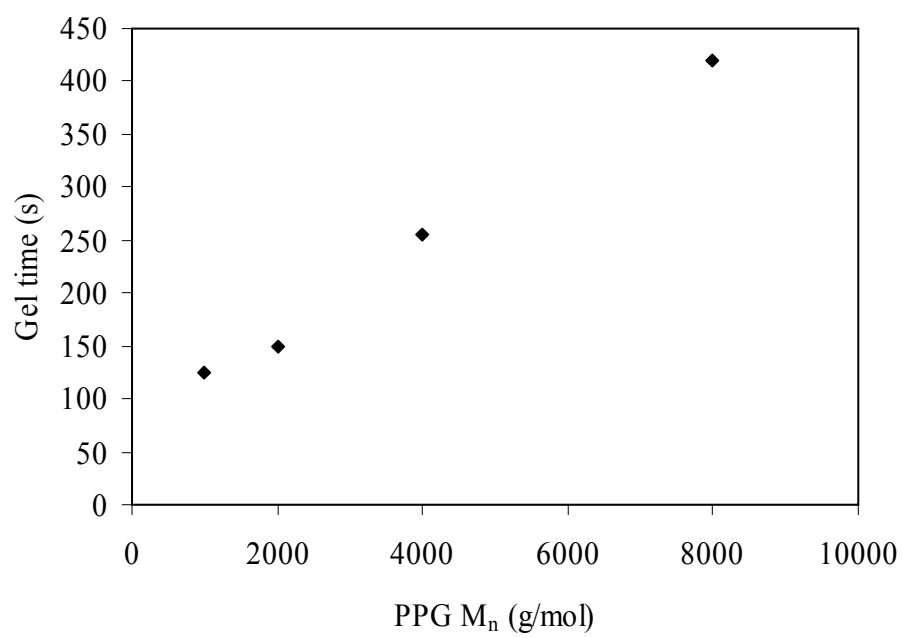


Figure 7.2. Gel times for PPG bisAcAc / PEG diacrylate networks as a function of PPG molecular weight.

Two different molar ratios of acrylate : acetoacetate were investigated in the preparation of PPG bisAcAc / PEG diacrylate networks. Both a 2.0:1.0 (assumes acetoacetate $f = 1$) and a 1.4:1.0 acrylate to acetoacetate molar ratio were used to synthesize carbon-Michael addition networks. Both ratios lead to successful network synthesis. However, the 1.4:1.0 ratio yielded higher tensile strengths, Young's moduli, and lower swelling despite the assumption of difunctionality of the acetoacetate group. These observations were consistent with less than difunctionality for each acetoacetate, which is reasonable based on the higher pK_a of the second acetoacetate proton and greater steric hindrance of the second enolate anion.⁶⁷⁴

7.4.3 Characterization of the PPG bisAcAc / PEG diacrylate Networks

Gel fraction analysis was performed in order to assess the effectiveness of oligomer incorporation into the network. Gel fraction analysis revealed a decrease in gel fraction with increased PPG molecular weight (Table 7.2). For the 1.4:1.0 acrylate to acetoacetate networks with 1.25 wt% DBU relative to PPG bisAcAc, a maximum gel fraction of 96% was observed for the PPG 1000 g/mol oligomer. Higher molecular weight PPG bisAcAc precursors lead to lower gel fractions. This result suggested the presence of dangling ends and unincorporated sol, which were more significant for networks containing higher molecular weight PPG bisAcAc precursors. In general, a slight decrease in the gel fraction was observed with increased acrylate to acetoacetate ratios (2.0:1.0), with the exception of the 2000 g/mol PPG bisAcAc, however these differences were generally close to the error of the gel fraction measurement ($\pm 5\%$). Incomplete reaction was proposed to account for the

⁶⁷⁴ Clemens, R. J.; Rector, F. D. A comparison of catalysts for crosslinking acetoacetylated resins via the Michael reaction. *J Coat Tech* **1989**, 61, 83-91.

low gel fractions of the higher molecular weight precursors, which is a potential consequence of low end group concentration, mobility, and lower functionality of the high molecular weight precursors. An alternate explanation presumed base catalyzed ester hydrolysis, which is promoted in the presence of moisture in the networks, was more significant for networks with lower crosslink densities. Networks were also synthesized using a lower amount of catalyst (0.027 equiv. relative to AcAc groups) on the premise that less catalyst would reduce the likelihood of ester hydrolysis. The use of lower catalyst levels resulted in only slightly higher gel fractions (1-12%, Table 7.2). This was attributed to both slower cure rates as well as decreased base catalyzed ester hydrolysis. Pavlinec and Moszner studied networks based on PPG bisAcAc of low molecular weight (425 g/mol), crosslinked with pentaerythritol tetraacrylate.⁶⁷⁵ In their case, a stronger, basic catalyst, 1,5-diazabicyclo[4.3.0]non-5-ene (DBN), was used at 2 mol% with a 2.0:1.0 acrylate to acetoacetate stoichiometry. Gel fractions ranging from 59 to 94% were obtained, prompting the use of photocrosslinking techniques to further consume acrylate groups and achieve higher gel fractions.

⁶⁷⁵ Pavlinec, J.; Moszner, N. Photocured polymer networks based on multifunctional β -ketoesters and acrylates. *J Polym Sci Part A: Polym Chem* **1997**, 10, 165-78.

Table 7.2. Gel fractions for PPG bisAcAc / PEG diacrylate networks.

PPG bisAcAc M _n (g/mol)	1.4:1.0 Acrylate to Acetoacetate Gel fraction (%)	2.0:1.0 Acrylate to Acetoacetate Gel fraction (%)	Low catalyst* 1.4:1.0 Gel fraction (%)
1000	96	88	97
2000	84	94	92
4000	85	81	88
8000	66	42	78

*0.027 equivalents of DBU catalyst relative to acetoacetate groups.

Dynamic mechanical analysis (DMA) was used to characterize the mechanical properties of the PPG bisAcAc / PEG diacrylate networks with the 1.4:1.0 acrylate to acetoacetate ratio (Figure 7.3). Increased rubbery plateau moduli were observed with a decrease in PPG molecular weight. The plateau moduli for the two lowest PPG molecular weights were nearly identical, contrary to expectations. The glass transition temperatures for the networks, which were measured as the tan delta maxima, indicated increasing glass transition temperature with decreasing PPG molecular weight. This result was expected since higher crosslink densities further restrict chain motions. A linear dependence between the glass transition temperature and inverse PPG bisAcAc molecular weight (Figure 7.4) was observed, which is consistent with previous studies for other well-defined networks.⁶⁷⁶

⁶⁷⁶ Andrady, A.L.; Sefcik, M.D. Glass transition in poly(propylene glycol) networks. *J Polym Sci: Polym Phys Ed* **1983**, *21*, 2453-63.

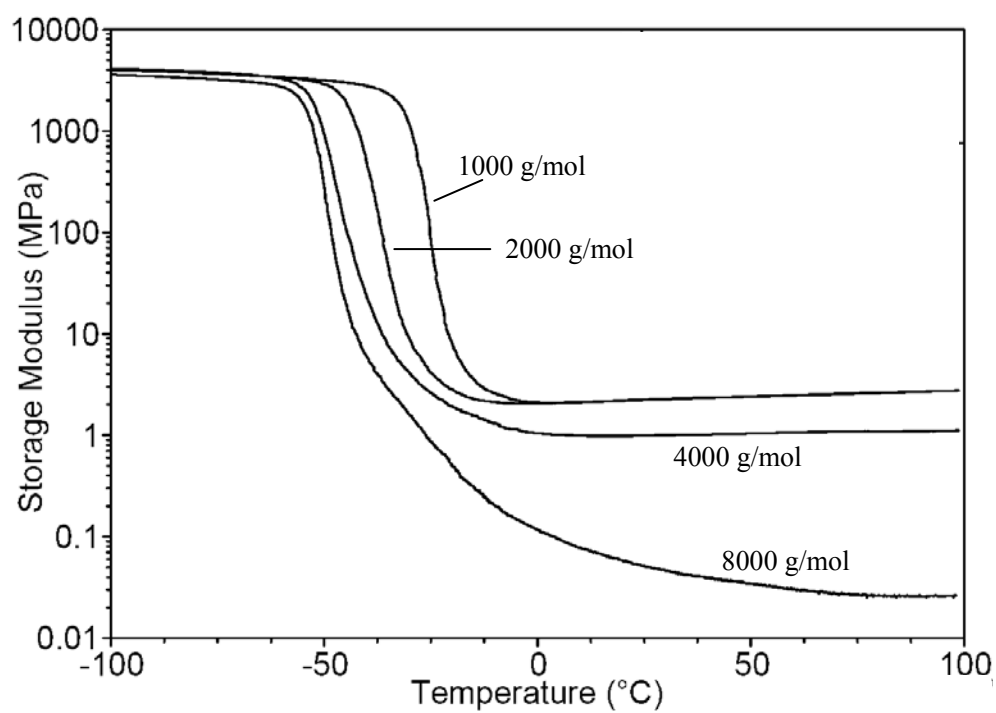


Figure 7.3. Storage modulus (E') plots for the PPG bisAcAc / PEG diacrylate networks with a 1.4:1.0 acrylate to acetoacetate ratio.

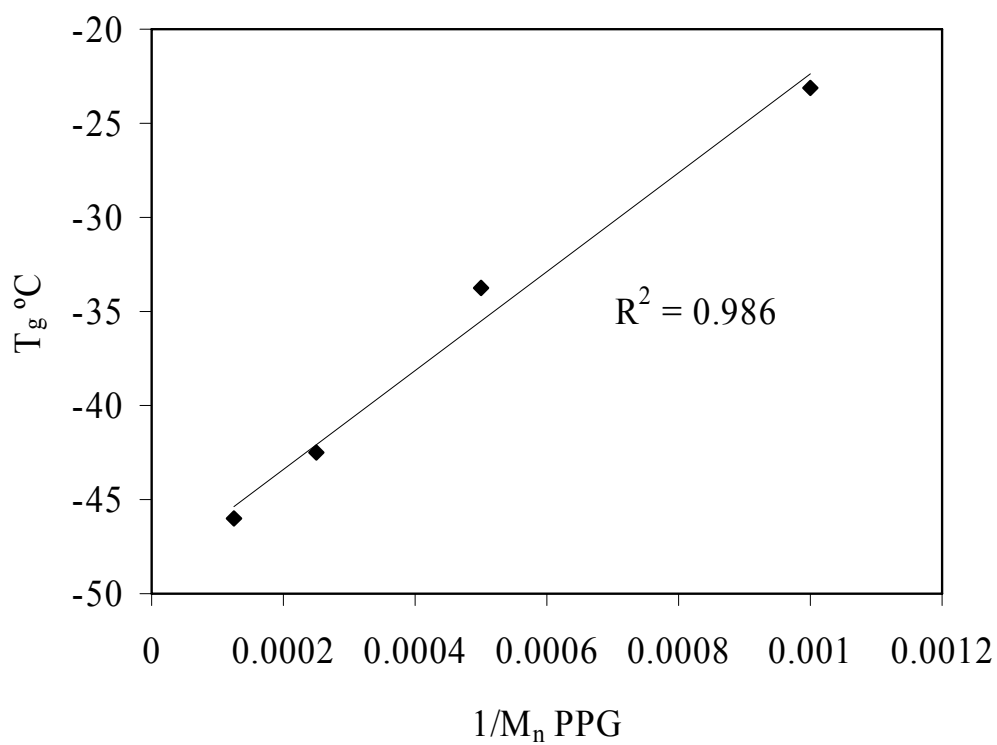


Figure 7.4. Glass transition temperatures of PPG bisAcAc / PEG diacrylate networks as a function of inverse PPG molecular weight as determined by SEC (1.4:1.0 acrylate to acetoacetate ratio).

Tensile measurements were performed on both the 1.4:1.0 and 2.0:1.0 acrylate to acetoacetate crosslinked networks in order to probe the effect of PPG bisAcAc molecular weight on the mechanical properties of the networks (Figure 7.5, Table 7.3). The 1000 g/mol, 2000 g/mol, and 4000 g/mol PPG bisAcAc networks exhibited low elongations (<100%), and elongation increased with molecular weight. Concurrently, stress at break and Young's moduli decreased with increasing PPG molecular weight, due to decreasing crosslink density. A marked change in properties was encountered for the 8000 g/mol PPG network. The elongation of the network increased dramatically (~900%), and the moduli and stress at break both dropped dramatically. This network was the only one consisting of PPG segments with molecular weights above the entanglement molecular weight ($M_e = 7700$ g/mol).⁶⁷⁷ The difference in mechanical performance compared to the lower molecular weight PPG bisAcAc precursors could result from a combination of macrophase separation as well as lower gel fraction for this network.

⁶⁷⁷ Aharoni, S. M. On entanglements of flexible and rodlike polymers. *Macromolecules* **1983**, 16, 1722-28.

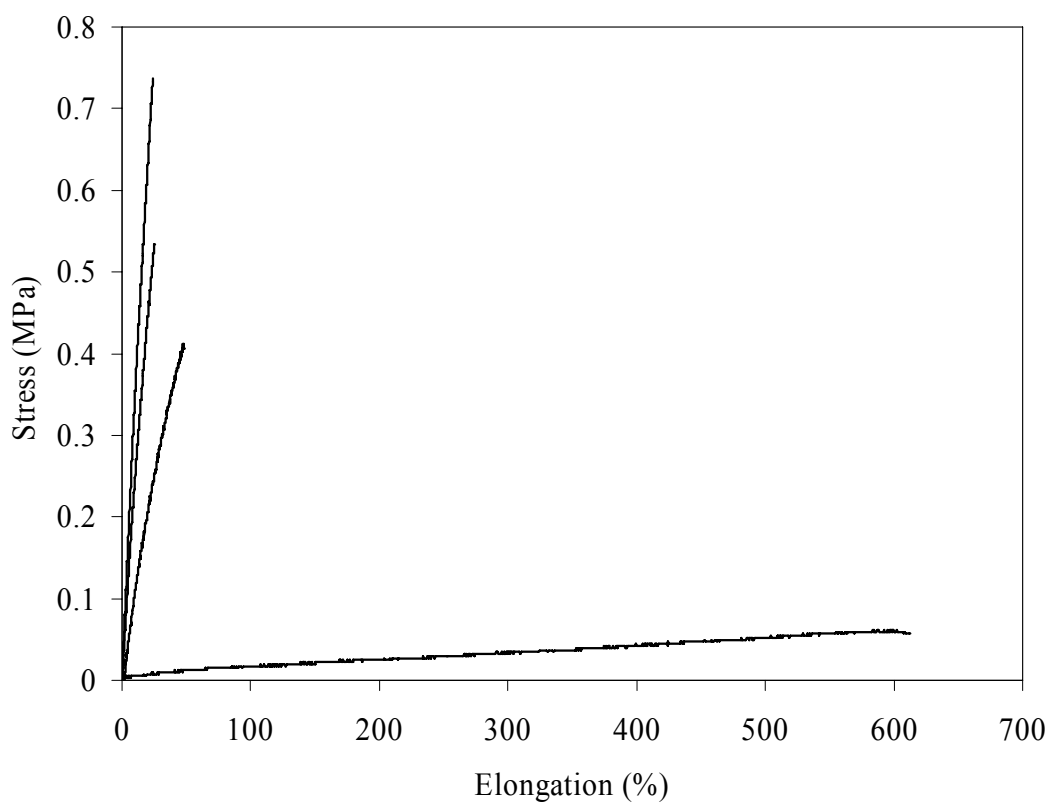


Figure 7.5. Stress-strain curves for PPG bisAcAc / PEG diacrylate networks containing 1.4:1.0 acrylate to acetoacetate ratios. Measurement was performed at 25 °C.

Table 7.3. Tensile properties of PPG-bisAcAc/ PEG diacrylate networks.

1.4:1.0 Acrylate to Acetoacetate Networks				
PPG M _n (g/mol)	Stress at Break (MPa)	Elongation (%)	Young's Modulus (MPa)	Toughness (MPa)
1000	0.70 ± 0.05	21 ± 2	3.96 ± 0.43	0.078 ± 0.013
2000	0.48 ± 0.07	23 ± 4	2.71 ± 0.14	0.061 ± 0.019
4000	0.39 ± 0.03	50 ± 2	1.26 ± 0.15	0.109 ± 0.008
8000	0.065 ± 0.02	570 ± 54	0.022 ± 0.004	0.229 ± 0.088
2.0:1.0 Acrylate to Acetoacetate Networks				
1000	0.48 ± 0.09	29 ± 6	2.11 ± 0.06	0.077 ± 0.029
2000	0.55 ± 0.07	51 ± 6	1.62 ± 0.07	0.158 ± 0.037
4000	0.44 ± 0.07	59 ± 10	1.20 ± 0.07	0.152 ± 0.049
8000	0.017 ± 0.006	920 ± 100	0.005 ± 0.002	0.109 ± 0.025

The molecular weight between crosslink points (M_c) is typically estimated from rubbery elasticity theory, which describes the relationship between elastic modulus and crosslink density.⁶⁷⁸ Assuming an affine network with tetrafunctional crosslink points and a Poisson's ratio of 0.5, Eq. 7.1 is defined as:

$$E = 3\rho RT/M_c \quad [7.1]$$

E = Young's modulus (Pa)

ρ = polymer density (g/cm^3)

R = gas constant (8.314 J/mol K)

T = temperature (K)

The resulting values of M_c calculated from the Young's moduli from tensile experiments are shown in Table 7.4. The M_c values approximately corresponded to the PPG bisAcAc precursor molecular weights for the lower molecular weight precursors (1000 and 2000 g/mol). The higher molecular weight sample (4000 g/mol) deviated significantly, and the 8000 g/mol network produced values which were unreasonably high, likely a consequence of the low gel fractions and macrophase separation for these networks. The M_c values for the networks prepared with the 2.0:1.0 acrylate to acetoacetate ratio were significantly higher than those obtained for the 1.4:1.0 ratio.

Swelling experiments were conducted on the networks in ethanol in order to further investigate the effect of molecular weight of the PPG chains on crosslink density (Table 7.4). As expected, the equilibrium solvent uptake increased with increasing PPG molecular weight. The swelling was greater for the 2.0:1.0 acrylate to acetoacetate networks, in agreement with

⁶⁷⁸ Calvet, D.; Wong, J.Y.; Giasson, S. Rheological Monitoring of Polyacrylamide Gelation: Importance of Cross-Link Density and Temperature. *Macromolecules* **2004**, *37*, 7762-71.

the lower tensile strengths. Based on the theory of rubbery elasticity, the equilibrium swelling of a network allows a calculation of the molecular weight between crosslink points, M_c .⁶⁷⁹

$$M_c = -V_s \rho_p (c^{1/3} - 0.5c) / (\ln(1-c) + c + \chi c^2) \quad [7.2]$$

V_s = molar volume of solvent (cc/g)

ρ_p = density of polymer (g/cc)

χ = Flory Huggins polymer-solvent interaction parameter⁶⁸⁰

c = relative concentration of polymer (dimensionless) = $(1 + \rho_p(W - W_o)) / \rho_s W_o$

ρ_s = density of solvent (g/cc)

W = equilibrium weight of swollen sample (g)

W_o = dry weight of sample (g)

In Eqn. 7.2 values of χ were utilized that reflected only poly(propylene glycol) which represented the majority of the networks.⁶⁸⁰ The values of M_c obtained from swelling data increased with PPG bisAcAc molecular weight but slightly differed from those obtained from tensile measurements. The M_c values obtained from both swelling and modulus measurements were consistent or greater than the precursor molecular weight, suggesting the absence of significant entanglements.

⁶⁷⁹ Pavlinec, J.; Moszner, N. Photocured polymer networks based on multifunctional β -ketoesters and acrylates. *J Polym Sci Part A: Polym Chem* **1997**, 10, 165-78.

⁶⁸⁰ Conway, B.E.; Nicholson, J.P. Some experimental studies on enthalpy and entropy effects in equilibrium swelling of poly(oxypropylene) elastomers. *Polymer* **1964**, 5, 387-402.

Table 7.4. Swelling properties of PPG bisAcAc / PEG diacrylate networks in ethanol and M_c values calculated from both swelling and tensile data.

PPG M_n (g/mol)	1.4 : 1.0 Acrylate to Acetoacetate			2.0:1.0 Acrylate to Acetoacetate		
	Equilibrium	M_c	M_c	Equilibrium	M_c	M_c
	Swelling (wt%)	Swelling (g/mol)	Tensile (g/mol)	Swelling (wt%)	Swelling (g/mol)	Tensile (g/mol)
1000	103 ± 1.5	1000	1900	136 ± 1.3	1500	3500
2000	180 ± 0.8	2800	2760	215 ± 1.6	3900	4600
4000	320 ± 1.3	8000	5900	293 ± 3.3	6800	6200
8000	1140 ± 38	77000	340000	1036 ± 273	76000	1.5E6

7.4.4 Sampling Experiments of the Crosslinking Reaction Involving SEC Analysis

Sampling experiments were pursued in order to study the progress of molecular weight and molecular weight distribution during crosslinking. Crosslinking reactions were performed using the 4000 g/mol PPG bisAcAc and PEG diacrylate. Samples were removed at regular intervals and subjected to SEC and ^1H NMR spectroscopic analysis which allowed measurement of both molecular weight and acrylate conversion. The broadening in the molecular weight distribution is clearly evident in the early stages of the reaction (Figure 7.6), and after only 3 min, multimodality is evident. The complexity of the SEC traces indicated that numerous species were present in the reaction mixture. The evolution of molecular weight (from both multi-angle laser light scattering (MALLS) and refractive index (RI) detectors) with diacrylate conversion is shown in Figure 7.7. The marked upturn in molecular weight near the gel point is typical of step growth crosslinking, where incremental conversion results in rapidly increasing molecular weight. The observed gel point occurred at 13 min, shortly after the last sample was removed. Flory developed a theory of gelation describing the critical conversion to reach the gel point (Eq. 4.3).^{681,682}

$$p_c = \frac{1}{[r + r\rho(f - 2)]^{1/2}} \quad [4.3]$$

p_c = conversion of multifunctional (AcAc) groups at the gel point

r = ratio of multifunctional (AcAc) to difunctional groups (acrylate) = 0.71

ρ = fraction of AcAc groups present on multifunctional unit = 1.0

f = functionality of the branch point = 4 (assumed)

For the acrylate to acetoacetate ratio of 1.4:1.0, the theoretical gel point occurs at 68 %

⁶⁸¹ Flory, P.J. Molecular Size Distribution in Three Dimensional Polymers. I. Gelation. *J Am Chem Soc* **1941**, 63, 3083-90.

⁶⁸² Chanda, M. "Advanced Polymer Chemistry", Marcel Dekker, New York, 2000.

acrylate conversion. Although the conversion at the gel point was not known, the acrylate conversion of the last sample (70%) is consistent with theoretical predictions.

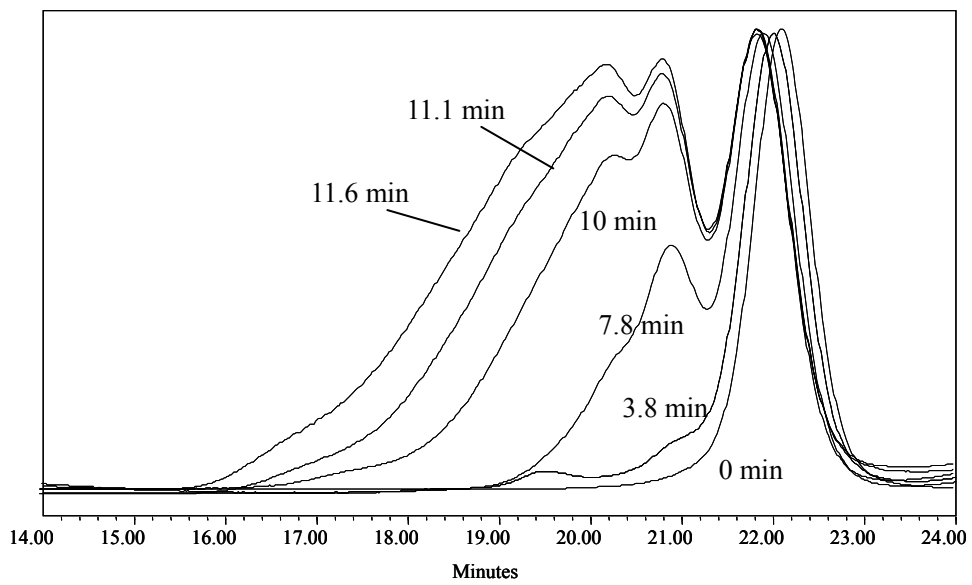


Figure 7.6. SEC traces from a PPG bisAcAc / PEG diacrylate crosslinking reaction.

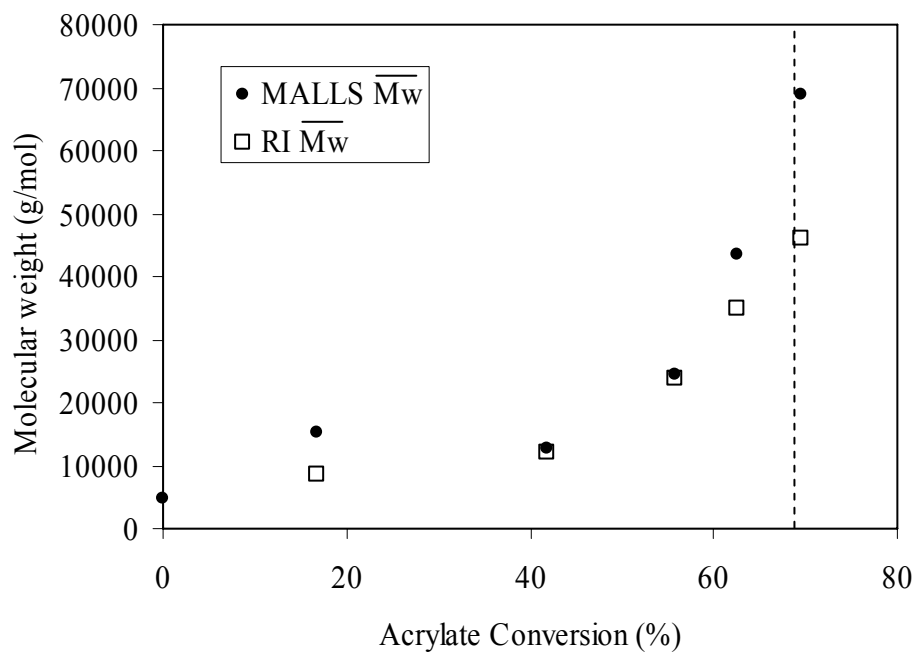


Figure 7.7. Weight-average molecular weight as determined by SEC MALLS and refractive index versus acrylate conversion determined by ^1H NMR spectroscopy. The experimental acrylate conversion slightly exceeds the theoretical value (vertical dashed line).

7.4.5 Kinetic Investigations of the carbon-Michael Addition Crosslinking Reaction

The kinetics of the base catalyzed Michael reaction are highly dependent on the base strength and concentration.⁶⁸³ Under the conditions of the present experiments, the consumption of acrylate groups follows pseudo first-order kinetics due to the fact that an equilibrium concentration of enolate ion is rapidly established, leading to the lack of dependence on acetoacetate concentration.⁶⁸⁴ The presence of a second labile acetoacetate proton leads to complexities in the kinetics at higher conversions. Kinetic investigations of the carbon-Michael addition reactions were pursued using ¹H NMR spectroscopy, which was effective in quantifying the conversion of acrylate groups. A simple first-order rate plot confirmed the first-order kinetics for the PPG bisAcAc / PEG diacrylate crosslinking reaction in DMSO-d₆ using DBU as a basic catalyst (Figure 7.8) at 25 °C.

Numerous basic catalysts are effective in the carbon-Michael addition reaction, including both homogeneous and heterogeneous organic and inorganic bases.⁶⁸³ An effective basic catalyst for the carbon-Michael addition possesses a pK_a of the conjugate acid near or above the pK_a of the abstractable protons of the acetoacetate group (pK_{a1} ~ 12, pK_{a2} ~ 13) (Table 7.5). Organic bases such as TMG and DBU, soluble inorganic bases such as tetramethylammonium hydroxide (TMAH) and sodium methoxide, and heterogeneous inorganic bases such as potassium *tert*-butoxide and potassium carbonate were investigated. TMAH provided the highest reaction rate and exhibited an observed *pseudo*-first-order rate

⁶⁸³ Mather, B.D.; Viswanathan, K.; Miller, K.M.; Long, T.E. Michael Addition Reactions in Macromolecular Design for Emerging Technologies. *Prog. Polym. Sci.* **2006**, *31*, 487-531.

⁶⁸⁴ Clemens, R. J.; Rector, F. D. A comparison of catalysts for crosslinking acetoacetylated resins via the Michael reaction. *J Coat Tech* **1989**, *61*, 83-91.

constant of $k_{\text{obs}} = 4.9 \times 10^{-3} \text{ s}^{-1}$. Interestingly, this strong hydroxide base did not lead to gel formation despite the high rate constant. This is likely due to nucleophilic attack and hydrolysis of the ester bonds contained in the precursors. Reducing the concentration of TMAH resulted in slower acrylate consumption but permitted gelation to occur after 13 min. The amidine bases DBU and TMG exhibited the next highest rate constants and also produced gels easily, likely due to their lack of nucleophilicity. The inorganic base sodium methoxide had a surprisingly low rate constant despite its complete solubility in reaction medium and relatively high basicity. The weak base potassium carbonate exhibited the lowest rate constant, but produced gel in 36 min. The activity of potassium carbonate was surprising due to its low pK_{a} , which is about 2 units below the pK_{a} of the acetoacetate protons. For the organic bases DBU and TMG, the acrylate conversion at the gel point was similar to the theoretical conversion. However, for the inorganic bases KOtBu and K_2CO_3 , higher conversion was needed to reach the gel point, presumably due to ester hydrolysis or preferential mono-adduct formation, which Clemens and Rector have reported earlier for alkoxide bases.⁶⁸⁵

⁶⁸⁵ Clemens, R. J.; Rector, F. D. A comparison of catalysts for crosslinking acetoacetylated resins via the Michael reaction. *J Coat Tech* **1989**, 61, 83-91.

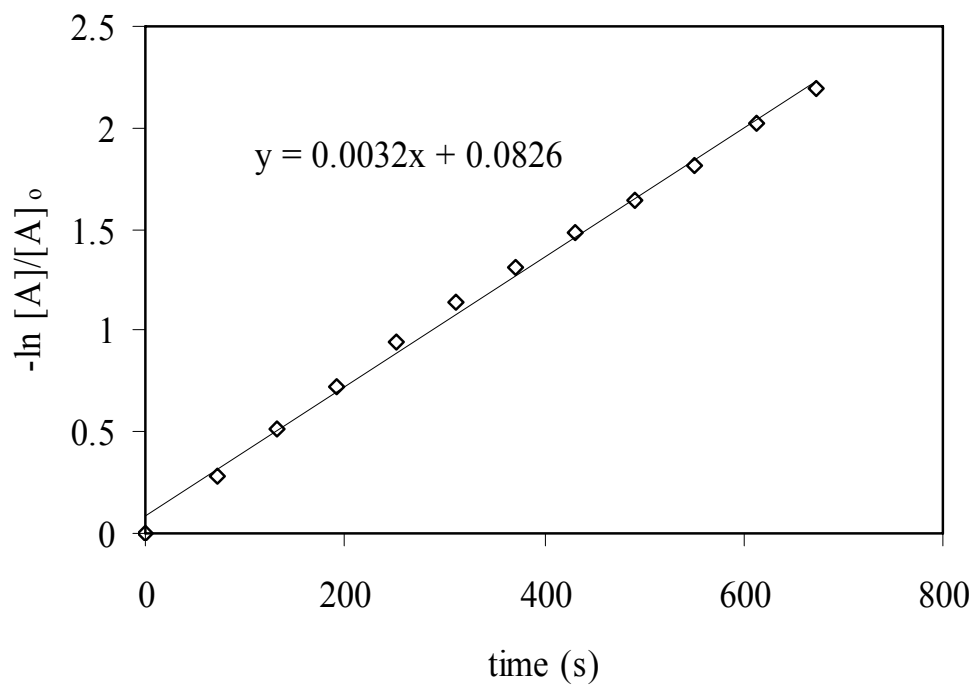


Figure 7.8. First-order rate analysis of acrylate concentration [A] from ^1H NMR spectroscopy for a PPG bisAcAc / PEG diacrylate crosslinking experiment in DMSO-d_6 using DBU as a basic catalyst.

Table 7.5. Kinetic data for the PPG bisAcAc / PEG diacrylate reaction using various basic catalysts. The pKa data is in aqueous solution.

Catalyst	Homogeneous	Gel time (min)	$k_{\text{obs}} (\text{s}^{-1}) \times 10^{-3}$	pK _a conj. acid*	P _{acryl} at gel point*
TMAH	Y	-	4.9	14	-
DBU	Y	5	4.7	12.5	78%
TMG	Y	6	3.2	13.6	73%
NaOMe	Y	-	1.2	15.5	-
K ₂ CO ₃	N	36	0.92	10.3	86%
KOtBu	N	12.5	2.8	19.2	92%

*Conversion of acrylate groups at the gel point

7.5 Conclusions

Networks based on PPG bisAcAc oligomers with a range of molecular weights were synthesized and characterized via mechanical testing, swelling, and gel fraction analysis. The gel fractions appeared to decrease with increasing oligomer molecular weight, and were markedly lower for the 8000 g/mol PPG bisAcAc precursor. This was attributed to incomplete reaction, macrophase separation, and lower functionality for this precursor. As expected, the glass transition temperature, tensile elongation and swelling ratio increased with the precursor oligomer molecular weight whereas the Young's modulus and tensile strengths decreased. Swelling and tensile measurements allowed calculation of the molecular weight between crosslink points (M_c). M_c values increased with precursor molecular weight but were greater than the precursor molecular weights, suggesting the absence of significant numbers of trapped entanglements in these networks. Sampling experiments involving SEC and ^1H NMR spectroscopy showed a rapid increase in molecular weight with time (or conversion) near the gel point and the measured conversion near the gel point was close to theoretical predictions. Kinetics experiments conducted using ^1H NMR spectroscopy demonstrated pseudo first-order kinetics and established reaction rates for a range of basic catalysts.

7.6 Acknowledgements

The authors would like to acknowledge the financial support of Rohm and Haas Company and the Department of Energy (DE-FG36-04GO14317).

Chapter 8. Synthesis of an Acid-Labile Diacrylate Crosslinker for Cleavable Michael Addition Networks

(Mather, B.D.; Williams, S.R.; Long, T.E. *Macromol. Chem. Phys.*, *submitted*)

8.1 Abstract

A novel acid-cleavable diacrylate crosslinker, dicumyl alcohol diacrylate (DCDA), was synthesized. DCDA was utilized as a difunctional Michael acceptor in the synthesis of acid-cleavable crosslinked networks via base-catalyzed Michael addition of telechelic poly(ethylene glycol) bis(acetoacetate). The hydrophilic networks that were chemically stable at ambient conditions had a rubbery plateau storage modulus of 1.2 MPa. Michael addition networks containing DCDA were degraded in the presence of catalytic quantities of acids such as trifluoroacetic acid (TFA), *p*-toluenesulfonic acid, and HCl to form completely soluble polymeric products. Michael addition networks composed of non-degradable diacrylate crosslinkers were chemically unchanged under identical reaction conditions and remained insoluble. Thermal degradation of DCDA containing networks was also investigated using thermogravimetric analysis (TGA), which confirmed the thermal reactivity and concentration of the acid-labile crosslink points.

8.2 Introduction

Acid-cleavable esters such as *tert*-butoxy carbonyl (t-BOC) esters and their derivatives have found widespread application in organic synthesis as protecting groups for nucleophilic

functional groups such as alcohols, phenols, amines, and thiols.⁶⁸⁶ These esters are quantitatively cleaved in the presence of catalytic quantities of acids such as trifluoroacetic acid (TFA)⁶⁸⁷ or *p*-toluene sulfonic acid.⁶⁸⁸ They are also readily cleaved with certain transition metals such as cerium ammonium nitrate,⁶⁸⁹ and may also be thermally deprotected.⁶⁹⁰ Acid-cleavable esters serve integral roles in peptide synthesis,^{687,691} and photoresists^{690, 692 - 694} in semiconductor technology. In the case of photoresists, a photo-acid generator (PAG) is blended with a *t*-BOC protected polymer. Exposure to ultraviolet light triggers acid production which cleaves the *t*-BOC group, resulting in a solubility change in the polymer.⁶⁹⁵ Due to the catalytic activity of the acid, the term

⁶⁸⁶ Greene, T. Protective groups in organic synthesis. 3rd ed.; Wiley: New York, 1999.

⁶⁸⁷ Pellois, J.P.; Wang, W.; Gao, X. Peptide Synthesis Based on *t*-Boc Chemistry and Solution Photogenerated Acids *J. Comb. Chem.* **2000**, 2, 355-60.

⁶⁸⁸ Reginato, G.; Mordini, A.; Caracciolo, M. Synthetic Elaboration of the Side Chain of (R)-2,2-Dimethyl-3-(*tert*-butoxycarbonyl)-4-ethynyloxazolidine: A New Regio- and Stereoselective Strategy to α -Functionalized α -Amino Alcohols. *J. Org. Chem.* **1997**, 62, 6187-92.

⁶⁸⁹ Hwu, J.-R.; Jain, M.; Tsay, S.-C.; Hakimelahi, G. Ceric ammonium nitrate in the deprotection of *tert*-butoxycarbonyl group. *Tetrahedron Letters* **1996**, 37, 2035-8.

⁶⁹⁰ Ahn, K.-D.; Koo, D.-I.; Willson, C. Synthesis and polymerization of *t*-BOC protected maleimide monomers: *N*-(*t*-butyloxycarbonyloxy)maleimide and *N*-[*p*-(*t*-butyloxycarbonyloxy)phenyl]-maleimide *Polymer* **1995**, 36, 2621-8.

⁶⁹¹ Merrifield, R.B. Solid Phase Peptide Synthesis. II. The Synthesis of Bradykinin. *J Am Chem Soc* **1964**, 86, 304-5.

⁶⁹² Yoo, J.-H.; Kim, S.-Y.; Cho, I.; Kim, J.-M.; Ahn, K.-D.; Lee, J.-H. A single component photoimaging system with styrene copolymers having *t*-BOC-protected quinizarin dye precursors and photoacid generating groups in a single polymer chain. *Polymer* **2004**, 45, 5391-5.

⁶⁹³ Fréchet, J.M.J.; Eichler, E.; Ito, H.; Willson, C.G. Poly(*p*-*t*-butoxycarbonyloxystyrene): A Convenient Precursor to *p*-Hydroxystyrene Resins. *Polymer* **1983**, 24, 995-1000.

⁶⁹⁴ Chang, S.Q.; Ayothi, R.; Bratton, D.; Yang, D.; Felix, N.; Cao, H.B.; Deng, H.; Ober, C.K. Sub-50 nm feature sizes using positive tone molecular glass resists for EUV lithography. *J Mater Chem* **2006**, 16, 1470-4.

⁶⁹⁵ Gabor, A. H.; Pruette, L. C.; Ober, C. K. Lithographic Properties of Poly(*tert*-butyl methacrylate)-Based Block and Random Copolymer Resists Designed for 193 nm Wavelength Exposure Tools. *Chem Mater* **1996**, 8, 2282-90.

chemically amplified resist,⁶⁹⁶ was adopted.

The Michael addition reaction, which involves the addition of nucleophiles to activated olefins, has generated recent interest in polymer synthesis.⁶⁹⁷ Michael addition chemistry is particularly suited for the synthesis of networks, due to the ability for room temperature curing and a wide range of functional crosslinkable oligomeric precursors. The Michael addition reaction enables applications in the synthesis of high-performance crosslinked resins,⁶⁹⁸ durable coatings⁶⁹⁹ and biodegradable hydrogels.⁷⁰⁰ The Michael addition is often employed in network synthesis and involves the reaction of acetoacetate functionalized precursors,⁷⁰¹ which are easily derived from hydroxyl containing precursors through a facile, uncatalyzed transesterification with *tert*-butylacetoacetate.⁷⁰²

In this manuscript, we report the synthesis of Michael addition networks containing a novel acid-cleavable diacrylate crosslinker, dicumyl alcohol diacrylate (DCDA). These networks benefit from facile room temperature curing and possess the unique property of being degradable in the presence of strong acids. The tertiary esters in DCDA cleave under

⁶⁹⁶ Fréchet, J. M. J.; Eichler, E.; Ito, H.; Willson, C. G. Poly(*p*-*t*-butoxycarbonyloxystyrene): A Convenient Precursor to *p*-Hydroxystyrene Resins. *Polymer* **1983**, 24, 995-1000.

⁶⁹⁷ Mather, B. D.; Viswanathan, K.; Miller, K. M.; Long, T.E. Michael Addition Reactions in Macromolecular Design for Emerging Technologies. *Prog. Polym. Sci.* **2006**, 31, 487-531.

⁶⁹⁸ Curliss, D. B.; Cowans, B. A.; Caruthers, J. M. Cure reaction pathways of bismaleimide polymers: a solid-state ¹⁵N NMR investigation. *Macromolecules* **1998**, 31, 6776-82.

⁶⁹⁹ Clemens, R. J.; Rector, F. D. A comparison of catalysts for crosslinking acetoacetylated resins via the Michael reaction. *J Coat Tech* **1989**, 61, 83-91.

⁷⁰⁰ Metters, A.; Hubbell, J. Network formation and degradation behavior of hydrogels formed by Michael-type addition reactions. *Biomacromolecules* **2005**, 6, 290-301.

⁷⁰¹ Clemens, R. J.; Hyatt, J. A. Acetoacetylation with 2,2,6-trimethyl-4H-1,3-dioxin-4-one: A convenient alternative to diketene. *J Org Chem* **1985**, 50, 2431-5.

⁷⁰² Witzeman, J. S.; Nottingham, W. D. Transacetoacetylation with *tert*-butyl acetoacetate: synthetic applications. *J Org Chem* **1991**, 56, 1713-8.

mild acidic conditions through a cationic mechanism to generate a diene by-product as well as polymer-bound carboxylic acid functionalities.

Previous work in our research laboratories has demonstrated the utility of acid-cleavable dimethacrylates in the synthesis of core-cleavable star polymers synthesized via anionic polymerization.⁷⁰³ Others have also reported the utility of acid-labile linkers in polymer science. For instance, Patrickios et al. have synthesized novel asymmetric aliphatic tertiary ester containing dimethacrylates and generated networks as well as star polymers via group transfer polymerization, which were hydrolyzable in the presence of TFA.⁷⁰⁴ Size exclusion chromatography (SEC) measurements over time were used to monitor the decomposition of core-cleavable star polymers into component arms. Ober et al. utilized aliphatic ditertiary ester-containing dimethacrylates and diacrylates to synthesize thermally degradable photocured networks.⁷⁰⁵ Decomposition of the networks via thermal treatment led to poly(acrylic acid) derivatives which were soluble in aqueous base.

Acid-cleavable networks may offer potential applications as drug delivery devices, and in particular, delivery of drugs to cancerous tumors, which relies on the lower pH within the surrounding tissue.⁷⁰⁶ Biodegradable Michael addition networks have been synthesized for

⁷⁰³ Kilian, L.; Wang, Z.-H.; Long, T. E. Synthesis and Cleavage of Core-Labile Poly(Alkyl Methacrylate) Star Polymers. *J Polym Sci: Part A: Polym Chem* **2003**, 41, 3083-93.

⁷⁰⁴ Kafouris, D.; Themistou, E.; Patrickios, C. Synthesis and Characterization of Star Polymers and Cross-Linked Star Polymer Model Networks with Cores Based on an Asymmetric, Hydrolyzable Dimethacrylate Cross-Linker. *Chem Mater* **2006**, 18, 85-93.

⁷⁰⁵ Ogino, K.; Chen, J.-S.; Ober, C. Synthesis and Characterization of Thermally Degradable Polymer Networks. *Chem Mater* **1998**, 10, 3833-8.

⁷⁰⁶ Murthy, N.; Thng, Y.; Schuck, S.; Xu, M.; Frechet, J. A Novel Strategy for Encapsulation and Release of Proteins: Hydrogels and Microgels with Acid-Labile Acetal Cross-Linkers. *J Am Chem Soc* **2002**, 124, 12398-9.

drug delivery applications,⁷⁰⁷ and acid-degradable networks have potential applications in tissue scaffolds. Hubbell et al. has synthesized biodegradable tissue scaffolds⁷⁰⁸ and tissue reinforcements⁷⁰⁹ using the Michael addition.

Applications of acid-cleavable networks in photolithography were studied by Reiser et al. with networks made from 2,5-dimethyl-2,5-hexanediol dimethacrylate.⁷¹⁰ It was found that partial cleavage of crosslink points resulted in local changes in tack, which allowed the adhesion of toner and circumvented solvent-based development. Fréchet and Willson also utilized acid-sensitive acetal linkages to develop novel acid-cleavable networks for photoresist technology.⁷¹¹ Fréchet applied this same acetal chemistry to create protein delivery devices which operate under acidic conditions such as those found in cancerous tissue.⁷¹² Rapid protein release at pH 5.0 was observed with these highly sensitive acetal linked networks.

⁷⁰⁷ Elbert, D.; Pratt, A.; Lutolf, M.; Halstenberg, S.; Hubbell, J. Protein delivery from materials formed by self-selective conjugate addition reactions. *J Control Release* **2001**, 76, 11–25.

⁷⁰⁸ Elbert, D.; Hubbell, J. Conjugate addition reactions combined with free-radical cross-linking for the design of materials for tissue engineering. *Biomacromolecules* **2001**, 2, 430-41.

⁷⁰⁹ Vernon, B.; Tirelli, N.; Bachi, T.; Haldimann, D.; Hubbell, J. A. *J Biomed Mater Res* **2003**, 64A, 447-56.

⁷¹⁰ Li, M. Y.; Liang, R. C.; Raymond, F.; Reiser, A. *J Imaging Sci* **1990**, 34, 259-64.

⁷¹¹ Yamada, S.; Medeiros, D.; Patterson, K.; Jen, W.-L.; Rager, T.; Lin, Q.; Lenci, C.; Byers, J.; Havard, J.; Pasini, D.; Frechet, J.; Willson, C. Positive and negative tone water processable photoresists: a progress report. *SPIE Proc: Advances in resist technology and processing* **1998**, 3333, 245-53.

⁷¹² Murthy, N.; Thng, Y.; Schuck, S.; Xu, M.; Frechet, J. A Novel Strategy for Encapsulation and Release of Proteins: Hydrogels and Microgels with Acid-Labile Acetal Cross-Linkers. *J Am Chem Soc* **2002**, 124, 12398-9.

8.3 Experimental

8.3.1 Materials

$\alpha,\alpha,\alpha',\alpha'$ -tetramethyl-1,4-benzenedimethanol (99%), *tert*-butylacetoacetate (98%), *p*-toluene sulfonic acid monohydrate (98%), trifluoroacetic acid (99%), 1,8-diazabicyclo[5.4.0]undec-7-ene (DBU, 98%) and 1,1,3,3-tetramethylguanidine (TMG, 99%) were purchased from Aldrich and used as received. Acryloyl chloride (96%) and triethylamine (99.5%) were purchased from Aldrich and distilled prior to use. Tetrahydrofuran was distilled from sodium and benzophenone under nitrogen prior to use. Poly(ethylene glycol) ($M_n = 600$ g/mol) was used as received. Poly(propylene glycol) bis(acetoacetate) ($M_n = 1000$ g/mol) was synthesized according to previously reported procedures.⁷¹³

8.3.2 Dicumyl alcohol diacrylate (DCDA)

$\alpha,\alpha,\alpha',\alpha'$ -tetramethyl-1,4-benzenedimethanol (6.25 g, 32.2 mmol) was dissolved in 100 mL dry tetrahydrofuran in a 500 mL round-bottomed flask containing a magnetic stirbar. Triethylamine (10.7 mL, 76.8 mmol, 2.38 equiv) were added via syringe. The flask was equipped with an addition funnel and 50 mL of dry THF were added to the funnel. Acryloyl chloride (5.70 mL, 74.9 mmol, 2.32 equiv) were syringed into the addition funnel. The reaction flask was cooled with an ice bath and the acid chloride was added dropwise to the reaction and the reaction was allowed to warm to room temperature. Stirring was continued

⁷¹³ Mather, B. D.; Miller, K. M.; Long, T. E. Novel Michael Addition Networks Containing Poly(propylene glycol) Telechelic Oligomers. *Macromol Chem Phys* **2006**, 207, 1324-33.

for 18 h. The triethylamine salt was filtered off and the reaction mixture was evaporated. The crude product was chromatographed on silica using chloroform eluent. The final product was obtained in 28% yield and was stored at -15 °C. ¹H NMR, CDCl₃ (δ, ppm): 7.33 (s, 4H), 6.34 (dd, 2H, *J*₁ = 17.4 Hz, *J*₂ = 1.6 Hz), 6.11 (dd, 2H, *J*₁ = 10.4, *J*₂ = 17.5 Hz), 5.77 (dd, 2H, *J*₁ = 10.3 Hz, *J*₂ = 1.6 Hz) 1.81 (s, 12H). ¹³C NMR (δ, ppm): 28.51, 81.74, 124.19, 129.77, 129.96, 144.17, 164.81 ppm. FAB MS: *m/z* = 302.151 [M]⁺, *m/z* = 302.15 (theoretical)

8.3.3 Poly(ethylene glycol) bis(acetoacetate)

Poly(ethylene glycol) (*M*_n = 600 g/mol) (3.0 g, 5.0 mmol) and *tert*-butyl acetoacetate (2.0 g, 12.6 mmol) were combined in a 50 mL round-bottomed flask containing a magnetic stirbar. The flask was heated under nitrogen at 150 °C for 2 h. A short-path condenser was adapted to the flask and vacuum from an aspirator was applied to remove *tert*-butanol byproduct. The condenser was removed and an additional aliquot of *tert*-butyl acetoacetate (2.0 g, 12.6 mmol) were added and the reaction was continued for another 1.5 h. Aspirator vacuum was applied a second time followed by high vacuum to remove excess reagents and byproducts. ¹H NMR was used to verify the presence of the acetoacetate end groups. ¹H NMR, CDCl₃ (δ, ppm): 5.01 (s, enol vinyl H), 4.28 (t, 4H, *J* = 4.4 Hz), 3.69 (t, 4H, *J* = 4.8 Hz), 3.62 (s, PEG CH₂), 3.46 (s, 4H), 2.25 (s, 6H).

8.3.4 Crosslinked Network Synthesis and Degradation

DCDA (152 mg, 0.50 mmol) was mixed with poly(ethylene glycol) bis(acetoacetate) (149 mg, 0.25 mmol) at room temperature for 2 min. DBU (3 uL, 0.020 mmol) and TMG (5

uL, 0.040 mmol) were added and mixed with the blend of crosslinkable precursors, resulting in an amber color due to the enolate anion formation. The blend gelled over a period of several hours. A sample of DCDA-poly(ethylene glycol) bis(acetoacetate) containing network (5 mg) was placed in dioxane (3.0 g) in a 20 mL sample vial containing a magnetic stirbar and *p*-toluenesulfonic acid (300 mg) was added. The sample degraded in 30 min into a homogeneous solution. The DCDA containing networks were also degraded in trifluoroacetic acid (TFA) solution. The DCDA containing Michael addition network (32 mg) was introduced to a solution of TFA in dichloromethane (20 vol%) and stirred at 25 °C. The network degraded in 50 s into a completely homogeneous solution. The network was also successfully degraded in concentrated HCl (35 wt%) into small, insoluble particles was achieved in 3 min at room temperature.

8.3.5 Characterization

¹H NMR was conducted using a Varian Inova 400 MHz spectrometer. Gel fraction analysis was conducted by immersing the samples in ethanol for 5 d, changing the ethanol every 24 h. Samples were dried after extraction in vacuum at 50 °C for 18 h and reweighed to obtain the gel content. Fast atom bombardment (FAB) mass spectrometry was conducted using a JEOL HX-110 dual focusing mass spectrometer in positive ion mode with xenon ion bombardment and a matrix of 3-nitrobenzyl alcohol with polyethylene glycol standards. Thermogravimetric analysis (TGA) was performed under a nitrogen atmosphere at a heating rate of 10 °C/min using a TA Instruments Hi-Res TGA 2950. Dynamic mechanical measurements were conducted on a TA Instruments Q-800 DMA under nitrogen at a heating

rate of 3 °C/min at 1 Hz frequency in film-tension mode. Tensile characterization was performed on an Instron model 5500R at 100%/min elongation using rectangular specimens and manual grips at ambient conditions.

8.4 Results and Discussion

8.4.1 Synthesis of Acid-Cleavable Networks

The acid-cleavable diacrylate crosslinker, DCDA, was synthesized in a single step from acryloyl chloride and $\alpha,\alpha,\alpha',\alpha'$ -tetramethyl-1,4-benzenedimethanol. The product oil was isolated through column chromatography and remained stable at -15 °C. Multinuclear NMR spectroscopy (Figure 8.1) and mass spectrometry were used to confirm the structure of the product. The diacrylate crosslinker maintained solubility in a range of solvents, potentially allowing miscibility and network formation with Michael addition donors of varying polarity. The Michael addition networks were synthesized through blending the DCDA crosslinker with a poly(ethylene glycol) bis(acetoacetate) ($M_n = 600$ g/mol) and adding base catalysts, such as DBU and TMG (Figure 8.2). This resulted in rapid gelation at 25 °C in air. The gel content of the network was determined through removal of sol through immersion in ethanol, which is a solvent known to dissolve the network precursors, for a period of 5 d, with daily replacement of the solvent. The gel content of the Michael addition networks were typically $89 \pm 2\%$.

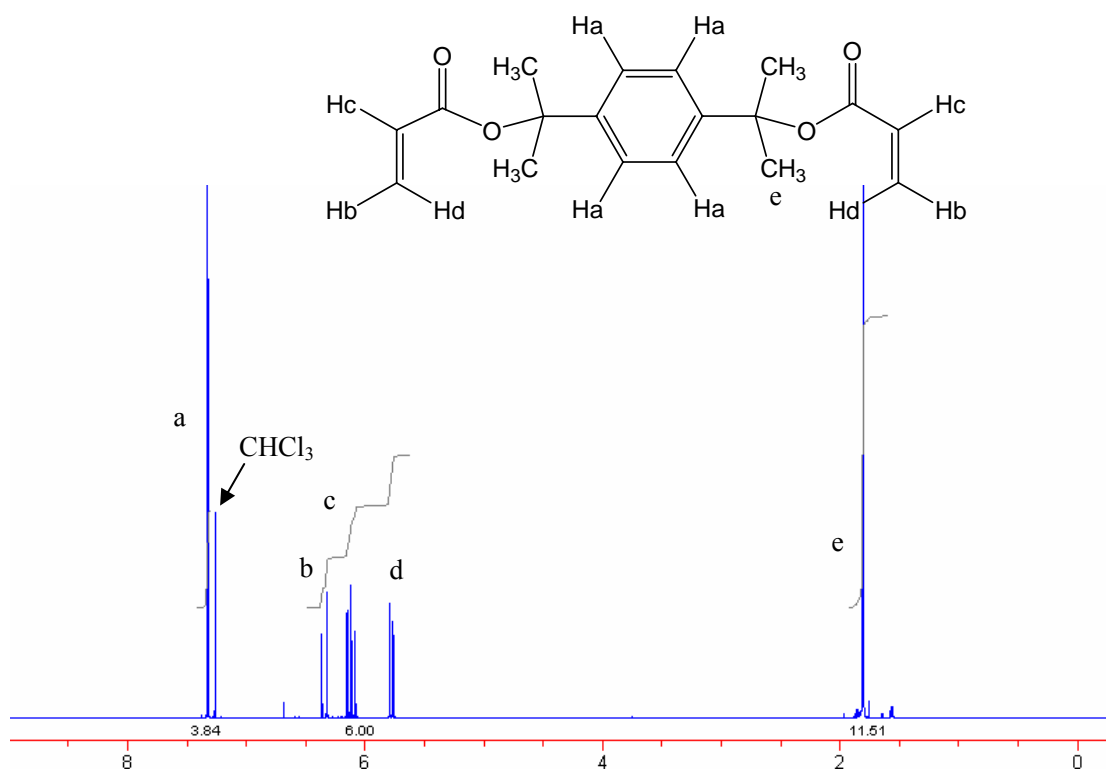


Figure 8.1. ^1H NMR spectrum of acid-cleavable diacrylate crosslinker, DCDA.

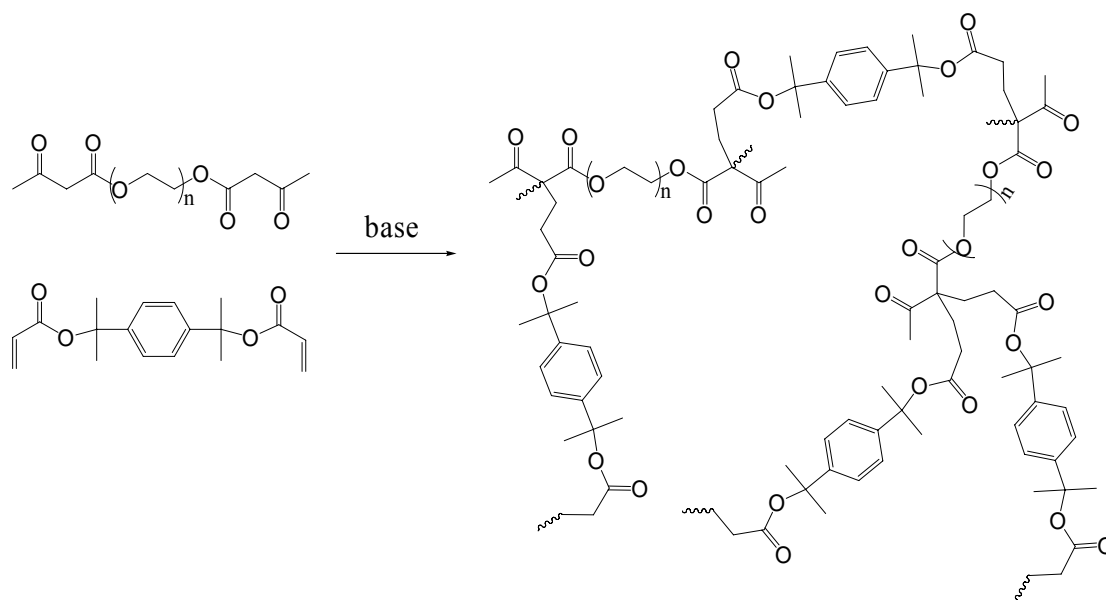


Figure 8.2. Synthesis of crosslinked networks via base catalyzed Michael addition.

8.4.2 Acid Catalyzed Degradation of Networks

The Michael addition networks containing DCDA were readily degraded using strong acid catalysts such as trifluoroacetic acid (TFA) in dichloromethane, concentrated HCl or *p*-toluenesulfonic acid (*p*-TSA) in dioxane (Figure 8.3) at 25 °C. The most effective acid was TFA, which converted the network into completely soluble components in 50 s in dichloromethane (20 vol%). The gel sample dissolved rapidly into soluble material and gel was not visible after 50 s. In the case of *p*-TSA (10 wt% in dioxane), the networks degraded into completely soluble components over a period of 30 min at 25 °C. In contrast, control networks did not degrade under these conditions. The presence of poly(ethylene glycol) linkages in the networks allowed limited swellability in water, permitting degradation in concentrated HCl (35 wt%), which completely converted the sample into a dispersion of insoluble particles within 3 min of stirring at room temperature. Photographs (Figure 8.4) revealed the complete disintegration of the acid-cleavable DCDA containing networks using *p*-TSA.

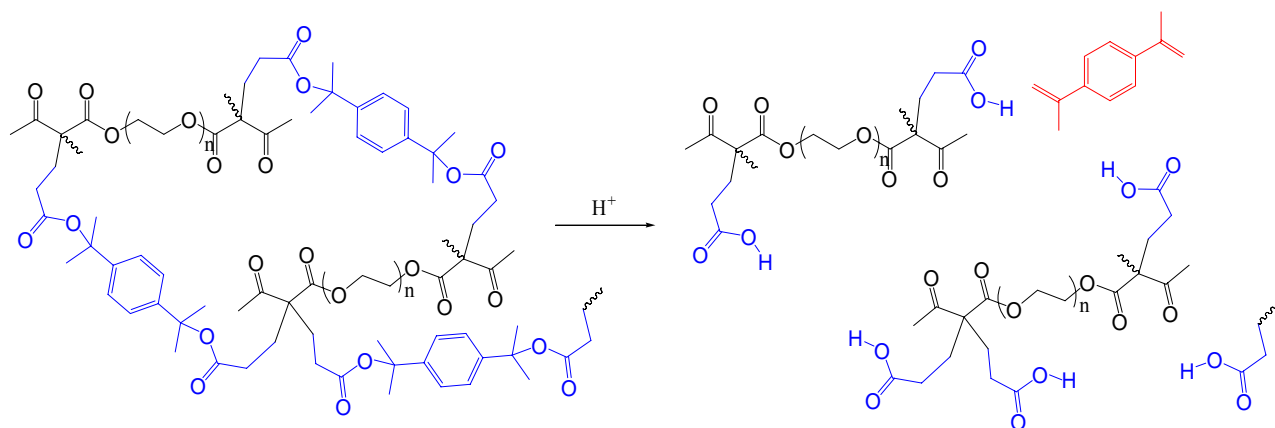


Figure 8.3. Degradation reactions of Michael addition networks containing DCDA using p-toluenesulfonic acid.

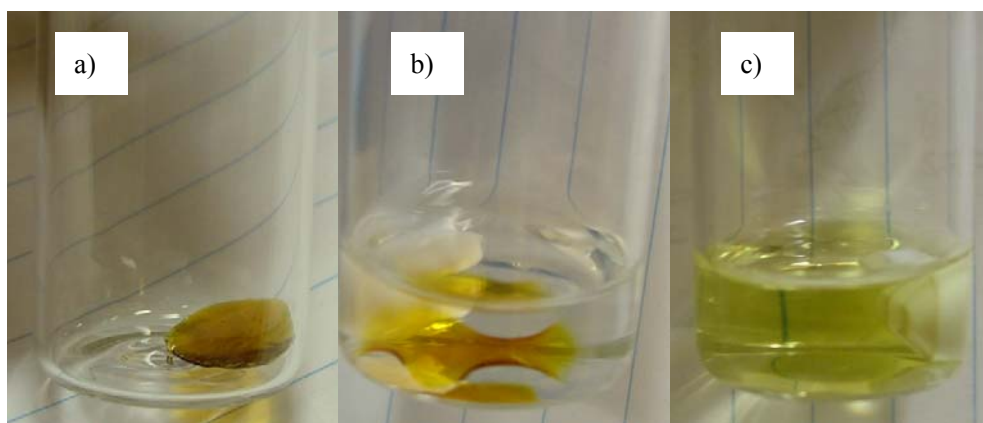


Figure 8.4. Pictures of the degradation of DCDA containing Michael addition networks using *p*-toluenesulfonic acid in dioxane. a) network sample as prepared, b) immersed in dioxane with *p*-toluenesulfonic acid, c) after degradation.

8.4.3 Thermal Degradation of Networks

The DCDA containing networks were also degraded thermally. Thermogravimetric analysis revealed a stepwise degradation process (Figure 8.5). An initial weight loss occurred at an onset temperature of 173 °C, which is consistent, but slightly higher than temperatures typically observed in the thermal deprotection of *t*-BOC protected compounds (210 °C).⁷¹⁴ The difference in degradation temperature may be attributed to the presence of residual base catalyst. The samples released nearly 28 wt% in that degradation step, which corresponded well to the weight loss from the volatile diene byproduct (theoretical weight loss = 26%).

⁷¹⁴ Ying, J.; Fréchet, J.; Willson, C. Poly(vinyl-*t*-butyl carbonate) synthesis and thermolysis to poly(vinyl alcohol). *Polym Bull* **1987**, 17, 1-6.

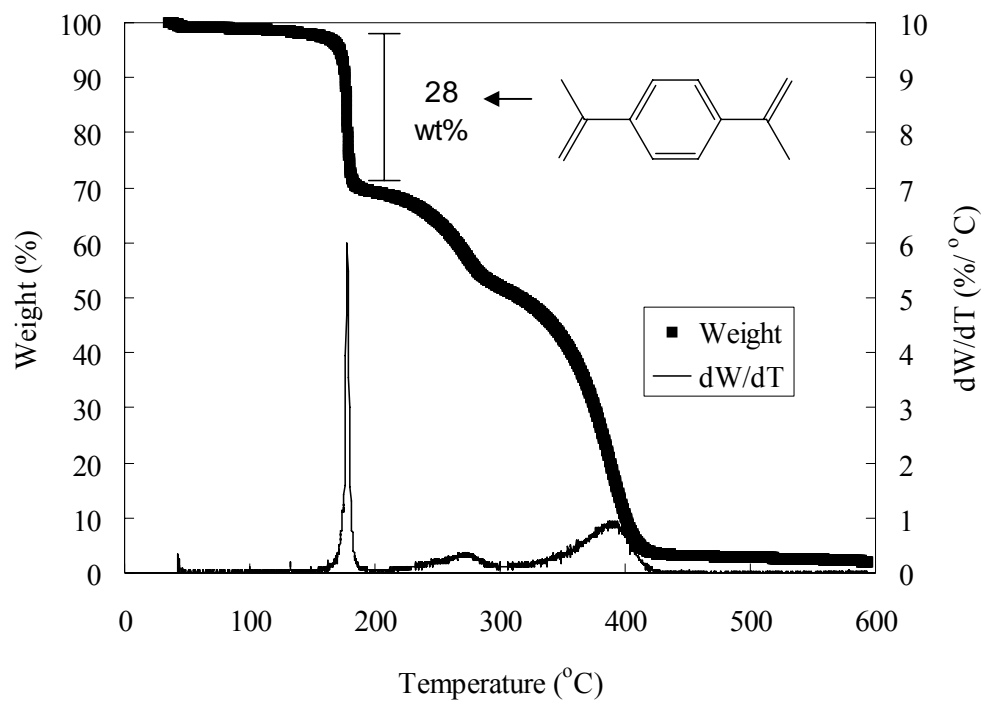


Figure 8.5. Thermogravimetric analysis (TGA) and derivative weight loss curve for DCDA containing network. The onset of weight loss at 173 °C corresponds to the theoretical mass of the diene byproduct of DCDA at complete conversion.

8.4.4 Mechanical Characterization of Networks

Dynamic mechanical analysis (DMA) of the acid-cleavable diacrylate containing networks (Figure 8.6) revealed a glass transition for the network at 17 °C (tan delta maximum), which was significantly higher than the T_g for PEG (-60 °C)⁷¹⁵ due to the restrictions on chain mobility imposed with the crosslink points. The T_g corresponded well with values obtained for PEG diacrylate free radically crosslinked networks ($T_g = 19$ °C for $M_n = 600$).⁷¹⁶ The rubbery plateau modulus for the network was 1.2 MPa, which corresponded to an elastomeric material. This modulus is in a typical range for networks composed of end-linked oligomers due to the relatively low crosslink density and mobility of the linear oligomeric chains in the network. The breadth of the tan delta peak was relatively narrow (full-width at half maximum, FWHM = 15 °C) and the peak was symmetric, indicating a relatively narrow distribution of segmental relaxation times. Cook et al. reported FWHM values as low as 21 °C for the tan delta curve of vinyl ester resins.⁷¹⁷ Generally, the breadth of the tan delta peak increases with crosslink density⁷¹⁷ and network cooperativity.⁷¹⁸

⁷¹⁵ Tormala, P. Determination of glass transition temperature of poly(ethylene glycol) by spin probe technique. *Eur Polym J* **1974**, 10, 519-21.

⁷¹⁶ Priola, A.; Gozzelino, G.; Ferrero, F.; Malucelli, G. Properties of polymeric films obtained from u.v. cured poly(ethylene glycol) diacrylates. *Polymer* **1993**, 34, 3653-7.

⁷¹⁷ Scott, T.; Cook, W.; Forsythe, J. Kinetics and network structure of thermally cured vinyl ester resins. *Eur Polym J* **2002**, 38, 705-16.

⁷¹⁸ Tyberg, C.; Bergeron, K.; Sankarapandian, M.; Shih, P.; Loos, A.; Dillard, D.; McGrath, J.; Riffle, J.; Sorathia, U. Structure–property relationships of void-free phenolic–epoxy matrix materials. *Polymer* **2000**, 41, 5053-62.

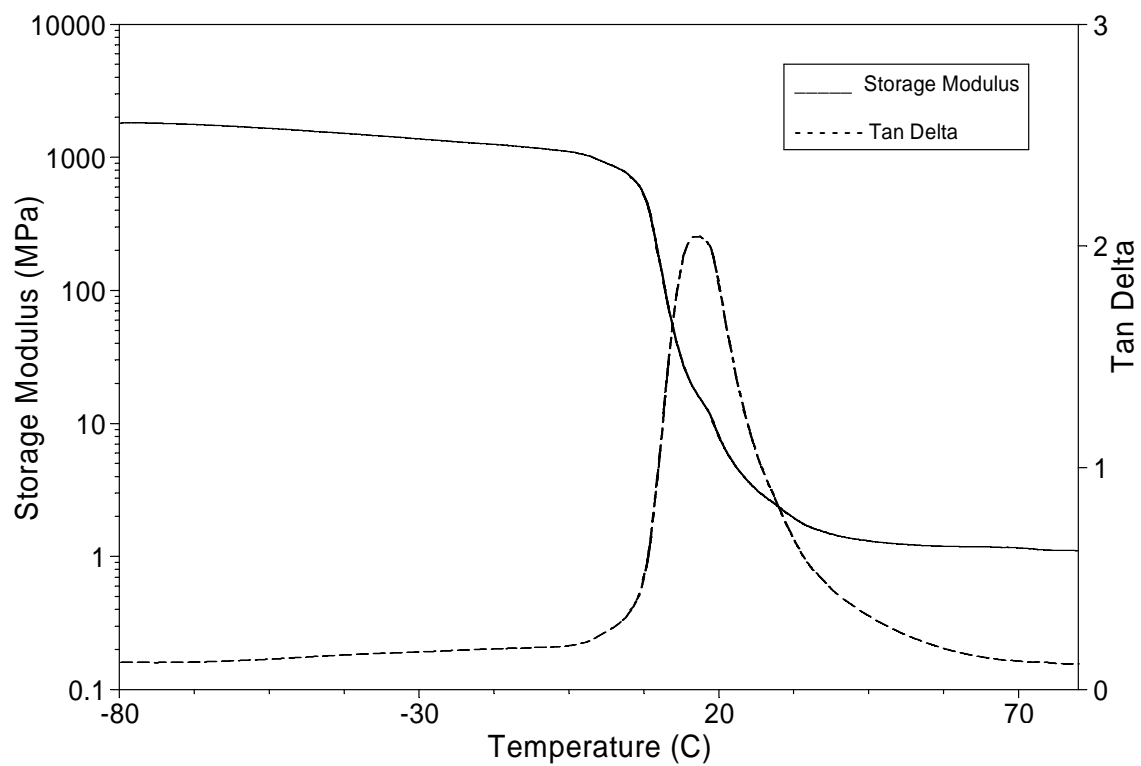


Figure 8.6. Dynamic mechanical analysis (DMA) of acid cleavable diacrylate network.

Tensile analysis (Figure 8.7) of the acid-cleavable diacrylate networks revealed a tensile strength of 0.39 ± 0.09 MPa and strain at break of $84 \pm 12\%$. The Young's modulus of the network was 0.75 ± 0.10 MPa. The networks did not exhibit a yield point in the tensile curves, likely due to the subambient glass transition temperature. These mechanical property values were consistent with previous measurements on Michael addition networks.⁷¹⁹ The corresponding molecular weight between crosslink points (M_c) obtained from the Young's modulus value was 9900 g/mol. This is significantly higher than the poly(ethylene glycol) bis(acetoacetate) molecular weight ($M_n = 600$ g/mol), and suggested less than difunctionality for the acetoacetate functional groups as well as the possible presence of dangling ends in the networks.

⁷¹⁹ Mather, B. D.; Miller, K. M.; Long, T. E. Novel Michael Addition Networks Containing Poly(propylene glycol) Telechelic Oligomers. *Macromol Chem Phys* **2006**, 207, 1324-33.

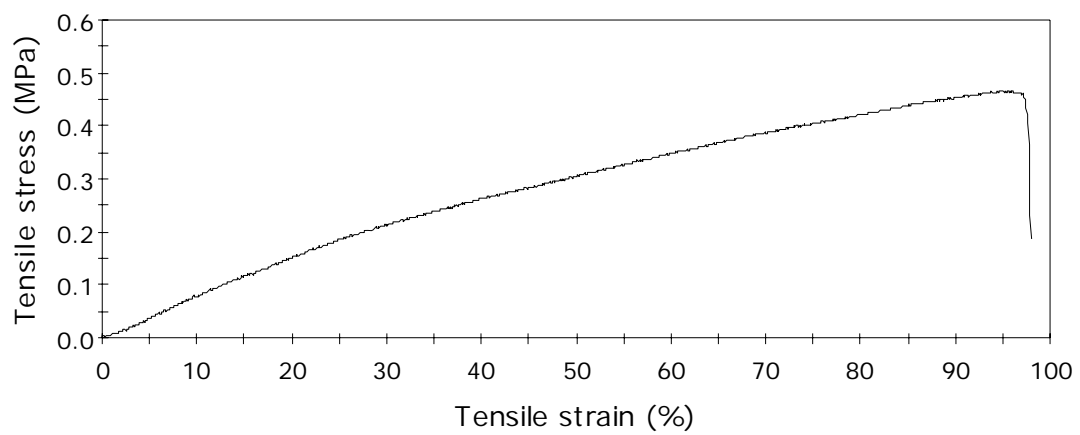


Figure 8.7. Tensile analysis of acid-cleavable Michael addition network.

8.5 Conclusion

This manuscript reports the first acid-cleavable network synthesized through Michael addition chemistry. A novel acid-labile diacrylate, DCDA, was synthesized in a single step from readily available starting materials. Networks containing DCDA were synthesized through facile base-catalyzed Michael addition of telechelic poly(ethylene glycol) bis(acetoacetate)s, which allowed curing at ambient temperature. The products had rubbery plateau modulus values of 1.2 MPa and glass transitions of 17 °C. Cleavage of the networks into soluble components was readily achieved in the presence of a variety of acids including trifluoroacetic acid in seconds. Thermal degradation was also achieved and thermogravimetric measurements revealed a sharp weight loss at 173 °C that corresponded closely to the expected weight loss for the diene byproduct.

8.6 Acknowledgement

The authors would like to acknowledge the financial support of Rohm and Haas Company and the Department of Energy (DE-FG36-04GO14317). This material is based upon work supported by the U.S. Army Research Laboratory and the U.S. Army Research Office under contract/grant number DAAD19-02-1-0275 Macromolecular Architecture for Performance Multidisciplinary University Research Initiative (MAP MURI).

Chapter 9. Synthesis and Morphological Characterization of Sulfonated Triblock Copolymers: Influence of High Sulfonate Levels and Poly(ethylene-*co*-propylene) Molecular Weight

(Mather, B.D.; Beyer, F.L.; Handlin, D.L. Long, T.E. *Polymer*, to be submitted)

9.1 Abstract

Sulfonated poly(styrene-*b*-ethylene-*co*-propylene-*b*-styrene) block copolymers containing short styrenic outer blocks (~1K) were synthesized via sequential anionic polymerization with subsequent hydrogenation and sulfonation. The central rubbery block molecular weight was systematically varied from 5K to 28K, which produced a range of triblock copolymers with varied degrees of entanglement ($M_c = 8100$). Dynamic mechanical analysis (DMA), small angle x-ray scattering (SAXS), atomic force microscopy (AFM), tensile testing, and rheological measurements were used to fully characterize the triblock polymers. The sulfonated block copolymers exhibited a rubbery plateau that lengthened upon neutralization of the sulfonic acid groups to the corresponding sodium salt. SAXS and tapping mode AFM both revealed microphase separated morphologies. Due to the low molar content of sulfonated polystyrene outer blocks, morphologies with a continuous rubber phase were expected, however, the absence of higher order peaks in the SAXS data prevented determination of the specific morphology. SAXS analysis revealed increased interdomain (Bragg) spacing with increasing poly(ethylene-*co*-propylene) molecular weight and decreased interdomain spacing upon neutralization. Tensile testing revealed increased tensile strengths

upon neutralization and generally higher elongations for higher molecular weight rubbery blocks due to higher levels of entanglement.

9.2 Introduction

Sulfonated block copolymer ionomers have re-emerged in recent years due to potential applications in fuel cells,⁷²⁰ proton and ion-conducting membranes,^{721 - 729} nanocomposites,^{730,731} and elastomers.⁷³² Ionomeric polymers include a number of commercial products

⁷²⁰ Kim, B.; Kim, J.; Jung, B. Morphology and transport properties of protons and methanol through partially sulfonated block copolymers. *J Membr Sci* **2005**, 250, 175-82.

⁷²¹ Liang, L.; Ying, S. Charge-mosaic membrane from gamma-irradiated poly(styrene-butadiene-4-vinylpyridine) triblock copolymer. *J Polym Sci B: Polym Phys* **1993**, 31, 1075 – 81.

⁷²² Mokrini, A.; Del Rio, C.; Acosta, J. L. Synthesis and characterization of new ion conductors based on butadiene styrene copolymers. *Solid State Ionics* **2004**, 166, 375-81.

⁷²³ Nacher, A.; Escribano, P.; Del Rio, C.; Rodriguez, A.; Acosta, J. L. Polymer Proton-Conduction Systems Based on Commercial Polymers. I. Synthesis and Characterization of Hydrogenated Styrene–Butadiene Block Copolymer and Isobutylene Isoprene Rubber Systems. *J Polym Sci Part A: Polym Chem* **2003**, 41, 2809-15.

⁷²⁴ Kim, B.; Kim, J.; Jung, B. Proton conductivities and methanol permeabilities of membranes made from partially sulfonated polystyrene-*block*-poly(ethylene-*ran*-butylene)-*block*-polystyrene copolymers. *J Membr Sci* **2002**, 207, 129-37.

⁷²⁵ Serpico, J. M.; Ehrenberg, S. G.; Fontanella, J. J.; Jiao, X.; Perahia, D.; McGrady, K. A.; Sanders, E. H.; Kellogg, G. E.; Wnek, G. E. Transport and Structural Studies of Sulfonated Styrene-Ethylene Copolymer Membranes. *Macromolecules* **2002**, 35, 5916-21.

⁷²⁶ Elabd, Y. A.; Walker, C. W.; Beyer, F. L. Triblock copolymer ionomer membranes Part II. Structure characterization and its effects on transport properties and direct methanol fuel cell performance. *J. Membr. Sci.* **2004**, 231, 181-8.

⁷²⁷ Won, J.; Park, H. H.; Kim, Y. J.; Choi, S. W.; Ha, H. Y.; Oh, I. H.; Kim, H. S.; Kang, Y. S.; Ihn, K. J. Fixation of Nanosized Proton Transport Channels in Membranes. *Macromolecules* **2003**, 36, 3228-34.

⁷²⁸ Kim, J.; Kim, B.; Jung, B.; Kang, Y. S.; Ha, H. Y.; Oh, I. H.; Ihn, K. J. Effect of Casting Solvent on Morphology and Physical Properties of Partially Sulfonated Polystyrene-*block*-poly(ethylene-*ran*-butylene)-*block*-polystyrene Copolymers. *Macromol Rapid Commun* **2002**, 23, 753-6.

⁷²⁹ Won, J.; Choi, S. W.; Kang, Y. S.; Ha, H. Y.; Oh, I. H.; Kim, H. S.; Kim, K. T.; Jo, W. H. Structural characterization and surface modification of sulfonated polystyrene-(ethylene-butylene)-styrene triblock proton exchange membranes. *J Membr Sci* **2003**, 214, 245-57.

⁷³⁰ Mauritz, K. A.; Storey, R. F.; Reuschle, D. A.; Tan, N. B. Poly(styrene-*b*-isobutylene-*b*-styrene) block copolymer ionomers (BCPI) and BCPI/silicate nanocomposites. 2. Na⁺BCPI sol-gel polymerization

such as Nafion™, which is an ion-conductive sulfonated fluoropolymer, and the tough, abrasion-resistant ethylene sodium methacrylate copolymer, Suryln™. Sulfonated block copolymers exhibit morphological differences from their non-ionic analogs due to the presence of ionic aggregates, which serve as additional physical crosslinks with microphase separation.^{733,734} According to the Eisenberg-Hird-Moore (EHM) model, ionomers contain multiplets, which consist of several ion pairs that overlap to form clusters and surrounding polymer chains of reduced mobility that give rise to a second, higher T_g .⁷³⁵ The ionic clusters dominate the properties of the polymer at low ion concentrations due to the corresponding large volume fraction of chains with reduced mobility (~50 vol% clusters at 4 mol% ion content).⁷³⁶ The strength of the association of ionic groups also increases the Flory-Huggins interaction parameter, χ , for microphase separation and enables lower block molecular weights for microphase separation since χN , where N is the degree of polymerization.⁷³⁷

Sulfonated block copolymers have generated interest as elastomers due the lengthening

templates. *Polymer* **2002**, 43, 5949-58.

⁷³¹ Mauritz, K. A.; Blackwell, R. I.; Beyer, F. L. Viscoelastic properties and morphology of sulfonated poly(styrene-*b*-ethylene/butylene-*b*-styrene) block copolymers (sBCP), and sBCP/[silicate] nanostructured materials. *Polymer* **2004**, 45, 3001-16.

⁷³² Chun, Y. S.; Weiss, R. A. The development of the ionic microphase in sulfonated poly(ethylene-*co*-propylene-*co*-ethylidene norbornene) ionomers during physical aging above T_g . *Polymer* **2002**, 43, 1915-23.

⁷³³ Eisenberg, A. Clustering of Ions in Organic Polymers. A Theoretical Approach. *Polymer* **1970**, 3, 147-154.

⁷³⁴ Mohajer, Y.; Tyagi, D.; Wilkes, G. L.; Storey, R. F.; Kennedy, J. P. New Polyisobutylene Based Model Ionomers. 3. Further Mechanical and Structural Studies. *Polymer Bulletin* **1982**, 8, 47-54.

⁷³⁵ Eisenberg, A.; Hird, B.; Moore, R. B. A New Multiplet-Cluster Model for the Morphology of Random Ionomers. *Macromolecules* **1990**, 23, 4098-107.

⁷³⁶ Eisenberg, A.; Kim, J. S., Introduction to Ionomers. John Wiley and Sons: New York, 1998.

⁷³⁷ Leibler, L. Theory of Microphase Separation in Block Copolymers. *Macromolecules* **1980**, 13, 1602-17.

of the rubbery plateau to higher temperatures compared to non-sulfonated analogs.^{738,739}

The higher temperature “service window” is a consequence of strong ionic interactions between sulfonated styrene residues, which reinforce the hard domains. Several workers have observed significantly improved high temperature (100 °C) tensile strengths for sulfonated block copolymers compared to non-sulfonated analogs.⁷⁴⁰⁻⁷⁴² In fact, the persistence of ionic interactions to 300 °C was established using variable temperature SAXS.⁷⁴³ Despite enhanced mechanical properties at high temperature, ionomers are often melt processible,⁷⁴⁴⁻⁷⁴⁶ particularly in the presence of ionic plasticizers such as zinc stearate.^{747,748} Above the

⁷³⁸ Bagrodia, S.; Wilkes, G. L.; Kennedy, J. P. New Polyisobutylene-Based Model Elastomeric Ionomers. VIII. Thermal-Mechanical Analysis. *J Appl Polym Sci* **1985**, 30, 2179-93.

⁷³⁹ Mani, S.; Weiss, R. A.; Williams, C. E.; Hahn, S. F. Microstructure of Ionomers Based on Sulfonated Block Copolymers of Polystyrene and Poly(ethylene-*alt*-propylene). *Macromolecules* **1999**, 32, 3663-70.

⁷⁴⁰ Balas, J. G.; Gergen, W. P.; Willis, C. L.; Pottick, L. A.; Gelles, R.; Weiss, R. A. Sulfonated block copolymers. US Patent 5239010, 1993.

⁷⁴¹ Pottick, L. A.; Willis, C. L.; Gelles, R. Selectively sulfonated block copolymers/extender oils. US Patent 5516831, 1996.

⁷⁴² Weiss, R. A.; Sen, A.; Pottick, L. A.; Willis, C. L. Block copolymer ionomers: 2. Viscoelastic and mechanical properties of sulphonated poly(styrene-ethylene/butylene-styrene) *Polymer* **1991**, 32, 2785-92.

⁷⁴³ Lu, X.; Steckle, W. P.; Hsiao, B.; Weiss, R. A. Thermally Induced Microstructure Transitions in a Block Copolymer Ionomer. *Macromolecules* **1995**, 28, 2831-9.

⁷⁴⁴ Mohajer, Y.; Tyagi, D.; Wilkes, G. L.; Storey, R. F.; Kennedy, J. P. New Polyisobutylene Based Model Ionomers. 3. Further Mechanical and Structural Studies. *Polymer Bulletin* **1982**, 8, 47-54.

⁷⁴⁵ Bagrodia, S.; Pisipati, R.; Wilkes, G. L.; Storey, R. F.; Kennedy, J. P. Melt Rheology of Ion-Containing Polymers. I. Effect of Molecular Weight and Excess Neutralizing Agent in Model Elastomeric Sulfonated Polyisobutylene-Based Ionomers. *J Appl Polym Sci* **1984**, 29, 3065-73.

⁷⁴⁶ Earnest, T. R.; MacKnight, W. J. Effect of Hydrogen Bonding and Ionic Aggregation on the Melt Rheology of an Ethylene-Methacrylic Acid Copolymer and its Sodium Salt. *J Polym Sci: Polym Phys Edn* **1978**, 16, 143-57.

⁷⁴⁷ Antony, P.; Bhattacharya, A. K.; De, S. K. Ionomeric polyblends of zinc salts of maleated EPDM rubber and poly(ethylene-*co*-acrylic acid). II. Effect of zinc stearate on processability *J Appl Polym Sci* **1999**, 71, 1257-65.

⁷⁴⁸ Duvdevani, I.; Lundberg, R. D.; Wood-Cordova, C.; Wilkes, G. L., Modification of Ionic Associations by Crystalline Polar Additives. In *ACS Symposium Series: Coulombic Interactions in Macromolecular Systems*, Eisenberg, A.; Bailey, F. E., Eds. American Chemical Society: Washington DC, 1986; Vol. 302, pp 185-99.

ionic T_g , ion hopping phenomena, which possess activation energies near 200 kJ/mol, are proposed to permit polymeric mobility and softening.⁷⁴⁹ Decreases in compression set⁷⁴⁰ while maintaining ambient tensile properties⁷⁴² were also observed earlier for sulfonated block copolymers. Furthermore, the sulfonation process leads to improved chemical resistance due to the lack of solubility of ionic domains in nonpolar solvents.

Sulfonated poly(styrene-*b*-ethylene/propylene-*b*-styrene) (SEPS) triblock copolymers with short styrenic end blocks (~1000 g/mol) and variable length poly(ethylene/propylene) (hydrogenated polyisoprene) rubber sequences containing 1,4-, 1,2- and 3,4-enchainment are presented herein. The short styrene outer blocks enabled the placement of a controlled number of metal sulfonate groups on the outer blocks, which contrasts from telechelic ionomers, which possess only a single ionic group at the terminus. An objective of this work is to elucidate the importance of the length of the rubbery block on morphology and mechanical properties relative to the critical molecular weight for entanglement. This work uniquely addresses a range of molecular weights, which were chosen to investigate the effects of entanglement in the rubbery block as well as the high sulfonation levels in the relatively short (1K) external blocks. Sulfonated block copolymers with relatively large styrenic blocks (~10-20K) and low levels of sulfonation (<20%) were studied earlier,⁷⁵⁰⁻⁷⁵³ and in

⁷⁴⁹ Hird, B.; Eisenberg, A. Sizes and stabilities of multiplets and clusters in carboxylated and sulfonated styrene ionomers. *Macromolecules* **1992**, *25*, 6466-74.

⁷⁵⁰ Chun, Y. S.; Weiss, R. A. The development of the ionic microphase in sulfonated poly(ethylene-*co*-propylene-*co*-ethylidene norbornene) ionomers during physical aging above T_g . *Polymer* **2002**, *43*, 1915-23.

⁷⁵¹ Mani, S.; Weiss, R. A.; Williams, C. E.; Hahn, S. F. Microstructure of Ionomers Based on Sulfonated Block Copolymers of Polystyrene and Poly(ethylene-*alt*-propylene). *Macromolecules* **1999**, *32*, 3663-70.

⁷⁵² Lu, X.; Steckle, W. P.; Weiss, R. A. Ionic Aggregation in a Block Copolymer Ionomer. *Macromolecules* **1993**, *26*, 5876-84.

⁷⁵³ Storey, R. F.; Baugh, D. W. Poly(styrene-*b*-isobutylene-*b*-styrene) block copolymers produced by

contrast, this manuscript deals with short styrenic blocks (1K) and higher levels of sulfonation (~50%).

Storey et al. studied similar short outer block sulfonated poly(styrene-*b*-ethylene-*co*-butylene-*b*-styrene) block copolymers, although these possessed shorter (~500 g/mol) outer blocks and a three-arm star-shaped structure.⁷⁵⁴ Wilkes and Storey also investigated linear telechelic ionomers, which contained a single ionic functionality at each polyisobutylene chain end.^{755 - 759} In many instances, three-arm telechelic ionomers are desirable due to the fact that trifunctionality leads to non-covalent network formation whereas difunctionality for dimeric associations leads to chain extension.⁷⁵⁶ In contrast, the multiple sulfonated styrene residues per chain end in our current work enable network formation with a linear architecture.

Small-angle X-ray scattering (SAXS) is critical for morphological investigations of traditional ionomers, microphase separated block copolymers, and block copolymer

living cationic polymerization. Part III. Dynamic mechanical and tensile properties of block copolymers and ionomers therefrom. *Polymer* **2001**, 42, 2321-30.

⁷⁵⁴ Storey, R. F.; George, S. E.; Nelson, M. E. Star-Branched Block Copolymer Ionomers. Synthesis, Characterization, and Properties. *Macromolecules* **1991**, 24, 2920-30.

⁷⁵⁵ Mohajer, Y.; Tyagi, D.; Wilkes, G. L.; Storey, R. F.; Kennedy, J. P. New Polyisobutylene Based Model Ionomers. 3. Further Mechanical and Structural Studies. *Polymer Bulletin* **1982**, 8, 47-54.

⁷⁵⁶ Bagrodia, S.; Wilkes, G. L.; Kennedy, J. P. New Polyisobutylene-Based Model Elastomeric Ionomers. VIII. Thermal-Mechanical Analysis. *J Appl Polym Sci* **1985**, 30, 2179-93.

⁷⁵⁷ Bagrodia, S.; Pisipati, R.; Wilkes, G. L.; Storey, R. F.; Kennedy, J. P. Melt Rheology of Ion-Containing Polymers. I. Effect of Molecular Weight and Excess Neutralizing Agent in Model Elastomeric Sulfonated Polyisobutylene-Based Ionomers. *J Appl Polym Sci* **1984**, 29, 3065-73.

⁷⁵⁸ Bagrodia, S.; Mohajer, Y.; Wilkes, G. L.; Storey, R. F.; Kennedy, J. P. New Polyisobutylene-Based Ionomers. 5. The Effect of Molecular Weight on the Mechanical Properties of Tri-Arm Star Polyisobutylene-Based Model Ionomers. *Polymer Bulletin* **1983**, 9, 174-80.

⁷⁵⁹ Mohajer, Y.; Bagrodia, S.; Wilkes, G. L.; Storey, R. F.; Kennedy, J. P. New Polyisobutylene Based Model Elastomeric Ionomers. VI. The Effect of Excess Neutralizing Agents on Solid-State Mechanical Properties. *J Appl Polym Sci* **1984**, 29, 1943-50.

ionomers.^{760 - 763} SAXS reveals the morphologies of block copolymers due to Bragg diffraction maxima that identify characteristic microphase separated morphologies in well-ordered samples. SAXS of ion-containing polymers typically displays an “ionomer peak” at a characteristic length scale of 2-6 nm, which is generally assigned to microphase separated ionic clusters.^{761,764 - 766} SAXS is particularly suited to the study of ionomers due to the greater electron density contrast afforded from ion-containing materials.

9.3 Experimental

9.3.1 Materials

Styrene (99%) and isoprene (99%) monomers were purchased from Aldrich and purified by vacuum distillation from calcium hydride and subsequent distillation from dibutylmagnesium. The monomers were stored under nitrogen at -15 °C until use. *Sec*-butyllithium (12% in hexanes/heptane) was purchased from FMC Lithium Co.

⁷⁶⁰ Serpico, J. M.; Ehrenberg, S. G.; Fontanella, J. J.; Jiao, X.; Perahia, D.; McGrady, K. A.; Sanders, E. H.; Kellogg, G. E.; Wnek, G. E. Transport and Structural Studies of Sulfonated Styrene-Ethylene Copolymer Membranes. *Macromolecules* **2002**, 35, 5916-5921.

⁷⁶¹ Mani, S.; Weiss, R. A.; Williams, C. E.; Hahn, S. F. Microstructure of Ionomers Based on Sulfonated Block Copolymers of Polystyrene and Poly(ethylene-*alt*-propylene). *Macromolecules* **1999**, 32, 3663-70.

⁷⁶² Tsujita, Y.; Hayashi, N.; Yamamoto, Y.; Yoshimizu, H.; Kinoshita, T.; Matsumoto, S. SAXS study on ionic aggregates of styrene-isoprene-sulfonated isoprene terpolymer ionomer *J Polym Sci Part B: Polym Phys* **2000**, 38, 1307-11.

⁷⁶³ Storey, R. F.; Baugh, D. W. Poly(styrene-*b*-isobutylene-*b*-styrene) block copolymers and ionomers therefrom: morphology as determined by small-angle X-ray scattering and transmission electron microscopy. *Polymer* **2000**, 41, 3205-11.

⁷⁶⁴ Lu, X.; Steckle, W. P.; Weiss, R. A. Ionic Aggregation in a Block Copolymer Ionomer. *Macromolecules* **1993**, 26, 5876-84.

⁷⁶⁵ Benetatos, N. M.; Heiney, P. A.; Winey, K. I. Reconciling STEM and X-ray Scattering Data from a Poly(styrene-*ran*-methacrylic acid) Ionomer: Ionic Aggregate Size. *Macromolecules* **2006**, 39, 5174-6.

⁷⁶⁶ Register, R.A.; Cooper, S.L. Anomalous small-angle x-ray scattering from nickel-neutralized ionomers. 1. Amorphous polymer matrixes. *Macromolecules*, **1990**, 23, 310-17.

Dibutylmagnesium (1.0 M in heptane) and triethylaluminum (1.0 M in hexanes), anhydrous 1,2-dichloroethane (99.8%) and citric acid (99.5%) were purchased from Aldrich and used as received. Nickel (II) 2-ethylhexanoate (8% in mineral spirits) was purchased from Shepherd Chemicals and used as received. Cyclohexane was purified using molecular sieves and alumina-containing columns under nitrogen.

9.3.2 Synthesis of Poly(styrene-*b*-isoprene-*b*-styrene) Triblock Copolymers

Polymerizations were conducted in a 600-mL glass reactor fitted with magnetic stirring, steam/cold water heating/cooling coils, a thermocouple and temperature controller as well as ports for introducing nitrogen, cyclohexane, monomers and initiators and for draining and venting.⁷⁶⁷ The reactor was filled with 400 mL dry cyclohexane under nitrogen and maintained at 40 °C. Styrene, 2.06 mL, (18.1 mmol) was injected into the reactor, and 1.60 mL *sec*-butyllithium (2.0 mmol, 1.25 M in hexanes) was subsequently added to rapidly form an orange color. The polymerization was allowed to proceed for 5 h and samples were periodically removed to ensure complete monomer conversion. Isoprene (55 mL, 550 mmol) was injected and the color immediately changed to light yellow. The polymerization was continued for 18.5 h and multiple samples were removed to ensure complete conversion of isoprene monomer. The final styrene aliquot (2.10 mL, 18.1 mmol) was injected and again polymerized for 5 h at 40 °C. Long polymerization times were used to ensure complete monomer consumption. The polymerization was then terminated with degassed methanol,

⁷⁶⁷ Hoover, J. M.; Ward, T. C.; McGrath, J. E. The influence of hydrogenation on star block copolymers based on tertiary-butylstyrene-isoprene-divinylbenzene. *Polym Prepr, Am Chem Soc, Div Polym Chem* **1985**, 26, 253-4.

precipitated into methanol, dried in vacuo at 50 °C, and stored in a freezer at -15 °C in the absence of inhibitor. SEC analysis of the samples and final product revealed block molecular weights of 1.2K-17.1K-0.5K (1.0K-19.9K-1.0K by ¹H NMR) and a molecular weight distribution (M_w/M_n) of 1.01.

9.3.3 Hydrogenation of Poly(styrene-*b*-isoprene-*b*-styrene) Triblock Copolymers

Hydrogenations were conducted in a similar reactor that was used for polymerizations. Nickel octoate/triethylaluminum hydrogenation catalyst was first prepared by adding a triethylaluminum solution in hexanes (4.8 mL, 1.0 M, 4.8 mmol) to a nickel 2-ethylhexanoate solution (5.7 mL, 1.34 mmol) in 20 mL dry cyclohexane dropwise with stirring under nitrogen. The catalyst solution was allowed to stir under nitrogen for 15 min prior to use. Poly(styrene-*b*-isoprene-*b*-styrene) (6.0 g) was dissolved in 100 mL dry cyclohexane under nitrogen and cannulated into the glass reactor fitted with magnetic stirrer and filled with 400 mL of cyclohexane. Finally, a few drops of catalyst solution were cannulated into the reactor and the reactor was pressurized to 90 psig with hydrogen gas and heated to 50 °C. Hydrogenation levels were monitored with periodic sampling, removing the catalyst with aqueous citric acid washes, and obtaining ¹H NMR spectra. The hydrogenations were performed to greater than 99% conversion of the olefinic sites. The catalyst was removed by washing with citric acid solution (10 wt%) for 24 - 48 h as described in the earlier literature.⁷⁶⁸

⁷⁶⁸ Hoover, J. M.; Ward, T. C.; McGrath, J. E. The influence of hydrogenation on star block copolymers based on tertiary-butylstyrene-isoprene-divinylbenzene. *Polym Prepr, Am Chem Soc, Div Polym Chem* **1985**, 26, 253-4.

9.3.4 Sulfonation of Poly(styrene-*b*-ethylene-*co*-propylene-*b*-styrene) Triblock Copolymers

Poly(styrene-*b*-ethylene-*co*-propylene-*b*-styrene) triblock copolymer (4.20 g) was charged to a 500-mL round-bottomed flask and dissolved in 140 mL cyclohexane at 50 °C. Acetyl sulfate (25 equivalents relative to styrene) was generated separately through the addition of sulfuric acid (10.1 g, 101 mmol) to acetic anhydride (16.6 g, 163 mmol) in 1,2-dichloroethane (100 mL) at 0 °C. After stirring vigorously, the acetyl sulfate was added to the polymer solution dropwise through an addition funnel. The sulfonation reaction proceeded for 24 h. The polymer was isolated through dripping the crude product into boiling water, which also served to remove the solvent. Water was repeatedly exchanged to completely remove the acetic and sulfuric acid impurities. The polymer was then dissolved in tetrahydrofuran and dialyzed against deionized water to further remove acidic impurities. Final isolation involved rotary evaporation of the aqueous suspension followed by drying at reduced pressure at 25 °C for 24 h.

9.3.5 Titration and Neutralization of Sulfonated Poly(styrene-*b*-ethylene-*co*-propylene-*b*-styrene)

Sulfonated SEPS block copolymer (0.116 g) was dissolved in tetrahydrofuran (30 mL) and titrated with standardized 0.023 M NaOH (aq) (0.75 mL) using thymol blue as an indicator. The degree of sulfonation (62%, relative to styrene content) was determined from the average of three titrations. A larger portion of polymer (3.89 g) was subsequently neutralized via addition of 45.1 mL (1 equiv) of 0.023 M NaOH. The neutralized polymer

was then isolated using rotary evaporation of the solvent mixture and drying under reduced pressure at 40 °C for 48 h.

9.3.6 Small Angle X-Ray Scattering (SAXS) Measurements

Block copolymers that contained pendant sulfonic acids were dissolved in THF and cast in Teflon™ molds whereas sodium sulfonated derivatives were cast from toluene/methanol (95/5 w/w). The films were dried in a vacuum oven at room temperature for 4 days and stored at -15 °C until use. SAXS data were collected on the Army Research Laboratory (ARL) SAXS instrument, located at Aberdeen Proving Ground, MD. $\text{Cu}_{\text{K}\alpha}$ X-ray radiation was generated using a Rigaku Ultrax18 rotating anode X-ray generator operated at 40 kV and 115 mA. A Ni foil was used to filter out all radiation except the $\text{Cu}_{\text{K}\alpha}$ doublet, with an average wavelength, λ , of 1.542 Å. The ARL instrument uses a Molecular Metrology camera with 300, 200 and 600 μm pinholes for X-ray collimation. Two-dimensional data sets were collected using a Molecular Metrology 2D multi-wire area detector located approximately 1.5 m from the sample. After azimuthal averaging, the raw data were corrected for detector noise, absorption, and background noise. The data were then placed on an absolute scale using a glassy carbon sample 1.07 mm thick, previously calibrated at the Advanced Photon Source of the Argonne National Laboratory as a secondary standard. The one-dimensional intensity data are given as a function of the magnitude of the reciprocal scattering vector, q , where $q = 4\pi \cdot \sin(\theta)/\lambda$, and 2θ is the scattering angle. All data reduction and analysis were performed using Wavemetrics Igor Pro v. 5.04.

9.3.7 Atomic Force Microscopy (AFM) Measurements

A Veeco MultiMode™ scanning probe microscope and a Nanoscope IVa controller were used for tapping-mode AFM. All sulfonated block copolymers were spun onto silicon wafers and dried under vacuum; imaging was performed at a set-point ratio of 0.6 at magnifications of 1 μm x 1 μm. Veeco's Nanosensor silicon tips having spring constants of 10-130 N/m were utilized for imaging.

9.3.8 Size Exclusion Chromatography

Size-exclusion chromatography (SEC) was performed at 40 °C in HPLC grade tetrahydrofuran at a flow rate of 1 mL/min using a Waters size exclusion chromatography instrument equipped with an autosampler, 3 in-line 5 μm PLgel MIXED-C columns. Detectors included a Waters 410 differential refractive index (DRI) detector operating at 880 nm, and a Wyatt Technologies miniDAWN multiangle laser light scattering (MALLS) detector operating at 45°, 90° and 135° and 690 nm, which was calibrated with polystyrene standards. The refractive index increment (dn/dc) was calculated online. All molecular weight values reported are absolute molecular weights obtained using the MALLS detector.

9.3.9 Dynamic Mechanical Analysis, Thermal and Rheological Studies

Dynamic mechanical measurements were performed on a TA Instruments Q-800 DMA under nitrogen at a heating rate of 3 °C/min at 1 Hz. The solvent cast samples were measured in film tension mode and cut into 5 mm wide strips using a razor blade. Rheological measurements were conducted using a TA Instruments AR 1000 rheometer in

parallel plate geometry using 25 mm plates and a 1 mm gap. Solvent cast films were cut to size and placed within the rheometer plates. Measurements of the storage modulus and loss modulus were performed between -30 °C and 60 °C and at a constant strain of 3%. Time-temperature superposition (TTS) allowed the development of master curves for the modulus measurements. Differential scanning calorimetry (DSC) was performed on a Perkin Elmer Pyris 1 instrument under a nitrogen flush at a heating rate of 10 °C/min. ¹H NMR spectroscopic data was collected in CDCl₃ on a Varian 400 MHz spectrometer at ambient temperature.

9.4 Results and Discussion

9.4.1 Sulfonated SEPS Triblock Polymer Synthesis

Poly(styrene-*b*-isoprene-*b*-styrene) (SIS) triblock copolymers were synthesized via anionic polymerization using sequential monomer addition (Figure 9.1). Anionic polymerization techniques allowed control of molecular weight and afforded narrow molecular weight distribution, well-defined block copolymers for subsequent fundamental studies (Table 9.1). SEC analysis during the polymerization demonstrated complete crossover as well as complete conversion of each block in the time intervals chosen, which established the absence of tapering between the blocks (Figure 9.2). Short styrene outer block (~1K) were targeted, while variable length rubber sequences (4K-28K) allowed a study of the effect of rubber block molecular weight.

Selective hydrogenation of the isoprene blocks was achieved using a conventional nickel/aluminum catalyst which is critical due to the reactivity of olefins towards subsequent

sulfonating reagents. The extent of hydrogenation was monitored with ^1H NMR spectroscopy which indicated conversion near 99% and above. Sulfonation was accomplished in a mixture of cyclohexane and dichloroethane using acetyl sulfate, which has been recognized as a mild sulfonating agent.⁷⁶⁹ Although excess sulfonating agent was used relative to styrene repeating units, the sulfonation of hydrogenated diene-containing block copolymers typically reached a maximum conversion near 50-60 mol%, as determined through titration measurements, which was presumed due to micelle formation during the reaction in cyclohexane/dichloroethane. In fact, solution turbidity was observed as sulfonation occurred. Low efficiencies were observed earlier in sulfonation of block copolymers with acetyl sulfate,^{770,771} and plateau levels of sulfonation from 60%⁷⁷² to 80%⁷⁷³ were noted in some cases. The sulfonated block copolymers were neutralized with stoichiometric quantities of sodium hydroxide, which was added to the sulfonic acid functionalized polymer solutions in THF.

⁷⁶⁹ La Combe, E.M.; Miller, W.P. Furansulfonic acids and their polymers. US Patent 3182042, 1965.

⁷⁷⁰ Kim, B.; Kim, J.; Jung, B. Proton conductivities and methanol permeabilities of membranes made from partially sulfonated polystyrene-*block*-poly(ethylene-*ran*-butylene)-*block*-polystyrene copolymers. *J Membr Sci* **2002**, 207, 129-37.

⁷⁷¹ Elabd, Y. A.; Walker, C. W.; Beyer, F. L. Triblock copolymer ionomer membranes Part II. Structure characterization and its effects on transport properties and direct methanol fuel cell performance. *J. Membr. Sci.* **2004**, 231, 181-8.

⁷⁷² Balas, J.G.; Gergen, W.P.; Willis, C.L.; Pottick, L.A.; Gelles, R.; Weiss, R.A. Sulfonated block copolymers. US Patent 5239010, 1993.

⁷⁷³ Elabd, Y.A.; Napadensky, E. Sulfonation and characterization of poly(styrene-isobutylene-styrene) triblock copolymers at high ion-exchange capacities. *Polymer* **2004**, 45, 3037-43.

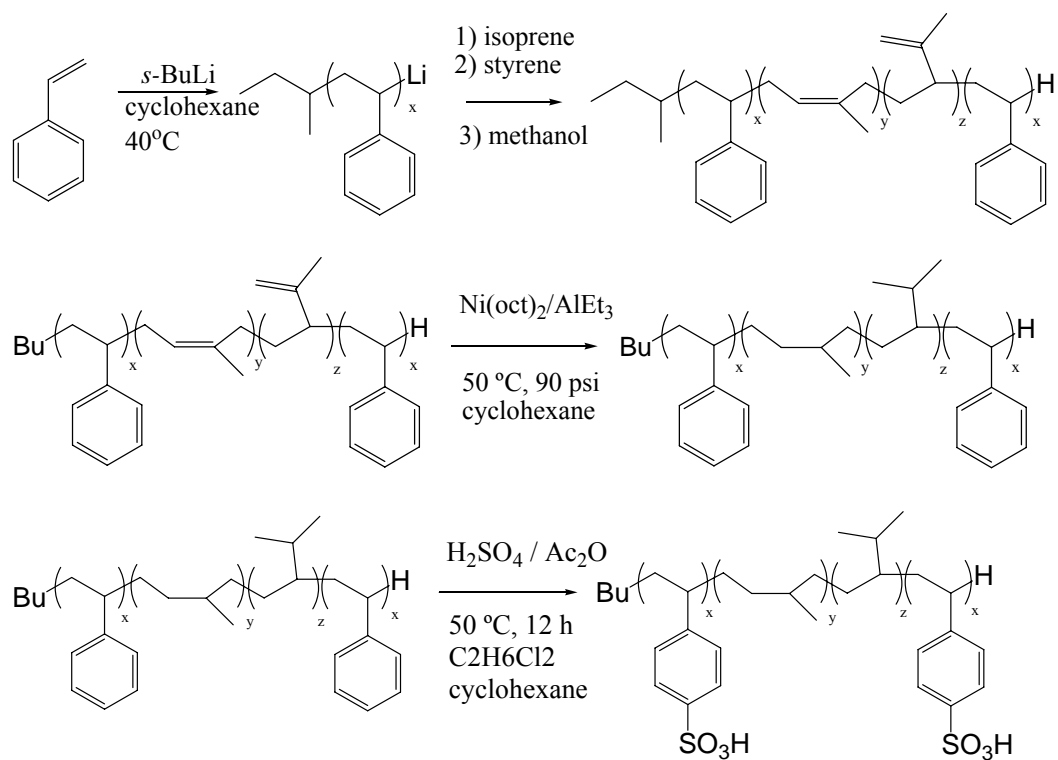


Figure 9.1. Synthesis of sulfonated block copolymers via sequential addition anionic polymerization.

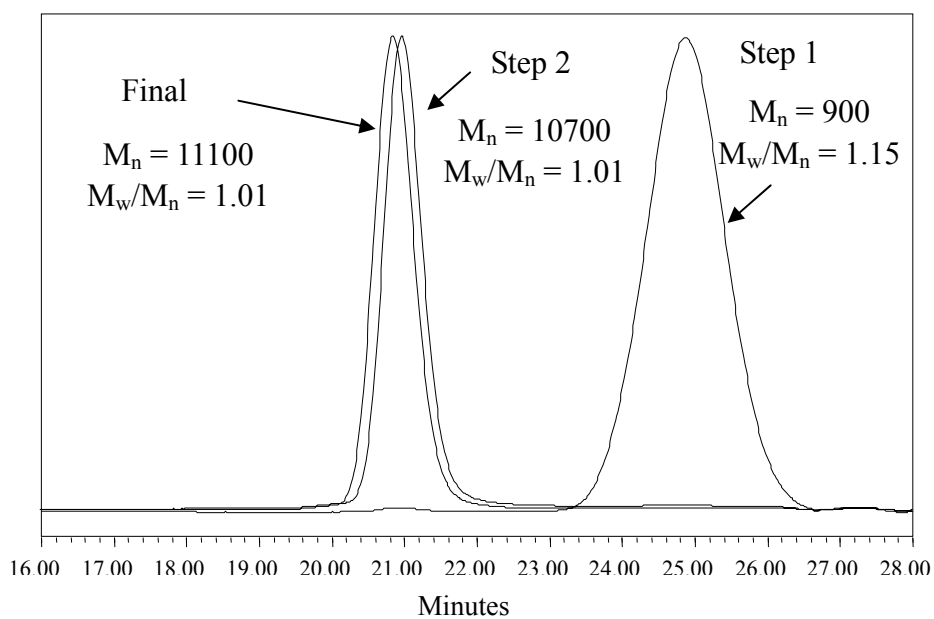


Figure 9.2. SEC analysis of aliquots removed from the polymerization reaction after each block (9K sample)

Table 9.1. Compositional analysis of block copolymers.

ID	Calculated SEC ^a Block Molecular Weights (g/mol)	Calculated NMR ^b Block Molecular Weights (g/mol)	M_w/M_n	Percent Styrene Content ^b (wt%)	Percent Hydrogenation (mol %) ^b	Percent Sulfonation ^c (mol % styrene)	SEPS T_g ^d (°C)
4K	1.2K-4.8K-1.7K	0.9K- 3.8K -1.0K	1.07	33.3	98.5	21	-53,-12
9K	1.0K-10.0K-0.4K	0.9K- 8.8K -1.1K	1.01	18.5	99.4	45	-54
20K	1.2K-17.1K-0.5K	1.0K- 19.9K -1.0K	1.01	9.1	99.8	62	-57
28K	1.0K-27.5K-0.8K	0.8K- 28.2K -1.4K	1.02	7.2	98.7	46	-56

^a SEC analysis, calculated from block molecular weights adjusted for hydrogenation

^b ¹H NMR analysis

^c Titration against 0.02 M NaOH_(aq) in tetrahydrofuran

^d DSC, 10°C/min, N₂

9.4.2 Dynamic Mechanical Analysis (DMA) of Sulfonated SEPS Triblock Polymers

Upon sulfonation, the block copolymers changed from viscous liquids to elastic solids. DMA of the sulfonated block copolymers revealed the microphase separated morphology (Figure 9.3). DSC measurements on the unsulfonated SEPS precursors revealed a single T_g in most cases near $-55\text{ }^\circ\text{C}$, however a second T_g near $-12\text{ }^\circ\text{C}$ was observed for the 5K sample, which had the highest styrene segment content. The Fox-Flory equation, which is based on free volume considerations, predicts a T_g of $15\text{ }^\circ\text{C}$ for 1000 g/mol endblocks based on a treatment by Storey and Baugh.⁷⁷⁴

The DMA revealed glass transitions in the sulfonated block copolymers that occurred at -45 to $-30\text{ }^\circ\text{C}$ ($\tan \delta$ peak), somewhat higher than the DSC measurement. Above this rubbery phase glass transition, a plateau in modulus existed for the sulfonic acid containing polymers that reached $60\text{ }^\circ\text{C}$, while the rubbery plateau for sodium sulfonate form reached nearly $150\text{ }^\circ\text{C}$. The high temperature mechanical performance of the ionomers was in agreement with the stronger association of ionic groups (SO_3Na) in comparison to the hydrogen bonding of sulfonic acid groups. Wilkes et al. observed a similar extension of the rubbery plateau upon neutralization for telechelic polyisobutylene ionomers from $25\text{ }^\circ\text{C}$ to $100\text{ }^\circ\text{C}$ ⁷⁷⁵ and Weiss et al. observed a similar trend for sulfonated SEPS possessing longer styrene blocks.⁷⁷⁶ The softening temperature of the ionomers in the present study was lower

⁷⁷⁴ Storey, R. F.; Baugh, D. W. Poly(styrene-*b*-isobutylene-*b*-styrene) block copolymers produced by living cationic polymerization. Part III. Dynamic mechanical and tensile properties of block copolymers and ionomers therefrom. *Polymer* **2001**, 42, 2321-30.

⁷⁷⁵ Bagrodia, S.; Wilkes, G. L.; Kennedy, J. P. New Polyisobutylene-Based Model Elastomeric Ionomers. VIII. Thermal-Mechanical Analysis. *J Appl Polym Sci* **1985**, 30, 2179-93.

⁷⁷⁶ Mani, S.; Weiss, R. A.; Williams, C. E.; Hahn, S. F. Microstructure of Ionomers Based on Sulfonated Block Copolymers of Polystyrene and Poly(ethylene-*alt*-propylene). *Macromolecules* **1999**, 32, 3663-70.

than the ionic T_g observed for sulfonated polystyrene, which occurred near 210 °C according to DMA at 1 Hz.⁷⁷⁷ However, it was noted earlier that the ionic T_g for sulfonated styrene-ethylene-butylene random copolymers (180 °C) was also significantly below sulfonated polystyrene.⁷⁷⁸

The magnitude of the rubbery plateau modulus appeared to be highest for the 5K rubber block sample and lower for 10K and above samples, but the differences in modulus were less distinguishable at higher molecular weights. This was attributed to the fact that the higher molecular weight samples were significantly above the critical molecular weight for entanglement for poly(ethylene-*co*-propylene) ($M_c = 8100$ g/mol).⁷⁷⁹ Loveday et al. observed near-superimposable storage modulus DMA curves for telechelic sulfonated polyisobutylene ionomers with molecular weights ranging from 20K to 50K (both above the entanglement molecular weight).⁷⁸⁰ For each rubber block molecular weight in the present study, the sodium sulfonated polymer had slightly higher moduli than the sulfonic acid-functionalized polymer in the dynamic mechanical spectrum. Wilkes et al. observed higher rubber plateau modulus values for neutralized telechelic sulfonated polyisobutylene ionomers compared to sulfonic acid analogues, indicating greater strength of the ionic association.⁷⁸¹

⁷⁷⁷ Hird, B.; Eisenberg, A. Sizes and stabilities of multiplets and clusters in carboxylated and sulfonated styrene ionomers. *Macromolecules* **1992**, *25*, 6466-74.

⁷⁷⁸ Nishida, M.; Eisenberg, A. Dynamic Mechanical Study of Sodium Sulfonated Random Ionomers Based on Hydrogenated Styrene-Butadiene Copolymer. *Macromolecules* **1996**, *29*, 1507-15.

⁷⁷⁹ Fetters, L. J.; Lohse, D. J.; Milner, S. T.; Graessley, W. W. Packing Length Influence in Linear Polymer Melts on the Entanglement, Critical, and Reptation Molecular Weights. *Macromolecules* **1999**, *32*, 6847-51.

⁷⁸⁰ Loveday, D.; Wilkes, G. L.; Lee, Y.; Storey, R. F. Investigation of the Structure and Properties of Polyisobutylene-Based Telechelic Ionomers of Narrow Molecular Weight Distribution. II. Mechanical. *J Appl Polym Sci* **1997**, *63*, 507-19.

⁷⁸¹ Bagrodia, S.; Wilkes, G. L.; Kennedy, J. P. New Polyisobutylene-Based Model Elastomeric Ionomers. VIII. Thermal-Mechanical Analysis. *J Appl Polym Sci* **1985**, *30*, 2179-93.

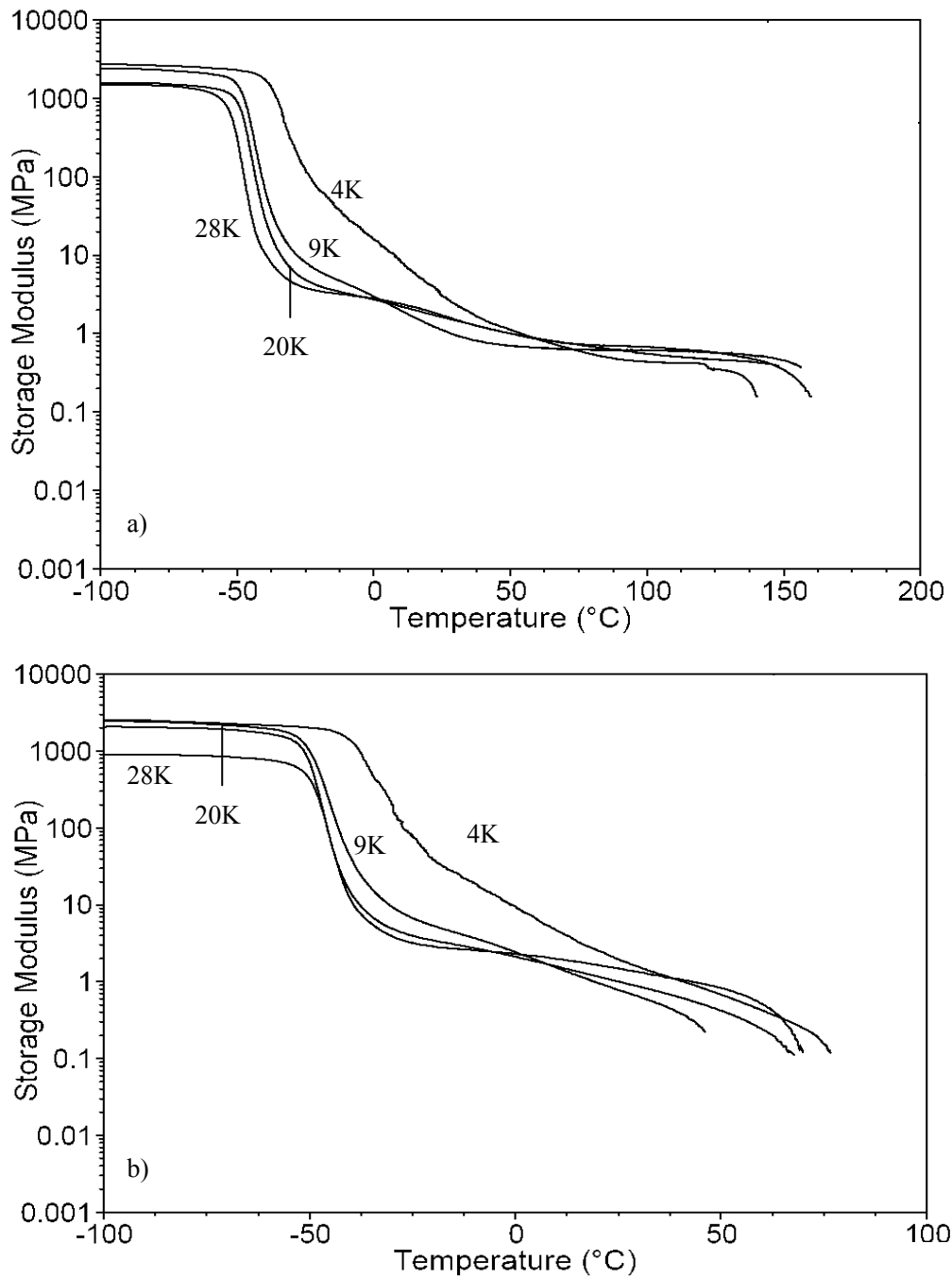


Figure 9.3. Dynamic mechanical analysis of sulfonated SEPS polymers a) sodium sulfonate form b) sulfonic acid form. The higher temperature service window for the neutralized polymers is due to the strong ionic interactions present.

The sodium sulfonated block copolymers all exhibited an intermediate transition in the dynamic mechanical spectrum, which appeared as a small decrease in storage modulus and a peak in the $\tan \delta$ curves near 25-60 °C and was not observed in the sulfonic acid forms. The transition broadened, diminished in magnitude, and increased in temperature with increased rubber block molecular weight. Similar, intermediate mechanical transitions in ionenes near 0 °C were attributed to molecular motions in the ion-rich phase.⁷⁸²

The dynamic mechanical behavior of the sulfonated block ionomers sharply contrasted with the classical behavior of random ionomers. For random ionomers, both the rubbery plateau moduli and glass transition temperatures increase dramatically with sulfonation level due to the higher physical crosslink density.^{783,784} In the current study, however, the multiplets and clusters were restricted to microphase separated domains and the continuous rubber domains were subject only to effects of entanglement and physical crosslink density due to the microphase separated domains. Thus, the block copolymers studied herein exhibited increased rubber phase glass transition temperatures with decreasing rubber block molecular weight. In a similar fashion, for covalent networks, the glass transition temperature increased linearly with inverse rubber block molecular weight,⁷⁸⁵ which is consistent with the trends observed for the sodium sulfonated block copolymers (Figure 9.4).

⁷⁸² Tsutsui, T.; Tanaka, R.; Tanaka, T. Mechanical relaxations in some ionene polymers. I. Effect of ion concentration. *J Polym Sci Polym Phys Ed* **1976**, 14, 2259-71.

⁷⁸³ Nishida, M.; Eisenberg, A. Dynamic Mechanical Study of Sodium Sulfonated Random Ionomers Based on Hydrogenated Styrene-Butadiene Copolymer. *Macromolecules* **1996**, 29, 1507-15.

⁷⁸⁴ Eisenberg, A.; Kim, J. S., *Introduction to Ionomers*. John Wiley and Sons: New York, 1998.

⁷⁸⁵ Andradý, A. L.; Sefcik, M.D. Glass transition in poly(propylene glycol) networks. *J Polym Sci: Polym Phys Ed* **1983**, 21, 2453-63.

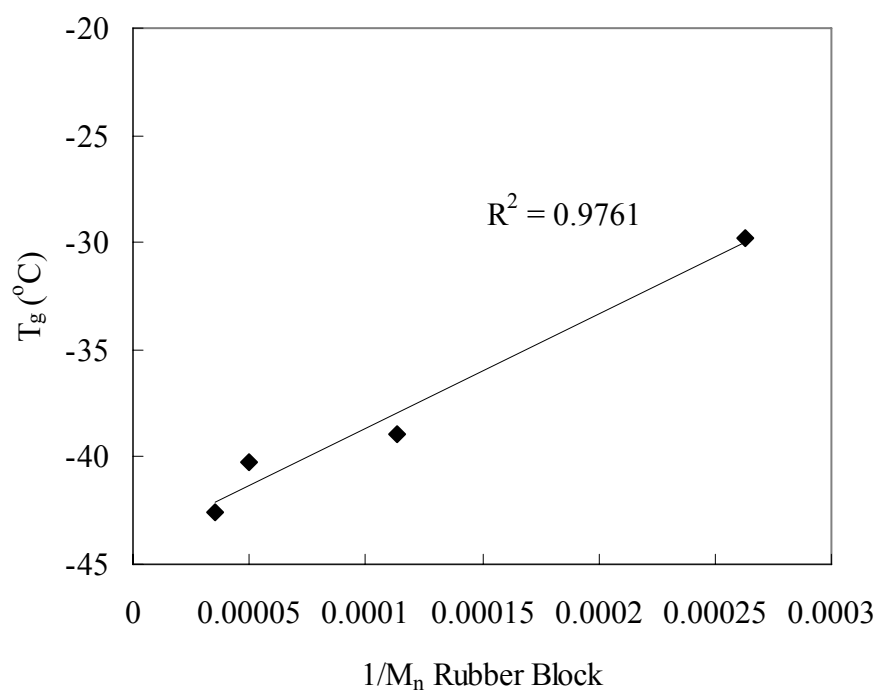


Figure 9.4. Glass transition temperatures of sodium sulfonated SEPS copolymers as a function of rubber block molecular weight.

9.4.3 Tensile Characterization of Sulfonated SEPS Polymers

Tensile characterization is an essential technique for the characterization of elastomers. The tensile properties of the sulfonated SEPS block copolymers are listed in Table 9.2. The sulfonic acid (SO₃H) functional polymers consistently exhibited lower tensile strengths than the corresponding salt (SO₃Na) forms (Figure 9.5). Generally, higher molecular weight rubber block samples exhibited higher elongations and similar tensile strengths. This is expected since higher strain must be applied to overcome greater levels of entanglements. Wilkes et al.⁷⁸⁶ and Loveday et al.⁷⁸⁷ also observed increasing elongation with molecular weight for three-arm sulfonated polyisobutylene telechelic ionomers and Storey et al. observed the same trend for sulfonated three-arm poly(styrene-*b*-ethylene-*co*-butylene-*b*-styrene) block copolymers.⁷⁸⁸ Storey et al. also observed that the polymers appeared brittle and mechanically weak at low rubber block molecular weights, and high elongations were only obtained at high rubber block molecular weights (120K).

⁷⁸⁶ Bagrodia, S.; Mohajer, Y.; Wilkes, G. L.; Storey, R. F.; Kennedy, J. P. New Polyisobutylene-Based Ionomers. 5. The Effect of Molecular Weight on the Mechanical Properties of Tri-Arm Star Polyisobutylene-Based Model Ionomers. *Polymer Bulletin* **1983**, *9*, 174-80.

⁷⁸⁷ Loveday, D.; Wilkes, G. L.; Lee, Y.; Storey, R. F. Investigation of the Structure and Properties of Polyisobutylene-Based Telechelic Ionomers of Narrow Molecular Weight Distribution. II. Mechanical. *J Appl Polym Sci* **1997**, *63*, 507-19.

⁷⁸⁸ Storey, R. F.; George, S. E.; Nelson, M. E. Star-Branched Block Copolymer Ionomers. Synthesis, Characterization, and Properties. *Macromolecules* **1991**, *24*, 2920-30.

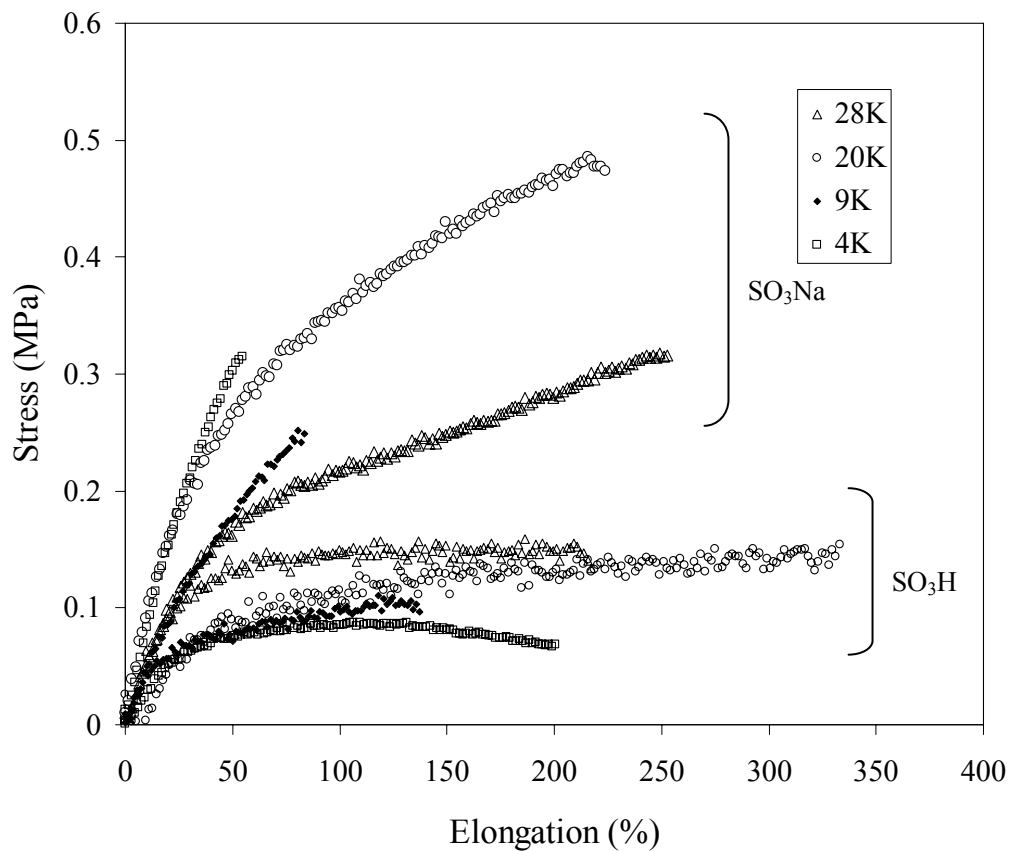


Figure 9.5. Tensile curves for sulfonated SEPS block copolymers.

Table 9.2. Tensile properties of sulfonated SEPS block copolymers and fitting parameters using model from van der Heide.

Polymer	Tensile Strength (MPa)	Elongation (%)	Young's Modulus (MPa)	E_{rubber} (MPa)	$E_{\text{composite}}$ (MPa)	M_c (g/mol)
4K Na ⁺	0.29± 0.03	55± 4	0.75± 0.086	0.26± 0.025	0.91± 0.077	9000
4K H ⁺	0.084± 0.004	210± 55	0.24± 0.017			
9K Na ⁺	0.25± 0.019	85± 5	0.49± 0.022	0.16± 0.013	0.58± 0.035	14000
9K H ⁺	0.091± 0.006	120± 15	0.27± 0.055			
20K Na ⁺	0.48± 0.027	220± 17	0.80± 0.16	0.122± 0.009	1.09± 0.16	19000
20K H ⁺	0.137± 0.009	270± 70	0.35± 0.072			
28K Na ⁺	0.31± 0.009	230± 17	0.61± 0.043	0.065± 0.002	0.83± 0.094	35000
28K H ⁺	0.143± 0.007	180± 50	0.56± 0.085			

The absence of a yield point was noted in the tensile curves for the sulfonated SEPS triblock copolymers, which indicated a lack of continuity of the hard phase.⁷⁸⁹ For the sulfonic acid-functionalized SEPS, stress relaxation due to sample flow was observed during the tensile experiment, leading to unexpected increases in Young's moduli with increased rubber block molecular weight. For the sodium sulfonated block copolymers, trends were not observed in Young's modulus or tensile strength. More strenuous sample drying conditions (60 °C, vacuum, 24 h, storage over P₂O₅) did not alter these observations.

The tensile data were fitted using a model developed by van der Heide et al. to describe polyurethanes, which was also subsequently applied to SBS elastomers (Figure 9.6, Table 9.2).⁷⁹⁰ This model assumes a phase separated system in which a composite modulus (E_c , containing contributions from the hard phase as well as rubber matrix) is observed at low strains followed by a rubber modulus (E_r) at higher strains. The fitting parameters for the sodium sulfonated block copolymers revealed a decrease in rubber modulus with increasing rubber block molecular weight, which is a consequence of decreasing physical crosslink density (Figure 9.7). The tensile data for the sulfonic acid-functionalized block copolymers were not fit due to the stress relaxation that occurred during testing. The effective molecular weight between crosslinks (M_c) for the sodium sulfonated polymers were calculated from rubbery elasticity theory based on the rubber moduli calculated from the van der Heide treatment. The M_c values increased with rubber block molecular weights as expected and

⁷⁸⁹ Bajaj, P.; Varshney, S.K. Morphology and mechanical properties of poly(dimethyl siloxane-*b*-styrene-*b*-dimethyl siloxane) block copolymers. *Polymer*, **1980**, 21, 201-6.

⁷⁹⁰ van der Heide, E.; Van Asselen, O. L. J.; Ingenbleek, G. W. H.; Putman, C. A. J. Tensile Deformation Behaviour of the Polymer Phase of Flexible Polyurethane Foams and Polyurethane Elastomers. *Macromol Symp* **1999**, 147, 127-37.

were similar to the rubber block molecular weights (Figure 9.7). Wilkes et al. calculated expected values of M_c from the Young's modulus of three-arm sulfonated polyisobutylene telechelic ionomers.⁷⁹¹

⁷⁹¹ Mohajer, Y.; Tyagi, D.; Wilkes, G. L.; Storey, R. F.; Kennedy, J. P. New Polyisobutylene Based Model Ionomers. 3. Further Mechanical and Structural Studies. *Polym Bull* **1982**, 8, 47-54.

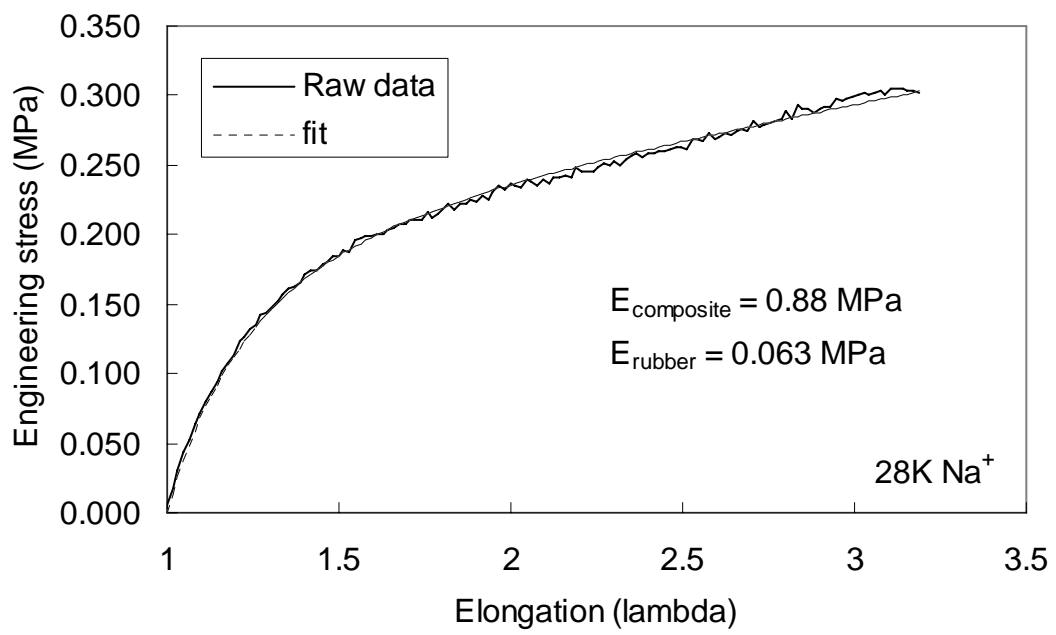


Figure 9.6. Typical tensile curve and fit from the model by van der Heide.

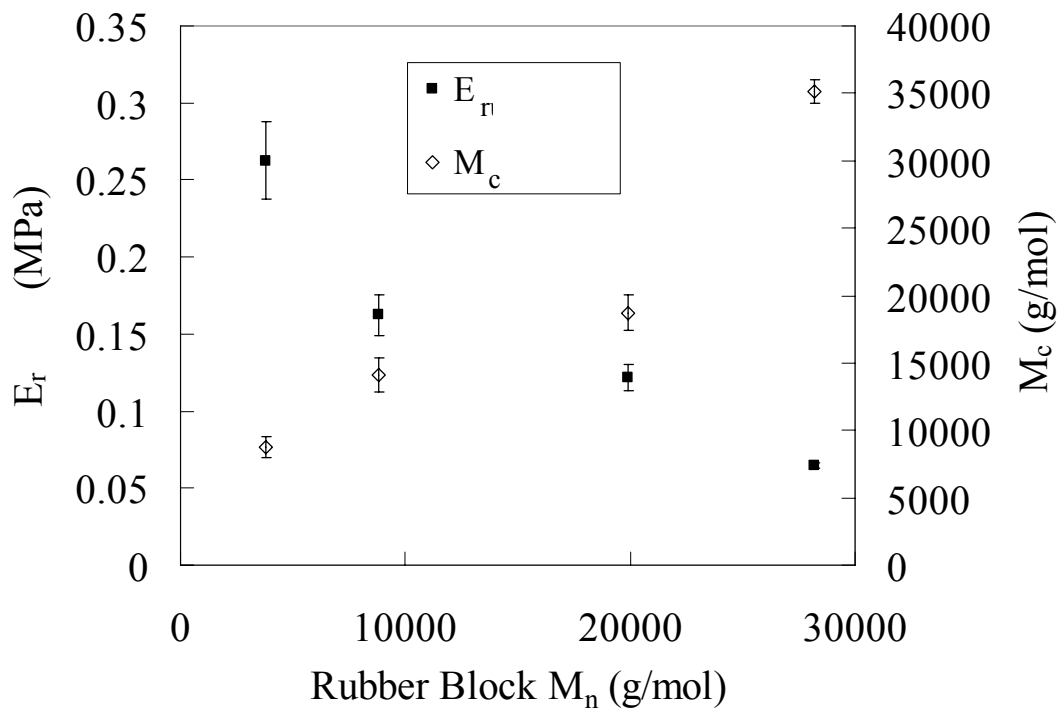


Figure 9.7. Trends in fitting moduli and molecular weight between crosslinks for the sodium sulfonated SEPS polymers.

9.4.4 Rheological Studies of Sulfonated Block Copolymers

Rheological studies were performed using oscillatory shear measurements in a parallel plate rheometer on solvent cast discs of polymers for the 5K (below the entanglement molecular weight) and 17K (above the entanglement molecular weight) sulfonated SEPS samples (both acid and Na⁺ salt forms). In the complex viscosity data, the absence of a Newtonian regime at low frequencies and the linearity of the log viscosity versus log frequency data suggested the presence of a physical network under the conditions studied (Figure 9.8a). For a network, a slope of -1 for the log viscosity versus log frequency is expected.⁷⁹² For the 17K sulfonated SEPS, a slope of -0.80 was observed for the sulfonic acid form whereas the sodium sulfonated produced a slightly higher slope of -0.84 and an improved linear fit. For the 5K sulfonated SEPS, lower slopes of -0.69 for the sulfonic acid and -0.72 for the sodium sulfonate form were observed. Over the frequency range studied, the 5K samples exhibited consistently higher complex viscosities, due to the higher ionic content and physical network density. MacKnight et al. also observed a linear plot of log complex viscosity versus log frequency for ethylene-sodium methacrylate random copolymers⁷⁹³ and Wilkes et al. observed a similar trend for excess neutralized three-arm telechelic sulfonated polyisobutylene in which the excess neutralizing agent was thought to contribute to the hard phase.⁷⁹²

The samples consistently exhibited high shear storage moduli (G') and did not appear to

⁷⁹² Bagrodia, S.; Pisipati, R.; Wilkes, G. L.; Storey, R. F.; Kennedy, J. P. Melt Rheology of Ion-Containing Polymers. I. Effect of Molecular Weight and Excess Neutralizing Agent in Model Elastomeric Sulfonated Polyisobutylene-Based Ionomers. *J Appl Polym Sci* **1984**, 29, 3065-73.

⁷⁹³ Earnest, T. R.; MacKnight, W. J. Effect of Hydrogen Bonding and Ionic Aggregation on the Melt Rheology of an Ethylene-Methacrylic Acid Copolymer and its Sodium Salt. *J Polym Sci: Polym Phys Edn* **1978**, 16, 143-57.

reach the terminal regime over the range of temperatures studied (-30-60 °C) (Figure 9.8b). Kennedy et al. also observed consistently high G' values near 10^5 Pa for zinc neutralized poly(methacrylic acid-*b*-isobutylene-*b*-methacrylic acid) and found that the modulus did not substantially decrease until 200 °C.⁷⁹⁴ The storage modulus data for the 5K SEPS samples were substantially higher than the storage modulus data for the 17K samples over the entire frequency range. Time-temperature superposition is often unsuccessful for random ionomers above a critical ion content due to multiple relaxation mechanisms,⁷⁹⁵⁻⁷⁹⁸ however, in our microphase separated system, the ionic domains were considered fixed, especially over the temperature ranges studied and thus a single relaxation mechanism was dominant.

⁷⁹⁴ Fang, Z.; Wang, S.; Wang, S. Q.; Kennedy, J. P. Novel block ionomers. III. Mechanical and rheological properties. *J Appl Polym Sci* **2003**, 88, 1516-25.

⁷⁹⁵ Eisenberg, A.; Kim, J. S., *Introduction to Ionomers*. John Wiley and Sons: New York, 1998.

⁷⁹⁶ Navratil, M.; Eisenberg, A. Ion Clustering and Viscoelastic Relaxation in Styrene-Based Ionomers. III. Effect of Counterions, Carboxylic Groups, and Plasticizers. *Macromolecules* **1974**, 7, 84-9.

⁷⁹⁷ Eisenberg, A.; King, M.; Navratil, M. Secondary Relaxation Behavior in Ion-Containing Polymers. *Macromolecules* **1973**, 6, 734-7.

⁷⁹⁸ Eisenberg, A.; Navratil, M. Ion Clustering and Viscoelastic Relaxation in Styrene-Based Ionomers. II. Effect of Ion Concentration. *Macromolecules* **1973**, 6, 604-12.

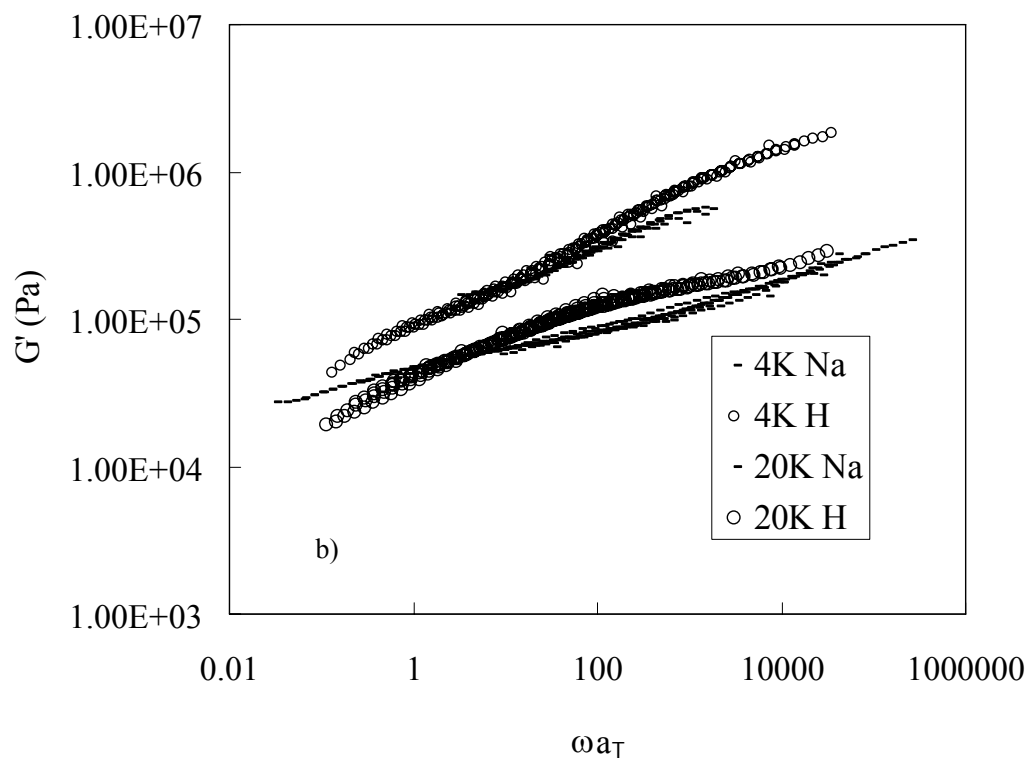
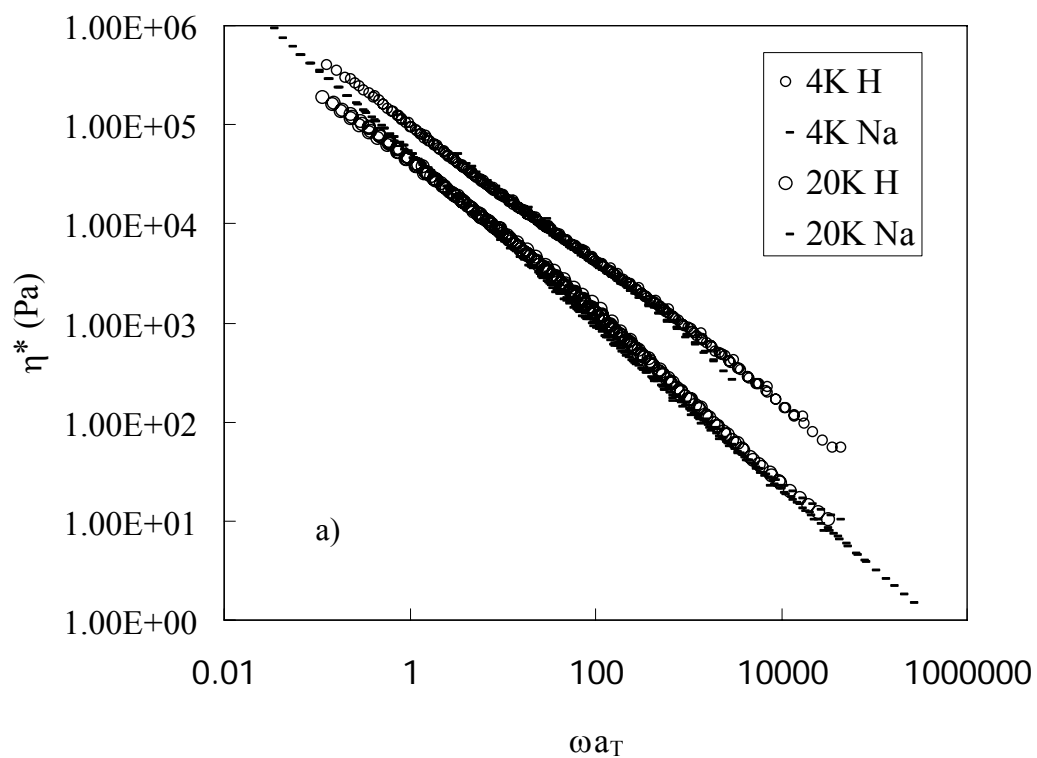


Figure 9.8 Complex viscosity (a) and storage modulus (b) master curves of 5K and 17K samples ($T_r = 20^\circ\text{C}$).

9.4.5 Small Angle X-Ray Scattering Characterization

SAXS is a powerful tool for the analysis of microphase separated systems and is sensitive to electron density fluctuations through a sample, making it useful for examining ionomers due to the presence of nanoscale ionic aggregates. The low volume fraction of styrene and the low degree of polymerization (DP) of the styrenic blocks in the unsulfonated precursor materials was expected to result in the absence of microphase separation. Thus, the unsulfonated 17K and 28K SEPS polymers did not produce a scattering maximum. The 10K SEPS sample produced a very weak scattering maximum at $q^* = 0.058 \text{ \AA}^{-1}$, corresponding to $d = 10.8 \text{ nm}$ in real space, indicating that the volume fraction of styrene was large enough to cause microphase separation. For the 5K SEPS sample, DSC measurements revealed two distinct glass transition temperatures, at $-53 \text{ }^\circ\text{C}$ and $-12 \text{ }^\circ\text{C}$, indicating substantial microphase separation.

The sulfonated SEPS block copolymers all produced single maxima in the one-dimensional scattering data. The scattering maximum arose from the partially sulfonated polystyrene domains, which were dispersed in the hydrocarbon ethylene/propylene matrix. The absence of higher-order peaks in the SAXS data revealed a lack of long-range ordering in these materials. Comparisons among scattering profiles for polymers with differing rubber block molecular weights provided some insight into the progression of the morphology with molecular weight. The intensities of the scattering maxima for the sulfonic acid functional polymers increased with decreasing molecular weight (Figure 9.9). This was expected due to the increase of the sulfonated styrene volume fraction with decreasing rubber content. Similar results were obtained by Weiss et al. when sulfonating

SEBS block copolymers to increasing levels.⁷⁹⁹

A second variation among the sulfonated samples is in the position of the maxima. In the microphase separated morphology, the position of the scattering maximum yields the average interdomain spacings, given in Table 9.3. The peak positions were obtained by fitting the scattering intensity with a Gaussian function and a linear background over a narrow q range encompassing the peak. The interdomain distances, which were calculated in this manner for the sulfonated block copolymers, ranged from 10 to 14 nm, and increased with increasing molecular weight. A similar trend was observed for the sodium sulfonated forms. Jerome *et al.* observed a similar trend of interdomain spacing with molecular weight for functionalized telechelic ionomers, where the interdomain spacing was proportional to the root-mean-square end-to-end distance.⁸⁰⁰ Loveday *et al.* also observed interdomain spacings near 10 nm for 10-20K polyisobutylene telechelic ionomers and a trend of increased interdomain spacing with molecular weight.⁸⁰¹ Similar interdomain spacings were observed for 15K telechelic sulfonated polyisoprenes.⁸⁰²

⁷⁹⁹ Lu, X.; Steckle, W. P.; Weiss, R. A. Ionic Aggregation in a Block Copolymer Ionomer. *Macromolecules* **1993**, *26*, 5876-84.

⁸⁰⁰ Sobry, R.; Fontaine, F.; Ledent, J.; Foucart, M.; Jerome, R. Morphology of Ionic Aggregates in Carboxylato- and Sulfonato-Telechelic Polyisoprenes As Investigated by Small-Angle X-ray Scattering. *Macromolecules* **1998**, *31*, 4240-52.

⁸⁰¹ Loveday, D.; Wilkes, G. L.; Lee, Y.; Storey, R. F. Investigation of the Structure and Properties of Polyisobutylene-Based Telechelic Ionomers of Narrow Molecular Weight Distribution. I. *J Appl Polym Sci* **1997**, *63*, 497-506.

⁸⁰² Venkatshwaran, L. N.; Tant, M. R.; Wilkes, G. L.; Charlier, P.; Jerome, R. Structure-property comparison of sulfonated and carboxylated telechelic ionomers based on polyisoprene. *Macromolecules* **1992**, *25*, 3996-4001.

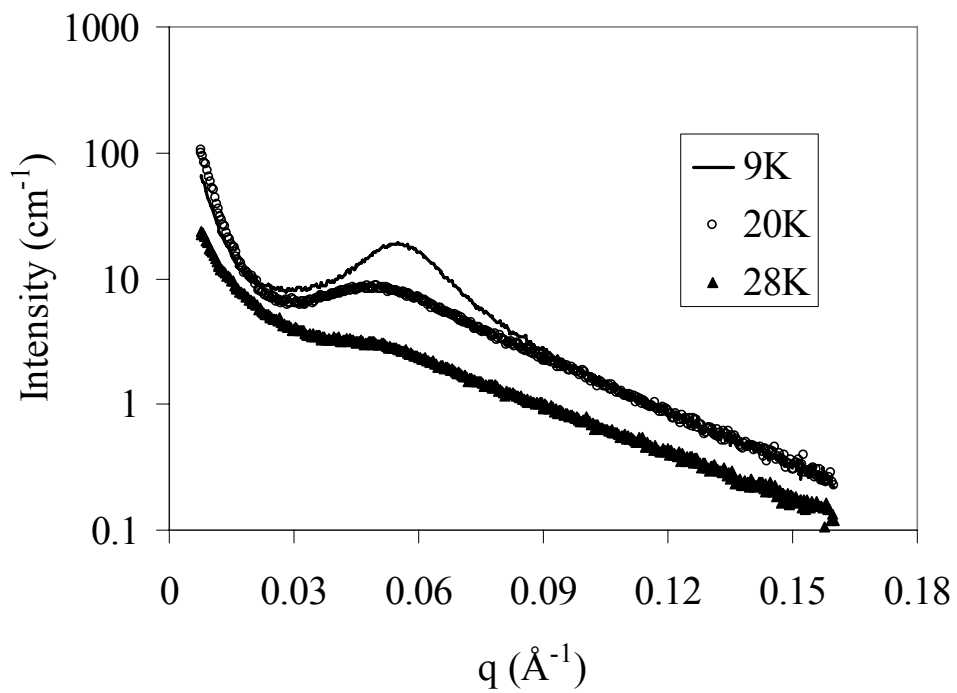


Figure 9.9. 1-D SAXS profiles for sulfonated block copolymers of varying rubber block molecular weights.

Table 9.3. Summary of scattering maxima position and Bragg spacing for sulfonated block copolymers.

Rubber Block M_n	Form	q^* (\AA^{-1})	d (nm)
4	SO ₃ H	0.060	10.4
4	SO ₃ Na	0.065	9.7
9	SO ₃ H	0.055	11.4
9	SO ₃ Na	0.061	10.3
20	SO ₃ H	0.049	12.6
20	SO ₃ Na	0.053	11.9
28	SO ₃ H	0.047	13.4
28	SO ₃ Na	0.049	12.9

The SAXS spectra of the sodium sulfonated polymers featured decreased Bragg spacings compared to the sulfonic acid polymers (Table 9.3). This was observed as a shift in the scattering maxima to higher q upon neutralization of the polymer (Figure 9.10). The smaller spacing between hard phases may arise from a “tightening” of the physical network structure due to the increased attractive forces between ionic groups compared to neutral sulfonic acid groups. Weiss observed a similar trend with oil-swollen sulfonated SEBS which was attributed to increasing strength of association.⁸⁰³ Weiss and coworkers also observed a broadening of the SAXS peak with increasing strength of association, with the breadth increasing in the order of “precursor” < “SO₃H” < “SO₃Na”. Such broadening is clearly visible in comparing the sulfonic acid containing polymers with the sodium sulfonated ionomers (Figure 9.10). The increased peak breadth was attributed to the hindered morphological development due to stronger interactions in the sodium sulfonated polymers. Other researchers have observed a shift in morphology due to sulfonation, such as from cylindrical to lamellar morphologies,⁸⁰⁴ apparently due to the increased drive for microphase separation and the thermodynamic driving force to minimize interfacial surface area.

⁸⁰³ Lu, X.; Steckle, W. P.; Weiss, R. A. Morphological Studies of a Triblock Copolymer Ionomer by Small Angle X-ray Scattering. *Macromolecules* **1993**, 26, 6525-30.

⁸⁰⁴ Balas, J. G.; Gergen, W. P.; Willis, C. L.; Pottick, L. A.; Gelles, R.; Weiss, R. A. Sulfonated block copolymers. US Patent 5239010, 1993.

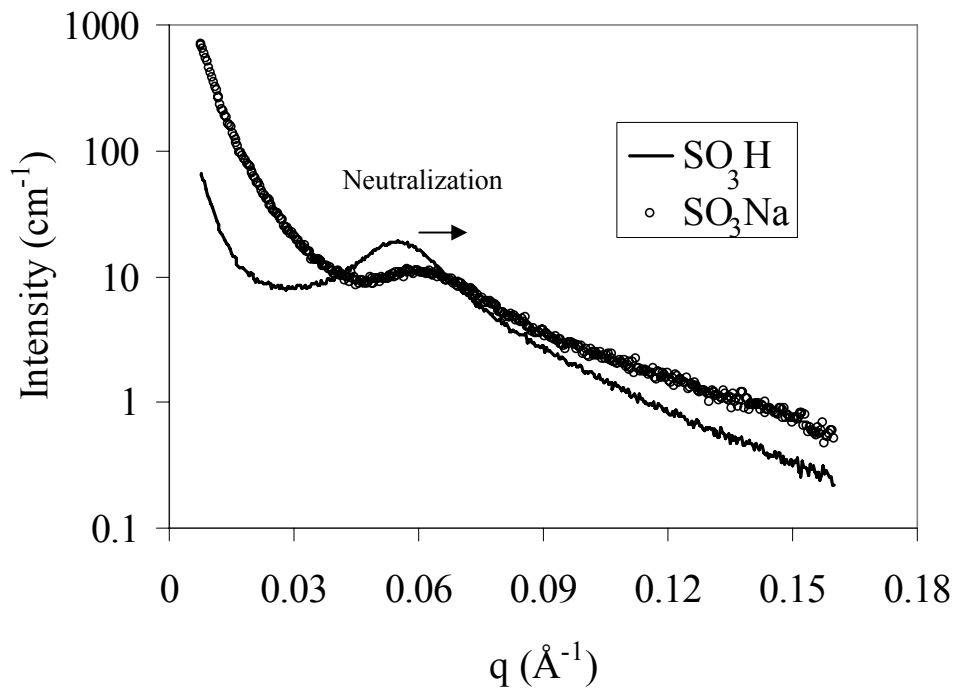


Figure 9.10. Effect of neutralization on the scattering maxima in the sulfonated block copolymer (10K sample).

Weiss et al. have studied similar sulfonated poly(styrene-*b*-ethylene-*co*-butylene-*b*-styrene) polymers and observed peaks in SAXS arising from both block copolymer microphase separation ($d = 10\text{-}30\text{ nm}$) as well as from ionic aggregation ($d = 2\text{-}6\text{ nm}$). Weiss et al. concluded that the ionic aggregates resided within the microphase separated styrene domains.^{805,806} Similar ionic peaks were also observed in Nafion™,⁸⁰⁷ however, an ionomer peak was not observed in the present studies. This may be due to the fact that films were prepared using solution casting, which was shown to suppress the ionomer peak.⁸⁰⁵ Also, the high level of sulfonation was shown to shift q values for the ionic peak above 0.2 \AA^{-1} (for 18 mol% sulfonation), which is an angular range that was not examined in this experiment.⁸⁰⁵

9.4.6 Atomic Force Microscopy (AFM) Characterization

Tapping mode AFM studies of the sulfonated block copolymers revealed microphase separation at the surface, with harder sulfonated styrene domains dispersed in a soft hydrogenated diene matrix apparent in the phase image (Figure 9.11). The smoothness and absence of structure in the topographic images (not shown) suggested that the structure present in the phase image indeed reflected “hard” and “soft” phases. The hard domains appeared to exhibit a spherical morphology as would be expected for the small styrene volume fractions. These domains are clearly not ordered in the material, corroborating the

⁸⁰⁵ Lu, X.; Steckle, W. P.; Weiss, R. A. Ionic Aggregation in a Block Copolymer Ionomer.

Macromolecules **1993**, 26, 5876-84.

⁸⁰⁶ Lu, X.; Steckle, W. P.; Weiss, R. A. Morphological Studies of a Triblock Copolymer Ionomer by Small Angle X-ray Scattering. *Macromolecules* **1993**, 26, 6525-30.

⁸⁰⁷ Mauritz, K. A.; Moore, R. B. State of Understanding of Nafion. *Chem. Rev* **2004**, 104, 4535-85.

lack of higher order peaks in the SAXS experiments. Similar images were obtained from spin-coated samples and slowly evaporated films, suggesting that the rate of evaporation was not preventing the ordering of the material. A cursory examination of the AFM images revealed hard domain spacings close to those obtained in SAXS experiments (~12-18 nm), however, these did not strongly correlate with rubber block molecular weight. Due to the strength of the tapping, however, multiple layers of thickness were likely sampled simultaneously, thereby preventing an accurate determination of the interdomain distances. AFM characterization of the unsulfonated precursor polymers did not reveal any surface texture.

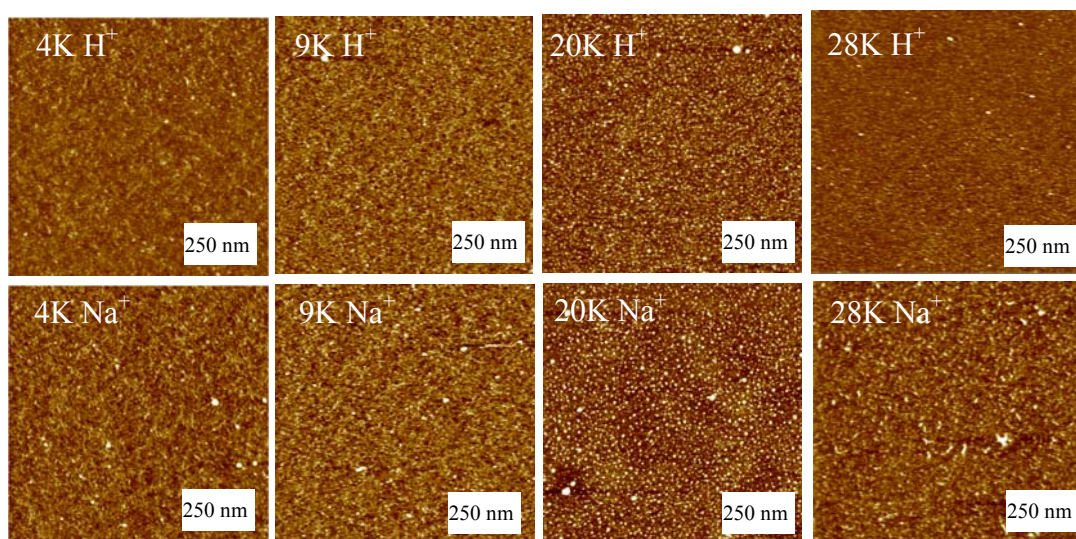


Figure 9.11. Tapping mode AFM phase images of the sulfonated block copolymer series.

Each image is 1 μm x 1 μm . Samples were spin-coated on silicon wafers and are unannealed.

9.5 Conclusions

Novel, short outer block sulfonated styrene-ethylene/propylene-styrene triblock copolymers were synthesized and characterized via small angle x-ray scattering (SAXS), dynamic mechanical analysis (DMA), tensile testing, rheology, and atomic force microscopy (AFM). The polymers exhibited microphase separation in which the minor component, sulfonated polystyrene formed a dispersed, hard phase in the soft, ethylene/propylene rubbery matrix. The sulfonated polystyrene phases appeared roughly spherical in shape, and no evidence of long-range order was observed. DMA revealed the presence of two glass transition temperatures and increasing rubber phase T_g with molecular weight. Tensile measurements showed increased elongation with molecular weight and higher tensile strengths for the sodium sulfonated polymers. Rheological measurements confirmed the presence of a non-covalent network structure. The interdomain spacing measured by SAXS increased with rubber block molecular weight and decreased upon neutralization of the block copolymers, suggesting a “tightening” of the network. AFM revealed phase separated morphologies at the surface, with similar length scales of phase separation.

9.6 Acknowledgements

The authors would like to acknowledge Carl Willis and Dale Handlin of Kraton Polymers for helpful discussions and Kraton Polymers for financial support. This material is based upon work supported by, or in part by, the U.S. Army Research Laboratory and the U.S. Army Research Office under grant number DAAD19-02-1-0275 Macromolecular Architecture for Performance (MAP) MURI.

Chapter 10. Morphological Analysis of Telechelic Ureido-Pyrimidone Functional Hydrogen Bonding Linear and Star-Shaped Poly(ethylene-*co*-propylene)s

(Mather, B.D.; Elkins, C.L.; Beyer, F.L; Long, T.E., *Macromolecular Rapid Communications*,
submitted)

10.1 Abstract

Ureidopyrimidone (UPy) end-functionalized linear and star-shaped poly(ethylene-*co*-propylene)s (hydrogenated polyisoprene) with molecular weights between 12K and 90K and narrow molecular weight distributions ($M_w/M_n < 1.10$) were synthesized via living anionic polymerization followed by chain-end modification reactions. UPy end-functionalized poly(ethylene-*co*-propylene)s of varying topology were studied with small-angle X-ray scattering (SAXS) and atomic force microscopy (AFM). These hydrogen bond end-functionalized polymers (0.45-1.14 mol% UPy end-groups) unexpectedly exhibited microphase separated domains with interdomain spacings of approximately 10-15 nm suggesting a solid-state clustering of the hydrogen bonding end-groups beyond simple dimerization. The interdomain spacings that were obtained from SAXS measurements systematically increased with molecular weight and decreased for monofunctional oligomers relative to telechelic analogs of the identical molecular weight. Variable temperature AFM measurements confirmed the presence of microphase separation at the surface for the star-shaped UPy end-functional poly(ethylene-*co*-propylene) and revealed a decrease in phase

contrast upon heating to 130 °C with retention of the microphase separated texture.

10.2 Introduction

Multiple hydrogen bonding enables the introduction of thermoreversible linkages and molecular recognition sites into novel macromolecular architectures through the tailoring of specific non-covalent intermolecular interactions.^{808 - 811} The association strength is a function of various environmental parameters such as temperature, solvent, humidity, and pH, and consequently, the thermomechanical and rheological properties are also controlled through a number of environmental variables. The strength of hydrogen bonding associations are further tunable using controlled polymerization strategies and molecular design of the hydrogen bonding scaffold. For example, DNA nucleotide bases possess association constants near 10^2 M^{-1} whereas synthetic quadruple hydrogen bonding ureidopyrimidone (UPy) arrays may possess association constants as high as 10^7 M^{-1} .⁸¹²

Hydrogen bonding interactions play a vital role in the development of self-assembling supramolecular structures.⁸¹³⁻⁸¹⁶ Lehn et al. studied the development of helical fibers from

⁸⁰⁸ Elkins, C. L.; Viswanathan, K.; Long, T. E. Synthesis and Characterization of Star-Shaped Poly(ethylene-co-propylene) Polymers Bearing Terminal Self-Complementary Multiple Hydrogen-Bonding Sites. *Macromolecules* **2006**, *39*, 3132-9.

⁸⁰⁹ Yamauchi, K.; Kanomata, A.; Inoue, T.; Long, T. E. Thermoreversible Polyesters Consisting of Multiple Hydrogen Bonding (MHB). *Macromolecules* **2004**, *37*, 3519-22.

⁸¹⁰ Mather, B. D.; Lizotte, J. R.; Long, T. E. Synthesis of Chain End Functionalized Multiple Hydrogen Bonded Polystyrenes and Poly(alkyl acrylates) Using Controlled Radical Polymerization. *Macromolecules* **2004**, *37*, 9331-7.

⁸¹¹ Yamauchi, K.; Lizotte, J. R.; Long, T. E. Synthesis and Characterization of Novel Complementary Multiple-Hydrogen Bonded (CMHB) Macromolecules via a Michael Addition. *Macromolecules* **2002**, *35*, 8745-50.

⁸¹² Sontjens, S. H. M.; Sijbesma, R. P.; van Genderen, M. H. P.; Meijer, E. W. Stability and Lifetime of Quadruply Hydrogen Bonded 2-Ureido-4[1H]-pyrimidinone Dimers. *J Am Chem Soc* **2000**, *122*, 7487-93.

⁸¹³ Brunsveld, L.; Folmer, B. J. B.; Meijer, E. W.; Sijbesma, R. P. Supramolecular Polymers. *Chem Rev*

complementary difunctional Janus wedge style recognition units.⁸¹⁷ Chiral complementary diacyldiaminopyridine and uracil-functionalized tartaric acids demonstrated formation of helical fibers, and the chirality of the precursors dictated the structure of the supramolecular helix.⁸¹⁸ Meijer et al. functionalized oligo-*p*-phenylenevinylenes with ureido-*s*-triazines, which formed associated helical structures in dodecane.⁸¹⁹ Rotello et al. also have observed giant vesicles, which were created from non-covalent, reversibly crosslinked, microspheres, and reversibly adsorbed polymer chains to surfaces through the association of diacylaminopyridine and thymine-functionalized polystyrene.⁸²⁰⁻⁸²² Furthermore, Rotello et al. also achieved reversible side chain functionalization using the diacylaminopyridine/thymine recognition pair.⁸²³

2001, 101, 4071-97.

⁸¹⁴ Hilger, C.; Drager, M.; Stadler, R. Molecular Origin of Supramolecular Self-Assembling in Statistical Copolymers. *Macromolecules* **1992**, 25, 2498-501.

⁸¹⁵ Lehn, J. M. Supramolecular polymer chemistry- scope and perspectives. *Polym Int* **2002**, 51, 825-39.

⁸¹⁶ Whitesides, G. M.; Simanek, E. E.; Mathias, J. P.; Seto, C. T.; Chin, D. N.; Mammen, M.; Gordon, D. M. Noncovalent Synthesis: Using Physical-Organic Chemistry To Make Aggregates. *Acc Chem Res* **1995**, 28, 37-44.

⁸¹⁷ Berl, V.; Schmutz, M.; Krische, M. J.; Khoury, R. G.; Lehn, J. M. Supramolecular Polymers Generated from Heterocomplementary Monomers Linked through Multiple Hydrogen-Bonding Arrays—Formation, Characterization, and Properties. *Chem Eur J* **2002**, 8, 1227-44.

⁸¹⁸ Gulik-Krzywicki, T.; Fouquey, C.; Lehn, J. M. Electron microscopic study of supramolecular liquid crystalline polymers formed by molecular-recognition-directed self assembly from complementary chiral components. *Proc Natl Acad Sci USA* **1993**, 90, 163-7.

⁸¹⁹ Schenning, A. P. H. J.; Jonkheijm, P.; Peeters, E.; Meijer, E. W. Hierarchical Order in Supramolecular Assemblies of Hydrogen-Bonded Oligo(*p*-phenylene vinylene)s. *J Am Chem Soc* **2001**, 123, 409-16.

⁸²⁰ Ilhan, F.; Galow, T. H.; Gray, M.; Clavier, G.; Rotello, V. M. Giant Vesicle Formation through Self-Assembly of Complementary Random Copolymers. *J Am Chem Soc* **2000**, 122, 5895-6.

⁸²¹ Thibault, R. J.; Hotchkiss, P. J.; Gray, M.; Rotello, V. M. Thermally Reversible Formation of Microspheres through Non-Covalent Polymer Cross-Linking. *J Am Chem Soc* **2003**, 125, 11249-52.

⁸²² Norsten, T. B.; Jeoung, E.; Thibault, R. J.; Rotello, V. M. Specific Hydrogen-Bond-Mediated Recognition and Modification of Surfaces Using Complementary Functionalized Polymers. *Langmuir* **2003**, 19, 7089-93.

⁸²³ Ilhan, F.; Gray, M.; Rotello, V. M. Reversible Side Chain Modification through Noncovalent

UPy groups exhibit unusually high association constants ($6 \times 10^7 \text{ M}^{-1}$ in chloroform) due to the presence of four hydrogen bonds in a configuration that minimizes repulsive interactions between opposing hydrogen bonding groups.^{824,825} This DDAA configuration (D = donor, A = acceptor) also results in self-complementary behavior, in contrast to nucleotide bases which are complementary (A-T, G-C). The planar structure of the UPy molecule and intramolecular hydrogen bonding assists in creating and maintaining a geometry that maximizes hydrogen bonding (Figure 10.1). The lifetime in solution of UPy dimers was reported as high as 170 ms in chloroform or 1.7 s in toluene.⁸²⁴ Meijer et al. have also demonstrated that molecules containing two UPy groups form reversible, non-covalent, supramolecular polymers in solution.⁸²⁶ These supramolecular polymers were formed through chain-extension resembling step-growth polymerization. Difunctional UPy molecules, which associate intramolecularly into cyclics at room temperature, were found to “polymerize” non-covalently via ring-opening with increased temperature.⁸²⁷

Interactions. “Plug and Play” Polymers. *Macromolecules* **2001**, 34, 2597-601.

⁸²⁴ Sontjens, S. H. M.; Sijbesma, R. P.; van Genderen, M. H. P.; Meijer, E. W. Stability and Lifetime of Quadruply Hydrogen Bonded 2-Ureido-4[1H]-pyrimidinone Dimers. *J Am Chem Soc* **2000**, 122, 7487-93.

⁸²⁵ Beijer, F. H.; Sijbesma, R. P.; Kooijman, H.; Spek, A. L.; Meijer, E. W. Strong Dimerization of Ureidopyrimidones via Quadruple Hydrogen Bonding. *J Am Chem Soc* **1998**, 120, 6761-9.

⁸²⁶ Sijbesma, R. P.; Beijer, F. H.; Brunsveld, L.; Folmer, B. J. B.; Hirschberg, J. H. K. K.; Lange, R. F. M.; Lowe, J. K. L.; Meijer, E. W. Reversible Polymers Formed from Self-Complementary Monomers Using Quadruple Hydrogen Bonding. *Science* **1997**, 278, 1601-4.

⁸²⁷ Folmer, B. J. B.; Sijbesma, R. P.; Meijer, E. W. Unexpected Entropy-Driven Ring-Opening Polymerization in a Reversible Supramolecular System. *J Am Chem Soc* **2001**, 123, 2093-4.

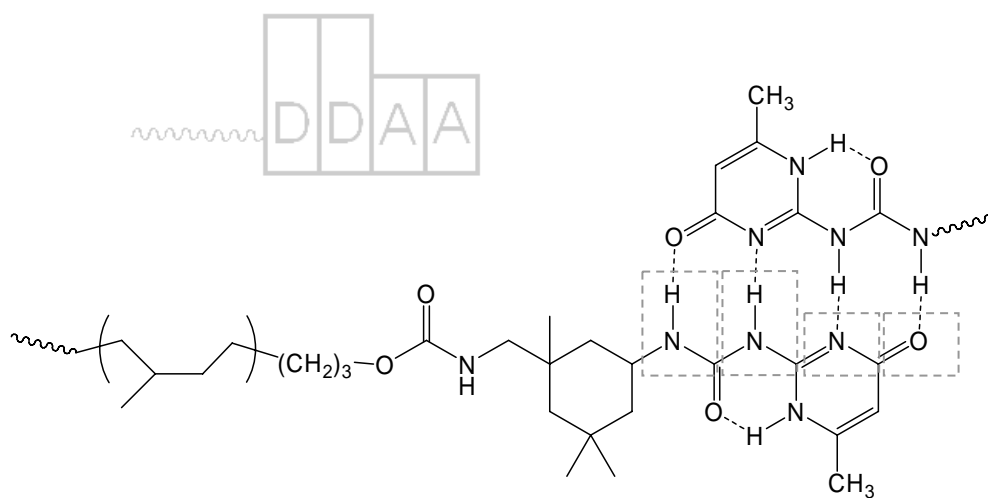


Figure 10.1. Ureidopyrimidone (UPy) quadruple hydrogen bonded dimer attached to poly(ethylene-*co*-propylene)s.

The UPy group has generated significant interest recently as efforts have transitioned from synthesizing functional low molecular weight molecules to high molecular weight polymers containing the UPy group. Meijer and coworkers demonstrated that end-functionalization of 3-arm poly(ethylene oxide-*co*-propylene oxide) oligomers with UPy groups converted the viscous liquid precursors into viscoelastic solids.⁸²⁸ The solution viscosity of these trifunctional oligomers decreased with the addition of monofunctional UPy “chain stoppers” and with increasing solvent polarity. Difunctional UPy functional siloxanes exhibited degrees of non-covalent polymerization of 20-100.⁸²⁹ In addition, the siloxanes exhibited endotherms in DSC measurements that were attributed to the melting of crystallites of UPy dimers. Guan et al. have incorporated the UPy group into polyurethanes to create intra-chain non-covalently cyclized polymers,⁸³⁰ and single molecule AFM studies demonstrated the mechanical disruption of intra-chain cyclic formations. Long and coworkers have introduced telechelic UPy functionality into polyesters via post-polymerization modification.⁸³¹ Melt rheological studies revealed hydrogen bond dissociation temperatures for telechelic poly(butylene isophthalate) near 80 °C and improved mechanical properties. Coates and coworkers have introduced the UPy group into polyolefins via copolymerization

⁸²⁸ Lange, R. F. M.; van Gurp, M.; Meijer, E. W. Hydrogen-Bonded Supramolecular Polymer Networks. *J. Polym. Sci. A: Polym. Chem* **1999**, 37, 3657-70.

⁸²⁹ Hirschberg, J. H. K. K.; Beijer, F. H.; van Aert, A. H.; Magusin, P. C. M. M.; Sijbesma, R. P.; Meijer, E. W. Supramolecular Polymers from Linear Telechelic Siloxanes with Quadruple-Hydrogen-Bonded Units. *Macromolecules* **1999**, 32, 2696-705.

⁸³⁰ Guan, Z.; Roland, J. T.; Bai, J. Z.; Ma, S. X.; McIntire, T. M.; Nguyen, M. Modular Domain Structure: A Biomimetic Strategy for Advanced Polymeric Materials. *J Am Chem Soc* **2004**, 126, 2058-65.

⁸³¹ Yamauchi, K.; Kanomata, A.; Inoue, T.; Long, T. E. Thermoreversible Polyesters Consisting of Multiple Hydrogen Bonding (MHB). *Macromolecules* **2004**, 37, 3519-22.

of a UPy functional α -olefin with 1-butene.⁸³² Dramatic improvements in tensile performance were observed as well as much stronger dependence of solution viscosity on concentration. Long has also developed both random copolymers.^{833,834} containing the UPy moiety as well as terminally functionalized polystyrene and polyisoprene.^{835,836} Random copolymers of a UPy-functionalized methacrylate monomer with 2-ethylhexylmethacrylate exhibited decreasing creep compliance with increasing UPy content. Furthermore, both broader plateaus in moduli as a function of frequency and higher modulus in melt rheological studies were observed. Random copolymers with *n*-butyl acrylate showed a linear relationship between T_g and UPy content, as well as stronger concentration dependence of solution viscosity compared to non-functional analogues. Telechelic functional polyisoprene exhibited hydrogen bond dissociation near 80 °C in melt rheological experiments.

Although significant attention has been devoted to the role of the UPy hydrogen bonding group on solution rheological performance, fewer studies have been devoted to understanding the solid state morphological implications of multiple hydrogen bonding groups. Recently, Meijer et al. reported the synthesis of telechelic

⁸³² Reith, R. L.; Eaton, F. R.; Coates, W. G. Polymerization of Ureidopyrimidinone-Functionalized Olefins by Using Late-Transition Metal Ziegler-Natta Catalysts: Synthesis of Thermoplastic Elastomeric Polyolefins. *Angew Chem Int Ed* **2001**, 40, 2153-6.

⁸³³ Elkins, C. L.; Park, T.; McKee, M. G.; Long, T. E. Synthesis and Characterization of Poly(2-ethylhexyl methacrylate) Copolymers Containing Pendant, Self-Complementary Multiple-Hydrogen-Bonding Sites. *J Polym Sci Part A: Polym Chem* **2005**, 43, 4618-31.

⁸³⁴ McKee, M. G.; Elkins, C. L.; Park, T.; Long, T. E. Influence of Random Branching on Multiple Hydrogen Bonding in Poly(alkyl methacrylate)s. *Macromolecules* **2005**, 38, 6015-23.

⁸³⁵ Yamauchi, K.; Lizotte, J. R.; Hercules, D. M.; Vergne, M. J.; Long, T. E. Combinations of Microphase Separation and Terminal Multiple Hydrogen Bonding in Novel Macromolecules. *J Am Chem Soc* **2002**, 124, 8599-604.

⁸³⁶ Yamauchi, K.; Lizotte, J. R.; Long, T. E. Thermoreversible Poly(alkyl acrylates) Consisting of Self-Complementary Multiple Hydrogen Bonding. *Macromolecules* **2003**, 36, 1083-8.

poly(ethylene-*co*-butylene)s with terminal UPy groups containing linear 1,6-hexylene linker groups with either urea, urethane or no additional functionality.⁸³⁷ The polymers that did not contain adjacent urea or urethane groups did not exhibit any phase texture in atomic force microscopy (AFM) studies. However, the introduction of adjacent urea or urethane groups resulted in additional hydrogen bonding interactions in the lateral direction. In particular, adjacent urea groups, which form two hydrogen bonds, produced 3-dimensional stacking of hydrogen bonding groups leading to distinct fibril-like hard phases. This combination of different modes of hydrogen bonding led to solid-like behavior, and improved tensile strengths and higher storage moduli in melt rheological experiments were observed for adjacent urethane or urea UPy-functionalized oligomers. Previous work from Meijer et al. involving UPy end-functionalized three-arm poly(ethylene oxide-*co*-propylene oxide)s with an asymmetric cycloaliphatic linker and adjacent urethane groups indicated the absence of microphase separation from SAXS analysis whereas a urea end-functional polymer without UPy groups did exhibit a scattering maximum.⁸³⁸

Long and coworkers recently reported the synthesis, thermal, mechanical, and rheological properties of UPy hydrogen bond functionalized star-shaped poly(ethylene-*co*-propylene)s (hydrogenated polyisoprene)⁸³⁹ with urethane groups linked

⁸³⁷ Kautz, H.; van Beek, D. J. M.; Sijbesma, R. P.; Meijer, E. W. Cooperative End-to-End and Lateral Hydrogen-Bonding Motifs in Supramolecular Thermoplastic Elastomers. *Macromolecules* **2006**, *39*, 4265-7.

⁸³⁸ Lange, R. F. M.; van Gorp, M.; Meijer, E. W. Hydrogen-Bonded Supramolecular Polymer Networks. *J. Polym. Sci. A: Polym. Chem* **1999**, *37*, 3657-70.

⁸³⁹ Elkins, C. L.; Viswanathan, K.; Long, T. E. Synthesis and Characterization of Star-Shaped Poly(ethylene-*co*-propylene) Polymers Bearing Terminal Self-Complementary Multiple Hydrogen-Bonding Sites. *Macromolecules* **2006**, *39*, 3132-9.

through an isophorone diisocyanate-containing asymmetric cycloaliphatic linker (Figure 10.1), and the present work focuses on the effect of polymer architecture on the morphology of these hydrogen bonding polymers. A significant difference was observed in the case of star-shaped UPy-functionalized polymers compared to telechelic linear polymers. The star-shaped UPy functional polymers exhibited higher Young's moduli, persistence of high melt viscosity to elevated temperatures (160 °C), and behaved more elastically than telechelic linear UPy-functionalized polymers. Due to the presence of multiple (~6) UPy sites, the star polymer was capable of forming a hydrogen bonded network. This manuscript describes the morphology of hydrogen bonding UPy functionalized poly(ethylene-*co*-propylene) polymers as a function of architecture (star-shaped vs. linear), molecular weight, and level of functionality. The influence of these structural parameters on morphology was studied using a combination of small-angle X-ray scattering (SAXS) and atomic force microscopy (AFM). This is the first report of SAXS measurements on UPy-containing star shaped polymers. SAXS is a powerful technique for characterizing microphase separated morphologies, and in particular, SAXS has found extensive use in the characterization of hydrogen bond containing polymer such as polyurethanes.⁸⁴⁰ In the present study, the presence of associating sites that contain heteroatoms (N, O) provides an adequate electron density difference with the hydrocarbon ethylene/propylene backbone, and consequently, UPy-based hydrogen bonded macromolecules well-suited for X-ray scattering characterization.

⁸⁴⁰ Sheth, J. P.; Unal, S.; Yilgor, E.; Yilgor, I.; Beyer, F. L.; Long, T. E.; Wilkes, G. L. A comparative study of the structure–property behavior of highly branched segmented poly(urethane urea) copolymers and their linear analogs *Polymer* **2005**, 46, 10180-90.

10.3 Experimental

10.3.1 Materials

UPy end-functional poly(ethylene-*co*-propylene)s were synthesized previously in our research laboratories via living anionic polymerization of isoprene followed by hydrogenation and post-polymerization modification.⁸⁴¹ Briefly, isoprene was polymerized from a protected hydroxyl alkyl lithium initiator, 3-(*tert*-butyldimethylsiloxy)-1-propyllithium. The polymerizations were terminated with methanol (to form monofunctional polymers), with ethylene oxide (to form telechelic polymers), or coupled with divinylbenzene (to form star-shaped polymers). The polymers were then hydrogenated to remove unsaturation using a nickel (II) octoate and triethylaluminum catalyst which improved the thermal stability and prevented crosslinking during subsequent acid-catalyzed deprotection. The deprotected hydroxyl terminated poly(ethylene-*co*-propylene)s were then reacted with isophorone diisocyanate followed by 6-methylisocytosine in the presence of DMSO to produce the final UPy-functionalized poly(ethylene-*co*-propylene)s.

10.3.2 Polymer Characterization

¹H NMR spectra were collected in CDCl₃ at 400 MHz with a Varian Unity Spectrometer. Glass transition and melting temperatures were determined using a Perkin-Elmer Pyris 1 cryogenic differential scanning calorimetry (DSC) at a heating rate of 20 °C/min under nitrogen, which was calibrated using indium (mp = 156.60 °C) and zinc (mp = 419.47 °C).

⁸⁴¹ Elkins, C. L.; Viswanathan, K.; Long, T. E. Synthesis and Characterization of Star-Shaped Poly(ethylene-*co*-propylene) Polymers Bearing Terminal Self-Complementary Multiple Hydrogen-Bonding Sites. *Macromolecules* **2006**, 39, 3132-9.

Glass transition temperatures are reported as the transition midpoint during the second heat. Molecular weights were determined at 40 °C in THF (HPLC grade) at 1 mL/min using polystyrene standards on a Waters 717+ Auto-sampler size exclusion chromatography (SEC) equipped with 3 in-line 5 µm PLgel MIXED-C columns, a Waters 2410 refractive index (RI) detector operating at 880 nm, and Wyatt Technologies miniDAWN multiple angle laser light scattering (MALLS) detector operating at 690 nm, which was calibrated with polystyrene standards. The refractive index increment (dn/dc) was calculated online. All molecular weight values reported are absolute molecular weights obtained using the MALLS detector. SEC analysis was not reliable for star-shaped UPy functional polymers, due to their association at SEC concentrations in THF, which was verified using dynamic light scattering.

10.3.3 Small-angle X-ray Scattering (SAXS) Measurements

UPy end-functionalized poly(ethylene-*co*-propylene)s were dissolved in THF and cast in Teflon molds. The films were dried in a vacuum oven and stored at -15 °C until use. $\text{Cu}_{\text{K}\alpha}$ X-ray radiation was generated using a Rigaku Ultrax18 rotating anode X-ray generator operated at 45 kV and 100 mA. A nickel filter was used to eliminate all wavelengths but the $\text{Cu}_{\text{K}\alpha}$ doublet, with an average wavelength of $\lambda = 1.542 \text{ \AA}$. The exact beam center and the sample-to-detector distance of approximately 1.5 m were calibrated using silver behenate.⁸⁴² The 3 m camera uses 3-pinhole collimation (300, 200 and 600 µm), and a sample-to-detector distance of approximately 1.5 m. Two-dimensional data sets were collected using a

⁸⁴² Huang, T. C.; Toraya, H.; Blanton, T. N.; Wu, Y. X-Ray-Powder Diffraction Analysis of Silver Behenate, a Possible Low-Angle Diffraction Standard. *J Appl Cryst* **1993**, 26, 180-4.

Molecular Metrology 2D multi-wire area detector. The data were corrected for detector noise, sample absorption, and background scattering, followed by azimuthal averaging to obtain intensity as a function of the scattering vector, $I(q)$, where $q = 4\pi \cdot \sin(\theta)/\lambda$ and 2θ is the scattering angle. The data were then placed on an absolute scale using a type 2 glassy carbon sample 1.07 mm thick, previously calibrated at the Advanced Photon Source in the Argonne National Laboratory, as a secondary standard. All data processing and analysis were done using Wavemetrics IGOR Pro 5.04 software and IGOR procedures written by Dr. Jan Ilavsky of Argonne National Laboratory.

10.3.4 Atomic Force Microscopy (AFM) Measurements

A Veeco MultiMode™ scanning probe microscope equipped with a heating/cooling scanner and a Nanoscope IVa controller was used for tapping-mode AFM. Polymer films were solution cast from THF and attached to metal sample discs with a special epoxy which does not release volatiles upon heating. Samples were imaged at a set-point ratio of 0.6 at magnifications of 1 μm x 1 μm . Veeco's Nanosensor silicon tips having spring constants of 10-130 N/m were utilized for imaging.

10.4 Results and Discussion

10.4.1 Polymer Synthesis

Living anionic polymerization with a protected hydroxyl functional initiator enabled the synthesis of well-defined linear, telechelic and star-shaped polymers. The subsequent quantitative hydrogenation, deprotection of the hydroxyl group, and final telechelic

functionalization led to novel UPy-containing linear monofunctional, telechelic and star-shaped polymers.⁸⁴³ The molecular weight characterization of the UPy end-functionalized poly(ethylene-*co*-propylene)s and the precursor polyisoprenes is summarized in Table 10.1. ¹H NMR spectroscopy allowed determination of the extent of UPy-functionalization, which was typically 90 to 100% for linear poly(ethylene-*co*-propylene)s and 75% for star-shaped polymers. The weight fractions of UPy hydrogen bonding groups in the polymers ranged from 0.7 to 3.0 wt% (Table 1).

Due to the strong tendency of UPy groups to dimerize, different architectures and levels of functionality of the macromolecules were expected to produce diverse associated structures in solution (Figure 10.2). Based on previous literature, the monofunctional linear polymers were expected to produce a simple dimer in solution, with twice the molecular weight of the original polymer. The dimeric hydrogen bonding association is a dynamic equilibrium between associated and dissociated molecules, which shifts to higher association at increased concentration. The telechelic linear polymers were expected to form extended chains with a degree of polymerization depending on the functionality and strength of the association as reported earlier by Meijer et al.⁸⁴⁴ Based on average functionality greater than two, the star-shaped polymer with peripheral functionality was expected to form a non-covalent network-like structure.

⁸⁴³ Elkins, C. L.; Viswanathan, K.; Long, T. E. Synthesis and Characterization of Star-Shaped Poly(ethylene-*co*-propylene) Polymers Bearing Terminal Self-Complementary Multiple Hydrogen-Bonding Sites. *Macromolecules* **2006**, *39*, 3132-9.

⁸⁴⁴ Sijbesma, R. P.; Beijer, F. H.; Brunsveld, L.; Folmer, B. J. B.; Hirschberg, J. H. K. K.; Lange, R. F. M.; Lowe, J. K. L.; Meijer, E. W. Reversible Polymers Formed from Self-Complementary Monomers Using Quadruple Hydrogen Bonding. *Science* **1997**, *278*, 1601-4.

Table 10.1. Molecular weight and molecular weight distribution of monofunctional, telechelic, and star-shaped polyisoprenes before and after hydrogenation and UPy functionalization.

Polymer Topology	Polymer	Precursor M_n (M_w/M_n)^a	UPy functional M_n (M_w/M_n)^a	Weight % UPy Groups
Linear monofunctional	12K-mono	14800 (1.04)	18800 (1.06)	1.0
	24K-mono	23000 (1.04)	22300 (1.27)	0.7
Linear telechelic	12K-telechelic	11000 (1.05)	12200 (1.10)	2.9
	24K-telechelic	24300 (1.08)	19100 (1.27)	1.4
Star	90K-star	90700 (1.37)	NT	1.1

^a Determined using SEC at 40 °C in THF with a MALLS detector. Precursor molecular weights. NT = not tested due to association in SEC solvent (THF).

Monofunctional

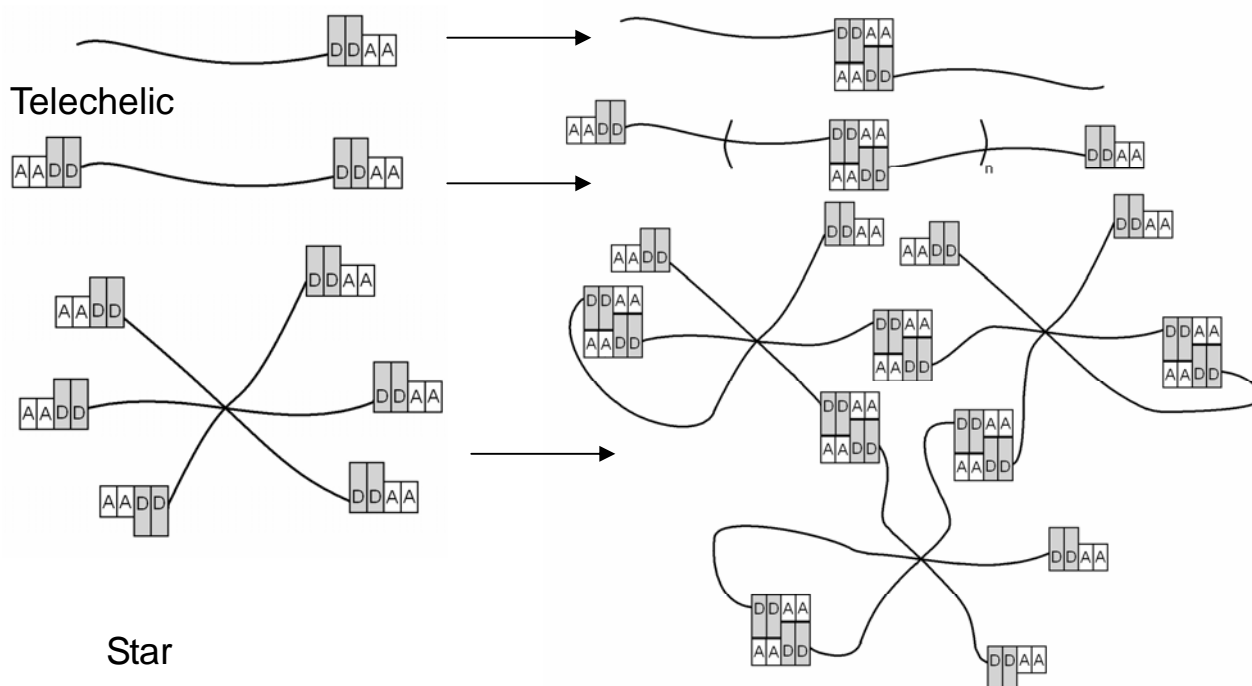


Figure 10.2. Representation of expected modes of association for different hydrogen bonding architectures in solution.

10.4.2 Small-angle X-Ray Scattering Studies

The UPy end-functionalized poly(ethylene-*co*-propylene)s bearing terminal functionality generated interesting scattering profiles, as shown in Figure 10.3. In general, all samples exhibited a single scattering maximum, which suggested the presence of a nanometer-scale structure, which was attributed to microphase separation of the hydrogen bonding domains within the rubbery ethylene-*co*-propylene matrix. The presence of microphase separation in the absence of solvent suggested UPy associations of greater than two, which is consistent with our previous rheological and DSC studies of telechelic UPy end-functional polyisoprenes.⁸⁴⁵ The presence of microphase separation was also consistent with DSC measurements of these polymers, which indicated that the UPy hydrogen bonding group did not alter the glass transition temperature.⁸⁴⁶ Mixing of the hydrogen bonding groups into the continuous ethylene-*co*-propylene matrix would be expected to increase the glass transition temperature, as previously observed for nucleobase end-functional polymers.⁸⁴⁷ The existence of microphase separation despite the low weight fraction of hydrogen bonding groups (0.7 to 2.9 wt%) suggested strong association of the polar UPy groups into aggregates. In addition, Stadler and coworkers, who studied urazole hydrogen bonding groups attached to polydiene backbones, claimed that the urazole sites microphase

⁸⁴⁵ Yamauchi, K.; Lizotte, J. R.; Hercules, D. M.; Vergne, M. J.; Long, T. E. Combinations of Microphase Separation and Terminal Multiple Hydrogen Bonding in Novel Macromolecules. *J Am Chem Soc* **2002**, 124, 8599-604.

⁸⁴⁶ Elkins, C. L.; Viswanathan, K.; Long, T. E. Synthesis and Characterization of Star-Shaped Poly(ethylene-*co*-propylene) Polymers Bearing Terminal Self-Complementary Multiple Hydrogen-Bonding Sites. *Macromolecules* **2006**, 39, 3132-9.

⁸⁴⁷ Mather, B. D.; Lizotte, J. R.; Long, T. E. Synthesis of Chain End Functionalized Multiple Hydrogen Bonded Polystyrenes and Poly(alkyl acrylates) Using Controlled Radical Polymerization. *Macromolecules* **2004**, 37, 9331-7.

separated at only 3 mol% when dispersed in a non-polar rubbery matrix.⁸⁴⁸ Stadler and coworkers also observed single SAXS peaks for urazoylbenzoic acid functionalized polybutadiene ($\sim 0.1 \text{ \AA}^{-1}$) and also concluded that these resulted from interparticle scattering from aggregates of the hydrogen bonding groups in the rubber matrix.^{849,850} However, in sharp contrast to UPy functional polymers, urazoylbenzoic acid functionalized polymers, are expected to aggregate since hydrogen bonding can occur from two sides of the molecule. For example, 4-phenylurazole functionalized polymers, which enable only a simple dimerization of functional groups, did not reveal SAXS maxima.⁸⁴⁹ Previous SAXS experiments by Meijer et al. involving UPy end-functionalized three-arm poly(ethylene oxide-*co*-propylene oxide)s with similar asymmetric cycloaliphatic linkers and adjacent urethane groups indicated no evidence of microphase separation.⁸⁵¹ The difference between these previous observations and the present results was presumed to arise from the lower polarity of the poly(ethylene-*co*-propylene) matrix compared to poly(ethylene oxide-*co*-propylene oxide), leading to a greater insolubility of the UPy groups in the matrix.

⁸⁴⁸ Dardin, A.; Stadler, R.; Boeffel, C.; Spiess, H. W. Molecular dynamics of new thermoplastic elastomers based on hydrogen bonding complexes: a deuterium nuclear magnetic resonance investigation. *Makromol Chem* **1993**, 194, 3467-77.

⁸⁴⁹ Hilger, C.; Stadler, R. Cooperative Structure Formation by Directed Noncovalent Interactions in an Unpolar Polymer Matrix. 7. Differential Scanning Calorimetry and Small-Angle X-ray Scattering. *Macromolecules* **1992**, 25, 6670-80.

⁸⁵⁰ Hilger, C.; Stadler, R. New Multiphase Architecture from Statistical Copolymers by Cooperative Hydrogen Bond Formation. *Macromolecules* **1990**, 23, 2095-7.

⁸⁵¹ Lange, R. F. M.; van Gurp, M.; Meijer, E. W. Hydrogen-Bonded Supramolecular Polymer Networks. *J. Polym. Sci. A: Polym. Chem* **1999**, 37, 3657-70.

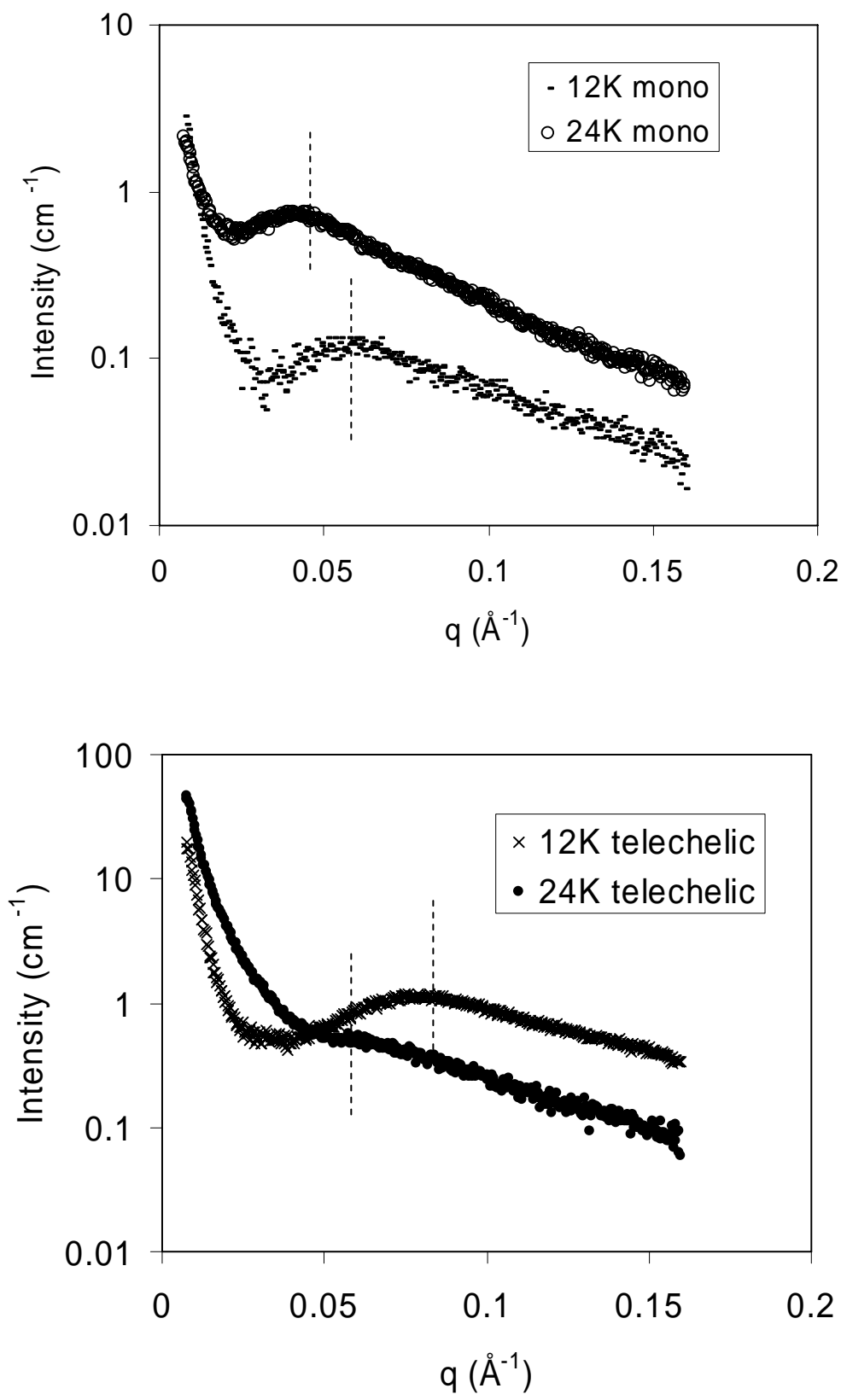


Figure 10.3. SAXS data for UPy-containing monofunctional (left chart) and telechelic (right chart) poly(ethylene-*co*-propylene)s polymers.

The hydrogen bonding polymers exhibited regular trends in the position of the scattering maxima with respect to molecular weight and architecture. The positions of the scattering maxima were calculated through fitting the sum of a Gaussian peak-shape and a linear baseline to the scattering data. The positions of the maxima were then used to determine the Bragg spacing, $d = 2\pi/q$, which corresponded to the average interdomain spacings of 8 to 16 nm (Table 10.2). A shift in the position of the scattering maxima to lower angles (or larger spacings) with increasing molecular weight (Figure 10.3) was observed. Both monofunctional (12K-mono and 24K-mono) and telechelic (12K-telechelic and 24K-telechelic) UPy end-functional poly(ethylene-*co*-propylene)s exhibited a shifting of the SAXS maxima to lower q with increasing molecular weight. The molecular weight between UPy groups was presumed to correlate with the distance between UPy-rich domains in a microphase separated morphology. Stadler et al. also observed a shifting of the SAXS maxima for urazoylbenzoic acid functionalized polybutadiene to higher q for higher levels of functionality (lower molecular weight between functional groups).⁸⁵² Jérôme et al. correlated Bragg spacing with molecular weight ($d \sim M_n^{0.5}$) for telechelic polyisoprene ionomers, and similar trends with molecular weight were apparent for the present UPy functionalized polymers.⁸⁵³

⁸⁵² Hilger, C.; Stadler, R. Cooperative Structure Formation by Directed Noncovalent Interactions in an Unpolar Polymer Matrix. 7. Differential Scanning Calorimetry and Small-Angle X-ray Scattering. *Macromolecules* **1992**, 25, 6670-80.

⁸⁵³ Sobry, R.; Fontaine, F.; Ledent, J.; Foucart, M.; Jerome, R. Morphology of Ionic Aggregates in Carboxylato- and Sulfonato-Telechelic Polyisoprenes As Investigated by Small-Angle X-ray Scattering. *Macromolecules* **1998**, 31, 4240-52.

Table 10.2. Scattering maxima and corresponding Bragg spacings for UPy functional poly(ethylene-*co*-propylene)s.

Polymer	q^* (\AA^{-1})	d (nm)
12K-mono	0.058	10.8 ± 0.1
12K-telechelic	0.078	8.1 ± 0.1
24K-mono	0.041	15.5 ± 0.1
24K-telechelic	0.059	10.7 ± 0.1
90K-star	0.074	8.5 ± 0.1

Upon further examination of the scattering data as a function of architecture, it appeared that a transition from monofunctional linear to telechelic linear functionality resulted in a shift of the maxima to higher angles (smaller real-space correlation distances), as illustrated in Figure 10.4. This effect was consistently observed for samples of different molecular weight, and was attributed to an increase in the overall concentration of hydrogen bonding groups while maintaining the molecular weight of the polymer. Although the telechelic UPy functional polymers did not possess perfect difunctionality ($f > 1.80$), their functionality was twice that of the monofunctional UPy functional polymers ($f > 0.90$).

The 90K-star polymer, which contained an average of eight 12K arms, and an average of six UPy groups due to incomplete functionalization, produced a single scattering maximum in a similar fashion to linear monofunctional and telechelic oligomers (Figure 10.5). However, the position of this peak was at a higher q value than the positions of the

scattering maxima for the 12K-mono or the 24K-telechelic, which suggested an even smaller distance between microphase separated domains of the UPy hydrogen bonding groups. The star architecture was viewed as a collection of linear, monofunctional 12 kg/mol arms joined together at their non-functional termini. Thus, the presence of intramolecular association is more probable, which would also contribute to a decrease in the size of the star-shaped polymer. Future efforts will involve modeling the scattering behavior of the UPy-containing polymers with models such as the Yarusso-Cooper model, in order to better understand the morphology of these unique polymers.^{854,855}

⁸⁵⁴ Benetatos, N. M.; Heiney, P. A.; Winey, K. I. Reconciling STEM and X-ray Scattering Data from a Poly(styrene-*ran*-methacrylic acid) Ionomer: Ionic Aggregate Size. *Macromolecules* **2006**, *39*, 5174-6.

⁸⁵⁵ Yarusso, D. J.; Cooper, S. L. Microstructure of Ionomers: Interpretation of Small-Angle X-ray Scattering Data. *Macromolecules* **1983**, *16*, 1871-80.

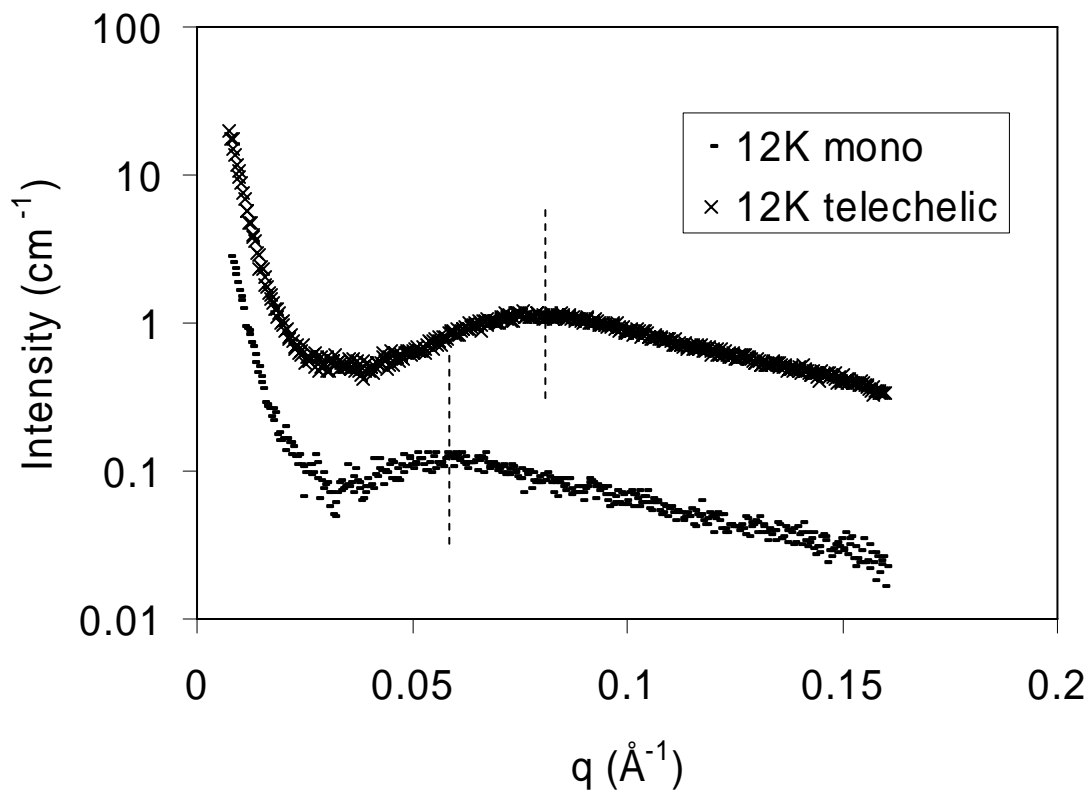


Figure 10.4. SAXS data showing the effect of functionality for 12 kg/mol polymers.

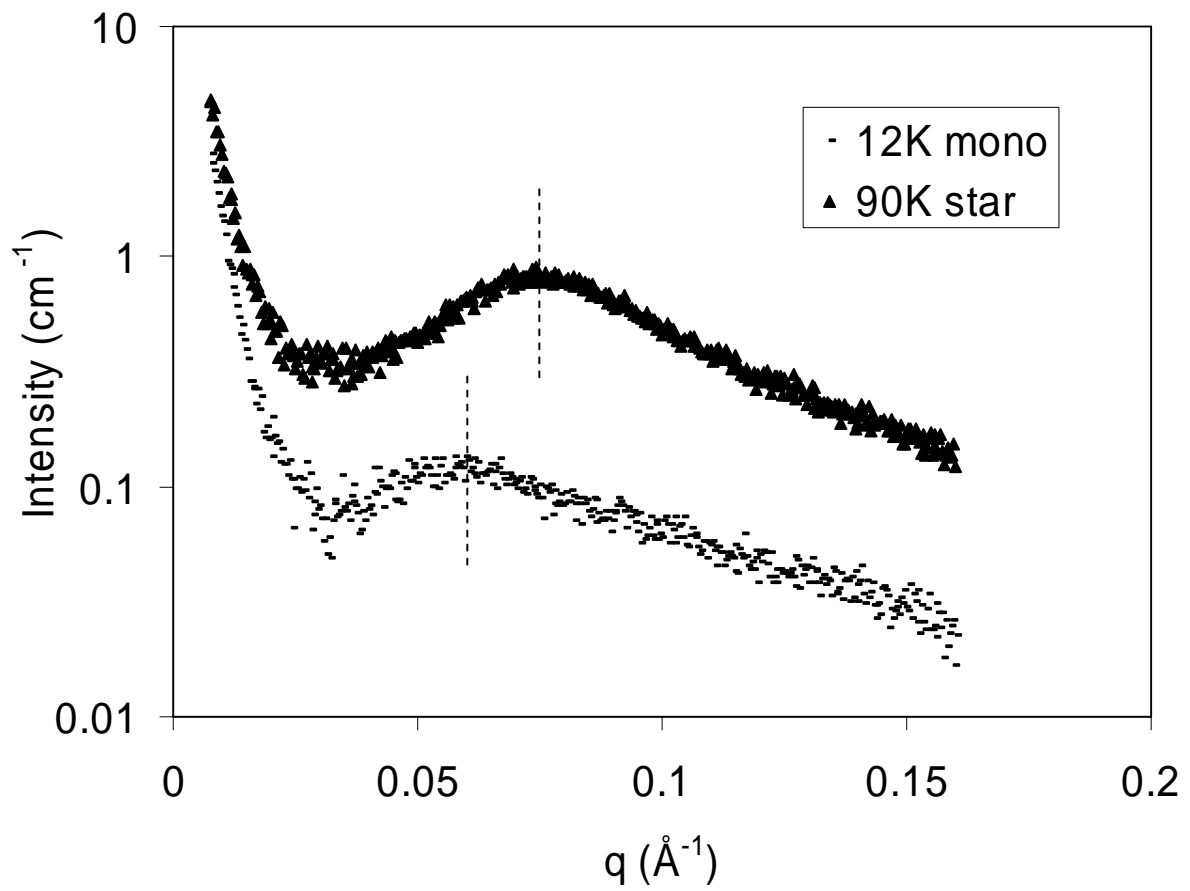


Figure 10.5. Scattering profile for star-shaped poly(ethylene-*co*-propylene) with UPy functional periphery and the 12K monofunctional polymer.

10.4.3 Atomic Force Microscopy

Tapping mode AFM studies were performed on the UPy end-functional poly(ethylene-*co*-propylene)s. It is well established that tapping mode AFM allows for detailed analysis of the surface morphology as well as topography.⁸⁵⁶ The UPy functionalized 90K star-shaped polymer was the only sample which clearly revealed a surface texture that was indicative of microphase separation (Figure 10.6). Numerous solvent casting procedures and annealing procedures were performed with the linear samples and a microphase separated surface texture was not observed. For the star-shaped architecture, it was proposed that the hard phases were less mobile in the rubbery ethylene-*co*-propylene matrix due to the central connection point in the star topology. Meijer et al. have also observed the absence of microphase separation on the surfaces of telechelic UPy functional poly(ethylene-*co*-butylene)s.⁸⁵⁷ In the case of urethane or urea groups bonded to the UPy functionality through symmetric 1,6-hexylene linkers, fibril-like surface textures were observed due to the lateral stacking of the urea groups, which differed strikingly from the images of the present star-shaped poly(ethylene-*co*-propylene). The differences observed in the AFM images of the present system, which also contains urethane groups, was proposed to arise from the asymmetry of the isophorone diisocyanate linker, which presumably prevents stacking of the urethane groups.

⁸⁵⁶ Maganov, S. N., Atomic Force Microscopy in Analysis of Polymers. In *Encyclopedia of Analytical Chemistry*, Meyers, R. A., Ed. John Wiley and Sons: Chichester, UK, 2000; pp 7432-91.

⁸⁵⁷ Kautz, H.; van Beek, D. J. M.; Sijbesma, R. P.; Meijer, E. W. Cooperative End-to-End and Lateral Hydrogen-Bonding Motifs in Supramolecular Thermoplastic Elastomers. *Macromolecules* **2006**, 39, 4265-7.

The phase image of the 90K star-shaped polymer exhibited 10-15 nm hard phases dispersed in a rubbery matrix. Typical interdomain distances as measured using AFM were 10-20 nm, although the spacing was not regular and long-range ordering was not apparent. Due to the low UPy content in the star polymer (1.1 wt%), the morphology was expected to consist of dispersed domains consisting of UPy groups. The 90K star-shaped polymer was subjected to variable temperature AFM in order to probe the structure of the hard phases upon dissociation of the hydrogen bonding groups (Figure 10.6). Interestingly, the hard phases persisted to 130 °C, which was the limit of our experimental temperature range, however, the phase contrast and apparent sizes of the hard phases both diminished significantly. Our laboratories have shown earlier that UPy associations contribute to the rheological behavior in the melt at elevated temperature.⁸⁵⁸ The melting phenomena of the double helical DNA molecule has provided a paradigm for tunable intermolecular interactions.⁸⁵⁹ More recently, similar well-defined hydrogen bond dissociation or “melting” was observed in solution studies of synthetic adenine and thymine functionalized acrylic polymers.⁸⁶⁰ Stadler et al. also observed the temperature sensitivity of hydrogen bonded structures in urazoylbenzoic acid functionalized polybutadiene using variable temperature SAXS.⁸⁶¹

⁸⁵⁸ McKee, M. G.; Elkins, C. L.; Park, T.; Long, T. E. Influence of Random Branching on Multiple Hydrogen Bonding in Poly(alkyl methacrylate)s. *Macromolecules* **2005**, 38, 6015-23.

⁸⁵⁹ Haq, I.; Chowdhry, B. Z.; Chaires, J. B. Singular value decomposition of 3-D DNA melting curves reveals complexity in the melting process. *Eur Biophys J* **1997**, 26, 419-26.

⁸⁶⁰ Lutz, J. F.; Thunemann, A. F.; Rurack, K. DNA-like "Melting" of Adenine- and Thymine-Functionalized Synthetic Copolymers. *Macromolecules* **2005**, 38, 8124-6.

⁸⁶¹ Hilger, C.; Stadler, R. Cooperative Structure Formation by Directed Noncovalent Interactions in an Unpolar Polymer Matrix. 7. Differential Scanning Calorimetry and Small-Angle X-ray Scattering. *Macromolecules* **1992**, 25, 6670-80.

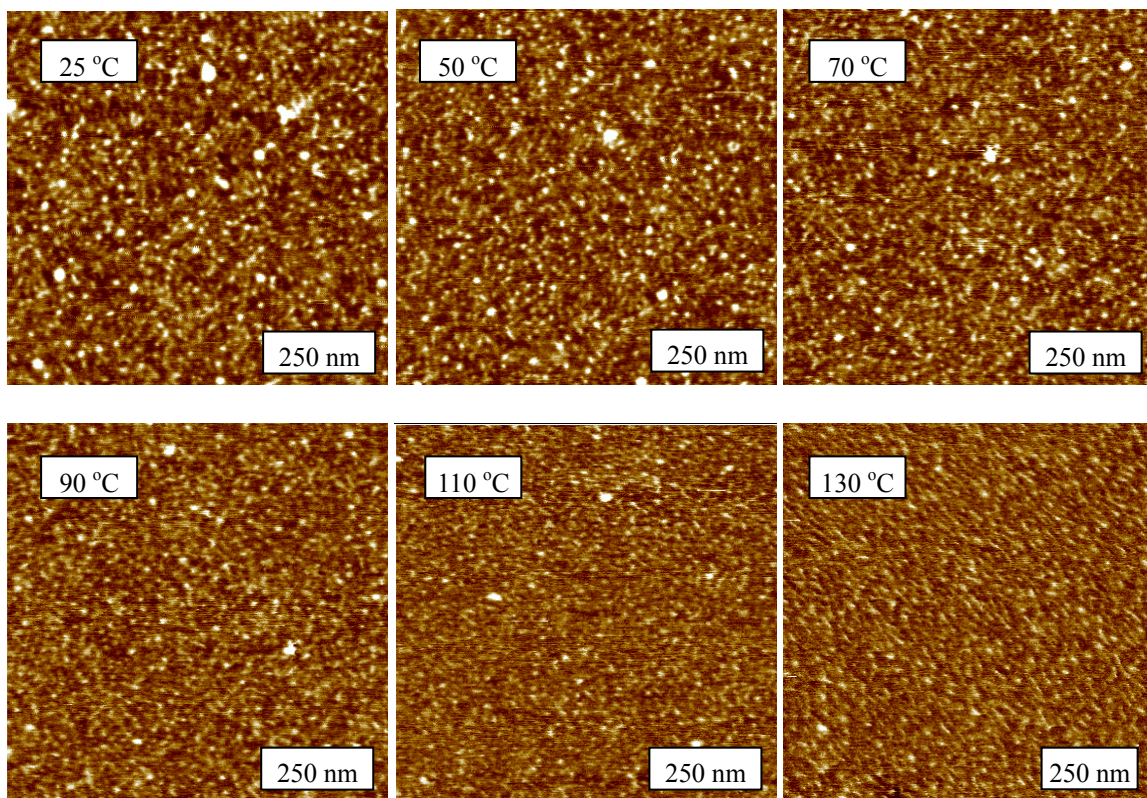


Figure 10.6. Variable temperature tapping mode AFM images of the UPy star-shaped polymer.

Each image is calibrated to the same phase range and measures 750 nm per side.

10.5 Conclusions

UPy end-functional poly(ethylene-*co*-propylene)s were found to form microphase separated morphologies as determined from small-angle X-ray scattering studies. The maxima in the SAXS data arose from interdomain scattering from the microphase separated UPy-rich domains within the ethylene-*co*-propylene hydrocarbon matrix. The presence of microphase separated domains in these polymers suggested an aggregation of the hydrogen bonding groups beyond simple dimerization, which would not produce a clear scattering peak in SAXS. The Bragg spacings corresponding to the scattering maxima followed trends with molecular weight and molecular architecture. Specifically, increased molecular weight between UPy groups lead to an increased spacing between domains, and increased functionality of telechelic polymers lead to decreased spacings between microphase separated domains. Variable temperature AFM revealed a decrease in phase contrast with heating to 130 °C.

10.6 Acknowledgements

This material is based upon work supported by, or in part by, the U.S. Army Research Laboratory and the U.S. Army Research Office under grant number DAAD19-02-1-0275 Macromolecular Architecture for Performance (MAP) MURI.

Chapter 11. Real-time Monitoring of Molecular Recognition of Complementary Ionic Guest Molecules with Hydrogen Bonding Block Copolymers Using Quartz-Crystal Microbalance with Dissipation (QCM-D)

11.1 Abstract

The molecular recognition between a water-soluble uracil functionalized phosphonium salt and an adenine containing block copolymer poly(9-vinylbenzyladenine-*b-n*-butyl acrylate-*b-9*-vinylbenzyladenine) surface was studied using quartz crystal microbalance with dissipation (QCM-D) measurements. Adsorption experiments revealed a frequency drop of 17.6 Hz associated with the adsorption. The uracil phosphonium salt was not completely rinsed from the surface with water, suggesting strong specific recognition. Control experiments with non-nucleobase containing poly(styrene-*b-n*-butyl acrylate-*b*-styrene) block copolymers revealed a frequency drop of 8.8 Hz, which was nearly completely reversible upon rinsing with water. X-ray crystallographic analysis of the uracil phosphonium salt revealed the competitive hydrogen bonding of water with the uracil group, which may play a role in the adsorption measurements.

11.2 Introduction

Hydrogen bonding enables the introduction of thermoreversible properties into macromolecules through the creation of specific non-covalent intermolecular interactions.⁸⁶² Recent interest in hydrogen bonding in both supramolecular⁸⁶³ and macromolecular⁸⁶⁴ design has inspired numerous new explorations. The strength of hydrogen bonding interactions is highly dependent on temperature, solvent, humidity and pH, thus allowing control of the degree of association through a number of environmental parameters.

Nucleobases, which exhibit association strengths near 100 M^{-1} , are ideal for introducing dynamic hydrogen bonding interactions into polymers.⁸⁶⁵ Rowan et al. noted that the behavior of the isolated nucleobases in synthetic polymers is quite different from their behavior in DNA where they are bound to a complementary base.⁸⁶⁶ Multiple complementary association modes are possible for nucleobases, including the classical Watson-Crick mode which is present in DNA as well as the less commonly observed Hoogsteen association mode.⁸⁶⁷ Furthermore, nucleobases exhibit several weak

⁸⁶² Yamauchi, K.; Lizotte, J. R.; Hercules, D. M.; Vergne, M. J.; Long, T. E. Combinations of Microphase Separation and Terminal Multiple Hydrogen Bonding in Novel Macromolecules. *J Am Chem Soc* **2002**, 124, 8599-604.

⁸⁶³ Brunsveld, L.; Folmer, B. J. B.; Meijer, E. W.; Sijbesma, R. P. Supramolecular Polymers. *Chem Rev* **2001**, 101, 4071-98.

⁸⁶⁴ Ilhan, F.; Galow, T. H.; Gray, M.; Clavier, G.; Rotello, V. M. Giant Vesicle Formation through Self-Assembly of Complementary Random Copolymers. *J Am Chem Soc* **2000**, 122, 5895-6.

⁸⁶⁵ Kyogoku, Y.; Lord, R. C.; Rich, A. The Effect of Substituents on the Hydrogen Bonding of Adenine and Uracil Derivatives. *Proc Natl Acad Sci USA* **1967**, 57, 250-7.

⁸⁶⁶ Sivakova, S.; Bohnsak, D. A.; Mackay, M. E.; Suwanmala, P.; Rowan, S. J. Utilization of a Combination of Weak Hydrogen-Bonding Interactions and Phase Segregation to Yield Highly Thermosensitive Supramolecular Polymers. *J Am Chem Soc* **2005**, 127, 18202-18211.

⁸⁶⁷ Ghosal, G.; Muniyappa, K. Hoogsteen base-pairing revisited: Resolving a role in normal biological processes and human diseases. *Biochemical and Biophysical Research Communications* **2006**, 343, 1-7.

self-association modes ($K_a < 10 \text{ M}^{-1}$),⁸⁶⁵ which compete with the complementary association modes.

Complementary hydrogen bonding interactions facilitate the introduction of guest molecules containing complementary recognition units. Others have shown the recognition of guest molecules through hydrogen bonding interactions in both solution⁸⁶⁸ and the solid state.⁸⁶⁹ Rotello et al. have used three-point hydrogen bonding between diacyldiaminopyridines and thymine to attach guest molecules containing flavin⁸⁷⁰ or POSS to polystyrene.⁸⁶⁹ Rotello has also used hydrogen bond functional polymers to reversibly attach polymers on surfaces,⁸⁷¹ and reversibly attach functional small molecules on polymers.⁸⁷² Ten Brinke et al. studied the blending of alkyl substituted phenols on poly(vinyl pyridine).⁸⁷³ Guest molecules can also increase the solubility of hydrogen bonding polymers, maintaining homogeneity during polymerization reactions.⁸⁷⁴ We recently reported on the introduction of phosphonium ionic guest molecules into hydrogen bonding block copolymers

⁸⁶⁸ Thibault, R. J.; Hotchkiss, P. J.; Gray, M.; Rotello, V. M. Thermally Reversible Formation of Microspheres through Non-Covalent Polymer Cross-Linking. *J Am Chem Soc* **2003**, 125, 11249-11252.

⁸⁶⁹ Carroll, J. B.; Waddon, A. J.; Nakade, H.; Rotello, V. M. "Plug and Play" Polymers. Thermal and X-ray Characterizations of Noncovalently Grafted Polyhedral Oligomeric Silsesquioxane (POSS)-Polystyrene Nanocomposites. *Macromolecules* **2003**, 36, 6289-6291.

⁸⁷⁰ Ilhan, F.; Galow, T. H.; Gray, M.; Clavier, G.; Rotello, V. M. Giant Vesicle Formation through Self-Assembly of Complementary Random Copolymers. *J Am Chem Soc* **2000**, 122, 5895-5896.

⁸⁷¹ Norsten, T. B.; Jeung, E.; Thibault, R. J.; Rotello, V. M. Specific Hydrogen-Bond-Mediated Recognition and Modification of Surfaces Using Complementary Functionalized Polymers. *Langmuir* **2003**, 19, 7089-93.

⁸⁷² Ilhan, F.; Gray, M.; Rotello, V. M. Reversible Side Chain Modification through Noncovalent Interactions. "Plug and Play" Polymers. *Macromolecules* **2001**, 34, 2597-601.

⁸⁷³ Valkama, S.; Ruotsalainen, T.; Kosonen, H.; Ruokolainen, J.; Torkkeli, M.; Serimaa, R.; ten Brinke, G.; Ikkala, O. Amphiphiles Coordinated to Block Copolymers as a Template for Mesoporous Materials. *Macromolecules* **2003**, 36, 3986-3991.

⁸⁷⁴ Stubbs, L. P.; Weck, M. Towards a Universal Polymer Backbone: Design and Synthesis of Polymeric Scaffolds Containing Terminal Hydrogen-Bonding Recognition Motifs at Each Repeating Unit. *Chem Eur J* **2003**, 9, 992-9.

with concomitant changes in morphology and physical properties.⁸⁷⁵

The quartz crystal microbalance (QCM) technique is a powerful technique for monitoring surface adsorption due to the high sensitivity of the quartz crystal to adsorbed mass. Recently, dissipative measurements of the oscillation have been coupled with QCM, allowing a measure of changes in viscous losses on the surface of the crystal. Hook et al. recently demonstrated the application of the quartz crystal microbalance technique to hydrogen bonding systems in the study of adsorption of DNA oligobases to complementary surface-anchored PNA.⁸⁷⁶ QCM has also found applications in biological systems, where recognition of antibodies and proteins can be studied.⁸⁷⁷ The sensitivity of the QCM technique is typically very high, allowing detection of very small amounts of adsorbed mass, even allowing detection of gases.⁸⁷⁸

In this manuscript, we discuss the molecular recognition of an adenine-containing surface with a complementary uracil-containing phosphonium salt (Figure 11.1). In DNA, hydrogen bonding and π -stacking interactions hold the double helix together, despite repulsive interactions between the phosphate ionic backbones. This is an inspiration for the

⁸⁷⁵ Mather, B. D.; Baker, M. B.; Beyer, F. L.; Green, M. D.; Berg, M. A. G.; Long, T. E. Multiple Hydrogen Bonding for the Reversible Attachment of Ionic Functionality in Block Copolymers. *Macromolecules* **2007**, Submitted.

⁸⁷⁶ Hook, F.; Ray, A.; Norden, B.; Kasemo, B. Characterization of PNA and DNA Immobilization and Subsequent Hybridization with DNA Using Acoustic-Shear-Wave Attenuation Measurements. *Langmuir* **2001**, *17*, 8305-12.

⁸⁷⁷ Hook, F.; Rodahl, M.; Brzezinski, P.; Kasemo, B. Energy Dissipation Kinetics for Protein and Antibody-Antigen Adsorption under Shear Oscillation on a Quartz Crystal Microbalance. *Langmuir* **1998**, *14*, 729-34.

⁸⁷⁸ Pasquinet, E.; Bouvier, C.; They-Merland, F.; Hairault, L.; Lebret, B.; Methivier, C.; Pradier, C. M. Synthesis and adsorption on gold surfaces of a functionalized thiol: elaboration and test of a new nitroaromatic gas sensor. *J Coll Int Sci* **2004**, *272*, 21-7.

current work, in which hydrogen bonds reversibly connect strongly interacting ionic molecules to a neutral polymer backbone.

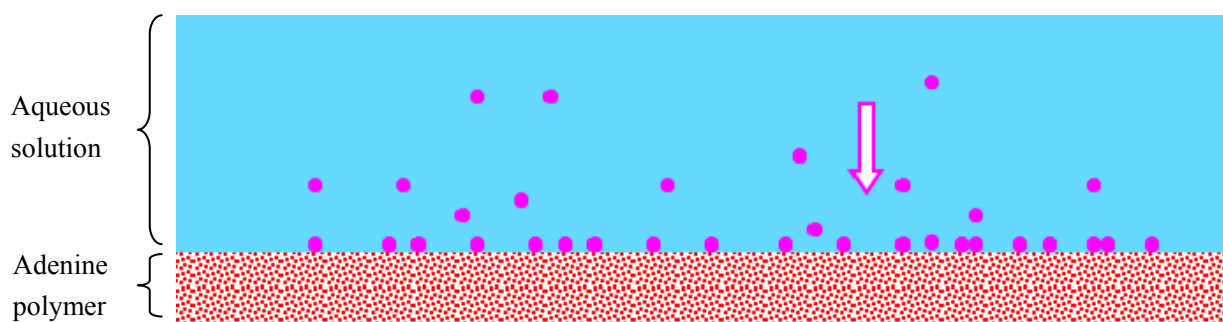
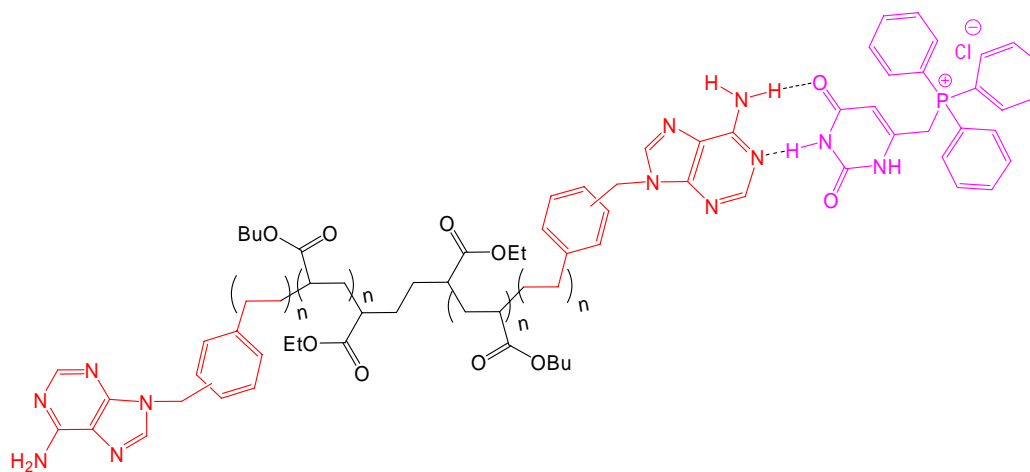


Figure 11.1. Molecular recognition of uracil containing phosphonium salt with complementary hydrogen bonding block copolymer.

11.3 Experimental

11.3.1 Materials

n-Butyl acrylate (99%) was purchased from Aldrich and purified using an alumina column and subsequent vacuum distillation from calcium hydride. *N*-*tert*-butyl-*N*-(1-diethylphosphono-2,2-dimethylpropyl)-*N*-oxyl (DEPN) nitroxide,⁸⁷⁹ DEPN₂,⁸⁸⁰ UPPh₃⁺⁸⁸¹ and 9-vinylbenzyl adenine⁸⁸² were synthesized according to the previous literature.

11.3.2 Polymerization of *n*-Butyl Acrylate from DEPN₂

DEPN₂ alkoxyamine (212 mg, 0.269 mmol) and DEPN nitroxide (31 mg, 0.105 mmol) were weighed into a 100-mL round-bottomed flask containing a magnetic stirbar. The flask was sealed with a three-way joint allowing introduction of reagents via syringe and application of vacuum and nitrogen. The flask was evacuated to 60 mtorr and refilled with high-purity nitrogen three times. Purified *n*-butyl acrylate (30 mL, 209 mmol) was added via syringe and the mixture was degassed with three freeze-pump-thaw cycles. Finally, the flask was immersed in an oil bath thermostated at 122 °C for 3 h. After the polymerization, residual

⁸⁷⁹ Grimaldi, S.; Finet, J. P.; Le Moigne, F.; Zeghdaoui, A.; Tordo, P.; Benoit, D.; Fontanille, M.; Gnanou, Y. Acyclic B-Phosphonylated Nitroxides: A New Series of Counter-Radicals for "Living"/Controlled Free Radical Polymerization. *Macromolecules* **2000**, *33*, 1141-7.

⁸⁸⁰ Mather, B. D.; Baker, M. B.; Beyer, F. L.; Green, M. D.; Berg, M. A. G.; Long, T. E. Multiple Hydrogen Bonding for the Reversible Attachment of Ionic Functionality in Block Copolymers. *Macromolecules* **2007**, Submitted.

⁸⁸¹ Klein, R. S.; Fox, J. J. Nucleosides. LXXVIII. Synthesis of Some 6- Substituted Uracils and Uridines by the Wittig Reaction. *J Org Chem* **1972**, *37*, 4381-6.

⁸⁸² Srivatsan, S. G.; Parvez, M.; Verma, S. Modeling of Prebiotic Catalysis with Adenylated Polymeric Templates: Crystal Structure Studies and Kinetic Characterization of Template-Assisted Phosphate Ester Hydrolysis. *Chem. Eur. J.* **2002**, *8*, 5184-91.

monomer was removed in vacuo (60 mtorr, 40 °C, 6 h). SEC analysis in THF revealed molecular weight data $M_n = 16500$, $M_w/M_n = 1.24$.

11.3.3 Synthesis of Adenine Containing Block Copolymer

Poly(*n*-butyl acrylate) homopolymer (4.83 g, $M_n = 16500$, $M_w/M_n = 1.24$) and 9-vinylbenzyladenine (0.99 g, 3.9 mmol) were added to a 50-mL round-bottomed flask with a magnetic stirbar. The flask was sealed with a three-way joint and evacuated to 60 mtorr and refilled with high-purity nitrogen three times. DMF (15 mL) was then syringed into the flask and the mixture was degassed with three freeze-pump-thaw cycles. The flask was then immersed in an oil bath at 122 °C for 5 h. After the polymerization, the polymer was isolated via precipitation into methanol. ^1H NMR (DMSO- d_6) revealed block molecular weights $A_{1.5K}$ - $nBA_{16.5K}$ - $A_{1.5K}$. ^1H NMR (400 MHz, DMSO- d_6 , 25 °C) (δ , ppm): 0.86 (t, CH_3 , 3H) 1.30 (q, $\text{COOCH}_2\text{CH}_2\text{CH}_2\text{CH}_3$, 2H), 1.5 (br, $\text{CH}_2\text{-CH-COO}$ and $\text{COOCH}_2\text{CH}_2\text{-}$), 1.75 (br, $\text{CH}_2\text{-CH-COO-}$, 1H), 2.2 (br, CH-COO- , 1H), 4.0 (br, COOCH_2 , 2H), 5.2 (br, Ph-CH_2 , 2H), 6.3 (br, Ph, 2H), 6.9 (br, Ph, 2H), 7.6 (br, NH_2 , 2H), 8.1 (br, adenine ring protons, 2H).

11.3.4 Synthesis of Poly(styrene-*b*-*n*-butyl acrylate-*b*-styrene) Block Copolymer

Poly(*n*-butyl acrylate) homopolymer (155 mg, $M_n = 23,700$, $M_w/M_n = 1.11$) and styrene (5 mL, 43 mmol) were added to a 50-mL round-bottomed flask with a magnetic stirbar. The flask was sealed with a three-way joint and the solution was degassed with three freeze-pump-thaw cycles. The flask was then immersed in an oil bath at 120 °C for 40 min. After the polymerization, the polymer was isolated via precipitation into methanol. ^1H

NMR (CDCl_3) revealed block molecular weights $\text{S}_{14.6\text{K}}\text{-nBA}_{23.7\text{K}}\text{-S}_{14.6\text{K}}$. SEC measurements in THF revealed a molecular weight of $M_n = 48400$, $M_w/M_n = 1.12$ (MALLS).

11.3.5 Characterization

Size exclusion chromatography (SEC) was performed at 40 °C in HPLC grade tetrahydrofuran at 1 mL/min using a Waters size-exclusion chromatographer equipped with an autosampler, 3 in-line 5 μm PLgel MIXED-C columns. Detectors included a Waters 410 differential refractive index (DRI) detector operating at 880 nm, and a Wyatt Technologies miniDAWN multiangle 690 nm laser light scattering (MALLS) detector, calibrated with PS standards. All reported molecular weight values are absolute molecular weights obtained using the MALLS detector. ^1H NMR spectroscopic data was collected in CDCl_3 on a Varian 400 MHz spectrometer at ambient temperature. A Veeco MultiMode™ scanning probe microscope was used for tapping-mode AFM. Polymer films were solution cast from chloroform on silicon. Samples were imaged at a set-point ratio of 0.6 at magnifications of 500 nm x 500 nm. Veeco's Nanosensor silicon tips having spring constants of 10-130 N/m were utilized for imaging. X-ray data was collected on an Oxford Diffraction Xcalibur™ diffractometer equipped with a Sapphire™ 3 CCD detector. The data collection routine, unit cell refinement, and data processing were carried out with the program CrysAlis(v1.171, Oxford Diffraction: Wroclaw, Poland, 2004). Structure solution and refinement were performed with the graphical user interface WinGX.⁸⁸³ The structures were solved by direct

⁸⁸³ Farrugia, L. J. WinGX: An Integrated System of Windows Programs for the solution, Refinement and Analysis of Single X-ray Diffraction Data. *J Appl Cryst* **1999**, 32, 837-8.

methods using SHELXS-97⁸⁸⁴ and refined using SHELXL-97. The final refinement model involved anisotropic displacement parameters for non-hydrogen atoms and a riding model for all hydrogens. The program package ORTEP-3 was used for molecular graphic generation.⁸⁸⁵

11.3.6 Quartz Crystal Microbalance with Dissipation (QCM-D) Measurements

Quartz crystal microbalance measurements were performed on a Q-Sense E4 operating in 7th overtone on AT-cut quartz crystals with gold electrodes with a fundamental frequency of 4.97 MHz. The instrument possessed a normal mass adsorption sensitivity of 3.5 ng/cm² and a maximum sensitivity of 1 ng/cm². The measurements were conducted at 25 °C at a flow rate of 150 uL/min. All aqueous solutions were prepared from Millipore water. Exposure to UPPh₃⁺ was conducted with solutions of 0.5 wt% concentration. Data analysis was performed using QTools software. The bare quartz sensor crystals were cleaned prior to use by exposure to UV/ozone for 10 min, followed by rinsing with water and drying with nitrogen. Polymer films were deposited on the wafers by spin-coating at 3000 rpm from chloroform solution at 0.37 wt% concentration. The sample was then dried annealed at 155 °C under vacuum.

11.4 Results and Discussion

11.4.1 Synthesis of Nucleobase Functional Hydrogen Bonding Block Copolymers

A novel, difunctional alkoxyamine initiator based on DEPN nitroxide, denoted DEPN₂,

⁸⁸⁴ Sheldrick, G. M. SHELX97. Programs for Crystal Structure Analysis. University of Gottingen, Gottingen, 1997.

⁸⁸⁵ Farrugia, L. J. ORTEP-3 for Windows - a version of ORTEP-III with a Graphical User Interface (GUI). *J Appl Cryst* **1997**, 30, 565.

was synthesized via conventional copper-promoted atom transfer radical addition techniques from a commercially available dihalide precursor.⁸⁸⁶ Adenine hydrogen bonding groups were introduced via a nucleobase-containing styrenic monomers, and 9-vinylbenzyladenine (Figure 11.2). The residual monomers and solvent were removed via precipitation into methanol, yielding purified polymer products. ¹H NMR spectroscopy was used to verify the presence of the nucleobases and to quantify the degree of polymerization of the outer blocks, based on the known poly(*n*-butyl acrylate) rubber block molecular weights that were determined from SEC in THF. The block molecular weights were A_{1.5K}-nBA_{16.5K}-A_{1.5K}. SEC was also carried out on the nucleobase functional block copolymers in THF, revealing narrow molecular weight distributions and monomodal traces for the final triblock copolymers. However, SEC was not suitable for the determination of hydrogen bonding block molecular weights due to the relatively short block lengths.

⁸⁸⁶ Matyjaszewski, K.; Woodworth, B. E.; Zhang, X.; Gaynor, S.; Metzner, Z. Simple and Efficient Synthesis of Various Alkoxyamines for Stable Free Radical Polymerization. *Macromolecules* **1998**, 31, 5955-7.

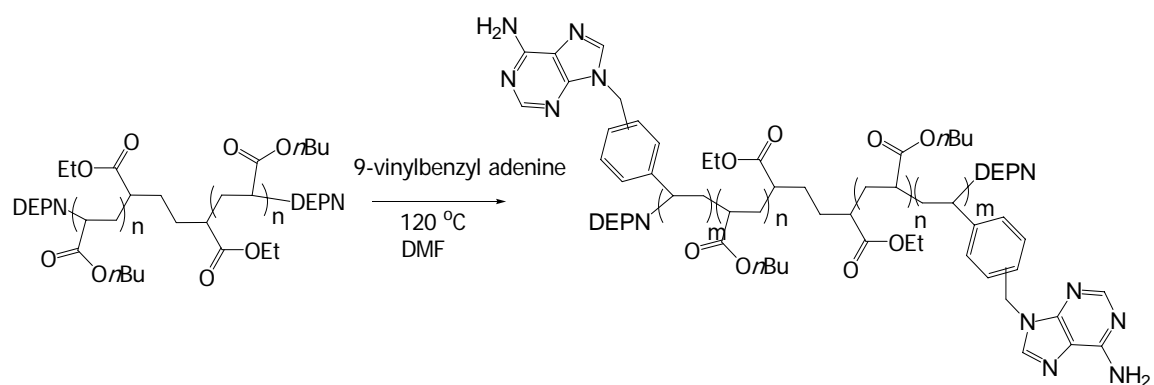


Figure 11.2. Synthesis of hydrogen bonding triblock copolymers containing adenine and thymine nucleobases from difunctional DEPN terminated poly(*n*-butyl acrylate).

11.4.2 Quartz Crystal Microbalance Measurements

The adenine containing block copolymer was spin coated onto the quartz crystal microbalance crystal with the gold electrodes. The polymer layer was annealed at 155 °C under vacuum to allow the development of morphology as observed using AFM (Figure 11.3). The hard domains at the surface (light color) suggest the accessibility of the adenine functional groups to solutions introduced to the film. SAXS measurements on this polymer previously established a cylindrical morphology.⁸⁸⁷ The spin-coated polymer film thickness (δ_{film}) was estimated from the frequency change (Δf) using the Sauerbrey equation:⁸⁸⁸

$$\Delta m = \rho_{\text{film}} \delta_{\text{film}} = \frac{C_{\text{QCM}}}{n} \Delta f \quad [11.1]$$

where ρ_{film} is the density of the film, C_{QCM} is an instrument constant (17.7 ng/cm²Hz), and n is the overtone number (Table 11.1). The film thickness estimated from the seventh overtone was 133 nm. Cross-sectional SEM measurements yielded a film thickness value of 127 nm, confirming the result from SEM. A control polymer, consisting of poly(styrene-*b*-*n*-butyl acrylate-*b*-styrene) (S_{14.6K}-nBA_{23.7K}-S_{14.6K}) was also spin-coated onto a quartz crystal, yielding a film thickness of 73 nm.

⁸⁸⁷ Mather, B. D.; Baker, M. B.; Beyer, F. L.; Green, M. D.; Berg, M. A. G.; Long, T. E. Multiple Hydrogen Bonding for the Reversible Attachment of Ionic Functionality in Block Copolymers. *Macromolecules* **2007**, Submitted.

⁸⁸⁸ Sauerbrey, G. The use of quartz oscillators for weighing thin layers and for microweighing. *Z. Phys.* **1959**, 155, 206-22.

Table 11.1. Film thickness of adenine containing polymer using QCM and SEM.

Surface	$\Delta f/n$ (Hz)	QCM Thickness (nm)	SEM Thickness (nm)
Adenine Polymer	-782	133	127
Control	-407	73	-

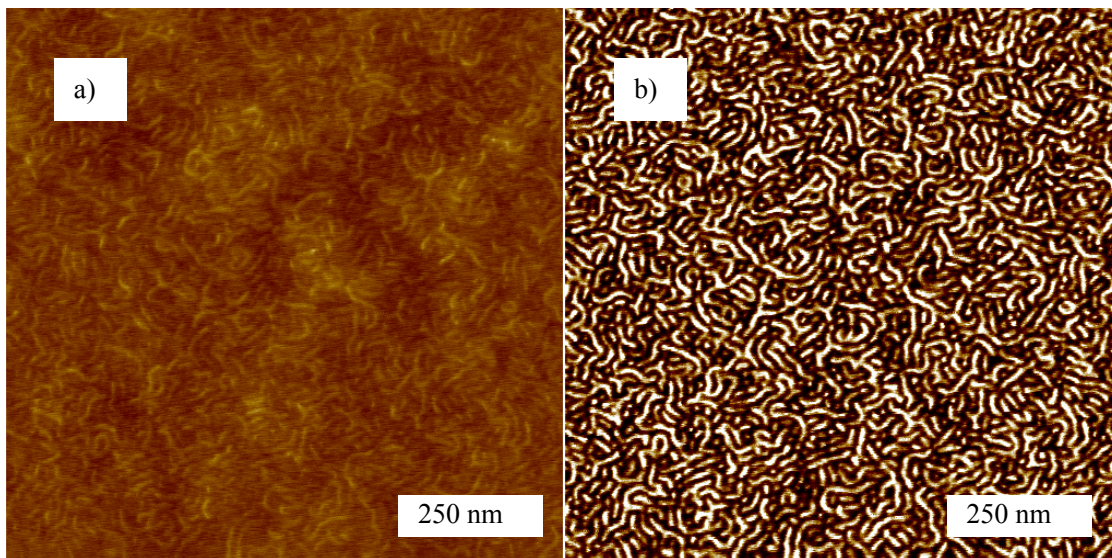


Figure 11.3. Tapping mode AFM a) height and b) phase images of adenine containing polymer spin coated on Si, from chloroform solution. Annealing was performed at 155 °C under vacuum for 18 h. Film thickness \sim 100 nm. Images are 1 μ m x 1 μ m. Full color variation corresponds to a 10 nm change in height (a) or 10 degrees of phase (b).

The adenine polymer coated quartz crystal was first exposed to humid air, in order to monitor the weight uptake due to moisture. The adenine-containing polymer surface adsorbed 45 ng/cm² of water almost immediately upon the exposure to the film to humid air (Figure 11.4, Table 11.2). In contrast, the control polymer exhibited nearly no change upon exposure to humid air. Both polymer surfaces were carefully kept dry prior to measurement, through storage in desiccator after drying in a vacuum oven at 155 °C. The greater water adsorption by the adenine containing polymer film was expected due to the polar, hydrogen bonding nature of the adenine functional groups. In contrast, the control polymer consisted of comparatively non-polar constituents (styrene and *n*-butyl acrylate).

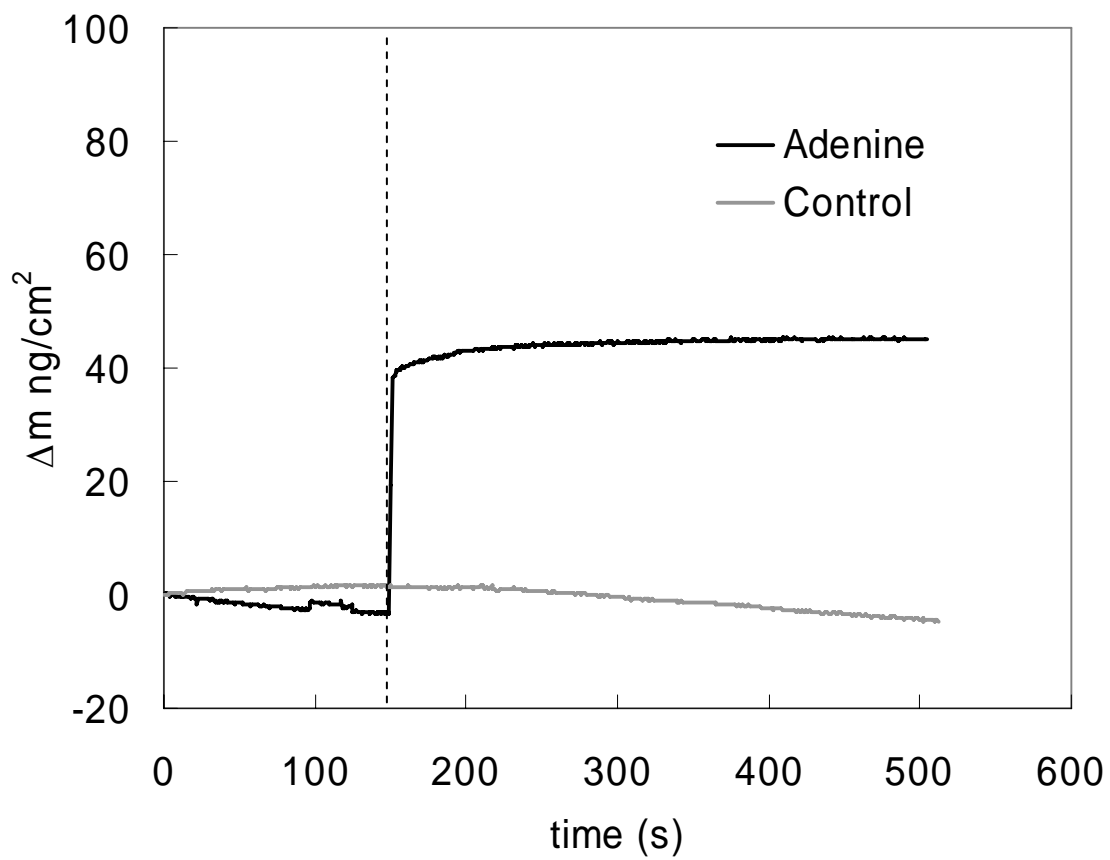


Figure 11.4. Changes in frequency (7th overtone) with exposure to humid air, 25 °C.

Table 11.2. Effect of moisture uptake on frequency and dissipation of adenine containing polymer and control polymer.

Surface	Δm (ng/cm ²)	$\Delta f/n$ (Hz) Moisture	ΔD Moisture ($\times 10^{-6}$)
Adenine Polymer	45	-2.7	-0.04
Control	-2	+0.2	+0.28

Exposure of the adenine-containing polymer to the complementary uracil-containing phosphonium salt (UPPh_3^+) was conducted by introducing the phosphonium salt in an aqueous solution (0.5 wt%). This required the previous exposure of the film to water. The frequency change observed upon introduction of UPPh_3^+ (-17.6 Hz) corresponded to a mass uptake of 317 ng/cm^2 . Upon rinsing with pure Millipore water, the uracil-containing phosphonium salt was partially desorbed (-289 ng/cm^2). The control polymer adsorbed UPPh_3^+ to a lower extent (157 ng/cm^2) than the adenine containing polymer. Furthermore, upon rinsing, the control polymer lost the majority of the phosphonium salt (-152 ng/cm^2). The greater adsorption and retention of the phosphonium salt by the adenine containing polymer was attributed to the complementary hydrogen bonding interaction.

The incomplete loss of UPPh_3^+ upon rinsing was thought to possibly arise from the permeation of the guest molecule into the bulk of the film. During the adsorption step (Figure 11.5), the weight uptake of the adenine-containing polymer continues gradually after an initial large change ($\sim 260 \text{ ng/cm}^2$). This may be attributed to permeation into the bulk of the film, whereas the initial weight uptake may represent rapid adsorption at the surface. Since the adenine containing polymer possesses a cylindrical morphology, there may be some continuity of the hard phases, which would facilitate permeation through these hard domains. Changes in the dissipation of the films were similar between the adenine containing polymer and the control polymer, during the UPPh_3^+ adsorption step (Table 11.3). The increase in dissipation is commonly observed with increased mass adsorption.

Hook et al. studied the adsorption of single stranded complementary or

single-mismatched DNA oligobases (15 bp) to PNA to surface.⁸⁸⁹ Hook observed higher levels of adsorption of the fully complementary DNA as well as greater retention upon rinsing with buffer solutions. These results were consistent with those observed in the current study.

⁸⁸⁹ Hook, F.; Ray, A.; Norden, B.; Kasemo, B. Characterization of PNA and DNA Immobilization and Subsequent Hybridization with DNA Using Acoustic-Shear-Wave Attenuation Measurements. *Langmuir* **2001**, *17*, 8305-12.

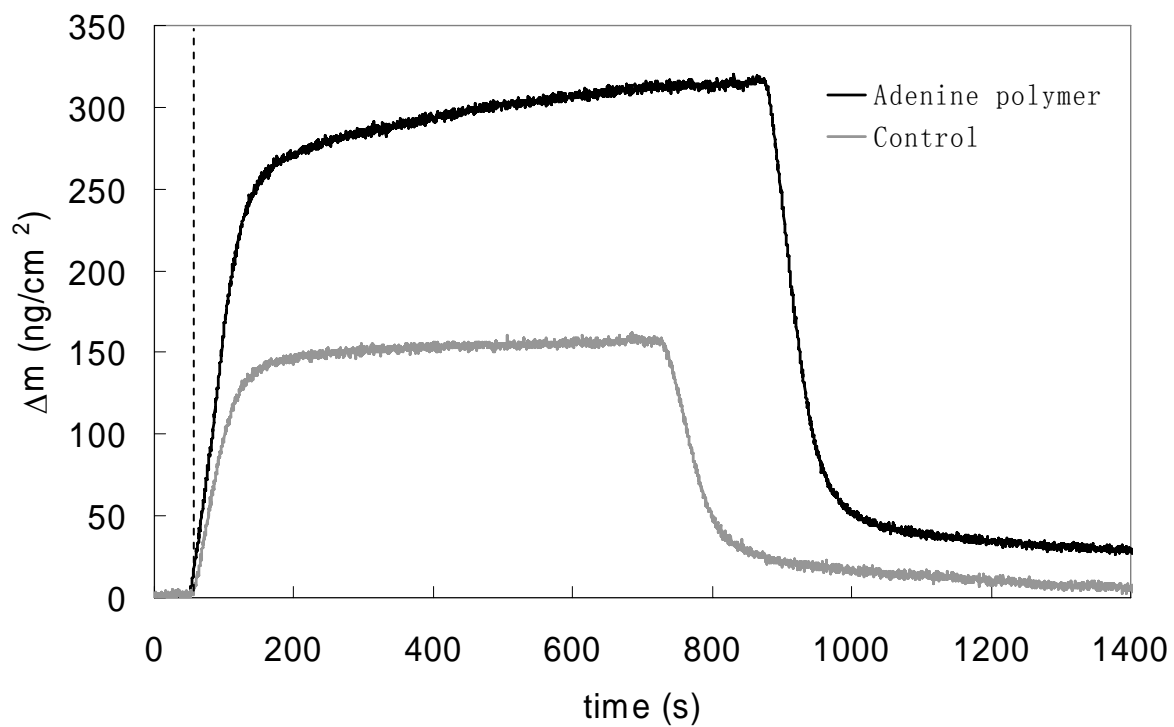


Figure 11.5. Changes in frequency (7th overtone) with exposure to UPPh_3^+ in water (0.5 wt%), 25 °C for adenine-containing and control block copolymer.

Table 11.3. Adsorption of UPPh_3^+ on adenine-containing and control block copolymers.

Surface	Adsorption (UPPh_3^+)			Rinsing (H_2O)		
	Δm (ng/cm^2)	$\Delta f/n$ (Hz)	ΔD ($\times 10^{-6}$)	Δm (ng/cm^2)	$\Delta f/n$ (Hz)	ΔD ($\times 10^{-6}$)
Adenine Polymer	317	-17.6	0.96	-289	+16.1	-1.01
Control	157	-8.8	0.97	-152	+8.6	-0.51

11.4.3 X-ray Crystallographic Studies of Uracil Phosphonium Salt

X-ray crystallography was carried out on the uracil-containing phosphonium salt (UPPh₃⁺) for the first time. Crystallization experiments were conducted in ethanol, which yielded a crystal structure in which thymine hydrogen bonding groups were dimerized through hydrogen bonding interactions (Figure 11.6). The distances between the carbonyl oxygens (O1) and hydrogen bonded nitrogens (N3) on the opposite uracil were 2.81 Å in each case. Uracil possesses a weak hydrogen bonding dimerization constant ($K_a = 6 \text{ M}^{-1}$).⁸⁹⁰ Ethanol was also observed in the crystal structure as disordered solvent and was not observed to hydrogen bond to the uracil group or to disrupt the dimerization. The chloride counterion was weakly hydrogen bonded to the uracil N1-H (3.11 Å, N to Cl distance) while maintaining a position relatively close to the phosphonium center (P to Cl distance 4.22 Å).

⁸⁹⁰ Kyogoku, Y.; Lord, R. C.; Rich, A. The Effect of Substituents on the Hydrogen Bonding of Adenine and Uracil Derivatives. *Proc Natl Acad Sci USA* **1967**, 57, 250-7.

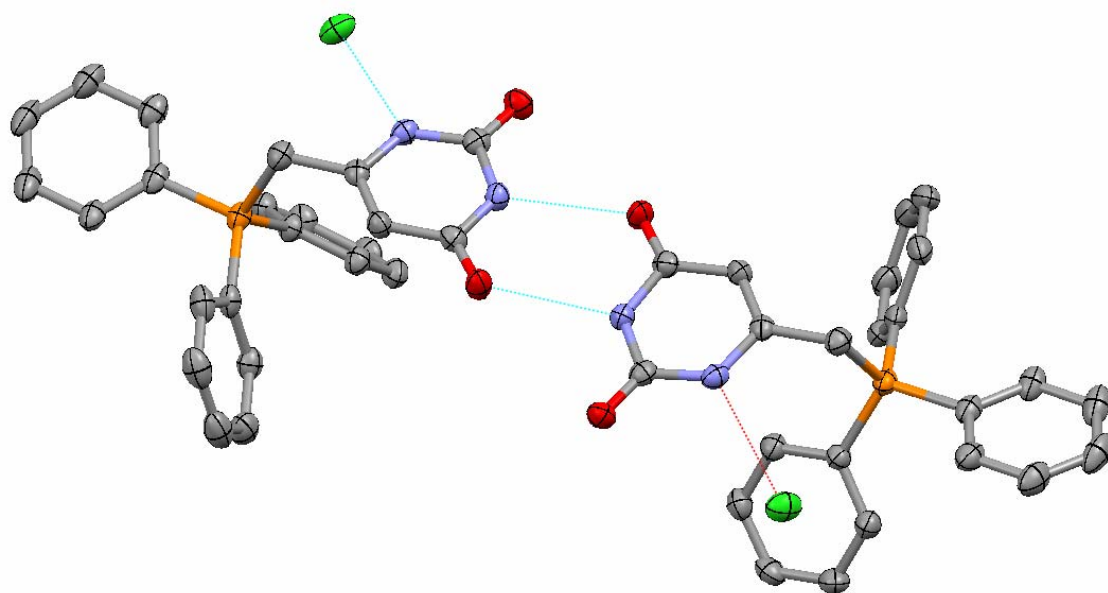


Figure 11.6. Molecular structure of UPPh_3^+ (50% probability displacement ellipsoids), crystallized from ethanol. Solvent molecules and hydrogens are omitted for clarity.

Crystallization of the phosphonium salt from a mixture of water and THF resulted in the incorporation of one water molecule hydrogen bonded to the uracil N3-H (Figure 11.7, 2.81 Å, O to N distance). The water hydrogens were also hydrogen bonded to chloride counterions on neighboring molecules (3.19 Å, O to Cl distance). As in the structure of UPh_3^+ crystals from ethanol, the chloride counterion was hydrogen bonded to the uracil N1-H (3.16 Å, N to Cl distance) and the distance to the phosphonium center was similar (4.31 Å, P to Cl). The strong hydrogen bonding capabilities of water were sufficient to disrupt the dimerization of the uracil groups. This hydrogen bond screening ability of water was thought to be responsible for the ability to remove UPh_3^+ from the adenine containing polymer film via rinsing. It is remarkable, however, that UPh_3^+ showed preferential adsorption to the adenine containing polymer despite the presence of water. Others have observed decreased hydrogen bonding association constants in the presence of water.⁸⁹¹

⁸⁹¹ Söntjens, S. H. M.; Sijbesma, R. P.; van Genderen, M. H. P.; Meijer, E. W. Stability and Lifetime of Quadruply Hydrogen Bonded 2-Ureido-4[1H]-pyrimidinone Dimers. *J Am Chem Soc* **2000**, 122, 7487-93.

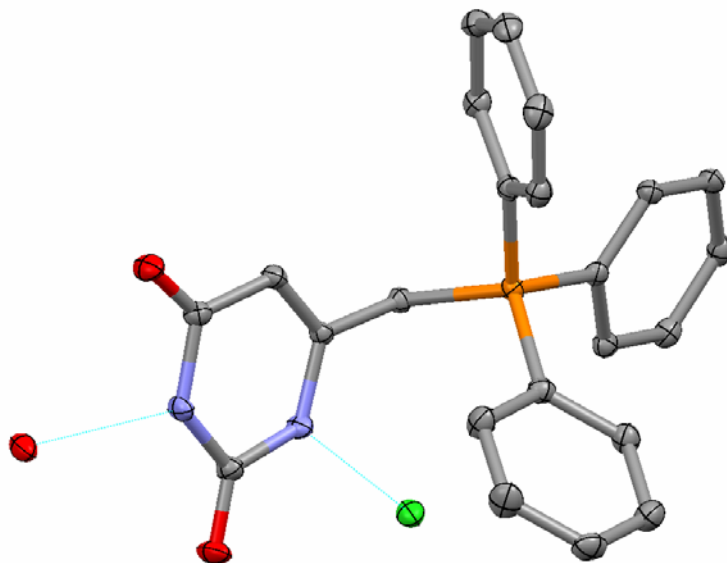


Figure 11.7. Molecular structure of UPPh_3^+ (50% probability displacement ellipsoids), crystallized from water/THF. Hydrogens omitted for clarity.

11.5 Conclusions

The molecular recognition between a water-soluble uracil functionalized phosphonium salt and an adenine containing block copolymer poly(9-vinylbenzyladenine-*b-n*-butyl acrylate-*b-9*-vinylbenzyladenine) surface was studied using quartz crystal microbalance with dissipation (QCM-D) measurements. Adsorption experiments revealed a frequency drop of 17.6 Hz associated with the adsorption. The uracil phosphonium salt was not completely rinsed from the surface with water, suggesting strong specific recognition. Control experiments with non-nucleobase containing poly(styrene-*b-n*-butyl acrylate-*b*-styrene) block copolymers revealed a frequency drop of 8.8 Hz, which was nearly completely reversible upon rinsing with water. X-ray crystallographic measurements of the uracil phosphonium salt revealed the competitive hydrogen bonding of water with the uracil group, which may play a role in the adsorption measurements.

11.6 Acknowledgement

This material is based upon work supported by, or in part by, the U.S. Army Research Laboratory and the U.S. Army Research Office under grant number DAAD19-02-1-0275 Macromolecular Architecture for Performance (MAP) MURI.

Chapter 12. Introduction of Central Diester Functionality in Polystyrenes Using Living Radical Polymerization for Graft Polyester Synthesis

12.1 Abstract

Novel, central diester functional polystyrenes were synthesized using nitroxide mediated polymerization from a difunctional alkoxyamine initiator (DEPN₂). The thermal stability of the functional polystyrenes was improved through the removal of the DEPN nitroxide end-groups, which was achieved through heating in the presence of thiol containing compounds. The removal of DEPN was confirmed with NMR spectroscopy and improved thermal stability was observed with TGA. The polystyrene diesters were then introduced into high temperature melt polyesterification reactions. The resultant polyester graft copolymers had polystyrene contents that were close to charged levels 2.5-10 wt%.

12.2 Introduction

Nitroxide mediated polymerization has gained attention recently as a technique for synthesizing narrow polydispersity linear and block copolymers with controlled molecular weights.⁸⁹² The use of unimolecular alkoxyamine initiators has increased in recent years, due to the control over the ratio of initiator to nitroxide as well as the possibility for

⁸⁹² Hawker, C.; Bosman, A.; Harth, E. New Polymer Synthesis by Nitroxide Mediated Living Radical Polymerizations. *Chemical Reviews* **2001**, 101, 3661-88.

introduction of functionality onto the polymer chain end.^{893,894}

Recently, our group has developed a difunctional alkoxyamine initiator, DEPN₂, which facilitates the synthesis of triblock copolymers by reducing the number of crossover steps compared to sequential polymerization and ensuring symmetric outer blocks.⁸⁹⁵ The DEPN₂ initiator also benefits from a continuous carbon chain, which prevents potential hydrolysis found in other difunctional initiators.⁸⁹⁶ Finally, the DEPN₂ initiator also introduces two ester functional groups into the center of the synthesized polymers.

Graft copolymers have unique molecular architecture which is tunable via a variety of parameters including arm molecular weight, graft density and composition. The unique architecture of graft copolymers results in novel rheological behavior.^{897,898} Graft copolymers have found utility in gene transfection,⁸⁹⁹ drug delivery and controlled release,^{900,901} and in

⁸⁹³ Gavranovic, G.; Csihony, S.; Bowden, N.; Hawker, C.; Waymouth, R.; Moerner, W.; Fuller, G. Well-Controlled Living Polymerization of Perylene-Labeled Polyisoprenes and Their Use in Single-Molecule Imaging. *Macromolecules* **2006**, 39, 8121 -7.

⁸⁹⁴ Mather, B.; Lizotte, J.; Long, T. Synthesis of Chain End Functionalized Multiple Hydrogen Bonded Polystyrenes and Poly(alkyl acrylates) Using Controlled Radical Polymerization. *Macromolecules* **2004**, 37, 9331-7.

⁸⁹⁵ Mather, B.; Long, T. Supramolecular triblock copolymers containing complementary molecular recognition. *PMSE Preprints* **2006**, 95, 304-5.

⁸⁹⁶ Robin, S.; Guerret, O.; Couturier, J.; Pirri, R.; Gnanou, Y. Synthesis and Characterization of Poly(styrene-*b*-*n*-butyl acrylate-*b*-styrene) Triblock Copolymers Using a Dialkoxyamine as Initiator. *Macromolecules* **2002**, 35, 3844-8.

⁸⁹⁷ Hempenius, M.; Zoetelief, W.; Gauthier, M.; Moller, M. Melt Rheology of Arborescent Graft Polystyrenes *Macromolecules* **1998**, 31, 2299 -2304.

⁸⁹⁸ Krishnamoorti, R.; Giannelis, E. Strain Hardening in Model Polymer Brushes under Shear *Langmuir* **2001**, 17, 1448 -52.

⁸⁹⁹ Unger, F.; Wittmar, M.; Kissel, T. Branched polyesters based on poly[vinyl-3-(dialkylamino)alkylcarbamate-*co*-vinyl acetate-*co*-vinyl alcohol]-graftpoly(D,L-lactide-*co*-glycolide): Effects of polymer structure on cytotoxicity. *Biomaterials* **2007**, 28, 1610-9.

⁹⁰⁰ Lo, C.-L.; Huang, C.-K.; Lin, K.-M.; Hsiue, G.-H. Mixed micelles formed from graft and diblock copolymers for application in intracellular drug delivery. *Biomaterials* **2007**, 28, 1225-35.

⁹⁰¹ Gref, R.; Rodrigues, J.; Couvreur, P. Polysaccharides Grafted with Polyesters: Novel Amphiphilic Copolymers for Biomedical Applications. *Macromolecules* **2002**, 35, 9861-7.

the modification of biopolymers such as chitosan,⁹⁰² dextran⁹⁰³ or cellulose derivatives⁹⁰⁴ to alter the hydrophilicity and impart unique solubility characteristics or for biomedical applications. Further applications exist in membranes for removal of heavy metals from wastewater.⁹⁰⁵

Graft copolymers are typically synthesized via one of several approaches: grafting to a preformed backbone using radical initiators,⁹⁰⁶ radiation,⁹⁰⁷ or linking chemistry,⁹⁰⁸ grafting from a macroinitiator,^{904 - 910} a polymer containing multiple initiation sites, and finally (co)polymerization of a macromonomer,^{911 - 913} a low molar mass polymer (typically $M_n <$

⁹⁰² Joshi, J.; Sinha, V. Ceric ammonium nitrate induced grafting of polyacrylamide onto carboxymethyl chitosan. *Carbohydrate Polymers* **2007**, 67, 427-35.

⁹⁰³ Li, Y.; Volland, C.; Kissel, T. Biodegradable brush-like graft polymers from poly(D,L-lactide) or poly(D,L-lactide-co-glycolide) and charge-modified, hydrophilic dextrans as backbone-in-vitro degradation and controlled releases of hydrophilic macromolecules. *Polymer* **1998**, 39, 3087-97.

⁹⁰⁴ Kang, H.; Liu, W.; He, B.; Shen, D.; Ma, L.; Huang, Y. Synthesis of amphiphilic ethyl cellulose grafting poly(acrylic acid) copolymers and their self-assembly morphologies in water. *Polymer* **2006**, 47, 7927-34.

⁹⁰⁵ Okieimen, F. E.; Sogbaïke, C. E.; Ebhoaye, J. E. Removal of cadmium and copper ions from aqueous solution with cellulose graft copolymers. *Separation and Purification Technology* **2005**, 44, 85-9.

⁹⁰⁶ Russell, K. Free radical graft polymerization and copolymerization at higher temperatures. *Prog Polym Sci* **2002**, 27, 1007-38.

⁹⁰⁷ Nasef, M.; Hegazy, E.-A. Preparation and applications of ion exchange membranes by radiation-induced graft copolymerization of polar monomers onto non-polar films. *Prog Polym Sci* **2004**, 29, 499-561.

⁹⁰⁸ Parrish, B.; Emrick, T. Aliphatic Polyesters with Pendant Cyclopentene Groups: Controlled Synthesis and Conversion to Polyester-graft-PEG Copolymers. *Macromolecules* **2004**, 37, 5863-5.

⁹⁰⁹ Li, H.; Zhao, H.; Zhang, X.; Lu, Y.; Hu, Y. A novel route to the synthesis of PP-g-PMMA copolymer via ATRP reaction initiated by Si-Cl bond. *Eur Polym J* **2007**, 43, 109-18.

⁹¹⁰ Chung, T. Synthesis of functional polyolefin polymers with block and graft architectures. *Prog Polym Sci* **2002**, 27, 39-85.

⁹¹¹ Lahitte, J.; Plentz-Meneghetti, S.; Peruch, F.; Isel, F.; Muller, R.; Lutz, P. Design of new styrene enriched polyethylenes via coordination copolymerization of ethylene with mono- or α,ω -difunctional polystyrene macromonomers. *Polymer* **2006**, 47, 1063-72.

⁹¹² Mespouille, L.; Degee, P.; Dubois, P. Amphiphilic poly(*N,N*-dimethylamino-2-ethyl methacrylate)-*g*-poly(ϵ -caprolactone) graft copolymers: synthesis and characterisation. *Eur Polym J* **2005**, 41, 1187-95.

⁹¹³ Sato, M.; Mangyo, T.; Mukaida, K. Thermotropic liquid-crystalline aromatic

10000) containing a polymerizable functional group. The macromonomer approach, which will be the focus of this manuscript, benefits from well-defined graft lengths and avoids the potential side reactions possible with the “grafting-to” approach. The synthesis of macromonomers is typically achieved using living polymerization techniques and they may be incorporated using radical polymerization,⁹¹² coordination polymerization⁹¹¹ or condensation routes.⁹¹³ Recently, even “click chemistry” was applied to the synthesis of graft copolymers.^{914,915}

Living radical polymerization possesses the advantage of producing grafts with well-defined lengths. Living radical polymerization gained attention recently as a useful tool for the synthesis of graft copolymers.⁹¹⁶ For instance, ATRP was used to graft PMMA onto a silyl chloride functionalized polypropylene.⁹¹⁷ ATRP was also utilized to graft poly(acrylic acid) side chains onto ethyl cellulose via an esterification with a haloacid halide.⁹¹⁸ The macromonomer approach has also been utilized with controlled radical polymerization. Dubois et al. utilized ATRP to copolymerize a methacrylate-terminated poly(ϵ -caprolactone)

polyester-graft-poly(2,6-dimethyl-1,4-phenylene oxide) copolymers. *Macromol. Chem. Phys.* **1995**, 196, 1791-9.

⁹¹⁴ Riva, R.; Schmeits, S.; Jerome, C.; Jerome, R.; Lecomte, P. Combination of Ring-Opening Polymerization and “Click Chemistry”: Toward Functionalization and Grafting of Polycaprolactone. *Macromolecules* **2007**, 40, 796-803.

⁹¹⁵ Parrish, B.; Breitenkamp, R.; Emrick, T. PEG- and Peptide-Grafted Aliphatic Polyesters by Click Chemistry. *J Am Chem Soc* **2005**, 127, 7404-10.

⁹¹⁶ Davis, K.; Matyjaszewski, K., *Advances in Polymer Science*, 159. Statistical, Gradient, Block and Graft Copolymers by Controlled/Living Radical Polymerizations. Springer-Verlag: New York, 2002; p 192.

⁹¹⁷ Li, H.; Zhao, H.; Zhang, X.; Lu, Y.; Hu, Y. A novel route to the synthesis of PP-g-PMMA copolymer via ATRP reaction initiated by Si-Cl bond. *Eur Polym J* **2007**, 43, 109-18.

⁹¹⁸ Kang, H.; Liu, W.; He, B.; Shen, D.; Ma, L.; Huang, Y. Synthesis of amphiphilic ethyl cellulose grafting poly(acrylic acid) copolymers and their self-assembly morphologies in water. *Polymer* **2006**, 47, 7927-34.

with *N,N*-dimethylaminoethyl methacrylate to make amphiphilic graft copolymers.⁹¹⁹ ATRP was also used to synthesize centrally difunctional aryl dibromide macromonomers to make poly(phenylene) graft copolymers.⁹²⁰ Relatively few works utilize nitroxide mediated polymerization for graft copolymer synthesis. Nitroxide mediated polymerization was also used in the synthesis of graft copolymer. For example, an alkoxyamine containing diphenylacetylene monomer was polymerized using coordination catalysis and was then used as a macroinitiator to polymerize styrene.⁹²¹ Also, nitroxides were used to mediate the polymerization of styrene from Barton ester functionalized poly(arylene ether sulfone)s.⁹²²

Polyesters have novel properties due to their biodegradability, potential crystallinity and recyclability. Graft polyesters have advantages in terms of the potential to create biodegradable amphiphilic molecules with potential drug delivery application.⁹²³ In the case of graft polyesters, macromonomers possessing alcohol or ester groups may be incorporated. Graft polyesters were prepared in melt polycondensation with dicarboxyterminated poly(2,6-dimethyl-1,4-phenylene oxide).⁹²⁴ In this report, we describe a route to centrally functionalized diester containing polystyrenes synthesized using nitroxide mediated

⁹¹⁹ Mespouille, L.; Degee, P.; Dubois, P. Amphiphilic poly(*N,N*-dimethylamino-2-ethyl methacrylate)-*g*-poly(ϵ -caprolactone) graft copolymers: synthesis and characterisation. *Eur Polym J* **2005**, 41, 1187-95.

⁹²⁰ Cianga, I.; Yagci, Y. New polyphenylene-based macromolecular architectures by using well defined macromonomers synthesized via controlled polymerization methods. *Prog Polym Sci* **2004**, 29, 387-99.

⁹²¹ Miura, Y.; Okada, M. Synthesis of densely grafted copolymers by nitroxide-mediated radical polymerization of styrene using poly(phenyl acetylene)s as a macroinitiator. *Polymer* **2004**, 45, 6539-46.

⁹²² Daly, W.; Evenson, T. Grafting of vinyl polymers to carboxylated poly(arylene ether sulfone) utilizing Barton ester intermediates and nitroxide mediation. *Polymer* **2000**, 41, 5063-71.

⁹²³ Li, Y.; Volland, C.; Kissel, T. Biodegradable brush-like graft polymers from poly(D,L-lactide) or poly(D,L-lactide-coglycolide) and charge-modified, hydrophilic dextrans as backbone-in-vitro degradation and controlled releases of hydrophilic macromolecules. *Polymer* **1998**, 39, 3087-97.

⁹²⁴ Sato, M.; Mangyo, T.; Mukaida, K. Thermotropic liquid-crystalline aromatic polyester graft-poly(2,6-dimethyl-1,4-phenylene oxide) copolymers. *Macromol. Chem. Phys.* **1995**, 196, 1791-9.

polymerization. These centrally functionalized polystyrenes possess narrow molecular weight distributions and controlled molecular weights and are suitable for incorporation in graft copolyesters or copolyamides or potentially, mikto-arm star polymers.

12.3 Experimental

12.3.1 Materials

Styrene monomer (Aldrich, 99%) was de inhibited prior to use via passage over alumina followed by distillation from calcium hydride under reduced pressure. 1-dodecanethiol (98%), dimethyl adipate (98%), 1,4-cyclohexanedimethanol (~30% cis/ 70% trans mixture) (99%), antimony (III) oxide (99%) and diphenylsulfone (97%) were obtained from Aldrich and used as received. 1,6-hexanediol (99%) was obtained from Avocado chemicals and was used as received. Titanium (IV) isopropoxide (97%) was obtained from Aldrich and was diluted with *n*-butanol to 0.01 g Ti/mL. DEPN₂ initiator was synthesized according to our previously reported procedure.⁹²⁵

12.3.2 Polystyrene Diester Synthesis

DEPN₂ initiator (150 mg, 0.19 mmol), and styrene (5 mL, 43 mmol) were combined in a 100-mL round-bottomed flask containing a magnetic stirbar. The flask was fitted with a 3-way joint allowing the introduction of nitrogen and the application of vacuum. The mixture was degassed by several freeze-pump-thaw cycles and immersed in an oil bath at 125 °C for 2

⁹²⁵ Mather, B.; Long, T. Supramolecular triblock copolymers containing complementary molecular recognition. *PMSE Preprints* **2006**, 95, 304-5.

h with stirring. The product was isolated through precipitation in methanol and was dried in a vacuum oven at 60 °C for 18 h. The conversion of the reaction was measured using ^1H NMR of the crude reaction product, through comparing the aromatic peaks with the olefin resonances. The conversion was determined at 32%, which enabled a calculation of the target molecular weight ($M_{n,\text{theo}} = 7500$). SEC revealed molecular weights of $M_{n,\text{actual}} = 6400$, $M_w/M_n = 1.23$. ^1H NMR, CDCl_3 (δ , ppm) 4.5-5.1 (br m, 2H, Ph-CH-O-N), 3.6-4.4 (br m, 12 H, OCH_2CH_3), 2.5-3.4 (br m, 8H, alkylene linker + $\text{CHP}=\text{O}$), 1.05 (br s, $\text{PO}(\text{CH}_2\text{CH}_3)_2$, 12H), 0.91 (br, $\text{COOCH}_2\text{CH}_3$, 6H), 0.73 (br, $\text{CC}(\text{CH}_3)_3$, 18H), 0.59 (s, $\text{NC}(\text{CH}_3)_3$, 18H).

12.3.3 Removal of DEPN from Polystyrene Diester

Polystyrene diester ($M_n = 5000$, $M_w/M_n = 1.45$) (1.18 g, 0.23 mmol) was weighed into a 100-mL round bottomed flask containing a magnetic stirbar. 1-dodecanethiol (0.611 g, 3.0 mmol) was added along with DMF (13 mL) and the mixture was degassed, followed by heating at 130 °C for 4 h. The product was isolated by precipitation into methanol and was dried in a vacuum oven at 60 °C for 18 h. SEC revealed molecular weights of $M_n = 5700$, $M_w/M_n = 1.41$.

12.3.4 Graft Polyester Synthesis

Polystyrene diester after DEPN removal ($M_n = 5700$, $M_w/M_n = 1.41$) (200 mg, 0.035 mmol), 1,6-hexanediol (3.73 g, 31.6 mmol), dimethyl adipate (5.00 g, 28.7 mmol), diphenylsulfone (3.0 g, 13.8 mmol) and titanium tetraisopropoxide (0.05 mL, 0.01 g Ti/mL, to achieve 60 ppm Ti) were combined in a 100-mL round-bottomed flask fitted with a

mechanical stirrer. The mixture was flushed with argon, and degassed with vacuum. The transparent mixture was heated to 200 °C for 2 h, then the temperature was raised to 220 °C for 3 h. Finally, the temperature was raised to 250 °C and vacuum was applied (30 min), resulting in distillation of the diphenylsulfone onto the flask walls and partial precipitation of the polystyrene diester. The reaction mixture was cooled and the polyester was dissolved in chloroform and precipitated in diethyl ether (5x), thereby removing any unreacted polystyrene diester, which was soluble in diethyl ether. The product was dried under vacuum at 60 °C for 18 h. ¹H NMR revealed that the graft polyester contained 2.5 wt% polystyrene. SEC analysis of the graft polyester revealed molecular weights of $M_n = 33600$, $M_w/M_n = 1.94$. Based on the polystyrene content and graft molecular weight, on average there was one polystyrene diester graft for every 6.8 polyester molecules.

A polystyrene graft polyester was synthesized containing a higher content of polystyrene diester. This polymer was synthesized with a mixture of 1,6-hexanediol and cis/trans-1,4-cyclohexanedimethanol in order to improve solubility of the polystyrene in the reaction mixture and attempt to create an amorphous polyester matrix. Thus, polystyrene diester after DEPN removal ($M_n = 5700$, $M_w/M_n = 1.41$) (432 mg, 0.076 mmol), 1,6-hexanediol (1.20 g, 10.2 mmol), dimethyl adipate (2.50 g, 14.4 mmol), diphenylsulfone (2.1 g, 9.7 mmol) 1,4-cyclohexanedimethanol (0.81 g, 5.6 mmol, mixture of cis/trans) and titanium tetraisopropoxide (0.025 mL, 0.01 g Ti/mL, to achieve 60 ppm Ti) were combined in a 100-mL round-bottomed flask fitted with a mechanical stirrer. The mixture was flushed with argon, and degassed with vacuum. The transparent mixture was heated to 200 °C for 3 h, and the temperature was raised to 220 °C for 3 h. Finally, antimony (III) oxide (200 ppm) and

additional diphenylsulfone (2.0 g, 9.2 mmol) were added and the temperature was raised to 250 °C for 1.5 h and finally vacuum was applied (20 min), resulting in distillation of the diphenylsulfone out of the reaction and partial precipitation of the polystyrene diester. The reaction mixture was cooled and the graft polyester was dissolved in chloroform and precipitated in diethyl ether (5 x), thereby removing any unreacted polystyrene diester, which was soluble in diethyl ether. The product was dried under vacuum at 60 °C for 18 h. ¹H NMR revealed that the graft polyester contained 4.8 wt% polystyrene and a 42 mol% incorporation of 1,4-cyclohexanedimethanol (relative to diol content). SEC analysis of the graft polyester revealed molecular weights of $M_n = 13700$, $M_w/M_n = 1.35$. Based on this analysis, on average there was one polystyrene diester graft for every 8.7 polymer molecules.

12.3.5 Characterization

¹H and ³¹P NMR spectra were collected using a Varian Inova spectrometer operating at 400 and 162 MHz, respectively. Thermogravimetric analysis (TGA) was performed under a nitrogen atmosphere at a heating rate of 10 °C/min using a TA Instruments Hi-Res TGA 2950. Differential scanning calorimetry was conducted on a TA Instruments Q1000 at a heating rate of 20 °C/min under a nitrogen purge. Size exclusion chromatography (SEC) of the polystyrene diesters was performed on a Waters 2690 chromatographer in THF at a flow rate of 1 mL/min at 22 °C with a T60A Viscotek Dual detector comprised of both a laser diffractometer and a viscometer which were calibrated using polystyrene standards. Size exclusion chromatography (SEC) of the graft polyesters was performed at 40 °C in THF at a flow rate of 1 mL/min using a Waters size exclusion chromatographer equipped with an

autosampler, three 5 μm PLgel Mixed-C columns, a Waters 2410 refractive index (RI) detector operating at 880 nm, and a miniDAWN multiangle laser light scattering (MALLS) detector operating at 690 nm, which was calibrated with polystyrene standards. A Veeco MultiModeTM scanning probe microscope was used for tapping-mode AFM imaging. Samples were imaged at a set-point ratio of 0.6 at magnifications of 1 μm x 1 μm . Veeco's Nanosensor silicon tips having spring constants of 10-130 N/m were utilized for imaging.

12.4 Results and Discussion

12.4.1 Synthesis of DEPN-Terminated Polystyrene Diesters

Nitroxide mediated polymerization allows controlled molecular weight and produces polymers with narrow polydispersity while enabling both block and graft copolymers. The polystyrenes with central diester (termed polystyrene diesters) functionality were synthesized in a single step using nitroxide mediated polymerization from a difunctional alkoxyamine initiator (DEPN₂) (Figure 12.1). The polystyrene diesters possessed similar appearance to polystyrenes synthesized using other techniques. A range of polystyrene molecular weights was obtained through varying the concentration of the initiator in the polymerization, while maintaining similar levels of conversion (Table 12.1).

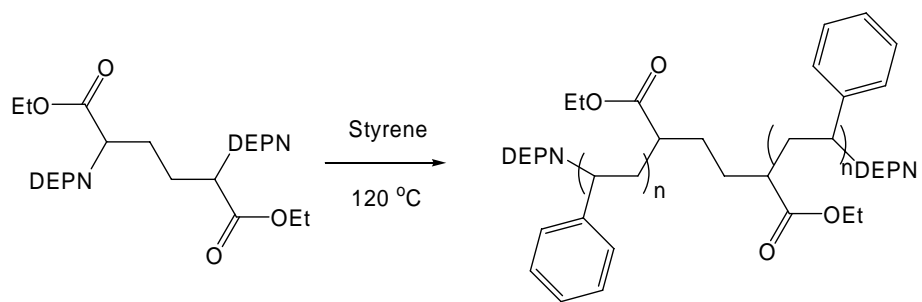


Figure 12.1. Synthesis of polystyrene diesters from DEP₂ initiator.

Table 12.1. Molecular weight characterization of polystyrene diesters.

Target M_n ^a	Conversion (%) ^b	Polystyrene diesters - DEPN		After DEPN removal		1 st weight loss (TGA) (wt%)
		M_n ^c	M_w/M_n	M_n ^c	M_w/M_n	
4800	35	5000	1.45	5700	1.41	5.4
7600	32	6400	1.23	n/a	n/a	4.3
14200	32	15100	1.41	15500	1.36	3.5

^a Based on conversion and initiator concentration

^b Conversion (¹H NMR)

^c Size exclusion chromatography (THF), RI detector

12.4.2 Removal of DEPN End-groups from Polystyrene Diesters

In order to introduce the polystyrene diesters into a high temperature melt polyesterification, the DEPN end groups, which possessed potentially reactive phosphate esters required removal. This was achieved through heating the polystyrene diesters in the presence of 1-dodecanethiol, a well known chain transfer reagent, which served to donate its labile hydrogens to the polystyrene radicals that would form in the reaction (Figure 12.2). After the reaction, the polystyrene was easily isolated through precipitation in methanol. The removal of DEPN was verified with ^1H NMR (Figure 12.3), which revealed the loss of resonances attributed to the *tert*-butyl and methyl groups on DEPN. Further evidence came from ^{31}P NMR, which demonstrated the absence of phosphorus after the reaction (Figure 12.4). Improvements in thermal stability were observed in TGA measurements, which indicated that the initial weight loss attributed to DEPN was absent in the DEPN-removed polystyrene diesters (Figure 12.5). There was no evidence of side reactions with the central ester functionality and NMR resonances corresponding to the ester functional groups (3.6-4.2 ppm) were still present in the product. Furthermore, molecular weights and distributions did not change significantly upon DEPN removal (Table 12.1). For instance a polystyrene diester with $M_n = 5000$ and $M_w/M_n = 1.45$ was chromatographed with SEC after DEPN removal and exhibited $M_n = 5700$ and $M_w/M_n = 1.41$.

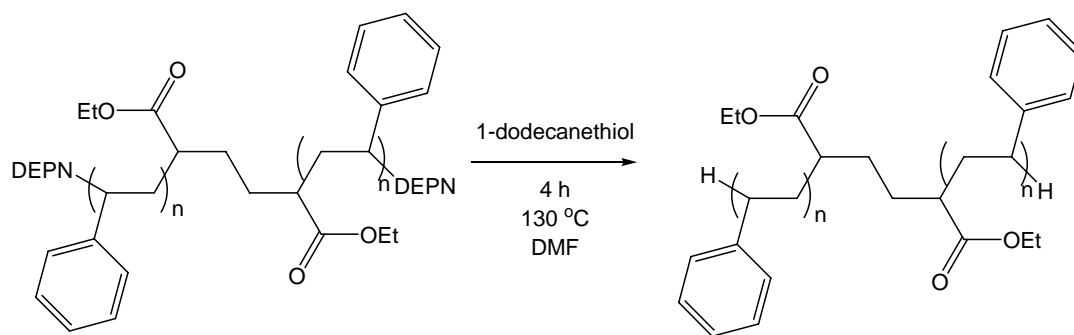


Figure 12.2. Removal of DEPN endgroups via heating with 1-dodecanethiol.

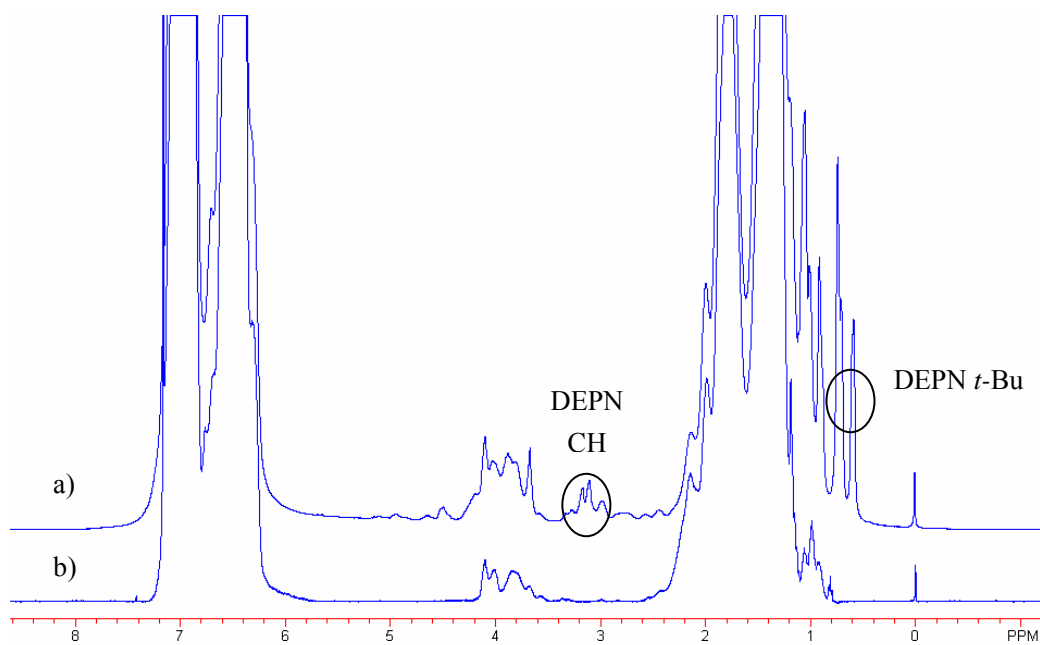


Figure 12.3. ¹H NMR spectrum of polystyrene diester (a) after removal of DEP (b). ($M_n = 5700$ after removal)

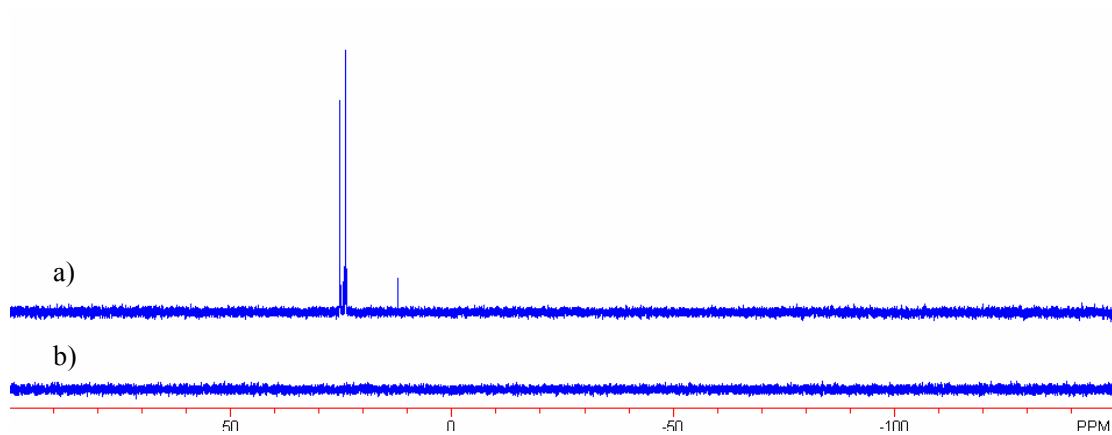


Figure 12.4. ^{31}P NMR data showing loss of DEPn from polystyrene diester (a) after reaction with 1-dodecanethiol (b). ($M_n = 5000$)

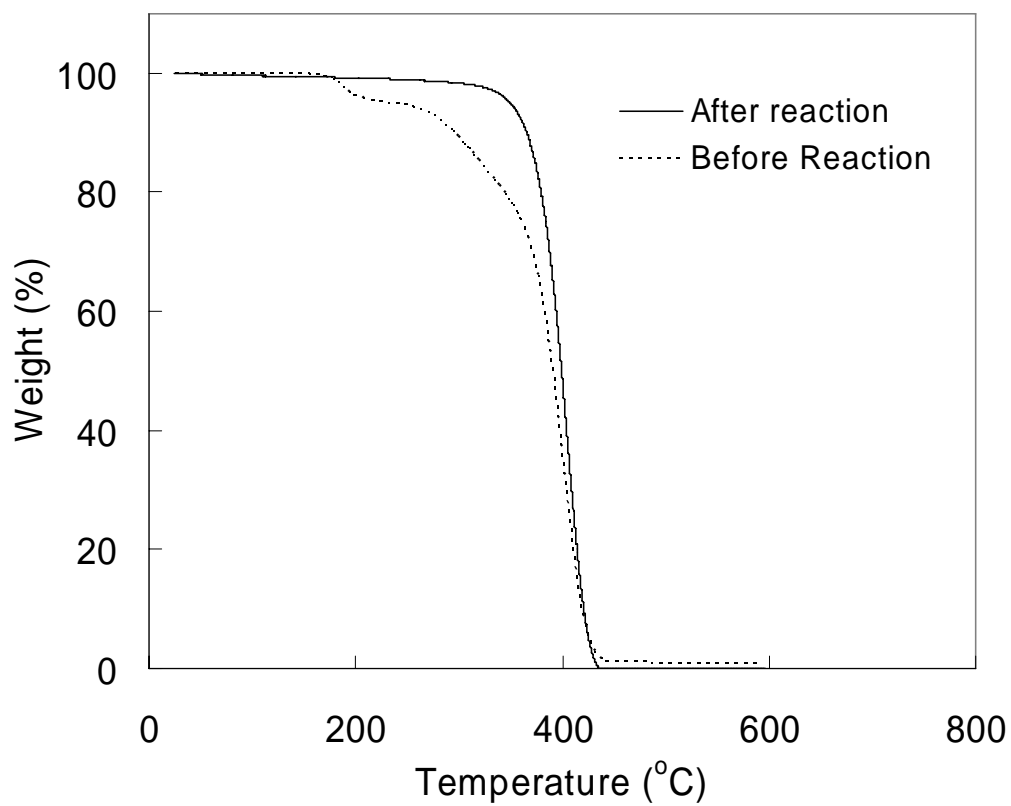


Figure 12.5. TGA data showing loss of DEPN endgroup and concomitant increased thermal stability after reaction with 1-dodecanethiol for polystyrene diester ($M_n = 5000$ g/mol).

12.4.3 Synthesis of Graft Copolymers

In order to synthesize polyester graft copolymers containing the polystyrene diesters, melt polymerization was employed. A non-polar aliphatic polyester backbone consisting of 1,6-hexanediol and dimethyl adipate was chosen to favor solubility of the polystyrene diesters. A solvent, diphenylsulfone was necessary, to allow the polystyrene diesters to remain soluble in the reaction medium. The lowest molecular weight polystyrene diester ($M_n = 5700$ g/mol, after DEPN removal) was utilized in the reaction to maximize the concentration of reactive ester groups. A slight excess (10 mol%) of 1,6-hexanediol monomer was introduced into the reaction, in order to favor reaction of the polystyrene diesters. The reaction was conducted over several hours using a temperature program typically employed with melt polyesters.⁹²⁶ During the final stage of the reaction, vacuum was employed to remove any unreacted 1,6-hexanediol. This also resulted in the loss of the diphenylsulfone solvent, resulting in some cloudiness, due to precipitation of unreacted polystyrene. After cooling, the polyester graft copolymer was dissolved in chloroform and precipitated 5 times into diethyl ether, a solvent which dissolved the low molecular weight polystyrene diesters. After this purification step, the product was analyzed with ^1H NMR spectroscopy, revealing a 2.5 wt% incorporation of polystyrene, which was close to the targeted level of incorporation (3.0 wt%). Due to the low content of polystyrene diester, the product polyester resembled poly(hexylene adipate), and which possesses a melting point of 58 °C.⁹²⁷

⁹²⁶ Lin, Q.; Unal, S.; Fornof, A. R.; Armentrout, R. S.; Long, T. E. Synthesis and characterization of telechelic phosphine oxide polyesters and cobalt(II) chloride complexes. *Polymer* **2006**, 47, 4085-93.

⁹²⁷ Brandrup, J.; Immergut, E. H., *Polymer Handbook*. 3rd ed.; Wiley: New York, 1989.

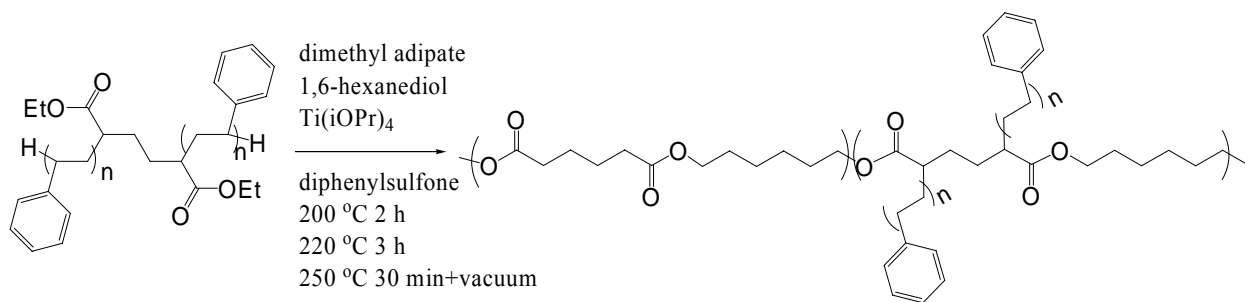


Figure 12.6. Synthesis of graft polyester containing polystyrene arms.

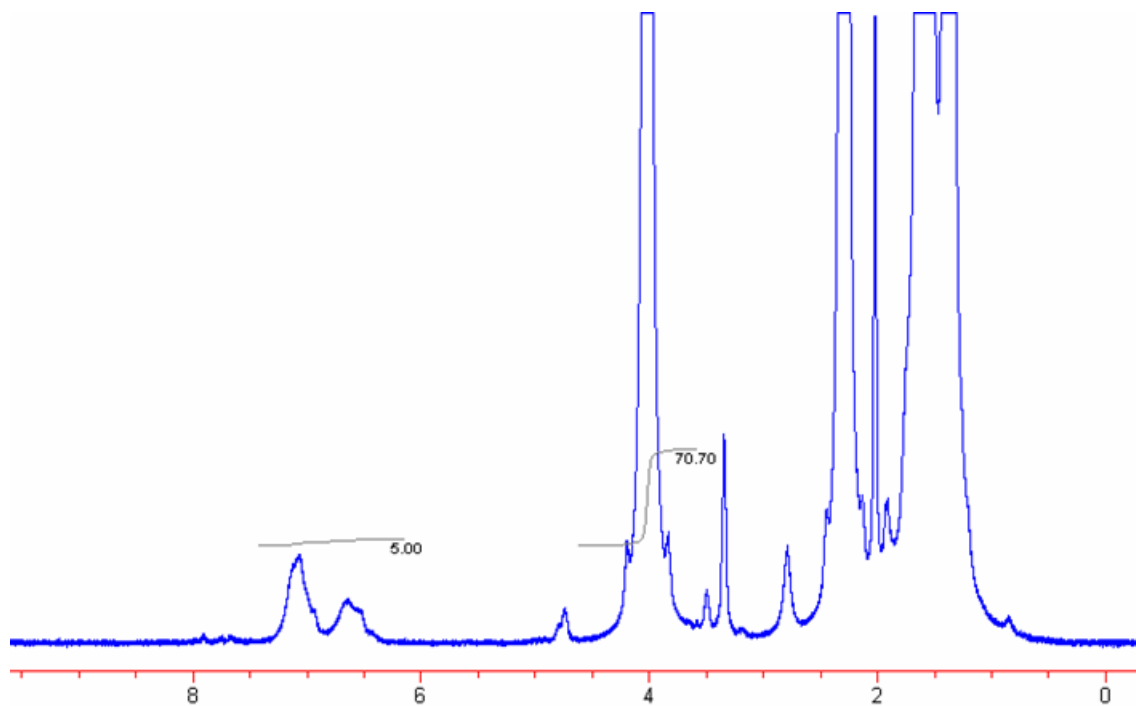


Figure 12.7. ^1H NMR spectrum of polyester graft copolymer (400 MHz, acetone- d_6).

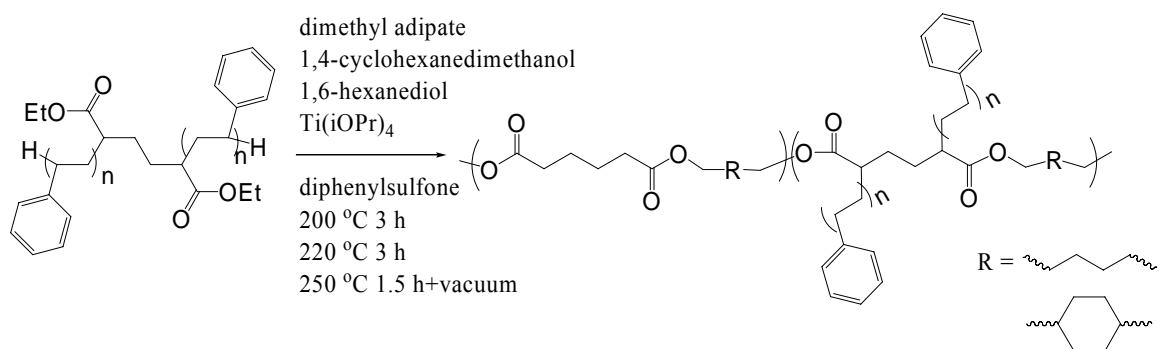


Figure 12.8. Graft polyester synthesis involving 1,4-cyclohexanedimethanol (cis/trans mixture).

Graft polyesters with a greater level of polystyrene incorporation (4.8 wt%, 5700 g/mol arms) were also synthesized (Figure 12.8). These polymers also contained 1,4-cyclohexanedimethanol (35 mol% of diol content, ~30% cis / 70% trans mixture) which decreased the level of crystallinity in the samples. However, a slow crystallization was evident at room temperature due to the low glass transition temperature (-51 °C). A melting temperature of 26 °C was observed with DSC. Atomic force microscopy was utilized to study the microphase separation in these systems. AFM phase images revealed a disordered multiphase morphology as shown in Figure 12.9. The polystyrene grafts were expected to microphase separate from the polyester backbone. Although graft copolymers typically exhibit less organized morphologies compared to block copolymers, some examples have shown well-ordered morphologies, for instance poly(methyl methacrylate-*g*-dimethylsiloxane) synthesized by McGrath et al.⁹²⁸

⁹²⁸ Smith, S. D.; DeSimone, J. M.; Huang, H.; York, G.; Dwight, D. W.; Wilkes, G. L.; McGrath, J. E. "Synthesis and characterization of poly(methyl methacrylate)-*g*-poly(dimethylsiloxane) copolymers. I. Bulk and surface characterization." *Macromolecules* **1992**, 25, 2575-81.

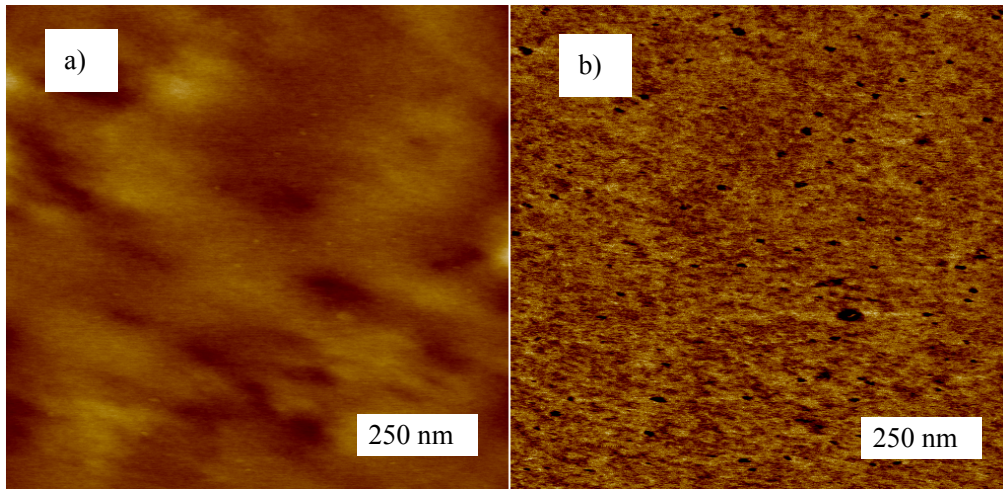


Figure 12.9. AFM a) height and b) phase images of a graft polyester with polystyrene arms $M_n = 5700$ g/mol.

12.5 Conclusion

A series of polystyrene diesters were synthesized using nitroxide mediated polymerization from a difunctional alkoxyamine initiator, DEPN₂. The polystyrene diesters were thermally treated in the presence of 1-dodecanethiol to remove the DEPN endgroups. This improved the thermal stability of the polystyrenes and removed potentially reactive phosphonate ester functional groups. The polystyrene diesters were introduced into a melt polyesterification, resulting in graft copolyesters containing polystyrene arms. The graft polyesters exhibited microphase separation in AFM images.

12.6 Acknowledgement

This material is based upon work supported by, or in part by, the U.S. Army Research Laboratory and the U.S. Army Research Office under grant number DAAD19-02-1-0275 Macromolecular Architecture for Performance (MAP) MURI.

Chapter 13. Future Directions - Introduction of Chiral Hydrogen Bonding Guest Molecules for Influence of Tacticity of Radical Polymerizations

13.1 Abstract

Hydrogen bonding monomers containing nucleobases (1-vinylthymine and 1-vinylbenzylthymine) were synthesized and polymerized in the presence or absence of complementary (adenine) hydrogen bonding derivatives possessing chirality. The influence of the chiral auxiliary guests on the tacticity of the polymers was analyzed by ^1H NMR spectroscopy. Polymerization of thymine-containing monomers in the presence of an acylated, chiral adenosine derivative yielded thymine containing polymers with similar ^1H NMR spectra to those obtained for radical polymerizations conducted in the absence of the chiral auxiliary. Analogous experiments with 1-vinylthymine produced similar results.

13.2 Introduction

Controlling the tacticity of radical polymerizations has presented a long-standing challenge for synthetic polymer chemists. Free radical polymerizations generally produce atactic polymers due to the symmetry of the sp^2 radical propagating chain end and the typically equal probability of reaction on either face.⁹²⁹ Stereocontrol is more commonly

⁹²⁹ Pino, P.; Sutter, U. W. Some aspects of stereoregulation in the stereospecific polymerization of vinyl monomers. *Polymer* **1976**, 17, 977-95.

afforded in the case of ionic or coordination polymerization.⁹³⁰ In cases of vinyl monomers with bulky substituents, radical polymerizations may result in some degree of syndiotacticity, due steric interactions between neighboring substituents.⁹²⁹ This is hypothesized to cause increased syndiotacticity in the polymerization of styrene conducted at lower temperatures.⁹³¹ The tacticity of radical polymerizations may be influenced through the use of chiral monomers.^{932,933}

The tacticity of radical polymerizations may also be altered through the use of species that associate reversibly or coordinate to substituents present on the polymer repeat units. Okamoto et al. observed the influence of Lewis acidic rare earth ions (Y, Sc, Yb) on the tacticity of acrylamide and alkylacrylamide polymerizations.⁹³⁴ Kamigaito et al. recently demonstrated the combination of metal catalyzed polymerization with stereocontrol via Lewis acids such as Y(OTf)₃ to influence the tacticity of *N,N*-dimethylacrylamide polymerizations.⁹³⁵ The coordination of the yttrium ions to neighboring amide substituents resulted in a tendency toward isotacticity (*m/r* = 82/12). Royles and Sherrington have used

⁹³⁰ Rodriguez-Delgado, A.; Chen, E. Y. X. Mechanistic Studies of Stereospecific Polymerization of Methacrylates Using a Cationic, Chiral ansa-Zirconocene Ester Enolate. *Macromolecules* **2005**, 38, 2587-94.

⁹³¹ Standt, U.; Klein, J. On the Stereoregularity of Radically Polymerized Polystyrene. *Makromol Chem Rapid Comm* **1981**, 2, 41-45.

⁹³² Porter, N. A.; Allen, T. R.; Breyer, R. A. Chiral Auxiliary Control of Tacticity in Free Radical Polymerization. *J Am Chem Soc* **1992**, 114, 7676-83.

⁹³³ Green, M. M.; Park, J.-W.; Sato, T.; Teramoto, A.; Lifson, S.; Selinger, R. L. B.; Selinger, J. V. The Macromolecular Route to Chiral Amplification. *Angew. Chem. Int. Ed.* **1999**, 38, 3138-54.

⁹³⁴ Isobe, Y.; Fujioka, D.; Habaue, S.; Okamoto, Y. Efficient Lewis Acid-Catalyzed Stereocontrolled Radical Polymerization of Acrylamides. *J Am Chem Soc* **2001**, 123, 7180-1.

⁹³⁵ Sugiyama, Y.; Sato, K.; Kamigaito, M.; Okamoto, Y. Iron-catalyzed radical polymerization of acrylamides in the presence of Lewis acid for simultaneous control of molecular weight and tacticity. *J Polym Sci, Part A: Polym Chem* **2006**, 44, 2086-98.

chiral auxiliaries that bond via metal-ligand interactions.⁹³⁶ Templated polymerizations also provide a route toward stereocontrol.⁹³⁷

Hydrogen bonding has only recently been employed as a means of influencing the tacticity of radical polymerizations. Hirano et al reported slight changes in tacticity for poly(*N*-isopropylacrylamide) that was polymerized in the presence of bulky diphosphates which hydrogen bonded to the NH of the monomer.⁹³⁸ Okamoto's⁹³⁹ and Kamigaito's⁹⁴⁰ group has used the hydrogen bonding between bulky fluoroalcohols and esters to influence the tacticity of radical polymerizations of vinyl ester monomers. Only slight changes in tacticity (greater syndiotacticity) were observed. More recently, more Kamigaito's group utilized more sophisticated triple hydrogen bonding between diaminopyridine acrylamide monomers and cyclic imide guests to influence tacticity of polymerizations.⁹⁴¹ As expected, the largest cyclic imide guest, naphthalimide, afforded the highest syndiotacticity ($r = 71\%$, versus 42% in the absence of naphthalimide).

⁹³⁶ Royles, J. L. R.; Sherrington, D. C. Transition metal complex-templated asymmetric free radical polymerisation. *Chem Comm* **1998**, 421-2.

⁹³⁷ Serizawa, T.; Hamada, K.; Akashi, M. Polymerization within a molecular-scale stereoregular template. *Nature* **2004**, 429, 52-5.

⁹³⁸ Hirano, T.; Kitajima, H.; Seno, M.; Sato, T. Hydrogen-bond-assisted stereocontrol in the radical polymerization of *N*-isopropylacrylamide with bidentate Lewis base. *Polymer* **2006**, 47, 539-46.

⁹³⁹ Habaue, S.; Okamoto, Y. Stereocontrol in Radical Polymerization. *Chem Record* **2000**, 46-52.

⁹⁴⁰ Koumura, K.; Satoh, K.; Kamigaito, M.; Okamoto, Y. Iodine Transfer Radical Polymerization of Vinyl Acetate in Fluoroalcohols for Simultaneous Control of Molecular Weight, Stereospecificity, and Regiospecificity. *Macromolecules* **2006**, 39, 4054-61.

⁹⁴¹ Wan, D.; Satoh, K.; Kamigaito, M. Triple Hydrogen Bonding for Stereospecific Radical Polymerization of a DAD Monomer and Simultaneous Control of Tacticity and Molecular Weight. *Macromolecules* **2006**, 39, 6882-6.

The reversible attachment of guest molecules to polymers via nucleobase hydrogen bonding has been investigated in both solution⁹⁴² and the solid state.^{943,944} Rotello et al. have used three-point hydrogen bonding between diacyldiaminopyridines and thymine to attach guest molecules containing flavin⁹⁴⁵ or POSS to polystyrene.⁹⁴³ Hydrogen bonding guest molecules can also increase the solubility of hydrogen bonding polymers via screening of polymer-polymer self-association, thereby maintaining homogeneity during polymerization reactions.⁹⁴⁶ Multiple complementary association modes are possible for nucleobases, including the classical Watson-Crick mode which is present in DNA as well as the less commonly observed Hoogsteen association mode.⁹⁴⁷ Furthermore, nucleobases exhibit several weak self-association modes ($K_a < 10 \text{ M}^{-1}$),⁹⁴⁸ which compete with the complementary association modes.

In this manuscript, we discuss the use of chiral auxiliaries containing hydrogen bonding groups for the influence of tacticity of radical polymerizations (Figure 13.1). In particular,

⁹⁴² Thibault, R. J.; Hotchkiss, P. J.; Gray, M.; Rotello, V. M. Thermally Reversible Formation of Microspheres through Non-Covalent Polymer Cross-Linking. *J Am Chem Soc* **2003**, 125, 11249-52.

⁹⁴³ Carroll, J. B.; Waddon, A. J.; Nakade, H.; Rotello, V. M. "Plug and Play" Polymers. Thermal and X-ray Characterizations of Noncovalently Grafted Polyhedral Oligomeric Silsesquioxane (POSS)-Polystyrene Nanocomposites. *Macromolecules* **2003**, 36, 6289-91.

⁹⁴⁴ Ilhan, F.; Gray, M.; Rotello, V. M. Reversible Side Chain Modification through Noncovalent Interactions. "Plug and Play" Polymers. *Macromolecules* **2001**, 34, 2597-601.

⁹⁴⁵ Ilhan, F.; Galow, T. H.; Gray, M.; Clavier, G.; Rotello, V. M. Giant Vesicle Formation through Self-Assembly of Complementary Random Copolymers. *J Am Chem Soc* **2000**, 122, 5895-6.

⁹⁴⁶ Stubbs, L. P.; Weck, M. Towards a Universal Polymer Backbone: Design and Synthesis of Polymeric Scaffolds Containing Terminal Hydrogen-Bonding Recognition Motifs at Each Repeating Unit. *Chem Eur J* **2003**, 9, 992-9.

⁹⁴⁷ Ghosal, G.; Muniyappa, K. Hoogsteen base-pairing revisited: Resolving a role in normal biological processes and human diseases. *Biochemical and Biophysical Research Communications* **2006**, 343, 1-7.

⁹⁴⁸ Kyogoku, Y.; Lord, R. C.; Rich, A. The Effect of Substituents on the Hydrogen Bonding of Adenine and Uracil Derivatives. *Proc Natl Acad Sci USA* **1967**, 57, 250-7.

we examine complementary nucleobase hydrogen bonding between adenine and thymine derivatives ($K_a = 130 \text{ M}^{-1}$ in chloroform)⁹⁴⁸ as a means to reversibly attach the chiral auxiliary. Chiral hydrogen bonding molecular recognition has also played a large role in supramolecular chemistry due to the ability to generate helical fibers and macroscopic structures through “programming” that the chirality provides.⁹⁴⁹ The use of chiral nucleobases is advantageous due to the ready availability of chiral sugar-containing nucleosides. The complementary nature of nucleobase hydrogen bonding is key to minimizing competition from self-association of the hydrogen bonding monomers or chiral auxiliary. Furthermore, nucleobase hydrogen bonding arrays are asymmetric, favoring specific orientation of the chiral auxiliary.

⁹⁴⁹ Gulik-Krzywicki, T.; Fouquey, C.; Lehn, J. M. Electron microscopic study of supramolecular liquid crystalline polymers formed by molecular-recognition-directed self-assembly from complementary chiral components. *Proc. Natl. Acad. Sci. USA* **1993**, 90, 163-7.

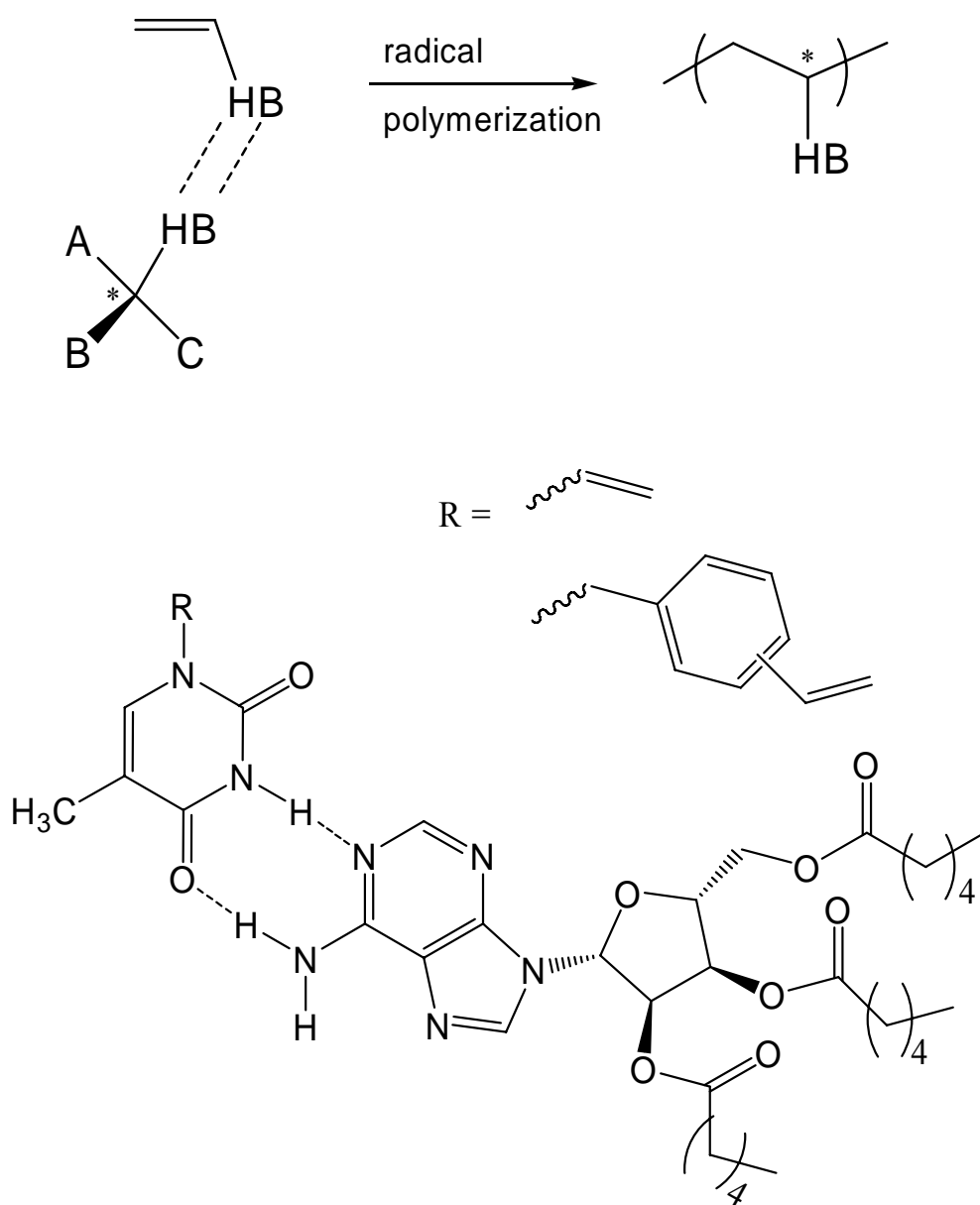


Figure 13.1. Polymerization of a hydrogen bonded complex of a chiral auxiliary and a complementary hydrogen bonding monomer.

13.3 Experimental

13.3.1 Materials

Adenosine (99%), azobis(isobutyronitrile) (AIBN, 98%), hexanoic anhydride (97%), pyridine (anhydrous, 99.8%), dimethyl sulfoxide (anhydrous, 99.9%), *N,N*-dimethylformamide (DMF, anhydrous, 99.8%), thymine (99%), 1,2-dibromoethane (99+%), hexamethyldisilazane (HMDS, 97%) sodium metal (99%) were obtained from Aldrich and used as received. *tert*-Butanol (99.5%) was obtained from Aldrich and was distilled from CaH₂ prior to use. 1-vinylbenzylthymine⁹⁵⁰ and 1-methacryloxythymine⁹⁵¹ were synthesized as previously described. V70 initiator was obtained from Wako Pure Chemicals.

13.3.2 Synthesis of 2',3',5'-trihexyladenosine (AdHex)

Adenosine (0.504 g, 1.88 mmol), hexanoic anhydride (1.200 g, 5.61 mmol, 3 equiv), pyridine (5 mL) and dimethyl sulfoxide (3 mL) were stirred at 25 °C for 16 h in a round bottomed flask. The solvents were removed under reduced pressure (60 mtorr, 40 °C) and the product was dissolved in hexane and washed with aqueous sodium bicarbonate. The solvent was evaporated and the product was purified via chromatography on silica gel, eluting with chloroform/methanol (95/5). AdHex was isolated as a colorless oil in 63% yield. ¹H NMR (DMSO-d₆, δ, ppm): 0.83 (m, 9H), 1.23 (m, 12H), 1.47 (m, 4H), 1.56 (m, 2H), 2.18 (t, 1H),

⁹⁵⁰ Sedlak, M.; Simunek, P.; Antonietti, M. Synthesis and ¹⁵NMR Characterization of 4-Vinylbenzyl Substituted Bases of Nucleic Acids. *J Heterocyclic Chem* **2003**, 40, 671-75.

⁹⁵¹ Akashi, M.; Tanaka, Y.; Iwasaki, H.; Miyauchi, N. Synthesis and Polymerization of New Vinyl Derivatives of Thymine. *Angew. Makromol. Chem.* **1987**, 147, 207-13.

2.28 (m, 3H), 2.38 (m, 2H), 3.49 (dd, 1H), 4.34 (q, 1H), 4.40 (dd, 1H), 5.65 (t, 1H), 6.05 (t, 1H), 6.19 (d, 1H), 7.39 (br s, 2H), 8.15 (s, 1H), 8.34 (s, 1H). FAB MS: 562.327 m/z [M+H]⁺, observed, 562.32 m/z [M+H]⁺ theoretical. $[\alpha]_D = -36.8^\circ$ (chloroform, 25 °C).

13.3.3 Synthesis of 1-(2-bromoethyl)thymine

Thymine (8.0 g, 63.5 mmol), HMDS (30 mL, 143 mmol, 2.25 equiv.) and DMF (5 mL) were stirred at 130 °C for 18 h. A short-path distillation head and receiving flask were fitted to the reaction flask and gentle (aspirator) vacuum was applied at 130 °C, resulting in distillation of the residual HMDS and DMF. 1,2-dibromoethane (30 g, 162 mmol, 2.55 equiv) and DMF (40 mL) were added and the mixture was stirred at 90 °C for 24 h. After cooling to room temperature, DMF and unreacted 1,2-dibromoethane were removed under reduced pressure (60 mtorr, 40 °C). The crude product was dissolved in THF (50 mL) and water (15 mL) was added to remove the silyl protecting groups, causing precipitation of thymine from solution. The mixture was dried with rotary evaporation and methanol was added. The unreacted thymine was filtered off with a sintered glass filter. The methanol solution was evaporated, yielding 1-(2-bromoethyl)thymine as a white powder, 3.52 g, 24% yield. ¹H NMR (DMSO-d₆, δ, ppm): 1.75 (s, 3H), 3.70 (t, 2H, J = 6.5 Hz), 4.02 (t, 2H, J = 6.5 Hz), 7.56 (s, 1H), 11.34 ppm (s, 1H).

13.3.4 Synthesis of 1-vinylthymine

Sodium (1.2 g, 52 mmol) was broken into small pieces and added to freshly distilled, dry *tert*-butanol (200 mL). The mixture was stirred at 50 °C for 24 h with a bubbler to release

hydrogen gas until all of the sodium was consumed. 1-(2-bromoethyl)thymine (3.52 g, 15.2 mmol) was added into the solution and stirred at 60 °C for 48 h. After the reaction, *tert*-butanol was removed under reduced pressure (60 mtorr, 40 °C) and water was added (100 mL) The solution was neutralized with HCl and the water was removed under reduced pressure (60 mtorr, 40 °C). The crude product was chromatographed on silica, eluting with chloroform/methanol (90/10). 1-vinylthymine was obtained as a cream-colored powder, 1.655 g, 72% yield. ¹H NMR (CDCl₃, δ, ppm): 1.99 (s, 3H), 4.91 (dd, 1H, *J*₁ = 9.3 Hz, *J*₂ = 2.2 Hz), 5.07 (dd, 1H, *J*₁ = 16.2 Hz, *J*₂ = 2.2 Hz), 7.21 (dd, 1H, *J*₁ = 15.8 Hz, *J*₂ = 9.8 Hz), 7.34 (s, 1H), 9.01 (br s, 1H). FAB MS: *m/z* = 153.066 [M+H]⁺ (experimental), *m/z* = 153.066 [M+H]⁺ (theoretical).

13.3.5 Free radical polymerization of 1-vinylthymine

1-vinylthymine (152 mg, 1.00 mmol) and AIBN (2 mg, 0.012 mmol, 1.3 wt% relative to monomer) were dissolved in DMSO-d₆ (1.000 g) and degassed with repeated cycles of vacuum (60 mtorr) followed by argon backfilling. The reaction was stirred at 65 °C for 48 h, followed by precipitation in methanol. The fine powder product was collected via syringe filter, dried under vacuum for 24 h, redissolved in DMSO-d₆ and precipitated a second time in methanol, followed by collection in a syringe filter. ¹H NMR (DMSO-d₆, δ, ppm): 0.7-2.5 (br m, 5H, backbone CH₂ + thymine CH₃), 3.5-5.3 (br m, 2H), 7-7.8 (br m, 0.2H), 10-10.8 (br s, 1H), 11-11.5 (br m, 0.16H)

13.3.6 Polymerization of 1-vinylthymine in the Presence of a Chiral Auxiliary

AdHex (864 mg, 1.54 mmol) and 1-vinylthymine (233 mg, 1.53 mmol, 0.99 equiv) and V70 initiator (60 mg, 0.169 mmol, 25 wt% relative to monomer) were dissolved in CDCl₃ (5.64 g) and degassed by purging briefly with argon. The mixture was stirred for 72 h at 25 °C under argon during which time the reaction became cloudy. The polymer was isolated via precipitation in methanol and filtered with a syringe filter.

13.3.7 Free radical polymerization of 1-vinylbenzylthymine

1-vinylbenzylthymine (106 mg, 0.44 mmol) and AIBN initiator (7.1 mg, 0.043 mmol, 6.7 wt% relative to monomer) were dissolved in DMSO-d₆ (1.14 g) and degassed by purging briefly with argon. The mixture was stirred for 24 h at 70 °C under argon during which time the reaction remained homogeneous. The polymer was isolated via precipitation in methanol. ¹H NMR (DMSO-d₆, δ, ppm): 1-2 (br, 6H, backbone + thymine CH₃), 4.4-4.9 (br, 2H, Ph-CH₂-N), 6-7.5 (br, 5H, Ph + thymine C=CH), 11.3 (br s, 1H, thymine NH).

13.3.8 Polymerization of 1-vinylbenzylthymine in the Presence of a Chiral Auxiliary

AdHex (210 mg, 0.374 mmol) and 1-vinylbenzylthymine (96 mg, 0.40 mmol, 1.06 equiv) and V70 initiator (4.0 mg, 0.013 mmol, 4.2 wt% relative to monomer) were dissolved in chloroform (1.05 g) and degassed by purging briefly with argon. The mixture was stirred for 24 h at 20 °C under argon during which time the reaction remained homogeneous. The polymer was isolated via precipitation in methanol. Poly(1-vinylbenzylthymine), 26 mg, was obtained as a white powder.

13.3.9 Characterization

¹H and ¹³C NMR spectroscopic data was collected in CDCl₃ on a Varian 400 MHz spectrometer at ambient temperature. FAB MS was conducted in positive ion mode on a JEOL HX110 Dual Focusing Mass Spectrometer using xenon ion bombardment, polyethylene glycol (PEG) standards and a 3-nitrobenzyl alcohol matrix. Optical rotation measurements were conducted on a Perkin Elmer 241 polarimeter using the sodium D line.

13.4 Results and Discussion

A chloroform soluble, chiral auxiliary containing adenine (AdHex) was synthesized in a single step from commercially available adenosine (Figure 13.2). The solubility in chloroform was a critical feature for the chiral auxiliary since hydrogen bonding interactions are screened by more polar solvents which typically dissolve nucleobase functionalized compounds such as DMSO, water or DMF. The acylation of the adenine hydroxyl groups occurred selectively over reaction with the adenine NH₂ as indicated by the presence of the NH₂ protons in the ¹H NMR spectrum (7.39 ppm, DMSO-d₆). The reaction was analogous to a literature procedure for acetylation of adenosine.⁹⁵² Acetylated adenosine was also synthesized according to the literature, however it proved insoluble in chloroform. The optical rotation of AdHex, ([α]_D = -36.8° chloroform, 25 °C) was similar to that of acetylated adenosine ([α]_D = -37.6°, DMSO-d₆, 25 °C) suggesting retention of chirality. The adenosine precursor possesses an optical rotation of -60° (H₂O, 24 °C) according to the literature.⁹⁵³

⁹⁵² Bajji, A. C.; Davis, D. R. Synthesis of the tRNA^{Lys},3 Anticodon Stem-Loop Domain Containing the Hypermodified ms2t6A Nucleoside. *J Org Chem* **2002**, 67, 5352-8.

⁹⁵³ Stecher, P. G.; Finkel, M. J.; Siegmund, O. H.; Szafranski, B. M., Merck Index. 7 ed.; Merck and Co: Rahway, NJ, 1960.

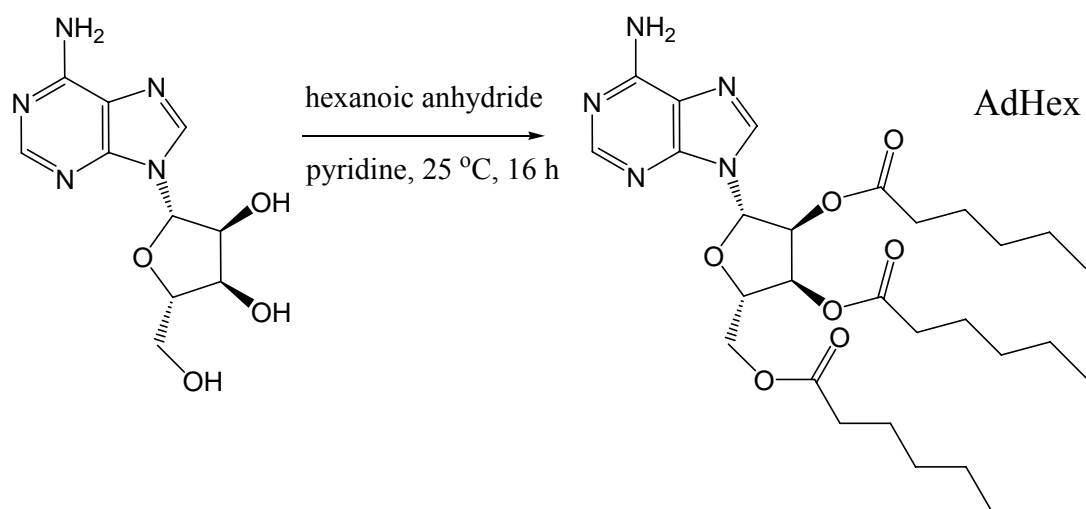


Figure 13.2. Synthesis of a chloroform soluble chiral auxiliary (AdHex) for polymerization of complementary thymine or uracil-containing monomers.

The chiral auxiliary was introduced into radical polymerizations of 1-vinylbenzylthymine, a monomer which possesses a phenyl group between the polymerizable vinyl group and the thymine nucleobase (Figure 13.3). The polymerization of 1-vinylbenzylthymine was first conducted in a polar solvent, DMSO-d₆, in the absence of the chiral auxiliary. In order to carry out the polymerization with the chiral auxiliary, conditions were chosen that were expected to maximize the level of association. Thus, the reactions were run in chloroform, at 20 °C, using a low-temperature initiator, V-70 and one equivalent of the AdHex. The polymerizations in both cases remained homogeneous and the resulting poly(1-vinylbenzylthymine)s were precipitated in methanol as a white powder. The ¹H NMR spectra of the polymers from these two separate routes are shown in Figure 13.4 (1-1.8 ppm, DMSO-d₆). Changes in tacticity of vinyl polymers, such as PMMA⁹⁵⁴ are often observed in ¹H NMR through the backbone or side-chain resonances. This typically provides information to the diad level (m = meso, r = racemic) or triad level (mm (isotactic), rr (syndiotactic), rm (heterotactic)). However, for polystyrene, tacticity is more difficult to obtain from NMR and detailed information is only obtained through quantitative ¹³C NMR.⁹⁵⁵ Unfortunately, for these polymers, the quantity of material obtained from the polymerizations was not sufficient to obtain ¹³C NMR spectra. Harwood and coworkers were able to assign proton NMR resonances to triad structures for substituted polystyrenes such as poly(4-acetylstyrene).⁹⁵⁶ The similarity of the proton NMR spectra for

⁹⁵⁴ Carriere, P.; Grohens, Y.; Spevacek, J.; Schultz, J. Stereospecificity in the Adsorption of Tactic PMMA on Silica. *Langmuir* **2000**, 16, 5051-3.

⁹⁵⁵ Pasch, H.; Hiller, W.; Haner, R. Investigation of the tacticity of oligostyrenes by on-line HPCL/¹H NMR. *Polymer* **1998**, 39, 1515-23.

⁹⁵⁶ Trumbo, D. L.; Chen, T.-K.; Harwood, H. J. Observation of Triad Sequences in a Polystyrene Derivative. *Macromolecules* **1981**, 14, 1138-9.

poly(1-vinylbenzylthymine) was interpreted to indicate similar tacticity. This lack of a clear difference suggested that the radical propagating chain end was too distant from the chiral center to be influenced.

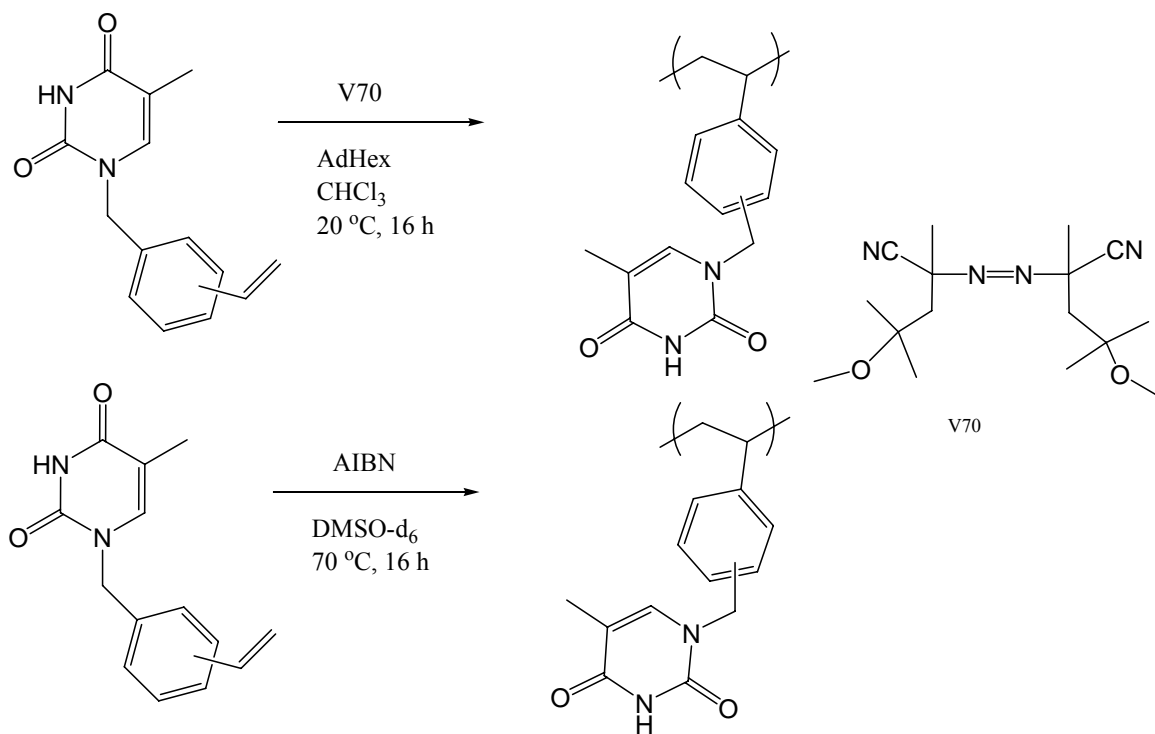


Figure 13.3. Polymerization of 1-vinylbenzylthymine with and without added chiral auxiliary AdHex.

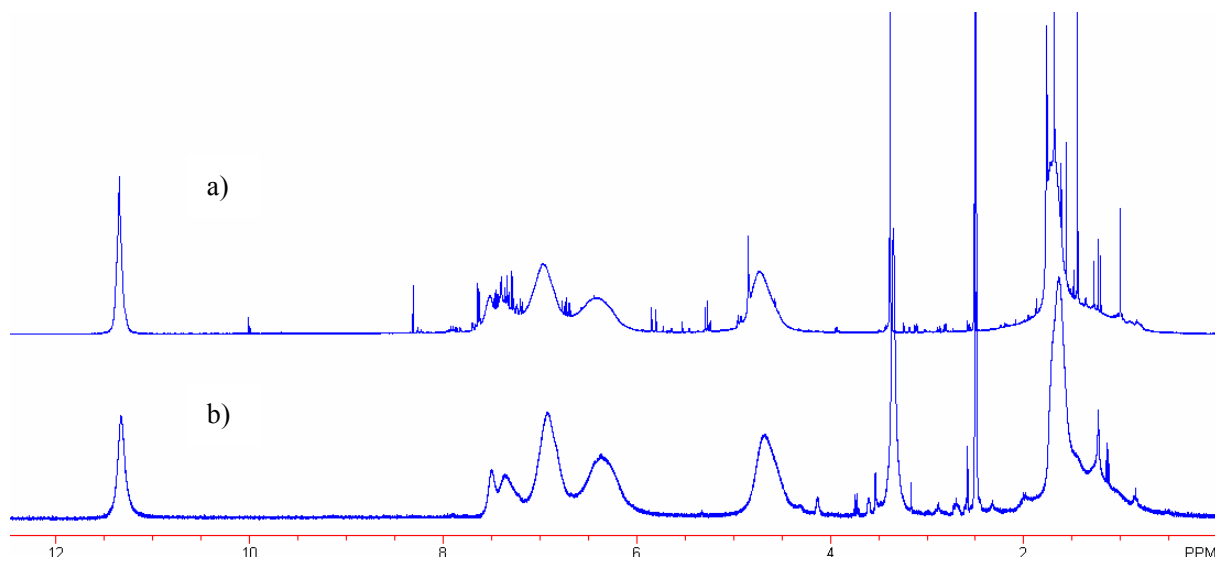


Figure 13.4. ¹H NMR spectra of poly(1-vinylbenzylthymine) polymerized in the absence (a) or presence (b) of chiral auxiliary AdHex. (DMSO-d₆). Sharp peaks represent impurities (residual monomer, solvents).

In order to bring the chiral center closer to the propagating radical chain end, hydrogen bonding monomers possessing shorter distances between the nucleobase and the vinyl group were pursued. Thus, 1-methacryloxythymine was synthesized according to a literature procedure.⁹⁵⁷ The methacrylate monomer also benefits from the ability to determine tacticity through ¹H NMR spectroscopy from the α -methyl resonances. However, this monomer was found not to homopolymerize even under conventional conditions (3 wt% BPO, DMSO, 80 °C, 16 h). The literature also confirmed difficulty in the polymerization of this monomer, reporting polymerization yields of only 7%.⁹⁵⁷ Alternately, 1-acryloxythymine was reported to provide higher polymerization yields (86%),⁹⁵⁷ but the synthesis of this monomer was unsuccessful despite repeated attempts. Michael addition side reactions of the acrylate group with the thymine NH were detected in ¹H NMR spectra and the literature reported low yields of the monomer (36%).⁹⁵⁷

Abandoning an acrylic nucleobase-containing monomer, attention was turned to a monomer with even shorter distance between the propagating center and the nucleobase. 1-vinylthymine was synthesized in four steps from thymine (Figure 13.5). This monomer was previously homopolymerized by Kondo et al. via free radical methods (AIBN, DMSO, 95 °C) with reported yields of 30%.⁹⁵⁸ The analogous 1-vinyluracil monomer was reported to yield nearly quantitative polymerization conversion, however, this was complicated by significant

⁹⁵⁷ Akashi, M.; Tanaka, Y.; Iwasaki, H.; Miyauchi, N. Synthesis and Polymerization of New Vinyl Derivatives of Thymine. *Angew. Makromol. Chem.* **1987**, 147, 207-13.

⁹⁵⁸ Kondo, K.; Iwasaki, H.; Nakatani, K.; Ueda, N.; Takemoto, K.; Imoto, M. Vinyl Compounds of Nucleic Acid Bases. 3. Polymerization and Copolymerization of *N*-Vinyl and *B*-Methacryloyloxyethyl Compounds of Nucleic Acid Bases and their Polymer-Polymer Interactions. *Die Makromolekulare Chemie* **1969**, 125, 42-7.

amounts of “cyclopolymerization” involving reaction of the internal double bond present in uracil as reported by Kaye.⁹⁵⁹

⁹⁵⁹ Kaye, H. Cyclopolymerization of *N*-Vinyluracil. *Macromolecules* **1971**, 4, 147-52.

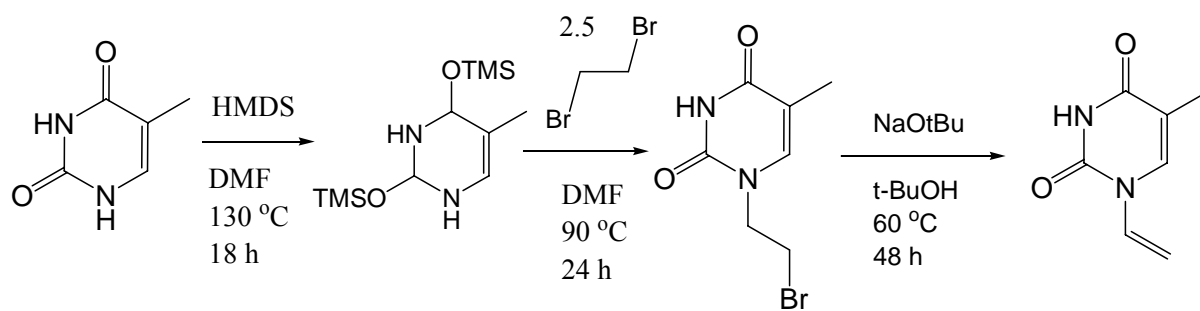


Figure 13.5. Synthesis of 1-vinylthymine.

1-vinylthymine was polymerized using conventional radical polymerization conditions (AIBN, DMSO-d₆, 65 °C). 1-vinylthymine was also polymerized in the presence of AdHex in CDCl₃ at 25 °C, with the low-temperature initiator V-70. This resulted in very low conversion, and the product was isolated via syringe filtering. As for the case of 1-vinylbenzylthymine, the ¹H NMR spectra were very similar (Figure 13.6) suggesting a lack of influence on tacticity. However, the most closely related common polymer, poly(*N*-vinyl pyrrolidone), requires ¹³C NMR spectroscopy for tacticity determination.⁹⁶⁰ The determination of the effect of the chiral auxiliary was complicated by the necessary low scale of the polymerization reactions and the low conversions obtained. Typically for quantitative ¹³C NMR, at least 300 mg of polymer is required.

⁹⁶⁰ Wan, D.; Satoh, K.; Kamigaito, M.; Okamoto, Y. Xanthate-Mediated Radical Polymerization of *N*-Vinylpyrrolidone in Fluoroalcohols for Simultaneous Control of Molecular Weight and Tacticity. *Macromolecules* **2005**, 38, 10397-405.

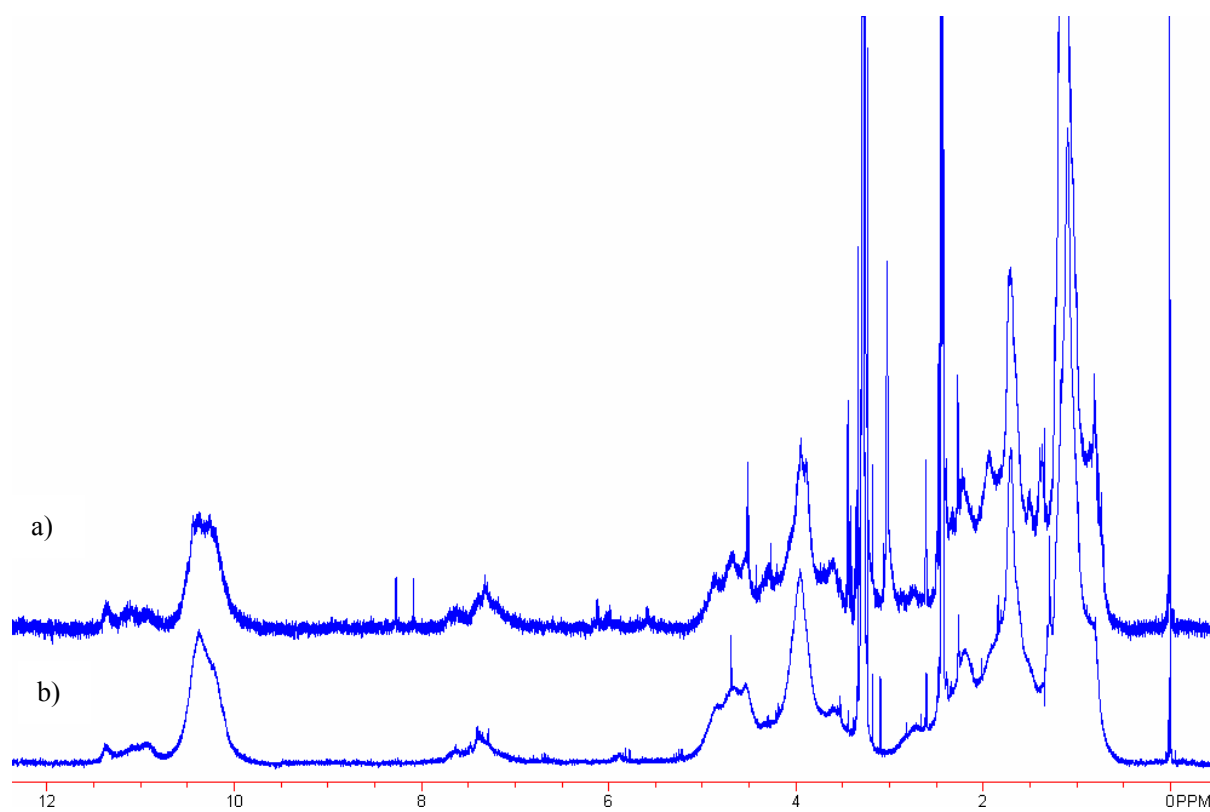


Figure 13.6. ^1H NMR spectrum of poly(1-vinylthymine) polymerized in the presence (a) and absence (b) of AdHex.

13.5 Conclusions

Hydrogen bonding monomers containing nucleobases (1-vinylthymine and 1-vinylbenzylthymine) were synthesized and polymerized in the presence or absence of complementary (adenine) hydrogen bonding derivatives possessing chirality. The influence of the chiral auxiliary guests on the tacticity of the polymers was analyzed by ^1H NMR spectroscopy. Polymerization of thymine-containing monomers in the presence of an acylated, chiral adenosine derivative yielded polymers with similar ^1H NMR spectrum to those obtained for radical polymerizations conducted in the absence of the chiral auxiliary.

13.6 Future Work

The next steps in this project involve finding reaction conditions or hydrogen bonding monomers which lead to high yields for polymerization. This is necessary in order to obtain necessary sample quantities for ^{13}C NMR analysis.

13.7 Acknowledgement

This material is based upon work supported by, or in part by, the U.S. Army Research Laboratory and the U.S. Army Research Office under grant number DAAD19-02-1-0275 Macromolecular Architecture for Performance (MAP) MURI.

Chapter 14. Future Directions- Rheological Studies of Hydrogen Bonding Copolymers with Reversible Attachment of Ionic Functionality

14.1 Abstract

Random copolymers of a phosphonium styrene monomer and *n*-butyl acrylate were synthesized in order to compare the covalent attachment of phosphonium ions to hydrogen bonding attachment. Hydrogen bonding attachment of ionic groups was achieved through blending of an adenine containing copolymer with a complementary uracil phosphonium salt. Partial miscibility of the uracil phosphonium salt with the 2.0 mol% adenine-functional copolymer was observed. Rheological studies indicated strong attachment of the uracil phosphonium salt, with rheological behavior of the blend mirroring that of the covalent copolymer across the range of temperatures studied. Covalent phosphonium copolymers with higher incorporation of the phosphonium salt monomer (30 mol%) resulted in increased T_g , a broad maximum in the small-angle X-ray scattering curve and multiple transitions above T_g in dynamic mechanical analysis, suggesting ionic aggregation.

14.2 Introduction

Ionic interactions have been studied in polymer systems for several decades.^{961- 963} These strong, electrostatic interactions possess enthalpies approximately one order of magnitude stronger than hydrogen bonding interactions (~200 kJ/mol).⁹⁶⁴ Furthermore, these coulombic interactions are non-specific and occur over longer distances than hydrogen bonding interactions. Ion-containing random copolymers which possess less than 15 mol% of ionic groups are termed ionomers. Typically, these ionomers consist of a relatively low dielectric constant, non-ionic, comonomer, which is designed to maximize ionic association. These ionomers possess ionic aggregates due to the association of the ionic species. Recently, Winey et al. thoroughly characterized these ionic aggregates via SAXS and STEM.⁹⁶⁵ The presence of the ionic aggregates in polymers results in improved high temperature mechanical properties and better toughness and abrasion resistance, as well as improved chemical resistance due to the insolubility of the ionic groups in hydrocarbon solvents. Decreases in compression set,⁹⁶⁶ tensile set, hysteresis and creep were also observed. Materials such as DuPont's Surlyn[®] (an ionomer of an ethylene methacrylic acid copolymer)

⁹⁶¹ Eisenberg, A.; Hird, B.; Moore, R. B. A New Multiplet-Cluster Model for the Morphology of Random Ionomers. *Macromolecules* **1990**, 23, 4098-107.

⁹⁶² Eisenberg, A. Clustering of Ions in Organic Polymers. A Theoretical Approach. *Macromolecules* **1970**, 3, 147-54.

⁹⁶³ Duvdevani, I.; Lundberg, R. D.; Wood-Cordova, C.; Wilkes, G. L., Coulombic Interactions in Macromolecular Systems. In *ACS Symposium Series*, Eisenberg, A.; Bailey, F. E., Eds. American Chemical Society: Washington DC, 1986; Vol. 302, pp 185-99.

⁹⁶⁴ Hird, B.; Eisenberg, A. Sizes and Stabilities of Multiplets and Clusters in Carboxylated and Sulfonated Styrene Ionomers. *Macromolecules* **1992**, 25, 6466-74.

⁹⁶⁵ Benetatos, N. M.; Heiney, P. A.; Winey, K. I. Reconciling STEM and X-ray Scattering Data from a Poly(styrene-*ran*-methacrylic acid) Ionomer: Ionic Aggregate Size. *Macromolecules* **2006**, 39, 5174-6.

⁹⁶⁶ Balas, J. G.; Gergen, W. P.; Willis, C. L.; Pottick, L. A.; Gelles, R.; Weiss, R. A. Sulfonated block copolymers. US Patent 5239010, 1993.

are typically used for golf ball covers, due to the outstanding mechanical properties conferred from the ionic association. Exxon studied sulfonated EPDM (ethylene propylene diene rubber) as a tough, chemical resistant elastomer.⁹⁶⁷ A further advantage of ionic polymers is the ability to conduct ions, which enables applications in ion-conducting membranes,⁹⁶⁸ fuel cells,⁹⁶⁹ electromechanical devices,⁹⁷⁰ water purification membranes⁹⁷¹ and breathable textiles for protection against chemical warfare agents.⁹⁷²

While the properties of ionomers are impressive, they come at the cost of processability. Due to the high temperature stability of ionic aggregates (which can persist to temperatures of 300 °C),⁹⁷³ these materials are often difficult to process via extrusion or melt compounding techniques due to their high melt viscosity.⁹⁷⁴ Earlier efforts to improve the processability of sulfonated EPDM centered on the addition of zinc stearate, which possesses long aliphatic

⁹⁶⁷ Agarwal, P. K.; Lundberg, R. D. Viscoelastic behavior of concentrated oil solutions of sulfo polymers. 2. EPDM and zinc sulfo-EPDMs. *Macromolecules* **1984**, 17, 1918.

⁹⁶⁸ Elabd, Y. A.; Walker, C. W.; Beyer, F. L. Triblock copolymer ionomer membranes: Part II. Structure characterization and its effects on transport properties and direct methanol fuel cell performance. *J. Membr. Sci.* **2004**, 231, 181-8.

⁹⁶⁹ Roy, A.; Hickner, M. A.; Yu, X.; Li, Y.; Glass, T.; McGrath, J. E. Influence of Chemical Composition and Sequence Length on the Transport Properties of Proton Exchange Membranes. *J Polym Sci, Part B: Polym Phys* **2006**, 44, 2226-39.

⁹⁷⁰ Akle, B.; Leo, D. J.; Hickner, M. A.; McGrath, J. E. Correlation of capacitance and actuation in ionomeric polymer transducers. *J Mater Sci* **2005**, 40, 3715-24.

⁹⁷¹ Takizawa, M.; Sugito, Y.; Oguma, N.; Nakamura, M.; Horiguchi, S.; Fukutomi, T. Charge-Mosaic Membrane Prepared from Microspheres. *J Polym Sci, Part A: Polym Chem* **2003**, 41, 1251-61.

⁹⁷² Rivin, D.; Meermeier, G.; Schneider, N. S.; Vishnyakov, A.; Neimark, A. V. Simultaneous Transport of Water and Organic Molecules through Polyelectrolyte Membranes. *J. Phys. Chem. B* **2004**, 108, 8900-8909.

⁹⁷³ Lu, X.; Steckle, W. P.; Hsiao, B.; Weiss, R. A. Thermally Induced Microstructure Transitions in a Block Copolymer Ionomer. *Macromolecules* **1995**, 28, 2831-9.

⁹⁷⁴ Weiss, R. A.; Fitzgerald, J. J.; Kim, D. Viscoelastic Behavior of Plasticized Sulfonated Polystyrene Ionomers. *Macromolecules* **1991**, 24, 1064-70.

chains as well a carboxylate ion, which “plasticized” the ionic aggregates when heated above its melting point (128 °C).⁹⁶³

The use of phosphonium cations to introduce ionic interactions has spurred recent research into phosphonium ionomers.^{975, 976} Phosphonium salts benefit from better compatibility with organic media compared to sulfonate and carboxylate salts. Random phosphonium containing ionomers possess thermoplastic elastomeric properties^{977,978} due to the presence of ionic aggregates,⁹⁷⁹ as in sulfonated and other ionomers. Furthermore, the ability of phosphonium salts to aggregate is tuned via the length of the substituents attached to phosphorus. Also, phosphonium salts possess greater thermal stability than the corresponding ammonium salts,⁹⁷⁵ which decompose via Hofmann elimination reactions at 200 °C.⁹⁸⁰ Phosphonium salts and ionomers often possess antibacterial⁹⁸¹ and phase transfer catalytic activity. Applications for phosphonium ionomers in the areas of ionically conductive

⁹⁷⁵ Unal, S.; McKee, M. G.; Massa, D. J.; Long, T. E. Synthesis and characterization of phosphonium-based telechelic polyester ionomers. *Polym Prep* **2005**, 46, 1028-9.

⁹⁷⁶ Ghassemi, H.; Riley, D. J.; Curtis, M.; Bonaplata, E.; McGrath, J. E. Main-Chain Poly(arylene ether) Phosphonium Ionomers. *Appl Organometal Chem* **1998**, 12, 781-5.

⁹⁷⁷ Arjunan, P.; Wang, H.-C.; Olkusz, J. A., *Functional Polymers*. American Chemical Society: Washington DC, 1998; Vol. 704, p 199-216.

⁹⁷⁸ Lindsell, W. E.; Radha, K.; Soutar, I.; Stewart, M. J. The preparation and characterization of phosphorus-terminated poly-1,3-butadiene: new telechelic ionomers. *Polymer* **1990**, 31, 1374-8.

⁹⁷⁹ Parent, J. S.; Penciu, A.; Guillen-Castellanos, A.; Liskova, A.; Whitney, R. A. Synthesis and Characterization of Isobutylene-Based Ammonium and Phosphonium Bromide Ionomers. *Macromolecules* **2004**, 37, 7477-83.

⁹⁸⁰ Burch, R. R.; Manring, L. E. *N*-Alkylation and Hofmann Elimination from Thermal Decomposition of R_4N^+ Salts of Aromatic Polyamide Polyanions: Synthesis and Stereochemistry of *N*-Alkylated Aromatic Polyamides. *Macromolecules* **1991**, 24, 1731-5.

⁹⁸¹ Kanazawa, A.; Ikeda, T.; Endo, T. Polymeric phosphonium salts as a novel class of cationic biocides. IX. Effect of side-chain length between main chain and active group of antibacterial activity. *J Polym Sci, Part A: Polym Chem* **1994**, 32, 1997-2001.

membranes, polymer battery components and water dispersable fiber sizings were envisioned.⁹⁷⁶

We propose the use of hydrogen bonding to allow reversible attachment of the ionic species. We propose that the thermoreversible properties conferred by hydrogen bonds will enable improved processability of ion-containing polymers. The reversible attachment of guest molecules to polymers via nucleobase hydrogen bonding has been investigated in both solution⁹⁸² and the solid state.^{983,984} Rotello et al. have used three-point hydrogen bonding between diacyldiaminopyridines and thymine to attach guest molecules containing flavin⁹⁸⁵ or POSS to polystyrene.⁹⁸³ Hydrogen bonding guest molecules can also increase the solubility of hydrogen bonding polymers via screening of polymer-polymer self-association, thereby maintaining homogeneity during polymerization reactions.⁹⁸⁶ Multiple complementary association modes are possible for nucleobases, including the classical Watson-Crick mode which is present in DNA as well as the less commonly observed Hoogsteen association mode.⁹⁸⁷ Furthermore, nucleobases exhibit several weak

⁹⁸² Thibault, R. J.; Hotchkiss, P. J.; Gray, M.; Rotello, V. M. Thermally Reversible Formation of Microspheres through Non-Covalent Polymer Cross-Linking. *J Am Chem Soc* **2003**, 125, 11249-52.

⁹⁸³ Carroll, J. B.; Waddon, A. J.; Nakade, H.; Rotello, V. M. "Plug and Play" Polymers. Thermal and X-ray Characterizations of Noncovalently Grafted Polyhedral Oligomeric Silsesquioxane (POSS)-Polystyrene Nanocomposites. *Macromolecules* **2003**, 36, 6289-91.

⁹⁸⁴ Ilhan, F.; Gray, M.; Rotello, V. M. Reversible Side Chain Modification through Noncovalent Interactions. "Plug and Play" Polymers. *Macromolecules* **2001**, 34, 2597-601.

⁹⁸⁵ Ilhan, F.; Galow, T. H.; Gray, M.; Clavier, G.; Rotello, V. M. Giant Vesicle Formation through Self-Assembly of Complementary Random Copolymers. *J Am Chem Soc* **2000**, 122, 5895-6.

⁹⁸⁶ Stubbs, L. P.; Weck, M. Towards a Universal Polymer Backbone: Design and Synthesis of Polymeric Scaffolds Containing Terminal Hydrogen-Bonding Recognition Motifs at Each Repeating Unit. *Chem Eur J* **2003**, 9, 992-9.

⁹⁸⁷ Ghosal, G.; Muniyappa, K. Hoogsteen base-pairing revisited: Resolving a role in normal biological processes and human diseases. *Biochemical Biophysical Research Communications* **2006**, 343, 1-7.

self-association modes ($K_a < 10 \text{ M}^{-1}$),⁹⁸⁸ which compete with the complementary association modes. We recently discussed the hydrogen bonding attachment of phosphonium ionic groups to nucleobase containing block copolymers.

In this chapter, we compare the non-covalent attachment of phosphonium salts to the covalent attachment (Figure 14.1). Assuming that ionic interactions are present in phosphonium containing polymers, one would expect effects on rheology due to ionic attractions and ionic aggregates. The use of hydrogen bonding to reversibly attach the ionic groups to the backbone should allow dissociation of these ionic groups and produce a lower viscosity.

⁹⁸⁸ Kyogoku, Y.; Lord, R. C.; Rich, A. The Effect of Substituents on the Hydrogen Bonding of Adenine and Uracil Derivatives. *Proc Natl Acad Sci USA* **1967**, 57, 250-7.

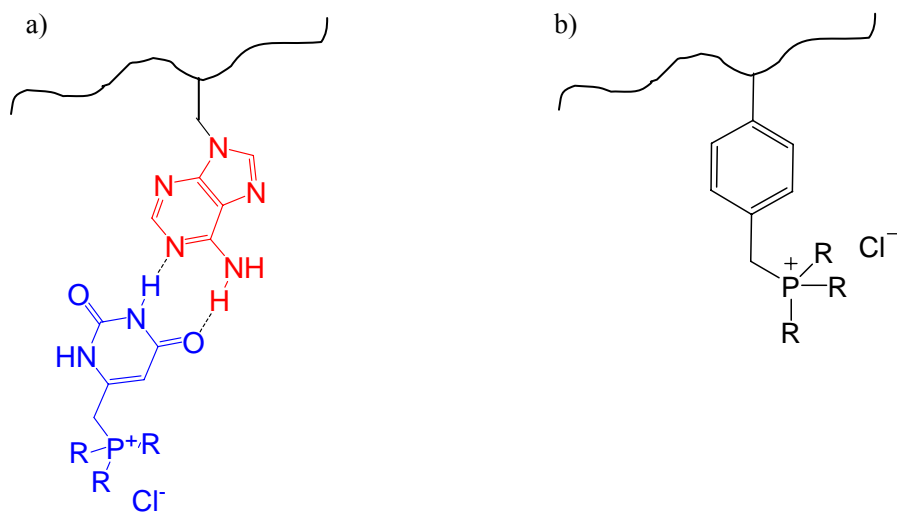


Figure 14.1. Pictorial representation of ionic groups hydrogen bonded to a polymer chain (a) as well as a covalent analog (b).

14.3 Experimental

14.3.1 Materials

n-Butyl acrylate (Aldrich, 99%) was deinhibited via passage through an alumina column. Azobis(isobutyronitrile) (AIBN, 98%), 2,6-di-*tert*-butyl-4-methylphenol (BHT, 99%), trioctylphosphine (90%, tech. grade), vinylbenzyl chloride (mixture of *meta* and *para* isomers, 97%) and 6-chloromethyluracil (98%) were obtained from Aldrich and used as received. 9-vinylbenzyladenine was synthesized as described elsewhere.⁹⁸⁹

14.3.2 Phosphonium Styrene Monomer Synthesis

Vinylbenzyl chloride (2.02 g, 13.2 mmol), BHT (10 mg) and hexanes (25 mL) were combined in a 100 mL round-bottomed flask containing a magnetic stirbar. The flask was sealed with a rubber septum and the solution was purged with argon using a long needle inserted into the solution and a vent needle. Trioctylphosphine (6.56 mL, 13.2 mmol at 90% purity) was injected via syringe and the reaction was heated to 60 °C and stirred for 24 h. The reaction was cooled to room temperature, upon which the product crystallized from the reaction medium. The product was separated by filtration and washed with cold hexanes. The product was recrystallized from hexanes. Yield 4.78 g, 69%. FAB MS: $m/z = 487.442$ $[M-Cl]^+$ (experimental), $m/z = 487.443$ $[M-Cl]^+$ (theoretical). ¹H NMR (CDCl₃, δ, ppm): 0.87 (t, 9H, CH₃), 1.23 (m, 24H, octyl CH₂), 1.42 (m, 12H, octyl CH₂), 2.41 (br, 6H, P-CH₂), 4.31 (d, 2H, $J = 13.9$ Hz, Ph-CH₂-P), 5.29 (dd, 1H, $J_1 = 11$ Hz, $J_2 = 4.3$ Hz, trans Ph-CH=CH₂),

⁹⁸⁹ Srivatsan, S. G.; Parvez, M.; Verma, S. Modeling of Prebiotic Catalysis with Adenylated Polymeric Templates: Crystal Structure Studies and Kinetic Characterization of Template-Assisted Phosphate Ester Hydrolysis. *Chem. Eur. J.* **2002**, *8*, 5184-91.

5.77 (dd, 1H, $J_1 = 17.3$ Hz, $J_2 = 11.1$ Hz, cis Ph-CH=CH₂), 6.68 (dd, 1H, $J_1 = 17.5$ Hz, $J_2 = 10.8$ Hz, Hz Ph-CH=CH₂), 7.3-7.45 (m, 4H, Ph). ³¹P NMR (CDCl₃, δ, ppm): 31.46, 31.57.

14.3.3 Uracil Phosphonium Salt

6-chloromethyluracil (1.001 g, 6.232 mmol) and trioctylphosphine (3.25 mL, 2.70 g, 7.29 mmol) were charged to a 100 mL round-bottomed flask containing a magnetic stirbar. Ethanol (40 mL) was added and a condenser was fitted to the flask. The reaction was heated to reflux using an external oil bath for 24 h. Excess solvent was removed using rotary evaporation. The resulting waxy solid was washed with diethyl ether and was dried overnight at room temperature under high vacuum. UP⁺ was obtained as a light brown solid (m.p. 179-181 °C) in 88% yield. ¹H NMR (DMSO-d₆, δ, ppm): 0.86 (t, 9H, $J = 6.8$ Hz), 1.26 (m, 24H), 1.37 (m, 6H), 1.49 (m, 6H), 2.37 (m, 6H), 3.77 (d, 2H, $J = 15$ Hz), 5.55 (m, 1H), 11.15 (s, 1H), 11.47 (s, 1H). ¹³C NMR (DMSO-d₆, δ, ppm): 13.96, 17.61, 18.06, 20.52, 22.08, 28.27, 28.8, 30.06, 31.22, 102.08, 145.18, 150.95, 163.37. ³¹P NMR (DMSO-d₆, δ, ppm): 33.68 ppm. FAB MS: $m/z = 495.4056$ [M-Cl]⁺ (experimental), $m/z = 495.41$ (theoretical).

14.3.4 Adenine Containing Copolymer

9-vinylbenzyladenine (0.392 g, 1.56 mmol), *n*-butyl acrylate (10 mL, 70.2 mmol), AIBN (30 mg, 0.32 wt% relative to monomer) and THF (33 mL) were combined in a 100 mL round-bottomed flask containing a magnetic stirbar. The flask was sealed with a rubber septum and the solution was purged with argon using a long needle inserted into the solution and a vent needle. The polymerization was conducted at 60 °C for 48 h. The product was

isolated as a viscous liquid polymer by precipitation in methanol/water (90/10 v/v) and dried at 50 °C under vacuum for 18 h. Yield 7.00 g (75%). ¹H NMR (CDCl₃) revealed a 9-vinylbenzyladenine content of 2.0 mol% as determined by comparing the integration of the benzyl CH₂ protons (5.25 ppm) and the *n*-butyl acrylate ester CH₂ protons (3.7-4.0 ppm). SEC in THF using a light scattering detector produced molecular weights of M_n = 17700, M_w = 32600, M_w/M_n = 1.84.

14.3.5 Phosphonium Salt Containing Copolymer

Phosphonium styrene monomer (1.42 g, 2.71 mmol), *n*-butyl acrylate (10 mL, 70.2 mmol), AIBN (25 mg, 0.24 wt% relative to monomer), THF (20 mL) and methanol (14 mL) were combined in a 100 mL round-bottomed flask containing a magnetic stirbar. The flask was sealed with a rubber septum and the solution was purged with argon using a long needle inserted into the solution and a vent needle. The polymerization was conducted at 60 °C for 48 h. The product was isolated by precipitation in methanol/water (90/10 v/v) and dried at 50 °C under vacuum for 18 h. Yield 4.16 g, 40%. ¹H NMR (CD₂Cl₂) revealed a phosphonium styrene content of 2.08 mol% as determined by comparing the integration of the phenyl protons (6.9-7.5 ppm) and the *n*-butyl acrylate ester CH₂ protons (3.7-4.0 ppm). SEC in THF using a light scattering detector produced a bimodal molecular weight distribution with M_{n1} = 21300, M_{w1} = 31000, M_{w1}/M_{n1} = 1.46 (98 wt% of sample), M_{n2} = 151900, M_{w2} = 780000, M_{w2}/M_{n2} = 5.12 (1.9 wt% of sample).

A copolymer with a higher content of phosphonium styrene monomer was also synthesized. Phosphonium styrene monomer (2.85 g, 5.44 mmol), *n*-butyl acrylate (3.7 mL,

26.6 mmol), AIBN (15 mg, 0.24 wt% relative to monomer) and methanol (30 mL) were combined in a 100 mL round-bottomed flask containing a magnetic stirbar. The flask was sealed with a rubber septum and the solution was purged with argon using a long needle inserted into the solution and a vent needle. The polymerization was conducted at 60 °C for 48 h. The product was isolated by precipitation in hexanes and dried at 50 °C under vacuum for 18 h. ¹H NMR (CD₂Cl₂) revealed a phosphonium styrene content of 30.0 mol% as determined by comparing the integration of the phenyl protons (6.9-7.5 ppm) and the *n*-butyl acrylate ester CH₂ protons (3.7-4.0 ppm). SEC in THF was attempted by Eastman and found to be unsuccessful due to adsorption to the column.

14.3.6 Blends of an Adenine Containing Copolymer with a Uracil Phosphonium Salt

Adenine containing copolymer (3.00g, 2.0 mol%, 3.8 wt% comonomer, 0.454 mmol adenine, M_w = 32600) was weighed into a vial. Uracil phosphonium salt (244 mg, 0.460 mmol) was added to the vial. Tetrahydrofuran (5 mL) followed by chloroform (5 mL) were added and the mixture dissolved completely. The solvent was removed via rotary evaporation and the sample was dried under vacuum at 50 °C for 18 h.

14.3.7 Characterization

¹H and ¹³C NMR spectroscopic data was collected in CDCl₃ on a Varian 400 MHz spectrometer at ambient temperature. FAB MS was conducted in positive ion mode on a JEOL HX110 Dual Focusing Mass Spectrometer using xenon ion bombardment, polyethylene glycol (PEG) standards and a 3-nitrobenzyl alcohol matrix. DSC was conducted

on a TA Instruments Q1000 DSC at a heating rate of 20 °C/min under nitrogen. Rheological studies were conducted on a TA Instruments G2 rheometer in parallel plate configuration at a frequency of 1 Hz using 5% strain. The samples were determined to be in the linear viscoelastic regime at this strain value.

14.4 Results and Discussion

A copolymer of 9-vinylbenzyladenine and *n*-butyl acrylate was synthesized using conventional free radical techniques (Figure 14.2). 9-vinylbenzyladenine is a styrenic nucleobase-containing monomer which was synthesized according to literature procedures. The *n*-butyl acrylate comonomer was chosen for the low glass transition temperature of poly(*n*-butyl acrylate) (-40 °C), which would cause the copolymers to exist as liquids at room temperature, and would facilitate rheological experiments of studying hydrogen bonding interactions which usually dissociate at temperatures below 100 °C. The polar solvent THF was utilized due to the limited solubility of the adenine containing monomer in less polar solvents (ethyl acetate). The copolymer contained a low level of adenine comonomer (2.0 mol%) and possessed a low molecular weight ($M_w \sim 32600$).

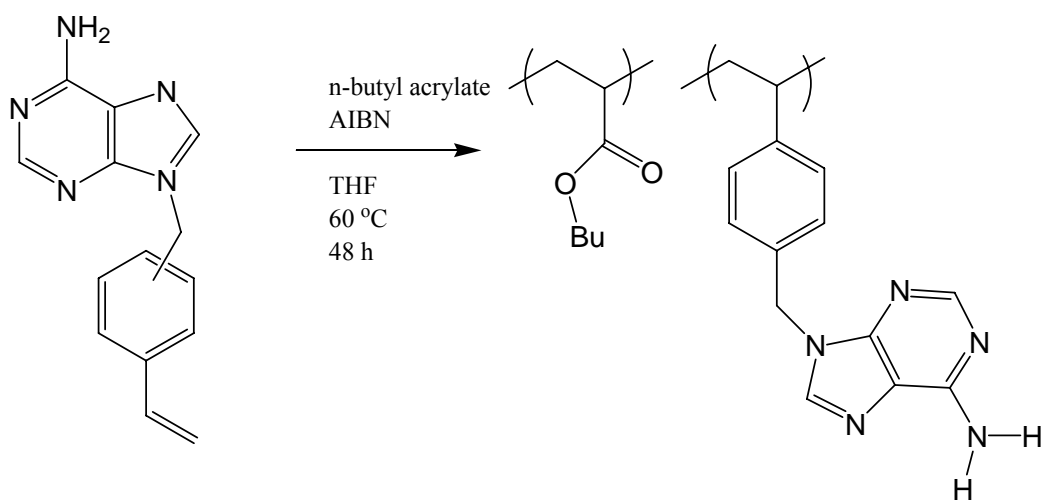


Figure 14.2. Synthesis of an adenine-containing random copolymer.

A phosphonium salt-containing copolymer was synthesized using a phosphonium containing styrenic monomer (Figure 14.3). Initially, polymerizations were conducted in THF, however, it was found that this resulted in very low incorporation of the phosphonium monomer into the polymer. Addition of methanol to the polymerization (40 vol%) resulted in improved incorporation (to 55% of targeted levels) and the polymerizations remained homogeneous. The mixture with THF was chosen to maintain the solubility of the poly(*n*-butyl acrylate) sequences, which are insoluble in methanol. The copolymers with the phosphonium monomer were also viscous liquids at room temperature and had similar comonomer levels compared to the adenine containing copolymers (2.08 mol%).

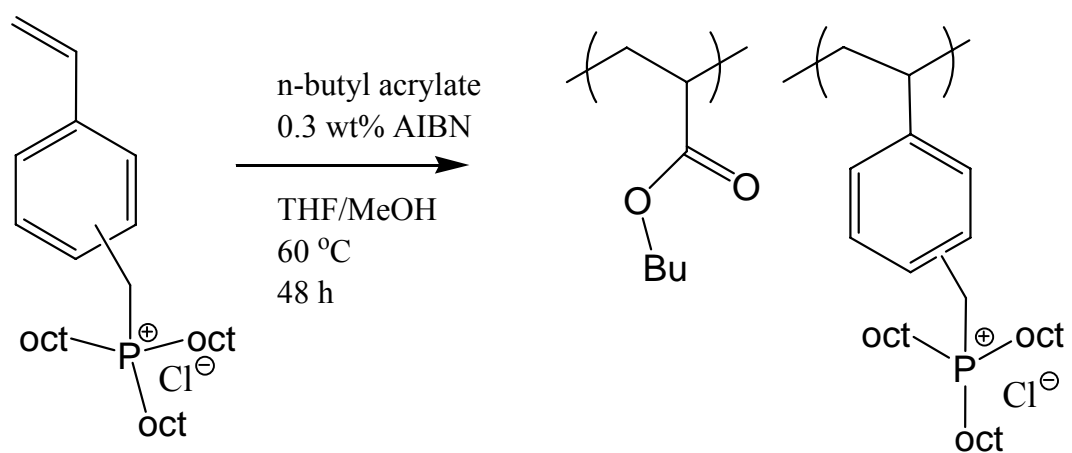


Figure 14.3. Synthesis of a phosphonium styrene containing random copolymer.

A copolymer with a higher content of phosphonium comonomer was synthesized using pure methanol solvent. This resulted in nearly quantitative incorporation of the phosphonium salt monomer (copolymer contained 30 mol%). SEC was challenging for the phosphonium containing copolymers. SEC in THF for the 2 mol% sample produced bimodal molecular weight distributions according to both light scattering (MALLS) and RI detectors. The main portion of the sample (98 wt%) possessed a molecular weight of $M_w = 31000$ ($M_w/M_n = 1.46$). A small portion of the sample (2 wt%) existed as a broad, high molecular weight peak $M_w = 780000$ ($M_w/M_n = 5.12$). No reason could be found for the presence of such high molecular weight material in the sample, and repeated synthesis produced the same result. SEC was attempted at Eastman on the 30 mol% copolymer, however, this resulted in adsorption to the columns and no signal was obtained. The adsorption of the 30 mol% copolymer suggested that similar effects could be responsible for the anomalous SEC of the 2 mol% samples.

DSC analysis of the 30 mol% phosphonium styrene copolymer (Figure 14.4) indicated a broad glass transition temperature centered at 10.7 °C over a range of about 35 °C. This T_g was significantly higher than that of *n*-butyl acrylate homopolymer (-40 °C), likely due to a copolymer effect, since the T_g of a pure phosphonium-containing styrenic polymer is expected to be above that of poly(*n*-butyl acrylate).

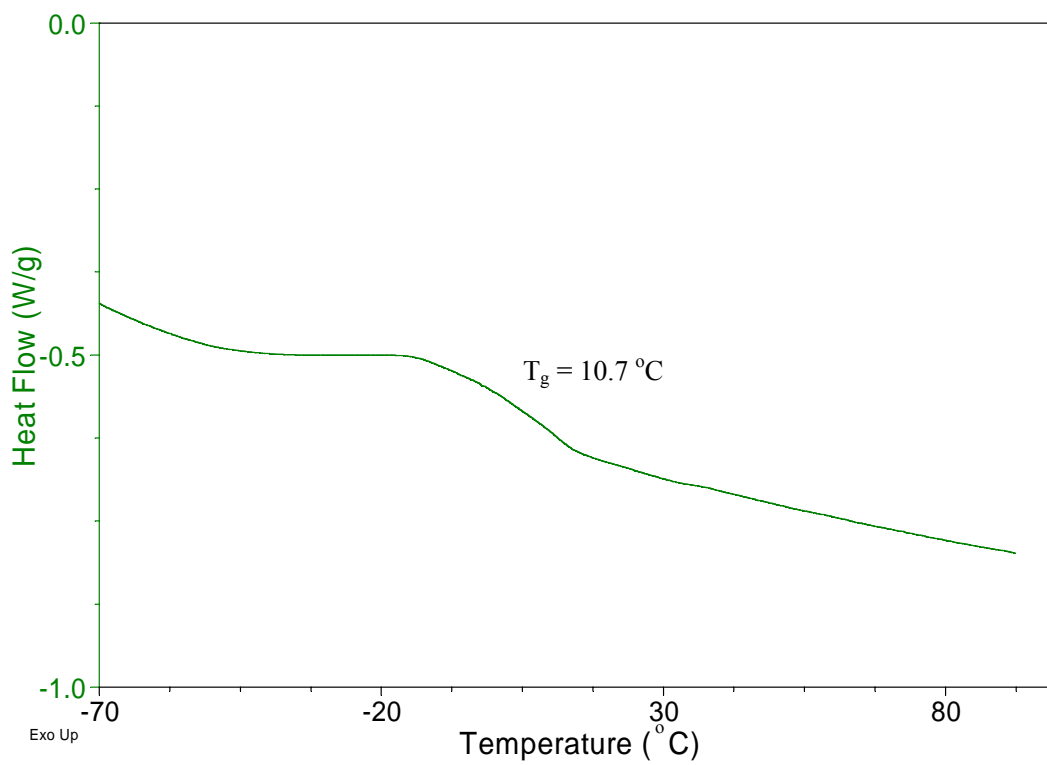


Figure 14.4. DSC analysis of phosphonium styrene copolymer (30 mol%).

Small-angle x-ray scattering was conducted on the 30 mol% copolymer, in order to look for ionic aggregates (Figure 14.5). X-ray scattering revealed a broad scattering maximum at $q = 3.75 \text{ nm}^{-1}$. The scattering maximum was weak, but it was located close to those observed for other ionomers. Winey et al. observed an ionomer peak at $q = 3.7 \text{ nm}^{-1}$ for poly(styrene-*co*-methacrylic acid) neutralized with copper (II) salts.⁹⁹⁰ The Yarusso-Cooper model, which was developed to model scattering from ionomeric aggregates,⁹⁹¹ was utilized to fit the scattering maxima. The fitting parameters for the Yarusso-Cooper model, the aggregate radius (R_1) and the radius of closest approach between aggregates (R_{ca}) matched closely with those observed by Winey et al. for the copper-neutralized styrene-methacrylic acid ionomers, whereas the volume of polymer per aggregate (V_p) was significantly lower (Table 14.1). The difference in the V_p values observed was attributed to the level of ionic groups present in the current copolymer (30 mol%) compared with the polymer studied by Winey (6.2 mol%). If the higher mole fraction in the current study resulted in the formation of more aggregates, then one would expect the volume of polymer per aggregate to decrease.

⁹⁹⁰ Benetatos, N. M.; Heiney, P. A.; Winey, K. I. Reconciling STEM and X-ray Scattering Data from a Poly(styrene-*ran*-methacrylic acid) Ionomer: Ionic Aggregate Size. *Macromolecules* **2006**, 39, 5174-6.

⁹⁹¹ Yarusso, D.J.; Cooper, S.L. Microstructure of Ionomers: Interpretation of Small-Angle X-ray Scattering Data. *Macromolecules* **1983**, 16, 1871-80.

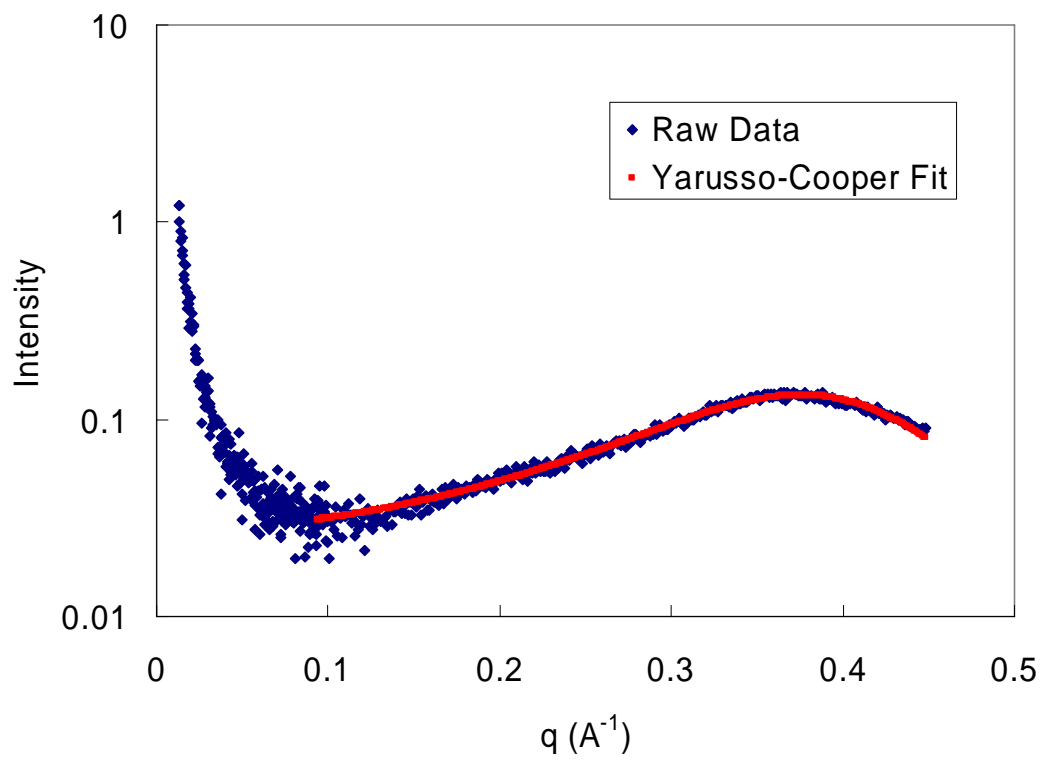


Figure 14.5. Small-angle X-ray scattering of 30 mol% phosphonium copolymer.

Table 14.1. Yarusso-Cooper fitting of scattering for 30 mol% phosphonium copolymer.

Sample	R_1 (nm)	R_{ca} (nm)	V_p (nm ³)
Phosphonium Copolymers	0.56	0.70	2.3
Styrene-methacrylic acid copolymers (Winey et al.) ⁹⁹²	0.50	0.71	4.2

⁹⁹² Benetatos, N. M.; Heiney, P. A.; Winey, K. I. Reconciling STEM and X-ray Scattering Data from a Poly(styrene-*ran*-methacrylic acid) Ionomer: Ionic Aggregate Size. *Macromolecules* **2006**, 39, 5174-6.

Dynamic mechanical analysis was utilized to study the 30 mol% phosphonium copolymer (Figure 14.6). The polymer, which was a tough, glassy solid, was melt pressed to obtain film samples. DMA revealed multiple transitions including a T_g at 20 °C (E'' maximum) and additional transitions near 38 and 56 °C. The primary maximum in the tan delta curve occurred at 45 °C. The additional transitions in the loss modulus curve were possibly attributed to dissociation of ionic aggregates. Teyssie et al. have observed multiple transitions in the loss modulus curve for telechelic quaternary ammonium ionomers based on polyisoprene. They observed rubbery plateaus for their materials which decreased in extent for longer alkyl chain substituents on the ammonium cation. For an bis(hexadecyldimethylammonium iodide) terminated polyisoprene, two peaks in the loss modulus curve were observed, one corresponding to the T_g of polyisoprene and one at about 35 °C, corresponding the dissociation of the ammonium ion aggregates and the end of the rubbery plateau.⁹⁹³

⁹⁹³ Charlier, P.; Jerome, R.; Teyssie, P.; Utracki, L.A. Viscoelastic Properties of Telechelic Ionomers. 2. Quaternized α,ω -bis(dimethylamino)polyisoprene. *Macromolecules* **1992**, 25, 617-24.

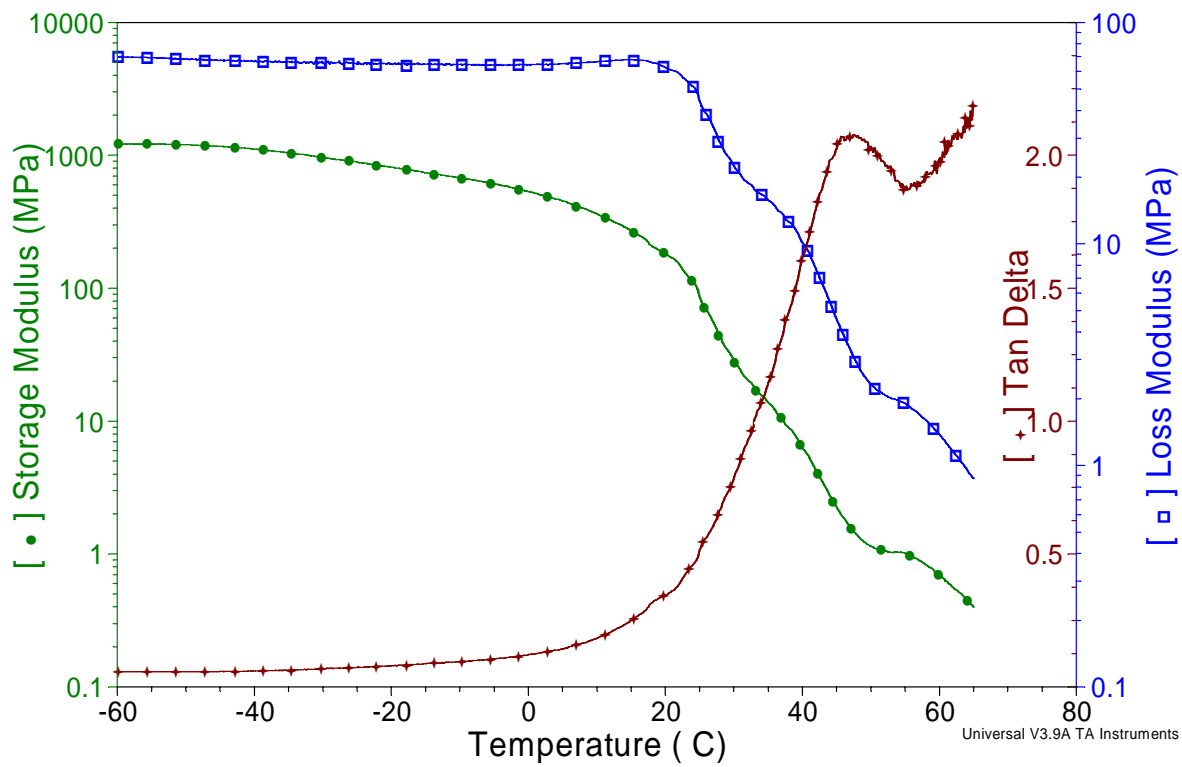


Figure 14.6. DMA analysis of 30 mol% phosphonium copolymer.

A uracil functionalized phosphonium salt was synthesized in a single step from 6-chloromethyluracil and trioctylphosphine. The salt was soluble in chloroform, a common solvent utilized to study hydrogen bonding systems. The uracil phosphonium salt was blended with the complementary 2.0 mol% adenine containing random copolymer at a 1:1 adenine to uracil molar ratio in chloroform solution. The blend appeared slightly cloudy, suggesting possible phase separation of the uracil phosphonium salt. The blend was characterized using differential scanning calorimetry, which allowed comparisons to the 2.0 mol% phosphonium copolymer and the pure adenine copolymer (Figure 14.7). Both of the copolymers and the blend exhibited nearly identical T_g values near $-50\text{ }^\circ\text{C}$. The blend of the uracil phosphonium salt with the adenine copolymer exhibited a small melting endotherm near $160\text{ }^\circ\text{C}$, which was characteristic of the crystalline uracil phosphonium salt. However, upon integration of this endotherm and calculating based on the composition of the blend, it was determined that only 30% of the uracil phosphonium salt was in the crystalline state. This suggests that 70% of the uracil phosphonium was dissolved into the adenine-functional random copolymer.

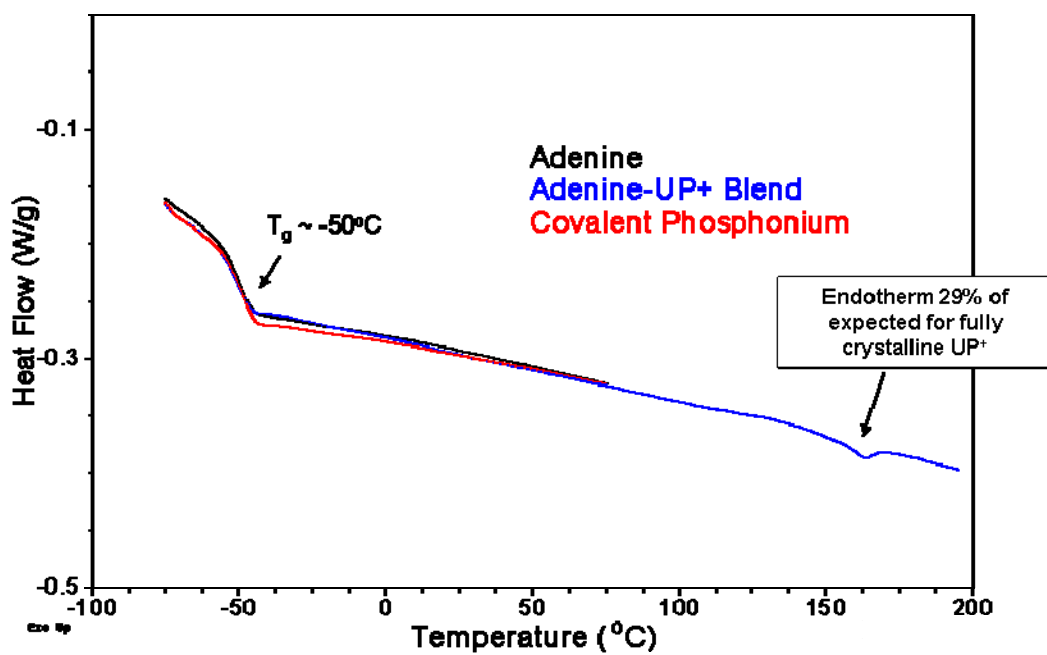


Figure 14.7. DSC analysis of blends of adenine- and phosphonium-functional random copolymers and blend of adenine copolymer with uracil phosphonium salt.

Constant frequency (1 Hz), variable temperature rheological studies were conducted on the blend of the adenine copolymer with the uracil phosphonium salt, and the individual adenine and phosphonium functional copolymers were also run as references. The viscosity of the adenine functionalized copolymer was the lowest out of the three polymers. The covalently bound phosphonium copolymer possessed melt viscosity values at 25 °C that were 2.7 times higher than the adenine copolymer. The increased melt viscosities observed for the covalent phosphonium copolymer could be attributed to either higher molecular weight, if the SEC data are reliable, or ionic interactions between polymer chains. The blend of the uracil phosphonium salt with the adenine copolymer produced melt viscosities that were nearly identical to the phosphonium copolymer, across the range of temperatures studied (25-100 °C). This suggested strong attachment of the phosphonium salt to the adenine copolymer, without significant disruption of hydrogen bonding interactions over the range of temperatures studied. The presence of dispersed crystals of the uracil phosphonium salt were not expected to result in the ~3 fold increased viscosity of the blend compared to the pure adenine functional polymer. This is due to calculations that reveal that only 2.3 wt% of the blend consists of phase separated uracil phosphonium salt, based on DSC results, and work from others shows negligible viscosity effects for particle dispersions at this low loading.⁹⁹⁴ The flow activation energies for each sample were similar, near 53 kJ/mol.

⁹⁹⁴ Rueb, C.J.; Zukoski, C.F. Rheology of Suspensions of Weakly Attractive Particles: Approach to Gelation. *J Rheol.* **1998**, 42, 1451-76.

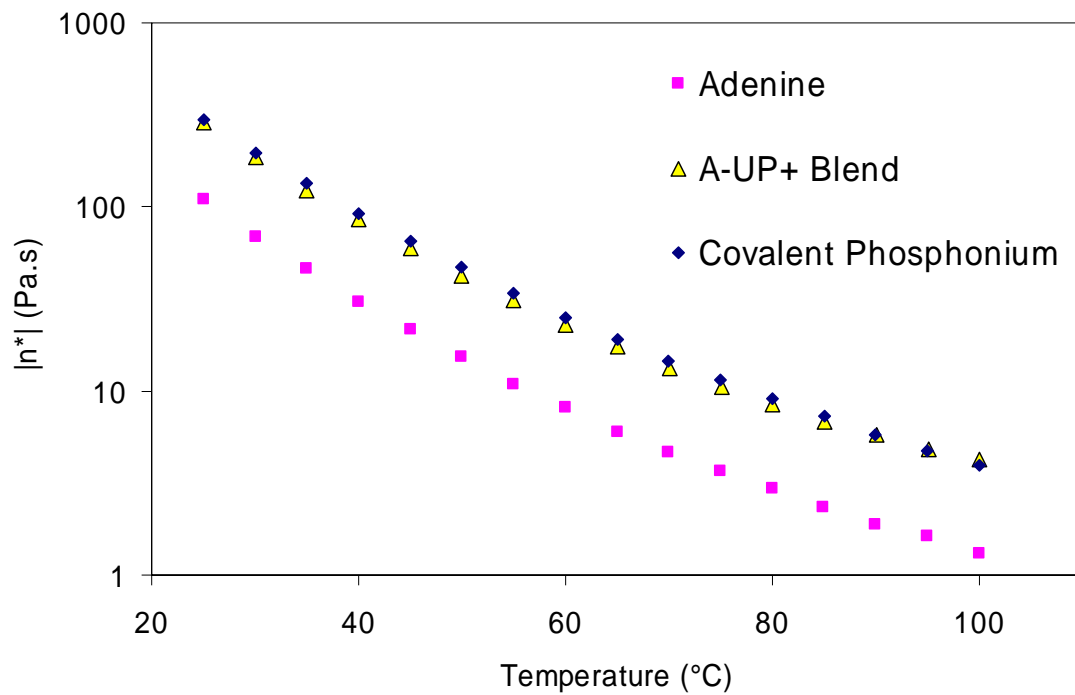


Figure 14.8. Rheological analysis of uracil phosphonium salt blend with adenine copolymer and comparisons with adenine and phosphonium copolymers.

14.5 Conclusions

Random copolymers of a phosphonium styrene monomer and *n*-butyl acrylate were synthesized in order to compare the covalent attachment of phosphonium ions to hydrogen bonding attachment. Hydrogen bonding attachment of ionic groups was achieved through blending of an adenine containing copolymer with a complementary uracil phosphonium salt. Partial miscibility of the uracil phosphonium salt with the 2.0 mol% adenine-functional copolymer was observed. Rheological studies indicated strong attachment of the uracil phosphonium salt, with rheological behavior of the blend mirroring that of the covalent copolymer across the range of temperatures studied. Covalent phosphonium copolymers with higher incorporation of the phosphonium salt monomer (30 mol%) resulted in increased T_g , a broad maximum in the small-angle X-ray scattering curve and multiple transitions above T_g in dynamic mechanical analysis. These findings suggest ionic aggregation in the high mole fraction phosphonium copolymer.

14.6 Future work

The next steps in this study are to examine the melt rheology of the blends at higher temperatures to attempt to observe the dissociation of the hydrogen bonding groups and secondly, to study phosphonium copolymers with intermediate comonomer contents, to determine the lower limit of phosphonium comonomer resulting in ionic aggregation.

14.7 Acknowledgement

This material is based upon work supported by, or in part by, the U.S. Army Research

Laboratory and the U.S. Army Research Office under grant number DAAD19-02-1-0275

Macromolecular Architecture for Performance (MAP) MURI.

Chapter 15. Overall Conclusions

Non-covalent interactions including nucleobase hydrogen bonding and ionic aggregation were studied in block and end-functional polymers synthesized via living polymerization techniques such as nitroxide mediated polymerization and anionic polymerization. Non-covalent interactions were expected to increase the effective molecular weight of the polymeric precursors through intermolecular associations. The influence of non-covalent association on the structure/property relationships of these materials were studied in terms of physical properties (tensile, DMA, rheology) as well as morphological studies (AFM, SAXS).

Terminal nucleobase functionality was studied in the form of uracil end-functionalized homopolymers of *n*-butyl acrylate synthesized through nitroxide mediated polymerization from novel functional initiators. Hydrogen bonding interactions were observed through increased melt rheology compared to non-functional analogs.

Nucleobase functionalized block copolymers, which consisted of microphase separated domains of nucleobase-functionalized blocks dispersed in a rubbery *n*-butyl acrylate matrix exhibited enhanced hydrogen bonding interactions due to the synergy of hydrogen bonding with microphase separation. Hydrogen bonding interactions were observed for blends of the complementary nucleobase-functionalized block copolymers in terms of increased specific solution viscosity as well as higher scaling exponents for viscosity with solution concentration. In the solid state, the blends exhibited evidence of a complementary A-T hard phase, which formed upon annealing, and dynamic mechanical analysis (DMA) revealed

higher softening temperatures.

Multiple hydrogen bonding interactions were utilized to reversibly attach uracil-functional quaternary phosphonium ionic guests to complementary adenine-functionalized triblock copolymers. The optically clear, compatible blends exhibited lower solution viscosity and lower softening temperatures, which were ascribed to screening of interchain hydrogen bonding interactions from the ionic guest molecules. A morphological transition from cylinders to lamellae was also observed due to selective uptake of the uracil phosphonium salt into the adenine containing hard domains and the resultant increased hard phase volume fraction. The molecular recognition between a water-soluble uracil functionalized phosphonium salt and an adenine-containing block copolymer surface was observed using quartz crystal microbalance with dissipation (QCM-D) measurements

Covalently attached ionic groups were studied in terms of sulfonated block copolymers synthesized via anionic polymerization. As for hydrogen bonding block copolymers, only low block molecular weights of the sulfonated blocks (1K) were necessary to achieve microphase separation. Strong ionic interactions resulted in greater extents for the rubbery plateau in DMA analysis.

In contrast to the physical networks consisting of sulfonated or hydrogen bonding block copolymers, covalent networks were synthesized using carbon-Michael addition chemistry of acetoacetate functionalized telechelic oligomers to diacrylate Michael acceptors. The thermomechanical properties of the networks based on poly(propylene glycol) oligomers were analyzed with respect to the molecular weight between crosslink points (M_c) and the critical molecular weight for entanglement (M_e). A novel acid-cleavable diacrylate

crosslinker was synthesized and utilized as a difunctional Michael acceptor in the synthesis of acid-cleavable crosslinked networks via Michael addition of telechelic poly(ethylene glycol) bis(acetoacetate).

VITAE

Brian Douglas Mather was born in Albuquerque, New Mexico, to Joseph Douglas Mather and Joan Cecile Voute. He was raised in New Mexico, Texas, California and Washington State, prior to returning to Albuquerque, New Mexico at age 16. He graduated from La Cueva High School in May 1998. He attended college at the University of New Mexico (UNM) and obtained his Bachelor's degree in Chemical Engineering in May 2002, graduating *summa cum laude*. Brian was involved with the engineering honor society Tau Beta Pi at UNM and won the Breece award and Donald F. Othmer awards for academic achievement. During college, Brian interned with Sandia National Laboratories working for Dr. Douglas Loy and Dr. Christopher Cornelius and conducted undergraduate research with Prof. James A. Brozik in the Department of Chemistry at UNM. It was during a summer internship at Virginia Tech in 2000, in which Brian worked for Prof. Timothy E. Long that he developed a strong interest in polymer research. The internship attracted Brian to return to graduate school at Virginia Tech where he worked for Prof. Timothy E. Long. Brian was a Cunningham Fellow at Virginia Tech and also won the Chevron-Phillips Chemical Professional Excellence Travel Award. Brian was fortunate to intern at Kraton Polymers in Houston, TX during the summer of 2004, where he worked with Dr. Carl L. Willis. Brian met his wife, Qian Zhang in the Chemistry Department of Virginia Tech in October 2003. Brian and Qian were married on January 5, 2005 in Albuquerque, New Mexico. After graduating in May 2007, he and his wife will begin work at Hewlett-Packard in San Diego, California.